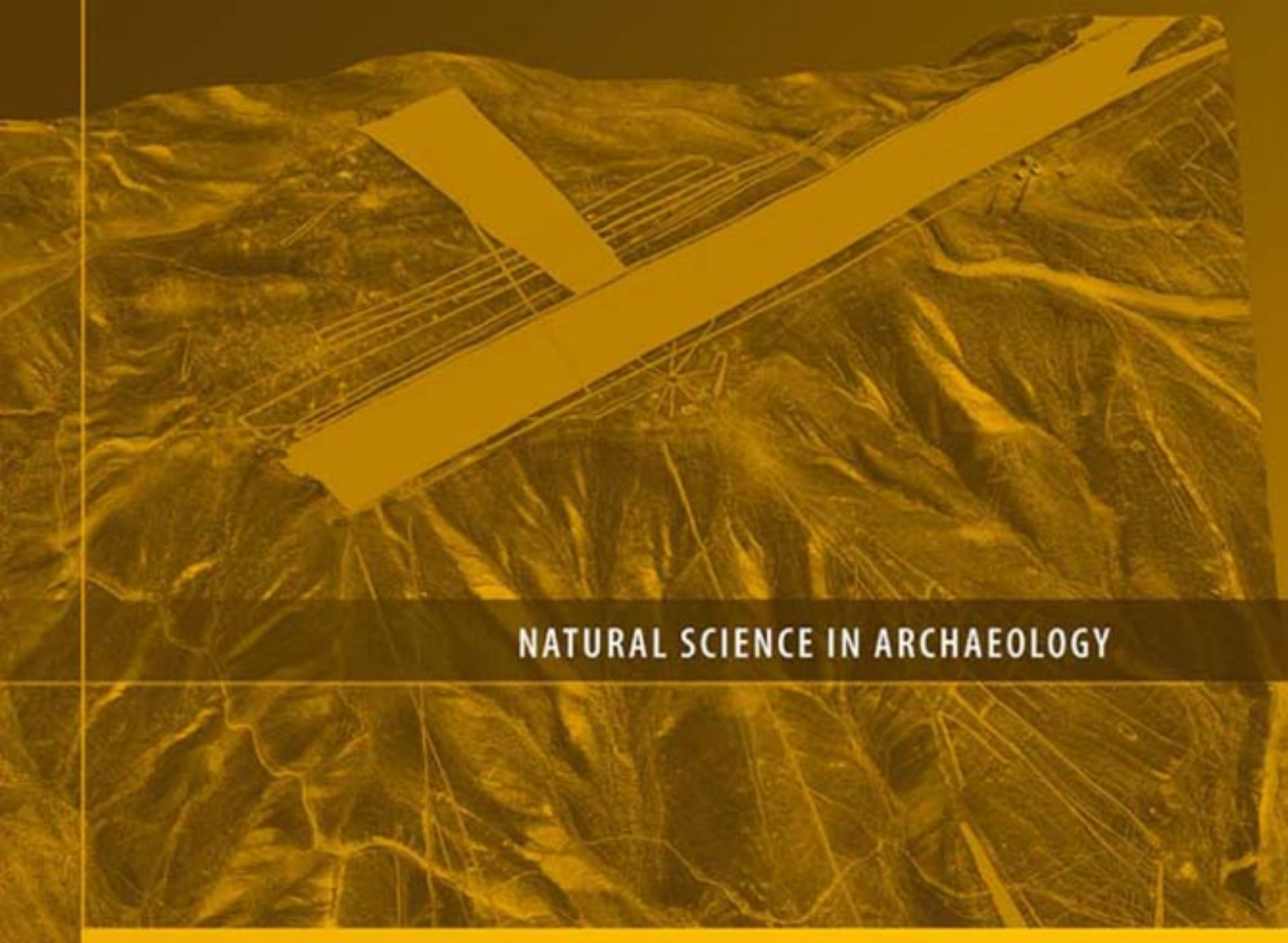

NATURAL SCIENCE IN ARCHAEOLOGY

M. Reindel · G. A. Wagner (Eds.)

New Technologies for Archaeology

Multidisciplinary Investigations in Palpa and Nasca, Peru

Springer

Natural Science in Archaeology

Series editors: B. Herrmann, G. A. Wagner

Markus Reindel · Günther A. Wagner (Eds.)

New Technologies for Archaeology

Multidisciplinary Investigations in Palpa and Nasca, Peru

With 223 Figures and 30 Tables

Springer

Volume Editors

Dr. Markus Reindel
Deutsches Archäologisches Institut
Kommission für Archäologie Außereuropäischer Kulturen (KAAK)
Dürenstr. 35-37
53173 Bonn
Germany
reindel@kaak.dainst.de

Prof. Dr. Günther A. Wagner
Geographisches Institut
Universität Heidelberg
Im Neuenheimer Feld 348
69120 Heidelberg
Germany
g.wagner@mpi-hd.mpg.de

Series Editors

Prof. Dr. Bernd Herrmann
Universität Göttingen
Institut für Anthropologie
Bürgerstraße 40
37073 Göttingen
Germany
bherrmann@gwdg.de

Prof. Dr. Günther A. Wagner
Geographisches Institut
Univesität Heidelberg
Im Neuenheimer Feld 348
69120 Heidelberg
Germany
g.wagner@mpi-hd.mpg.de

ISBN: 978-3-540-87437-9 e-ISBN: 978-3-540-87438-6

DOI 10.1007/978-3-540-87438-6

Library of Congress Control Number: 2008936494

Natural Science in Archaeology ISSN: 1613-9712

© Springer-Verlag Berlin Heidelberg 2009

This work is subject to copyright. All rights are reserved, whether the whole or part of the material is concerned, specifically the rights of translation, reprinting, reuse of illustrations, recitation, broadcasting, reproduction on microfilm or in any other way, and storage in data banks. Duplication of this publication or parts thereof is permitted only under the provisions of the German Copyright Law of September 9, 1965, in its current version, and permission for use must always be obtained from Springer. Violations are liable to prosecution under the German Copyright Law.

The use of general descriptive names, registered names, trademarks, etc. in this publication does not imply, even in the absence of a specific statement, that such names are exempt from the relevant protective laws and regulations and therefore free for general use.

The research project reported in this book was financed by the German Federal Ministry of Education and Research under the grant no. 03REX1VP. The authors are responsible for the contents of this publication.

Cover picture: Geoglyphs on the Sacramento ridge, SW of the town of Palpa. Institute of Geodesy and Photogrammetry, ETH Zurich

Cover design: deblik, Berlin

Printed on acid-free paper

9 8 7 6 5 4 3 2 1

springer.com

Preface

In 2002 the multidisciplinary research project "Nasca: development and adaptation of archaeometric techniques for the investigation of cultural history" (*Nasca: Entwicklung und Adaption archäometrischer Techniken zur Erforschung der Kulturgeschichte*) started, funded by the German Federal Ministry of Education and Research (*Bundesministerium für Bildung und Forschung, BMBF*) in its priority program "New scientific methods and technologies for the humanities" (*Neue Naturwissenschaftliche Methoden und Technologien für die Geisteswissenschaften, NTG*). This new project continued and in a certain way fulfilled a lasting goal of the ministry to integrate different branches of scientific activities and to foster the transfer of expertise gained in natural sciences to the humanities and vice versa. Archaeometry, by definition the application of scientific methods in archaeological investigation, has been a major focus of the priority program since its beginnings in 1989.

After funding numerous fruitful research projects that developed new archaeometric techniques mostly in bilateral cooperation, an even greater outcome was expected from a more multifaceted approach with the participation of various scientific disciplines around a well-defined, archaeological research topic. Furthermore, it was intended to establish a project outside the traditional research areas in central Europe or the Mediterranean. It was the great merit of the person formerly in charge of the BMBF priority program, Dr. Edgar Pusch, to develop these far-reaching perspectives and we are extremely grateful that after a rigorous screening our project among other interesting ones was selected for funding.

Our project was in a favourable situation because it met precisely the requirements defined by the BMBF, having developed a challenging research design centered on the puzzling problem of the Nasca lines in the desert of southern coastal Peru. The initial archaeological steps were financed by the Swiss-Liechtenstein Foundation for Archaeological Research Abroad (SLSA) and we are not only grateful for this support of the archaeological activities, but even more for this unique opportunity to develop a key project which in many ways became exemplary and trend-setting for future research activities. We also received very valuable financial support from the Japan Maria Reiche Fund, which enabled us to build a little museum in the center of Palpa where we can now present the results of our scientific work to the public.

We were always supported and assisted in the organization and management of the project by the project-executing institution at the Research Center Jülich, especially its representatives, Dr. Hans-Joachim Krebs and Dr. Sabine Gerhard. It was their idea to organize not only meetings and workshops in Germany, but also a field conference directly in the research area, in Palpa, where the base camp of our field campaigns was located. Five days of very intensive talks and discussions and the following excursion with about 70 participants of the field conference, among them the project members, Peruvian partners and colleagues, and international specialists from many different countries, reflected very well the special spirit of this project group: the concentration of knowledge in an interdisciplinary project in direct contact with the areas of research yielded an exceedingly high output of scientific results in an excellent working atmosphere.

At this point we as the coordinators and at the same time the editors of this volume, which constitutes the final report of our research project, would like to thank all our German, Swiss, Peruvian, and other international colleagues for their dedicated work in this very productive cooperative effort to develop new methods and technologies for archaeological investigation and to advance the knowledge of the ancient South American cultures.

In Peru we always received optimal support from the authorities and the cooperating institutions. We are indebted to the National Institute for Cultural Heritage (Instituto Nacional de Cultura, INC) for always handling the permits for our archaeological investigations in a nonbureaucratic and effective manner, and we especially thank the former director of the INC, Dr. Luis Guillermo Lumbreras, for his steady support of and interest in our project. We also thank our direct partners at the regional department of the INC, Rubén García and Susana Arce, for their very friendly and effective cooperation.

The realization of the high goals of our project, sometimes resulting in a very tight working schedule, would not have been possible without the support of the German embassy, which not only aided at the administrative level, but also enabled the logistics; exchanging research equipment and samples for the analyses in laboratories in Germany were crucial for the success of this project. We are especially grateful to the ambassador Dr. Roland Kliesow and the attaché for cultural affairs, Jens Urban, for their support and sincere interest as well as their visits to Palpa and participation in public activities of the project in Lima and Palpa.

Our special thanks go to our Peruvian colleagues and friends in Nasca and Palpa, for their hospitality and for their patience while introducing us to their fascinating world and showing us the enigmas of their pre-Hispanic history. Without their knowledge and careful observations, but also the ability to assimilate quickly new skills and at the same time to adapt to the sometimes seemingly strange behavior of the "gringos" who populated the Palpa valleys for a short time every year, they contributed a great deal to the success of the project. Our host for several years at the Fundo Jauranga, merits special mention: Don Oscar Tijero, who not only followed our research activities

with special interest, but also transmitted to us his fascination for the local history and motivated some of the most successful archaeological activities of the project.

In summary, after five years of intense research activities with a multitude of scientific results, new insights into Andean history, the development of new technologies for archaeology being useful also in other regions of the world, countless publications in different disciplines, public presentations and documentaries on radio and television, the people of Palpa will be astonished when they realize that the slogan they coined many years ago for their little forgotten desert town, turns out to be quite accurate: *Palpa es más de lo que te imaginas* (Palpa is more than you can imagine).

Bonn and Heidelberg — *Markus Reindel*
August 2008 — *Günther Wagner*

Contents

1 Introduction – New Methods and Technologies of Natural Sciences for Archaeological Investigations in Nasca and Palpa, Peru 1
Markus Reindel and Günther A. Wagner

Part I Geoarchaeology

2 Man and Environment in the Eastern Atacama Desert (Southern Peru): Holocene Climate Changes and Their Impact on Pre-Columbian Cultures 17
Bernhard Eitel and Bertil Mächtle

3 Built on Sand: Climatic Oscillation and Water Harvesting During the Late Intermediate Period 39
Bertil Mächtle, Bernhard Eitel, Gerd Schukraft and Katharina Ross

Part II Geophysics

4 Beneath the Desert Soil – Archaeological Prospecting with a Caesium Magnetometer 49
Jörg W. E. Fassbinder and Tomasz H. Gorka

5 Quantum Detection Meets Archaeology – Magnetic Prospection with SQUIDs, Highly Sensitive and Fast 71
Sven Linzen, Volkmar Schultze, Andreas Chwala, Tim Schüler, Marco Schulz, Ronny Stolz and Hans-Georg Meyer

6 Viewing the Subsurface in 3D: Sediment Tomography for (Geo-)Archaeological Prospection in Palpa, Southern Peru 87
Stefan Hecht

7 **The Field of Sherds: Reconstructing Geomagnetic Field Variations from Peruvian Potsherds** 103
Florian Stark, Roman Leonhardt, Jörg W.E. Fassbinder and Markus Reindel

Part III Bioarchaeology

8 **From Hunters to Regional Lords: Funerary Practices in Palpa, Peru** . . 119
Johny Isla Cuadrado

9 **Talking Bones: Bioarchaeological Analysis of Individuals from Palpa** . . 141
Elsa Tomasto Cagigao

10 **Who Were the Nasca? Population Dynamics in Pre-Columbian Southern Peru Revealed by Ancient DNA Analyses** 159
Lars Fehren-Schmitz, Susanne Hummel and Bernd Herrmann

11 **Humans and Camelids in River Oases of the Ica–Palpa–Nazca Region in Pre-Hispanic Times – Insights from H-C-N-O-S-Sr Isotope Signatures** 173
Peter Horn, Stefan Hölzl, Susanne Rummel, Göran Åberg, Solveig Schiegl, Daniela Biermann, Ulrich Struck and Andreas Rossmann

12 **The Nasca and Their Dear Creatures – Molecular Genetic Analysis of Pre-Columbian Camelid Bones and Textiles** 193
Rebecca Renneberg, Susanne Hummel and Bernd Herrmann

Part IV Archaeochronometry

13 **Of Layers and Sherds: A Context-Based Relative Chronology of the Nasca Style Pottery from Palpa** 207
Niels Hecht

14 **The Clock in the Corn Cob: On the Development of a Chronology of the Paracas and Nasca Period Based on Radiocarbon Dating** 231
Ingmar Unkel and Bernd Kromer

15 **Cold Light from the Sediments of a Hot Desert: How Luminescence Dating Sheds Light on the Landscape Development of the Northeastern Atacama** 245
Annette Kadereit, Steffen Greilich, Clemens Woda and Günther A. Wagner

16 Light Thrown on History – The Dating of Stone Surfaces at the Geoglyphs of Palpa Using Optically Stimulated Luminescence 271
Steffen Greilich and Günther A. Wagner

Part V Geomatics

17 Virtual Archaeology – New Methods of Image-Based 3D Modeling . . 287
Armin Gruen

18 Virtual Flight Over the Nasca Lines – Automated Generation of a Photorealistically Textured 3D Model of the Pampa de Nasca . . 307
Martin Sauerbier

19 Context Matters: GIS-Based Spatial Analysis of the Nasca Geoglyphs of Palpa 321
Karsten Lambers and Martin Sauerbier

20 A Model Helicopter Over Pinchango Alto – Comparison of Terrestrial Laser Scanning and Aerial Photogrammetry 339
Henri Eisenbeiss

21 Perspectives and Contrasts: Documentation and Interpretation of the Petroglyphs of Chichictara, Using Terrestrial Laser Scanning and Image-Based 3D Modeling 359
Peter Fux, Martin Sauerbier, Thomas Kersten, Maren Lindstaedt and Henri Eisenbeiss

22 Pottery Plotted by Laser – 3D Acquisition for Documentation and Analysis of Symmetry of Ancient Ceramics 379
Hubert Mara

Part VI Archaeometallurgy

23 Gold in Southern Peru? Perspectives of Research into Mining Archaeology 393
Thomas Stöllner

24 Fingerprints in Gold 409
Sandra Schlosser, Robert Kovacs, Ernst Pernicka, Detlef Günther and Michael Tellenbach

Part VII Summary

25 Life at the Edge of the Desert – Archaeological Reconstruction of the Settlement History in the Valleys of Palpa, Peru 439
Markus Reindel

References 463

Index 505

Contributors

Göran Åberg Bavarian State Collection for Palaeontology and Geology, Munich, Richard-Wagner Straße 10, 80333 Munich, Germany, goranelin@hotmail.com

Daniela Biermann Obere Beutau 79, 73728 Esslingen, Germany, daniela.biermann@t-online.de

Andreas Chwala Institute of Photonic Technology e.V., POB 100239, 07702 Jena, Germany, andreas.chwala@ipht-jena.de

Henri Eisenbeiss ETH Zurich, Institute of Geodesy and Photogrammetry, ETH Hönggerberg HIL D 43.2, 8093 Zurich, Switzerland, henri.eisenbeiss@geod.baug.ethz.ch

Bernhard Eitel Institute of Geography, University of Heidelberg, Im Neuenheimer Feld 348, 69120 Heidelberg, Germany, bernhard.eitel@geog.uni-heidelberg.de

Jörg W.E. Fassbinder Bavarian State Department for Monuments and Sites, Archaeological Prospection, Hofgraben 4, 80539 Munich, Germany, joerg.fassbinder@BLFD.Bayern.de

Lars Fehren-Schmitz Johann Friedrich Blumenbach Institute of Zoology and Anthropology, Historical Anthropology and Humanecology, Georg-August-University Goettingen, Bürgerstraße 50, 37073 Göttingen, Germany, lfehren@gwdg.de

Peter Fux Museum Rietberg Zürich, Gablerstrasse 15, 8002 Zürich, Switzerland, peter.fux@zuerich.ch

Tomasz H. Gorka Bavarian State Department for Monuments and Sites, Archaeological Prospection, Hofgraben 4, 80539 Munich, Germany, gorka@geophysik.uni-muenchen.de

Steffen Greilich Radiation Research Department, Risø National Laboratory for Sustainable Energy, Technical University of Denmark, Frederiksborgvej 399, 4000 Roskilde, Denmark, Steffen.Greilich@risoe.dk

Armin Grün ETH Zurich, Institute of Geodesy and Photogrammetry, ETH Hönggerberg HIL D 43.2, 8093 Zurich, Switzerland, agruen@geod.baug.ethz.ch

Detlef Günther ETH Zurich, Department of Chemistry and Applied Biosciences, Laboratory of Inorganic Chemistry, HCI G 113, Wolfgang-Pauli-Straße 10, 8093 Zurich, Switzerland, detlef.guenther@inorg.chem.ethz.ch

Niels Hecht, M. A. German Archaeological Institute (DAI), Commission for Archaeology of Non-European Cultures (KAAK), Bonn, Dürenstraße 35–37, 53173 Bonn, Germany, nihecht@web.de

Stefan Hecht Institute of Geography, University of Heidelberg, Im Neuenheimer Feld 348, 69120 Heidelberg, Germany, stefan.hecht@geog.uni-heidelberg.de

Bernd Herrmann Johann Friedrich Blumenbach Institute of Zoology and Anthropology, Historical Anthropology and Humanecology, Georg-August-University Göttingen, Bürgerstraße 50, 37073 Göttingen, Germany, bherrma@gwdg.de

Stefan Hölzl Bavarian State Collection for Palaeontology and Geology, Munich, Richard-Wagner Straße 10, 80333 München, Germany, s.h@lmu.de

Peter Horn Bavarian State Collection for Palaeontology and Geology, Munich, Richard-Wagner Straße 10, 80333 München, Germany, p.horn@lrz.uni-muenchen.de

Susanne Hummel Johann Friedrich Blumenbach Institute of Zoology and Anthropology, Historical Anthropology and Humanecology, Georg-August-University Göttingen, Bürgerstraße 50, 37073 Göttingen, Germany, shummel1@gwdg.de

Johny Isla Cuadrado Instituto Andino de Estudios Arqueológicos (INDEA), Lima, Av. Mariátegui 155, Dpt. 111, Jesús María, Lima 11, Perú, isla-nasca@amauta.rcp.net.pe

Annette Kadereit Luminescence Laboratory, Institute of Geography, University of Heidelberg, Im Neuenheimer Feld 348, 69120 Heidelberg, Germany, annette.kadereit@geog.uni-heidelberg.de

Thomas Kersten HafenCity University (HCU) Hamburg, Department Geomatics, Hebebrandstraße 1, 22297 Hamburg, Germany, thomas.kersten@hcu-hamburg.de

Robert Kovacs ETH Zurich, Department of Chemistry and Applied Biosciences, Laboratory of Inorganic Chemistry, HCI G 141, Wolfgang-Pauli-Straße 10, 8093 Zurich, Switzerland, robert.kovacs@inorg.chem.ethz.ch

Bernd Kromer Forschungsstelle Radiometrie der Heidelberger Akademie der Wissenschaften, c/o Institut für Umweltphysik, Heidelberg, Im Neuenheimer Feld 229, 69120 Heidelberg, Germany, bernd.kromer@iup.uni-heidelberg.de

Karsten Lambers University of Konstanz, Zukunftskolleg, Department of Computer Science, P.O. Box 697, 78457 Konstanz, Germany, karsten.lambers@uni-konstanz.de

Roman Leonhardt Department of Applied Geoscience and Geophysics Chair of Geophysics, University of Leoben, Peter-Tunner-Straße 25–27, 8700 Leoben, Austria, roman.leonhardt@mu-leoben.at

Maren Lindstaedt HafenCity University (HCU) Hamburg, Department Geomatics, Hebebrandstraße 1, 22297 Hamburg, Germany, maren.lindstaedt@hcu-hamburg.de

Sven Linzen Institute of Photonic Technology e.V., POB 100239, 07702 Jena, Germany, sven.linzen@ipht-jena.de

Bertil Mächtle Institute of Geography, University of Heidelberg, Im Neuenheimer Feld 348, 69120 Heidelberg, Germany, bertil.maechtle@geog.uni-heidelberg.de

Hubert Mara Vienna University of Technology, Institute of Computer Aided Automation, Pattern Recognition and Image Processing Group, Favoritenstrasse 9/183-2, 1040 Vienna, Austria, mara@prip.tuwien.ac.at

Hans-Georg Meyer Institute of Photonic Technology e.V., POB 100239, 07702 Jena, Germany, hans-georg.meyer@ipht-jena.de

Ernst Pernicka Curt-Engelhorn-Zentrum Archaeometrie (CEZA) Mannheim, An-Institut der Universität Tübingen, D6, 3, 68159 Mannheim, Germany, ernst.pernicka@cez-archaeometrie.de; Eberhard-Karls-Universität Tübingen, Institut für Ur- und Frühgeschichte und Archäologie des Mittelalters, Abteilung für Jüngere Urgeschichte und Frühgeschichte, Schloss Hohentübingen, 72070 Tübingen, Germany, ernst.pernicka@uni-tuebingen.de

Markus Reindel German Archaeological Institute (DAI), Commission for Archaeology of Non-European Cultures (KAAK), Dürenstraße 35–37, 53173 Bonn, Germany, reindel@kaak.dainst.de

Rebecca Renneberg Graduate School Human Development in Landscape, Universitätsklinikum Schleswig-Holstein, Arnold-Heller-Straße 3, 24105 Kiel, Germany, rrenneberg@gshdl.uni-kiel.de

Katharina Ross Institute of Geography, University of Heidelberg, Im Neuenheimer Feld 348, 69120 Heidelberg, Germany, ninaross@gmx.de

Andreas Rossmann Isolab GmbH Laboratorium für Stabil-Isotopenanalytik, Woelkestraße 9/I, 85301 Schweitenkirchen, Germany, isolab_gmbh@t-online.de

Susanne Rummel Bavarian State Collection for Palaeontology and Geology, Munich, Richard-Wagner Straße 10, 80333 München, Germany, susanne.rummel@iaag.geo.uni-muenchen.de

Martin Sauerbier ETH Zurich, Institute of Geodesy and Photogrammetry, ETH Hönggerberg HIL D 43.2, 8093 Zurich, Switzerland, martin.sauerbier @geod.baug.ethz.ch

Solveig Schiegl Institut für Ur- und Frühgeschichte und Archäologie des Mittelalters, Abteilung Ältere Urgeschichte und Quartärökologie, Schloss Hohentübingen, Burgsteig 11, 72070 Tübingen, Germany, solveig.schiegl @uni-tuebingen.de

Sandra Schlosser Curt-Engelhorn-Zentrum Archaeometrie (CEZA) Mannheim, An-Institut der Universität Tübingen, D6, 3, 68159 Mannheim, Germany, sandra.schlosser@cez-archaeometrie.de

Tim Schüler Thüringisches Landesamt für Denkmalpflege und Archäologie, Humboldtstraße 11, 99423 Weimar, Germany, SchuelerT@tlda.thueringen.de

Gerd Schukraft Institute of Geography, University of Heidelberg, Im Neuenheimer Feld 348, 69120 Heidelberg, Germany, gerd.schukraft@geog.uni-heidelberg.de

Volkmar Schultze Institute of Photonic Technology e.V., POB 100239, 07702 Jena, Germany, volkmar.schultze@ipht-jena.de

Marco Schulz Institute of Photonic Technology e.V., POB 100239, 07702 Jena, Germany, marco.schulz@ipht-jena.de

Florian Stark Department für Geo- und Umweltwissenschaften, Bereich Geophysik, Ludwig-Maximilians-Universität, München, Theresienstraße 41, 80333 Munich, Germany, stark@geophysik.uni-muenchen.de

Thomas Stöllner Deutsches Bergbau-Museum Bochum, Forschungsstelle Archäologie und Materialwissenschaften, Fachbereich Montanarchäologie, Herner Straße 45, 44787 Bochum, Germany, thomas.stoellner@bergbaumuseum.de; Fakultät für Geschichtswissenschaften, Institut für Archäologische Wissenschaften, Lehrstuhl für Ur- und Frühgeschichte, Universitätsstraße 150, 44780 Bochum, Germany, thomas.stoellner@ruhr-uni-bochum.de

Ronny Stolz Institute of Photonic Technology e.V., POB 100239, 07702 Jena, Germany, ronny.stolz@ipht-jena.de

Ulrich Struck Berlin Museum of Natural History, Invalidenstraße 43, 10115 Berlin, Germany, ulrich.struck@museum.hu-berlin.de

Michael Tellenbach Reiss-Engelhorn-Museen Mannheim, C5, Zeughaus, 68159 Mannheim, Germany, michael.tellenbach@mannheim.de

Elsa Tomasto Cagigao Pontificia Universidad Católica del Perú (PUCP), Departamento de Humanidades, Av. Universitaria cdra. 18, San Miguel, Lima 32, Perú, etomast@pucp.edu.pe

Ingmar Unkel Department of Physics, Nuclear Physics, Lund University, Professorsgatan 1, 22100 Lund, Sweden, ingmar.unkel@geol.lu.se

Günther A. Wagner Institute of Geography, University of Heidelberg, Im Neuenheimer Feld 348, 69120 Heidelberg, Germany, g.wagner@mpi-hd.mpg.de

Clemens Woda Helmholtz Center Munich, German Research Center for Environmental Health, Institute of Radiation Protection, Ingolstädter Landstraße 1, 85764 Neuherberg, Germany, clemens.woda@helmholtz-muenchen.de

Chapter 1
Introduction – New Methods and Technologies of Natural Sciences for Archaeological Investigations in Nasca and Palpa, Peru

Markus Reindel and Günther A. Wagner

1.1 Natural Sciences in Archaeology

Applications of natural sciences in archaeology have actually a long tradition. In particular the chemical composition of metal artefacts was sporadically used for more than two hundred years, mainly for the purpose of material classification. One of the earliest examples is the quantitative analysis of Roman coins in 1799 by Martin Heinrich Klaproth in Berlin, a chemist who is better known as the discoverer of the element uranium. Based on the material composition of dominant remains, the Danish archaeologist Christian Jürgensen Thomsen formally introduced in the 1820s the three-age system of prehistoric archaeology into three consecutive time periods: the Stone Age, the Bronze Age, and the Iron Age.

Especially during the second half of the twentieth century, natural scientific approaches in archaeology experienced a nearly explosive increase. It became obvious that, when trying to reconstruct the past as comprehensively as possible, the archaeologist needs to take into consideration all sources of relevant information including those which are hidden to the naked eye, being the foremost tool of an archaeologist's perception, and which are only revealed by scientific studies. Terms such as 'science-based archaeology' or simply 'archaeometry' are used for this new discipline. Originally coined in 1958 as the title for a journal (M. Aitken, in Olin, 1982, p. 142) and subsequently also used for an international symposium, 'archaeometry' was increasingly adapted within the past few decades for this field of research. It is acknowledged in the meantime by most archaeologists as an indispensable and integral part of archaeology.

M. Reindel (✉)
German Archaeological Institute (DAI), Commission for Archaeology of Non-European Cultures (KAAK), Dürenstraße 35-37, 53173 Bonn, Germany
e-mail: reindel@kaak.dainst.de

M. Reindel, G.A. Wagner (eds.), *New Technologies for Archaeology*, Natural Science in Archaeology, DOI 10.1007/978-3-540-87438-6_1,
© Springer-Verlag Berlin Heidelberg 2009

1.2 Archaeometry

In our understanding 'archaeometry' designates the development and application of natural scientific methods and concepts in order to contribute to the solution of cultural–historical questions (Wagner, 2007). In this multidisciplinary, most extensive scope, archaeometry is the interface between the natural and the cultural–historical sciences. Archaeometry is both archaeology by ultimate aim ($\alpha\rho\chi\alpha\iota\sigma\nu$), but natural science by approach ($\mu\epsilon\tau\rho\sigma\nu$). In this broad definition all disciplines of natural sciences that may contribute to archaeology are included, that is, not only physics, chemistry, and mathematics, but also the biological sciences, anthropology, geological sciences, astronomy, and remote sensing. Inasmuch as all of these disciplines describe natural phenomena quantitatively they readily identify themselves with the $\mu\epsilon\tau\rho\sigma\nu$ aspect of archaeometry.

As part of cultural history, which generally is concerned with the behaviour of past man, archaeology is the study of the material remains of man's past with the aim to get broad insights into ancient human cultures, specifically their tools, techniques, economy, works of art, language, ideas, beliefs, customs, and so on. In achieving this goal, natural sciences enter archaeology twofold: first, by their application to inorganic artifacts (e.g., chemical analysis of ceramics) as well as biomaterials (e.g., isotopic studies of bones). Second, natural objects and phenomena as such are of archaeological importance for reconstructing the former environmental situation, such as landscape and climate. Because the natural environment sustains culture, the understanding of the interaction between nature and culture requests combined efforts of both the cultural–historical as well as the natural sciences, and thus the archaeo-environment is a subject of archaeometry.

Archaeometric projects should focus on relevant archaeological questions (e.g., prehistoric chronology), to which one tries to contribute by gaining primary data with an appropriate method (e.g., ^{14}C), followed by scientific evaluation (e.g., reliability and meaning of the age value) and ultimately by archaeological interpretation (e.g., chronological significance). In other words, at first an archaeological question needs to be transformed into a natural scientific one, and then the scientific result needs to be translated back into an archaeological one. Archaeological topics, for which commonly archaeometric support is demanded, comprise mainly the identification, manufacture, and provenance of material remains, as well as the geophysical prospection, dating, and archaeo-environment of whole sites.

The occasionally raised dispute of whether archaeometry is research in its own or service to archaeology, is needless in such cooperation. There are cases where an archaeological problem triggers the development of a new technology, and other cases where an available technology stimulates the archaeologist towards fresh questions. An intensive and sustained interchange between natural scientists generating the data and those interpreting them

archaeologically obviously is required. The archaeologist should be familiar with the archaeometric possibilities to define accessible aims, and the natural scientist must understand the archaeological problems in order to optimize his or her efforts towards their solution.

1.3 Archaeometry in South America

Archaeometry is a quite recent discipline in American archaeology. The majority of archaeological investigations in South America is concentrated in the Andean region where the research area of the Nasca–Palpa project is located. Therefore the following overview of archaeometric approaches in South American archaeology focuses on this western part of the subcontinent and, of course, cannot be comprehensive. Rather it highlights the most important publications in an exemplary fashion.

One of the foremost interest and most traditional issues in archaeometry is chronometry. Right from the beginning of numeric dating with physical methods after the discovery of the radiocarbon (^{14}C) method by W.F. Libby, the American archaeologist J. Bird introduced this new method in Andean archaeology (Bird 1951). Radiocarbon dating is now the most widely used method for numeric dating and is an integral part of all major archaeological projects. The chronological placement of some of the most important cultures in South America such as the Valdivia culture relies mainly on radiocarbon dating (Marcos 1988). A large number of radiocarbon dates of the Central Andean area have been published by Ziolkowski et al. (1994), although many of these dates are lacking a detailed description of the archaeological context of the samples.

Other physical dating methods have been used only in very isolated cases in South America. Thermoluminescence (TL) dating for ceramics has been applied in coastal Ecuador (Reindel 2007; Alvarez 1995). Optically stimulated luminescence (OSL) was tested for the dating of the Nasca lines, actually in the same area where the Nasca–Palpa project later took place (Rink and Bartoll 2005). Obsidian hydration was applied soon after its discovery to date the early cultures of Ecuador (Evans and Meggers 1960). But until today this method could not be established as a reliable dating tool in South America, due to the problems of temperature and moisture changes over time, which heavily affect the dating results. However, recently good results have been achieved for dating obsidian objects in the extremely dry environment of the Nasca region on the south coast of Peru (Eerkens et al. 2008). Another product of volcanic activity, the deposition of tephra layers, which reach far into the coastal areas and can be correlated with datable eruptions of well-studied volcanoes of the cordilleras, has been successfully applied in Ecuador for dating and studying the impact of environmental change on pre-Columbian societies (Mothes 1998).

The analysis of inorganic materials is another original field of archaeometry. Recently the exact knowledge of the composition of minerals and metals is used

especially for provenance studies. The investigations of metal and ceramic production, led by I. Shimada on the north coast of Peru, may serve as an example of one of the most diversified long-term projects aimed at the reconstruction of pre-Hispanic procurement of raw materials and craft production (Shimada and Wagner 2007).

The chemical and mineralogical characteristics of ceramics, which are the most numerous findings by archaeologists, are investigated by thin sections, x-ray spectrometry, and neutron activation analysis (NAA). The available techniques have been applied in the last few years to trace the production centres and the distribution of ceramics in the Nasca region (Vaughn and Neff 2004; Vaughn et al. 2006; Vaughn and Gijseghem 2007). Mössbauer spectrometry was used to determine details of the production process of ceramics (Wagner et al. 2003b). With the development of laser ablation and inductively coupled plasma-mass spectrometry (LA-ICP-MS) it is now possible to analyze the mineralogical composition of ceramics and their decoration using only minimal amounts of sample material and thus nearly without destruction (Dussubieux et al. 2007; Vaughn et al. 2005).

In sharp contrast to the Old World, metal production played a minor role in South American cultures, except for the extensive use of gold ornaments in some regions such as Colombia and northern Peru. A representative overview of metal weapons and tools is given by Mayer (1986, 1992, 1994, 1998). The metallurgy has been studied especially in the Central Andean area (Root 1949; Lechtman 1979; Lechtman and Macfarlane 2005). Nondestructive techniques have been applied to analyze the composition of metals and to test by this means the authenticity of museum objects (Rovira 1990). Important advances in the study of copper and bronze production have been achieved on the north coast of Peru (Epstein and Shimada 1983; Merkel et al. 1994). Neutron activation analysis has also been applied to trace the provenance of metal objects (Gordus et al. 1996; Chapdelaine et al. 2001).

Inasmuch as the cordilleras of the Andes are active volcanic regions, obsidian is available in many places and has been used throughout the entire history of human occupation of South America. The study of obsidian artefacts, raw material sources, and trade routes has thus become a fruitful field of archaeological investigation. Glascock (2002) gives a summary of the obsidian provenance research in the Americas. Ecuador is one of the main regions where detailed studies on obsidian production and exchange among the pre-Hispanic cultures have been carried out (Burger et al. 1994; Bellot-Gurlet et al. 2008). And again, the central Andean area has produced the largest number of publications on this topic (Glascock et al. 2007; Burger et al. 2000, 2006). The Quispisisa obsidian source in the Peruvian department of Ayacucho is of special importance for our project because according to the available studies it was the major source for obsidian of the Nasca–Palpa region (Burger and Glascock 2000; Vaughn and Glascock 2005). Obsidian sources have been investigated also farther to the south, in Argentina and Chile (e.g., Giesso et al. 2008).

Anthropological studies have made great progress in South America since the establishment of systematic long-term projects, especially following the discovery of the royal tombs of Sipan and the related investigations of the Moche culture of the north coast of Peru. Traditional anthropological research has been carried out by Verano on different sites in the Andes (Verano 1997a,b, 2003, 2005). The discovery of mummies in regions with optimum conservation conditions, like the Chachapoyas region on the eastern slope of the Peruvian Andes as well as the extremely arid environment of the Atacama desert, fostered the establishment of a research cluster led by the Peruvian anthropologist Guillén (Guillén 2002, Guillén et al. 2004). Another focus of anthropological studies was the interdisciplinary projects of the Tiwanaku and the Wari cultures (Blom et al. 2003; Tung 2007). These studies were complemented by the most recent developments in anthropology, namely palaeogenetic studies. The few available pioneering publications in this field (Lewis et al. 2005, 2007; Shimada et al. 2006; Shinoda et al. 2006) are far away from giving a comprehensive picture of human population history, but they open a window to a fascinating field of future research being enlarged by the contribution of Fehren-Schmitz et al. in this volume.

Another new archaeometric analytical tool, which has been successfully applied in anthropological as well as in palaeobiological and palaeoecological studies, are stable isotopes. Examples of the Andean area illustrate the wide use of isotope studies for archaeology. Strontium isotopes have been used to investigate seasonality and the palaeodiet of the Chiribaya polity in southern Peru (Knudson et al. 2007; Knudson and Buikstra 2007). Isotope studies have also contributed to the history of maize in South America, which played an important role in the rise of Andean civilizations (Gil et al. 2006; Tykot 2006).

Palaeoecological studies always played an important role in the investigation of the early stages of South American populations. In the context of the general discussion of climate change and its influence on human societies, palaeoecological and especially palaeoclimatological studies have been intensified in the last years. Except for a few publications about the Amazon lowlands dealing with the influence of palaeoclimate on human development (e.g., Araujo et al. 2005) most studies are centered on the cordilleras of the Andes and Pacific coast of South America (e.g., Weng et al. 2006). Clearly, the most discussed topic is the El Niño phenomenon, which has far-reaching implications for human development on the central Andean coast. Studies have focussed on the early periods (Sandweiss 2003; Sandweiss et al. 2004; Keefer et al. 2003) as well as late periods where El Niño events are assumed to have had a major impact on pre-Hispanic societies (e.g. Satterlee et al. 2000). These studies are complemented by geoarchaeological investigations of long-term climate change influencing the occupation of the extreme south coast of Peru in the early periods (Lavallée et al. 1999; Usselmann et al. 1999). Later periods have been studied recently in the Titicaca region (Stanish 2003; Calaway 2005). Similar studies are available from the southern part of South America (Latorre et al. 2003; Iriarte 2006; Maldonado and Villagran 2002).

Geophysical prospection is far behind recent developments especially in Europe, where in the last decades the geophysical survey has become an integral part of most archaeological projects. In South America, geophysical techniques have been applied in major interdisciplinary projects. Magnetometry, conductivity, and resistivity surveys were pioneered in a project on the Amazonas delta in Brazil (Roosevelt 1991, 2007). The same techniques were employed in geophysical surveys in the Peruvian and Bolivian highlands, in Tiahuanaco and Pucara, for the detection of stone architecture (Williams et al. 2007; Klarich 2008). Successful magnetometry, electromagnetometry, and resistivity surveys have been applied also in the investigation of monumental architecture in the Casma valley of northern Peru (Fuchs et al. 2006). Another single study, using GPR, electrical, and electromagnetic methods, has been reported from northwestern Argentina (Martino et al. 2006; Osella et al. 2005).

Similar to geophysical prospection methods, remote sensing, which is widely used and in continuous development in Europe, is only beginning to be applied in South American archaeology (Baltsavias et al. 2006). Photogrammetric methods have been employed to map a limited area of the geoglyphs of the Pampa de Nasca in southern Peru (Hawkins 1974). In the same area a project of the Technical University of Dresden is developing a geographic information system using photogrammetric and satellite data (Teichert and Richter 2001; Richter 2007). Satellite data are also beginning to be used for the monitoring of cultural heritage sites as in the case of Machu Picchu (Hernandez 2006). But the systematic use of satellite and other remote sensing data for archaeological prospection and field research, as it is being realized in pilot projects in the Maya area in Mesoamerica (Saturno et al. 2007), still remains a challenging task for the future of South American archaeology.

Archaeobotanic studies have also advanced in the last few years through new analytical methods, giving fresh insights especially in early processes of plant domestication in South America. The archaeobotanists Pearsall and Piperno have greatly advanced traditional systematic studies of botanical remains as well as the use of new technologies (Pearsall 2000, 2004; Piperno and Pearsall 1998). Starch grain analysis allows for the identification of minimal plant remains in archaeological contexts even under humid conditions, opening new ways for the reconstruction of tropical agriculture and plant domestication (Chandler-Ezell et al. 2006; Perry et al. 2007). Phytoliths, the mineralized remains of certain plant components, are also very useful for the reconstruction of the plant inventory in humid environments or even in burnt contexts. In the last years sample databases for South America have been built up and were used in archaeological studies (Piperno 2006, 2008).

Also in contrast to the Old World, where the domestication of animals played a crucial role in the process of sedentarization and the rise of complex societies, the use of domestic animals played a minor role in South America. The only major animals in the Andes used for transport, but also as an important source of meat and wool, were the camelids. A comprehensive

overview of camelid studies can be found in Mengoni et al. (2001). The other relevant publications for the study of the domestication and use of camelids in South America are mentioned in the contribution by Renneberg et al. (this volume) on palaeogenetic studies of camelids.

1.4 Archaeology of the South Coast of Peru

Because of the lack of any known writing system in pre-Columbian times, archaeology is the only means for the reconstruction of cultural history in South America. Archaeological investigation from its beginning has paid special attention to the central Andean area because this region was the homeland of the most developed culture in South America at the arrival of the Europeans in the sixteenth century, the Inka culture, and because it was one of the few regions in the world where complex societies emerged about five thousand years ago. In recent years great advances have been achieved in the understanding of the mechanisms for the rise of early complex societies in the central Andes, in part as a result of the interdisciplinary cooperation between archaeology and natural sciences.

The earliest findings in the central Andean area date to the beginning of the Holocene. The Archaic period, which ends about 2000 BC, is still poorly known. Recent investigations have shown that the origins of early complex societies must be dated to the fourth millennium BC. This timeframe almost equals the chronological placement of the early urban societies in the Old World. With the recent findings of early monumental architecture and other spectacular discoveries, such as the royal tombs and beautifully decorated temple buildings on the north coast of Peru, the central Andean area occupies a prominent place in worldwide archaeological research.

Archaeological research began in Peru at the end of the nineteenth century with the work of Max Uhle. He recognized cultural styles that allowed the comparison of cultural developments based on stylistically similar artifacts, namely the Inka and Tiahuanaco style. He also identified regional styles that represented independent cultural developments. After the first investigations at the central and north coast of Peru, Uhle carried out archaeological excavations in the Ica valley on the south coast of Peru. There he discovered remains of the Nasca culture which previously had been studied merely in museum collections. Uhle recognized the Nasca-style as representing a regional development and considered it the earliest culture of this region.

Some years later Julio C. Tello discovered at the Paracas peninsula the remains of an even earlier culture. This Paracas culture was contemporaneous with the Chavin culture, represented by another horizon style which Tello had discovered before at Chavin de Huantar and in the Casma valley in northern Peru. This chronological system of horizon and regional cultures in the 1950s and 1960s was further developed by J.H. Rowe and his team. He based his work

on collections from the Ica valley where he intended to develop a master sequence for the cultures of the central Andean area. Hence the south coast of Peru has considerable importance for the systematic study of the central Andean cultures. However, in the years after 1960 the focus of archaeological investigation shifted to the central coast and highlands where a great number of early monumental sites pointed to the place of origin of complex societies in the Andes.

In archaeological terms the south coast of Peru is considered the part between the Cañete valley to the north down to the Acari valley in the south. In contrast to the rich alluvial fans of the central and northern valleys, the agricultural lands of the south coast are limited and offer fewer resources for the development of an agriculturally based economy. This is reflected by the lack of major complexes of monumental architecture on the south coast, which is a characteristic of the pre-Hispanic societies farther to the north. However, for the strategy of archaeological research, especially of settlement patterns, this has the advantage that the valleys of the south coast represent well-defined and clearly delimited settlement territories. This is especially true in the Nasca region where the research area of the Nasca–Palpa project is located.

The Nasca region is defined by the ten tributaries of the Rio Grande de Nasca (Fig. 1.1) which is the only river that reaches the Pacific Ocean after crossing the coastal cordillera, which is a particular geomorphologic feature of this part of the Peruvian coast. The most famous archaeological culture of this region is the Nasca culture (200 BC–600 AD) which is characterized by polychrome painted vessels that can be found in many museums all over the world. On the other hand, the Nasca culture became famous for the geoglyphs that cover large areas of the desert plateaus between the fertile river valleys.

The largest site of the Nasca culture is Cahuachi in the Nasca valley. Despite long-term archaeological investigations it is not clear whether this site represents the central place of a political entity or a center for religious pilgrimage. Until the start of the Nasca–Palpa project, few data were available to answer this question. Archaeological research centered mostly on the esthetically attractive artefacts and the enigmatic geoglyphs of the Nasca culture. Settlement pattern studies and the investigation of the cultural and ecological context seemed to be of minor importance. The Paracas culture (800–200 BC), which preceded the Nasca culture, was poorly investigated. Only one single site of the Initial period (1500–800 BC) and one of the Middle Archaic period (approx. 4000 BC), respectively, had been studied. The same was true for later periods, the Middle Horizon (600–1000 AD), the Late Intermediate period (1000–1400 AD), and the Inka period (1400–1532 AD).

Therefore the Nasca valleys and especially the northern tributaries around the actual town of Palpa presented ideal conditions for the study of settlement patterns and cultural development of pre-Hispanic societies in a specific region:

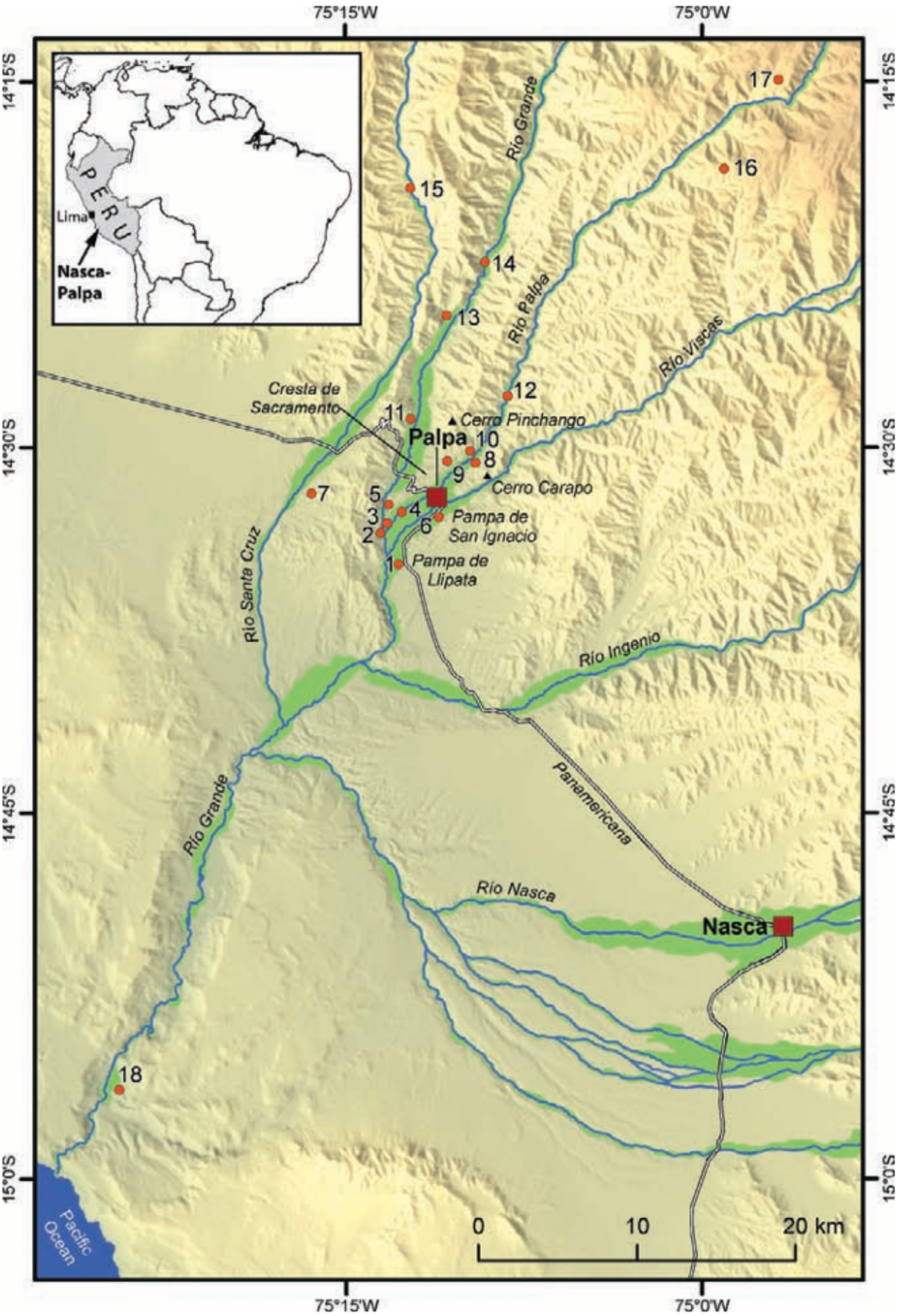

Fig. 1.1 Research area of the Nasca–Palpa project. Red dots indicate major sites mentioned in the contributions to this volume. 1. Pueblo Nuevo, 2. La Muña, 3. Estaquería, 4. Jauranga, 5. Los Molinos, 6. Hanaq Pacha, 7. Ciudad Perdida de Huayurí, 8. Mollake Chico, 9. Pinchango Alto, 10. Pinchango Viejo, 11. Pernil Alto, 12. Chichictara, 13. Parasmarca, 14. Lucriche, 15. Jaime, 16. Letrayoc, 17. Pacapacarí, 18. Monte Grande. (Graphic: V. Soßna.)

(1) The research in the river oases of the eastern Atacama desert represents a well-defined settlement territory.
(2) Surface findings and the results of previous studies indicated a large indigenous occupational history beginning in archaic times and ending with the Inka occupation.
(3) Due to the desert environment the conditions for preservation of archaeological findings, even organic materials, were excellent.
(4) The geoglyphs of the region are unique and well known worldwide, but at the same time their function and meaning in their cultural context remained unsolved and enigmatic.

1.5 Conception of the Nasca–Palpa Project

Inasmuch as archaeometry is largely based on scientific and technological expertise, the rapid progress of natural sciences carries a great potential that needs steadily to be taken advantage of for archaeology. The German Federal Ministry for Education and Research (*Bundesministerium für Bildung und Forschung, BMBF*) realized this potential and established in 1989 the research funding program 'Neue naturwissenschaftliche Methoden und Technologien in den Geisteswissenschaften' (new natural scientific methods and technologies in the humanities). The emphasis of the program lay originally on the adoption of new methods from natural sciences and their specific technological development for the benefit of humanity. In the course of the program it was recognized that a most effective means was combining various promising techniques around a central and important archaeological issue. In this manner not only the dialogue with archaeology but also among the different scientific disciplines could be enhanced. This concept stood in 2002 at the start of the Nasca–Palpa project *Entwicklung und Adaption archäometrischer Techniken zur Erforschung der Kulturgeschichte* (development and adaption of archaeometric techniques for the investigation of cultural history).

In the Palpa region, in the northern part of the Nasca drainage, the conditions for the establishment of such a multidisciplinary research program were excellent. Since 1997 archaeological investigations had been carried out with the financial support of the Swiss-Liechtenstein Foundation for Archaeological Research Abroad (SLSA), centered on the geoglyphs of the Nasca culture. In many cases research questions emerged that could not be solved with archaeological methods alone. It became clear, for example, that climate and landscape changes must have had considerable influence on the settlement patterns. The task of the documentation of the geoglyphs, which extended over hundreds and thousands of meters, as well as the topographic survey of the numerous extended settlements and landscape features could not be achieved with traditional methods of terrestrial surveying.

The lack of a reliable chronology based on numerical data was a major task in the context of the reconstruction of local settlement history. The complex population history could not be investigated with the analysis of settlement patterns and anthropological studies alone.

Imported raw materials, such as obsidian from the highlands or seashells from the Pacific Ocean, show clearly that the societies in the research area maintained complex trade relations which constituted an important base of their economy. The provenance and the processing of raw materials could only be investigated with adequate methods of archaeometric analysis. Especially interesting is the investigation of luxury goods such as gold and other precious objects.

Finally, it became clear that the systematic management of the rich data of the different kinds produced by the multidisciplinary project were a great challenge for the archaeologists, but at the same time held a great potential for analytical methods available today through geographic information systems (GIS).

In principle, a broad spectrum of archaeometric methods was on hand for this program. Our conception was to employ the different disciplines in a way that they would complement and interchange with each other in order to achieve quantitative as well as qualitative novel insights into the complex prehistory of southern Peru. This implied, of course, also new technological developments according to specific conditions in this near-equator region.

The pre-Columbian cultures in the desert belt of southern Peru were exposed to a harsh climatic environment. This requires a detailed knowledge of the climatic conditions and their effects on landscape and vegetation, hitherto unknown for this region. Therefore, geoarchaeological studies seemed to be of foremost importance for detecting climate changes and understanding their impact on pre-Columbian cultures at the edge of the Atacama desert in southern Peru.

The localization and extension of archaeological structures beneath the soil without digging was achieved by geomagnetic prospection and sediment tomography, whereby the problem of nearly surface-parallel geomagnetic field-lines presented a methodological challenge.

The biogenic remains, well preserved under the arid conditions of the Palpa region, initiated their bioarchaeological analysis and molecular-anthropological examinations. In particular, isotopic studies revealed the subsistence strategy and the migration patterns of humans.

Of crucial importance in prehistory is archaeochronometry. The achievement of a solid, highly resolving chronology of the Paracas and Nasca periods, based on radiocarbon, has implications far beyond our study area. Luminescence dating of the sediments sheds light on the landscape development. The successful dating of stone surfaces at the geoglyphs using luminescence is one of the new technologies.

Also new is the development and application of geomatics with its three-dimensional photorealistic modelling of the landscape, the GIS-based

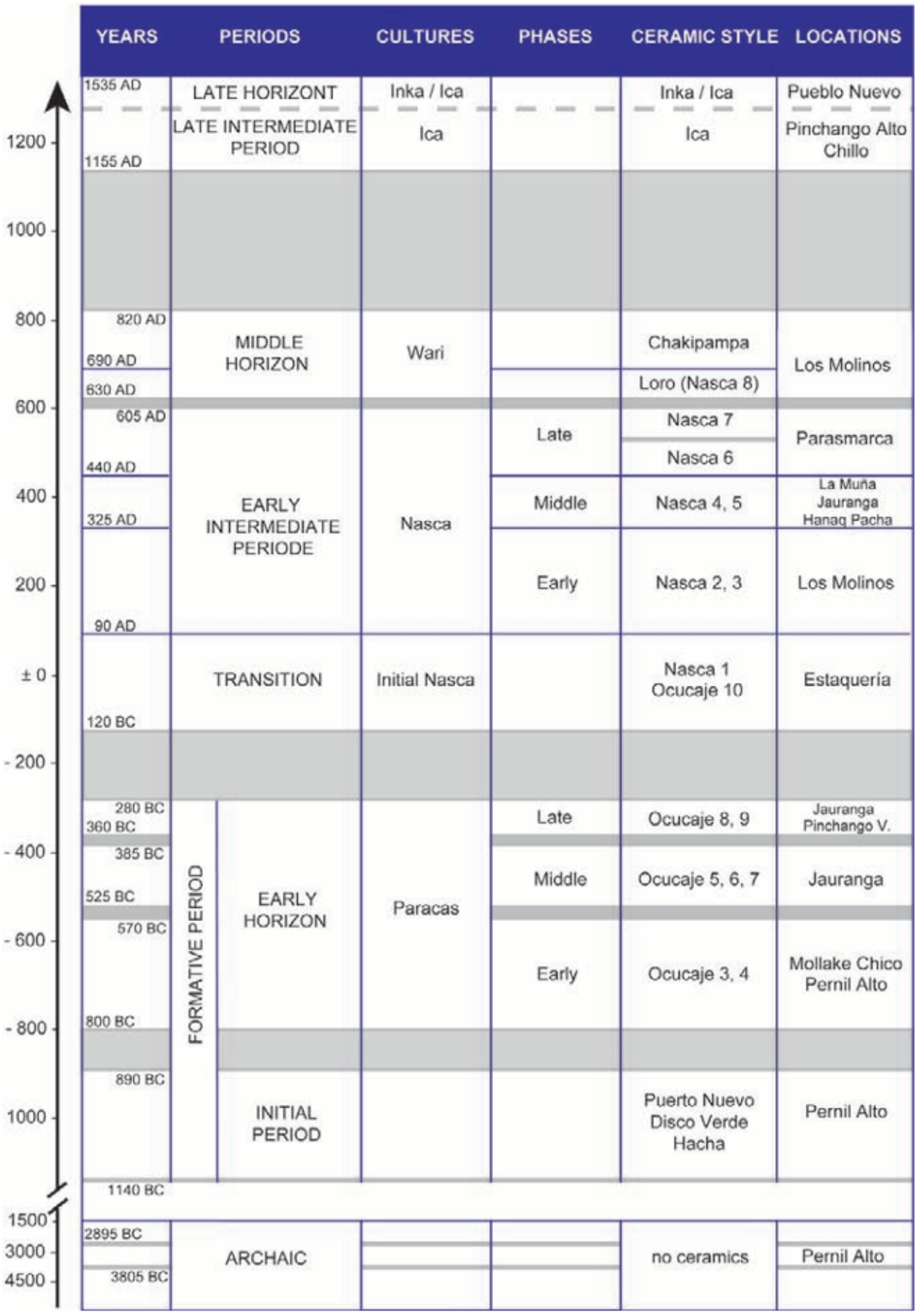

Fig. 1.2 Chronological table containing the archaeological and the physical dating results of the Nasca–Palpa project. (After Unkel 2006)

modelling and spatial analysis of the geoglyphs of Palpa and Nasca, as well as the documentation and interpretation of prehistoric petroglyphs with laser scanning, photogrammetry, and satellite imagery.

Finally, archaeometallurgy and archaeoceramology employ geological and geochemical methods to identify the sources and to investigate the working of metals and ceramics. Thus, trading patterns and the technological skills of the Paracas and Nasca periods may be revealed.

The nuclear area of the Nasca–Palpa project was the valleys of the rivers Grande, Palpa, and Viscas of the Palpa province, in the northern part of the Nasca drainage. A systematic archaeological survey was carried out in the area between the confluence of the rivers Grande and Ingenio, up to the upper courses of the rivers at an elevation of about 2000 m. The research area thus comprises mainly the footzone of the Andes. For comparative reasons some sites of the neighbouring valley Santa Cruz, in the catchment areas of the valleys and in the lower course of the Rio Grande valley were studied (Fig. 1.1). Especially the radius of the geoarchaeological investigations goes far beyond the nuclear research area.

About 800 sites are registered in the database, 450 of which are settlements dating to different periods of pre-Hispanic history. In the course of the surveys the sites were dated according to the published chronological models. For a more detailed chronological placement, test excavations were carried out at many places. Furthermore, for nearly every major chronological period a large-scale excavation was designed in order to document the characteristics of each epoch in well-defined archaeological contexts. The most important sites mentioned in the contributions to this volume are marked on the map of Fig. 1.1.

In the course of the project and during the process of analysis of the findings the chronology was refined. Cooperation with the chronometric project especially yielded a great number of archaeological as well as geomorphological dates. As a result, the Palpa region now holds probably the most detailed chronology of landscape and cultural history in South America. The chronological table with its archaeological and physical numeric ages for the research area of the Nasca–Palpa project is represented in Fig. 1.2.

Part I
Geoarchaeology

Chapter 2
Man and Environment in the Eastern Atacama Desert (Southern Peru): Holocene Climate Changes and Their Impact on Pre-Columbian Cultures

Bernhard Eitel and Bertil Mächtle

Abstract Geoarchaeological evidence for Holocene palaeoclimates in the eastern Atacama desert is compiled to reconstruct the palaeoenvironmental history in the Andean foreland. In contrast to earlier assumptions that El Niño events controlled the environment of pre-Columbian people in the Ica–Nazca region, major hydrological changes, triggered by oscillations of the summer monsoon in the western Andes, concurred with cultural changes.

Loess deposits, phytoliths, and snail shells indicate that during the early and middle Holocene the eastern Atacama desert was a grassland until the third millennium BC. With the aridisation hunter–gatherer people concentrated on favourable sites along the river oases, which were flooded seasonally by reliable rains in the western Andes. During the rise of the Paracas culture the increasing population density went hand in hand with the formation of more complex societies. After ~200 BC the Nasca displaced the Paracas culture. Approximately four centuries later the aridisation of the region accelerated and the Nasca settlements shifted eastwards into the valleys of the Andean footzone. With even more reduced summer rains in the western Andes, the river oases dried up. Finally, shortly after 600 AD, the Nasca culture collapsed.

A new hydrological oscillation took place after ~1100 AD. Monsoonal rains reached the Andean foreland again and narrowed the desert to ~40 km. During the following Late Intermediate Period (LIP), pre-Columbian people re-occupied the eastern Atacama desert until the sixteenth century AD. The Little Ice Age, with its coldest temperatures between the seventeenth and nineteenth centuries AD, was a very dry period in the study area, so that LIP settlements were abandoned and desert conditions reappeared lasting until today.

B. Eitel (✉)
Institute of Geography, University of Heidelberg, Im Neuenheimer Feld 348, 69120 Heidelberg, Germany
e-mail: bernhard.eitel@geog.uni-heidelberg.de

M. Reindel, G.A. Wagner (eds.), *New Technologies for Archaeology*, Natural Science in Archaeology, DOI 10.1007/978-3-540-87438-6_2,
© Springer-Verlag Berlin Heidelberg 2009

2.1 Introduction: Geoarchaeology – A Young Discipline

'Geoarchaeology' deals with the interaction between man and environment in archaeological contexts. Using modern techniques of natural sciences ('archaeometry', Wagner 2007) geoarchaeological research is a young discipline investigating the impact of environmental changes on humans and societies, and vice versa. This includes the reconstruction of archaeo-landscapes and the ancient geomorphodynamics having formed such environments. Geoarchaeology can be focussed on sedimentological (geo-)archives within archaeological sites (on-site studies), or it uses landforms, rocks, deposits, and soils as geoarchives for palaeoenvironmental reconstruction (off-site studies). The added value of geoarchaeological research is that the result is a dataset which is independent of archaeological findings and interpretations (Eitel 2007). The assembly of historical or archaeological data and of numeric dating (e.g., radiocarbon or luminescence) provides the chronological time frame for palaeogeographical reconstructions.

Within the Nasca–Palpa project, geoarchaeological research integrates archaeological results and data from geophysics, from geomorphology and soil science, from isotope analyses and palaeogenetics, and fits them in a new chronological framework derived from AMS-^{14}C dating (Unkel 2006) and OSL-dating (data of A. Kadereit compiled in Mächtle 2007). The palaeoenvironmental reconstruction confirms the notion that desert-margin areas such as the eastern border of the Peruvian Atacama desert respond as reactive areas very sensitively to climate changes (Eitel 2006, 2007). Furthermore the study demonstrates that hydrological fluctuations in such drylands have had a deep impact on the development of early cultures (e.g., Issar and Zohar 2004; Eitel et al. 2005a; Kuper and Kröpelin 2006). It supports the hypothesis that desert-margin areas are hotspots of the onset and change of cultural development in general (Eitel 2007).

2.2 Geographical Setting of the Palpa Region

The Humboldt upwelling system, which is controlled by the presence of southerly winds and the pattern of the coastal ocean circulation, borders the west coast of South America between 45°S and 4°S (Longhurst 1998). The cold sea and different degrees of sea versus land surface roughness lead to divergent air masses along the coast and force the air to sink. Thus the eastern ridge of the South Pacific High is regionally intensified, preventing convection and causing the aridity of the Atacama desert in northern Chile and in Peru. The Pacific High can join the Bolivia High over the Andean Altiplano forming a very stable anticyclone system (Mächtle 2007). In particular off southern Peru the upwelling is pronounced due to the submarine Nazca Ridge (Schweigger 1959). Strong winds support this system culminating during July and August in the austral

winter (Strub et al. 1998). In contrast to the desert strip north of Lima, which is characterised by heavy rainfall events during El Niño years, and to parts of the southern Atacama desert (Chile), which can be hydrologically influenced by strong westerlies with advective rains (Caviedes 2005), in southern Peru the desert remains dry. The only source of humididy is coastal fog.

In the study area between the Pisco–Ica region in the north and the Nazca–San Juan region in the south (13°–15°S/southern Peru) the desert strip is ~90 km wide, which is 10–30 km more than farther north along the coast between Ica and Lima. This is caused by the Cordillera de la Costa reaching ~170 km in length and ~1500 m in altitude, and consisting of Palaeozoic igneous rocks and Mesozoic to Tertiary sedimentary layers. For Peru, the existence of this mountain range is unique. To its east, a ~20 km broad hyperarid basin, the Ica–Nazca depression, formed by Tertiary and Quaternary tectonics, contains terrigeneous and marine deposits. With an altitude between 150 and 500 m the depression separates the Cordillera de la Costa from the Andean Cordillera Occidental, which rises steeply to more than 4000 m a.s.l. Large Pleistocene pediments in the eastern basin form the transition zone to the foothills of the Andes that belong to the desert, too (Fig. 2.1).

The pediments reach back in the lower parts of the Andean valleys. Built up by Tertiary and Pleistocene deposits they underwent the final sedimentary overprint ~50 ka ago (Eitel et al. 2005a; Greilich et al. 2005; Mächtle 2007;

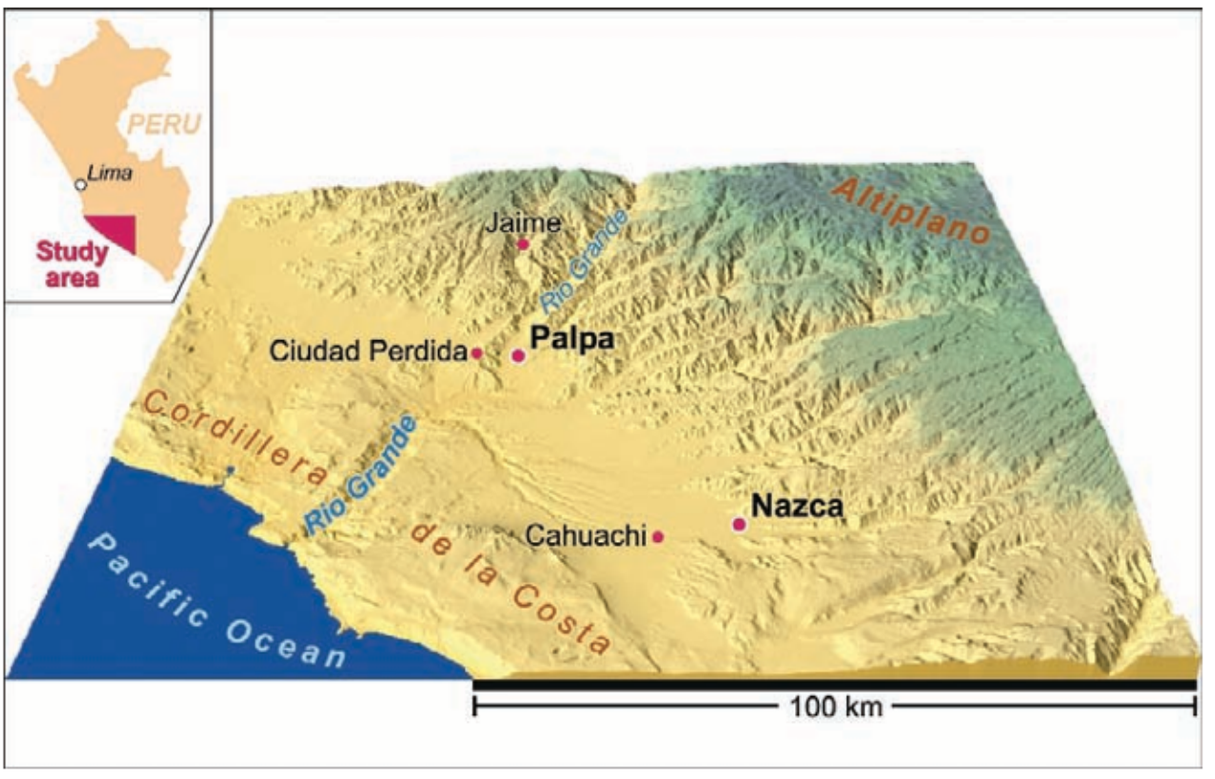

Fig. 2.1 Study area in southern Peru (block-diagram generated by SRTM-data is distorted). It reaches from the Pacific Ocean to the semi-arid western Altiplano rim of the Andes (>4300 m a.s.l.). Green colours indicate mean annual precipitation >100 mm per year. Note that the Rio Grande is the only perennial river with headwaters northeast in the Western Cordillera

Steffen et al. 2007). This shows that all valleys, incising the pediments, must be relatively young (<50 ka). At present the valleys are either river oases fed by ephemeral rivers (in the study area only the Rio Grande has perennial runoff) or dry valleys (*quebrada* systems). In the study area, from north to south, the rivers Rio Santa Cruz, Rio Grande, Rio Palpa, Rio Viscas, Rio Ingenio, and Rio Nazca flow down from the Andean highlands, providing the ecological basis for agriculture in the desert. These drainage systems reach far back to the high semi-arid Andes whereas the quebradas are autochthonous dry valley systems with much smaller catchments in the arid footzone of the Andes.

Whereas the input of humidity from the Pacific Ocean is restricted to fog in the Cordillera de la Costa, the eastern desert margin is hydrologically affected by summer rains (November–May), when Amazonian monsoonal thunderstorms seasonally cross the Cordillera Occidental and can reach the uppermost river catchments which subsequently flow down to the desert-strip in the western Andean foreland. The water supply over the Andes by convection to higher tropospheric layers is confirmed by $\delta^{18}O$ and $\delta^{2}H$ values in teeth and hair from humans and animals (Hölzl et al. 2007). At present, in the study area the eastern desert margin is botanically characterized by ephemeral summer rains resulting in the cactus belt 1200–1800 m a.s.l. in 60–90 km distance from the coast (Mächtle 2007).

The region is a typical example for a geomorphologically and ecologically very sensitive tropical environment (~14°S) due to the prominent hydrological gradient (Eitel 2006) from the semi-arid Andean highlands down to the hyperarid coastal desert. Already weak hydrological oscillations at its eastern margin can trigger considerable shifts of the desert margin with related severe environmental changes as has been demonstrated for western Namibia (Eitel et al. 2005b, 2006) and southern Peru (Eitel et al. 2005a; Mächtle 2007). Thus, with respect to ancient cultures, the study area is a high-risk region in particular for people depending on agricultural production.

Various remnants from different pre-Columbian cultures occur in the valleys of the study area near Palpa. Except for isolated stone-rings in the outer coastal desert, Pernil Alto is the oldest hitherto known human-occupied archaeological site. Situated in the Rio Grande valley the earliest recorded funerary contexts date back to the fourth millennium BC. The overlying Initial period settlement of Pernil Alto dates to the second millenium BC (Reindel and Isla 2006a,b). Ceramics emerged after 1500 BC extending to the Paracas (860–200 BC) and the Nasca cultures (200 BC–650 AD). The latter are famous due to their geoglyphs as a UNESCO world cultural heritage. After the collapse of the Nasca culture the region was only sparsely populated until ~1000 AD. A reoccupation of the footzone of the Andes and the eastern part of the basin of Ica–Nazca took place during the Late Intermediate period which lasted until the Inka dominance in the fifteenth century AD and the Spanish conquest in the sixteenth century.

This chapter presents a chronological synopsis of environmental changes at the eastern margin of the Atacama desert. The work is based on results of extended geomorphological and geoarchaeological investigations between 2002

and 2008 in the study area between Ica and Nazca (southern Peru). It combines evidence from geoarchives, in particular from sediments, soils, landforms, and from archaeological findings in order to reconstruct cultural and climatic developments and breaks. It is intended to show that

- Periods with accelerated cultural development or collapse coincide chronologically with environmental changes.
- Climate changes have strongly influenced the development of pre-Columbian cultures.
- The development of pre-Columbian cultures in the study area follows – at least in parts – analogous principles as they are known from Old World drylands.

2.3 Geoarchaeological Chronology since the Early Holocene

The synopsis focuses on the Holocene. For the late Pleistocene there are only a few hints to environmental conditions in the study area. Debris flows (*huaycos*) mostly consisting of removed pediment deposits show ages of 14–11.3 ka (A. Kadereit in Mächtle 2007). Periodically moister conditions than at present are also confirmed by snail shells (*Scutalus chiletensis granulatus Weyrauch sp.*) in the Andean footzone. This suggests that the late Pleistocene global warming trend coincides with moister conditions due to higher monsoonal summer precipitation in the eastern Atacama desert-margin during the Pleistocene–Holocene transition.

2.3.1 Loess Deposits: Occurrence and Age

A (peri-)desert loess (according to Pye and Sherwin 1999; Goudie and Middleton 2006) covers wide land surfaces of the study area. For the Palpa region first described by Eitel et al. (2005a), it is a prominent marker for a former Holocene humid period in the eastern Atacama desert.

2.3.1.1 Loess Distribution and Genesis Mechanism

Loess occurs in a small NW–SE oriented belt between ~50 and ~90 km from the Pacific Ocean. It covers slopes and pediments above ~450 m a.s.l. in the eastern Ica–Nazca depression and extends up to ~2200 m a.s.l. in the Cordillera Occidental. In the Andean valleys between 1200 and 1700 m a.s.l. it forms a continuous loess cover of ~50 cm thickness whereas in the footzone of the mountains and in higher regions only loess patches remain. No signs of stratification or cementation of the deposits have been observed. Chemical analyses, in particular different types of Cd-bonds, point to postsedimentary alteration (Mächtle and Eitel 2008).

Transported into the coastal desert by the Andean rivers and local quebradas most of the silt derives from fluvial deposits. High amounts of volcanic compounds (in parts up to 50%; Mächtle 2007) indicate transportation from pyroclastic rocks of the Cordillera Occidental down to the Andean foreland. Blown out from floodplains by the predominant southerly winds, the dust could only get accumulated areawide if vegetation fixed the material (e.g., Goudie and Middleton 2006). Therefore the loess indicates a cactus-grassland in the actually hyperarid eastern Atacama desert. This is confirmed by the finding that 1 mg of the loess acid-insoluble fraction contains ~500 grass phytoliths (Schiegl in Mächtle 2007). In the western part of the Ica–Nazca depression the sands, which have been left over and form large dunefields, are the correlated sediments to the windblown dust deposits (Fig. 2.2).

The above-mentioned *Scutalus* shells were found below the bottom of loess deposits too (Mächtle et al. 2006a,b; Mächtle 2007). AMS-^{14}C ages (all data calibrated with OxCal 3.10 acc. to Reimer et al. 2004 and corr. southern

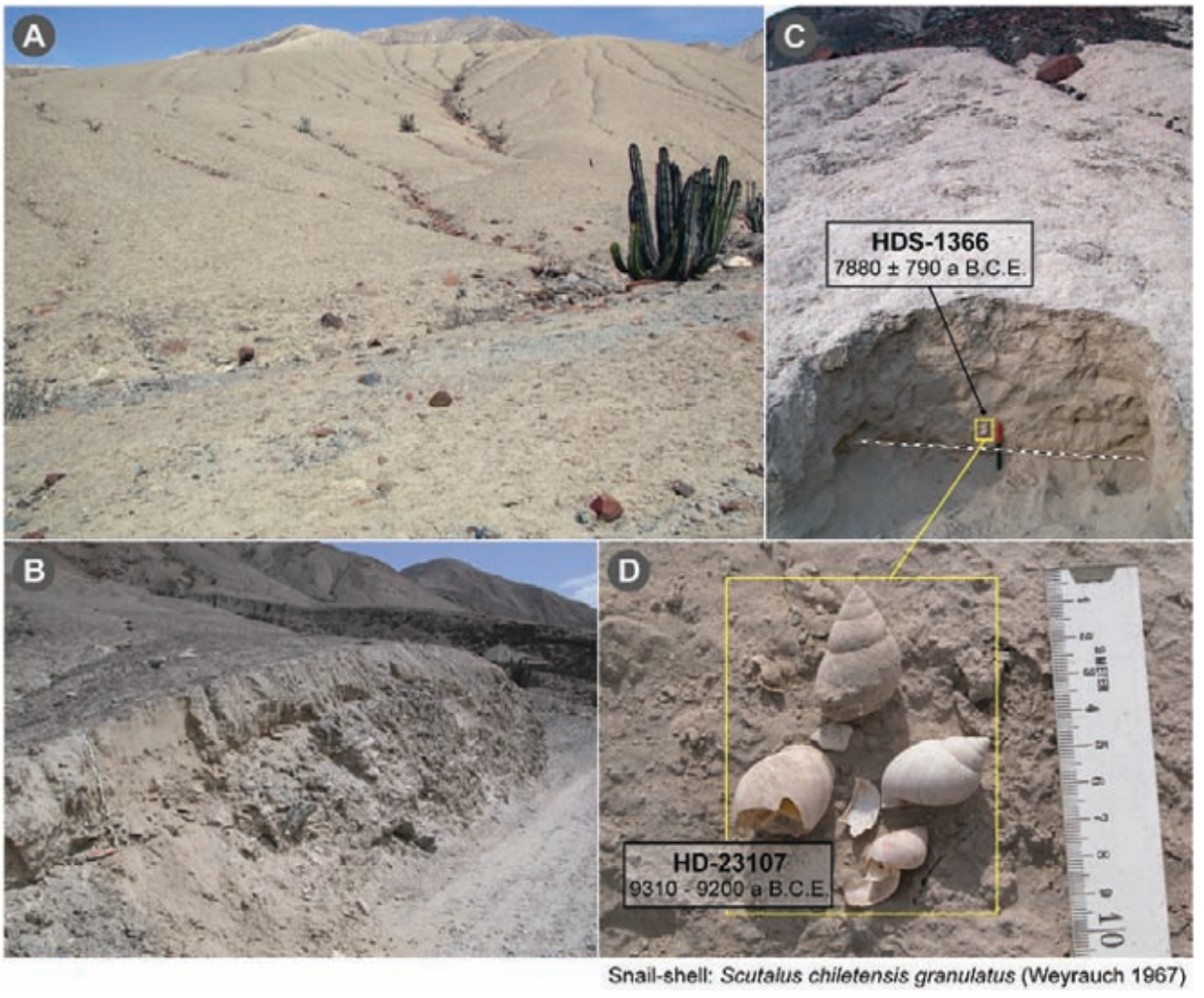

Fig. 2.2 (**A**) and (**B**): Loess covers at Jaime (Rio Santa Cruz valley) and loess deposit with *Scutalus* snail shell from Chichictara ~10 km east of Palpa (**C**) and (**D**); (**B**) confirms the aeolian origin of the desert loess covering even convex surfaces ~50 cm thick. In (**C**) the age of the loess deposition and in (**D**) the age of the snail shells confirm the early Holocene humid period in the eastern Atacama of southern Peru

hemisphere effect –41±14 a) of snail shell give 12,390–12,140 cal BP (LuS50018) and 11,310–11,200 cal BP (Hd-23107). The loess deposition started after the death of the snails at the transition to the Holocene ~11,560 years ago (Kadereit et al. this volume). Farther on, the onset of the loess deposition is assured by loess snails (*Pupoides albilabris peruvianus Weyrauch* sp.) in its deepest layers (11,750–11,400 cal BP, LuS50060; Mächtle 2007). The Holocene age of the loess is also confirmed by 14 OSL dates ranging between 11.17±1.15 and 4.15±0.36 ka (Eitel et al. 2005a; Mächtle 2007).

2.3.1.2 Geoarchaeological Interpretation

The early and mid-Holocene loess deposition suggests that the eastern Atacama in southern Peru (Ica–Nazca region) was more humid at that time than at present. In the desert-margin area west of the Andes open semiarid grasslands and perennial or ephemeral rivers (actually quebradas) provided good living conditions for human hunters and gatherers since the end-Pleistocene initial occupation of southern America.

This situation changed dramatically, most likely in the course of the second millennium BC. First, the end of the aeolian loess deposition ~4 ka ago, and second, the subsequent onset of deposition of fluvial loams in the river oases due to increased loess erosion (see Section 2.3.2), both pieces of geomorphic evidence, must be interpreted as a strong aridisation of the region. Henceforth the local quebradas dried up, and fluvial activity was restricted to the big rivers flowing down from the Andean uplands (from north to south: Rio Santa Cruz, Rio Grande, Rio Palpa, Rio Viscas, Rio Ingenio, Rio Nazca). Silt production decreased due to reduced fluvial sediment transportation. The vegetation cover disappeared, dust fixation ended, erosion only by episodic rainfall began, and the coastal desert expanded to the east.

People had to concentrate on the ecologically favourable oases along the ephemeral or perennial rivers, or to leave the region. This concurs with the oldest known settlement in the region, Pernil Alto in the Rio Grande valley, which was occupied at least since 1300 BC (Reindel and Isla 2006a,b). Stable settlements and agricultural production went hand in hand with the development of ceramics, presumably due to accelerating population density. The oldest graves thus far discovered derive from the end of the Archaic period (Isla this volume; Reindel this volume) and likely indicate the first societal differentiation processes in this region during the transition to the Initial period (Fig. 1.1 of Chap. 1 of this volume).

2.3.1.3 Palaeoclimatological Considerations: The Role of the Bolivia High

The causes for the early and mid-Holocene humid phase are uncertain. At the same time, global warming led to more relative air moisture in general. In a regional context it is most likely that, particularly for the Atacama desert, the latitudinal position of the Bolivia High is responsible for the moisture transport

from the Amazon Basin over the Andes to the study area. At its northern margin the stable anticyclone drives the moisture transport to the west coast. A shift of the anticyclone of only a few hundred kilometres farther north or south led to intensified or to reduced east–west transport of Amazon air (Fig. 2.3). It must be stressed that leeward effects in tropical mountains are not very important because the moisture transport happens not advectively as in the subtropics or higher latitudes but by convection up to heights >12 km.

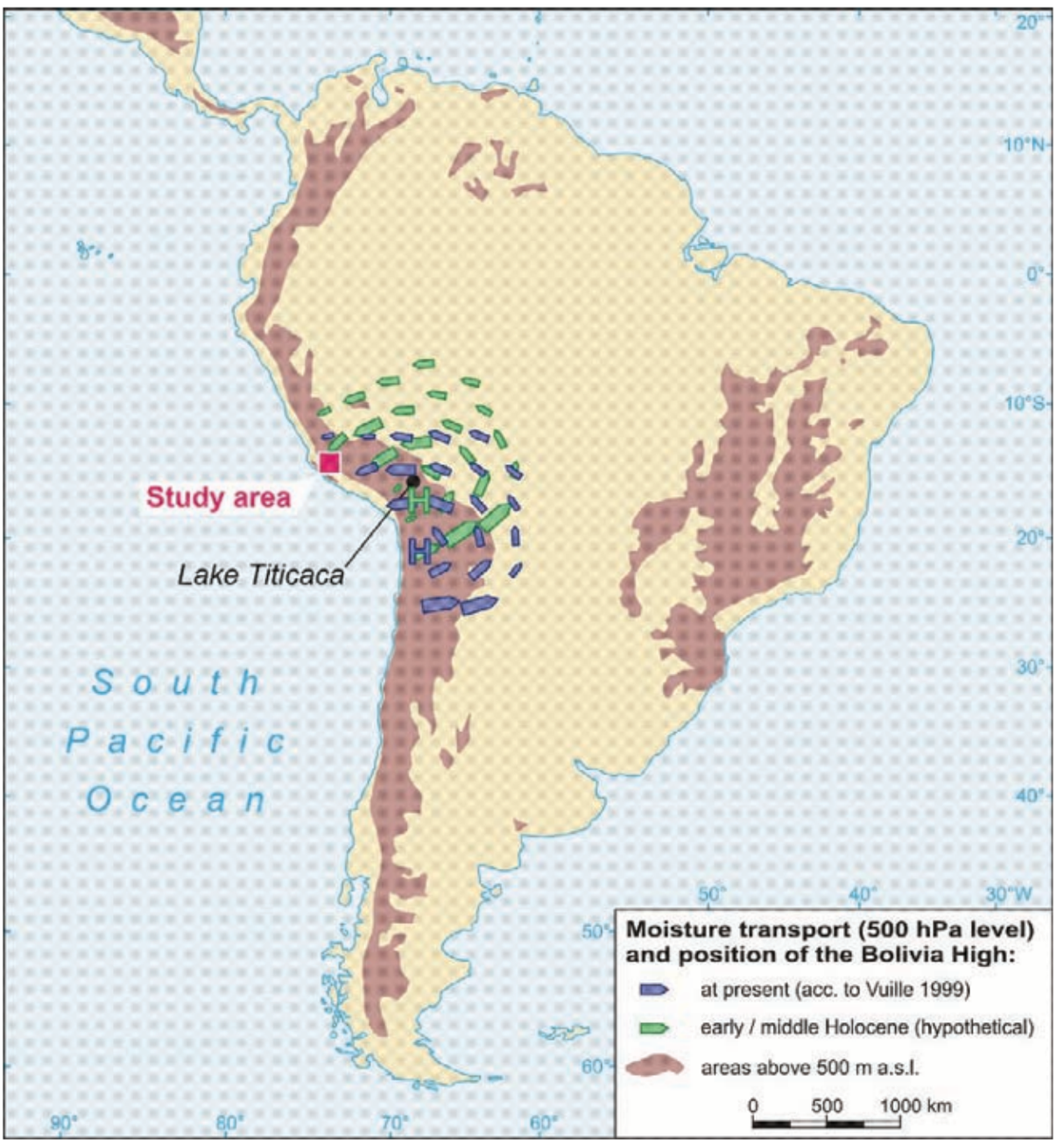

Fig. 2.3 Transport trajectory of humid Amazon air in the 500 hPa level at the northern margin of the Bolivia High (according to Vuille 1999, leading to dry conditions in the study area). The figure shows that a weak latitudinal shift of the anticyclone can provide dramatic hygroclimatical changes with more humid conditions (*green*) in the study area at the eastern desert margin in the Palpa region. This constellation seems to be responsible for the humid phase in the early and mid-Holocene, and ~800 years ago

The aridisation of the eastern Atacama desert-margin coincides with an increasing insolation farther south over the Bolivian Altiplano since ~4000 years ago (Mächtle 2007) due to perihel-position during the austral summer season (Baker et al. 2001). It is obvious that – assuming the steering role of the Bolivian High – this came together with drier conditions because the study area got in a more peripheral position with regard to the anticyclonic moisture transportation (Fig. 2.3).

2.3.2 Fluvial Deposits in the River Oases

With the onset of the Paracas culture during the eighth century BC and the following the Nasca period from the second century BC to the seventh century AD most of the loess deposits were already eroded in the Andean foreland. Only loess patches remained. This allowed the construction of the geoglyphs by removing the re-exposed desert pavement on a pedogenic vesicular layer of the pediment surfaces (Eitel et al. 2005a; Lambers 2006). Only in the valleys of the Cordillera Occidental farther east did loess remain preserved even by a sparse vegetation cover.

From the Early Paracas to the Middle Nasca periods no geomorphic evidence is known for catastrophic flash floods and for intense removal of deposits in the river oases. At Jauranga, downstream of Palpa, an old terrace, which was continuously settled, and various graves, which are buried by loamy sediments (Reindel and Isla 2006a,b) confirm stable geomorphic conditions with reliable ephemeral high-floods for centuries. These floods occurred only in the oases of the big rivers with catchment areas in the high Cordillera Occidental with reliable monsoonal summer rains. More local river systems in the Andean footzone remained dry (quebradas). Nasca lines crossing terrace series and the quebrada floors show that the valleys have been flooded in pre-Nasca times for the last time. Only small quebrada floor channels provide evidence for weak episodic runoff events in younger times (Fig. 2.4). This is a clear signal for lasting aridity.

Not until the Late Nasca period, which started in the fifth century AD, did the runoff even in the major valleys become more and more accentuated with enforced sediment reworking (Unkel et al. 2007). In drylands this is typical for a proceeding aridisation with long-lasting droughts and short but heavy rainfall events causing high and turbulent floods.

2.3.2.1 Geoarchaeological Findings

Whereas the earliest settlements in western Peru were situated along the coast (seventh–sixth millennia BC) or in middle altitudes on hills and water divides between the valleys (Dillehay et al. 1989), since the third millennium BC settlements concentrated along the river oases. Perhaps north–south oriented contacts

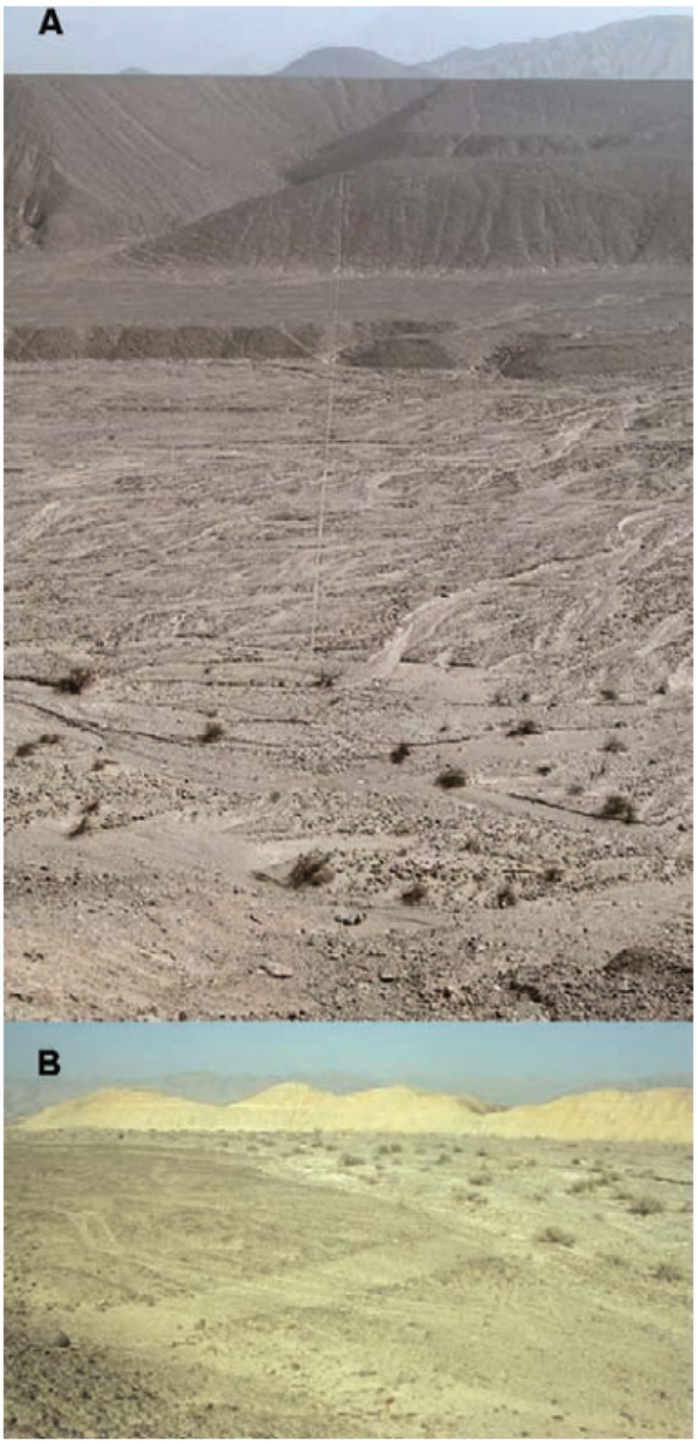

Fig. 2.4 (**A**) Nasca line (geoglyph) crossing a quebrada south of Palpa. The existence of the line exemplarily illustrates that the valley floor has never been flooded since the Nasca period. Only a small channel in the foreground provides evidence for weak episodic runoff events during the past two millennia. (**B**) Geoglyph in quebrada Zorral, south of Palpa, showing the same fact: since the construction of the geoglyph the quebrada runoff did not flood the whole valley. That is a clear sign of lasting aridity with only weak episodic rains (even during pluvial times) without any disastrous El Niño floods

changed to west–east interaction during this time, because the eastern Atacama dried up and the desert prevented longitudinal exchange. In the study area after 800 BC cultural development peaked for the first time with the well-organised and pronounced social structure of the Paracas culture. During the Nasca period (second century BC–seventh century AD) societal differentiation accelerated by increasing population density in the oases as indicated by settlement hierarchy in the Palpa valleys, by the necropolis of La Muña west of Palpa, or the temple complex of Cahuachi in the Nasca valley (Isla and Reindel 2006a,b).

Paracas and Nasca buildings are constructed with adobe. It is typical for dryland constructions along river oases to use adobe for buildings. This is again a clear sign for nearly permanent absence of local rainfall and for a water supply exclusive of the river.

Since ~200 AD the central settlements shifted more and more to the north-east entering the valleys of the Cordillera Occidental (Mächtle 2007). This is most likely a response to increasing aridity and reduced summer monsoon intensity, because the relief in the steep valleys and the difficult conditions in the narrow strip of mountainous river oases make the occupied areas less favourable for agriculture than the broad floodplains in the mountain foreland farther west. At the end of the sixth century AD the aridity culminated and the Nasca society collapsed. Based on new observations in the Andean highlands one can assume that most people migrated to the Altiplano rim (Reindel 2007, pers. comm.) with its colder but more humid environment (Fig. 2.5).

The collapse of the Nasca culture at the end of the sixth century AD is not a unique event. According to our current knowledge, at the same time the Moche culture in northern Peru and the Atacameña culture in northern Chile came to an end (Shimada et al. 1991; Nuñez 1992). It is interesting that in the Ayacucho region at the same period the Huari settlements concentrate along river courses too, whereas formerly the people had settled on higher surfaces and had worked on rainfed terraces (Isbell 2001).

2.3.2.2 Palaeoclimatological Considerations

Most hints for the aridisation during the first millennium AD derive from archaeological findings and interpretations. Important palaeoenvironmental evidence originates from Lake Titicaca. After the third century AD the rapidly rising lake level (Binford et al. 1997) coincides with accelerated aridisation of the study area and points to a more southern position of the Bolivia High which causes more precipitation in the Titicaca Basin and reduced rainfall in the Ica–Nazca region (Fig. 2.3).

The hydrologically sensitive living space of the Nasca people responded dramatically even to weak climate changes. Mächtle (2007) assumed only a rainfall reduction of ~100 mm/a, which seems not very much at first, but it could have halved the total annual precipitation and could have stopped the runoff in the lower parts of the valleys. Once again this is a telling example for the high sensitivity of desert-margin areas and the risks for human societies in such regions. After the aridisation of the eastern Atacama desert since the third or second millenium BC and the concentration of the people on the river oases this further-enforced arid pulse affected the river runoff and finally deprived the Nasca people of their livelihood.

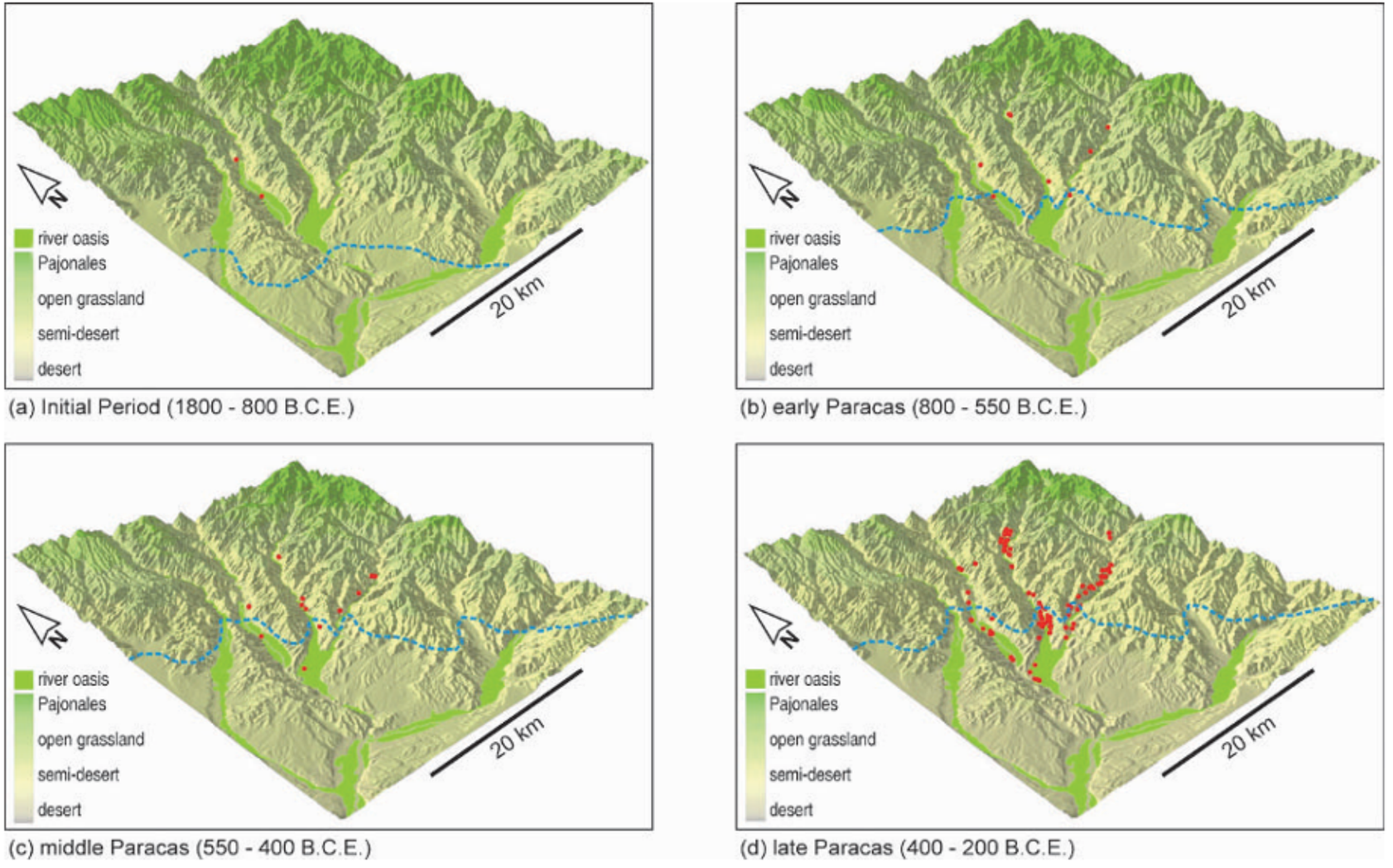

Fig. 2.5 (a) Settlement patterns and the palaeoenvironmental conditions from the Initial period until the present (Mächtle 2007). Note the shifting desert-margin due to changing intensity of the monsoonal rainfall during the austral summer

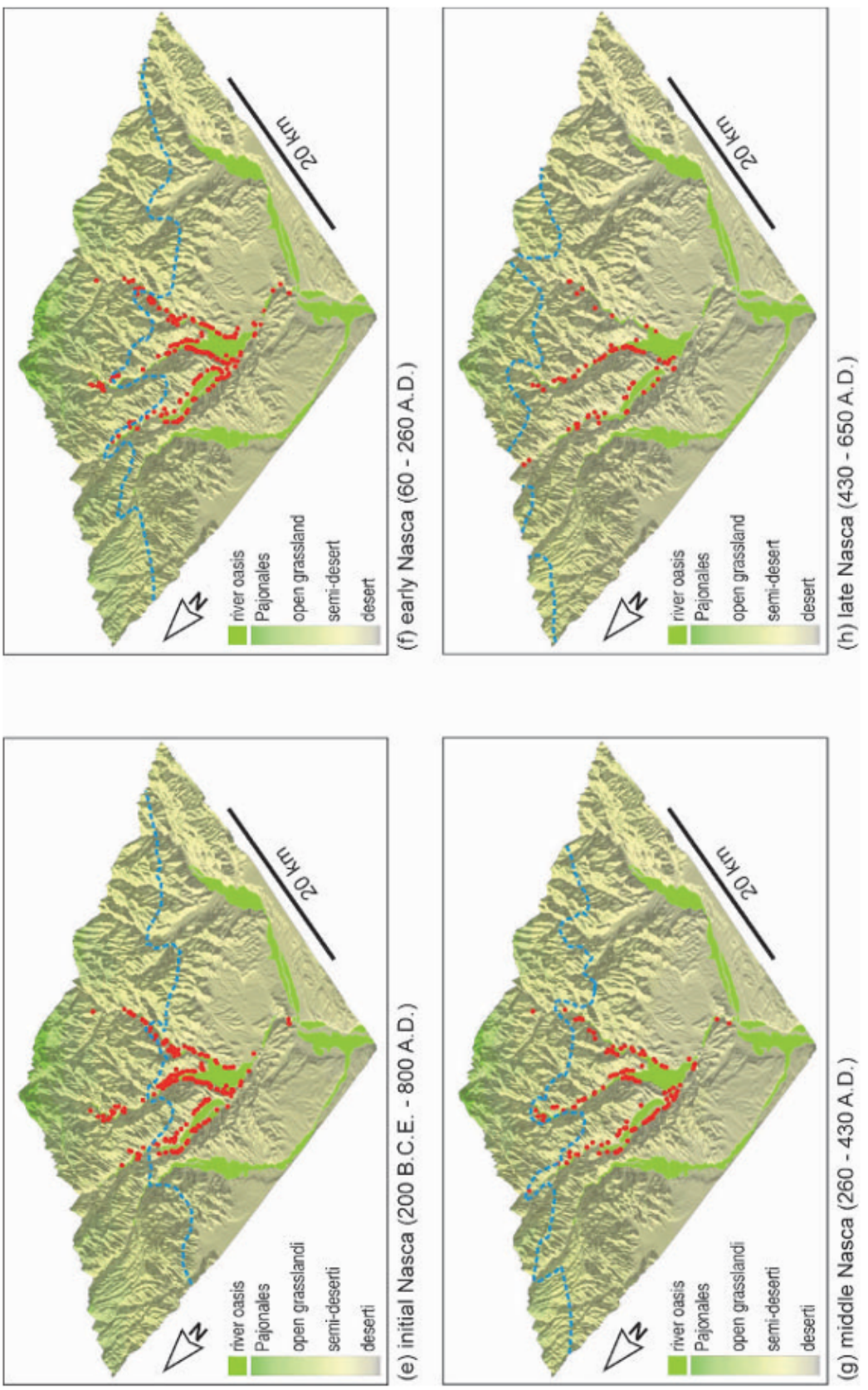

Fig. 2.5(b) (Continued)

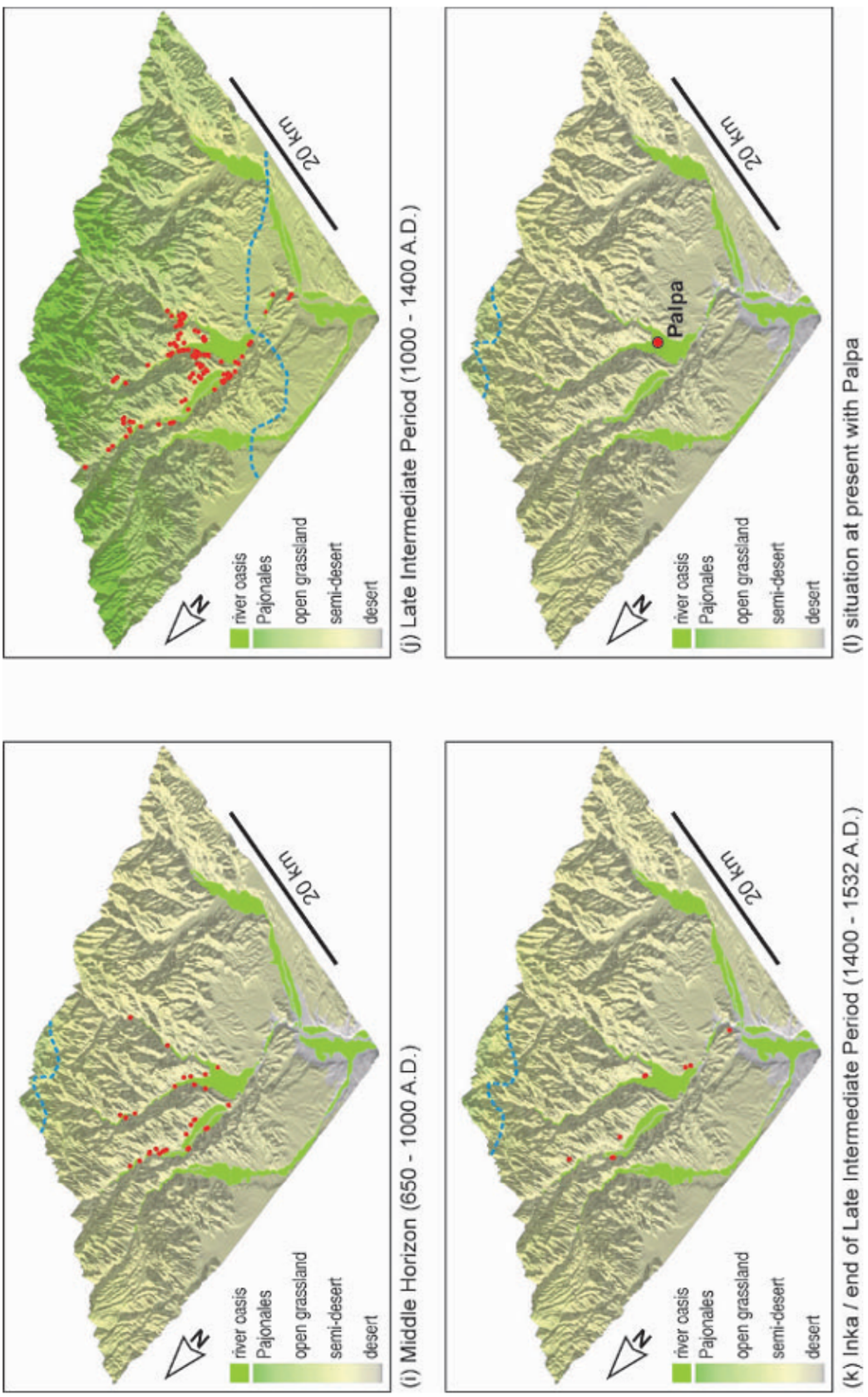

Fig. 2.5(c) (Continued)

2.3.3 *Recurring Humidity in the Fourteenth Century AD: Sedimentary Evidence*

Geoarchives in the study area give evidence that the very dry period lasted not longer than the fourteenth century AD. Radiocarbon and luminescence dated terrace deposits indicate recurring fluvial dynamics in all river oases of the region (Mächtle 2007; Unkel et al. 2007) by a sedimentary aggradation of older terrace systems during the following centuries (Fig. 2.6). The burying of older surfaces by more or less sandy sediments must be interpreted as geomorphic evidence for more precipitation in the river catchments of the western Andes with flooding of large parts of the valleys. This is indicated at first by the deposits in the Rio Grande valley, as its catchment area reaches farther east into the Cordillera Occidental than other rivers of the neighbouring valleys do.

In addition to the terrace deposits in the major valleys, some isolated debris flows based on slack Pleistocene pediment remnants indicate very local heavy rainfall events. At La Muña (Fig. 2.1) radiocarbon and OSL dating confirm repeated geomorphic dynamics between ~1320 and 1770 AD. This time span encompasses exactly the humid phase as indicated by other sedimentary archives.

Where the valley joins the lower Rio Grande valley the age of the Rio Santa Cruz floodplain confirms the pluvial phase too, but it marks coevally the onset

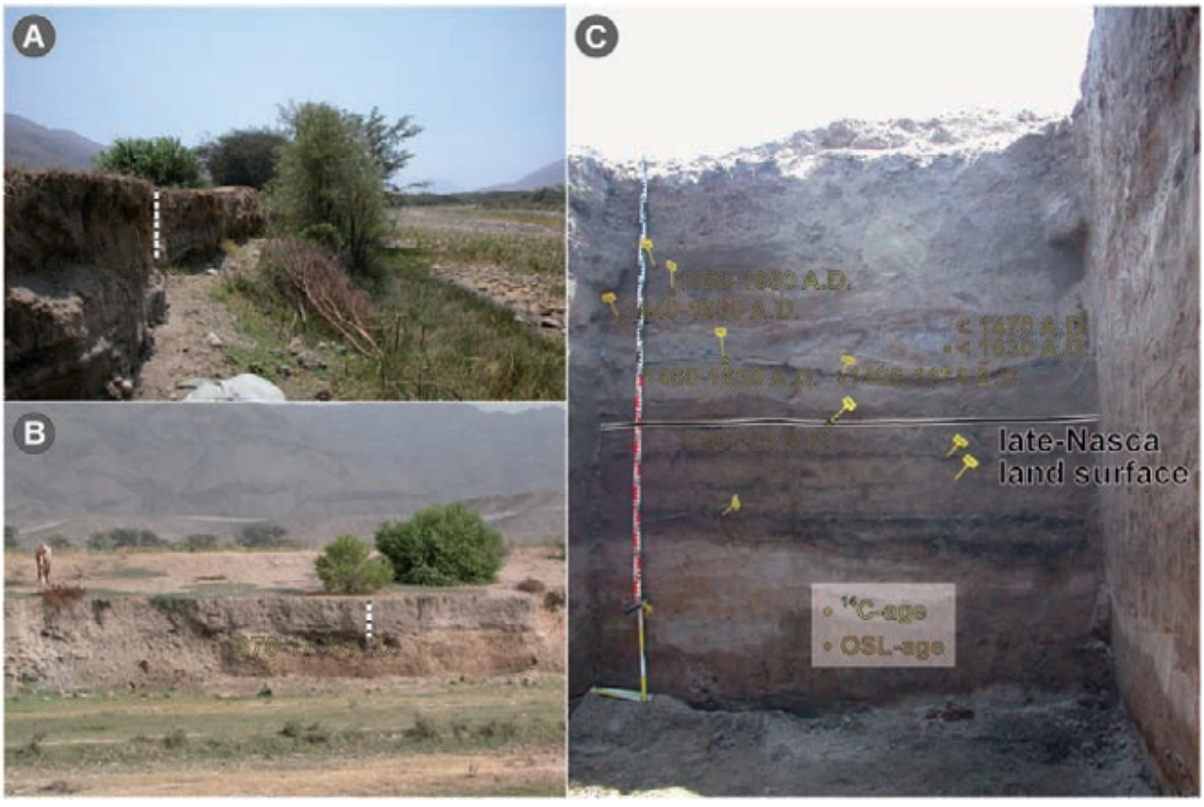

Fig. 2.6 Typical terrace deposits consisting of two sedimentary layers (some km west of Palpa). The upper units (*yellow bars*) belong to the humid phase in the eastern Atacama desert after the fourteenth century AD

of the final turnover to desert conditions, lasting from the seventeenth century AD. The surface of the ancient floodplain is characterized by sandy and silty deposits marked by cracks when the fine-grained deposits dried up (Fig. 2.1). Wood pieces provided a radiocarbon age of 1520–1660 cal AD. At this time the valley floor was flooded for the last time (Unkel 2006; Unkel et al. 2007). At present the fluvial deposits are mostly covered by unconsolidated dunes fixed in parts by bushes.

2.3.3.1 Geoarchaeological Evidence for the Pluvial Phase

Archaeological studies confirm the interpretation of the geomorphic archives. Many settlements show that during the Late Intermediate period people have reoccupied even the eastern Atacama desert. LIP buildings generally are constructed from stones and not adobe as during Nasca times. This is most likely because adobe is not stable enough under more humid conditions. It seems possible that the people migrated down from the semi-arid highlands bringing their traditional building techniques to the western lowlands. In the Palpa region the most prominent example is the Ciudad Perdida de Huayuri located in the mountain range between the Rio Santa Cruz and the Rio Grande valley. Geoarchaeological studies can help to reconstruct the ancient environmental conditions for the recolonisation of the eastern desert. Many geoarchaeological findings in the valleys of the Andean footzone show that the people settled under more humid environmental conditions which were characterised by reliable monsoonal rains. This justifies designating the period as the accentuated pluvial phase.

In the mountainous footzone of the Andes near Jaime (Santa Cruz valley, ~1,200 m a.s.l.) rills in the loess cover, which are oriented parallel to contour lines, have been identified as remnants of rainfed agricultural systems. The loess deposits in the formerly irrigated fields contain up to fivefold more phytoliths of grasses than the nonirrigated areas. The phytoliths derive mainly not from roots so that it is most likely that they were mixed up with the loess by field work (Schiegl in Mächtle 2007). Water concentration was used to intensify grass growth for livestock farming because irrigation channels brought water which was collected locally in deep rills of the northern flank of the valley. The excavated material was dated preliminarily (large standard deviation) to 820±340 years (Kadereit in Mächtle 2007). This altogether shows that local summer rainfall must have occurred reliably in an area which belongs at present to the eastern Atacama desert.

Water harvesting is also a typical feature in the Ciudad Perdida de Huayuri and its vicinity. The stone-built ancient city (Fig. 2.7) was built in a solitary valley of a mountainous ridge separating the Santa Cruz River and the Rio Grande River in the Andean foreland. Rainfed agricultural terraces cover the slopes, in particular in erosion rills in order to retain runoff and use the water. More obvious are small anthropogenic channels which have served as water samplers. They led the water to dammed quebradas as known from the Thar

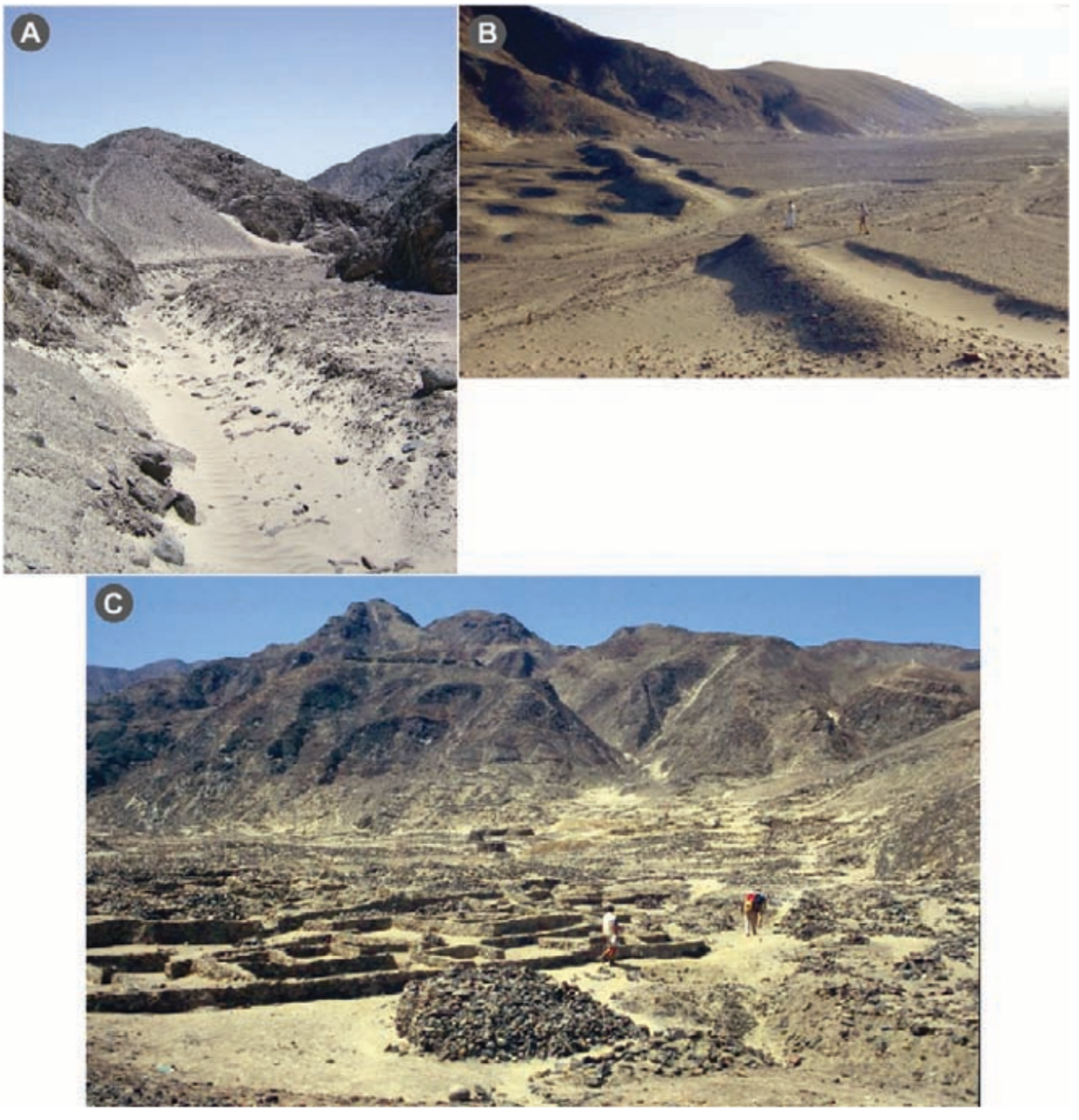

Fig. 2.7 Ciudad Perdida de Huayuri (**C**). The small photographs show a water collector (**A**) and a sand dam (**B**)

desert in India (Kolarkar 1997) as 'khadin', in Arabia as 'snail', or in northern Africa as 'tussur' (Hornetz and Jätzold 2003). Similar systems with sand dams are used in Namibia (Stengel 1965). Such systems (cf. Mächtle et al. this volume) with a ratio between catchment area and water consumption area of 5:1 up to 25:1 only make sense in a semi-arid climate with more than 50 mm and less than 250 mm mean annual precipitation. The water infiltrates the sandy deposits which save it for up to two years. Such systems are highly efficient and make ~50–60% of the harvested water usable. For more detailed hydrological, pedogeochemical, and geoarchaeological data from the LIP water-harvesting system in Ciudad Perdida see Mächtle et al. (2008). First calculations allow us to assess that semi-arid conditions with 100–200 mm summer rain prevailed in the Ciudad Perdida region during the LIP period. This is noteworthy because it

shows that for a period of three or four centuries the desert strip was only half as broad as before and at present, and it makes clear that the desert margin has shifted very quickly during the past centuries.

The studies make it likely that the Spanish conquerors arrived when the Andean footzone was still characterized by semi-arid conditions. The collapse of the LIP culture, which at this time was more or less dominated by the Inca empire, seems not only to be triggered by introduced diseases but also by climate changes leading over again to desert conditions after the seventeenth century AD.

The cultural change during the LIP has also been observed at other places in southern Peru. For example, the Wawakiki spring site, Ilo region in southern Peru (17°S), at present a hyperarid environment, exhibited intensive land-use from the twelfth until the fourteenth century AD (Late Chiribaya period; Zaro and Alvarez 2005). Water transporting channels, settlements, and fields were first destroyed in the fourteenth century. It had been assumed that El Niño high floods destroyed the constructions (Keefer et al. 2003), but the lack of coarse clasts in the deposits, and the presence of decomposed organic material (decomposition needs soil humidity) point to increased runoff over longer times most likely fed by rains in the catchment area. Subsequently, as in the Palpa region, the Wawakiki site had been widely abandoned in the beginning of the seventeenth century too when the region dried up again.

2.3.3.2 Palaeoclimatological Causes for the Humid Phase

The observed palaeoenvironmental changes in the Palpa–Nazca region are generally compatible with the findings from drilling sites off the Peruvian coast. Sediment input into marine deposits off Lima after 1250 AD are interpreted as intensified El Niño events with high sediment discharge into the Pacific Ocean (Rein et al. 2004). This may be the case for northern Peru and may agree with El Niño as marine events, but in the study area in southern Peru the good state of preservation of Nasca geoglyphs excludes heavy El Niño rainfall. The example of recent El Niño events such as 1997/1998 shows that the marine phenomenon did not trigger heavy rain in the desert of southern Peru.

High sediment discharge of ephemeral rivers is rather a signal of increased rainfall in the Cordillera Occidental caused by an intensified summer monsoon. This is supported by the fact that the coastal cultures in Peru did not depend on unpredictable El Niño rainfall but on reliable summer rain in the Andes flooding the seasonal rivers even in the coastal desert. The moisture transport over the Andes works at its best during stable La Niña phases whereas during marine El Niño events the atmospheric circulation leads to an anticyclone over the Amazon basin which hinders rainfall in the mountains (Caviedes 2005). In the Nazca–Palpa region the pluvial phase was perhaps supported by a weak northern shift of the Bolivia High during the first parts of the Little Ice Age which lasted until the mid-nineteenth century.

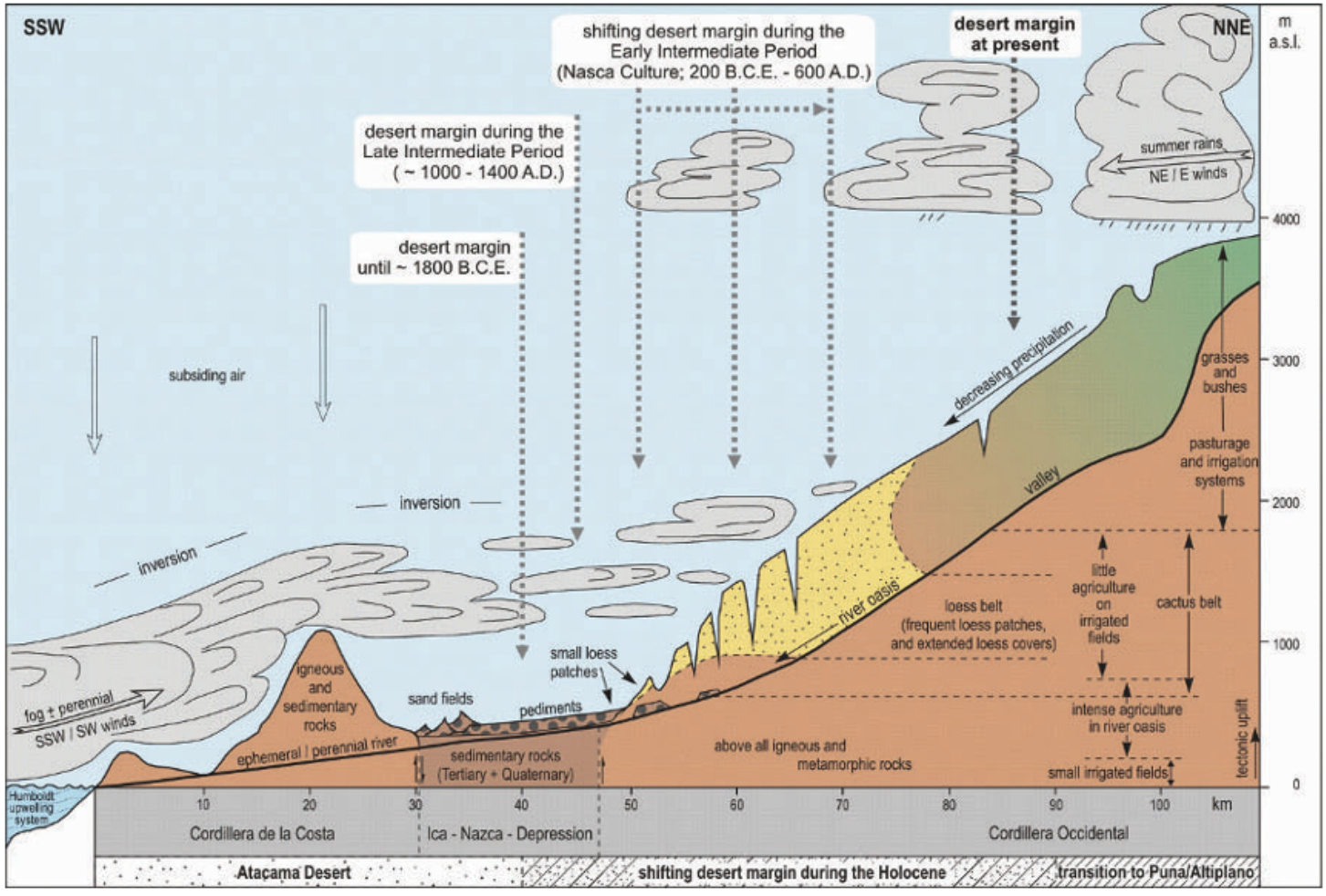

Fig. 2.8 Schematic geomorphological cross-section through the study area near Palpa including geological and vegetation characteristics. The arrows indicate the likely desert margins during the last millennia. The eastern desert was affected by multiple climatic changes indicated by dramatic shifts of the desert margin. Environmental changes triggered early cultural development and had a deep impact on pre-Columbian cultures

Hitherto, several terrestrial-based studies misinterpreted geoarchives in southwestern Peru ignoring the hydrological control of the rivers by the monsoonal summer rains in the Andes (Grodzicki 1994; Satterlee et al. 2000; Keefer et al. 2003). Even ephemeral high floods might just as well be explained in the light of varying spatial influence of the South American summer monsoon. The model of a shifting eastern desert margin (Fig. 2.8) explaining Holocene environmental changes in today's hyperarid northern Atacama desert was first presented by Eitel et al. (2005a). Meanwhile the concept has also been used to explain changes in settlement patterns in the Lima region (Goldhausen 2005). Therefore, the model might be well suited to explain cultural changes as observed in the greater area of southern Peru.

2.4 Conclusion

The study area in the footzone of the western Andes is a typical desert-margin area. Such areas are defined as highly sensitive regions which respond rapidly to hygroclimatic changes by environmental turnover. The transition from desert to grassland ecosystems is characterised by shifting desert-margin shifts. Therefore, desert-margin areas can be defined as reactive spatial systems with low resilience where the desert-margin oscillates within some hundred or some thousand years (Eitel 2007). Such subtropical and tropical desert-margin areas are hotspots of early culture development, not only in the Old World but also in the Americas, because they provide good living conditions, they are warm, generally provide fertile soils, seasonal aridity reduces the danger of pathogens, and – if still available – they provide good hunting conditions to big herbivores. But such climatically sensitive regions are regions at risk and in general societies are highly vulnerable to hydrological changes.

Abrupt or sneaky environmental changes trigger individual and societal adaptation processes, and at last to the point of societal collapse and migration. This does not mean a revival of geodeterminism. The geodeterministic hypothesis as well as the opposite theory of free human behaviour exists from the antagonism between nature and human beings, but regarding both as compounds of the same environmental system we can see that there are multiple interactions. This system can be triggered by internal and external stimuli.

In the Ica–Nazca region the development of the pre-Columbian cultures can exemplify the deep impact of environmental changes on culture development. This includes the establishment of stable agricultural settlements along the river oases and the stimulation of adaptation processes as there are divisions of work and societal differentiation, and the displacement of settlements. In addition, the study shows that disastrous flash floods, especially El Niño events, were not the causes of major changes in settlement patterns. There is no clue for 'disaster-determinism' because flood events did not destroy the living conditions of the people in the long run. This was the case when climatic changes led to complete environmental

turnover in the seventh and seventeenth centuries AD when the Nasca and, respectively, LIP–Inca societies collapsed due to accelerated aridisation.

Finally, it is noteworthy that the collaboration between natural scientists and archaeologists provided a lot of added value. The synopsis showed how geoarchives and archaeological findings complement each other, and how this provides new comprehensive insights in the history of the man–environment system. The Nasca–Palpa project adds not only one more regional study to the huge number of such ventures. It provides new approaches to understand basic early cultural processes by testifying to the findings of the Old World independently in the New World, it successfully adopts the model of monsoonally controlled shifting desert margins from the Namib desert to the northern Atacama desert in order to explain environmental changes, and it fits the results into the supraregional climatological frame by explaining aridisation in the Nazca region and simultaneous high lake levels in the Titicaca Basin easily by weak shifts of the Bolivia High. The comprehensive approach of a multidisciplinary collaboration has offered new perspectives for future geoarchaeological research.

Chapter 3
Built on Sand: Climatic Oscillation and Water Harvesting During the Late Intermediate Period

Bertil Mächtle, Bernhard Eitel, Gerd Schukraft and Katharina Ross

Abstract For the first time in South America, we found specific constructions for water harvesting from the Late Intermediate period. Their configuration allows the precise reconstruction of mean annual precipitation during that time. In that area, enhanced precipitation enabled the people to cultivate the desert. The remains of human occupation give evidence of a short climatic oscillation in the northern Atacama desert around ~1300 AD.

3.1 Introduction: Man and Desert Environment in the Palpa Region

Former human occupation of present-day deserts was often coupled with a replacement of the desert environment by grasslands due to more humid conditions in the past. The emergence of adequate water resources was the essential condition for colonisation. In desert environments, remains of human occupation represent geoarchives and give evidence of palaeoenvironments. Furthermore, remnants of human adaption strategies to dryland ecosystems – for example, water harvesting structures – may allow accurate quantitative estimations of past average rainfall.

At present, the study area around Palpa (14.5°S, southern Peru) belongs to the hyperarid northern Atacama desert. The mean annual precipitation does not exceed 10 mm. During the Holocene, several hygric fluctuations occurred in that area due to climatic changes (Eitel and Mächtle this volume). During the Early and Middle Holocene, enhanced moisture transport across the Andes to the west triggered the development of grasslands and the sedimentation of desert margin loess. The desert retreated. In Late Holocene times, increased aridity forced pre-Columbian people to settle along the river oases. For several centuries the civilisations of Paracas and Nasca flourished there.

B. Mächtle (✉)
Institute of Geography, University of Heidelberg, Im Neuenheimer Feld 348, 69120 Heidelberg, Germany
e-mail: bertil.maechtle@geog.uni-heidelberg.de

M. Reindel, G.A. Wagner (eds.), *New Technologies for Archaeology*, Natural Science in Archaeology, DOI 10.1007/978-3-540-87438-6_3,
© Springer-Verlag Berlin Heidelberg 2009

They made a good choice: along the lowland river oases, year-round extensive irrigation farming was possible, whereas in the more humid, but colder highlands the yield was reduced due to a short vegetation period, low temperatures, and winds. In addition, highland farming was limited to small lots on hillsides and the high plateaus were usable only as pasture. Thus, during periods of reliable and adequate runoff, the people moved from the highlands to the lowland river oases.

This is confirmed by the fact that the highlands were populated at all times, whereas only during specific periods were the ecologically favoured lowland river oases of coastal Peru the hotspots of sedentariness. This was the case for the Paracas and Nasca civilisations of southern coastal Peru (Reindel and Isla 2006) during the period from 800 BC–650 AD, but also for the Moche culture of northern coastal Peru. After that time, declining rainfall in the highlands induced a critical decrease of runoff in the river oases and led to the abandonment of lowland settlements. During the following Middle Horizon of Andean archaeology, the highland civilisations of Huari and Tiahuanaco evolved and the lowland river oases became too dry for humans (Fig. 1.2 of Chap. 1, this volume).

An increase of rainfall and river discharge, at the latest starting during the thirteenth century, once more allowed the occupation of lowland sites during the Late Intermediate period around Palpa. A synchronous expansion is reported for the Chiribaya culture farther to the south (summarised in Satterlee et al. 2000). Simultaneously, on the northern coast of Peru, the Chimu empire was established after a period of depopulation during the Middle Horizon.

It is striking that the hotspots of pre-Columbian cultural development seem to coincide at each point in time with the ecologically most favoured regions! During the more humid Early and Late Intermediate periods the coastal civilisations prospered along the lowland river oases, whereas during the dry Middle Horizon highland civilisations advanced and the coastal civilisations collapsed.

In this chapter, we focus on the Late Intermediate period. After the depopulation of the Middle Horizon, a new civilisation flourished along the river oases in the Palpa region. Far away from the common water resources of the river oases, a new kind of city emerged for the first time. For a short time, they got their water from springs fed by local rainfall. However, the environmental conditions soon deteriorated. Situated closest to the advancing desert, the people of one of these cities, the Ciudad Perdida de Huayurí, had to decide: exodus or adaption.

3.2 Adaption Strategies to Dryland Environments

Dryland environments are chacterised by rare, but intense, rainfall. With rising aridity, the frequency of rainfall events decreases, but the magnitude increases. Under these conditions, the infiltration of water into sediments is small. This results in high amounts of water loss due to surface runoff. However, for thousands of years people have developed strategies to adapt to this situation: they concentrated the runoff of large areas on small plots. That way, they

created artificial areas of increased humidity, which could be used for agriculture or drinking-water production. This method is called "water harvesting".

Water harvesting means gathering and storing surface runoff by several technologies and has been a well-known adaption to arid and semi-arid environmental conditions for thousands of years all over the world. Water harvesting systems are the check-dams of southern Arabia, the Tussurs (which means 'sediment storage') of the African Anti-Atlas, the Karez of Central Asia and, in particular, the Khadin systems in the Thar desert of India. Some of these systems are more than 3000 years old (summarised in Pandey et al. 2003).

From coastal South America, only the 'albarrada' water harvesting system was known (e.g., Stothert 1995). During research within the Nasca–Palpa project, we discovered a system hitherto unknown and corresponding to the Indian Khadin, around Ciudad Perdida de Huayurí (Fig. 3.1). It is striking that

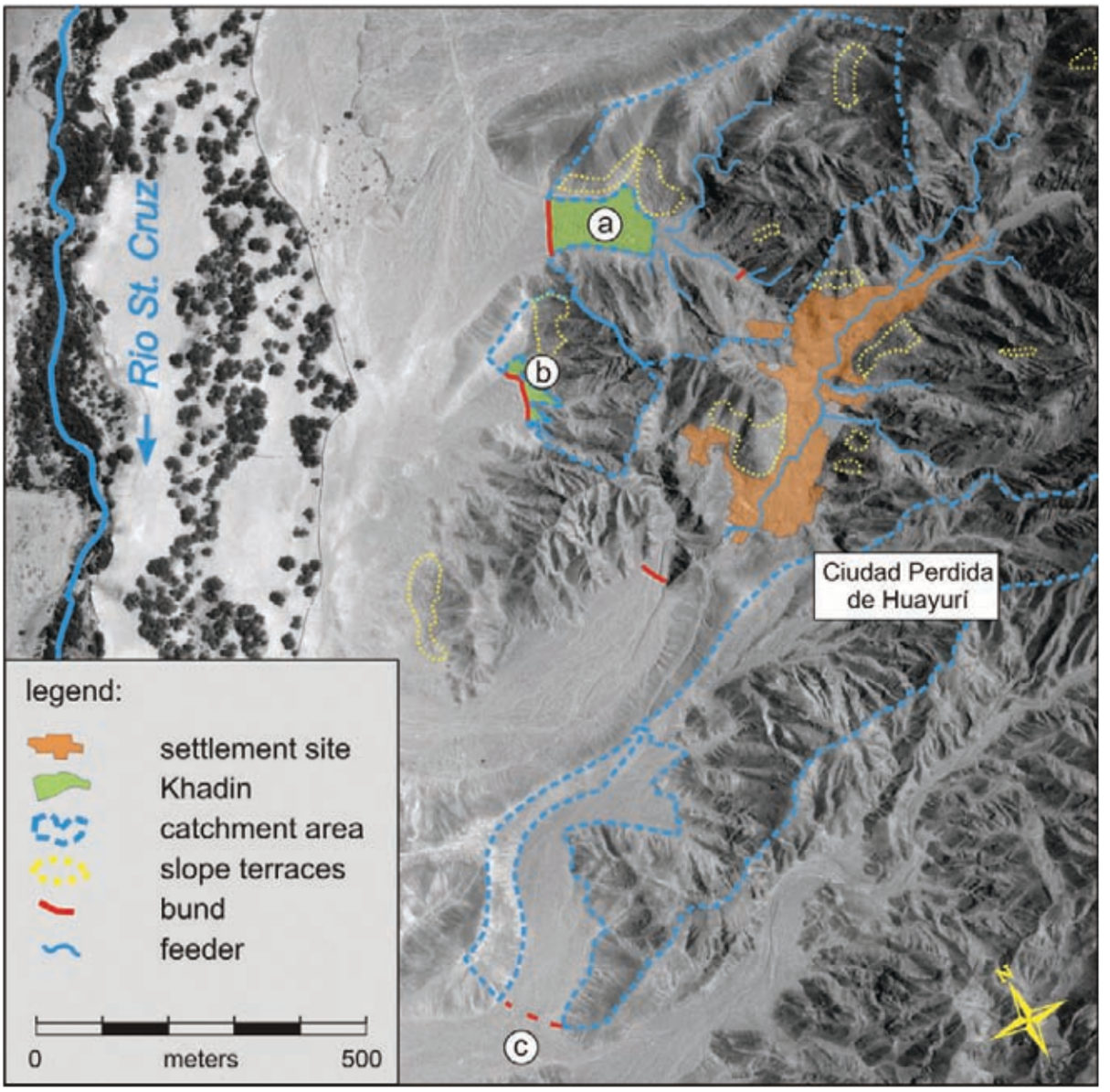

Fig. 3.1 Aerial view of Ciudad Perdida de Huayurí and adjacent Khadin areas (a and b). The bund at 'c' remained unfinished. (Borders of catchments and Khadin areas according to Ross (2007); Aerial photo: Servicio Aerofotográfico Nacional, Lima, Peru.)

people of Peru and India independently came up with the same answer to the challenges of desert margins.

3.3 The Water Harvesting of Ciudad Perdida de Huayurí

Today, the Ciudad Perdida de Huayurí remnants are located in the hyperarid Andean foreland (see Fig. 2.1 in Eitel and Mächtle this volume), which is unsuitable for water harvesting. Therefore, the Khadin plants we found are testimony to more humid conditions during the Late Intermediate period. Khadin means 'cropped area'.

The Khadin system is well studied by Kolarkar (1997). A Khadin is located in a seasonally dry valley (Fig. 3.2). A bund is built of loose sediments with a solid core of rocks, to stop rare surface runoff. In addition, it collects loose sediments, which are useful for water storage. The collected water seeps down and improves soil water conditions. For a successful operation of the Khadin, some typical features are necessary (Fig. 3.3):

- Rocky upland in the catchment so that only a minimum of rainfall is retained by talus deposits
- Debris retaining walls on steeper ditches

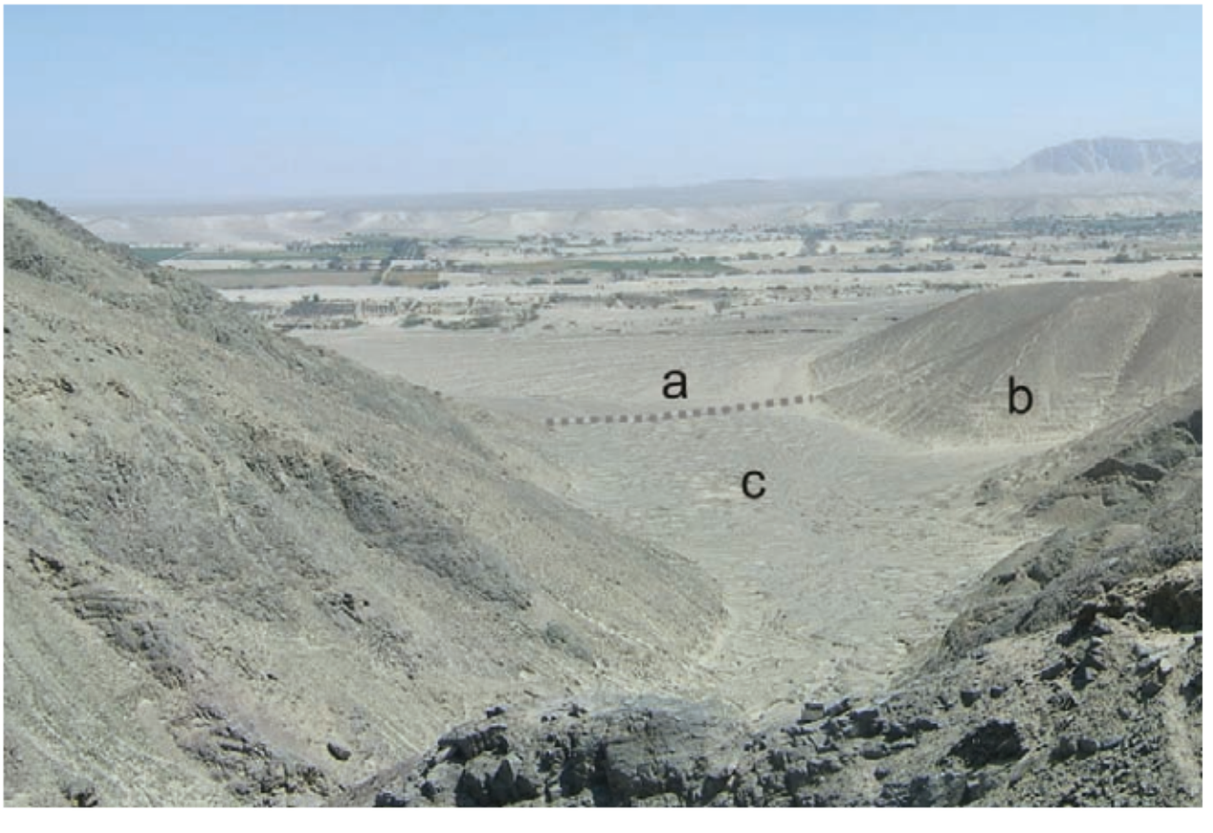

Fig. 3.2 Dry valley, blocked by a bund (**a** and dotted line, for detail see Fig. 3.3d). On the lower slopes terraces were built (**b**). The valley fill was used as cropping area, the "Khadin" (**c**)

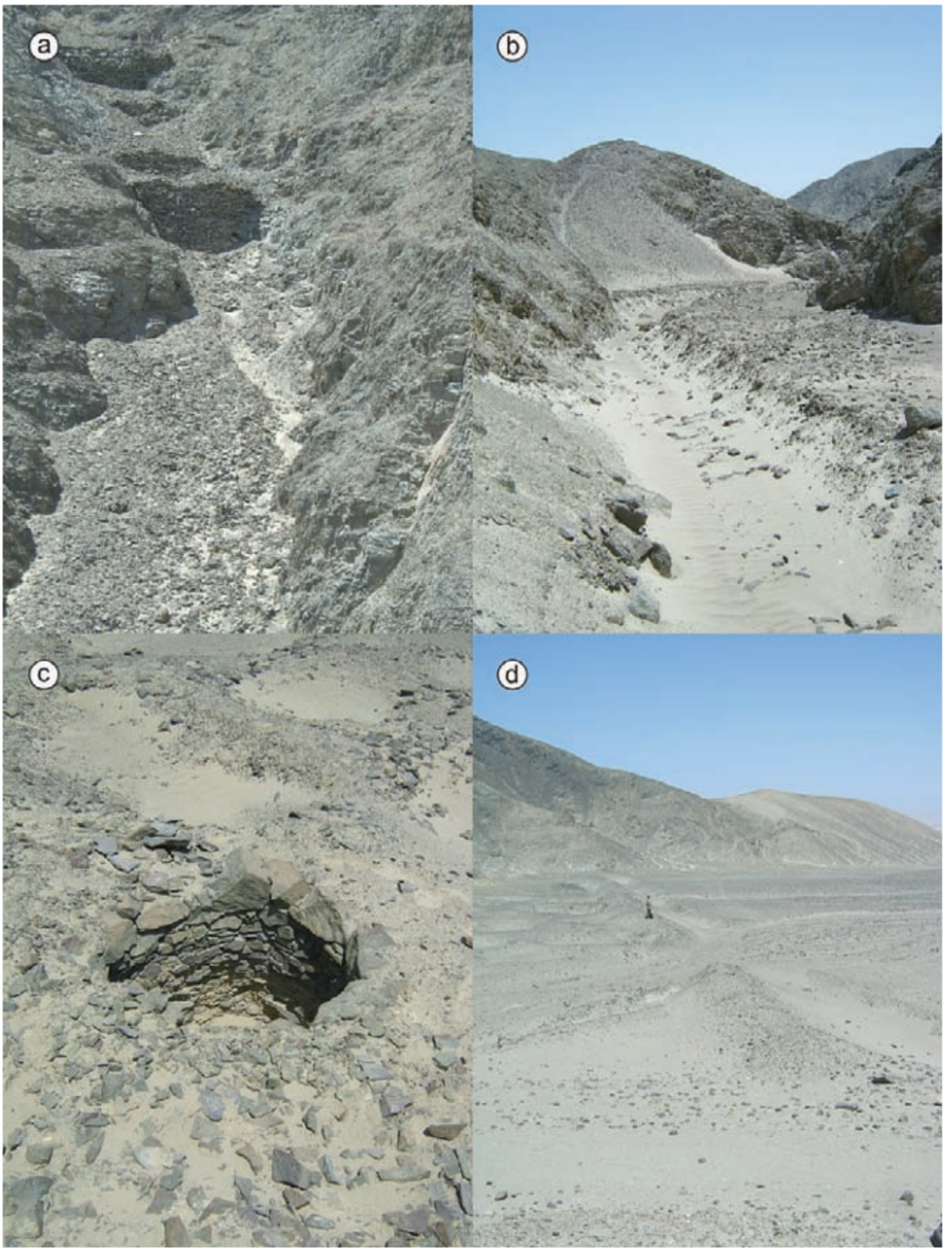

Fig. 3.3 Features of water harvesting installations in Ciudad Perdida de Huayurí: (**a**) debris retaining wall, bare rocks; (**b**) feeder for collected surface runoff; (**c**) cistern or well; (**d**) Khadin bund

- A feeder to drain surface runoff during short rainfall events to the Khadin pond
- Sandy storage sediments to hold the concentrated runoff
- A bund to stop surface runoff

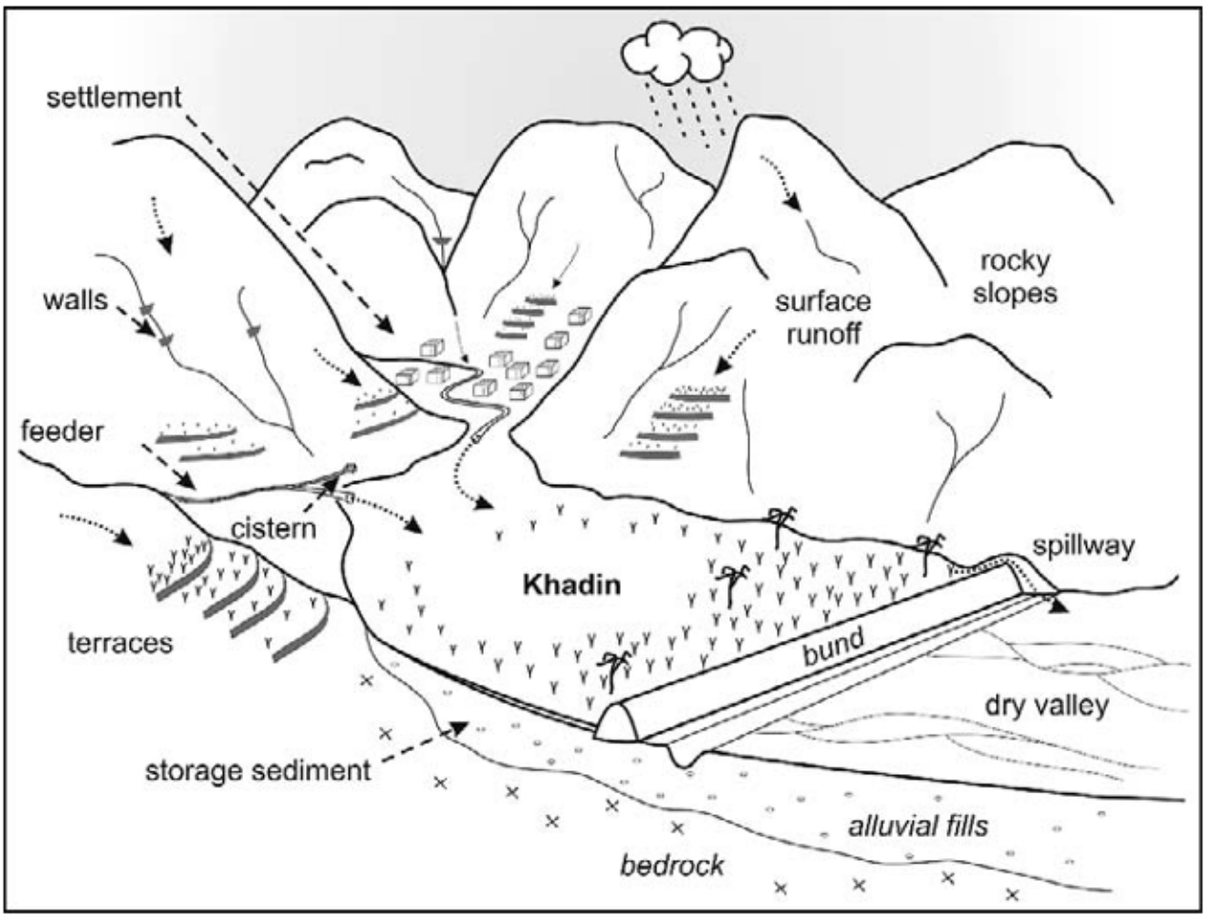

Fig. 3.4 Schematic drawing of the Khadin system, found in Ciudad Perdida de Huayurí. During singular rainfall events the surface runoff is collected by feeders and channelled to the Khadin bund. The runoff will be stopped and the water infiltrate into the sandy sediment. It may be gathered by cisterns or wells. The Khadin area is used for cropping. On the slopes, terraces are built for cropping as well. Steeper ditches are protected by debris retaining walls

- A spillway to prevent destruction of the check dam during extreme rainfall events
- A well or cistern to capture drinking water

All these features of India's Khadins we found around the Ciudad Perdida de Huayurí (see Fig. 3.4). Other feeders were built to protect the settlement against flooding.

3.3.1 Technical Parameters of the Khadin Plant

In general, the water requirement of agricultural crops exceeds 250 mm by far. Thus, in arid environments, rainfed cropping is impractical. The Khadin system concentrates and stores surface runoff on a small plot, producing plant-available

water much higher than the minimum requirement. This makes at least one crop a year possible.

Typically, the ratio between the catchment and the Khadin pond ranges from 25:1 down to a minimum of 15:1, depending on mean annual precipitation and the retention capacity of the catchment area (Kolarkar 1997). Therefore, under environmental conditions of 75–150 mm total precipitation cropping will be possible. Around Ciudad Perdida de Huayurí, the catchment:Khadin pond ratio is about 15:1 (Khadin 'a') and 22:1 (Khadin 'b'), respectively, calculated from aerial photographs. According to observations from the Thar desert (Kolarkar 1997), this ratio is equivalent to ~100–150 mm mean annual precipitation, around ten times more than today.

The water harvesting was completed by rainfed farming terraces on the lower slopes, feasible by additional water from above, which is described from arid northwest Africa by Kutsch (1982). Runoff from the bare rocks of the higher slopes was concentrated in narrow cascading terraces. The terraces stored around twice the amount of past mean annual rainfall. For cropping, less than 200 mm of concentrated precipitation is not adequate. Thus, most likely the terraces were used for pasture (Ross 2007).

The Khadins tell us more than the mean annual precipitation during the past. They also show the high annual variability of rainfall in drylands: one check-dam ('c' in Fig. 3.1) obviously remained unfinished. Abundant rainfall during a series of wet years may have conveyed that the area was also useful for water harvesting. The people started to build a new bund, but stopped after a short time. Most likely the rainfall suddenly ceased. Our modern knowledge of Khadins explains the stop of construction works: due to the catchment:Khadin pond ratio of merely 6:1 for Khadin 'c' agriculture would never have been possible.

3.3.2 Age of the Khadin

Several organic remains in the Khadin bund of Khadin 'b' such as dung from camelids, wood, and cotton were dated. During construction or repair of the bund, they were incorporated by people. The results of age determination are shown in Table 3.1.

These ages show the minimum age of the Khadin bund, which corresponds to the archaeological findings from the Late Intermediate period in the periphery.

Table 3.1 ^{14}C-Ages of Organic Remains in the Khadin Bund[a]

Sample No.	Type	Lab. No.	^{14}C-Age BP	Cal Yrs AD (1 σ)
Pe 583/2	Cotton	Hd-25997	666±34	1297–1391
Pe 583/2	Dung	Hd-25998	764±35	1262–1292
Pe 583/2	Wood	Hd-26002	759±34	1264–1292

[a]Calibrated with INTCAL04 and CALIB5 (Reimer et al. 2004).

3.4 Conclusion

Further investigations will show how long the Khadins have been used. In order to reconstruct the climatic changes during the last millennium, we have to know when the Ciudad Perdida de Huayurí was founded and when the construction of Khadins began. That will allow us to estimate the rate of aridification during that time. For sure, the foundation of this settlement was induced by the onset of reliable rainfall in the Andean foreland, which implies the retreat of desert. The kickoff to developing water resources by water harvesting was induced by the climate deterioration during the transition to the Little Ice Age. The desert readvanced. Soon after, around the fifteenth century AD, the people in India's Thar desert were forced to devise their Khadin system, independently of the people in Peru. At that time, the critical threshold of resilience was exceeded in the Andean foreland and the people had to leave. Thus, in several aspects the boom of Ciudad Perdida de Huayurí was "built on sand".

Part II
Geophysics

Chapter 4
Beneath the Desert Soil – Archaeological Prospecting with a Caesium Magnetometer

Jörg W.E. Fassbinder and Tomasz H. Gorka

Abstract Large area prospection with highly sensitive caesium magnetometers up to now has been one of the most successful geophysical prospecting methods in archaeology. The application of this method on pre-Hispanic cultures provides a perfect framework and has a high potential capacity for further development of magnetometry and archaeological prospection methods in general. Both shallow inclination as well as the low intensity of the geomagnetic field near the equator requires an adaption and modification of the caesium magnetometer. In the case of the geoglyphs of the Peruvian Atacama desert – a UNESCO World Heritage site since 1994 – the prospecting results are exemplified in detail. Magnetometry enables us to visualise not only the traces of numerous lightning strikes in the desert but also the traces of thus far unknown archaeological structures and older invisible lines beneath the multiphase trapezoidal geoglyphs. Magnetometry therefore turns from pure geophysics to a perfect archaeological tool for studying ancient sites without destruction.

4.1 Introduction

The geoglyphs of Nasca and Palpa commonly known as the Nasca lines in southern Peru are among the world's greatest archaeological enigmas. Thousands of geometric and biomorphic figures cover the desert pampas between Nasca and Palpa. The interpretation of these structures, which is still a matter of considerable debate, depends on the accurate mapping of visible but moreover also invisible structures beneath the soil. Mapping of the topographically visible structures has been done by remote sensing techniques and satellite image processing (Reindel et al. 2003; Lambers 2006). For the documentation

J.W.E. Fassbinder (✉)
Bavarian State Department for Monuments and Sites, Archaeological Prospection, Bayerisches Landesamt für Denkmalpflege, Ref. Archäologische Prospektion, Hofgraben 4, 80539 Munich, Germany
e-mail: joerg.fassbinder@BLFD.Bayern.de

M. Reindel, G.A. Wagner (eds.), *New Technologies for Archaeology*, Natural Science in Archaeology, DOI 10.1007/978-3-540-87438-6_4,
© Springer-Verlag Berlin Heidelberg 2009

of possible patterns beneath the ground, however, geophysical prospecting methods were required.

Here we report on the results of the recent interdisciplinary investigation of five main geoglyph complexes and on a couple of supplementary archaeological sites in the vicinity of Palpa with a high-resolution caesium magnetometer, conducted for the first time on those remarkable Peruvian sites. The development of new magnetometer configurations combined with mineral magnetic measurements and characterisation of the soils and sediments not only revealed previously obliterated lines as well as other hitherto unknown features beneath the surface, but also gave a better archaeological understanding of the prospecting results. All these discoveries have been achieved by nondestructive geophysical methods and may therefore serve as an important archaeological tool for further research on this extraordinary UNESCO World Heritage site.

4.2 Archaeological Background

Over an area of several 100 km^2 on the 'Pampa de Nasca', the pediment plain on the western slope of the Andes, ancient cultures have carved an array of geometrical figures of varying size and precision into the ground by the removal of the dark desert pavement and exposure of the bright loess sediment below (Eitel et al. 2005a,b; Aveni 2000a,b). The Atacama desert between northern Chile and southern Peru is one of the Earth's driest areas. Hardly any precipitation reaches the desert floor, thus erosion by water runoff has been rare for centuries. For that reason, the 'Nasca lines' have survived almost unaltered up to the present. It was not until 1926 that the western world took notice of the geoglyphs (Kroeber and Collier 1926; Mejía Xesspe 1942). Because the Pampa de Nasca was included in the UNESCO World Heritage List, it attracted most of the public's attention. The other areas of high geoglyph concentration, such as the Palpa region, have been widely neglected. Hence, Cresta de Sacramento, Cerro Carapo, Pampa de Llipata, and Pampa de San Ignacio, all in the Palpa region, were chosen as the new areas for integrated archaeological and geophysical investigations (Fig. 1.1 of the introduction to this volume).

There are numerous hypotheses and speculations about the meaning of the 'Nasca lines', the most popular of which have been astronomical calendars (Reiche 1969) and pathways for religious ceremonies (Reinhard 1996). The lack of good documentation, however, has thus far made it difficult to test recent hypotheses against archaeological data (Lambers 2006). The question of the cultural meaning of the geoglyphs is almost inextricably linked with the question about their age. Many of the geoglyphs superimpose each other, as they were in use for several centuries and grew considerably over time (Lambers 2006). Therefore, the stratigraphic sequence of their construction can be recognised. New geoglyphs were frequently added and existing ones enlarged or remodelled. In this process, large trapezoids often covered older lines. During

their construction the stones of the desert pavement between the existing lines were removed, rendering the older lines and other structures invisible on the surface (Gorka et al. 2007; Lambers 2006).

4.3 Magnetic Properties of Archaeological Soils – An Overview

The occurrence of small-sized and small-scale magnetic anomalies such as these, measured approximately 30 cm above the surface, can be ascribed both to magnetic enhancement processes and to remanence forming processes beneath the topsoil (Le Borgne 1955; Fassbinder 1994). The former may occur due to the enrichment of magnetic minerals in the archaeological features; the latter may appear as a result of remanence enhancement or destruction processes. Both processes cannot easily be discriminated by the simple measurement of the total Earth's magnetic field above the ground. The shape and the intensity of a single magnetic anomaly are determined not only by the structure itself but also by the resulting vector of the induced and the remanent magnetisation. For archaeological interpretation of the magnetic field data it is therefore necessary to understand the formation pathways of magnetite, maghemite, and greigite, along with the occurrence of other rock-bearing magnetic minerals, for example, titanomaghemite, as well as the type and origin of the different remanent magnetisations.

Mineral magnetic characterisation of soils and sediments can be done in the laboratory by rock magnetic analysis methods such as the measurement of the natural remanent magnetisation (NRM), the magnetic susceptibility χ, the frequent dependent magnetic susceptibility χ_{FD}, the anhysteretic remanent magnetisation (ARM), the saturation isothermal remanent magnetisation (SIRM), and by the measurement of the hysteresis parameters. These data not only categorise the type of mineral but also determine the particle size. Direct identification of magnetic minerals can be done by Curie-temperature analysis (e.g., the detection of magnetite by the Verwey transition; Verwey and Haayman 1941) or by crystallographic methods, particularly by the determination of the lattice constant by a Guinier-diffractometer. For a more comprehensive description of the rock magnetic properties see also Soffel (1991), Dunlop and Özdemir (1997), and Evans and Heller (2004).

For induced magnetisation it is necessary to understand the formation processes of the ferrimagnetic minerals in soils and sediments:

(1) Maghemite (γ-Fe_2O_3)

   (a) By the oxidation of magnetite derived from weathered rocks. Those maghemites have grain sizes in the range of mm and are therefore mostly multidomain. This process was also detected on magnetic soils derived from titanomagnetites (Fitzpatrick and Le Roux 1976).

(b) Depending on the grain size, lepidocrokite (γ-FeOOH) dehydrates at temperatures of 260–300°C to maghemite (Scheffer et al. 1959; Schwertmann and Taylor 1979).
(c) In the presence of organic material goethite transforms to maghemite (Schwertmann and Fechter 1984; Anand and Gilkes 1987; Stanjek 1987).
(d) By the oxidation of siderit ($FeCO_3$) under moderate temperature (Van der Marel 1951; Schwertmann and Heinemann 1959).

(2) Magnetite (Fe_3O_4)

The occurrence of pure magnetite in soil was not recognised for a long time, because the fine-grained magnetite crystals oxidise easily to maghemite. The first proof of the occurrence of magnetite in soils was given by Maher and Taylor (1988) and Fassbinder et al. (1990). However, the pedogenic formation of magnetite in soils is still under debate and discussed controversially. Thus far there exist three pathways to the neoformation of magnetite in soils:

(a) Synthesis experiments yielded magnetite by the controlled oxidation of Fe^{2+} to magnetite (David and Welch 1956). This inorganic pathway could also be responsible for the magnetite formation in soils (Maher and Taylor 1988).
(b) The intracellular formation of magnetite by magnetotactic soil bacteria was demonstrated by Fassbinder et al. (1990) and Fassbinder and Stanjek (1993).
(c) Evidence for dissimilatory iron-reducing bacteria (GS-15) was found by Lovley et al. (1987) in sediments; this could also be a potential source of magnetite in soils.

(3) Greigite (Fe_3S_4)

The occurrence of greigite was reported from freshwater sediments and marine sediments (e.g., Dell 1972) as well as from soils (Stanjek et al. 1994). There exist two pathways which may be responsible for the formation of greigite in soils and sediments.

(a) Synthesis experiments from Uda (1965) showed the possible geochemical pathways yielding greigite.
(b) Mann et al. (1990) reported the occurrence of magnetotactic greigite bacteria in freshwater sediments. Stanjek et al. (1994) reported the first occurrence of biogenically formed greigite in a soil of southern Bavaria.

For the remanent part of the magnetic anomalies it is necessary to understand the formation of remanent magnetisations:

(1) Natural remanent magnetisation NRM

Every rock, sediment, and soil containing ferri- or antiferromagnetic minerals, exhibits in addition to the induced magnetisation in the Earth's

field, a natural remanent magnetisation (NRM). This magnetisation could be of different origin.

(2) Thermoremanent magnetisation TRM

The heating of any material such as rocks, clays, bricks, soils, or sediments to high temperatures (>600°C) and cooling them in the Earth's magnetic field produces a thermoremanent magnetisation. This thermoremanence is always parallel to the field in which it was acquired. Its intensity is proportional to the strength of the ancient Earth's magnetic field. Heating and the use of manmade fires of archaeological sites are therefore easily recognisable by the uniform magnetic anomalies parallel to the Earth's magnetic field. Additionally the use of fireplaces and kilns forms new ferrimagnetic minerals such as maghemites.

(3) Detrital remanent magnetisation DRM

The sources of detrital particles that form new sedimentary rocks are the erosion products of igneous, metamorphic, or other sedimentary rocks. The detrital remanent magnetisation is acquired when the sediments are deposited and consolidated. The DRM is inherently weak, because it represents only a partial realignment of the original NRM vectors. Nevertheless the partial mechanical destruction of this remanence by the contruction of the geoglyphs may result in a detectable magnetic anomaly.

(4) Lightning-induced remanent magnetisation LRM

Lightning strikes cause a strong LRM in nature. Within a few m up to 40 m radius from a strike, the surface soils, sediments, and rocks experience a DC field of short duration and varying intensity that remagnetises part of the NRM in the area. The lightning overprint is easily recognisable in the magnetogram by its extreme intensity compared to other structures, but moreover by its typical star-shaped positive and negative magnetic anomalies pointing in all directions and interlacing each other (Fig. 4.8). Never before have lightning strikes been magnetically detected in a higher density than on plateaus of Nasca and Palpa.

4.4 Caesium Magnetometry

In terms of soil and rock magnetic conditions it was an exceptional challenge to detect structures beneath the desert soil, particularly beneath the geoglyphs (Fassbinder and Hecht 2004; Fassbinder and Reindel 2005). Because of the extremely dry underground and due to unsorted large gravel below the surface, resistivity surveying as well as radar prospecting seemed to be inappropriate for archaeological purposes. Therefore magnetometry was chosen as one of the nondestructive techniques of site exploration that was supposed to be the most efficient tool for detecting and mapping possible features beneath the lines and trapezoids (Gorka et al. 2007).

4.4.1 Total Field Measurements

In general, magnetic survey methods rely on the ability of magnetometers to measure small deviations of the Earth's magnetic field associated with buried archaeological remains (Aitken, 1974; Scollar et al. 1990). In effect, archaeological

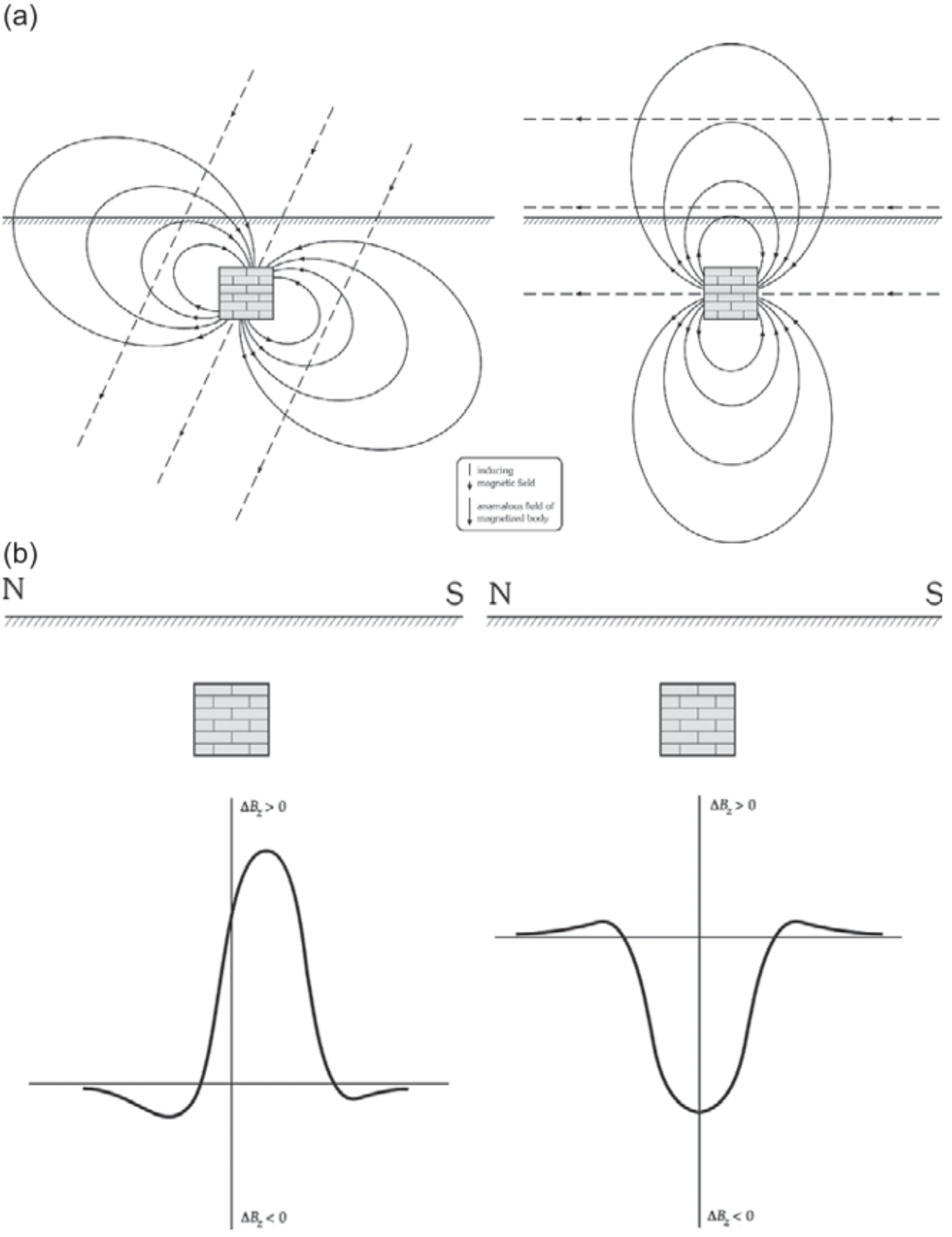

Fig. 4.1 (**a**) Sketch of the dipole archaeological body in the Earth's magnetic field. (**b**) Calculated response of the total field, for example, caesium magnetometer in Europe and in Peru

structures such as ditches, pits, or kilns act as magnetic dipoles which produce distortions and resulting anomalies in the Earth's magnetic field (Fig. 4.1a,b).

The magnetic prospecting technique is a passive survey method; therefore it is essential to discriminate between diurnal variations of the Earth's magnetic field and the disturbances caused by the lack of the homogeneity in the soil and by buried archaeological features, respectively. By mapping slight variations of the Earth's magnetic field and the transformation and visualisation of these anomalies to a grayscale plot of the data, detailed plans of sites can be obtained with the advantage that the site remains untouched.

The principle of the magnetic prospecting technique that was applied to the geoglyphs is based on the measurement of the total intensity of the Earth's magnetic field. The instrument employed is a high-resolution total field caesium magnetometer (Scintrex Smartmag SM4-G Special) with a sensitivity of ±0.01 nT (Nanotesla; for comparison: the intensity of the total Earth's magnetic field in the Pampa of Peru oscillated around 24,000 nT, the diurnal variations depending on the sun activity were in the range of 10–30 nT). For geophysical purposes, in order to reach the highest possible sensitivity combined with a maximum speed of prospection, the so-called 'duo-sensor' configuration (Becker 1999) was chosen. The probes were mounted on a wooden frame and were carried in a zigzag-mode 30 cm above the ground (Fig. 4.2). Bearing in mind that the geoglyphs of Nasca and Palpa are a UNESCO World Heritage Site and therefore should remain undamaged, a handheld system for all

Fig. 4.2 The caesium Smartmag system, SM4G-Special, in the field, mounted on a wooden frame to provide constant distance from the ground, the most suitable arrangement for prospecting on the geoglyph ground cover with gravel and stones

measured complexes was preferred. Moreover, as gravel and pebbles up to several cm in diameter cover the surface of the geoglyphs, this arrangement of the measuring device was the only possible configuration to provide a constant distance between the magnetometer and the topsoil. The sampling frequency of the magnetometer (10 readings per second) provided the measurement of a 40 m profile of the grid (40 × 40 m) in less than 30 s, maintaining the spatial resolution of approximately 10–15 cm at a normal to fast walking speed. Every 5 m, in addition to the magnetic data, a manual switch set a signal, required for the correct interpolation of data during the subsequent laboratory processing work.

The linear changes in the daily variation of the geomagnetic field were reduced to the mean value of the 40 m sampling profile and alternatively to the mean value of all data of a 40 m grid. Here it is assumed that the variation of the Earth's magnetic field during one profile length of 40 m follows a linear increase or a linear decrease of the intensity. If so, it is possible to eliminate this variation for each traverse line by a reduction in the mean line value. Alternatively in magnetically quiet periods it is also useful to calculate the mean value of the whole 40 × 40 m square. This avoids the disappearance of the linear structures parallel to the profile. To create discrete field values a resampling program setting the data to 25 × 25 cm was used.

Additionally by this procedure the difference between the measurement of both magnetometer probes and the theoretically calculated mean value of the Earth's magnetic field was obtained. This intensity difference gave the apparent magnetic anomaly, which was then influenced by the magnetic properties of the archaeological structure, the soil magnetism, and the geology. To cancel the natural micropulsations of the Earth's magnetic field a bandpass filter in the hardware of the magnetometer processor was used.

At least 97% of the magnetometer data in a 40 m grid on common archaeological sites varies in the range of ±10.0 nT from the corrected mean value of the geomagnetic field. The stronger anomalies can be ascribed to burned structures or to pieces of iron containing slag or iron rubbish. In situ burning, iron pieces, and the traces of lightning strikes are easily distinguishable by their different direction of magnetic dipole anomalies but also by their high intensities (>±50.0 nT).

4.4.2 The Horizontal Gradiometer

Due to the flat inclination of the Earth's magnetic field and the intensity of only 24.000 nT, which is only half of what can be measured in Europe, simple anomalies created more complicated patterns and were more difficult to interpret (Tite 1966; Clark 1996; Fassbinder and Gorka 2007). To overcome this problem and to enhance the visibility of magnetic data, two sensors were arrayed for the first time in a horizontal gradiometer configuration (Fig. 4.3).

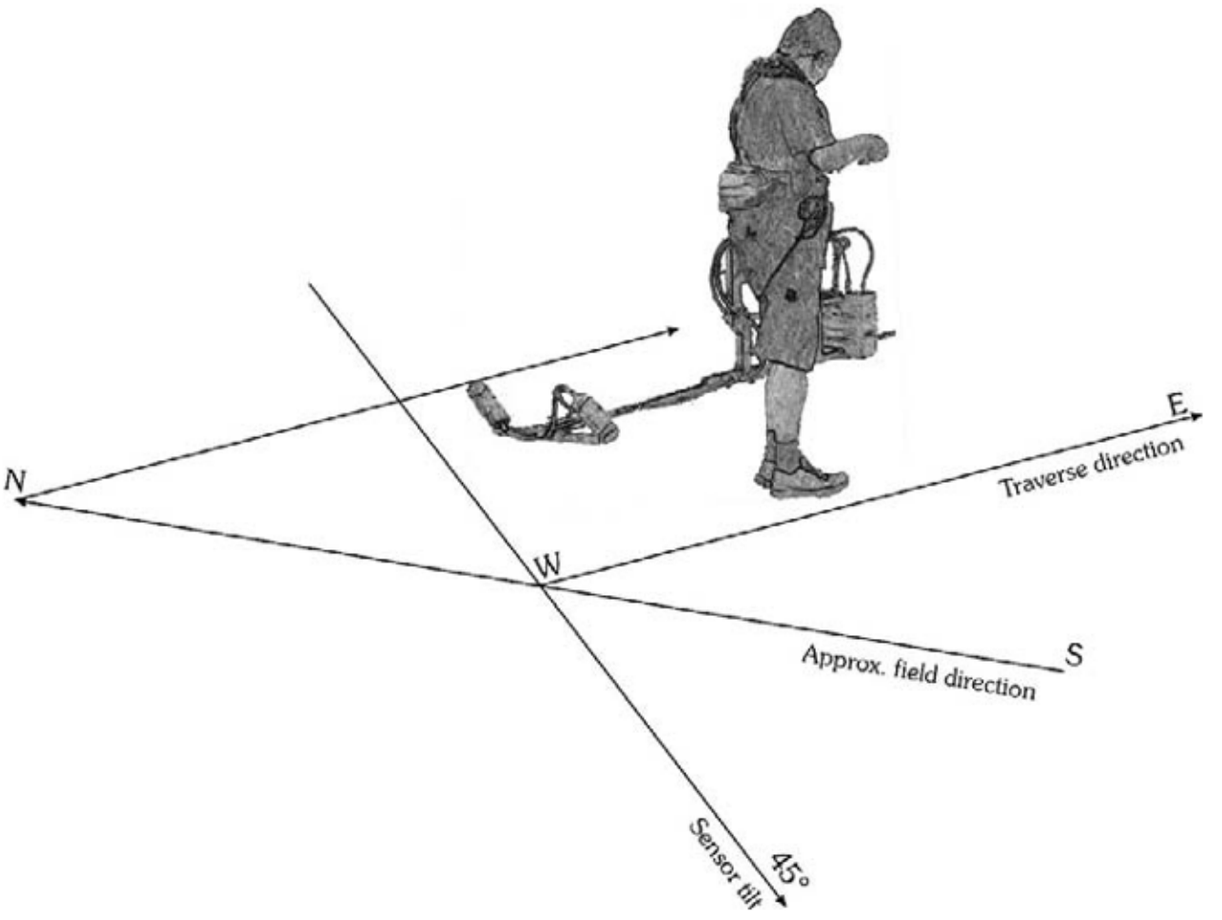

Fig. 4.3 Sketch of a total field caesium magnetometer in the horizontal gradiometer configuration

In order to optimise the results it was necessary to set up a layout of the grid and to keep the probes in the north–south direction, walking at the same time along the west–east arranged traverses.

For the horizontal gradiometer, the probes were positioned in the same manner as used before for the total field measurements. This enabled the recalculation of all former measurements as a gradiometer mode. The application of the magnetometer in such an arrangement, in combination with the results of the total magnetic field data, enabled the crucial data enhancement to visualise thus far unseen archaeological features. This allowed tracing older lines that had been obliterated during the construction of the larger trapezoids on the same site.

4.4.3 Image Processing

For data processing the discrete magnetometer readings were imported to Geoplot (Geoscan Research), ArcheoSurveyor (DWConsulting), and Surfer (Golden Software) and converted into greyscale values ranging from 0 = white

to 99 = black. The 'DeSlope' and 'Edge Match' filtering of each 40 m grid allowed the correction of the linear variations of the Earth's magnetic field.

The horizontal gradient was processed by ArcheoSurveyor (DW Consulting) by the calculation of the difference between the two probes, which gave a similar result to the dB/dBz value of the SQUID magnetometer configuration (Linzen et al. this volume). For image processing, similarly to the total field data, the magnetometer readings were converted into greyscale values ranging from 0 = white to 99 = black.

4.5 Magnetometry on the Geoglyphs of Palpa

In the framework of the Nasca–Palpa project, since 1997 the geoglyphs in the vicinity of Palpa (Fig. 4.4) have been documented and analysed, combining archaeological, archaeometric, and photogrammetric techniques (Reindel et al. 2003; Lambers 2006). Unlike the biomorphic figures, geometric geoglyphs can be found in the whole Pampa. The trapezoidal form, however, is the most abundant and occurs even more frequently than a zigzag line. Sixty-two percent of the biggest geoglyphs are trapezoids, thus, they have greater dimensions and cover more space of the desert territory than any other drawing. Aveni (2000a,b), for example, counted 227 geometric geoglyphs that are bigger than 15 m^2. The long axis of the typical trapezoid is about 10 times longer than the short one with an average ratio of about 400 × 40 m.

The natural topography and shape of the area enforces the arrangement and layout of the geoglyphs. For example, at San Ignacio it is clearly visible that the zigzag lines always reach the edge of the flat area, covering the farthest available parts of the site. Also the axis of the trapezoid follows the natural layout of the site. That means that the construction of the figures was not planned and dictated by cosmic ideas on a 'sheet of paper' but simply followed the geographical setting. The direction was given by the topography and not by the direction of stars, water pipes, or other (Aveni 2000a,b).

4.5.1 The Trapezoid Near Llipata

Apart from some first test measurements in 2003, the large trapezoid from Llipata (Table 4.1A) was the first geoglyph site measured in total in March 2004. The direction of its main axis is northeast–southwest. The measured area on the plateau approximates 640 × 200 m (see Fig. 4.4a,b). The site has been quite destroyed and 'overprinted' by an old football field that was earlier used by the children from neighbouring villages. Analysing the magnetic image of the total field measurement (dynamics ±13.0 nT), a large number of archaeological anomalies that might be ascribed to traces of pits, small fireplaces, and post-holes could be recognised. The most remarkable features and outstanding

(a)

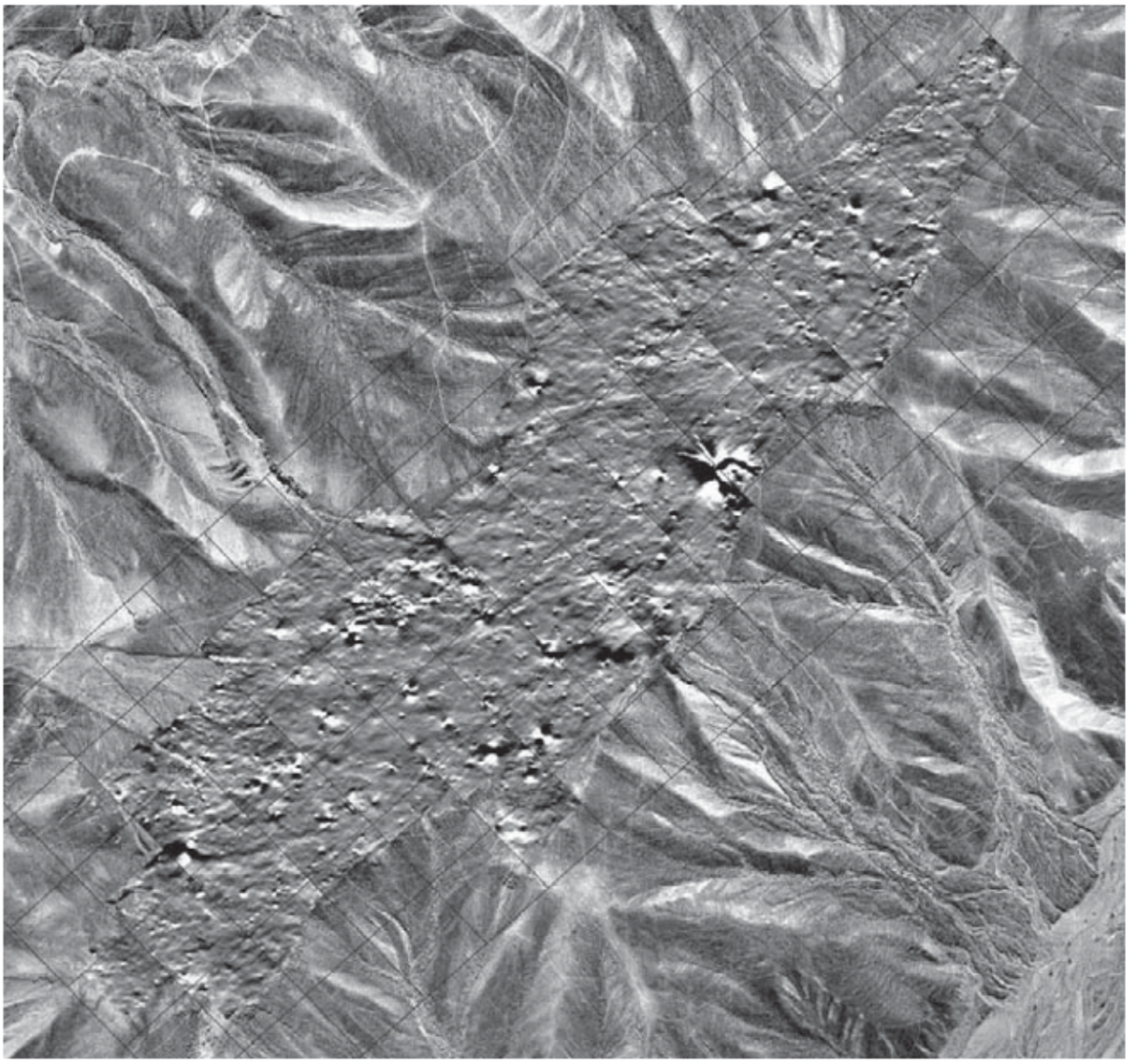

(b)

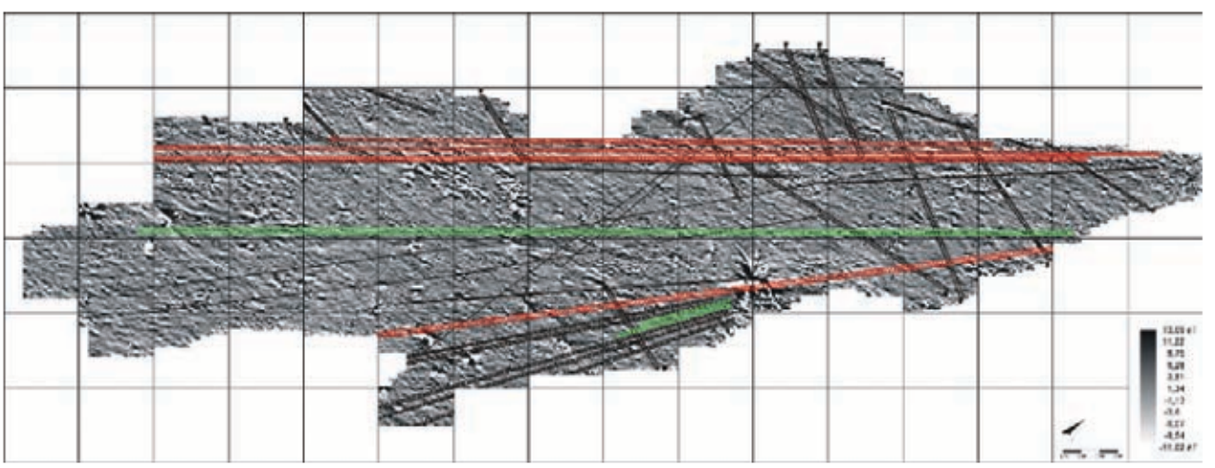

Fig. 4.4 (**a**) Magnetogram of geoglyphs on the site Llipata (PP01-36) overlaid on the orthophoto (K. Lambers) of the area. *Grey* shade plot caesium total field magnetometer data, dynamics ±13.0 nT, in 99 greyscale values, 40 m grid). (Orthoimage courtesy of Institute of Geodesy and Photogrammetry, ETH Zürich.) (**b**) Gradiometer data and the interpretation of geophysical results (T. Gorka) representing the lines detected by magnetic prospecting (*green*)

Table 4.1 Geoglyph Sites Surveyed by Caesium Magnetometer Between 2003 and 2007

	Site Name	Project Name	Official Name
A	Llipata	PAP379	PP01-36
B	Yunama	PAP64	PV67A-15/16
C	Sacramento	PAP51A	PV67A-47
D	Carapo	PAP283A	PV67B-55
E	San Ignacio	PAP365	PP01-49

results are the exceptionally strong star-shaped anomalies (up to ±700 nT), which originate from lightning strikes.

Data processing with the new horizontal gradiometer data reveals further features, namely the traces of older lines that are no longer visible on the surface, because they have been superimposed and obliterated by the construction of the later trapezoid.

4.5.2 The Trapezoid Near Yunama

The geoglyph complex from Yunama (B, PV67A-15/16, Fig. 4.5a,b and Table 4.1), to the northwest of Palpa, has nearly the same orientation as the plateau Cresta de Sacramento on which it is located. It consists of a shorter rectangular area and a longer trapezoid linked at their northeast ends, and is moreover underlain by several older lines.

The size of the area, 440 × 200 m, is slightly smaller than the Llipata trapezoid. The magnetic image of the total field measurement (Fig. 4.5b) revealed for the first time some regular anomalies indicating the presence of constructions and buildings on the site (Fassbinder et al. 2007). In particular, the area of the rectangular geoglyph is free of granite rocks with their high magnetic susceptibilities and due to the topographical conditions also free of lightning strikes. For that reason the magnetic image much better exposes geoglyph construction elements of interest. Even in the total field magnetic image, older lines (e.g., line 58) are detectable and easily visible.

The central element of the Yunama site (A, PV67A-15/16) is a trapezoidal geoglyph (52). Close to its northeast end it crosses an obliquely oriented, earlier meandering line (55).

This line, together with an interconnected similar one (56), originally formed the northern part of the site. In this early stage, the geoglyphs represent a typical combination of different types found at other sites as well. Later on, by removing the stones of the desert pavement between the two lines, the northern part of the site was converted into a large rectangular geoglyph (57).

Except for the stones heaped along the geoglyph borders and the stone platforms at both ends of the trapezoid, nothing can be seen on the surface, neither from the aerial photos nor from the ground perspective. Magnetometry

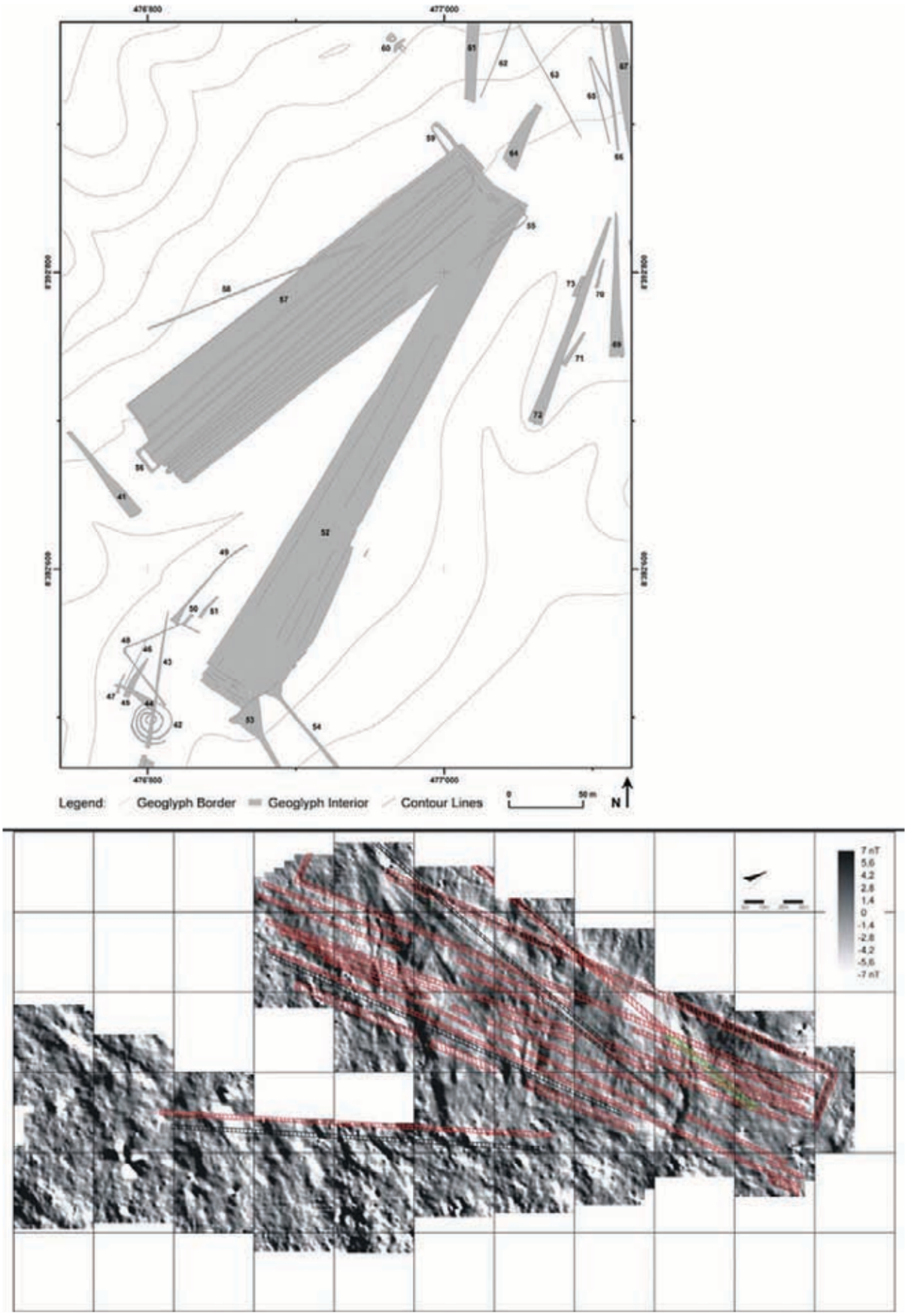

Fig. 4.5 Yunama. (**a**) Detailed map of the geoglyph site PV67A-15/16. The geoglyph assemblage drawn after an aerial photograph. A stratigraphical sequence of different phases of construction and reworking as discussed in the text can be shown here. (**b**) Result of the magnetic prospecting image of the Yunama geoglyph and the interpretation of geophysical results (T. Gorka). Dynamics ±7.0 nT in 99 grey scales, grid size 40 × 40 m; the total Earth's magnetic field ~24.000 nT

for the first time allowed an insight beneath the ground (Fig. 4.5b). The detailed analysis of the resulting magnetogram shows that trapezoid 52 has a different geological background than rectangle 57. The granite rock, abundant on the southern part of this site, has the highest magnetic susceptibility, which shows up in a typical manner as a magnetic dipole, making interpretation more difficult. The additional magnetic overprint appears as extreme starlike magnetic anomalies. This is due to the exposure to the edge of the plateau and therefore the occurrence of a couple of lightning strikes.

In addition to the afore-mentioned lines 55 and 56, many other structures and thus far unknown lines, specifically line 58 are clearly visible in the grey shade plot of the total field data (Fig. 4.5b). Some of the structures might be ascribed to the remains of buildings. Easier to interpret, however, is the occurrence of pits. They are filled with material of higher magnetic susceptibility such as burnt material or probably pottery sherds. The distribution of some of the pits is not erratic; rather they were arranged to divide the trapezoid along its longer axis into three equal sections.

From the hillside on the western part of the site, a straight line runs in the northeast direction towards rectangle 57 (green line, Fig. 4.5b). It was cut by the northern section of line 56 and is therefore older. However, the stratigraphic relation with rectangle 57 was not clear on the basis of evidence from surface observations and aerial images alone. Magnetometry helped to resolve this question by revealing a continuation of line 58 beneath the rectangular geoglyph 57. The line points directly to one of the stone platforms at the end of trapezoid 52 and ends in a pit.

4.5.3 The Trapezoid Complex Sacramento Near the Reloj Solar

The Sacramento geoglyph complex was the largest site measured within the project, reaching approximately 720 × 200 m. It covers at least three trapezoids, zigzag lines, and spirals as well as single lines. The results of the magnetometer survey show again, in addition to more than 30 lightning strikes, the traces of pits, fireplaces, and probably postholes (Figs. 4.6a,b and 4.7). Reprocessing the data as a horizontal gradiometer plot reveals, however, numerous single lines that were thus far unknown in the topographical mapping and aerial images (Fassbinder and Gorka 2007, Lambers 2006).

4.5.4 The Carapo Geoglyph Complex

The trapezoid of Cerro Carapo about 1.5 km to the east of the centre of Palpa, located on the elevated plain between the Rio Palpa and the Rio Viscas, was prospected in April 2006. The complex is formed by a large trapezoid which

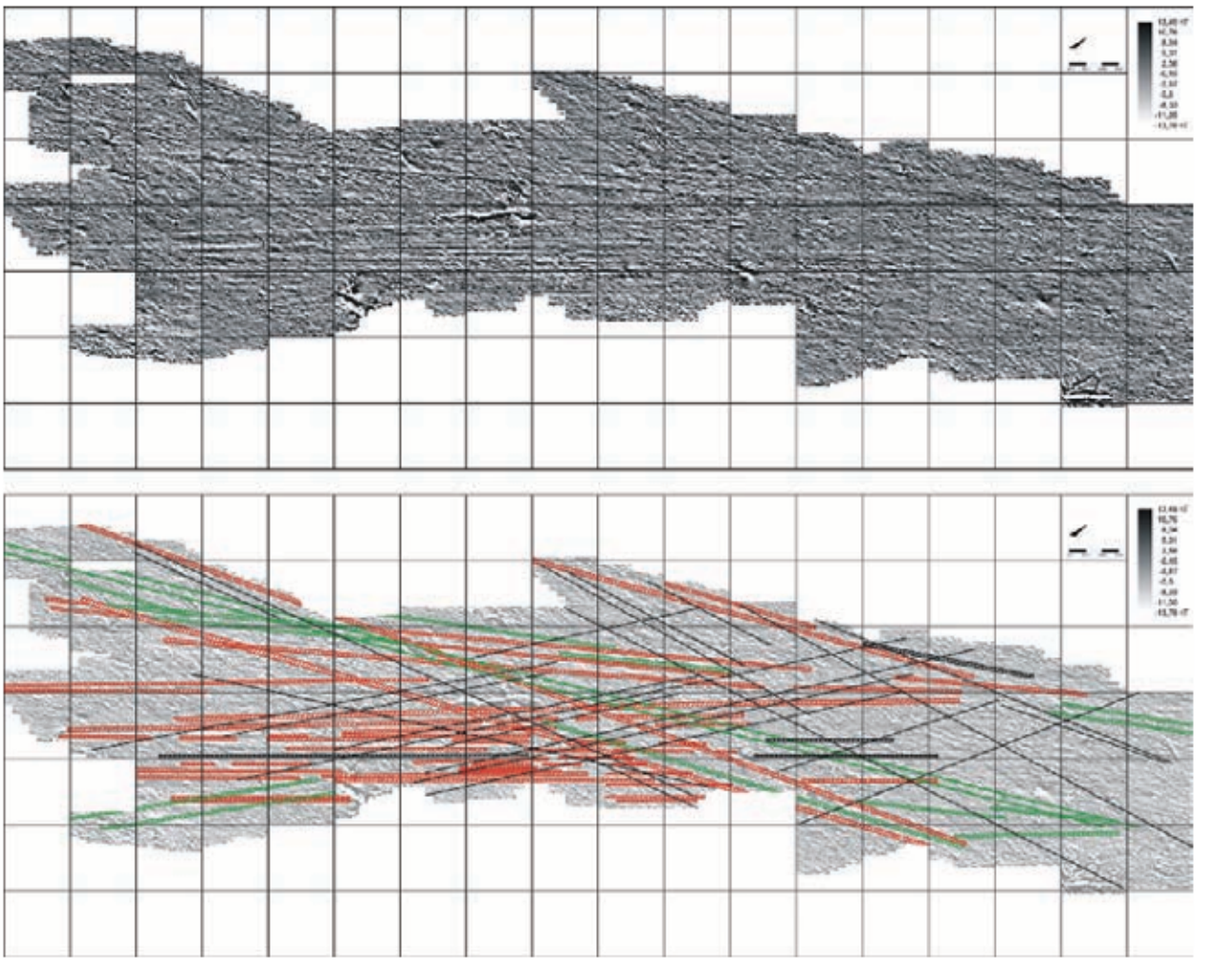

Fig. 4.6 Sacramento. Magnetogram of the geoglyph site PV67A-47. (**a**) Magnetogram of the horizontal gradiometer data, dynamics ±13.5 nT in 99 grey scales, grid size 40 × 40 m. (**b**) Gradiometer data and the interpretation of geophysical results (T. Gorka) representing the lines detected by magnetic prospecting (*green*)

superimposes several zigzag lines, older lines, but is also 'covered up' and superimposed by a settlement of the Late Intermediate period (Fig. 4.8a,b).

4.5.5 The San Ignacio Complex

The San Ignacio geoglyph complex is the largest archaeological trapezoidal site of the Palpa area. Separated by the valley of the Rio Palpa, the Rio Viscas, and the town of Palpa, it forms the counterpart to the Sacramento geoglyph complex and the Reloj Solar. Five trapezoids about 2 km long are visible from the ground. Our magnetometer prospecting area, 320 × 240 m in size, however, covered the central part of this large complex (Fig. 4.9). To take full advantage of the newly developed magnetometer system, an exact layout of the grid with the traverse lines in the east–west direction, was made for the first time. The survey area covered the plain reaching the edge of the plateau. It enclosed the measurements of the stone platforms on the very border of the terrain. A detailed description and interpretation of the results is still in progress.

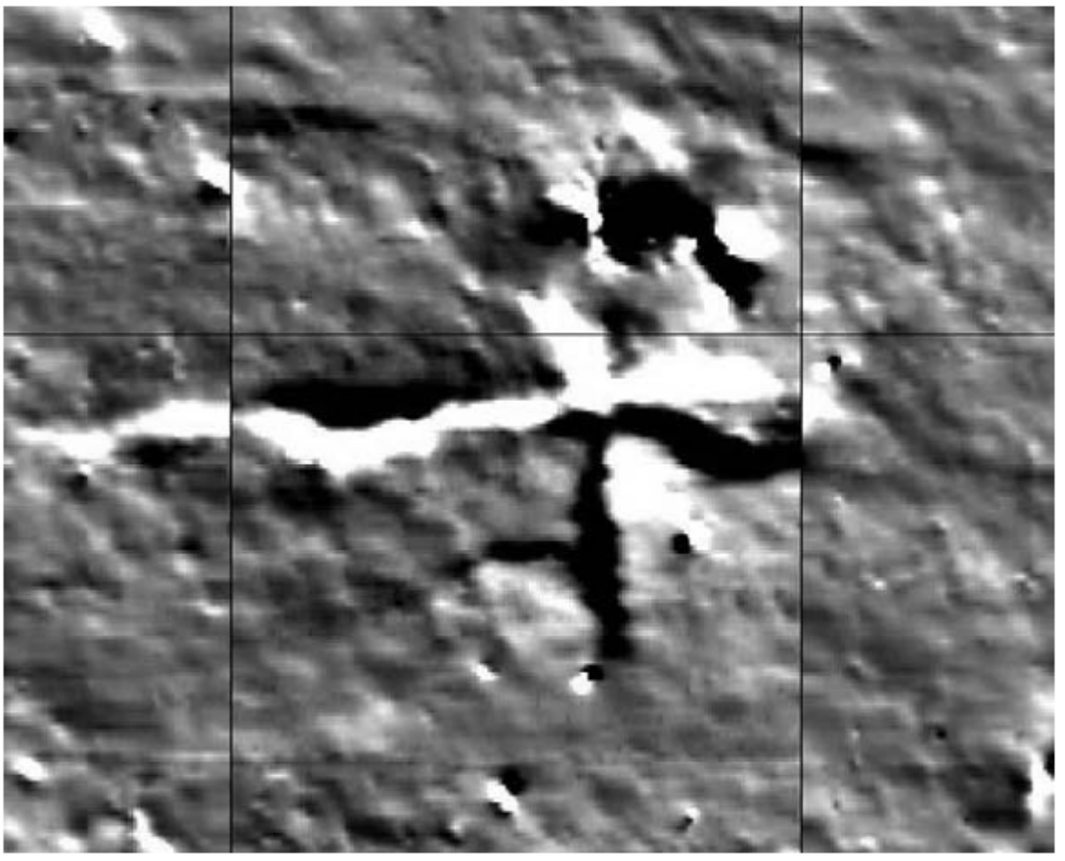

Fig. 4.7 Sacramento. Cutout of the magnetogram site PV67A-47 showing the typical star-shaped magnetic structure of a lightning-induced magnetic anomaly. Dynamics ±30.0 nT in 99 grey scales, grid size 40 × 40 m

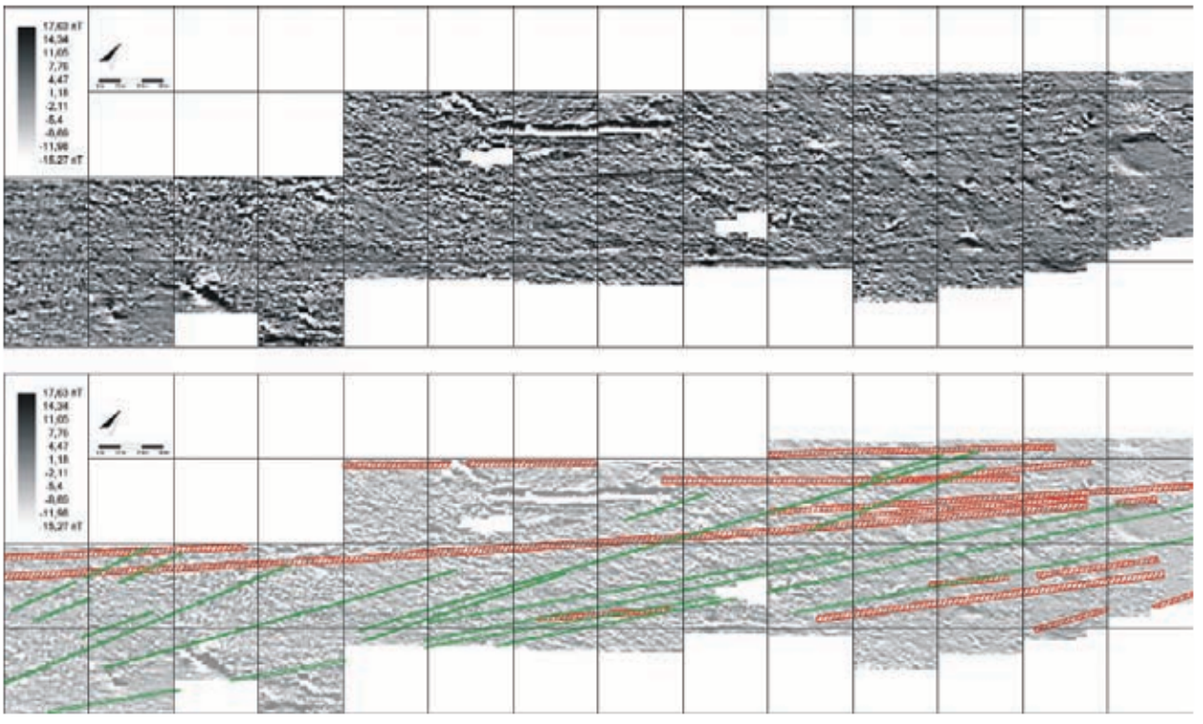

Fig. 4.8 Carapo. Magnetogram of the geoglyph site PV67B-55. (**a**) Magnetogram of the horizontal gradiometer data, dynamics ±17.5 nT in 99 *grey* scales, grid size 40 × 40 m; the total Earth's magnetic field ~24.000 nT. (**b**) Gradiometer data and the interpretation of geophysical results (T. Gorka) representing the lines detected by magnetic prospecting (*green*)

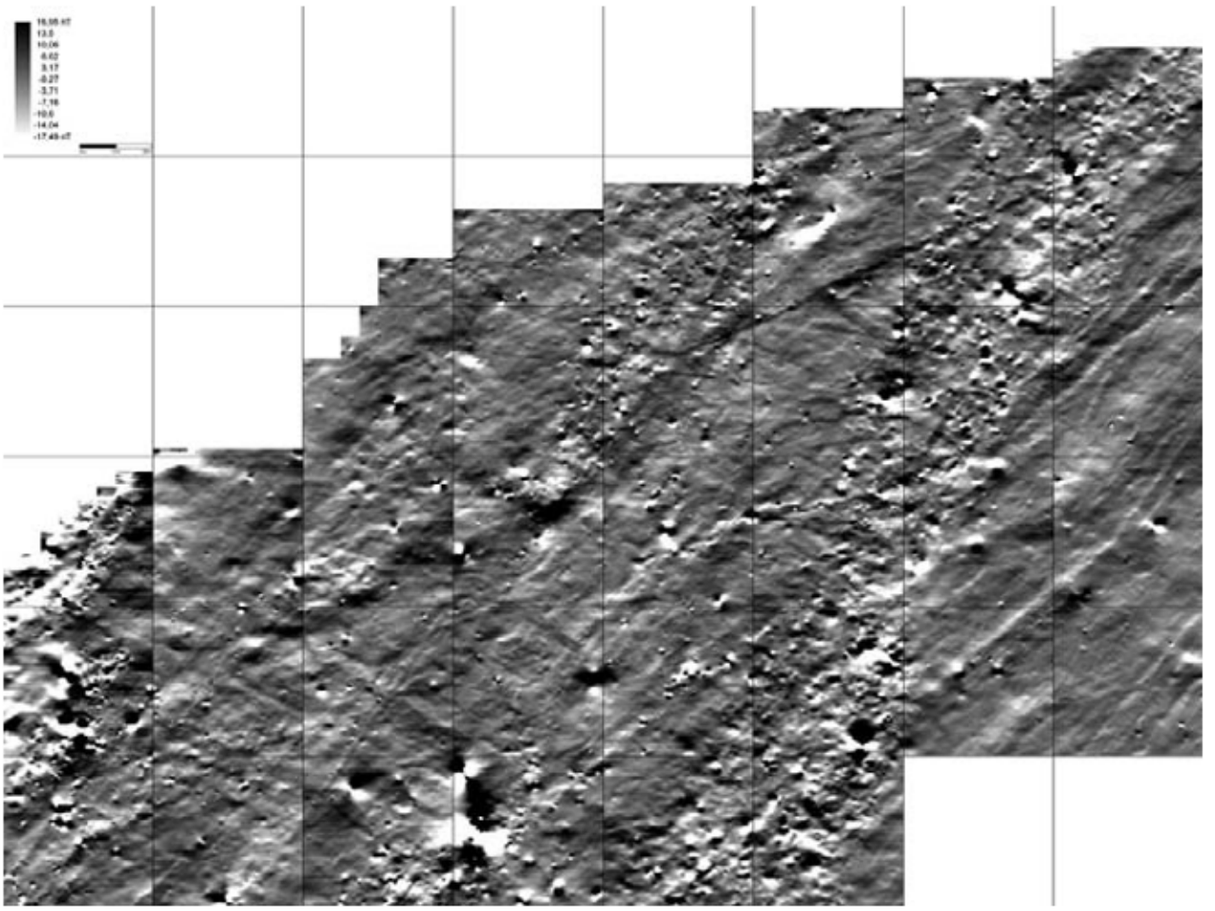

Fig. 4.9 San Ignacio. Magnetogram of the total field prospection of the geoglyph site PP01-49. Dynamics ±17.5 nT in 99 *grey* scales, grid size 40 × 40 m; the total Earth's magnetic field ~24.000 nT

4.6 Magnetometry of Newly Discovered Settlements

Comparative caesium magnetometer and resistivity measurements were performed for the first time on the area of irrigated fields close to the Fundo Jauranga.

Due to the intensive irrigation and land use by the farmers, it was nearly impossible to get any successful results by aerial prospecting. Two fields of around 160 × 120 m and 240 × 160 m were chosen. Therefore again geophysical prospecting remains the only tool for the detection and mapping of the archaeological structures (Hecht and Fassbinder 2004; Fassbinder 2007). The magnetic images revealed some structures from ancient settlement activity but were also dominated by the traces of the old river sediments. The differentiation of heavy minerals by the river flow, and the diversity in size of the gravel dominate the magnetogram (see figures in Chap. 6, this volume). Because of the long wave anomalies, it is obvious that they occur in deeper parts of the soil. This stands out in contrast to the very sharp anomalies generated by the field system, the ploughing, and the small irrigation canals.

4.6.1 Estaqueria

The SQUID magnetometer measurement of the Estaqueria site by the Jena group inspired us to develop the horizontal gradiometer (Chwala et al. 2001). Although from the archaeological point of view the resulting finding may be poor, magnetically, however, this result revealed again the potential of the geophysical methods. Figure 4.10a,b presents the comparison of the total field and the gradiometer measurements (Linzen et. al. this volume).

4.6.2 Cutamalla

The archaeological site of Cutamalla discovered by M. Reindel's team in 2006 (Fassbinder and Ebner 2007), is one of the newly discovered settlements near Laramate in the highlands of the Andes (Fig. 4.11a). Stone fundaments made mainly of granite rocks are partly visible from the ground. The settlements consist of an oval about 40 m in diameter. The single houses are rosette-oriented around the oval and form a flowerlike ground pattern.

The resulting magnetic map of the site (Fig. 4.11b) is a textbook example of only remanence-based magnetic anomalies. All the granite rocks with their

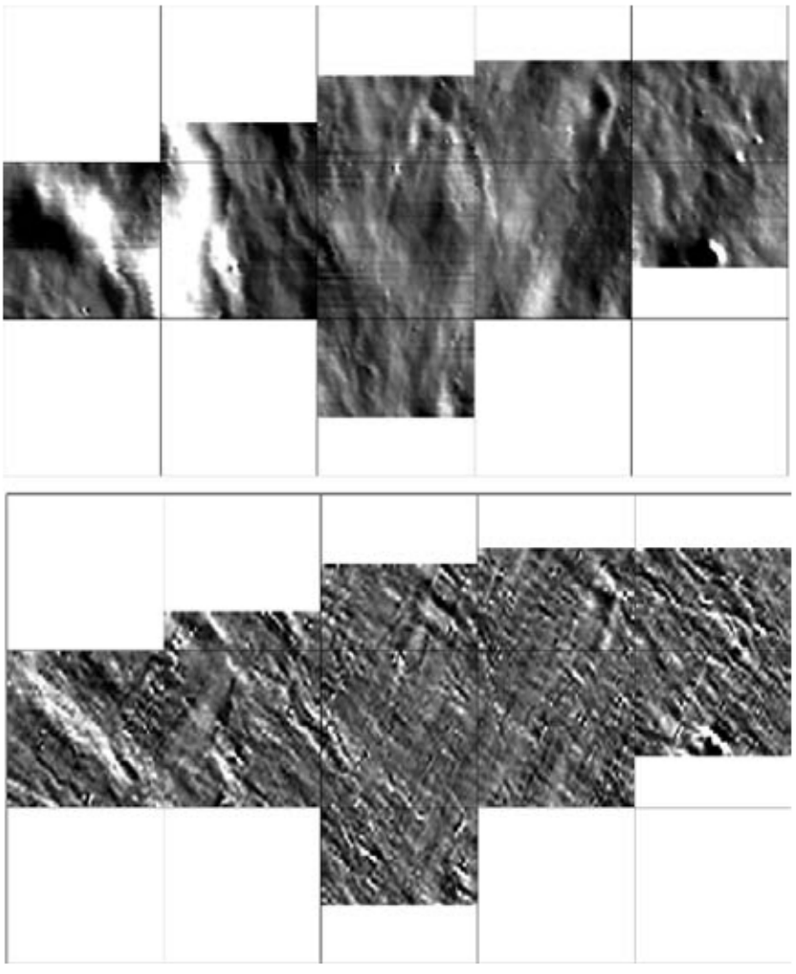

Fig. 4.10 Estaqueria. (**a**) Magnetogram of the total field prospecting of the site. Dynamics ±7.5 nT in 99 grey scales, grid size 40 × 40 m; the total Earth's magnetic field ~24.000 nT. (**b**) Magnetogram of the horizontal gradiometer data, dynamics ±7.5 nT in 99 *grey* scales, grid size 40 × 40 m

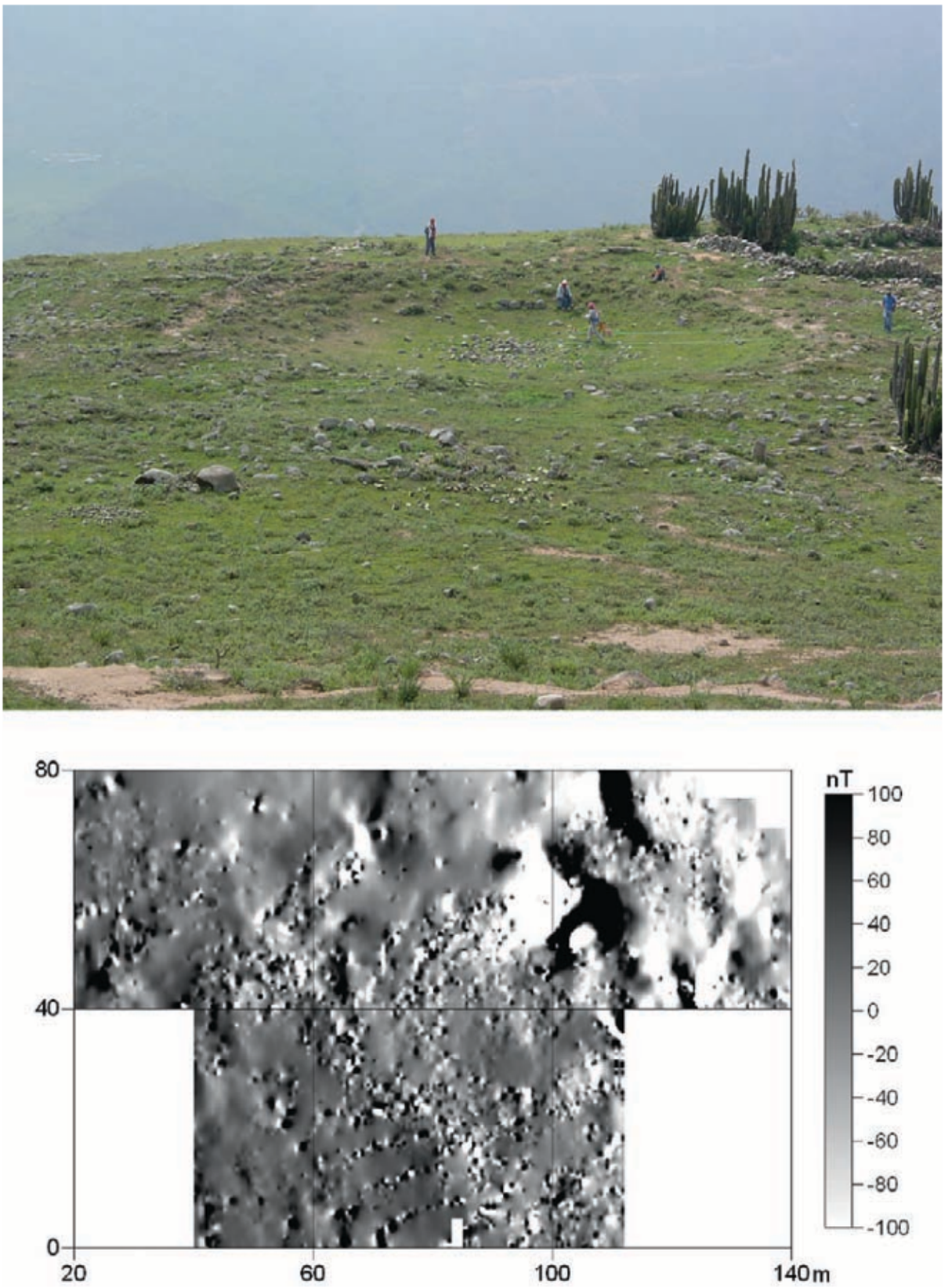

Fig. 4.11 Cutamalla. (**a**) Photograph of the site during magnetometer prospecting 2007. Note the circular outline of the sunken court (Photo: M. Reindel). (**b**) Magnetogram of the total field prospection of the site. Dynamics ±100 nT in 99 *grey* scales, grid size 40 × 40 m; the total Earth's magnetic field ~23.000 nT

extremely high remanent magnetisations are erratically aligned like little dipole magnets along the house fundaments. Although they also show relative magnetic susceptibility values of up to 30×10^{-6} [SI-units] (measured by a handheld Kappa-bridge SM 30, ZH-Instruments, Czech Republic) the induced magnetisation plays no role in the resulting magnetogram. The four star-shaped anomalies, as in the case of geoglyphs, are the results of lightning strike magnetisation.

4.7 Conclusion

The magnetic prospecting method relies on the fact that almost all common soils of the world reveal enhancement of magnetic minerals in the topsoil (Fassbinder et al. 1994). As the desert of the southern Peruvian coast is one of the driest regions in the world with less than 5 mm rain per year, it is necessary not only to verify all responsible processes for the formation of magnetic minerals in the topsoil but also the types of remanent magnetisations.

The outcome of the contribution to the project was that predominantly on almost all measured sites the remanence-based magnetic anomalies dominate the results, of which the Cutamalla site, where all measured archaeological anomalies trace back only to the natural remanent magnetisation of the granite rocks is an extraordinary example. As already discussed, DRM-based magnetic anomalies may be formed, for example, by the mechanical destruction of the remanence of the sediments beneath a geoglyph. Wind and water are responsible for the accumulation of heavy minerals such as the iron oxides. Enrichment of these minerals in a topographic depression such as geoglyph lines or old riverbeds will be visible in the magnetogram. The thermoremanent magnetisation dominates the magnetic anomalies of fireplaces. Although they might have nothing to do with archaeological structures it should be mentioned that extreme magnetic anomalies of lightning strikes which occur on the flat area of the trapezoid could be attracted by archaeological structures such as pylons or towers which were excavated by Reindel et al. (2004) at the geoglyph sites Llipata and Yunama.

All geoglyphs in this area were first mapped with photogrammetric means. This basic documentation was then revised and complemented by on-site field observations. Archaeological fieldwork encompassed a detailed description of

Table 4.2 Some Typical Magnetic Susceptibility Values

	Type of Rock or Sediment	Magnetic Susceptibility [$\times 10^{-6}$ SI]
A	Loess soil	0.8–5.8
B	Quartzite	0.008–0.5
C	Granite	11–30
D	Stone detritus	0.5–1.9
E	Pottery	3.2–9,0

Measured in situ by the handheld Kappa-bridge SM-30 (ZH-Instruments, Czech Republik).

each geoglyph, the recording of associated finds (mainly ceramics), the registration of the stratigraphic sequence of the geoglyphs, and trench excavations. Finally, magnetic prospecting and the development of the horizontal gradiometer configuration enabled the detection of thus far unknown and unseen geoglyph lines and revealed further structures beneath the desert.

4.8 Final Summary

1) The total field magnetometry combined with the development of the horizontal gradiometer as an additional tool is the most suitable configuration to detect the structures near the geomagnetic equator.
2) Destruction of the detrital remanent magnetisation by construction and walking on the geoglyph lines is detectable and verifiable by magnetometers.
3) It is possible to detect older stratigraphic layers of the geoglyph constructional phases and give a relative chronological description of the site.
4) Enrichment of magnetic minerals by wind and water separation may contribute to the detection of magnetic anomalies on geoglyph lines as well.
5) The detection of lightning strikes in the desert may contribute to the understanding of a changing climate.

Acknowledgements The fieldwork was undertaken under permission by the Instituto Nacional de Cultura (INC), Lima. The German Embassy, Lima, supplied us with logistic support. The project was funded by the German Federal Ministry of Education and Research (BMBF) through their priority programme NTG (Neue naturwissenschaftliche Methoden und Technologien in den Geisteswissenschaften). To all these colleagues and institutions we would like to express our sincere gratitude. Special thanks to Markus Reindel and Günther Wagner and Bernhard Eitel for substantial discussions during the fieldwork, and last but not least to our workers in the field: Alberto, Eduardo, and Manolo; they were the ones who 'pulled the lines'!

Chapter 5
Quantum Detection Meets Archaeology – Magnetic Prospection with SQUIDs, Highly Sensitive and Fast

Sven Linzen, Volkmar Schultze, Andreas Chwala, Tim Schüler, Marco Schulz, Ronny Stolz and Hans-Georg Meyer

Abstract A new measurement system was built for magnetic prospection in archaeology. The new device extends the capability of fluxgate- and caesium magnetometer-based systems to large-area mapping as well as high magnetic and lateral resolution. The SQUID system passed its first toughness test during a survey in the Peruvian Palpa region in 2005. Within a couple of days an impressive magnetic database of several hectares was created. This georeferenced archaeological and geological information is used for specific excavations and contributes to the comprehension of the historical contexts of the Palpa region.

5.1 Introduction

5.1.1 Magnetic Prospection for Archaeology

Within the last decades the importance of geophysical methods for archaeological investigations increased steadily (Scollar et al. 1990; Clark 1996; Wagner 2007). The impetus is the desire to get an image of buried structures before or – in special cases – instead of an excavation. In this context the magnetic prospection has significant impact. The method belongs to the passive geophysical ones, because no external excitation has to be applied to generate the physical measurand. One detects local variations of the earth's magnetic field by lateral moving of adequate sensitive magnetic sensors some centimetres above the ground. The so-acquired two-dimensional map represents the morphology of the ground from a magnetic point of view. That means a magnetic contrast occurs if a variation of magnetic susceptibility or permanent magnetisation exists. The origin of such variations is either geological or archaeological. The importance of magnetic prospection for archaeology arises from the variety of

S. Linzen (✉)
Institute of Photonic Technology e.V., POB 100239, 07702 Jena, Germany
e-mail: sven.linzen@ipht-jena.de

M. Reindel, G.A. Wagner (eds.), *New Technologies for Archaeology*, Natural Science in Archaeology, DOI 10.1007/978-3-540-87438-6_5,
© Springer-Verlag Berlin Heidelberg 2009

processes during or after human settlement activities which result in detectable magnetic markers. A prominent example is the magnetic detection of wood post and palisade holes even after complete decomposition of the used timber. Here, bacteria involved in the decomposition process leave the magnetic traces (Fassbinder et al. 1990).

Nowadays, caesium magnetometer systems are the state-of-the-art devices used for archaeometry (Fassbinder 2007; Neubauer 2001; Linford 2003). A magnetic prospection of a maximum area of about 2 ha can be performed with these manually carried or pushed systems within a day. The required lateral measurement point density leads to a typical distance between measured lines of 0.5 m which results in a meanderlike walking with a total distance of 10 km per ha with a double sensor system and a corresponding physical strain on the operator. However, the complete investigation of the area of an expanded earthwork or a former city corresponds to a prospection of several hectares. To fulfil such requirements a new magnetic prospection technique was developed within the German BMBF project No. 03SCX4JY. The new system was successfully applied in the wide-ranging valleys of Rio Palpa and Rio Grande. Its efficiency enables a new field of archaeometry: the search for buried archaeological sites within large areas by use of magnetic prospection.

5.1.2 Why Quantum Detection and SQUIDs?

As a consequence of the required increase of magnetic prospecting efficiency, a car-driven measurement system was developed. The maximum measurement speed should be at least 20 km/h which corresponds to an efficiency of 2 ha/h for a double sensor system and 0.5 m line spacing. A measurement point density of 1 point each 10 cm in the moving direction results in a necessary sampling rate of about 60 Hz for the magnetic measurement system. In general, it is challenging to construct a magnetic sensor which has both a high sensitivity and a broad bandwidth (which allows high sampling rates). Today only the Superconducting Quantum Interference Device (SQUID) fulfils these requirements. Its bandwidth is only limited by the corresponding electronics which linearise the sensor characteristics. These Flux Locked Loop electronics (FLLs) have bandwidths up to the MHz range. In addition to this enormous bandwidth the SQUID is the most sensitive detector of magnetic flux known (Clarke and Braginski 2004). It enables us to detect magnetic flux variations which correspond to small fractions of the flux quantum. To illustrate that fact, Fig. 5.1 shows a comparison of various sensors with respect to their magnetic field sensitivity within a bandwidth of 10 Hz. SQUIDs designed and fabricated at the IPHT Jena for different applications exhibit a noise-limited magnetic field resolution of about 20 Femtotesla ($1\ \mathrm{fT} = 10^{-15}\ \mathrm{T}$), which is about 200 times better than the resolution of caesium magnetometer systems. Using SQUID gradiometer sensors, however, this factor is somewhat smaller for large sensor-source distances (see Schultze et al. 2008 for

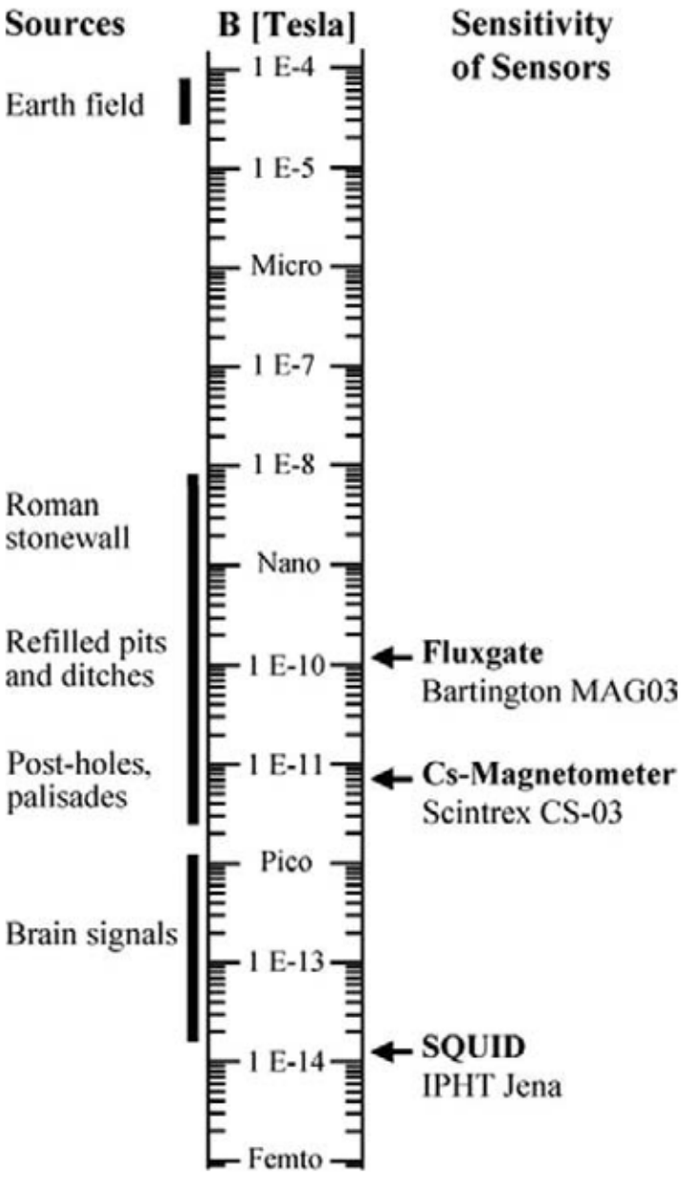

Fig. 5.1 Sensitivity of various magnetic field sensors. Note the logarithmic scale of the magnetic flux density B in the middle of the figure. The peak-to-peak noise was integrated within 0.01 and 10 Hz to calculate the noise-limited sensitivity values of the various sensors, shown on the right. The examples of archaeological sources on the left represent only qualitative levels based on experimental experience. The magnitudes depend on the specific conditions of an archaeological site (structural extent and depth, soil composition, measurement distance, etc.). For comparison the level of human brain signals which are measurable only with SQUIDs in a shielded environment are plotted

details). To recapitulate, the SQUID sensors are predestined for a highly sensitive and fast prospection system.

5.2 The New Measurement System

5.2.1 The SQUID Gradiometer

To make the SQUID sensors applicable for outdoor usage several problems had to be solved. A main issue is the permanent presence of the earth magnetic field, which is more than 10^9 times stronger than the smallest field change the SQUID can detect (Fig. 5.1). Thus, a linear movement in the earth magnetic field of vectorial sensors such as SQUID or fluxgate magnetometers results in signals which are mainly produced by small sensor tiltings or rotations, unavoidable in prospection practice. In addition, a magnetic shielding, which allows, for example, the visualisation of the human brain activity by means of SQUIDs

in biomagnetics, is not applicable. The only way out is the detection of a spatial derivative of the magnetic field in one direction instead of the field component itself by use of a SQUID gradiometer instead of a magnetometer. Such first-order gradiometers, especially designed for geophysical purposes, have been developed and fabricated at the IPHT Jena in $Nb/AlO_x/Nb$ technology (Stolz et al. 2001).

The planar-type gradiometers used have a size of $2 \times 6\ cm^2$ dominated by the two square superconducting antenna loops (Fig. 5.2). If the magnetic flux density B penetrating the antenna is slightly different between the two loops, a tiny electrical current results, which is finally detected by the inductively linked micrometer-sized SQUID structure. In this way, a formidable noise-limited resolution of 16 fT/cm is achieved (peak-to-peak value, integrated within 10 mHz and 100 Hz). The ideal gradiometer is insensitive against a homogeneous B-Field because then the fluxes in both antenna loops are identical. However, the real gradiometer still shows a little sensitivity because of tiny imperfections. Our gradiometer reaches a ratio between gradiometric and magnetometric sensitivity (intrinsic balance) of 10.000 which can be increased to 10^7 by use of SQUID reference magnetometer data (Stolz et al. 2004).

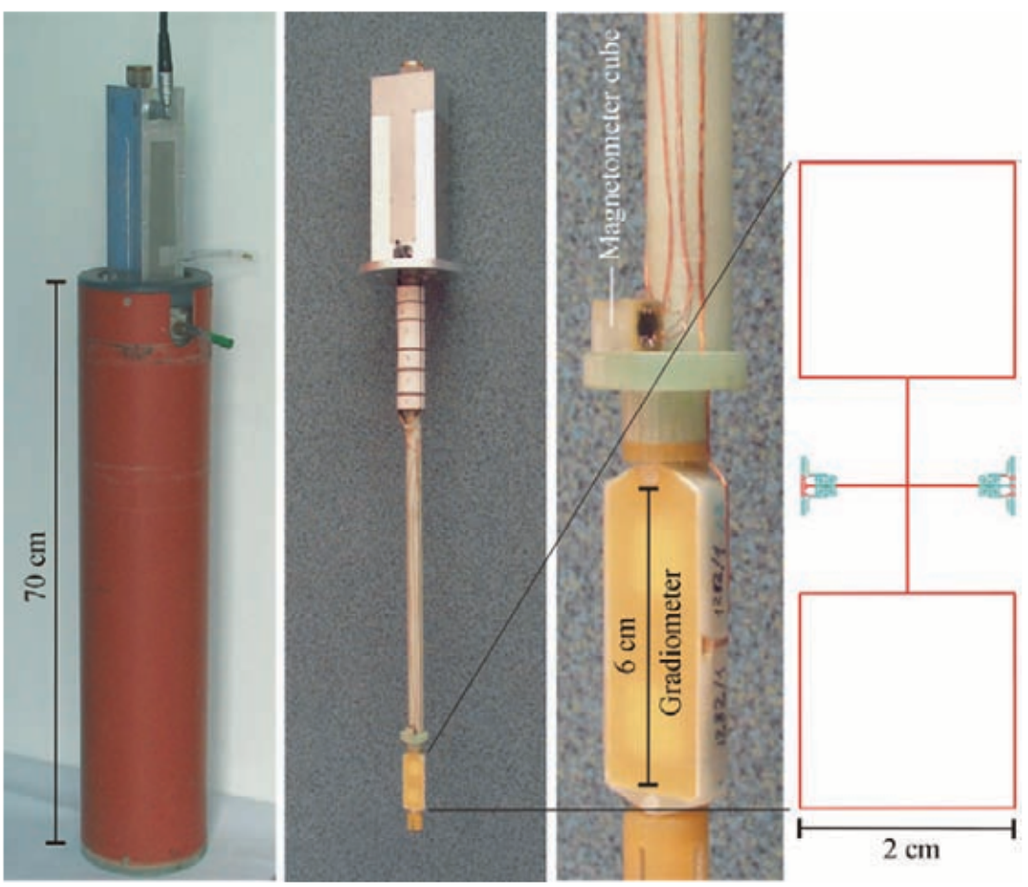

Fig. 5.2 Complete cryostat, the inset with FLL electronic box on top, and the lower end of the inset with encapsulated SQUID gradiometer and reference magnetometer cube (f. l. t. r.). The right drawing shows the gradiometer design

With these very promising gradiometer properties a first step towards the SQUID-based prospecting system was done. Next, the necessary sensor cooling setup was realised. Determined by the used Niobium thin film material, the SQUID sensors have to be cooled below a temperature of 9.2 K for functionality. In standard stationary applications the SQUIDs operate at 4.2 K inside cryostats, thermally well-isolated vessels filled with liquid helium. These cryostats had to be adapted for nonstationary and unshielded conditions. The result is a complete glass-fibre reinforced plastic (GRP) cryostat with an inset made from the same material serving as carrier for the SQUID gradiometer and the additional SQUID reference sensors (Fig. 5.2). The cryostat contains two litres of liquid helium. It has to be refilled every two days. The refilling is a nonspectacular operation of about 15 minutes using a storage Dewar with, for example, 60 L of liquid helium and a small transfer tube. Because of medical and industrial usage helium is available worldwide, in less-developed countries at least in the capital city. For the campaign in Peru, for instance, we carried a storage Dewar together with our measurement equipment from the capital Lima to the Palpa area using a pick-up car.

5.2.2 The Measurement Cart

Partly contrary requirements have to be fulfilled for the measurement vehicle which has to carry the cryostats with the SQUID sensors inside. The device has to provide a save movement even over rough ground with more than 20 km/h for hundreds of line kilometres of prospection. On the other hand, no magnetic material and – especially in the vicinity of the sensor – no electrical conducting material can be used for construction. Conductive parts would lead to magnetic disturbances because of eddy current generation during movement in the earth's magnetic field. Thus, the body construction holding the cryostats as well as the moveable parts such as the four wheels are again made from GRP. Mechanically crucial parts such as the wheel suspension, the wheel bearing, and any screws are made from synthetic materials, too.

The cart allows a manually pushed as well as a car-pulled measurement modus (Fig. 5.3). The latter favourite one is applied for large-area prospecting; the first one is used for smaller areas on which driving is impossible, unwanted, or not efficient. The unavoidable magnetic disturbances of the pulling motor vehicle are reduced to an acceptable value by a distance to the SQUID sensors of 6 m and some further compensation of the gradiometer data during software postprocessing.

In addition to the maximal three cryostats the cart carries a differential GPS and an inertial system for precise position measurement with centimetre resolution at a sampling rate of 10 Hz. These data as well as the data streams of all SQUID sensors are bundled and synchronised by self-made electronics. This data acquisition unit includes very low noise 24-bit AD converters for digitising

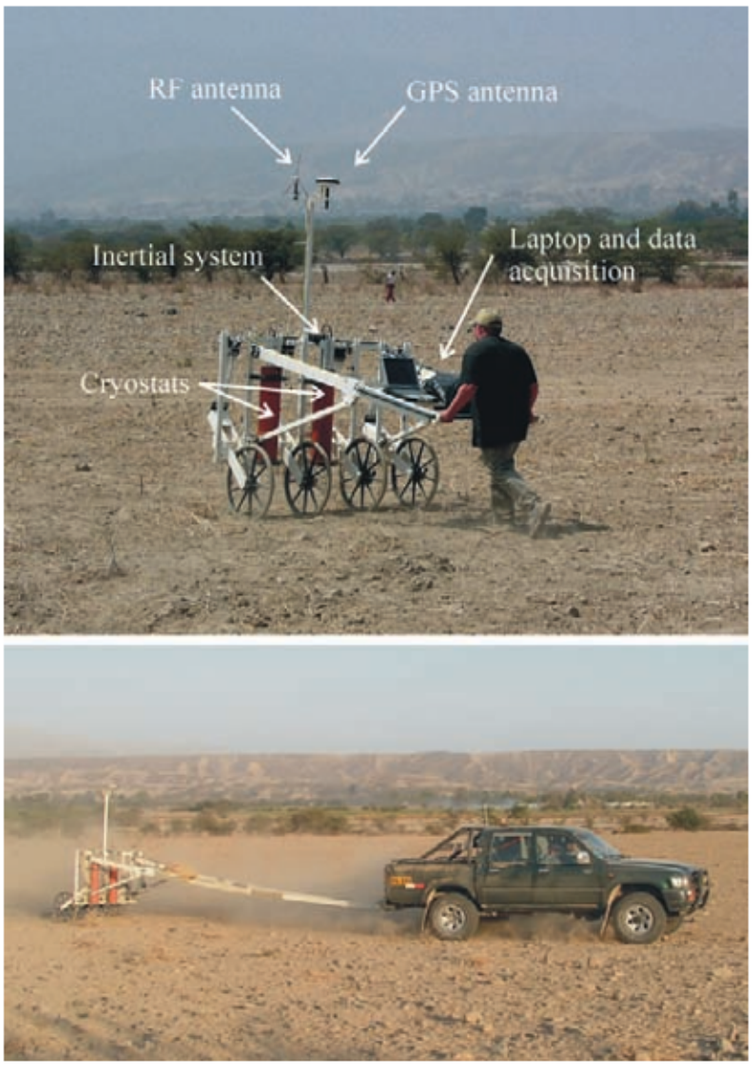

Fig. 5.3 New measurement system during manual and motorised prospection in the Palpa valley. The marked RF antenna in the upper image receives as part of the differential GPS system the position data from the stationary GPS base station located on a field edge (not visible)

all SQUID signals at a 1 kHz sampling rate, a fully autonomous power supply based on lithium ion batteries, and an Ethernet link via glass-fibre cable to the operator's laptop. This is either fixed on the cart in the pushed mode or placed inside the car for the motorised one. The operator can observe in real-time all SQUID signals and has control over the cart's actual position. In addition, the Labview program visualises the coverage status of the area showing all previously measured traces. Within a measurement break of some minutes a first magnetogram similar to subsequently shown figures can be calculated by just starting a Matlab script. Details of the data processing steps can be found in Linzen et al. (2007).

5.3 The Prospection in Peru

The new prospection system passed its first toughness test outside Germany in the south of Peru in autumn 2005. Six different sites were mapped manually and motorised inside an about 200 ha wide region located 3 km southwest of Palpa (Fig. 5.4). Manual measurements were performed on two sites, in the area of

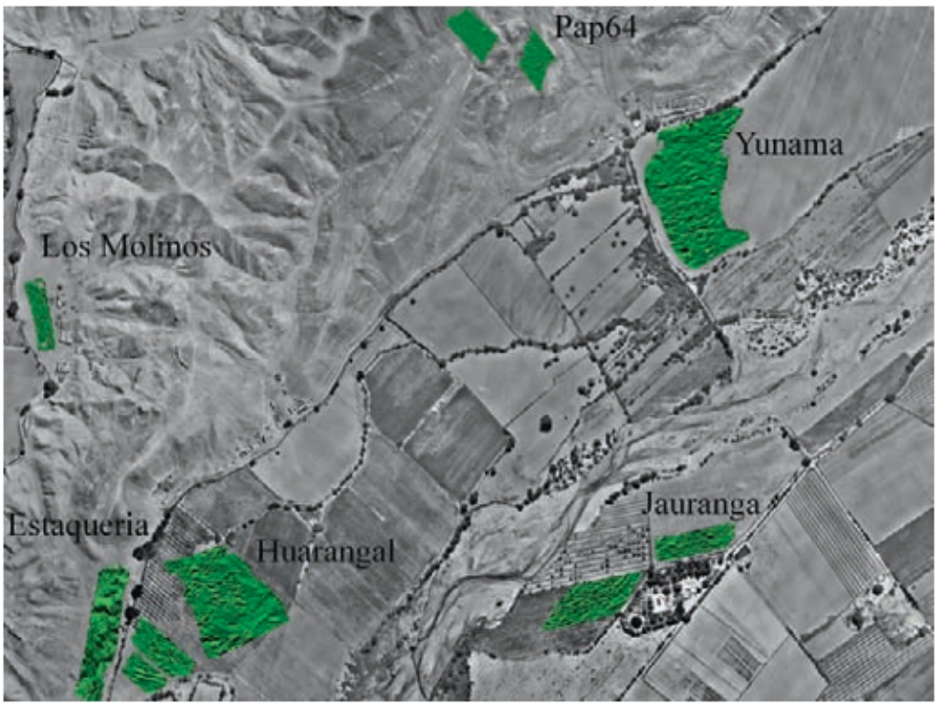

Fig. 5.4 Overview of all measurements performed by the new SQUID measurement system within the Palpa region. The mapped magnetograms are georeferenced and embedded in green colour into the 1.2 × 1.6 km^2 wide orthophoto. (The latter is used by courtesy of the Institute of Geodesy and Photogrammetry, Swiss Federal Institute of Technology, Zürich.)

PAP 64 (PV67A-013-016) for preserving the geoglyph's surface and partly on the Yunama field for comparing with motorised measurements. The archaeological aim of the prospection was the search for settlements especially of the Paracas period. Subsequently, we present a selection of measurement results taken from the Yunama and Estaqueria area west of the Palpa River and close to the hillside of the low mountain range with the PAP 64 (PV67A-013-016) geoglyph. Further results are from Jauranga, an area quite close to the east bank of the Palpa River (Fig. 5.4). Not explicitly shown are the recorded magnetic maps from Los Molinos and the PAP 64 (PV67A-013-016) part. In the latter, magnetic traces of old optically invisible lines could be found, an effect investigated and reported in detail by Fassbinder, this volume.

5.3.1 Yunama and Jauranga

Firstly, we want to illustrate exemplarily the potential of the new system by means of the Yunama area (PAP 734; PV67A-273), on which the first SQUID measurements in Peru were performed. The dusty loess soil of Yunama shows no obvious sign of archaeological structures. However, the south part of the area was previously investigated by different geophysical methods; also several excavations were realized with a subsequent closure of the opened pits. These activities and other structures are represented by the manual and the motorised SQUID

measurements in a nearly identical manner (Linzen et al. 2007). Thus, it was possible to use subsequently only the fast motorised modus on the large areas.

The first complete prospection of the area with a length of 300 m from the south excavation zone up to the hillside in the north could be realised (Fig. 5.5). The magnetogram appears bumpy in large sections, generated by rubble sediments. A separation of settings of boulders from the Paracas time from natural formations is difficult: excavations show both within a depth of 0.7–2 m. On closer inspection, especially in the southeast magnetogram part, a network of

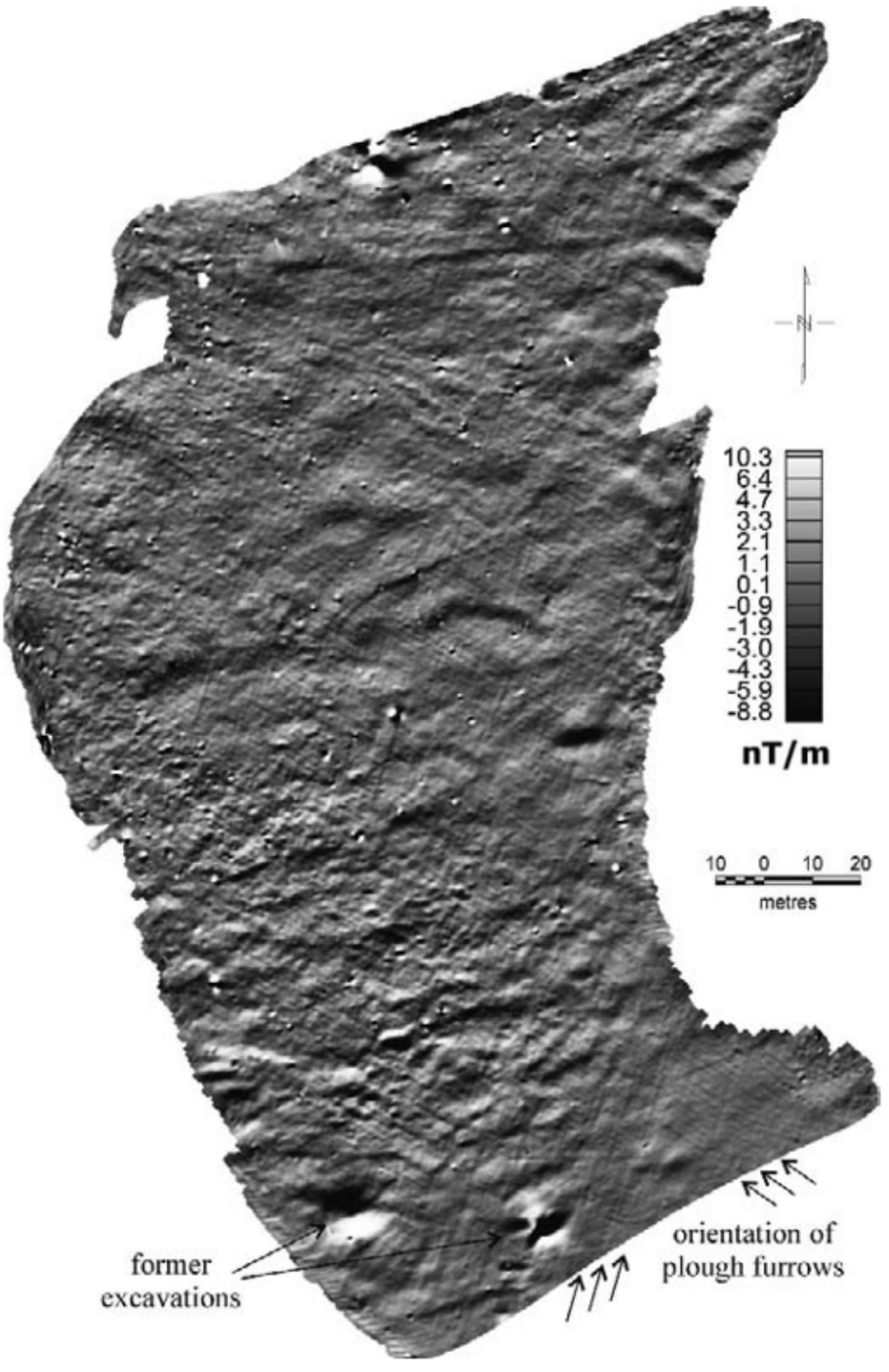

Fig. 5.5 SQUID Gradiometer data of the Yunama area recorded by motorized prospection. The pronounced anomalies in the south represent refilled pits of former excavations

thin lines from southwest to northeast and from southeast to northwest is visible. Here plough traces of different ages are represented magnetically. The probably youngest orientation of plough furrows is visible in the corresponding orthophoto (Fig. 5.6). This figure shows the advantage of the synchronous

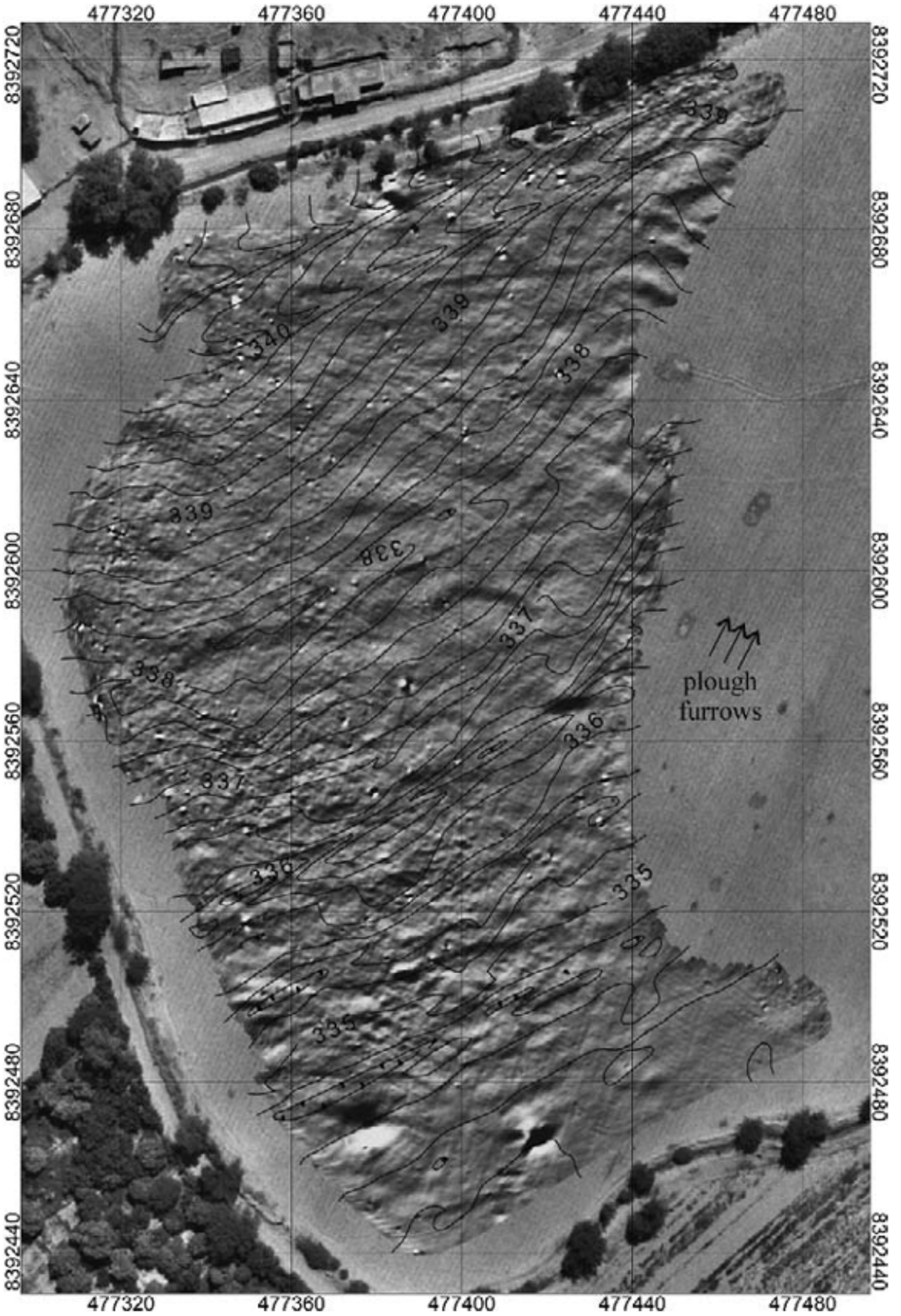

Fig. 5.6 Georeferenced Yunama gradiometer data embedded into the orthophoto using the synchronously recorded GPS data. These are the basis for the additionally plotted altitude levels also. (UTM zone 18 South, WGS-84 ellipsoid, all values in metres)

recording of SQUID sensor data and differential GPS information. The prospected magnetograms are always georeferenced with local x–y-coordinates in the worldwide UTM or in other systems (e.g., the German Gauß-Krüger). Thus the magnetogram can be directly embedded into a georeferenced orthophoto or linked to a GIS database without an additional photogrammetric survey. Furthermore, the UTM altitude data can be used for terrain modelling and finding local correlations in advance of an excavation.

To examine mainly the geological aspects, SQUID measurements on two areas around the Jauranga property are discussed next. The east prospection borders from the north on the finding-place of widespread adobe walls from the Paracas period. The magnetogram is dominated by pronounced plough furrows in a nearly east–west direction (Fig. 5.7). However, some linear structures point along southwest–northeast, the orientation of the excavated adobe walls. The altitude of the second prospected western area is on average two metres lower than the first one. On this lower terrace, structures of the old riverbed, that is,

Fig. 5.7 Two measured Jauranga maps (*green*) embedded into the orthophoto showing the current riverbed of the Rio Palpa in the northwest part

sediments located about 1.5 m below the surface, were detected magnetically (Fig. 5.7). These structures illustrate amongst others the close relation between the found settlement and the nearby Rio Palpa which currently has a larger distance of about 200 m.

5.3.2 *Estaqueria*

Next we show measurements to demonstrate the usefulness of the SQUID system for locating archaeological structures such as settlement sites.

The 80 × 240 m^2 wide Estaqueria area was prospected in addition to the measurements of the eastern Haurangal area (Fig. 5.8). The hilly site is currently used neither as farmland nor for housing. Paths cross the area; one leads

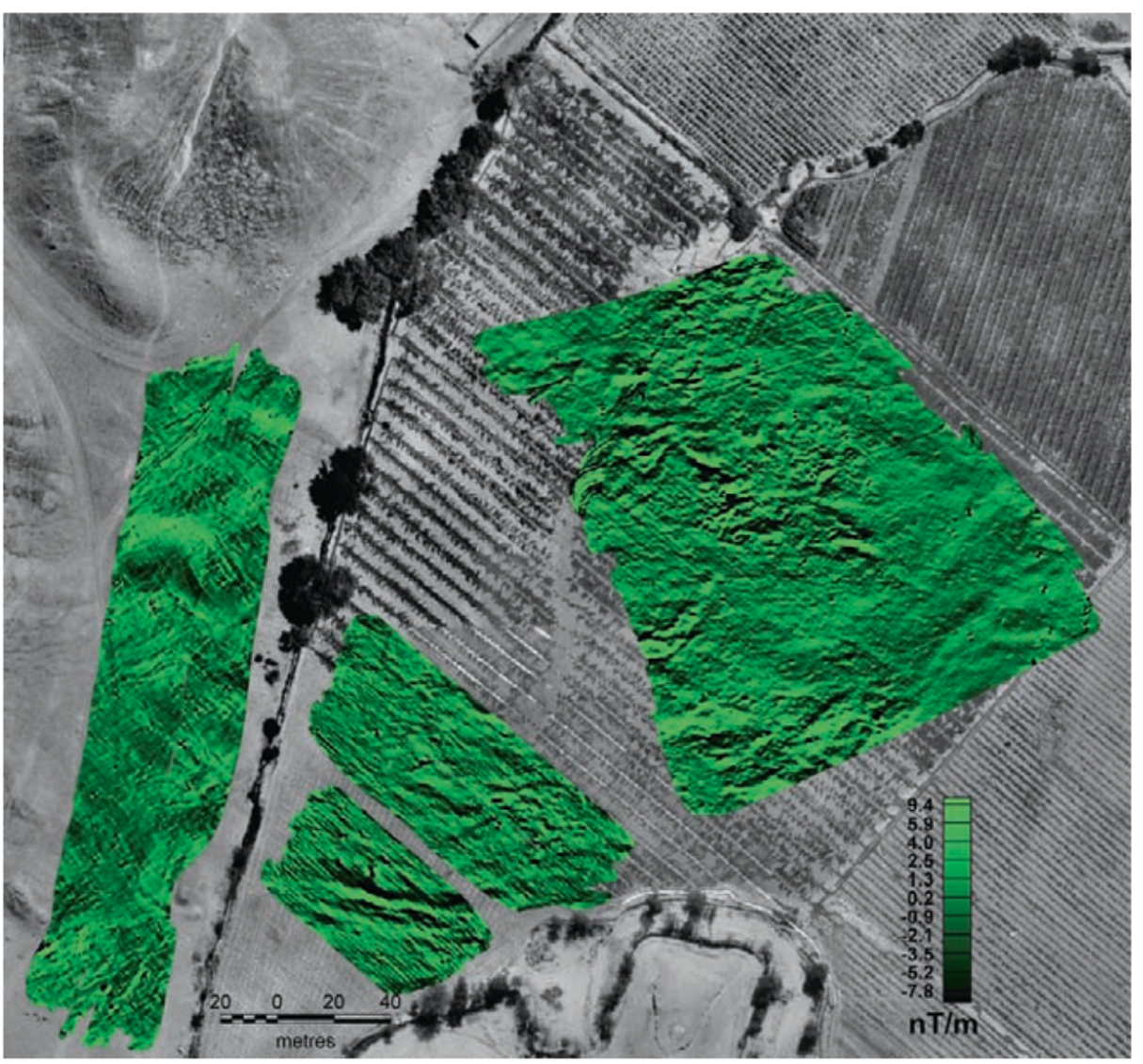

Fig. 5.8 SQUID gradiometer maps of Estaqueria (*left*) and Haurangal (*middle* and *right*) embedded into the orthophoto. Note the northwest-oriented dell and the path on the left side of the Estaqueria map which leads to Los Molinos and the Rio Grande valley

to the bordering Rio Grande valley in the west. The magnetogram (Figs. 5.8 and 5.9) shows rectangular structures with southeast–northwest orientation (in addition to geological formations correlated with the closed hillside). One part of them is marked by a square (Fig. 5.9).

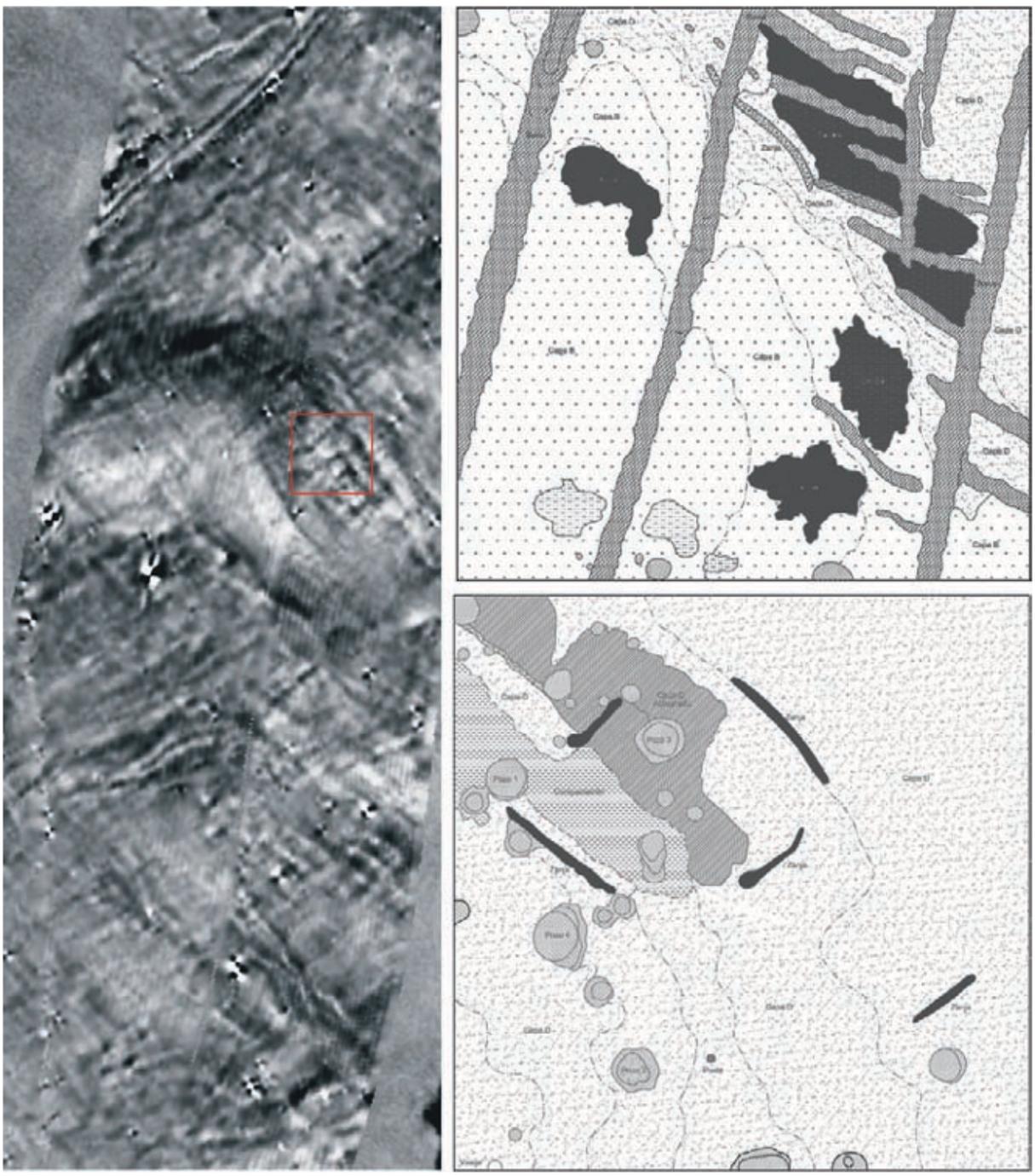

Fig. 5.9 Detail of the Estaqueria magnetogram (*left*) and excavation schemes of the first and second cut (*upper* and *lower right*, respectively). The square on the magnetogram marks the excavated area. The excavation area and the schemes have a size of $10 \times 10\ m^2$. The first cut of about 15 cm depth is dominated by old plough furrows along SW–NE and ash fields (*dark*). The scheme of the second cut shows small trenches (*dark*) and a couple of round pits. Both schemes exhibit sequences of different soil composition and compaction along SE–NW (various hatching)

Triggered by our magnetic mapping, this area of $10 \times 10\ m^2$ was the object of excavations by Markus Reindel and Johny Isla in 2006. Although the expected adobe wall formation was not found, a settlement area of the Initial Nasca period was discovered. The settlement site seems to be related to the nearby archaeological site Estaqueria (PAP 70-73; PV67A-001-004) where test excavations had been realized in 1997 (Reindel et al. 1999). A variety of human activities seems to be responsible for the detected magnetic signature. Ash fields were found within the first 15 cm. A set of trenches, indicating a house floor plan, also fits the magnetic map (Fig. 5.9). Furthermore, the many filled pits with dimensions of up to 1 m in diameter and 80 cm in depth contribute to the gradiometer's signal (Fig. 5.10). For a deeper understanding of the magnetic signatures, however, additional measurements of the magnetic susceptibility on excavated samples are necessary. The excavations were successfully continued in the north part of Estaqueria in 2007.

Fig. 5.10 Photographs of the excavated area on the Estaqueria site. The upper one shows the $10 \times 10\ m^2$ area of Fig. 5.9 but with west orientation. The pit on the lower one has a diameter of 65 cm and a depth of 80 cm

5.3.3 Comparison of SQUID and Caesium Magnetometer Data

Before the excavation campaign in the Estaqueria area was started by M. Reindel and J. Isla in 2006, caesium magnetometer measurements were performed manually by J. Fassbinder providing a direct comparison with the SQUID gradiometer data. A first view of both the magnetometer and gradiometer data gives completely different impressions (Fig. 5.11a,c). The magnetometer image shows mainly long periodic structures which represent the geologic formation of the hillside situation. In contrast, the gradiometer image has a couple of quite sharp features which belong to the surface layers (approximately the first metre). The enhancement of surface sensitivity results mainly from the stronger dependence of the gradiometric signal $G = dB_y/\mathrm{d}z$ on the distance r to the magnetic source ($G \sim 1/r^4$) in comparison to the dependence of the magnetic field $B = \left|\vec{B}\right| = \sqrt{B_x^2 + B_y^2 + B_z^2}$ itself on r ($B \sim 1/r^3$).

The effect is further pronounced by the higher SQUID gradiometer sensitivity discussed in detail by Schultze et al. (2008). A kind of bridging between the caesium total field magnetometer signal and the vectorial signal of one SQUID

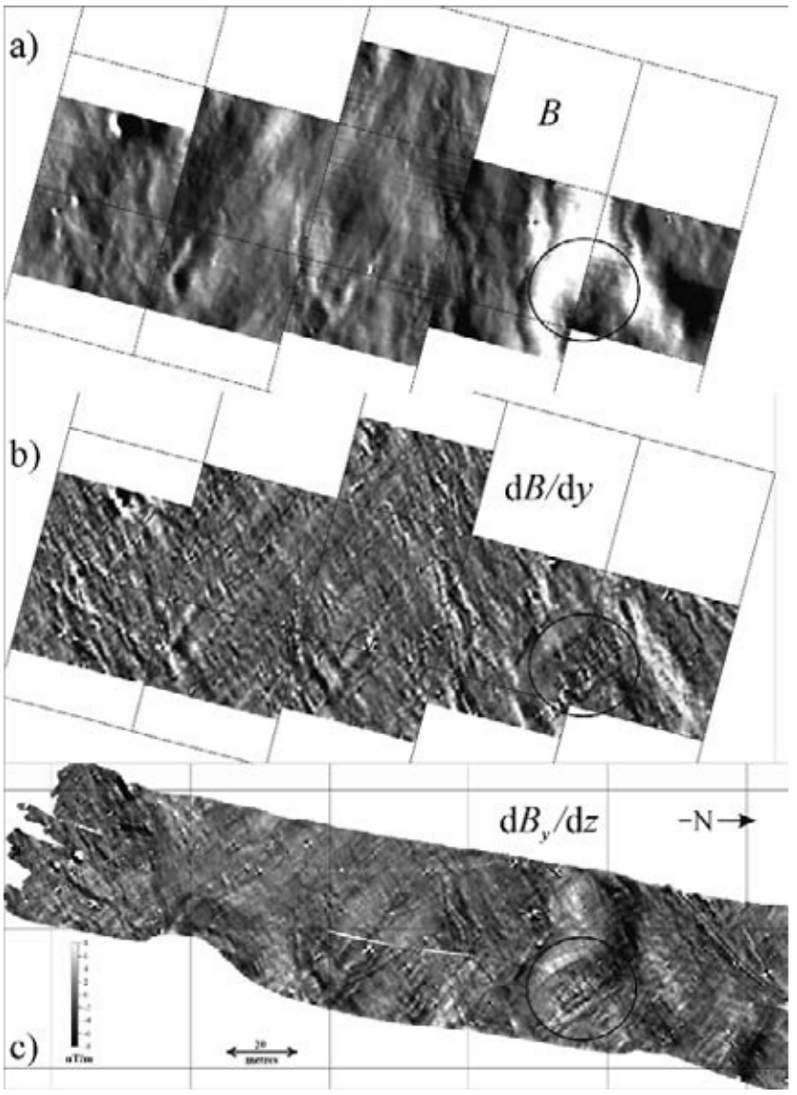

Fig. 5.11 Comparison of Cs-magnetometer measurements (**a**) and (**b**) performed by J. Fassbinder and SQUID-gradiometer data (**c**) on the Estaqueria area. Image (**b**) was calculated by T. Gorka from the magnetometer data (**a**) by forming a lateral gradiometer. The encircled area shows the above-discussed archaeological structure which is visible only in the two gradiometric datasets

gradiometer was realised by J. Fassbinder and T. Gorka forming a software gradiometer (Fassbinder and Gorka 2007, this volume). The lateral component dB/dy with y as the (approximate) east–west-direction was calculated for the Estaqueria case by use of couples of caesium magnetometer data points with a distance of 50 cm in y. The result is shown in Fig. 5.11b; it can be compared with the directly measured SQUID gradiometer component dB_y/dz with y in the same east–west-direction (Fig. 5.11c). In this way, some features of the SQUID gradiometer map can be recognised in the processed Cs magnetometer data as well.

This kind of comparability allows a more common analysis and interpretation of prospecting data from caesium magnetometers and SQUID gradiometers in general. Furthermore, combined surveys can profit from the individual advantages of each system.

5.4 Summary and Outlook

A new SQUID gradiometer-based system was developed for magnetic prospection in archaeology. The device provides a new quality of prospection speed and magnetic resolution which allows the search for buried archaeological structures within large areas, in general impossible with the hitherto existing technology. Comprehensive georeferenced magnetic maps were generated during a short survey in the Palpa region in 2005. Successful excavations were carried out on the basis of the SQUID data. The new system confirmed its applicability within various subsequent prospections in several countries.

We currently are working on the generation of depth information and reconstruction of buried structures using the data from a set of SQUID gradiometers. Having this information available would mean the next step in magnetic prospection.

Acknowledgements The authors would like to thank Markus Reindel, Johny Isla, and Jörg Fassbinder for their support in Peru as well as for the scientific teamwork during the whole project. Many thanks to Pablo See for his hospitality in Lima and help with the liquid helium transfer. Beate Träger from the German Embassy in Lima enabled the transport of our equipment. Thanks to the German BMBF for financial support.

Chapter 6
Viewing the Subsurface in 3D: Sediment Tomography for (Geo-)Archaeological Prospection in Palpa, Southern Peru

Stefan Hecht

Abstract This contribution focuses on the application of geophysical methods for geoarchaeological prospection. At first, methodological bases of sediment tomography are presented, especially the use of earth resistivity tomography (ERT) and seismic refraction tomography (SRT) in case of on-site and off-site studies. Then, the results of the measurements within the Nasca–Palpa project are explained in more detail. The results of the measurements at Jauranga show that one strength of the earth resistivity tomography is the possibility to separate different types of fluvial sediments, whereas the seismic velocities give valuable information about the bedrock and the thickness of the overlying loose sediments wherein archaeological findings could be clearly identified. Former loam excavation pits could be detected by the specific use of 3D tomographies. The comparsion of 2D and 3D geoelectric data at Yunama showed a very good agreement between the different datasets. Several former soil surfaces could be reconstructed, that were covered subsequently by high-flood sediments of the River Palpa. We present the results of the geoelectric measurements at the archaeological site PAP-83(PV66-057) in comparison to the results of archaeological excavations. Anomalies of extremely high resistivity values could be identified as layers of straw mats, whereas relatively lower resistivity values represent adjacent adobe walls. The results of all 2D and 3D geoelectric tomographies are validated clearly by the archaeological excavations.

S. Hecht (✉)
Institute of Geography, University of Heidelberg, Im Neuenheimer Feld 348, 69120 Heidelberg, Germany
e-mail: stefan.hecht@geog.uni-heidelberg.de

M. Reindel, G.A. Wagner (eds.), *New Technologies for Archaeology*, Natural Science in Archaeology, DOI 10.1007/978-3-540-87438-6_6,
© Springer-Verlag Berlin Heidelberg 2009

6.1 Introduction: Sediment Tomography for (Geo-)Archaeological Prospection – On-Site and Off-Site Studies

The application of tomographical methods in medicine for the X-ray examination of our bodies for years has been part of the standard repertoire in a variety of medical examinations. Meanwhile, different geophysical methods are also available for the 'X-ray examination' of the shallow subsurface for locating archaeological findings. The use of geophysical methods in the context of geoarchaeology offers two main fields of application. These methods can be used to map archaeological structures directly within archaeological sites with high resolution at a small scale (on-site studies). On the other hand, geophysical investigations in the wider environment of archaeological findings may yield valuable information about landscape evolution or environmental changes in close connection with cultural changes (off-site studies). In contrast to detailed on-site studies, information about larger distances is decisively important for landscape-evolution aspects. According to these different requirements different methods or equipment configurations come into operation. The term 'sediment tomography' is used in this contribution generally for the application of geophysical procedures in which two-dimensional slices of the underground are produced. Conversely, the construction of 'real' tomographies requires a three-dimensional data set.

6.2 Methodological Bases of Sediment Tomography

An important advantage of using geophysical methods for sediment tomography is the nondestructive, complete, and in most cases high-resolution investigation of archaeological sites along a measuring line or across a measuring area. In the past, merely punctual information could be derived from results of landscape reconstruction (e.g., drilling data). Moreover, the areas between the drill holes always held uncertainties as to the interpretation of the data. But the acquisition of complete detailed information is an indispensable prerequisite for the recognition of archaeological structures at a small scale, such as wall remains, postholes, or pits.

A difficulty frequently met when interpreting geophysical data is the ambiguity of the measurements (e.g., Lange 2005; Kirsch and Rabbel 1997). For the reconstruction of the shallow subsurface there often exist several possible solutions explaining the data. In the case of favourable measuring conditions, however, the doubts can be reduced to questions of detail. Another difficulty consists in the correct interpretation of the results inasmuch as data anomalies of the measured parameters can reflect both natural variations of the sediment structures as well as archaeological findings. Because of that, the interdisciplinary cooperation of geoscientists and archaeologists is particularly important to exclude misinterpretations of the geophysical data.

For archaeological and geoarchaeological questions geoelectric and refraction seismic procedures offer different possible applications. Although refraction seismic methods are particularly well suited to delimit loose sediments from bedrock, Earth Resistivity Tomography (ERT) is mainly appropriate for distinguishing different types of loose sediments and the identification of archaeological structures. Therefore, refraction seismic methods are rather used for off-site studies whereas earth resistivity tomography is suitable for both off-site and on-site studies (Hecht 2007).

6.2.1 Earth Resistivity Tomography (ERT)

The principle of geoelectric measuring is to determine the specific electrical resistivity value of the subsurface. For the identification of natural or anthropogenic structures with this method it is presupposed that the values of the electrical resistivity differ significantly from each other. A methodical difficulty consists in the very large fluctuation of the resistivity values of specific materials (rocks or substrata; Table 6.1). This means a certain measurement cannot be assigned directly to a certain material or specific type of rock or sediment. Therefore, additional information from drilling data, from other geophysical measuring methods, or from archaeological data is particularly important for an exact interpretation of the results.

The electrical characteristics of rocks or soil are marked by different influence factors. The most substantial ones are the chemical and mineralogical composition, the rock structure, and the porosity (Greinwald and Thierbach 1997). The water content is reflected in the grain-size composition of loose sediments and therefore plays a particularly important role in the resistivity values. Fine-grained substrata are able to store precipitation water better than coarse-grained sediments, which rather tend to dryness because of a higher permeability. Due to these factors large ranges of the specific electrical resistivity may appear for certain rocks or substrata. The unit of the specific electrical resistivity is Ωm.

Table 6.1 Specific electrical resistivity values for selected rocks and substrata

Soil, sandy	150–7.000 Ωm
Soil, loamy	50–9.000 Ωm
Soil, clayey	20–4.000 Ωm
Sand	1.000–10.000 Ωm
Silt	10–1.000 Ωm
Clay	1–1.000 Ωm
Limestone	100–7.000 Ωm
Granite	300–30.000 Ωm

Source: Compilation according to Greinwald and Thierbach (1997).

The procedure of earth resistivity tomography developed from the common four-point methods (Friedel 1997; Berktold 1997). Hereby, the electrical resistivity is measured by two electrodes, which deliver the current to the underground (current electrodes), and another two electrodes are used to measure the resistivity values (potential electrodes). A slice (*tomos*, Greek for plate, cut) of the underground resistivity distribution is generated by a large number of four-point measurements with the help of multielectrode systems, for example, with a line of 100 electrodes at a distance of 1 m each. Depending on the electrode array, several hundred to several thousand individual measurements are necessary to generate such a tomography. A two-dimensional outlay of the electrodes provides the determination of a three-dimensional distribution of the electrical resistivity values in the underground. This procedure is also based on the four-point methods mentioned above. Strictly speaking, only a 3D-measurement is a tomography in the real meaning.

Different electrode arrays show different sensitivities concerning the lateral or vertical resolution of the resistance distribution. The dipole–dipole array of the electrodes provides the best results with regard to the lateral variability of a resistivity measurement (e.g., Lange 2005; Kneisel 2003) and is thus very well suited particularly for the detailed mapping of archaeological structures. In the case of 3D measuring, the pole–pole array in most cases offers the best compromise for small-scale measuring with narrow distances of the electrode units (Loke and Barker 1996). For the interpretation of geoelectric data the software Res2DInv and Res3DInv were used.

6.2.2 Seismic Refraction Tomography (SRT)

The principle of refraction seismics is based on the appearance of different P-wave velocities in different rocks or substrata. For a successful use of these methods the velocities must differ considerably from each other. With the help of a signal transmitter (e.g., hammer) seismic waves are produced, which can be registered by receivers (geophones) usually arranged along a line. In the case of seismic refraction studies, only the first breaks of the P-waves, which arrive faster at the receivers in comparison with reflection waves or surface waves, are looked at. Dynamic wave effects, such as amplitudes, frequencies, and the like are not taken into account in general. The specific rock type cannot be derived directly from a velocity value at a seismic refraction measurement (Lankston 1990), similarly to the case of the earth resistivity tomography. Figure 6.1 shows the large varieties of the P-wave velocities for different rocks and substrata, which means that additional data are required for the correct interpretation of the data.

Different procedures for the interpretation of seismic refraction data exist. Standard inversion methods such as the intercept-time method as well as the generalized reciprocal method (GRM) (Palmer 1981) belong to the most common approaches for the interpretation of refraction seismic data (Kirsch and Rabbel 1997). It is the great advantage of these methods that as a result

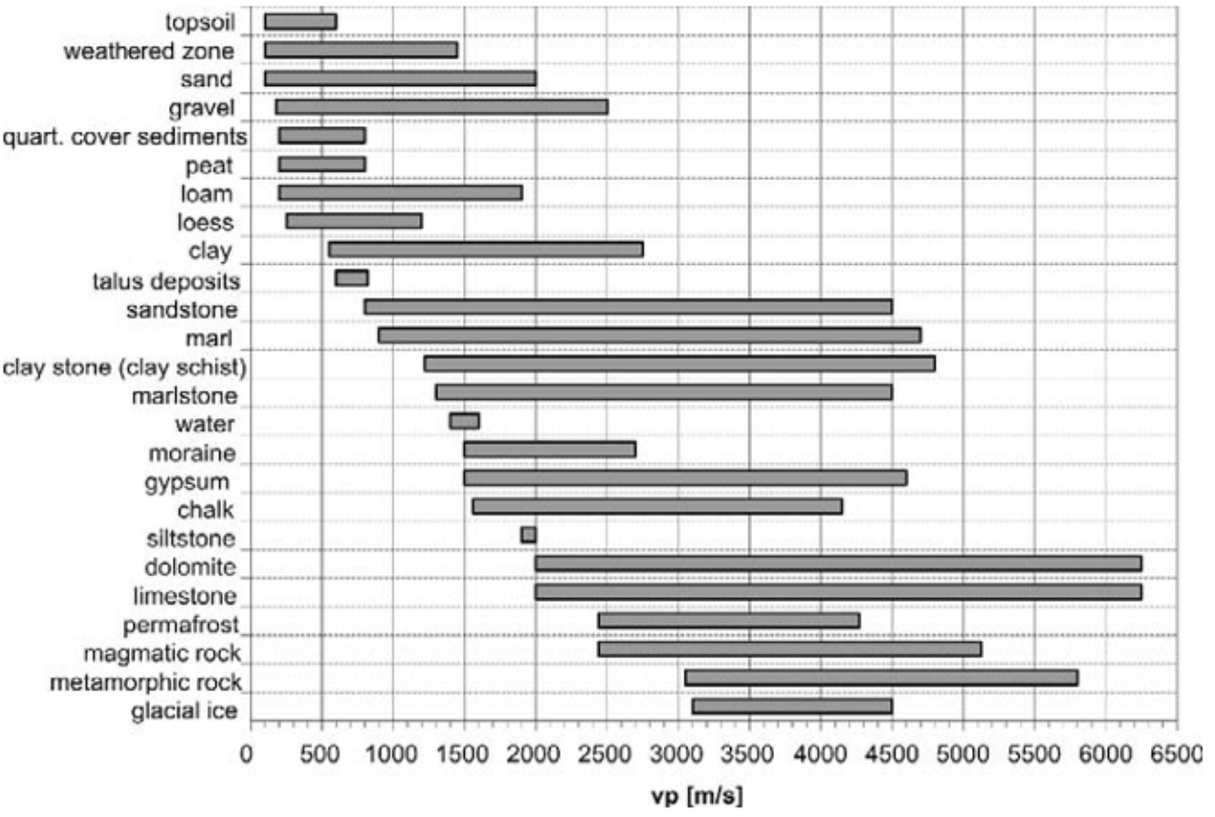

Fig. 6.1 Velocities of seismic P-waves in different media. This compilation is based on values from Fertig (1997) and was amended with additional data from numerous authors. Indicated are the ranges in which data were measured. In some cases small ranges are shown because of a lack of sufficient data (e.g., siltstone; Hecht 2003)

relatively sharp layer boundaries are reconstructed. The depth and the topography of layer boundaries can be determined hereby.

The application of raytracing methods, allowing the comparison of synthetic traveltime data with the measured data, should be used to check the quality of the resulting underground model (Hecht 2001). Gradual (iterative) improvement of the model must be done until good agreement of measured and calculated data is obtained (Sandmeier and Liebhardt 2005). The seismic refraction tomography reveals the distribution of the P-wave velocities along a measuring section with high depth resolution. This procedure needs dense coverage with traveltime data over the complete study area (Utecht 2005). For optimal results, overlaying receiver spreads by as much as half the spread length should be employed. For the interpretation of seismic traveltime data the software packages Reflexw and Rayfract were used.

6.3 Results of Sediment Tomography in the Context of the Archaeological Research in Palpa

The application of the innovative geophysical methods for sediment tomography within the Nasca–Palpa project was carried out in close collaboration with the archaeologists J. Isla and M. Reindel and in collaboration with

J. Fassbinder who made magnetic measurements at the same locations (Fassbinder this volume). The aim of all examinations was not only the adaptation of the methods to the conditions of the hyperarid desert area in southern Peru but also the further development of both seismic and geoelectric methods. Seismic measuring was generally applied on the fluvial terraces of the Rio Palpa to distinguish loose sediments from the underlying bedrock. This was done with regard to landscape evolution, because the thickness and the structure of the terraces yield valuable information about the sedimentation history, which plays an important role in the reconstruction of environmental changes in the river catchment areas (Eitel and Mächtle this volume). For geophysical prospection on archaeological sites, earth resistivity tomography was mainly used. Because most of the measuring was carried out for archaeological purposes, the following case studies also focus on ERT. The example of Jauranga shows the results of seismic and geoelectric tomographies in direct evaluation, whereas the comparison of 2D and 3D geoelectric data is presented for the location of Yunama. At the archaeological site PAP-83(PV66-057) we can present the results of the geoelectric measurements in comparison to the results of archaeological excavations.

6.3.1 Case Study Jauranga: Earth Resistivity Tomography and Seismic Refraction Tomography

The archaeological site Jauranga is situated in the river oasis of the Rio Palpa where fine-grained alluvial deposits cover wide parts of the fluvial terraces (Fig. 6.2). First of all, seismic refraction (including raytracing and seismic tomography) was used to locate the boundary between the loose sediments and the underlying bedrock. Overlapping receiver spreads of 24 geophones each provided the necessary data coverage of first breaks along the seismic profile. The data were interpreted with the help of standard inversion methods (including raytracing) as well as SRT. Figure 6.4 shows the result of the tomographical analysis with large contrasts in seismic velocities: the loose sediments near the surface are characterised by P-wave velocities of about 200–600 m/s. A further differentiation vertically or laterally of the fluvial sediments was not possible, however, unmistakably higher velocities of seismic P-waves appear in the underlying bedrock (2500–3000 m/s). The depth of the groundwater table could only be determined correctly with additional help of standard inversion methods. These results illustrate that the structure of the fluvial terrace is rather simple, giving useful hints for the reconstruction of the sedimentation history of the Rio Palpa (Fig. 6.3).

The geoelectric measuring along the identical profile line at Jauranga provided a surprising result: by means of various 2D resistivity tomographies, the loose sediments could be further differentiated laterally: fine-grained sediments,

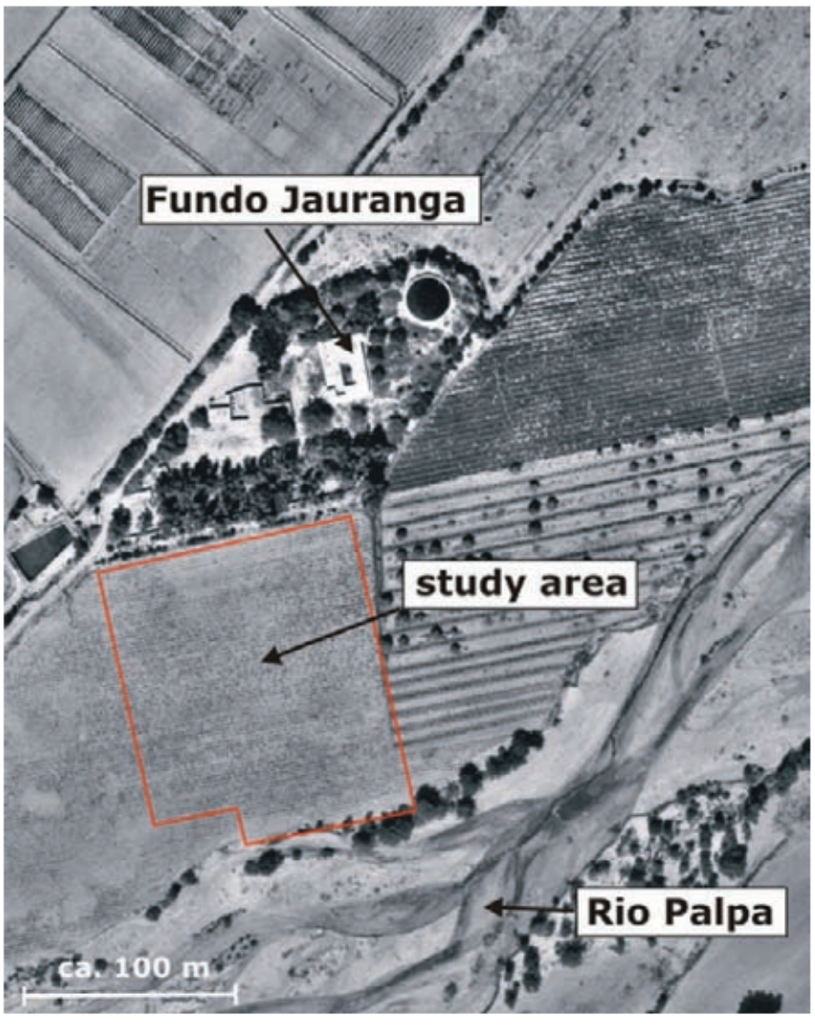

Fig. 6.2 Aerial view of Fundo Jauranga, Palpa showing the investigation area between the Fundo Jauranga and the Rio Palpa. (Aerial photo with kind permission of A. Grün, ETH Zürich)

which belong to high-flood events ('fluvial sediment 1' in Fig. 6.4), alternate with more coarse-grained sediments of distinctly higher resistivity levels ('fluvial sediment 2' in Fig. 6.4). The transition between the two different sediment types also marks the boundary between two different fluvial terraces, which could not be separated by geomorphological features. No embankment or

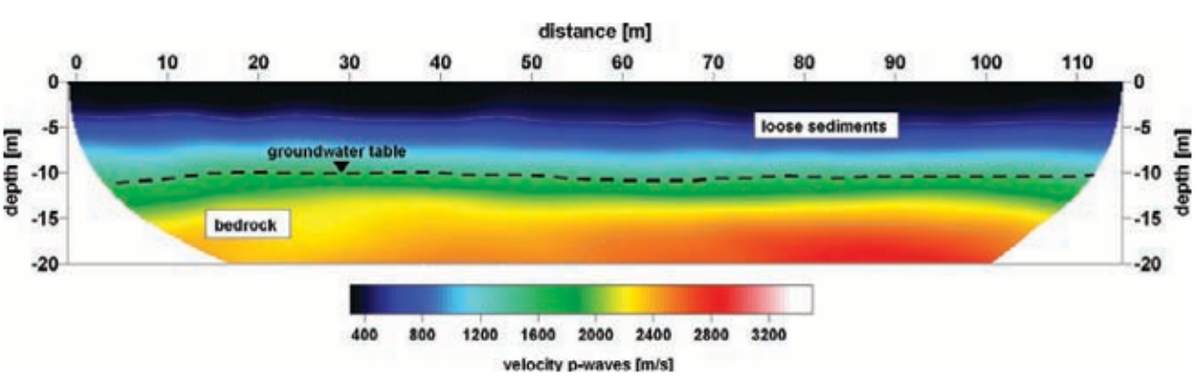

Fig. 6.3 Result of the seismic refraction tomography (SRT) on a fluvial terrace at Jauranga, Palpa. The ground-water level was identified additionally with standard inversion methods. The clear distinction between loose rock and compact rock underground is due to large velocity contrasts of seismic P-waves

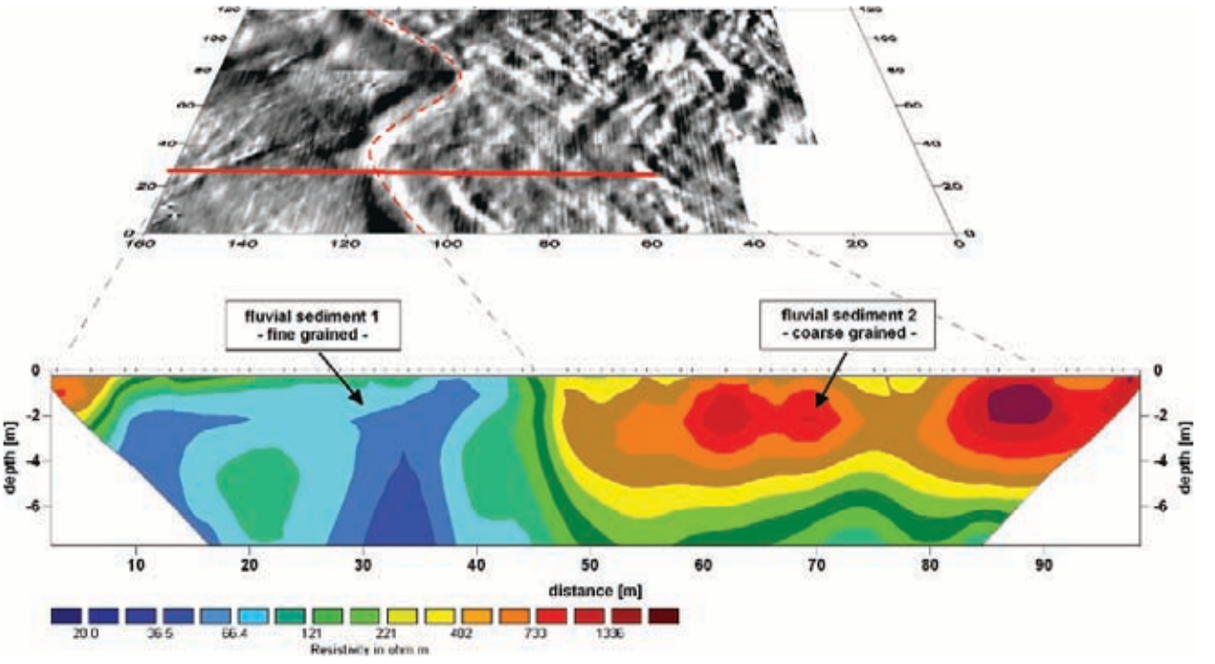

Fig. 6.4 Comparison of the results of magnetic measurements (above) and earth resistivity tomography. Note the distinct boundary in the middle of the profile which separates two different sediment types and therefore marks the transition between two different fluvial terraces of the Rio Palpa. 'Fluvial sediment 1' belongs to fine grained high-flood deposits whereas 'fluvial sediment 2' represents more coarse-grained gravel or sand. This boundary could not be recognized on the surface but is also visible in the magnetic data (*red curve*). At Jauranga, archaeological findings are limited to the area of the fine grained 'fluvial sediment 1'

terrace is visible on the surface. In this case, Wenner and Schlumberger arrays were used for the measuring of 2D geoelectric tomographies.

Figure 6.4 shows in addition that the terrace limit can also be recognized in the magnetic data. This was not expected at the beginning because large penetration depths are usually not reached with magnetic measuring. This result opens up new possibilities for the use of magnetic prospection also for geomorphologic purposes.

The basis of the 3D geoelectric tomographies at Jauranga was provided by J. Fassbinder, who carried out magnetic measurements at the same location (Fig. 6.4). His results showed distinct anomalies in the magnetic data, which indicated archaeological structures only in the area where 'fluvial sediment 1' occurs. To obtain more precise information about the depth position of these potential archaeological findings, 3D geoelectric tomographies were carried out. Therefore, arrays with 10×10 electrode units in pole–pole configuration were installed. The results of the resistivity tomographies revealed well-defined areas of higher resistivity values (>300 Ωm), which are interpreted as anthropogenic structures, enclosed by loam of lower resistivity values (<200 Ωm). The data match very well with the results of the magnetic measurements. Some of the electric and magnetic anomalies were confirmed by archaeologists as former loam excavation pits (A in Fig. 6.5; Reindel this volume).

In the field of 3D geoelectric tomography it was possible to implement some technical innovations concerning data acquisition. A new cable configuration for

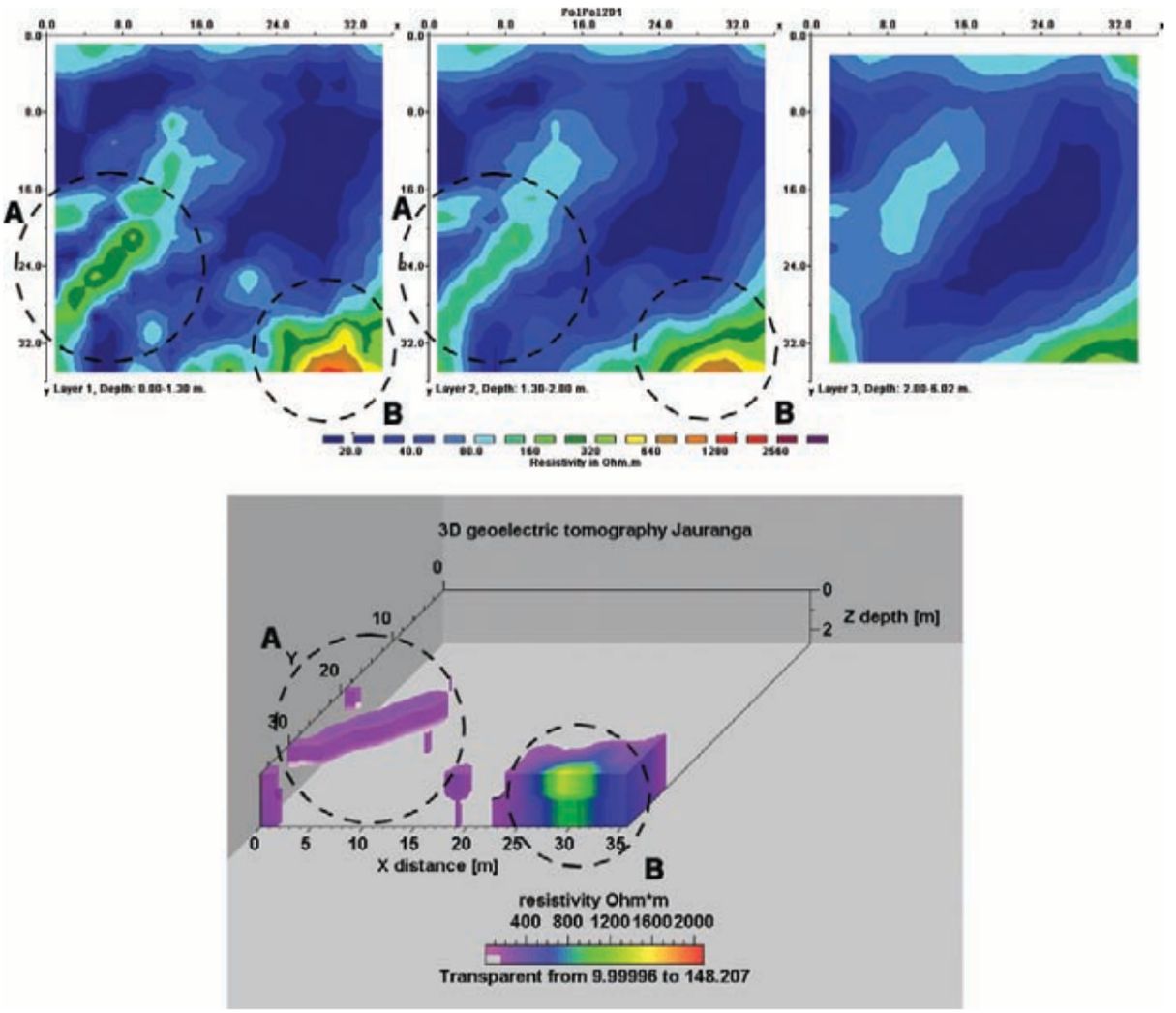

Fig. 6.5 3D geoelectric tomography at Jauranga (10 × 10 electrode units, pole–pole array). Above: horizontal distribution of the electrical resistivity values in different depth layers. From left to right: 0–130, 130–280, 280–602 cm. Below: 3D display of only the highest resistivity values. (**A**) former loam excavation pits (confirmed by archaeological excavations); (**B**) wall remnant (?)

an easier setup of electrode arrays was established as well as the implementation of an interactive configuration tool for 2D arrays in the data acquisition software (Geotom).

6.3.2 Case Study Yunama: Comparison of 2D with 3D Earth Resistivity Tomography

A similar geomorphological configuration to that of Jauranga can be found at the archaeological site Yunama, which is also located on a fluvial terrace, but on the other side of the Palpa river (Fig. 6.6). Burial places on the terrace gave first indications of archaeological structures in the underground just as did some remarkable magnetic anomalies detected by J. Fassbinder. On this basis,

Fig. 6.6 Outlay of cables for 3D geoelectric tomography on a fluvial terrace of the Rio Palpa at Yunama (array of 10 × 10 electrodes with a unit electrode spacing of 3 m)

geoelectric measuring was performed to identify the assumed archaeological findings in the underground with high precision. Several parallel geoelectric sections with narrow unit electrode spacings of 1 m were to provide resistivity data with high resolution.

The dipole–dipole configuration was applied to identify lateral structures such as archaeological findings. In addition, rectangular electrode arrays for 3D geoelectric tomography were laid out at the same location. Figure 6.7 shows the resistivity values of two combined 3D geoelectric tomographies for different depth layers. Each array consists of a rectangular grid with 10 × 10 electrodes and a spacing of 3 m. The blue colours in Fig. 6.7 represent low resistivity values and therefore indicate fine-grained high-flood sediments (resistivity values $<150\ \Omega$m), whereas the green, yellow, and red colours stand for higher resistivity values, which are related either to more coarse-grained fluvial sediments or to archaeological structures. It is not easy to decide, however, whether these anomalies are caused by natural sediment variations or if they represent man-made structures.

The comparison of these results with the results of the 2D surveys in Fig. 6.8 helps to clear up this ambiguity. The two resistivity profiles at $y = 70$ and $y = 75$ show clear horizontal layer boundaries at 2 and 4 m depth with relatively abrupt transitions to the next lower or upper levels. These different levels are supposed to having been former soil surfaces in Nasca times, which were later covered by high-flood events of the Rio Palpa. Archaeological excavations at Yunama confirmed this assumption, even though parts of the high resistivity

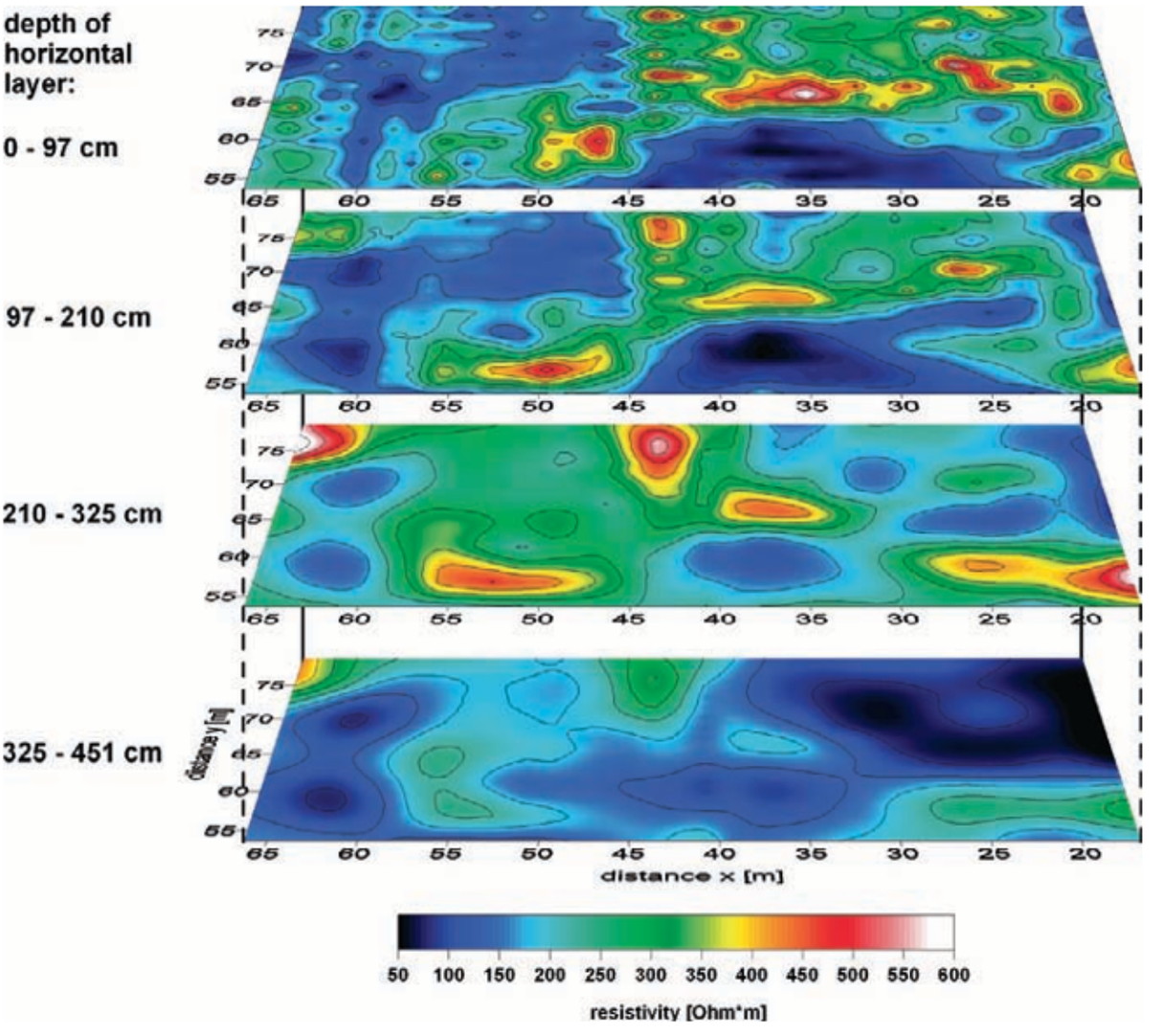

Fig. 6.7 Results of 3D geoelectric tomography at Yunama. Low resistivity values (blue, <150 Ωm) occur in fine-grained high-flood sediments; higher resistivity values are due to more coarse-grained deposits or may represent archaeological structures. Note the almost right-angled shape of some of the anomalies (two adjacent pole–pole arrays with 10 × 10 electrodes each, unit electrode spacing 3 m)

values were related to coarse-grained fluvial deposits. Figure 6.8 also shows the very good agreement of 2D and 3D geoelectric tomographies concerning this case study. By comparison of the tomograms it turned out that 3D mapping is especially useful for generating a (floor) plan of archaeological structures, whereas 2D tomographies deliver more accurate data, especially for the reconstruction of deep-lying structures.

6.3.3 Case Study PAP-83 (PV66-057): Resistivity Data Compared to the Results of Archaeological Excavation

The archaeological site PAP-83 (PV66-057) has been known as a Nasca settlement for a long time (Fig. 6.9). Although the site was heavily affected by grave robbers, magnetic measurements by J. Fassbinder revealed data that

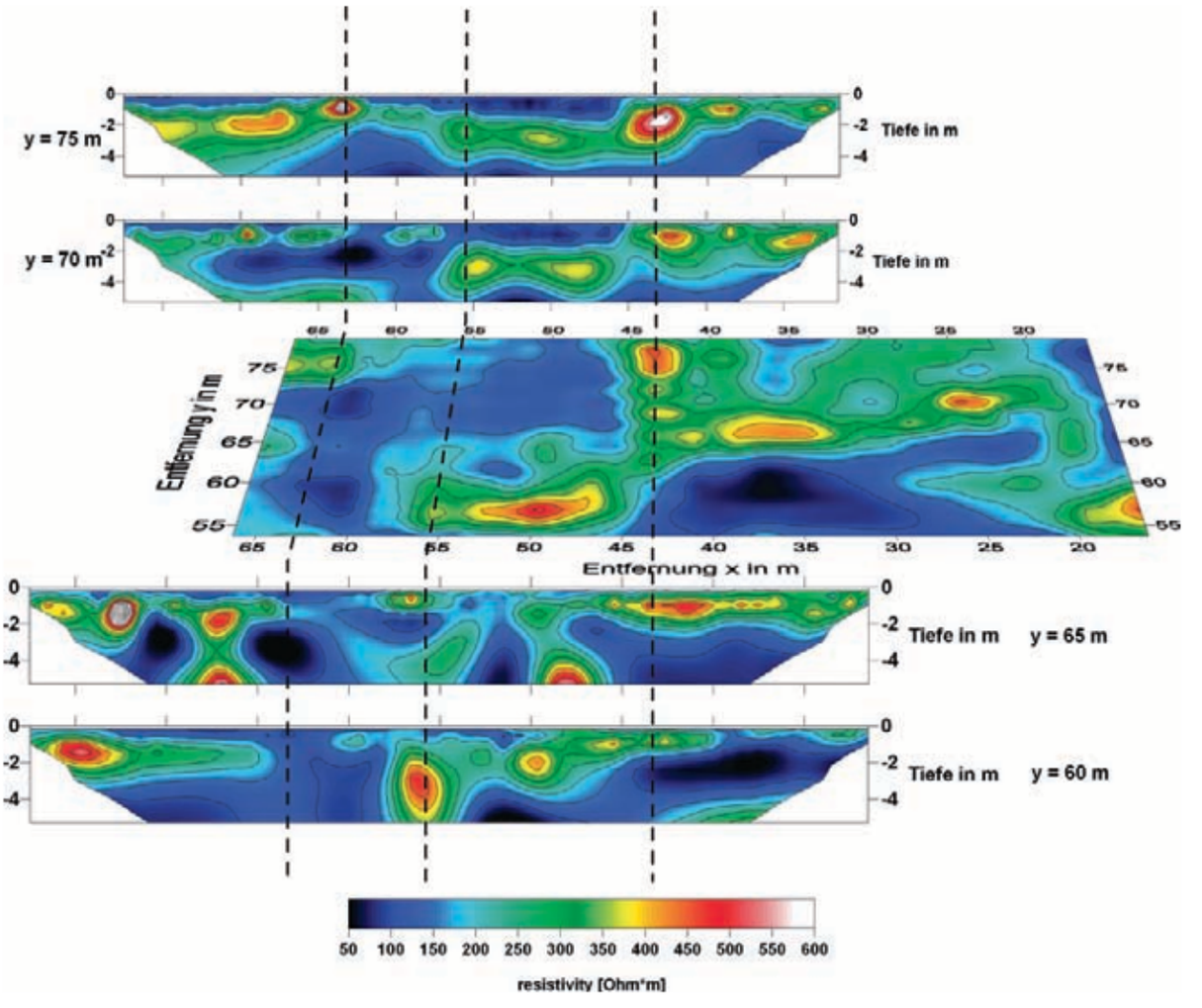

Fig. 6.8 Comparison of the results of 3D geoelectric measuring (depth layer 92–210 cm) with the results of several 2D profiles (dipole–dipole array, unit electrode spacing 1 m). 2D and 3D tomographies show a very good correlation concerning the resistivity values. Note the horizontal layer boundaries of 2D tomographies especially at $y = 70$ m, which may indicate former soil surfaces in the Nasca period

pointed to archaeological structures in the shallow subsurface, too. In the area of magnetic field work we carried out 2D and 3D geoelectric tomographies, to obtain more precise data of depth and topology of archaeological findings. In the case of 2D tomographies, a narrow unit electrode spacing of 0.5 m was used to acquire resistivity data of spatial resolution as high as possible. Schlumberger surveys were chosen to achieve the required lateral exactness. The 3D geoelectrical tomographies were measured with the pole–pole array and a unit electrode spacing of 1.5 m. From the beginning, it was planned to carry out archaeological excavations in interesting parts of the investigation area, not only to verify the right positions of archaeological findings deduced from the data but also for a detailed evaluation of the geoelectric data as a whole.

Figure 6.10 shows the resistivity values of two adjacent 3D tomographies at the archaeological site PAP-83 (PV66-057) for the uppermost layer (0–105 cm depth). Extremely high resistivity values of more than 1,00,000 Ωm appeared at

Fig. 6.9 Measuring field at the archaeological site PAP-83 (PV66-057), Rio Grande Valley

the upper and the lower part of the array (red). Furthermore, several circular anomalies (green and yellow) attracted attention. The latter anomalies could be clearly identified in the field as small pits made by tomb raiders searching for the Nasca treasures. The pits were later refilled with loose material, so that these parts show much higher resistivity values than the consolidated sediments of the surrounding area.

In the course of archaeological excavations it became clear that the big red spot in the upper part of the measuring field (Fig. 6.10, *y* distance approx. 14–22 m) with the highest resistivity values was due to layers of straw mats. The high proportion of organic material and the very loose layering caused these

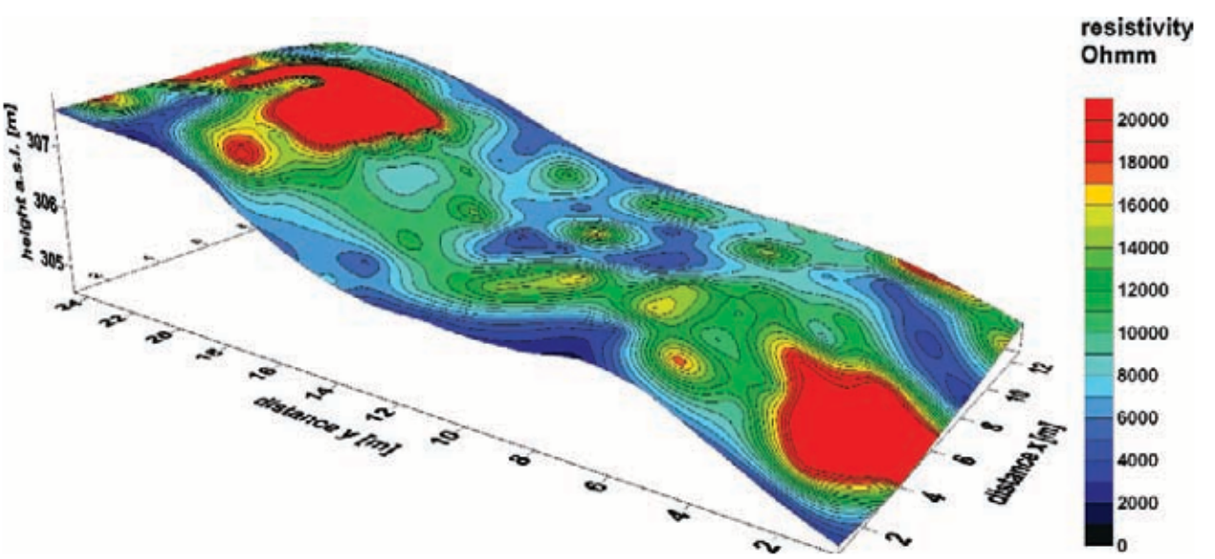

Fig. 6.10 Result of two collated 3D geoelectric tomographies at the Nasca settlement PAP-83 (PV66-057): distribution of the specific resistivity in the depth layer 0–105 cm. The red coloured areas with extremely high resistivity values represent layers of straw mats (Fig. 6.11; pole–pole array, unit electrode spacing 1.5 m)

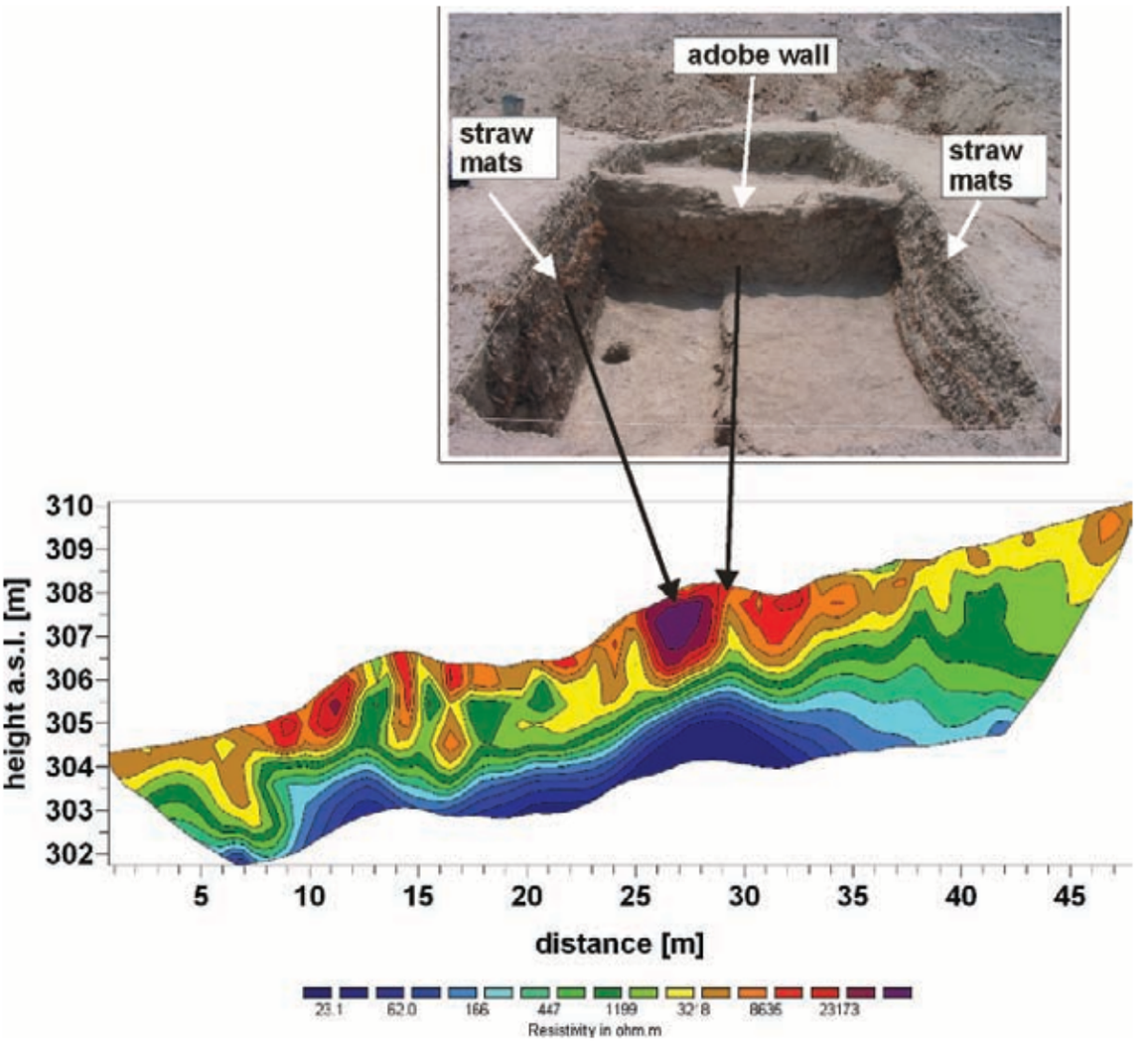

Fig. 6.11 Result of 2D tomography at PAP-83 (same area as Fig. 6.10, $x = 6$ m, Schlumberger array, spacing: 0.5 m) and comparison with archaeological excavation (*above*). The layers of straw mats with extremely high resistivity values (*red*) and the adobe wall are clearly represented in the geoelectric data. Other parts of the tomography (e.g., 10–20 m) show anomalies which are probably also due to archaeological findings

values. As seen in Fig. 6.11, the straw mats adjoin adobe walls of relatively lower resistivity values (ca.1000–5000 Ωm). Figure 6.11 also shows the result of a 2D Schlumberger survey in the same area. The straw mats and the adobe wall were identified clearly in the tomogram. Resistivity values <1000 Ωm at the basis indicate the underlying bedrock (blue), whereas the first 1–2 m of the shallow subsurface seem to be very heterogeneous with possible archaeological structures also in the lower part (distance approx. 10–20 m) of the geoelectric profile.

The strength of 'real' 3D geoelectric tomographies is the possibility of slicing the whole dataset in any desired direction. Hence, archaeological findings can be visualized completely and set apart from the ambient soil or substratum. Figs. 6.12 and 6.13 display slices in x- and y-directions for the upper half of the measuring field displayed in Fig. 6.10.

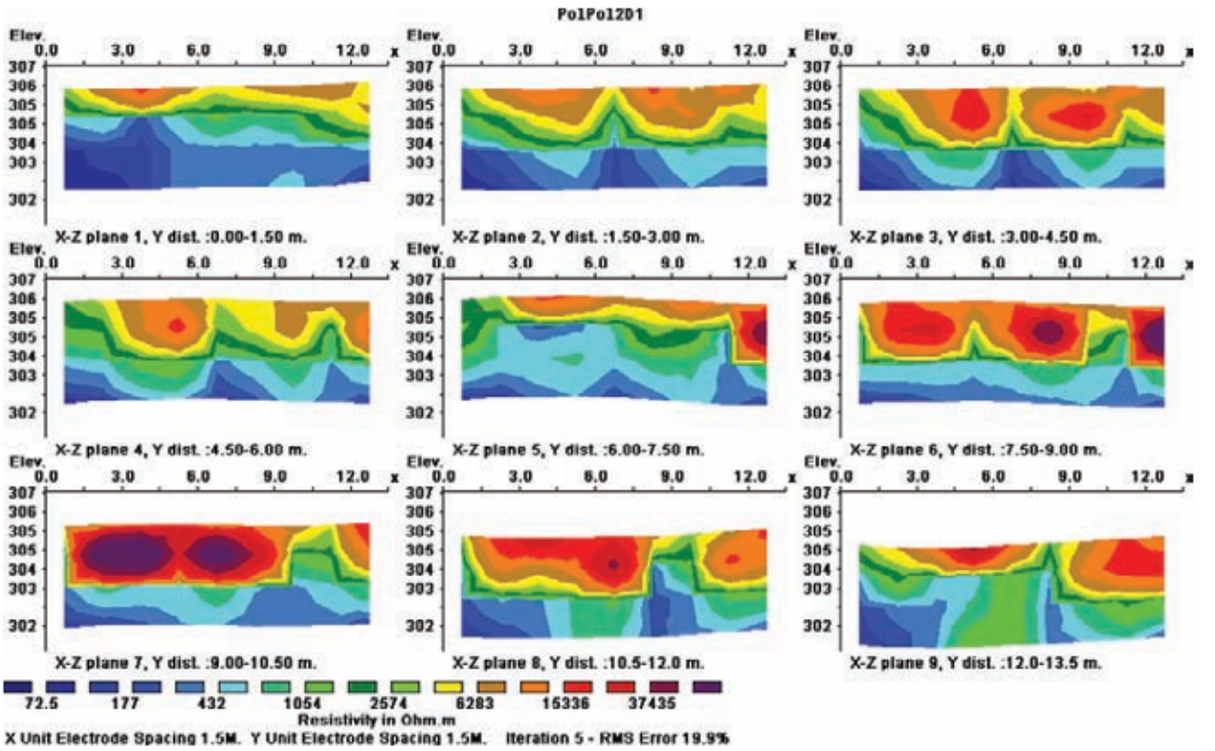

Fig. 6.12 Vertical slices in x-direction through a collated 3D dataset measured at PAP-83 (PV66-057) of the *upper half* of the area displayed in Fig. 6.10 (pole–pole array, unit electrode spacing 1.5 m). The anomaly of high resistivity values (layers of straw mats, Fig. 6.11) appear between $y = 7.5$ m and $y = 10.5$ m (*red*)

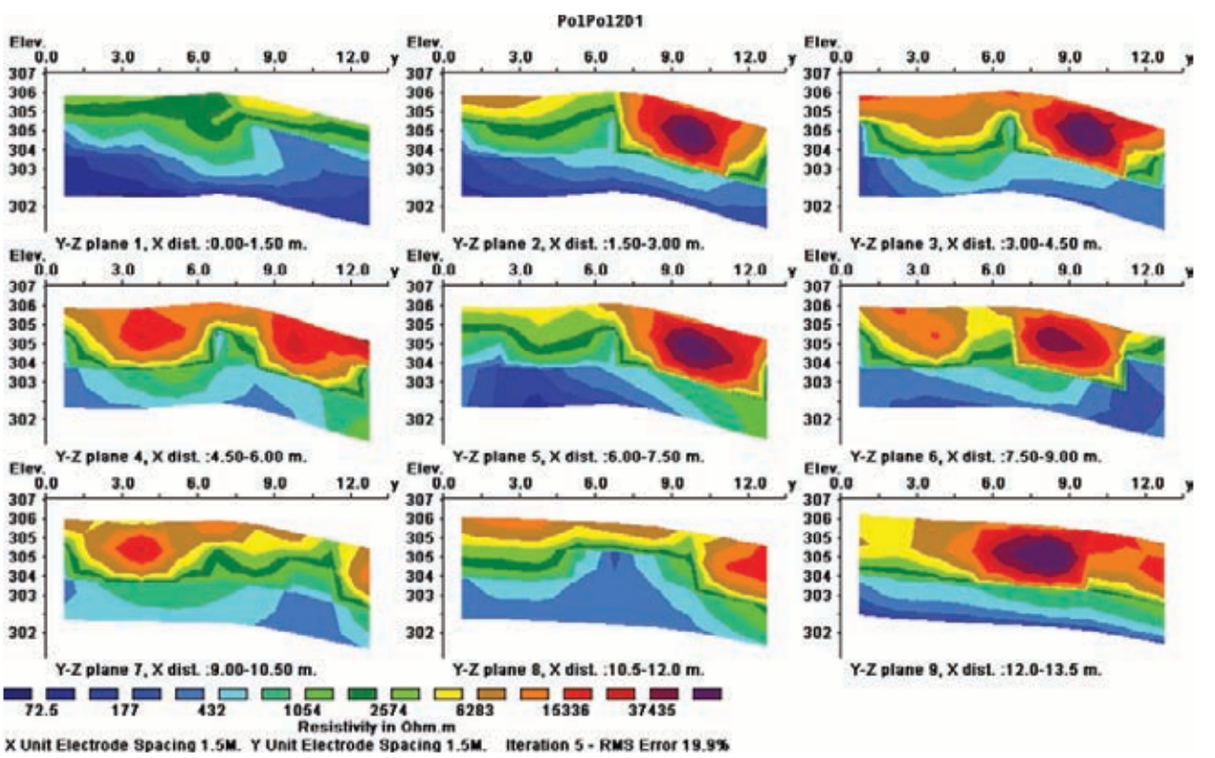

Fig. 6.13 Vertical slices in y-direction through a collated 3D dataset measured at PAP-83 (PV66-057), *upper half* of the area displayed in Fig. 6.10 (pole–pole array, unit electrode spacing 1.5 m). The anomaly of high resistivity values (layers of straw mats, Fig. 6.11) appear between $x = 3$ m and $x = 9$ m (*red*)

6.4 Conclusions and Outlook

The application of sediment tomography in the hyperarid environment of southern Peru produced promising results in the context of (geo-)archaeological investigations. Although the main focus of sediment tomography was the geoelectric investigation for archaeological prospection, the results of seismic refraction tomography revealed valuable data, particularly in the field of landscape evolution. Information on soils and sediment structures even of the deeper subsurface is an essential prerequisite for the interpretation of archaeological sites or settlements with regard to the environment and its changes through history (Hecht 2007). Our results show that the combination of geoelectric and magnetic surveys is exceptionally suitable for archaeological purposes. Magnetic measurements can quickly yield detailed information about very large areas on the basis of which more narrowly focused investigations, such as earth resistivity tomography, can provide precise information about the depth and topology of archaeological structures (Hecht and Fassbinder 2004).

If possible, 2D and 3D geoelectric surveys should be performed together, because of the different strengths of each procedure: 3D measurements are appropriate to obtain a clear layout of archaeological structures, whereas 2D tomographies, especially in case of dipole–dipole arrays, normally provide more detailed data along a line because of the higher spatial resolution. Therefore, the improvement of the spatial resolution of 3D geoelectric surveys is one big challenge for the future from a methodological point of view. In addition, the measuring time in extremely dry substrata is two to three times longer than under humid conditions and should be reduced. To learn more about the characteristics of resistivity values of archaeological findings it is of particular importance that the results of the tomographies be compared to archaeological excavations directly. The more geophysical and archaeological data are compared, the better the interpretation of resistivity tomographies should be even if no excavations are carried out. Moreover, a better understanding of geoelectric data on archaeological sites will help to achieve a better understanding of the archaeological sites themselves.

Chapter 7
The Field of Sherds: Reconstructing Geomagnetic Field Variations from Peruvian Potsherds

Florian Stark, Roman Leonhardt, Jörg W.E. Fassbinder and Markus Reindel

Abstract Well dated potsherds of Peruvian ceramics, comprising nine different cultural phases from 1000 BC to 1400 AD were studied providing the unique opportunity to establish a geomagnetic field intensity curve for Peru. Rock magnetic experiments revealed magnetite and maghemite as main carrier of the thermoremanent magnetization (TRM). Archaeointensities are determined using a Thellier-type technique (MT4), including checks for magnetomineralogical changes during laboratory treatment and multidomain (MD) bias. Additionally, TRM anisotropy tensors and cooling rate dependencies are measured and corrected for. Both experiments, carried out for the first time on Peruvian ceramics, emphasise that these corrections are critical factors in archaeointensity determinations. Our new high quality data set shows that the average intensity of the investigated cultural phases is about 35% higher than the present day local geomagnetic field. Besides three intensity maxima at 350 ± 50 BC, 210 ± 120 AD and 720 ± 100 AD a significant decline around 250 ± BC, complying with today's magnetic field strength is found. Comparing the new established intensity curve with French and Syrian data, almost no concordance is found. Beneath the intensity maximum in the year 200 AD two further outliers of the epoch of the Middle Horizon (620–820 AD) and the epoch of the Late Intermediate Period (1000–1400 AD) give hints of three archaeomagnetic jerks, which fit very well to the French jerks.

F. Stark (✉)
Department für Geo- und Umweltwissenschaften, Bereich Geophysik,
Ludwig-Maximilians-Universität, München, Theresienstraße 41,
80333 Munich, Germany
e-mail: stark@geophysik.uni-muenchen.de

M. Reindel, G.A. Wagner (eds.), *New Technologies for Archaeology*,
Natural Science in Archaeology, DOI 10.1007/978-3-540-87438-6_7,
© Springer-Verlag Berlin Heidelberg 2009

7.1 Introduction

Our earth is shielded by its magnetic field, which largely protects us from solar wind and cosmic radiation. This shield, however, underwent dramatic changes in the earth's history. Even during the past centuries recordings of observatories and mariners revealed a significant attenuation of the earth's magnetic field (McElhinny and Senayake 1982; Jackson et al. 2000). Firm conclusions about the reasons and the consequences of this decrease, however, cannot be drawn from this short period of direct observation. In order to extend the observational time range beyond direct field measurements conducted during the last three centuries, information can only be gathered by palaeomagnetic or archaeomagnetic data.

Burned archaeological and historical materials such as kilns, bricks, tiles, and pottery record the direction and intensity of the ambient geomagnetic field during cooling. This stored information is then reconstructed by archaeomagnetic techniques. Since the pioneering work of Thellier in the 1930s archaeological material has been recognised as an excellent recorder of geomagnetic field variations over the past few thousand years.

A considerable amount of archaeomagnetic intensity data, especially of the last three millennia, is already available. However, the geographic distribution of these sites is very poor. As a matter of fact, most of these studies have been carried out on samples from the northern hemisphere, providing a detailed temporal geomagnetic field evolution of high spatial resolution within Europe (e.g., Kovacheva et al. 1998; Chauvin et al. 2000; Genevey and Gallet 2002). For other regions of the globe, in particular the southern hemisphere, both temporal and spatial resolution are far less developed. Results from Africa (e.g., Odah 1999), Asia (e.g., Shaw et al. 1999), North America (e.g., Bowles et al. 2002), and South America (e.g., Gunn and Murray 1980; Yang et al. 1993) indicate distinct differences between the observed regional geomagnetic field variations, which are likely related to the secular variation of the earth's field. In addition to poor global and temporal coverage, a significant amount of archaeomagnetic data was obtained in the 1960s–1980s and is likely to be affected by unrecognised errors to the determinations. Usually, an intrinsic anisotropy in acquisition of a TRM is observed in historical material. In particular, pottery samples show strong magnetic anisotropy which could lead to archaeointensity errors of 30–60% for wheel-thrown pottery (Rogers et al. 1979). A further error source in archaeointensity determination is the difference between cooling rates in the laboratory and in the historical past (e.g., Fox and Aitken 1980).

In many older studies the possible bias of these processes is not taken into consideration. Therefore, in combination with the insufficient global and temporal coverage of archaeomagnetic data, a reconstruction of the evolution of the global magnetic field is significantly hampered. These restrictions can only be overcome by new high-quality data, in particular, from poorly constrained areas such as South America.

In addition to an improvement of global field models, well-defined regional archaeomagnetic records can also be used to date burned archaeological materials. For an unambiguous predication the full archaeomagnetic vector (inclination, declination, and intensity) is needed. This vector can often be obtained from kilns. Samples from bricks, tiles, and ceramics provide mostly only information about the intensity.

Sixty very well dated potsherds of Peruvian ceramics were recovered during excavations in several sites in the Palpa area. These potsherds, comprising nine different cultural epochs from 1000 BC to 1400 AD, give the unique opportunity to establish a geomagnetic field-intensity curve for this region of the southern hemisphere. The independently known ages are well determined by means of pottery style and a combination of radiocarbon methods and stratigraphical layering of the archaeological finds. A modified Thellier-type technique, including checks for magnetomineralogical changes during laboratory treatment, as well as multidomain (MD) remanence bias was used. TRM (thermoremanent magnetisation) anisotropy tensors and cooling rate dependencies are determined and corrected for. Based on our new data a regional intensity variation curve for Peru during the last three millennia is established.

7.2 Sample Description

All potsherds used for this study were recovered during the excavations at the surrounding area of Palpa in South Peru (14.32°S; 75.11°E). They comprise a timeframe of nine different cultural periods of ancient Peru (Table 7.1). Each of these periods is represented by five different sherds (samples). The earliest investigated ceramics were produced during the late Initial period, followed by the different phases of the Paracas period and the Nasca period. The latest investigated ceramics are from the Middle Horizon and the subsequent Late Intermediate periods. Moreover, there were further potsherds available. They dated from the Paracas, Nasca, and Late Intermediate periods. However, they were less well dated and thus could only roughly be associated to their periods. Altogether 60 different potsherds were investigated.

Clay is the starting material of ceramic manufacture. It was found in the river oases near the settlements of ancient Peruvians. Important for the archaeomagnetic investigations are the small entries of ferrous minerals in the clay, which are able to acquire a remanent magnetisation. The most frequent minerals are magnetite (Fe_3O_4), maghemite (γ-Fe_3O_4), and hematite (α-Fe_3O_2). The ancient Peruvian ceramics developed enormously between 1000 BC and 1400 AD. The Nasca people especially excelled in the production of pottery, which is unlike that of other Peruvian cultures. Each cultural phase

Table 7.1 Chronology of the investigated potsherds

Period/Phase	Timeframe	Origin	Pottery Style
Initial Period	1140–890 BC	Pernil Alto	Hacha/Pernil Alto
Early Paracas	800–550 BC	Mollake	Ocucaje 3
Paracas	600–200 BC	Jauranga	Ocucaje 5 to 9
Middle Paracas	550–370 BC	Jauranga	Ocucaje 5/6
Late Paracas	370–200 BC	Jauranga	Ocucaje 8
Late Paracas	370–200 BC	Jauranga	Ocucaje 9
Nasca	100–440 AD	La Ventilla	Nasca 1 to 5
Early Nazca	90–325 AD	Los Molinos	Nasca 3/4
Middle Nazca	325–440 AD	La Mina	Nasca 5
Middle Horizon	620–820 AD	Los Molinos	Loro
Late Intermediate period	1000–1400 AD	Chillo	Ica
Late Intermediate period	1150–1400 AD	Chillo	Ica

The pottery styles are very distinguished for every historical phase. When possible the new datings of Unkel (2006) were used.

has more or less its own style. Therefore the pottery is used as a cultural marker.

Nevertheless, only little is known about the manufacturing and burning techniques. About two-thirds of the sherds are of grey and black colour, which indicates that the pottery was burned under a reducing atmosphere. The remaining sherds show reddish colours, which were generated during firing in oxidising condition. The firing took place in pits, where the attained temperature should be sufficient to record exclusively the ambient ancient magnetic field during cooling. Furthermore, the effect of different cooling rates between the ancient procedure and treatment in the lab has to be considered. We assume that the pottery was left in the fire pit until it cooled down. A slow cooling rate of 6–12 h, suggested by archaeologists, faces an about 55 times higher cooling rate in the lab. Due to magnetomineralogical interactions, which could lead to an over- or underestimation of intensity, this effect must not be ignored.

Although it is assumed that there was no wheel-thrown pottery, there is still a considerable anisotropy effect which stems from the preferential alignment of the magnetic particles during shaping of the pottery. Both effects are corrected by determining a cooling rate correction factor (CR) and a tensor of anisotropy (ATRM). In order to test the effect of the anisotropy correction, a modified sampling technique is introduced. Two samples (5 mm) are taken from each sherd. One is drilled perpendicular to the surface, the other within the plane of the sherd (Fig. 7.1). After intensity determination and successfully applying the ATRM correction factor, these two values of a sherd need to converge. To analyse the magnetomineralogy in the potsherds, a third specimen is used for standard rock magnetic investigations.

Fig. 7.1 Typical Peruvian potsherd sampled with our newly introduced technique. One specimen was drilled perpendicular, and the other within the plane of the potsherd

7.3 Magnetic Mineralogy

For a better understanding of the behaviour of the samples during the archaeointensity experiments, magnetomineralogical investigations were conducted in the geophysical laboratory at the University of Munich. The goal of the magnetomineralogical experiments is to identify magnetic phases and estimate their domain states. Therefore one specimen of each sherd was investigated. Isothermal remanent magnetisation (IRM) acquisition, backfield curves, hysteresis loops at room temperature, and thermomagnetic curves ($B = 33$ mT, $T_{max} = 700°C$) were measured for one specimen of each sherd using a variable field translation balance (VFTB). After heating the sample to 700°C, the IRM/backfield measurements were repeated.

Deduced from thermomagnetic measurements, magnetite, respectively, impure magnetite, is the dominating magnetic material. In addition, some sherds also contained hematite and maghemite, whereas maghemite was exclusively found in grey and black sherds.

Two different types of thermomagnetic curves can be identified. Type 1 has one Curie temperature T_C ranging between 550 and 585°C and shows an almost reversible curve indicating magnetite as the main carrier of the remanence. The cooling cycle is generally slightly below the heating cycle after heating to 700°C, signifying a transformation of a magnetic phase to a non- or a less-magnetic phase (Fig. 7.1a). The difference between the heating and cooling cycles is more pronounced when a second magnetic fraction with T_C ranging between 595 and 630°C is found, which is only observed in grey and black potsherds (Type 2). This phase is not, or only to a very limited extent, present in subsequent cooling runs (Fig. 7.1b). It is interpreted as maghemite, which could have T_C values ranging from 590 to 640°C (Dunlop and Özdimir 1997). This high stability of maghemite during the heating run up to 630°C can be explained by Al^{3+} and/or Mg^{2+} substitutes.

Heating to 700°C, however, leads to a transformation of maghemite towards the less-magnetic hematite. This conclusion is supported by IRM/backfield measurements after the 700°C heating/cooling run, which show an increase of

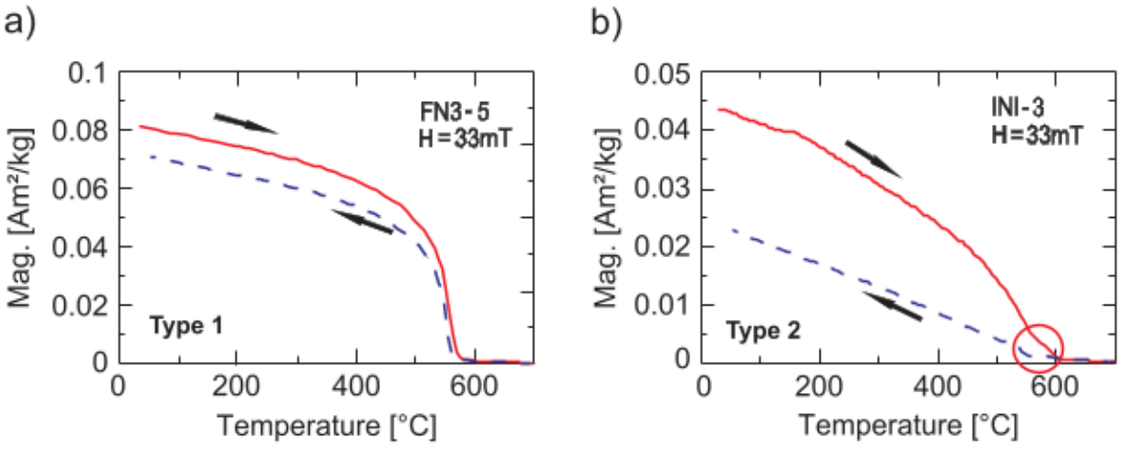

Fig. 7.2 Two different types of thermomagnetic curves can be identified. Solid lines show heating, and dashed lines cooling cycles. (**a**) Shows an almost reversible behaviour with magnetite as the dominating magnetic phase. (**b**) In addition to magnetite, maghemite (*circle*) is present in the heating cycle, which is no longer found during cooling

the high coercivity fraction. In order to test the reversibility of heating and subsequent cooling cycles, some specimens containing maghemite were heated successively to different maximal temperatures with the final temperature of 700°C. All of them showed reversible behaviour at least to a temperature of 550°C (Fig. 7.2).

7.4 Archaeointensity Determination

To determine the archaeointensity, we used minicores with a diameter of 5 mm and a length of 4 mm. Using minicores has the advantage of short heating and cooling cycles, which saves time and keeps thermal alteration on a very low level. Moreover, sample material is saved. All thermal experiments (Thellier, magnetic anisotropy, and cooling rate determination) were conducted under atmospheric conditions in a MMTD20 thermal demagnetiser with, if necessary, an ambient laboratory field of 30 μT. The remanence was measured in a 2G SQUID magnetometer, housed in a magnetic shielded room in the palaeomagnetic laboratory of the University of Munich in Niederlippach. Subsequent to the Thellier experiments we perfomed the anisotropy and cooling rate determinations on the same specimens and instruments.

7.4.1 Thellier Experiments

All techniques of palaeo- and archaeointensity determinations are based on a linear relationship between an applied magnetic field and an acquired TRM. The natural remanent magnetisation (NRM) is replaced step by step with a partial thermoremanent magnetisation (pTRM) in a known laboratory field

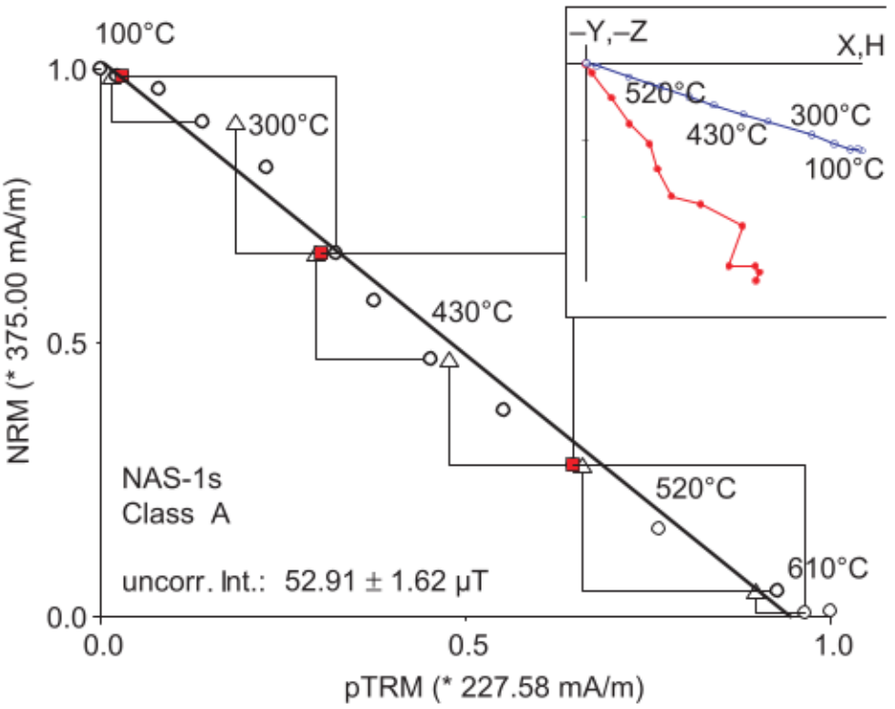

Fig. 7.3 Representative example of a successful Thellier-type experiment. The black line shows the linear fit, which was used to calculate the intensity. Additionally, the orthogonal projection (*blue open circles*) evinces a dominating single magnetic component

and plotted in an NRM–pTRM diagram. Figure 7.1 illustrates a typical NRM–pTRM diagram of a successful Thellier-type experiment on a specimen from the Nasca period. Ideally the measured points plot in a straight line, with the slope of the straight line being a measure for the archaeointensity. To determine the archaeointensities a modified Thellier-type technique (MT4; Leonhardt et al. 2003) was applied, including checks for magnetomineralogical alterations during laboratory treatment and multidomain remanence bias. Heating and cooling cycles take 45–60 min and the samples were remagnetised along their Z-axis. The obtained data were analysed and selected by the default criteria of the ThellierTool4.1 (Leonhardt et al. 2004). Furthermore, the orthogonal projection was examined as an additional selection criterion. Only segments containing the characteristic magnetic component were analysed, respectively (Fig. 7.3).

7.4.2 Magnetic Anisotropy

In order to determine the anisotropy correction factor for each specimen subjected to Thellier experiments, we used the approach of Leonhardt et al. (2006) which is based on a technique suggested by Veitch et al. (1984). To obtain the tensor of ATRM we repeatedly heated the cylindrical specimens in an ambient field of 30 µT along the $+Z$, $+Y$, $-Y$, $+X$, $-X$, $-Z$ axes. To test the stability of the specimens a final heating step in the $+Z$-direction was performed. Prior

thermomagnetic measurements revealed high unblocking temperatures for most specimens. Therefore we performed the anisotropy experiments at a temperature of 610°C. The investigated potsherds revealed a strong anisotropy of TRM and were generally characterised by oblate anisotropy ellipsoids, showing a strong axis perpendicular to the surface of the sherd and an easy plane within the surface. The calculated correction factor varied between the values of 0.71 and 1.47. In most cases specimens taken parallel to the surface showed higher correction factors than their corresponding perpendicular specimens.

7.4.3 Cooling Rate Determination

Since the 1980s there have been some theoretical and experimental investigations concerning the influence of cooling rates on TRM acquisition (e.g., Fox and Aitken 1980; McClelland Brown 1984). They show that differences in cooling rates can lead to a misjudgement of intensity data. The presence of noninteracting single-domain (SD) particles results in higher TRMs after a slow cooling run, whereas MD particles would acquire lower TRMs. In order to determine the cooling rate correction factor, the specimens were heated in a laboratory field to 610°C followed by a fast cooling run as in the Thellier experiments. The specimens cooled down from 610°C to room temperature within 21 min. The second step was a slow cooling run with the same constraints as before. This cool-down process lasted about 8 h, which is similar to the estimated historic cooling rate in ceramic production. Finally the fast cooling run was repeated to check the stability of the magnetic minerals.

Comparing both intensities of TRM of the fast cooling runs, we noticed only a small deviation. The CR correction factor, which corresponds to the ratio of slow versus fast cooled TRM, overweighed alteration distinctly (Fig. 7.2). In all cases, the acquired TRMs are higher after the slow cooling run which suggests

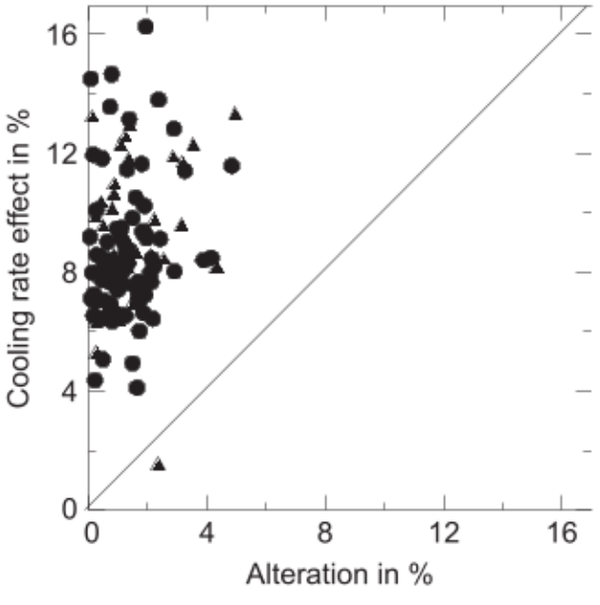

Fig. 7.4 The cooling rate effect overweighs the alteration of magnetic minerals. Alteration is calculated from the difference of the two fast cooling runs. The *black dots* are specimens, passing the standard criteria of the ThellierTool 4.1.The other specimens (*triangle*) failed these criteria

prevailing SD states. The overestimation of uncorrected intensities of 120 measured specimens would range from 1.5 to 16.3% with a mean value of 8.8% (Fig. 7.4).

7.5 Archaeointensity Results

120 specimens of 60 different sherds were investigated, with 73 suitable for archaeointensity determination. This relatively high success rate of ~61% is the result of a high physical and chemical stability of the specimens. For example, the success rate of volcanic samples ranges from 10 to 20% (Valet 2003). Two thirds of these determinations cover a fraction of 70 to 100% of the NRM, whereas the rest range from 30 to 70%. The quality factors vary between 2.7 and 46.4 with a mean value of 17.8 testifying to the high quality of the archaeointensity determination.

Unfortunately only two samples from the Early Paracas phase could be successfully evaluated. Most rejected specimens failed due to alteration during heating. Further specimens were quashed due to overlay of several magnetic components and multidomain effects. Almost half of the samples revealed a small magnetic component in a low temperature range (<200°C), which is probably of viscous origin. This small component was followed by a well-defined origin-pointing component in the middle and high temperature range, which is interpreted to stem from the initially acquired TRM. For some specimens the main component could not be isolated before reaching a temperature of ~350°C. Presumably some ceramics were used as cooking vessels and have therefore acquired a small but significant secondary TRM. Older potsherds from the Initial period and Paracas period particularly revealed strong magnetic overprints. Therefore, for some of these sherds a characteristic remanent magnetisation (ChRM) could not be isolated and their results were consequently quashed.

7.6 Discussion

7.6.1 Reliability of the Results

In the course of archaeointensity determinations one encounters inevitable potential error sources which could lead to a strong scatter of the results. Potsherds with high inaccuracies in their dating are one of these error sources. For this study, we can limit this error, because we used well-dated potsherds using different dating methods (pottery style, radiocarbon methods, and stratigraphical layering) with accuracy up to ±50 years.

According to Rogers et al. (1979) neglecting the anisotropy effect could result in misinterpretation of intensities of sometimes more than 30%. In our

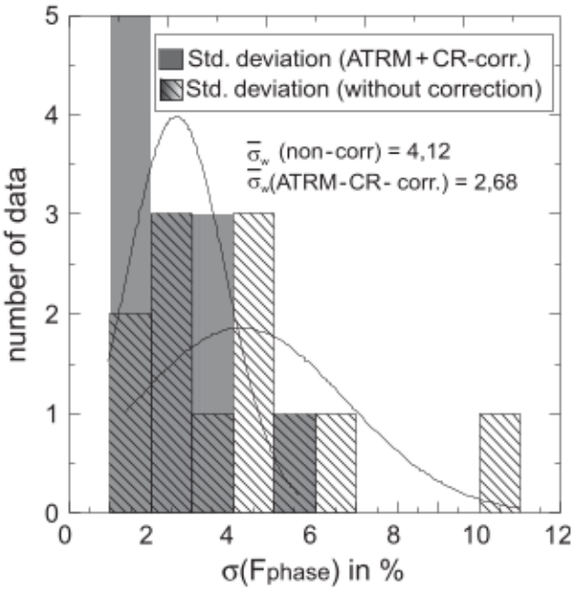

Fig. 7.5 This diagram shows the standard deviation of the magnetic intensity of each cultural phase. After applying ATRM and CR correction the scatter decreases significantly, which testifies to the efficiency of these corrections

case some specimens revealed even higher anisotropy errors up to 41%. The newly introduced sampling technique of two perpendicular-oriented samples is very suitable to test the efficiency of the anisotropy correction. Before ATRM correction, the two specimens of a sherd exhibit a significant scatter. In almost all cases, the two values match very well after correction.

Furthermore, disregarding cooling rate differences between treatment in the laboratory and the ancient manufacturing process would cause an overestimation of the archaeointensities in the case of SD-carried remanence which is present in most archaeological materials. Applied CR correction factors eliminated the bias on average 8.8%. By using both the ATRM and CR correction factors, the scatter within a cultural phase was reduced significantly. The mean standard deviation of the cultural phases decreased from 4.12 to 2.68 μT (Fig. 7.1). To analyse the specimens we applied a modified Thellier technique (MT4), which is accepted as a reliable tool to determine palaeo- and archaeointensities, particularly due to its checks for alteration and MD bias.

To calculate the archaeointensities of a cultural phase the sum of the individual uncertainties of the specimens caused by deviation from the straight line segment, anisotropy correction, and cooling rate correction are factored in following Leonhardt et al. (2006). The reciprocal of this overall uncertainty is used as a weighting parameter to determine the mean value of a sherd. All intensities of the sherds of a cultural phase were exerted to calculate the weighted average using their individual standard deviation as weighting parameter (Fig. 7.5).

7.6.2 Archaeointensity Development in Peru

Based on the new data a regional intensity-variation curve for Peru from 1000 BC to 1400 AD is established (Fig. 7.2). This curve shows that the averaged

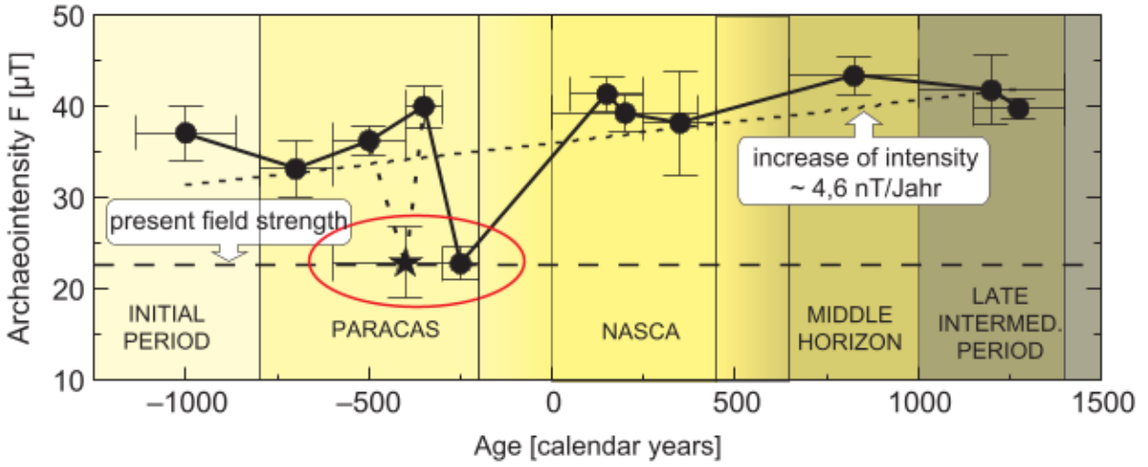

Fig. 7.6 The newly established intensity curve for Peru. In addition to the minimum at the end of the Paracas period the local intentensity was 10–20 μT higher than the present field. Furthermore, such an intensity curve could be used as a dating tool (ellipse).The value of five not-so-well dated sherds (star) seems to date from the Late Paracas phase

intensity for this investigated stretch is about 35% higher than the present local field. Besides three intensity maxima at 350 ± 50 BC (Late Paracas Oc.8, 40 μT), 210 ± 120 AD (Early Nasca, 41 μT), and 720 ± 100 AD (Middle Horizon, 43 μT) a significant decline in the year 250 ± 50 BC (Late Paracas Oc.9) to 25 μT, complying with today's local field strength is recognised. Furthermore, we have an additional set of potsherds available, which are dated from 400±200 BC comprising the whole Paracas period. The archaeointensity determinations of these samples revealed the same low value of 25 μT as the Late Paracas Oc.9 samples. Therefore, we can assume that these sherds date from the same late Paracas phase. As a consequence this high-quality intensity curve supports dating of archaeological materials.

Old datasets of this region from earlier studies indicate an enormous scatter of the intensity values and exhibit mostly higher intensities in comparison to the new dataset. This difference is interpreted to be related to unrecognised errors in the old intensity values (e.g., magnetic anisotropy, cooling rate differences, alteration, and MD effects were mostly not considered; Fig. 7.6).

7.6.3 Comparison with Contemporaneous Datasets of Other Regions and Continents

Comparing the virtual axial dipole moments (VADM) of the newly obtained dataset (representing the South American continent) with European, Asian, and global data, processed by Yang et al. (2000) shows distinct differences, in particular in comparison to the European dataset.

The Asian curve behaves to a certain extent similarly to the Peruvian data. Between 1000 AD and the present, the VADM of all continents evidence a significant decrease. The red curve with triangles (Fig. 7.3) which represents the

global field development (Yang et al. 2000) is dominated by European data and therefore is similar to the European curve. When comparing the newly established intensity curve with French and Syrian data (Fig. 7.4), the differences between Europe and South America are also apparent. In contrary to a slow increase of the Peruvian archaeointensities between 1000 BC and 1300 AD, the intensities of the European and Syrian data decline. In addition there is no comparable decline between 300 BC and 200 AD. There is a different evolution of the regional magnetic field of Peru, France, and Syria. The continental differences of the local field strength, which is related to the nondipole contribution in the earth's magnetic field, demonstrate the importance of temporally and spatially well-distributed data for establishing any global field model. The lack of high-quality data particularly from the southern hemisphere can thus significantly restrict the application and interpretation of such models.

Additionally, the Peruvian intensity curve was investigated for intensity peaks which were found in French archeomagnetic data. These peaks are defined as archeomagnetic jerks, if there they coincide with sharp cusps in geomagnetic field directions (Gallet et al. 2003; Figs. 7.7 and 7.8).

Beneath the intensity maximum in the year 200 AD two further outliers of the epoch of the Middle Horizon (620–820 AD) and the epoch of the Late Intermediate period (1000–1400 AD) give hints of three archaeomagnetic jerks, which fit very well to the French jerks. Moreover, the newest model calculations of the archaeodirections of this region (Leonhardt and Fabian 2007) assume archaeomagnetic jerks for Peru.

Recent investigations (e.g., Gallet et al. 2005) indicate a possible connection between the occurrence of archaeomagnetic jerks (AMJ) and climatic changes.

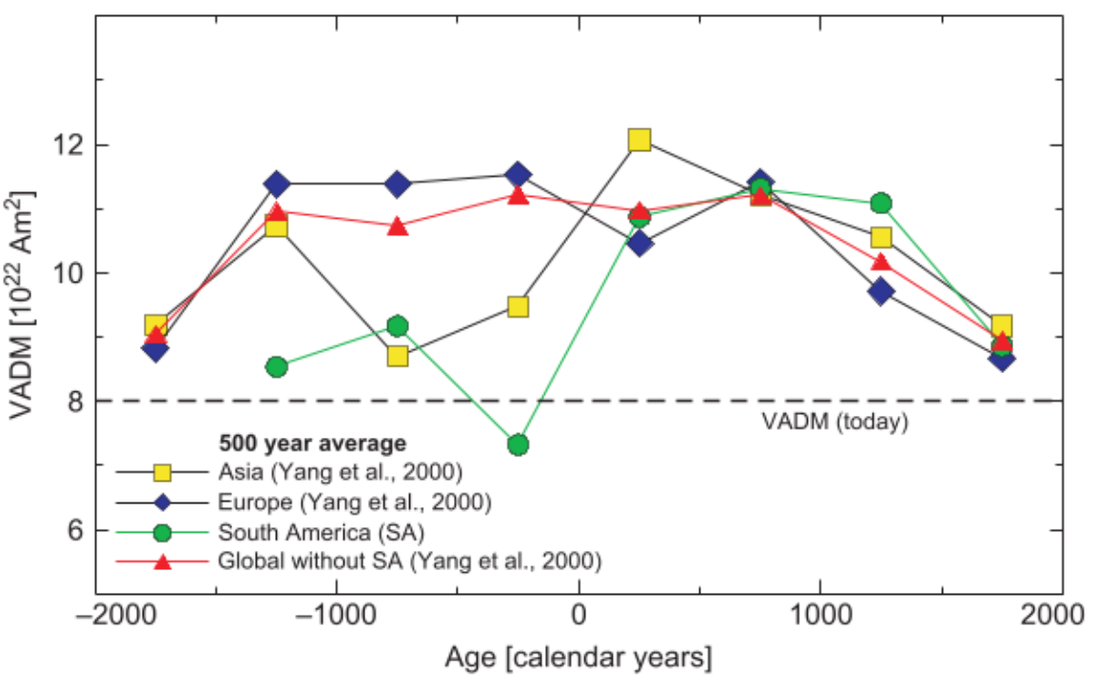

Fig. 7.7 Comparing the intensity evolution of different regions: almost no concordance is found among European, Asian, and South American data

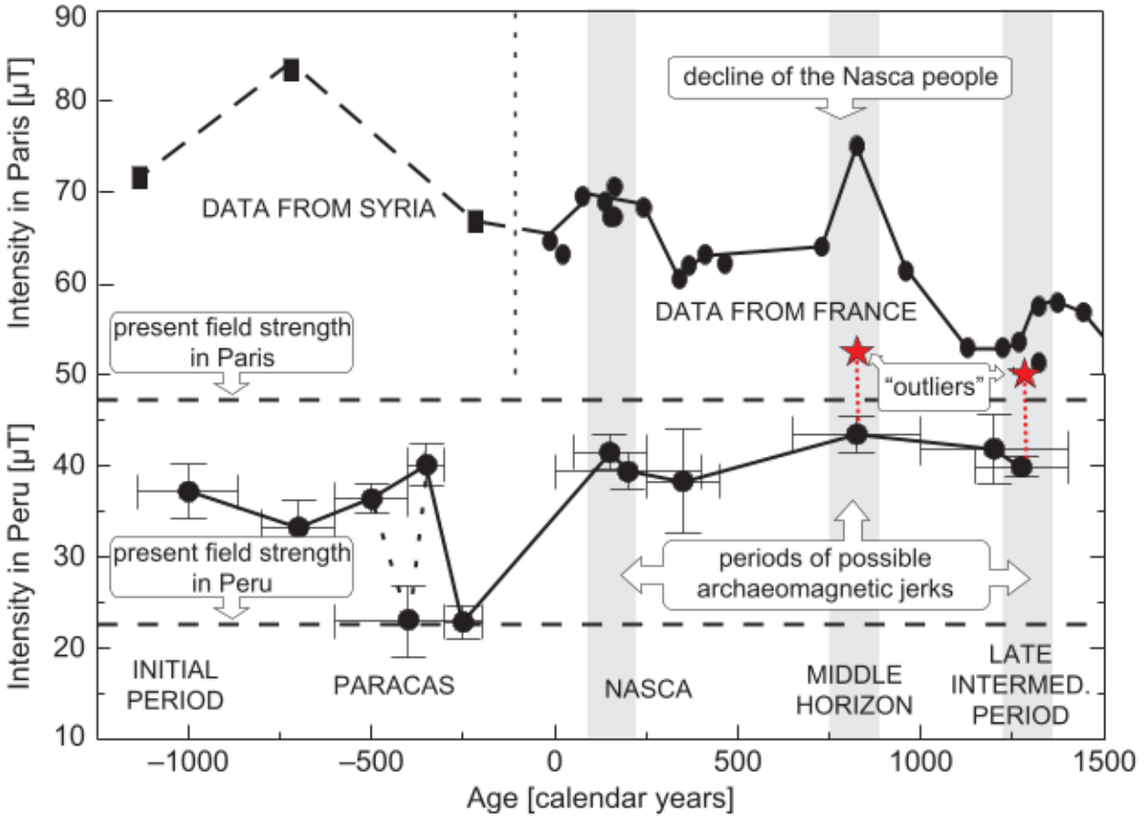

Fig. 7.8 The comparison of the Syrian/French data (*upper curve*; after Gallet et al. 2003) to the new Peruvian data (*lower curve*) reveals a different evolution. Two outliers of the Peruvian data (*red stars*) could give a hint of archaeomagnetic jerks. These potential AMJ seem to coincide with the French AMJ (*grey bins*)

Comparing potential jerks of the new Peruvian intensity curve with the fluctuations of the lake level of Lake Titicaca and the degree of desertification of the Peruvian west coast could suggest that a short-term increase of the earth's magnetic field, interpreted as AMJ, coincides with a decrease of the sea level of the nearby Lake Titicaca and an increase of aridisation (Eitel and Mächtle this volume). Up to now, however, the resolution of the new dataset is by far too small to support or reject this hypothesis.

7.7 Conclusion

The investigated Peruvian ceramics are an excellent recorder of the ancient magnetic field. For the first time magnetic anisotropy and cooling rate corrections were applied to a Peruvian dataset. Mean values for nine cultural epochs based on up to five independent potsherds each, are characterised by low standard deviations after applying the corrections. As expected, our results indicate lower intensity values than previously published uncorrected archaeointensity data from Peru. We were able to establish a reliable intensity curve describing the geomagnetic field evolution from 1000 BC to 1400 AD which can also be used as a dating tool. This curve shows significantly stronger field

values, compared to the present-day field, throughout the past. Only at about 250 BC similarly 'low' field values as today's are observed. In order to verify the presence of intensity peaks and resulting consequences as suggested for archaeomagnetic jerks in France, however, the resolution is not yet sufficient.

Part III
Bioarchaeology

Chapter 8
From Hunters to Regional Lords: Funerary Practices in Palpa, Peru

Johny Isla Cuadrado

Abstract During the pioneering work of Max Uhle, Julio C. Tello, and Alfred Kroeber in the Ica, Palpa, and Nasca valleys on the southern Peruvian coast, hundreds of funerary contexts mainly belonging to the Paracas, Nasca, and Wari cultures were discovered, but only few studies and analyses have been made of these large collections. The same is valid for other collections excavated during the past century in the Palpa and Nasca region. Within the Nasca–Palpa Archaeological Project, more than 200 funerary contexts belonging to different cultural periods were excavated in various sites of the Palpa valleys. The earliest evidence of graves in the Palpa valleys dates to the Archaic period although the most numerous sample are those from Paracas and Nasca times. With a gap during the Initial Period and only little evidence from the Middle Horizon, funerary contexts cover the time from 3500 BC to 900 AD. This chapter presents a summary of the research carried out concerning the funerary practices, describing the main features observed for each epoch, in order to have a better idea of the mortuary customs existing in each period and the changes occurring through time. The chapter concludes with a brief outline of the funerary patterns found and their relation to the characteristics of each society's structure.

8.1 Introduction

During the research of the Nasca–Palpa Project, over 200 funerary contexts were excavated in various locations of the Palpa valleys, on the southern Peruvian coast. These funerary contexts belong to different epochs and cultural periods, spanning the time from 3500 BC to 900 AD. Although not the largest in the region, representative funerary context samples of all occupational periods

J. Isla C. (✉)
Instituto Andino de Estudios Arqueológicos (INDEA), Lima, Av. Mariátegui 155, Dpt. 111, Jesús María, Lima 11, Perú
e-mail: isla-nasca@amauta.rcp.net.pe

M. Reindel, G.A. Wagner (eds.), *New Technologies for Archaeology*, Natural Science in Archaeology, DOI 10.1007/978-3-540-87438-6_8,
© Springer-Verlag Berlin Heidelberg 2009

are now available for the first time allowing us to define the characteristics of the funerary pattern through a long period of time.

The study of funerary contexts plays a crucial role in the analysis of ancient social structures, as it provides us with the possibility of coming into almost direct contact with the cultural traditions of the pre-Hispanic people of the Nasca region, their physical conditions, and their forms of social organization in general. In this regard, it can be said that the individuals' cultural customs and position in society are more precisely preserved in funerary contexts (Chapman and Klavs 1981; O'Shea 1981). In other words: "a person treated differentially in death was probably also so treated in life; this differential treatment reflects the social structure of the society" (Goldstein 1981: 54).

Based on this approach, this article presents a summary of the research carried out in over 200 excavated funerary contexts, describing the main features observed for each epoch, from the oldest ones in the Archaic Period to the most recent ones from the Middle Horizon, thus developing a better idea of the mortuary customs existing in each epoch and the changes occurring through time. The chapter concludes with a brief outline of the funerary patterns found and their relation to the characteristics of each society's structure. Finally, it is worth mentioning that due to the nature of this book and the rich, broad, and varied sample studied, only the most general results are shown here. More exhaustive analyses are currently underway and will be presented in detail in the future.

8.2 Background

Before the twentieth century, various objects from looted cemeteries in the southern coast of Peru were already known, coming especially from the Palpa and Nasca valleys. Most objects belonged to the Paracas and Nasca cultures, whose gravelots were thoroughly looted due to the existence of tombs containing elaborate textiles and polychrome pottery. The richness of these materials attracted the interest of both archaeologists and collectors.

Consequently, in the first years of the twentieth century, almost all archaeological expeditions to the southern coast focused mainly on the search for cemeteries with intact tombs containing objects from these cultures. The most important excavations of that time include the one carried out in 1926 and 1927 by Julio C. Tello and his team in several sites of the Nasca region, especially in Las Trancas valley, where over 400 funerary contexts of the Nasca and Wari cultures were excavated (Tello and Mejía 1967). Not less important were the expeditions made between 1925 and 1929 in various cemeteries on the Paracas peninsula near Pisco, where over 600 Paracas funerary contexts were excavated (Tello and Mejía 1979). It was during these years that the first scientific records of Paracas, Nasca, and Wari burials were made. Most recently, the Italian Mission lead by Giuseppe Orefici excavated over 200 funerary contexts

belonging to the Nasca and Wari cultures at different sites in the Nasca valley (Orefici 1992; Orefici and Drusini 2003).

In contrast to the large number of currently excavated tombs, the information on such contexts remains unpublished or access to it is still limited. Data on the excavation and the description of some funerary contexts were made available through diverse publications, most of them published several years after their discovery (Strong 1957; Proulx 1970; Mason 1926; Neudecker 1979; Kroeber and Collier 1998; MAAX UNMSM 2002).

Systematic studies based on these contexts are also scarce. They include studies by Carmichael (1988) and Isla (2001a), based on a group of some 350 tombs of Nasca and Wari affiliation, where the first data on such ancient cultures' mortuary customs are found. Taking this background into account, it is important to present the study of the more than 200 funerary contexts excavated in the Palpa valleys, which are part of the Nasca–Palpa Project collection.

8.3 Sample Presentation

During the Nasca–Palpa Project, numerous funerary contexts of different cultural periods were excavated. These contexts come from several sites located in the Grande, Palpa, and Viscas valleys, although most of them were excavated in Los Molinos, La Muña, Jauranga, Pernil Alto, Hanaq Pacha, Parasmarca, and Lucriche, where area excavations have been carried out. The sample analyzed in this study comprises 219 funerary contexts excavated between 1997 and 2007, 166 of which were found intact, and 53 were partially or almost totally looted. Notwithstanding this situation, it is noteworthy that data and materials were recovered even from the latter burials, allowing us to determine their cultural affiliation with a high level of certainty. Contexts with unknown affiliation were not included in this study.

The distribution of these funerary contexts according to time periods (Fig. 8.1) shows that most of them (over 80%) belong to the Paracas (62) and Nasca (114) cultures, two of the most important social groups of the Andes, which settled in different valleys and ecological zones of Rio Grande basin, where numerous remains of their notable cultural development can be found. The other funerary contexts correspond to the Archaic Period (9) and the Middle Horizon (34), the latter being represented by the presence of the Wari culture on the southern coast. There are still gaps with respect to the Initial Period and the Late Intermediate Period. From these periods only few looted graves are known.

Due to the region's arid conditions and the sites' preferred location at the border of valleys, most funerary contexts were well preserved and, consequently, they permitted recovering complete data on the type of grave and funerary structure as well as the individuals and their associated offerings.

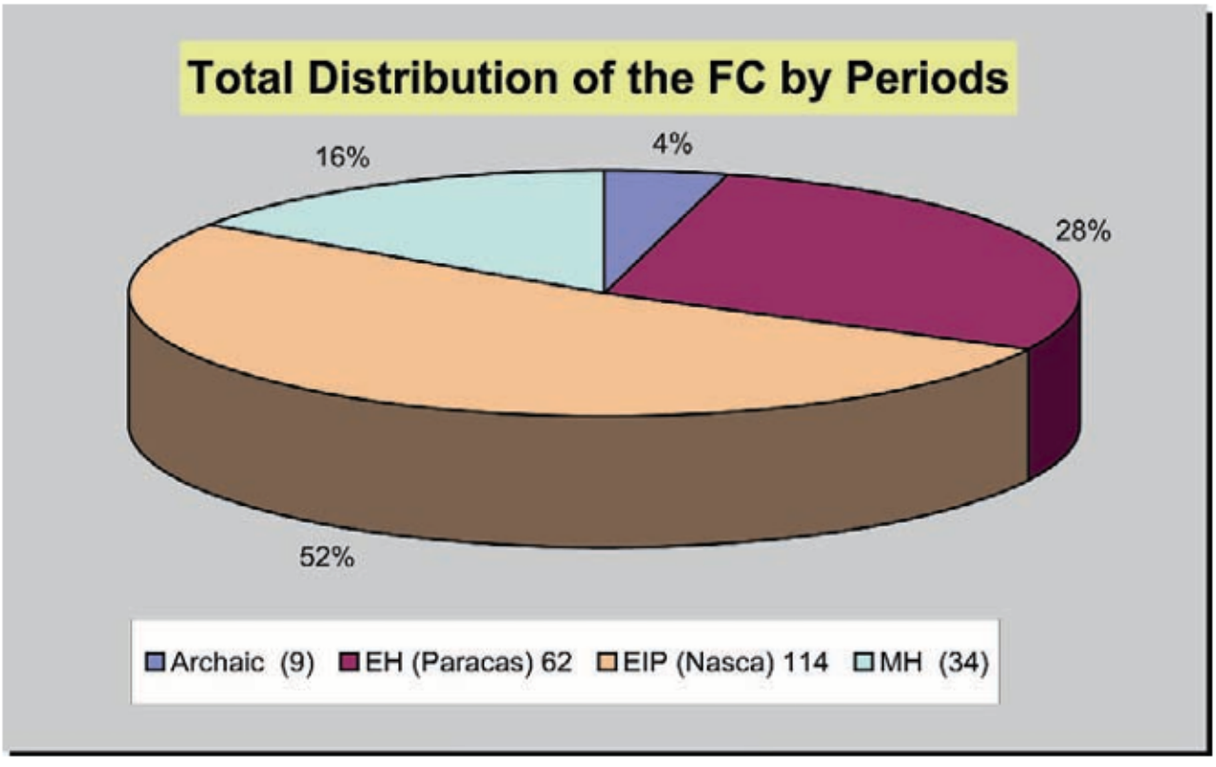

Fig. 8.1 Distribution of the funerary contexts (FC) by periods

Only in some sites where the funerary contexts were found at great depths on the valley bottom, in ravines or areas affected by the expansion of agricultural fields, the land's dampness hindered the preservation of organic materials (textiles, vegetables, etc.). In these cases, only damaged skeletal remains were found, together with some offerings such as pottery vessels, shell and bone objects, as well as lithic artifacts.

8.4 Methodology

Detailed descriptions of the excavation process, condition of the findings, tomb contents, and so on, were made for each funerary context. Likewise, records were kept of the individual's position and orientation, gender, and age, and also of the location and type of the associated objects. The textual information was complemented with general and detailed photographs and additional technical drawings to offer a better picture of each context.

Once the sample was documented, the first step of analysis was to define the chronological position and the cultural affiliation of each funerary context. Several aspects were considered: stratigraphic relations, associated artifacts, and numeric dating. Except for the contexts of the Archaic Period, whose chronological positions were determined based on stratigraphic data and radiocarbon dating, for all other cases cultural affiliation was based on stratigraphic relations and associated artifacts, that is, pottery. Furthermore, for the Paracas and Nasca cultures, in most cases the chronological placement could be

identified by style phases, following the relative chronology sequences proposed for both cultures (Menzel et al. 1964; Rowe 1960a,b; see N. Hecht in this volume). Moreover, numerous C14 datings confirmed the chronological position of the funerary contexts (Unkel 2006; Unkel et al. 2007).

Subsequently funerary contexts were examined independently according to cultural groups, mainly bearing in mind aspects related to the type of grave, treatment of the individual, and composition and location of funerary goods (Binford 1971; Tainter 1978; Brown 1995). Other variables such as gender, age, position, and orientation were also taken into account and recorded in statistical tables, although at this stage of the study they were used only as referential data. Where the sample is limited, broader descriptions were provided to identify the features that characterize the contexts of each time period.

8.5 Funerary Contexts of the Archaic Period

The first evidence of the Archaic Period comes from Pernil Alto, a site in the Rio Grande valley, where nine intact funerary contexts were excavated located under Initial Period constructions (see Reindel in this volume). Radiocarbon dates obtained from these contexts' samples determined an age between 3800 and 3000 BC, corresponding to the Middle Archaic Period. Previously, in the entire Rio Grande basin, only one funerary context of this Period had been excavated in Cahuachi, Nasca valley (Isla 1990).

The evidence documented in Pernil Alto shows that during the Archaic Period the burials were put into large pits dug into the natural soil. Generally, pits have circular or oval shapes, measuring 2.5–3.0 m in diameter, and were 0.8–1.0 m deep. Remains of floor surfaces, fire areas, and a large amount of organic remains found inside the pits suggest that they were part of the houses of that time, which were reused after abandonment for funerary purposes. Burials with two to three individuals per pit were placed separately within a layer of fill.

In these individual burials mostly the body was placed in a lateral flexed position, with the head to the side and the arms folded over the pelvis (Fig. 8.2). Two bodies were laid in a dorsal extended position, with the head tilted back. In every case the body presented a well-defined orientation and all of them were wrapped in woven mats of vegetable fiber, which usually covered the whole body up to the head. Moreover, some bodies were tied with vegetal-fiber ropes with a knot near the neck. In only two cases seed beads were found as part of the funerary goods. Finally, after placing the individual and their offerings in the pit, these were filled with a layer of dirt and vegetable remains over which, a long time later, the Initial Period structures were built.

A special case is a funerary context (CF-10) found at some distance to the others, inside a small depression dug into the natural terrain, under the Initial Period structures. It is the grave of an individual lying in a ventral extended position, with the arms along the sides of the body and one leg flexed. The skull

Fig. 8.2 Middle Archaic burial from Pernil Alto (CF-15), and some offerings from CF-10

rests on the right parietal and is forced toward the back, facing northeast. It was covered with a mat made with vegetal fibers. This individual was not wrapped in the mats seen in other cases; instead, the body was barely covered by a layer comprised of willow sticks, canes, and leaves which also showed evidence of intentional burning. This feature would indicate the existence of some mortuary ritual that entailed partial body incineration. Offerings associated with this context included sea snails, mollusks, bone and shell beads, deer horns (Fig. 8.2), gourds, carved bones, and lithic artifacts.

To date, the features documented in the Pernil Alto burials match similar contexts registered in other contemporary sites, such as Chilca and La Paloma, quite well where individuals wrapped in mats were buried under the houses' floors or in abandoned houses (Engel 1980: p. 108; Quilter 1989: p. 26). The differences observed in the bodies' position and orientation also coincide with the characteristics recorded in other Middle Archaic and Late Archaic sites excavated in the southern and central coast of Peru (Engel 1960, 1980, 1987), where a well-defined burial pattern is yet to be found.

8.6 Funerary Contexts of the Paracas Culture

In addition to the more than 600 funerary contexts of the Paracas culture excavated in 1925 on the Paracas Peninsula (Tello and Mejía 1979), the findings of the Nasca–Palpa Project in various sites of the Palpa valleys constitute the

most numerous sample of funerary contexts of that period scientifically excavated on the south coast of Peru. The sample comprises 62 funerary contexts. Most of them belong to the Late Paracas epoch (50) and were excavated at the Jauranga site. From the 12 remaining contexts, only 6 belong to the Early Paracas epoch and were excavated in Mollake Chico and Pernil Alto, and the other 6 belong to the Middle Paracas epoch and were excavated in Jauranga.

From the six Early Paracas contexts, one was excavated in Mollake Chico, a site in the middle Palpa valley, where a unique Ocucaje 3 funerary structure was discovered (Isla and Reindel 2006a). This funerary structure includes a 1.8 × 2.5 m rectangular chamber, dug into the natural soil only 1.1 m below the surface. Its walls were lined with vertically placed large flat stones with a length of up to 60 cm. The type of cover of this structure is unknown but evidence shows that after depositing the bones and funerary goods, it was completely filled. The burnt and incomplete remains of 17 individuals, including children and adults, were found inside the chamber, together with complete, but broken vessels, necklace beads, a golden ring, and an obsidian point among other artifacts that showed influences from the coast and northern highlands. In accordance with the described features, it is clearly a special case that cannot be compared to any other site on the southern coast. This underscores the need to continue investigating new evidence that would help to interpret it.

The other five Early Paracas funerary contexts, which were different from the ones at Mollake Chico, were excavated in Pernil Alto. For the most part, they are burials placed within simple pits dug into the natural soil, cutting adobe structures from the Initial Period. In two cases (CF-6 and 9) they are individual burials placed in a dorsal extended position on the bottom of the pit, with the arms extended along the sides of the body and the legs slightly flexed. In both cases the bodies were wrapped in plain cotton cloths. A third context (CF-7), the most complete of the five, was covered by stones and pieces of adobe. Two individuals were found inside the pit, lying in a dorsal extended position, with the arms folded over the abdomen and pelvis. Both bodies were wrapped in plain cotton cloths and tied with cords. Two Ocucaje 3 pottery vessels were found on the skeletons as offerings. To date, this is the only case of a double burial of the Paracas period.

In another sector of Pernil Alto, further looted funerary contexts of the Early Paracas epoch (Ocucaje 4) were studied. A considerably large tomb stands out among them. It was dug into the natural soil, and is comprised of a deep pit which constitutes the funerary chamber, and a roof made of huarango beams, stones, and mud. The offerings found in this tomb included carved sea snails, obsidian points, and pottery vessel fragments (Fig. 8.3). This type of tomb constitutes one of the immediate precedents of the barbacoa-covered tombs, which would become one of the most frequent grave types during the development of the Nasca culture.

Funerary contexts of the Middle Paracas and Late Paracas epochs come mainly from Jauranga, a site located in the middle Palpa valley, where the remains of an important Paracas settlement, occupied uninterruptedly from

Fig. 8.3 Early Paracas grave goods from Pernil Alto (PAP-265; PV66-133)

550 to 120 BC, have been discovered (Isla et al. 2003, Reindel and Isla 2006). During excavations in Jauranga, an interesting, over 3.5 m deep stratigraphic sequence was documented, with a related series of superimposed quadrangular structures. Likewise, 80 intact funerary contexts were excavated in different layers, 49 belonging to the Paracas culture, and 31 to the Nasca culture. From the Paracas contexts, only 6 belong to the Middle Paracas epoch, and the remaining 43 to the Late Paracas epoch.

Middle Paracas funerary contexts are few and were found in the layers corresponding to the first occupations of the site. Burials were deposited within simple pits dug into the natural soil or between the first abandoned structures, mainly laid in a dorsal extended position with extended or flexed legs and arms along the sides of the body or folded over the chest or pelvis (Fig. 8.4). Some exceptional cases present bodies placed slightly flexed in a lateral position, with the skulls resting on one of their sides. Generally, the bodies are oriented

Fig. 8.4 Child burial from the Middle Paracas epoch found at Jauranga (PAP-150; PV67A-011)

towards the northwest and the skulls look up or are slightly raised to look northwest. There is only one case of an infant placed in fetal position looking northeast. These bodies were probably wrapped in plain cloths like those in Pernil Alto, but the dampness of the soil barely permitted the preservation of the bones, spindles, and pottery vessels left as offerings. In almost all cases it can be seen that Middle Paracas contexts maintain the features of the Early Paracas epoch.

The sample is more numerous for the Late Paracas funerary contexts, and it has been possible to clearly define some common traits. Except for the three contexts described below, all contexts constitute individual children or adult burials placed inside pits dug into the underlying structures, and also inside pots and jars which were converted into funerary urns. Pit burials mainly contain adults placed in a dorsal extended position, with the legs extended or flexed, and the arms lying along the sides of the body, following the same pattern observed for the previous epochs. A smaller group of burials was placed in a seated posture within simple pits, legs flexed to the chest and arms folded to the chest or around the legs. Due to the area's dampness, only a few cases presented remains of plain cloths covering the bodies. Stones or adobes placed on or around the bodies were more frequent, acting as a cover or burial sign.

Burials in funerary urns were relatively few and were used mainly for children, who were placed in a seated flexed posture inside the pots or jars, which were partially broken to introduce the bodies. This type of burial seems to appear in the Late Paracas epoch and, as shown later, it was more frequent during the time of the Nasca culture.

The associated offerings of most Late Paracas funerary contexts include mainly pottery vessels, obsidian points, stone artifacts, and shell beads. Objects found in the best-preserved contexts include necklace beads, obsidian points, bone and wood artifacts, pieces of cotton cloths, gourds, and spindle-whorls.

Finally, it is worth mentioning a group of Late Paracas funerary contexts that include individual and multiple burials placed within five rectangular chambers made of mud and adobes (Fig. 8.5). The chambers are low and located one beside the other, forming a single group established in one single moment during the Ocucaje 8 phase. The three largest and best built chambers contained between three and seven individuals (including children and adults) that had been placed in a dorsal extended or lateral flexed position. Due to the reduced size of the chamber, the bodies were tightly placed one beside the other, and sometimes piled up in two or three levels. Likewise, numerous pottery vessels were left as offerings in each chamber. In these three cases, intentional burning traces were found with the individuals' bones, the offering vessels, and the internal walls of each chamber being affected. In contrast, the other two chambers were smaller and simpler, and each one contained only the remains of one person, placed in a flexed position, with no offerings. Unlike the other chambers, no traces of burning were found.

Again, we have a unique context that cannot be compared to other sites on the southern coast. It is clear that this is a special case that reveals a variation in

Fig. 8.5 Burial chambers containing single and multiple interments at Jauranga

the funerary ritual of the Paracas culture, which shows a well-prepared structure, the use of multiple burials, and intentional body burning. They may be family graves or graves of individuals related by some degree of kinship or a special circumstance in death. In any case, significant differences in the individual's mortuary treatment are observed more clearly in this period, perhaps reflecting differences in the social status of the individuals.

8.7 Funerary Contexts of the Nasca Culture

In the history of the Nasca culture research, the search and study of funerary contexts have been one of the goals that guided fieldwork of diverse archaeological expeditions carried out from the beginning of the last century in the Rio Grande basin. Since then, over 400 funerary contexts of the Nasca culture were excavated and recorded with some scientific rigor at different sites and cemeteries found in the Ica, Palpa, and Nasca valleys (Strong 1957; Tello and Mejía 1967; Proulx 1970; Mason 1926; Neudecker 1979; Carmichael 1988; Kroeber and Collier 1998; Silverman 1993; Orefici and Drusini 2003).

Funerary contexts are among the most frequent features found in the Nasca settlements that were studied during the development of the Nasca–Palpa Project in the Palpa valleys (Reindel and Isla 2001, 2006a,b). The sample analyzed in this study includes 114 contexts of different epochs, 21 of which belong to the Early Nasca, 88 to Middle Nasca, and only 5 to the Late Nasca epoch. Most Early Nasca contexts were excavated in Los Molinos, whereas Middle Nasca contexts were excavated mainly in the Jauranga, Hanaq Pacha, and La Muña sites.

The studies carried out on the funerary contexts of the Nasca culture indicate that during this period there was some standardization in the forms of burials;

Table 8.1 Distribution of the Nasca funerary contexts by burial type

Epoch	Early Nasca	Middle Nasca	Late Nasca	Sub Total
Urns	6	23	0	29
Pits	11	41	4	56
Barbacoas	4	24	1	29
Total	21	88	5	**114**

all phases show the same types of graves (Table 8.1), a similar treatment of the individuals, and the presence of the same objects as part of the funerary goods (Carmichael 1988, 1995: p. 169; Isla 2001a). From this perspective, the funerary contexts excavated in Palpa basically share the same characteristics and follow the same aspects.

8.7.1 Types of Graves

The most frequent types of graves include urn, pit, and barbacoa burials. Each one of them presents variations that depend on the size of the funerary structure as well as its preparation and finish. The large tombs excavated in La Muña (see below) constitute special cases that, undoubtedly, are related to the social status of the individuals buried there.

Urn burials account for 25.4% of the sample, and are generally made using pots or jars placed inside holes or pits of different depths. In most cases, the pits were dug into layers of fill or abandoned houses. After placing the individuals, the pits were filled up and covered by a layer of mud that included some stones and adobes. The majority of individuals buried in this type of grave are children younger than six years, usually placed in a seated posture, with legs flexed to the chest, or flexed in a lateral position. Occasionally, young or adult individuals are found placed in a seated posture, legs flexed, and arms around the legs. Generally, the burials of this category are quite simple, with individuals barely wrapped in simple cloths. Depending on their status, they may or may not include some offerings, although they usually have one to four pottery vessels.

The second type of graves consists of tubular pits, 1.5–2.0 m deep with a variable circular or oval floor 0.5–1.2 m in diameter. These types of pits amount to 50% of the sample and constitute the most frequent type of graves in all epochs of the Nasca culture (Carmichael 1998:186). In this case, the pit itself is the funerary chamber, and close to its entrance it is lined with carefully arranged medium-sized stones. In this type of tomb, the individual and the funerary goods were placed on the bottom of the pit over a thin sand layer. The pit was filled up and then a seal made of a layer of mud that sometimes included stones or adobes placed on top of the tomb. In most of these cases, the walls of the tombs do not present any type of finish, although occasionally there are pits whose walls have been lined with mud, adobe, or stones within mud mortar. In

some cases wooden poles of huarango trees were placed vertically along the wall, sometimes also in a tilted position, giving the impression of a tilted roof.

Also, there are pits that have a small roof or cover similar to the barbacoa tombs (see below), made of tied canes and huarango beams, on top of which a thin layer of leaves from the pacae tree and a mud covering were placed. Burials in this class of grave mainly contain young and adult individuals placed in seated or extended positions, although some children are also found.

Finally, the barbacoa-roofed/covered tombs amount to 25.4% of the sample, and generally they are larger and better built than the previously described graves. This suggests that they may have been used for people of higher status within the society (Isla 2001b). Most of these tombs date to the Middle Nasca epoch and were excavated in Los Molinos, La Muña, and Hanaq Pacha.

The main characteristic of these tombs is the presence of a funerary chamber with oval or quadrangular shape, 1.5–2.0 m long, set in a pit dug into the natural layer at a depth that varied between 1.5 and 3.0 m. The chambers usually have walls of adobe or stones in mud mortar, although the walls may also be formed by the natural terrain only. After placing the individual and the offerings, the chamber was covered with a quite solid roof made of a bed of huarango beams, later covered by tied canes, pacae leaves, stones, and, finally, sealed with a layer of mud (Fig. 8.6). This type of roof is locally known as barbacoa. The chambers could have an empty space under the roof, or were filled before placing it. After covering the chamber, the tomb shaft was filled up to the surface level, and a tomb sign made of a vertical cane or a small adobe and mud structure was

Fig. 8.6 Some grave goods found in an Early Nasca tomb in Estaquería (PAP-69; PV67A-005)

placed close to it. In all cases, the tombs contained the remains of a single individual (mainly adults), placed in an extended, dorsal position, legs flexed to one side.

8.7.2 Treatment of the Individual

Data regarding the treatment of individuals are very scarce, mainly due to the bad preservation of the bodies. Except for the examples observed in Los Molinos, where the terrain permitted a good preservation of organic remains, in the other cases the soil's dampness barely allowed the conservation of bones and pottery offerings.

For this reason, we can only say that all cases consisted of individual burials, which were placed predominantly in two positions: extended and seated. In the first case, the bodies were placed in a dorsal extended position, legs flexed upwards or to one side of the body. The arms were extended along the sides of the body or folded over the chest or the pelvis. In most cases, the head was tilted back slightly, facing southwest and west, although there are others that face towards other directions. This is a quite frequent position in Nasca contexts scarcely mentioned in the literature. In the second case, the individuals were placed in a seated position, knees to the chest. and arms between the chest and legs or wrapped around the legs. Only in a few cases remains from one or two plain fabrics covering the bodies were preserved. In tombs of higher status, individuals wrapped in fine plain fabrics decorated with elaborate three-dimensional fringes were also found (Fig. 8.7).

8.7.3 The Funerary Goods

The funerary goods documented in the Nasca tombs in Palpa contain a great variety of offerings, mainly comprising pottery vessels, stone artifacts, or other nonperishable materials. In accordance with the preservation level, diverse organic remains were also found. Each tomb contained 1–12 pottery vessels. The organic remains include a great variety of vegetables and fruits (maize, manioc, sweet potato, beans), maybe food to be taken by the deceased on the journey to the afterlife. They were usually contained in pottery vessels or squash containers. Similarly, guinea pigs, shrimp, and mollusk remains were also found.

8.7.4 Tombs of La Muña

The archaeological evidence shows that during the Middle Nasca epoch, the Nasca society reached its highest development level, and therefore there was a marked social differentiation (Silverman and Proulx 2002; Isla and Reindel 2006a,b). In La Muña, a special cemetery from this epoch was identified. It

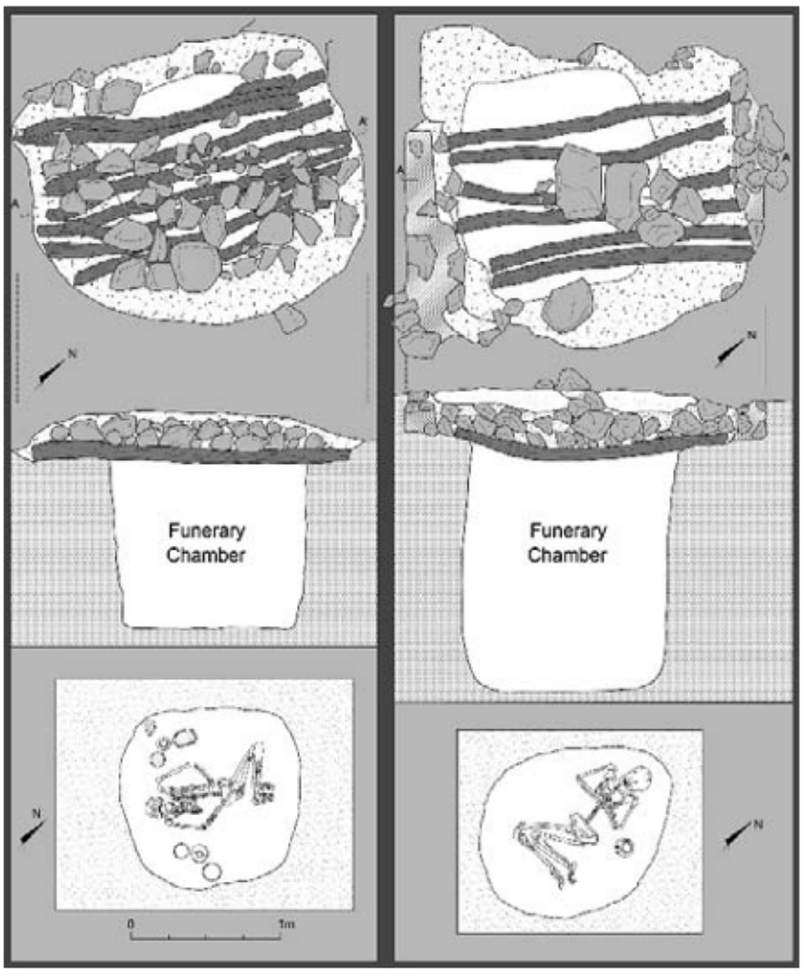

Fig. 8.7 Drawings of two barbacoa tombs from Hanaq Pacha (PAP-733; PV67B-155)

contains more than a dozen looted tombs, which were arranged on several long platforms, demarcated by large adobe walls. Six of these tombs were excavated during the fieldwork of the Nasca–Palpa Project (Isla and Reindel 2006b).

Although looted, in all the tombs data related to the construction of the funerary structure and its contents were registered. In this way, each tomb's general layout could be reconstructed quite precisely. The construction of these tombs began with the digging of a large and deep pit into the natural layer, where, at a variable depth of 5–7 m, the funerary chamber was built (Fig. 8.8). Such chambers measure 2 × 2.5 m in width and 1.8 m in height, and were made of adobe walls placed against the natural wall of the pit. The chamber floor was made of a layer of compacted mud with a highly regular surface on which was placed a thin layer of river sand. Due to the looting of the tombs, there were no details on the individual's position and funerary goods, but in every case only one skeleton per tomb was found. After placing the individual the chamber was covered by a roof made of thick huarango beams placed one beside the other, over which a layer of pacae leaves and cane branches was laid. Finally, the entire roof was covered by a thick layer of mud and stones. After this, the pit shaft was filled almost to the surface level, where a roofed platform and a rectangular floor enclosure with a small internal yard were built.

Despite having been being looted, a large amount of objects that were originally part of the funerary goods were found inside the tombs (Fig. 8.9).

Fig. 8.8 Excavation of one of the largest tombs (CF-4) of La Muña (PAP-79; PV66-049)

The materials recovered in each tomb include many fine pottery vessels and broken panpipes. Likewise, dozens of beads made from diverse semiprecious stones, *Spondylus* shell beads, and gold and copper beads were found. Additionally, in one of the tombs (CF-4) five complete *Spondylus* shells were found, one of them having a zoomorphic face carved on the inside; five obsidian points

Fig. 8.9 Grave goods found in some tombs of La Muña (PAP-79; PV66-049)

and four golden earrings shaped like chili peppers were also found. In another tomb (CF-6) 19 golden earrings shaped like killer whales were found.

Without doubt, the tombs of La Muña are among the most exceptional funerary contexts excavated in the Rio Grande basin so far. Their characteristics indicate the existence of marked social differences between groups of individuals in the Nasca society (Reindel and Isla 2001; Isla and Reindel 2006b).

8.8 Funerary Contexts of the Middle Horizon

The Middle Horizon on the southern coast, which corresponds to the occupation of the Wari culture in the region, is represented by the Loro and Chakipampa styles of Epoch 1, and by the Atarco, Viñaque, and Pachacámac styles of Epoch 2 of the Middle Horizon (Menzel 1964, 1968). The funerary contexts of the Middle Horizon excavated in Palpa come mainly from three sites, which are located in different sections of the Rio Grande valley: Los Molinos, Parasmarca, and Lucriche (Fig. 1.1 of Chap. 1 this volume). A total of 34 funerary contexts were excavated in these sites (16% of the sample), where the main features that characterize the period's funerary customs have been documented.

Although some traits observed in the Nasca culture continue into the Middle Horizon, the occupation of the Wari culture introduced substantial changes to the burial patterns of the region, especially regarding the mortuary treatment of the individuals. One of the most remarkable traits of that time was the sepulture of multiple burials. Adults and children were placed in pits and chambers that were covered with large stones or barbacoa roofs. In some of the most important graves, quadrangular stone structures were placed at the entrances of the chambers.

Albeit limited, the sample of the Middle Horizon in Palpa allows the identification of three main grave types: simple or uncovered pits, barbacoa and roofed pits surrounded by a quadrangular stone structure, and roofed funerary chambers with a stone enclosure in the upper part.

Examples of the first type have been excavated in Los Molinos and Hanaq Pacha, where individual burials can be observed. They were placed in simple pits that do not present any special structure or preparation. The pits had a circular or oval outline and were completely filled. Usually a covering of mud, which sometimes contained adobes or stones, was placed on top of the grave. The pits contain the remains of one single individual, usually in a seated position, with the legs flexed to the chest and the arms wrapped around the legs. Exceptional cases include bodies in a lateral flexed position, arms folded to the chest, or in dorsal extended position with the head tilted back. Due to the soil's dampness, in all cases only pottery vessels (Loro and Chakipampa style) were conserved as part of the offerings.

On the other hand, pit tombs with roofs made of slabs or wooden beams are similar to barbacoa-covered graves described for the Nasca culture. In this case,

the pits themselves, which were of circular, oval, or boot shapes, served as funerary chambers where the individual and the offerings were placed. Subsequently, the pit entrance was covered by large slabs or by huarango beams which, in turn, were covered by boulders and a thick layer of mud. Finally, once the chamber entrance was sealed, a layer of fill was put in place with a wooden stick or an adobe brick as a grave marker. In this type of graves, it is common to see quadrangular structures surrounding the pit entrance, simulating to some extent the Nasca elite tombs excavated in La Muña. In accordance with the tomb size and the importance of the individuals, these structures were built with a simple line of upright stones or double-faced, 50 cm high stone walls. The remains of wooden posts located in the interior corners evidence the existence of light roofs at the level of the surrounding terrain.

Fourteen tombs of this type have been excavated in Parasmarca, two of them intact and the other twelve looted, but showing the same characteristics. According to the evidence recorded in the two intact tombs, one of them contained the remains of an infant placed in a semi-flexed, lateral position, surrounded by eight vessels. The other contained the remains of two individuals, a child and an adult, with the former seemingly moved from its original position, and the latter placed in a seated flexed position. The offerings included twelve pottery vessels, one copper needle, and beads, as well as ceramic and stone spindle-whorls. Unfinished *Spondylus* beads were found near the walls that delimited the upper part of the grave structure. In both cases the vessels belong to the Loro style of Middle Horizon Epoch 1.

Finally, tombs with chambers were documented for the first time in Lucriche, a site located in the middle reaches of the Rio Grande valley, where five looted funerary structures have been excavated, that show the same construction traits (Fig. 8.10). They consisted of carefully built tombs with

Fig. 8.10 Funerary structure and offering found in CF-5 from Lucriche (PAP-180; PV66-219)

quadrangular-floor funerary chambers, 2 × 2 m long and 1.5–2.0 m deep. These chambers were built with 1.2–1.5 m high stone walls, and were roofed with large slabs and thick huarango beams which were covered with a layer of mud and stones. After placing the individual and the offerings, the tomb was covered with a thick layer of fill and on its upper part was placed a quadrangular or rectangular enclosure made of thin stone walls up to 1.5 m high.

In all cases, the materials recovered in these tombs included the remains of the bones of two or more individuals (children and adults), as well as pieces of several pottery vessels from Middle Horizon Epoch 2. The goods also included pottery figurines and spindle-whorls, shell and bone beads, copper sheets and needles, semi-precious stone beads, obsidian points, and chipped tools.

It is worth mentioning that in one of the corners of the tombs (CF-1), a small quadrangular space delimited by stones was found, containing the remains of five infants placed tightly one beside the other, as well as two offering vessels. In addition, the intact burials of three infants placed in small sand-filled pits were found in the backfill on top of the roof of another tomb (CF-5). Child burials such as the ones described here are frequent in Middle Horizon tombs (Isla 2001a,b), and undoubtedly were part of a common funerary context together with the individuals placed inside the chambers.

8.9 Summary and Final Comments

After the study carried out by Patrick Carmichael (1988) on a group of funerary contexts of the Nasca culture, this is the first study based on a collection of funerary contexts of similar size, but from known archaeological contexts of one single region that covers almost the entire cultural sequence known on the south coast of Peru. The analysis of such contexts allowed us to identify quite precisely the traits that characterized each epoch, and the changes they underwent through time. The following is a summary of the performed study, which highlights the implications for the development of sociopolitical structures in different time periods on the south coast of Peru.

The Archaic Period contexts excavated in Pernil Alto present common traits in their mortuary customs, which are characterized by individual burials, usually placed in flexed position and wrapped in mats within abandoned houses. These traits are not any different from the ones found in other contemporary contexts, located in other sites of the central and southern coast of Peru (Engel 1966, 1980). Except for some special cases, these burials usually present no associated offerings, and this indicates an absence of significant social differences between the people of that time. Nevertheless, evidence documented in Pernil Alto shows that the people of that time had a sedentary life, with a wide mobility that gave them access to distant areas, such as the coast and the highlands.

After the Late Archaic contexts excavated in Pernil Alto, the studies in the Palpa valleys present a 2000-year gap until the Initial Period. The remains of a relatively complex settlement of the Initial Period were found also in Pernil Alto; it was built with mud walls and housed a stable sedentary population that lived from agriculture. To date, it is the first settlement of that time known in the whole Rio Grande basin, and some of its aspects can be compared to the Hacha site in the Acari valley (Robinson 1994). However, no funerary context corresponding to this occupation period is yet known.

On the other hand, the evidence of the development of the Paracas culture in the Palpa valleys is copious and varied (Reindel and Isla 2007). Likewise, funerary contexts are also more numerous and better represented, especially those from the Late Paracas epoch. The study has allowed us to observe some common traits. Most of the funerary contexts contain individual burials placed in urns or pits in an extended, flexed, or sitting position. Urn burials are mainly for infants, in fetal or seated position. Only one case showed a double burial in Pernil Alto. On the other hand, multiple burials, such as the ones excavated in Jauranga, are special cases which, in turn, are quite different from the multiple burials found in the cemeteries of the Paracas Peninsula (Tello and Mejía 1979). The same can be said for the funerary context in Mollake Chico, which contained the incomplete and burnt remains of 17 individuals. Without a doubt, these are particular cases that represent a variation in the funerary customs of the Paracas period, which will be better interpreted based on future evidence.

On the other hand, although the funerary goods generally do not present any marked differences, in some cases they have differed slightly in the quantity and quality of the objects, and this may evidence social differences between some individuals. This is more clearly seen in the chamber burials excavated in Jauranga, where in the same funerary complex we found individuals with many associated vessels, and some with none at all.

Although in the excavated funerary contexts in Palpa we did not recover clear evidence that might have indicated higher status or elite membership of some of the individuals, the settlement data documented in the Palpa valleys show that during this period the Paracas culture was well established and achieved significant socioeconomic development (Reindel this volume). This was particularly evident in the Late Paracas epoch, when the number of settlements and therefore the population, and the production of geoglyphs and high-quality crafts, increased. Products from distant areas excavated in Paracas contexts in Palpa prove the existence of well-organized exchange networks, mainly between the coast and the highlands.

The significant developments of the Paracas culture in Palpa and other valleys on the south coast set the foundations for the subsequent successful development of the Nasca culture, whose artistic and cultural achievements are widely known. Accordingly, the study of the funerary contexts of the Nasca culture also shows more defined and elaborate features.

Particularly, there is an almost exclusive occurrence of individual burials in three types of graves, urns, pits, and barbacoas, that do not present major changes throughout all phases of the Nasca period. Urn burials account for almost 30% of the sample, and are mainly used for children, who were placed in three dominant positions: seated, flexed, and extended with flexed legs. Carmichael recognized in his studies about other Nasca funerary contexts only two frequent postures: seated and flexed (Carmichael 1995). It seems that the extended position with flexed legs is more frequent in pit and barbacoa tombs, as in the case of Los Molinos, Hanaq Pacha, and La Muña. Both types of graves tend to be larger in the Middle Nasca epoch. At the same time, funerary goods from Nasca tombs are richer and more varied, with more marked differences among them. This result was obtained by cross-checking information on the construction of the graves and the quality of the funerary offerings, rather than comparing depth variables and the number of objects as Carmichael did (1995: 170, Table 8.1). In this context it seems to be clear that the tombs excavated in La Muña were built for individuals of the highest status in the Nasca society, and constitute the clearest examples to illustrate such differences (Isla and Reindel 2006b).

The archaeological data recovered in the Palpa valleys show that during the Nasca period the society reached its highest political, economic, and social development level, which resulted in the establishment of larger settlements with a higher number of inhabitants, an increase in the number of geoglyphs, the construction of larger and better prepared graves, such as La Muña's, and a greater craft specialization, among other features. This evidence suggests that during the Middle Nasca epoch, the society was organized in social classes, with an elite that was governed by true regional lords.

After the collapse of the Nasca culture, the Palpa valleys, as happened with a large part of the Rio Grande basin and the southern coast in general, came under the influence of the Wari culture, which introduced some remarkable changes to the mortuary customs. During the Middle Horizon the grave types of the Nasca culture remained in use, that is, urn, pit, and barbacoa burials. However, quadrangular stone structures were added around the entrance and near the surface of higher status graves in Epoch 1, as if they were imitating the La Muña grave type. In Epoch 2 graves, these quadrangular structures are small stone enclosures that surround the entire upper part of the funerary chamber. The sitting position with flexed legs became dominant, although there are some burials placed in flexed or extended positions. The number and the treatment of the bodies changed in this period. It is worth mentioning that during this time the individual burials continued to be predominant, but almost 30% of the sample included two or more bodies per grave, usually one adult and several children. Due to the poor preservation of the bodies no bundle burials were observed (Isla 2001a).

The continuity of some funerary traits of the preceding period show the long-lasting traditions of the funerary customs, which were adopted with some minor changes by the new social structure. Nevertheless, the most significant

changes mentioned above must be understood in a context of greater social complexity embodied by the Wari culture in the Andes.

Finally, it must be stressed that this study represents a step forward in the research of funerary patterns, some of which are described here for the first time. In this regard, it must be taken into account that in several cases the sample was very limited, and in others it presents gaps that are yet to be filled. In spite of this, the obtained results are encouraging and further research will surely help to improve the concepts presented in this chapter.

Chapter 9
Talking Bones: Bioarchaeological Analysis of Individuals from Palpa

Elsa Tomasto Cagigao

Abstract Bioarchaeology, the scientific discipline that studies past societies through human remains, has had an uneven development in Peru. One of the zones of lesser development has been the south coast, probably due to the lack of scientifically recovered collections accessible to investigators. Most studies centre on the skull: cranial deformations, trephinations, and trophy heads, but little is known about the biological characteristics and levels of adaptation of the prehistoric human populations that inhabited the area.

In this work we present the results of the osteological analysis of 198 individuals recovered from funerary contexts excavated by the Nasca–Palpa Archaeological Project. The levels of adaptation of Archaic, Paracas, Nasca, and Middle Horizon populations are evaluated through demography, comparative statures, spongiosclerosis, and trauma analysis. The tendencies found suggest that the best levels were achieved during the Archaic, and the worst in Paracas. Other important findings include a differential distribution of trauma among women and men in Paracas and Nasca times, suggesting gendered activities. Finally, there is a rising through time of trauma attributable to interpersonal violence, reaching the highest point in Nasca, when also two cases of possible child abuse are identified

9.1 Introduction

Bioarchaeology is a more or less recent development of the physical anthropological sciences. The term 'bioarchaeology' proposed by Dr. Jane Buikstra in a symposium held in 1976, makes reference to a new approach, focusing on the cooperative work between archaeologists and biological anthropologists in order to deal with new questions from a problem-oriented standpoint (Buikstra 1991). It also refers to the

E. Tomasto Cagigao (✉)
Pontificia Universidad Católica del Perú (PUCP) Departamento de Humanidades, Av. Universitaria cdra. 18, San Miguel, Lima 32, Perú
e-mail: etomast@pucp.edu.pe

M. Reindel, G.A. Wagner (eds.), *New Technologies for Archaeology*, Natural Science in Archaeology, DOI 10.1007/978-3-540-87438-6_9,
© Springer-Verlag Berlin Heidelberg 2009

study of faunal and botanical remains found in archaeological contexts (Buikstra 2006). In this chapter we use it only in reference to human remains.

Among the issues addressed by bioarchaeology are the differential health and adaptation levels within and between populations, the diet, patterns of activity, genetic relations, human migrations, paleopathology, trauma, and paleodemography. In 30 years of existence, this discipline not only has enriched significantly the knowledge of past societies, but as Ortner (2006) points out, because culture is an important component of human societies, human biology is better understood in the context of the associated culture.

Throughout these years, in addition to the metrical and morphological examination of bones with the assistance of X-rays and tomography, new and more sophisticated techniques, such as DNA and isotope analysis or electron microscopy have been incorporated as current practices in bioarchaeology. Also, the strong development of forensic anthropology in relation to human rights violations in the last decade opened the door to new issues, such as the identification of perimortem trauma and patterns of violence in past societies (Martin and Frayer 1997).

In Peru the development of bioarchaeology has been uneven. The first insights into this discipline come from the pioneering investigations of Pedro Weiss (1958, 1961), who studied osteological collections coming from all around Peru and proposed the approach of the 'cultural osteology', defined as the study of human remains from the standpoint of its cultural context. Unfortunately this approach didn't have continuity and there was a 30-year period of very scarce studies of human remains in Peru, mainly accomplished by physicians and dentists who weren't familiar with the cultural contexts. A special mention should be made regarding the isolated studies on the human remains of Cerro Paloma (Benfer 1986, 1990). Then, from the decade of the 1990s on there was a strong development of this kind of studies related to the creation of Centro Mallqui, a cultural institution devoted to the preservation and investigation of pre-Hispanic human remains. Also, the study of human remains has flourished in the north coast, alongside with renewed interest in the archaeology of the Moche culture that followed the spectacular discovery of The Lord of Sipan. Finally, in recent years other bioarchaeological contributions have clustered around the discovery of Inka funerary contexts near Puruchuco (central coast) and archaeological research in the Cotahuasi Canyon in the southern highlands.

Surprisingly, the south coast, located between the Cañete and Acarí valleys, an area that was the scene of important pre-Hispanic cultural developments such as Paracas and Nasca has received little attention by bioarchaeologists. The major reason for that is probably the lack of accessible collections of human remains coming from scientifically controlled excavations. The main south coastal collections are still those gathered by Julio C. Tello and his team in the early twentieth century. According to published data (Tello and Mejía 1979) almost 1000 individuals were recovered from funerary contexts on the Paracas Peninsula. The expeditions to the Nasca valley, on the other hand,

yielded more than 400 individuals of Nasca and Middle Horizon affiliation, as recorded in Tello's field notes (Isla, personal communication). The management of these enormous quantities of material and information was very difficult from the beginning. That's why the inventory and cataloguing of Tello's collections, housed at the National Museum of Archaeology, Anthropology and History of Peru, are still in process, and until very recently the access to them was very limited. As a result, in addition to researches focusing on deformed and trepanned skulls as well as trophy heads, (Allison et al 1981, Baraybar 1987, Browne et al 1992, Guillen 1995, Verano 2003, Williams et al 2001) only Kellner (2002) and Rhode (2006) had the opportunity to apply extensively to this collection some of the new methods developed in the field of bioarchaeology.

Another important group of scientifically excavated human remains are those recovered by the Italian mission in the Nasca valleys. Nevertheless, the bioarchaeological publications about this collection of 237 individuals are very general (Orefici and Drusini 2003) or of difficult access (Drusini 1987, 1988; Drusini et al. 1988; Visconti di Modrone 1988).

In this context, the knowledge of the biological characteristics and adaptation levels of the populations that inhabited the Peruvian south coast in pre-Columbian times is still in process of building. In this sense, the contribution of the present research has three main branches: first, the careful documentation of biological aspects of a scientifically excavated collection of human remains which temporal span covers the most important periods of cultural development of the south coast; second, the building of new knowledge or the adding to the existing one about the paleodemography, biological characteristics, levels of adaptation and health, paleopathology, and trauma of these populations; and third, perhaps the most important, the raising of new questions about the changes observed throughout the time, underlying the need for more bioarchaeological research in the area.

9.2 The Sample

The present research focuses on the osteological analysis of 198 individuals coming from funerary contexts discovered by the Nasca–Palpa Archaeological Project during the 1997–2006 field seasons (Isla this volume). The sample comprises about 4500 years, from the Archaic period to the Middle Horizon (ca. 3800 BC–900 AD), but not all the periods are equally represented. The largest samples are those of the Paracas and Nasca periods, with 84 and 92 individuals, respectively. Next, the Middle Horizon has 19 individuals and the Archaic period is represented by 3 individuals. Two gaps exist in the sequence, one in the Initial Period and the other in Initial Nasca. Also, the periods following the Middle Horizon are not represented.

The state of preservation of the skeletons is variable, mainly due to post-depositional events such as illegal excavations, farming, or vegetation rooting. Also, some skeletons were cremated. As can be seen in Table 9.1, the sample is

Table 9.1 Distribution of individuals by cultural period and state of preservation

	Complete	Incomplete	Very incomplete	Only Skull	Mummy or Bundle	Total
Archaic	2	1	–	–	–	**3**
Paracas	22	25	37	–	–	**84**
Nasca	39	27	23	1	2	**92**
Middle Horizon	10	3	2	4	–	**19**
Total	**73**	**56**	**62**	**5**	**2**	**198**

more or less split into three categories: 73 skeletons had 95% of elements present and well preserved and 56 lacked some parts such as the small bones or the epiphysis. As a result we had 128 skeletons complete enough to perform most analyses. The remaining 62 were represented only by small fragments; nevertheless some of them gave information on periostosis, stress indicators, and trauma. There were also five skulls found with no association to the body, two of which were trophy heads. Finally, there was a funerary bundle of an infant and an adult mummy.

Because of these differences of preservation the number of individuals per analysis is different and is specified in each case.

9.3 Methods for Recording and Analysis

Each individual was cleaned with soft brushes and in some cases also with wooden or metal sticks. In a few cases, after a careful evaluation of the bone strength, we used drops of water to clean some very important traits that were not clearly visible. After cleaning, each skeleton was laid out in anatomical position and a general photography was done. The next steps were the filling of the inventory form, attribution of sex, age estimation, and measurements for stature, according to Buikstra and Ubelaker (1994).

For the estimation of the age of children the standards of Gaither (2004), Moorrees et al. (1963), Scheuer and Black (2000), and Ubelaker (1989) were applied. In the same way, for the estimation of adult age, the standards of Suchey (1986), Lovejeoy et al. (1985), Buckberry and Chamberlain (2002), and Iscan et al. (1984; also Iscan and Loth 1986) were used. The state of preservation of teeth made the use of root transparency impossible. The sample was divided into age categories according to Baker et al. (2005), Scheuer and Black (2000), and Tomasto (1998, 2005).

Stature was calculated with the formulae of Genovés (1967). The recording and analysis of teeth, in relation to inventory, caries, and lineal enamel hypoplasia (LEH) were done following Hillson (1996, 2000). Finally, all the pathologies, trauma, stress indicators, and other anomalies were carefully recorded in descriptive and photographic ways. The descriptions included the location, type, extension,

severity, degree of activity, and possible cause of the observed changes. All the information was arranged in an Excel database. After the analysis each skeleton was carefully packed with acid-free paper, put into polyethylene bags, and arranged in cardboard boxes. The forms, photos, as well as the database are part of the archives of the Nasca–Palpa Archaeological Project.

9.4 Results

In this section we present the biological characteristics of the sample as revealed through four indicators: demography, comparative stature, spongiosclerosis, and trauma.

As mentioned before, because of the differences of preservation the number of individuals per analysis is diverse. Also, for most analyses the samples weren't large enough to give statistically significant results, but there are clear tendencies that suggest important changes occurring in these populations throughout time.

9.4.1 Demography

Demographic analysis was not applied to the Archaic period, which was represented by only three individuals. For the construction of mortality curves for the remaining cultural periods, nine age cohorts were created as follows.

1: Infancy: individuals smaller than 1 year old
2: Early childhood: 1–7 years
3: Late childhood: 7–12 years
4: Puberty: 12–15 years
5: Adolescence: 15–20 years
6: 20–30 years
7: 30–40 years
8: 40–50 years
9: Individuals older than 50 years

There were a number of adults whose age could not be calculated because of the bad preservation of the diagnostic features. They were included in the statistical calculations but not in the graphics. Only the Paracas and Nasca samples could be divided into epochs. In this way, the sample used for the construction of mortality curves is composed by 163 individuals distributed as shown in Table 9.2.

Figures 9.1, 9.2 and 9.3 show the mortality curves for each period. As can be expected, the 'total' curves follow the shape of the largest subsamples: Late Paracas and Middle Nasca, respectively. The curves for the epochs with small

Table 9.2 Sample used for the construction of mortality curves

	Early	Middle	Late	Total
Paracas	10	5	50	**65**
Nasca	21	60	–	**81**
Middle Horizon	17			**17**
Total				**163**

samples are shown only as a reference but the analysis focuses on the largest samples.

The shape of the Late Paracas and total Paracas curves don't agree with the expected curve for preindustrial societies (Weiss 1973) because juvenile mortality shows three differences. First, the mortality in the first cohort is very low. Second, instead of a continuous falling from the first to the 15th year, there is a small rise in the cohort of 1 to 7 years. And third, after a fall in the cohort of 7–12 years, the curve increases again in the cohort of 12–15 years. The small rise in the second age group is probably an artefact of the low levels on the first. Taken together, these features are probably related to special funerary treatments for the smallest children, which are not uncommon in traditional societies. However, the levels of mortality in the cohort of 12–15 years are atypical and could be the reflection of some stressor affecting this age group.

The Early Nasca curve resembles the Paracas in the small rise in the cohort of 12–15 years, although the Nasca level agrees better with the expectable mortality in this age group. The Middle and 'total' Nasca curves, on the other hand, clearly show the 'U' shape expected for this kind of society (Weiss 1973). The relatively low adult mortalities could be related to the number of adults

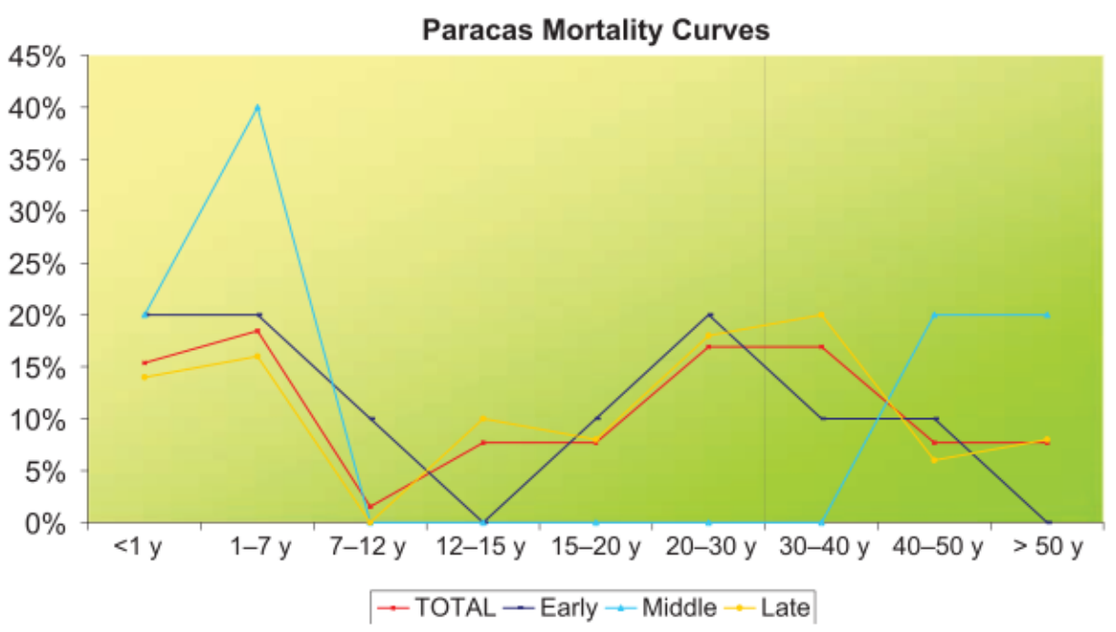

Fig. 9.1 Paracas mortality curves

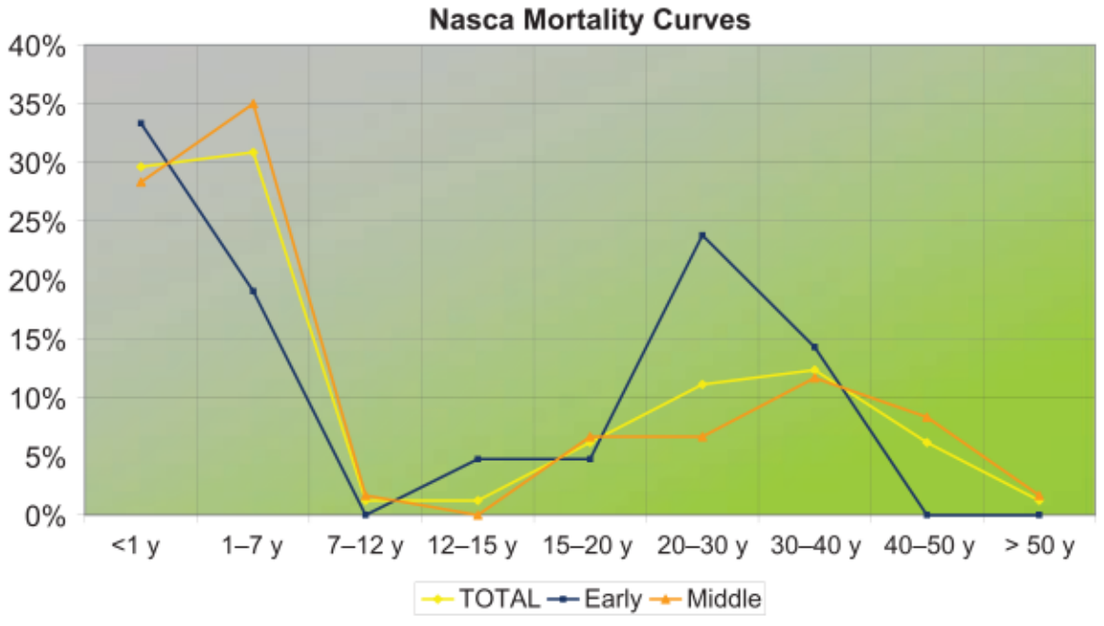

Fig. 9.2 Nasca mortality curves

whose age could not be calculated. For the Middle Horizon we found a similar 'U' shape.

The distribution by sex among the adults is shown in Fig. 9.4. As can be seen, the Paracas and Nasca samples are more or less evenly distributed, but the Middle Horizon sample is composed almost exclusively of females. This is completely unusual and most probably is related to differential mortuary treatments for males and females.

In sum, the demographic analysis shed light in three aspects of the studied societies: first, low levels of infant mortality in Paracas, which most probably

Fig. 9.3 Middle Horizon mortality curve

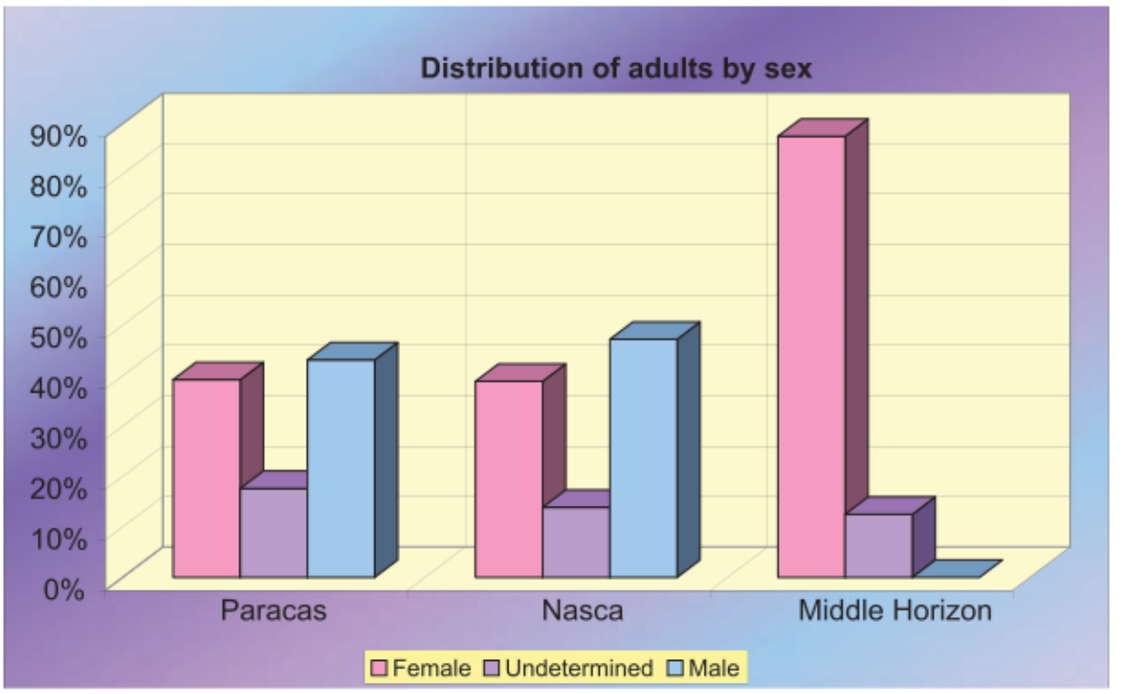

Fig. 9.4 Distribution of adults by sex

are related to funerary practices; second, an abnormally high mortality in the cohort of 12–15 years in Paracas and maybe also in Early Nasca; and third, the lack of male skeletons in the Middle Horizon sample, a feature probably related to differential funerary treatments for males and females.

9.4.2 Stature Achieved in Adulthood

The genetic potential to achieve a determinate stature in adulthood is hampered by factors such as diet, diseases, and general environment (Angel 1984; Frisancho 1977; Frisancho et al. 1975; Gaither 2004; Larsen 1987; Rose et al. 1984; Scheuer and Black 2000). That's why stature is used as a measure of comparison between populations.

In the present research, due to the differential preservation already explained, the sample available for the calculation of average statures was composed of 42 individuals distributed as shown in Table 9.3. The average statures for males and females in each cultural period can be seen in Fig. 9.5.

Table 9.3 Sample used for the calculation of statures

	Archaic	Paracas	Nasca	Middle Horizon	Total
Male	2	10	11	0	**23**
Female	1	6	9	3	**19**
Total	**3**	**16**	**20**	**3**	**42**

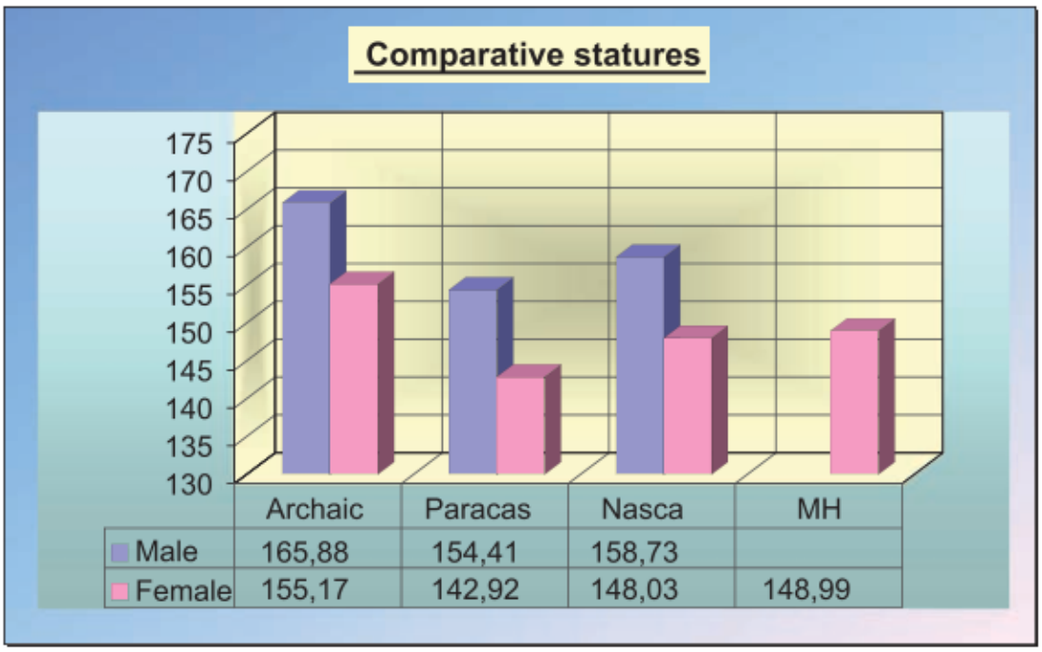

Fig. 9.5 Comparative statures

The first outstanding feature is the high average statures of the archaic individuals in comparison to all the later cultural periods. The lowest statures are those of Paracas, while Nasca and the Middle Horizon have similar averages, at least among females, which are intermediate between Paracas and the Archaic.

More or less 3000 years separate the Paracas from the Archaic period. In that time a population change could occur, but currently there is neither positive nor negative evidence for that (Fehren-Schmitz, personal communication). Supposing that the population change didn't take place, the differences in the statures would mean worse living conditions in Formative times, compared to the Archaic, and a gradual improvement of them throughout Nasca and the Middle Horizon. As we show later, there are other indicators suggesting bad living conditions in Paracas times.

9.4.3 Spongiosclerosis

Spongiosclerosis, the abnormal growing of spongy bone (Ortner 2003) is frequently related to anaemia. This is caused by the increase of the red marrow housed inside the bone in response to lowered levels of systemic oxygen. This increase also affects the bone (Buikstra and Ubelaker 1994; Klepinger 1992; Kruger 1990; Larsen 1987; Ortner 2003) and occurs more frequently in the cranial vault and in the roofs of the orbits. There are several causes for anaemia, but as long as the genetic factors responsible for sickle cell anaemia and thalassemia are absent from pre-Hispanic populations (Ortner 2003) the span of possible aetiologies is reduced to nutritious factors and disease.

Table 9.4 Sample used for the recording of spongiosclerosis

	Archaic	Paracas	Nasca	MH	Total
Children	0	21	26	7	**54**
Females	1	11	9	7	**28**
Males	2	9	7	0	**18**
Total	**3**	**41**	**42**	**14**	**100**

Spongiosclerosis may be confused with periostosis, the deposition of new bone on the existing surfaces, but the pattern of changes can be differentiated through X-rays or histological analysis. Also the close examination of the borders of cranial fragments can give a clue to the kind of lesion observed, as was the case in the present research. In this way, the fragmentation of most skulls due to the pressure of the fill inside the tombs was an advantage. Therefore, the presence or absence of spongiosclerosis was recorded in a sample consisting of 100 individuals whose skulls were at least 75% preserved, even though most of them were fragmented. The distribution of the sample by sex, age, and cultural period can be seen in Table 9.4.

Figure 9.6 shows the percentages of individuals affected by spongiosclerosis in each of the cultural periods under study. None of the three Archaic individuals shows evidence of spongy bone increase in the skull. The Nasca sample has the next lower frequency, reaching a level of 4.8% whereas Paracas and the Middle Horizon have similar frequencies, of 25.6 and 21.4%, respectively.

The first conclusion that can be drawn from Fig. 9.6 is again related to the bad living conditions in Paracas times, which have the highest frequency of the whole series. On the other hand, as long as the consumption of maize is often

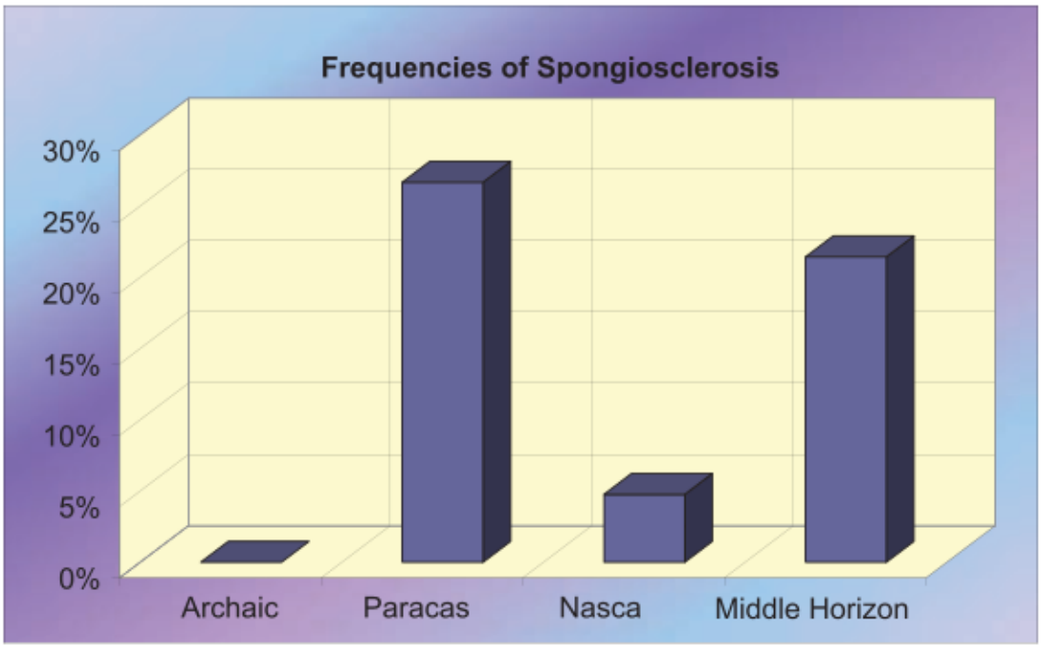

Fig. 9.6 Frequencies of spongiosclerosis

mentioned as one of the potential causes for anaemia, a possible interpretation to the changes observed could be the decrease in the consumption of this staple in Nasca times and similar levels in Paracas and the Middle Horizon. Nevertheless, the isotope analysis suggests a completely different scene (Horn et al. 2007). In view of these facts, other alternative interpretations could be an earlier weaning in Nasca, or the existence of diseases diminishing the levels of blood iron in Paracas and the Middle Horizon. Most probably the causes are a complex mix of several factors and more research will be needed to answer the raised questions.

9.4.4 Trauma

The interpretation of trauma in skeletal populations is not easy. In some cases as in healed trephination the participation of a specialist is indubitable but in most fractures, dislocations, mutilations, and cuts the interpretation is not so straightforward. In general the causative factors for trauma can be divided in two large groups. We have accidents related to the risk implicit in some daily activities, and on the other hand there is the diversity of behaviours that can be classified under the label of interpersonal violence. These behaviours can happen in a variety of contexts such as ritual and domestic spaces or situations of general violence occurring in wars.

The mechanism of production of many fractures is well known, such as the Colles' fracture, produced by falls on the hand. Falls are often the result of an accident, but can also be produced in situations of interpersonal violence. Depending on the context, this fracture could be classified as accidental or not. In archaeological cases we don't have the detail of the circumstances surrounding the production of a trauma, so the only possible approximation to an interpretation is the attribution of lesions to its more apparent cause, according to the mechanisms of production described in the literature (Angulo 1995; Ballesteros 2002; Byers 2002; Capasso et al. 1999; Galloway 1999), keeping in mind that this classification is arbitrary to some degree.

In the sample under investigation, 72 individuals with fractures, mutilations, possible trephinations, and cut marks were identified. The fractures on the ribs, feet, wrists, hands (except for the Bennett's fracture), ankles, and mid-diaphysis of clavicles were classified as possibly accidental. On the other hand, the depressive fractures of the skull vault, ring fractures of the cranial base, lines of fracture on the middle extreme of clavicles, cut marks, 'parry' fractures of the ulna, lesions in the hand bones that could be related to blows given with the fist, and rib fractures suggesting child abuse were classified under the category of possible interpersonal violence. Finally, there were some kinds of trauma that were classified as miscellaneous, such as some depressions over the inion that have been interpreted as healed trephinations (Weiss 1958) or the result of the use of cradleboards (Capasso et al. 1999). The dislocations of the temporomandibular joint were also classified as miscellaneous.

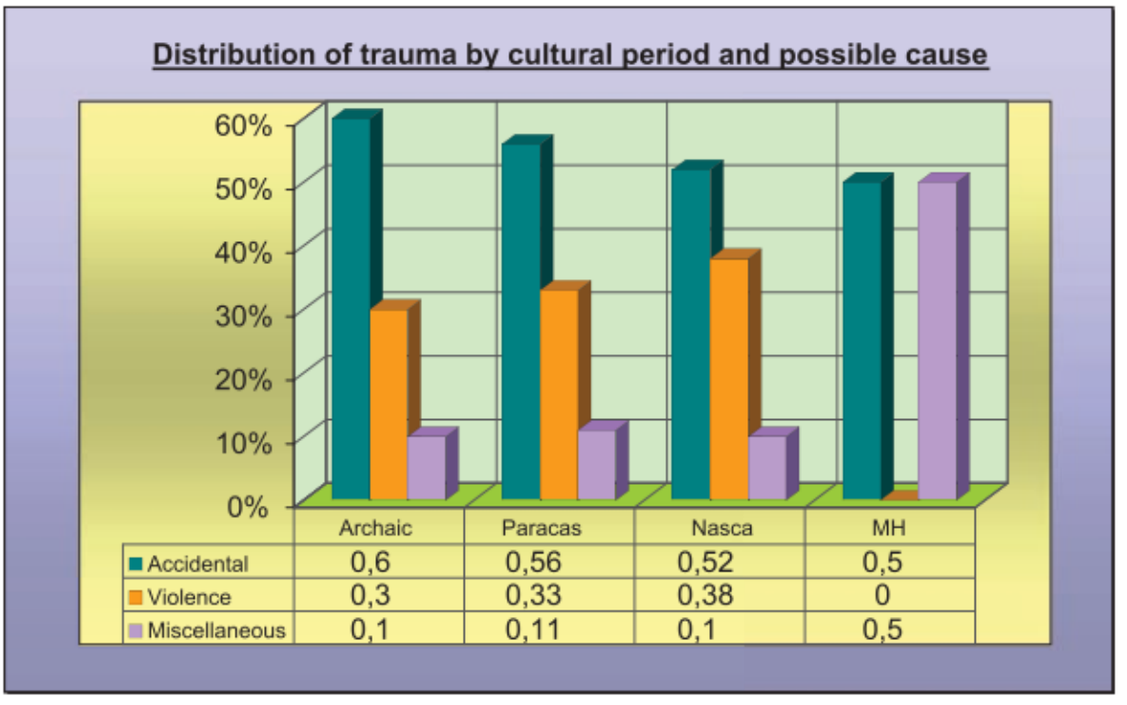

Fig. 9.7 Frequencies of trauma by cultural period and possible cause

Figure 9.7 shows the distribution of trauma by cultural period and possible cause. The decrease in frequency of accidental traumas from the Archaic to the Middle Horizon is clearly seen, whereas in contrast, the frequency of traumas possibly related to violence increases through time.

The detailed evaluation of lesions by cultural period shows that in the Archaic sample most lesions concentrate on the hands, wrists, ribs, and feet and are evenly distributed between both males and the only female. The majority of lesions can be attributed to accidents and there are only three that may have been the result of violence: a small depressive fracture on the left frontal of the female, a fracture with angulation of the right second metatarsal of this same individual, and a parry fracture on the right ulna of a male. Finally, under 'miscellaneous' there is a suprainion depression, not associated to cranial deformation (Fig. 9.8).

Fig. 9.8 'Supra-inion like' depression in an Archaic skull

In Paracas the frequency of possibly accidental traumas is lower than the Archaic frequency but still reaches more than 50%. Conversely the traumas possibly related to interpersonal violence increase a little, whereas the miscellaneous cases stay at the same level as before (Fig. 9.7).

In the first category, the incidence of trauma between males and females is similar, although the fractures to the inferior limb related to males are slightly more frequent. In general the inferior limb is, at the same time, the region more commonly affected, particularly the feet. On the other hand, among the 'possibly violence' category there are many depressive fractures on the skull, as well as a couple of cases of line fractures in the middle extreme of the clavicle whose most reported cause in clinical cases is a strong blow to the shoulder (Angulo 1995; Galloway 1999). Particularly interesting is a perimortem ring fracture of the skull base that was identified in an occipital which also showed another possible perimortem fracture running through the prominence (Fig. 9.9). The bone probably pertained to a female and was found in a unique Early Paracas burial found in Mollake Chico (Isla and Reindel 2006a,b; Isla this volume). Equally outstanding is the burial of an adult male who was deposited inside a funerary urn, with an obsidian projectile point embedded between the ribs, without the skull and showing cut marks in the axis (Figs. 9.10 and 9.11). Also it's interesting to note that 62% of the cases that could be attributed to violence were found in a type of funerary contexts, recorded for the first time for Paracas. These burials show evidence of cremation and secondary treatment of some individuals (Isla and Reindel 2006a,b, 2007; Isla this volume). Finally, the miscellaneous cases in Paracas are referred to suprainion depressions associated with occipital flattening.

In Nasca times there is again a decrease in the frequency of traumas attributable to accidents and an increase in those attributable to violence, whereas the miscellaneous keep the same level as before (Fig. 9.7). In contrast to the Paracas sample, in Nasca the most frequent accidental traumas occur in the superior limb and are exclusive to the females. There are also some traumas in the inferior limbs, which are more frequent among the males.

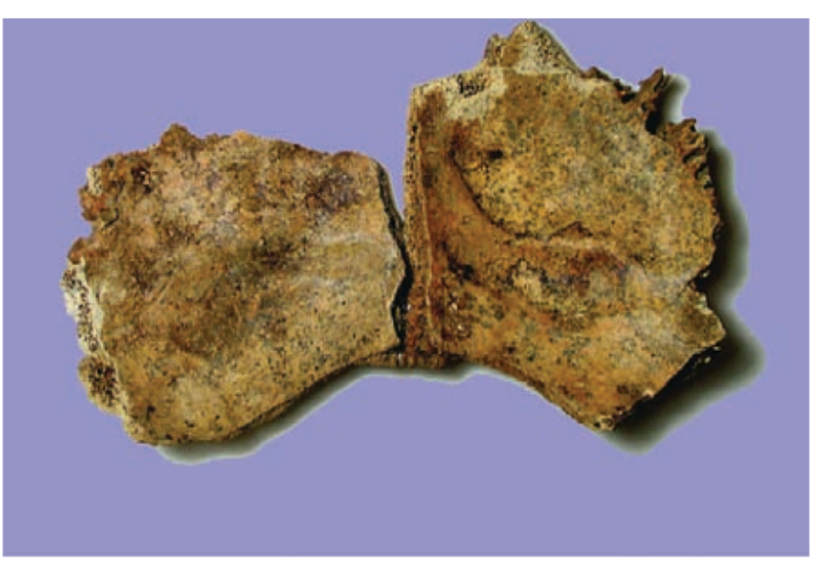

Fig. 9.9 Occipital with perimortem fractures

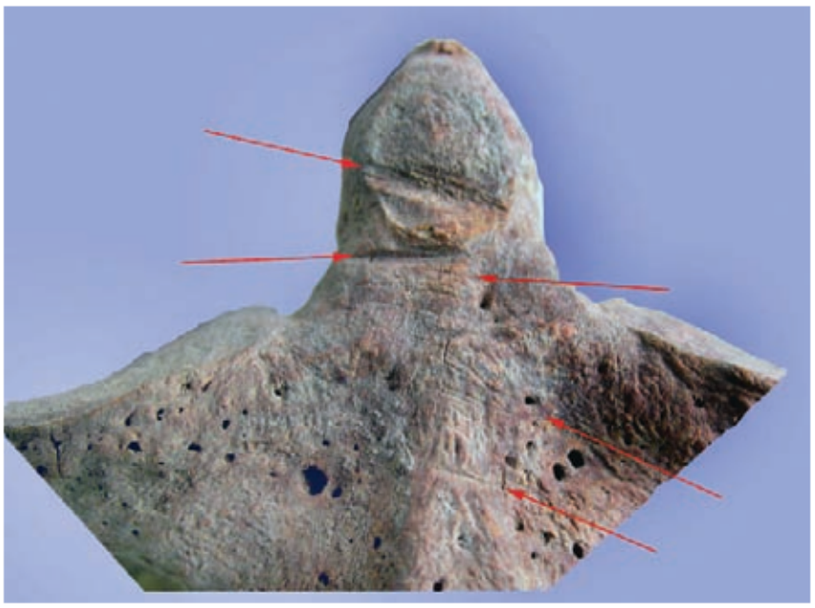

Fig. 9.10 Axis with cut marks

Among the traumas attributable to violence we didn't find the depressive fractures to the skull that were so frequent in Paracas, except for a small depression in the lambdoid suture of a child, 5–6 years old. At this point it's important to mention that there are two cases suggestive of child abuse. In the first case, an infant 6–12 months old had a transverse fracture to the proximal diaphysis of the right femur. The fracture was in the process of healing and possibly occurred a month or so before the child's death. In the second case a child 8 to 16 months old had five fractured ribs. They showed at least two stages of healing, some with a thin layer of fibrous bone and others with fibrous bone changing to lamellar (Fig. 9.12). In general, bone fractures in small children are very infrequent because the growing skeleton is very flexible and particularly, the most common cause for fractures occurring in children less than three years old is child abuse (Pierce et al. 2004 Walker et al. 1997). Finally, rib fractures showing different stages of healing are considered as highly diagnostic for child abuse (Silberberg 2007; Walker et al. 1997).

Fig. 9.11 Burial of a decapitated adult male who had a projectile point embedded between the ribs

Fig. 9.12 Fractured ribs of a child, showing different stages of healing

Other examples attributable to violence in the Nasca sample are a couple of parry fractures to the ulna and a Bennett's fracture to the first metatarsal. A case that deserves special mention is an obsidian point embedded in the superior left articulation of the third cervical vertebra of an adult male (Fig. 9.13). He was found inside a partially disturbed burial, so the original state of the interment is not known, nevertheless, at the moment of the excavation the skull was absent. The conjunction of both facts strongly suggests that this is another example of decapitation as that described for Paracas.

Fig. 9.13 Projectile point embedded in the third cervical vertebra of an adult male

In the miscellaneous Nasca group there are not the suprainion depressions found in the two preceding periods. Instead the bulk of this category is referred to dislocations in the temporomandibular joint, found only in females.

Finally, the traumas in the Middle Horizon sample are very scarce: two females showed fractures in a rib and in a metatarsal, respectively. On the other hand, the miscellaneous category is composed of cases so badly preserved that it was very difficult to classify the lesions.

In sum, various tendencies were found from the trauma analysis. First, the cases attributable to accidents decrease through time whereas those that could be related to violence increase. Among the first the association between inferior limb trauma and males in Nasca times and to a lesser degree in Paracas is interesting. In the same line is the association between upper limb fractures and females in Nasca. Both tendencies could be related to differential activities performed by both sexes. In regard to the second category of trauma, Paracas and Nasca show evidence of decapitation, although in Nasca the skull depressive fractures that were so frequent in Paracas disappear. Nevertheless, in Nasca two cases suggestive of child abuse were registered. Finally, the suprainion depressions appear only in pre-Nasca times

9.5 Discussion and Conclusions

This research sheds light on a series of issues that give more questions than answers. The most interesting conclusions are drawn from the largest samples, Paracas and Nasca, and the following discussion centres in these cultural periods. It's possible that some of the findings, such as the absence of cranial fractures in Nasca may be an artefact of the sample size. Nevertheless other tendencies must be taken as a standpoint from which new investigations should be oriented. In this way it's important to note that Kellner (2002) obtained some similar and some different results in her analysis of 272 Nasca and Middle Horizon individuals recovered by Tello in the Las Trancas valley, which are discussed below.

The results can be divided in two main streams: there are some findings that are more biological although tightly attached to cultural practices, whereas others are related mainly to cultural behaviours. In the first group there are various indicators suggesting bad living conditions in Paracas. Among these indicators are: the high mortality in the cohort of 12–15 years in Paracas and maybe also in Early Nasca, the high levels of spongiosclerosis and the short average stature in Paracas. At this point it's important to note that our Paracas sample compares unfavourably to the averages obtained for other populations such as Moche (Verano 1994), Chiribaya (Burgess 1999), Nasca (Orefici and Drusini 2003; Kellner 2002), Wari or Middle Horizon (Orefici and Drusini 2003; Kellner 2002), and Chincha (Orefici and Drusini 2003) whereas the statures in Nasca and the Middle Horizon are more or less similar to the published averages for other pre-Hispanic Andean populations.

In regard to the frequencies of spongiosclerosis it's interesting to note that Kellner (2002) found low levels in Early Nasca (8%), even lower in Middle Nasca (6%), and then an increase in Late Nasca (12%) and the Middle Horizon (10%). The lower levels of our sample are also in Middle Nasca. This information, taken together, suggests that health improved continuously from Paracas times to Middle Nasca, at least in regard to the frequencies of anaemia.

In the second group, demographic analysis revealed the probable distinctive funerary treatments for children younger than age one and for women in Paracas and the Middle Horizon, respectively. The sample of the Middle Horizon is too small and more excavations will be needed to confirm the difference observed. Nevertheless, in the case of Paracas it's interesting to note that the differential treatment affects only a group of infants, as long as 15% of the recovered skeletons correspond to this age cohort. According to the shape of the expected curve, the level of mortality in this group should be about 30%, which means that one half of death infants should have been disposed in some different way. In this regard, Parker Pearson (2002) presents a similar example from the Early Bronze Age in the former Yugoslavia, where most children were interred under the houses and only some special ones were taken to the adults' cemetery. In the case of Paracas the funerary practices are beginning to be explored (Isla this volume) and more deep investigations will be needed to understand them. Nevertheless, the contexts recently discovered suggest that those practices were varied and complex. The fact that 62% of fractures attributable to violence in Paracas were found in a different type of burial, points also in this direction, as well as the funerary treatment given to the possible decapitated male, who was buried in a funerary urn, a treatment frequently used for children.

Other findings that could be related to cultural behaviours are the distributions of traumas attributable to accidents in Paracas and Nasca, with upper limb fractures frequently associated with the Nasca females, whereas the lower limb lesions are more recurrent among the Paracas and Nasca males. This differentiation could be related to gendered activities and it will be necessary to review the objects associated with those individuals.

The increase through time of traumas attributable to violence is another finding that must be highlighted. The highest point of the curve is reached in Nasca, when two cases of probable child abuse were also identified. This increase of violence is at odds with the improvement of living conditions in Nasca times that was discussed before. At this point a question rises about the reasons that allow the appearance of child abuse in a society. In this regard, Walker (1994) found a short frequency of child abuse in early European and Native American populations, and considers that child abuse is a recent phenomenon related to the collapse of social control and the lack of support mechanisms that the parents had in the past due to the proximity of the extended kin groups. In the same way, Wheeler et al. (2007) state that child abuse is related to high levels of social stratification and political integration and is used to prepare the children to live in unequal conditions. In this way, the increase of indicators of violence in Nasca times agrees with other

archaeological evidence of social complexity for this epoch. More investigations will be needed to expand this as well as the other issues found, in order to better understand the complex relationship between culture and human biology in the south coast of Peru.

Chapter 10
Who Were the Nasca? Population Dynamics in Pre-Columbian Southern Peru Revealed by Ancient DNA Analyses

Lars Fehren-Schmitz, Susanne Hummel and Bernd Herrmann

Abstract Through the analysis of ancient DNA from human mortal remains it is possible to gain access to a biohistoric archive containing relevant information about the structure of prehistoric populations. The data obtained help to answer questions related to migration processes and population relationships that could not be answered by the methods of cultural science alone. The aim of this study was to show to what extent the cultural evolution of the southern Peruvian Palpa area was accompanied by processes of population exchange. Bone and tooth samples of over 200 individuals from prehistoric burial grounds from southern Peru were collected and examined with the methods of ancient DNA analysis. The study focuses on the matrilineal population dynamics by the analysis of mitochondrial genetic markers. Mitochondrial haplogroups and types could be successfully determined for over 100 individuals from different archaeological periods. The obtained data were compared with mitochondrial data from recent Native American populations. The results allow us to describe to what extent cultural changes were influenced by allochthonous contributions to the gene pool and how changes in the socioecological complexity of the cultures affected the genetic composition of the Palpa valley population. Also, a significant differentiation of ancient coastal and highland populations in southern Peru is detectable as are changes in the mitochondrial haplogroup distribution patterns as a result of the emergence of the extensive highland empires in later South American prehistory.

L. Fehren-Schmitz (✉)
Johann Friedrich Blumenbach Institute of Zoology and Anthropology, Historical Anthropology and Humanecology, Georg-August-University Goettingen, Bürgerstraße50, 37073 Göttingen, Germany
e-mail: lfehren@gwdg.de

M. Reindel, G.A. Wagner (eds.), *New Technologies for Archaeology*, Natural Science in Archaeology, DOI 10.1007/978-3-540-87438-6_10,
© Springer-Verlag Berlin Heidelberg 2009

10.1 Introduction

One of the recurrent questions of archaeological science is how far cultural change in a geographic region is connected to changes in the biological population structure, for example, by migration. The progression of archaeological theories from cultural history, processual archaeology, and postprocessual archaeology to the present developments were always accompanied by changes in the perception of migration as a potential factor in cultural evolution (Anthony 1990). There are many possible scenarios for the cause of cultural changes reaching from pure autochthonous developments or cultural diffusion with a stable population to culture change through population replacements by processes of migration or invasion (Burmeister 2000). Although changes in the material culture can be detected in the archaeological record by typological comparison, methods of cultural science allow no definite decision if new craft styles, ritual behavior, and so on were introduced by immigrating people or other mechanisms of diffusion. The only archive that can be used to resolve this question is humans themselves.

Through the use of molecular genetic methods it is possible to gain access to a nonbiographic archive containing all relevant information about the biological composition of a population. Uniparental inherited genetic markers such as mitochondrial DNA (mtDNA) and the nonrecombining proportion of the Y-chromosome (nryDNA) have proven valuable for the reconstruction of the global spread of Homo sapiens and therewith the understanding of longer term global patterns of human diversification (Underhill and Kivisild 2007). Analyses of the maternal inherited mtDNA and paternal inherited nryDNA from recent populations were successfully used to throw light on the processes – source populations, number of migrants, migration dates, routes, and so on – accompanying the initial colonisation of the Americas (e.g., Torroni et al. 1993), Europe (e.g., Richards et al. 1998), and Australia (e.g., Hudjashov et al. 2007). Comparisons of the data from both genetic markers also allowed the analysis of sex-specific mobility patterns and therewith human migrational behavior (e.g., Wilder et al. 2004). All those studies use DNA from recent populations to reconstruct historic migration processes by utilising methods and calculations of population genetics.

Through the development of methods and techniques to analyse ancient DNA (aDNA) from pre-/historic specimen physical anthropology gained an analytic tool that also allows the access to such genetic data from populations and cultures that vanished long ago. Instead of deducing historic processes from a recent genetic as-is state, these methods allow a diachronic comparison of the genetic relationship of ancient populations. Furthermore the analysis of ancient DNA allows, for example, the reconstruction of complex genealogies from individuals buried in prehistoric burial grounds as shown for the Bronze Age Lichtenstein Cave near Osterode, Germany (Schilz 2006) or species determination from prehistoric animal remains (Renneberg et al. this volume).

To conduct such investigations, methods and techniques developed for the analysis of DNA from living organisms have to be adapted to the specific characteristics of aDNA, DNA degradation patterns have to be examined, and methods of contamination control and prevention have to be improved. So the constant development of new methods and techniques is an essential need for palaeogenetic science. Detailed information on possible applications, methods, specifics, and possible problems faced with the analysis of aDNA are compiled in some review articles (e.g., Paabo et al. 2004; Willerslev and Cooper 2005) and two monographs published by the Palaeogenetics Group of the Department of Historic Anthropology, Göttingen (Herrmann and Hummel 1995; Hummel 2003).

10.1.1 The Peopling of South America from a Genetic Perspective

Important insights into the initial colonisation of the New World have been gained through molecular genetic studies – particularly through the analyses of mtDNA – of recent Asian and Native American populations. Today it is generally agreed that the first humans entered the Americas through or along the Beringian land bridge. Controversy arises when it comes to the timing, the precise route, and the number of major migrations. The most parsimonious model by today's state of knowledge from genetic data is a single initial migration with relatively few individuals about 20,000–14,000 years ago along a Pacific coastal route (Merriwether et al. 1995; Silva et al. 2002; Schurr 2004; Lewis et al. 2007). The assumption of rapid spread of the people along the Pacific coast from Beringia to southernmost South America and therewith a pre-Clovis colonisation of the Americas is consistent with archaeological data (Dixon 2001) and the assured early ^{14}C dates of South American archaeological contexts such as Monte Verde, Chile (Dillehay 1999). Demographic simulations also prove that even for a small founding population by this route it would be possible to cover such a distance – Alaska to Tierra del Fuego – in relatively short time (e.g., 1000 years) under retention of an effective population size (Fix 2002).

Despite the richness of their cultures and the richness of environments that they inhabit, the Native Americans harbor a low level of genetic diversity. This is probably a consequence of the previously described terms of the initial peopling. Nearly all Native American mtDNA-haplotypes belong to four ancestral lineages, the mt-haplogroups labled A, B, C, and D (Torroni et al. 1993). These lineages are widely found throughout the Americas, but there is a lot of variation in frequencies among populations and geographic regions. A fifth founding mitochondrial haplogroup, designated X, is only found in indigenous populations of northern North America (Dornelles et al. 2005). All of those five major matrilineages (mt-haplogroups) were represented by only one (Schurr 2004) or a few (Tamm et al. 2007) sublineages (mt-haplotypes) in the initial founding population. The mt-haplogroups have a definite Asian

ancestry and the genetic data indicate that the ancestral source population probably originated in south-central Siberia from where it migrated to Beringia and then into the New World (Schurr 2004).

In the case of the Y-chromosomal DNA most male Native Americans belong to the two principal founding lineages C and Q (nomenclature: Y-Chromosome Consortium 2002). Haplogroup Q dominates with about 75% and for South America especially the subhaplogroup Q-M3 can be found, a group not existent outside the Americas (Underhill et al. 2001).

Although understanding of the further peopling of North America has significantly progressed in the last years this is not the case for South America. There is compelling archaeological and genetic evidence to suggest that the continent was peopled by 14–13,000 years ago (Dillehay 1999; Fuselli et al. 2003) but there is no agreement regarding the number of initial migrations and the migration routes (Lalueza et al. 1997; Rothhammer et al. 2001; Keyeux et al. 2002; Lewis et al. 2007). South America has a unique pattern of genetic diversity. Western (Andean) populations show a higher level of within-population diversity but short genetic distances to each other when compared to eastern (Amazonian) populations (Fuselli et al. 2003; Lewis et al. 2005).

There is a very specific regional distribution of mitochondrial haplogroup frequencies (Fig. 10.1; Fehren-Schmitz 2008) and a high frequency of mt-Haplotypes that are unique and not shared between different regions. Recent genetic comparison of modern Native American populations from all over South America based on mitochondrial Hyper Variable Region I (HVR I) sequences show that although there are regional differences in the patterns of genetic variation the low overall variance among these regions gives no evidence for several migrational waves (Lewis et al. 2007). Even if this makes it most parsimonious that the continent was peopled by one founding population, the exact routes, and if this wave split in different groups when passing the Isthmus of Panama remains uncertain. This lack of knowledge partly can be attributed to the circumstance that all available hypotheses regarding these questions are based on the analysis of recent Native American populations. There are only a few aDNA studies from South America with reliable results (e.g., Shimada et al. 2004; Moraga et al. 2005; Shinoda et al. 2006). Unfortunately most of these studies have neither a sample size that allows relevant population genetic calculations nor diachronic developments of settlement areas. The palaeogentic investigations conducted within the Nasca–Palpa project are the first large-scale, diachronic aDNA studies for South America.

10.1.2 Aims and Goals of the Palaeogenetic Investigations of Human Remains from the Palpa Area

One of the aims of the study presented here was to prove that large-scale ancient DNA investigations can be used to reveal complex population dynamics in

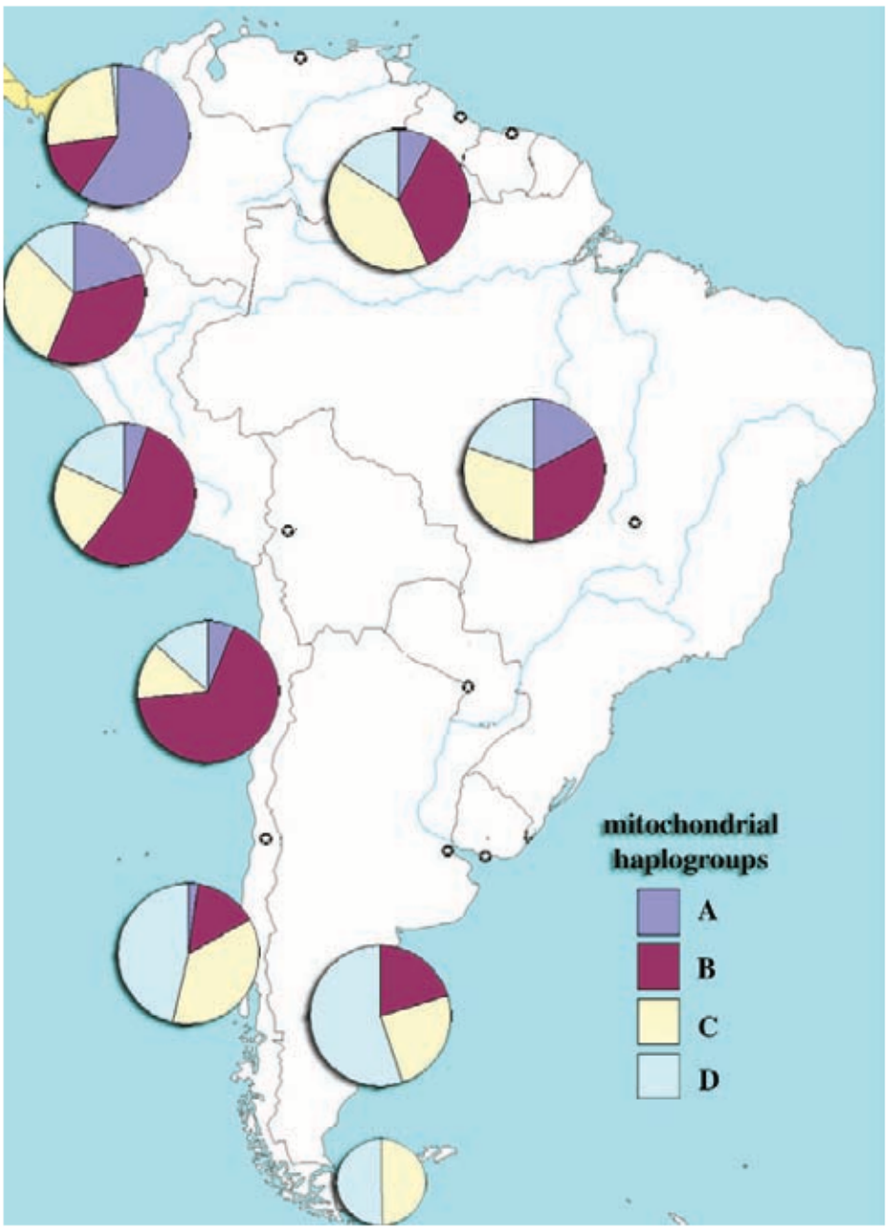

Fig. 10.1 Recent regional distribution of mitochondrial haplogroup frequencies in native South American populations. For this illustration a reduced dataset is used. Refer to Fehren-Schmitz (2008) for a more detailed distribution map. (Data used: Torroni et al. 1993; Merriwether et al. 1995; Ward et al. 1996; Rickards et al. 1999; Moraga et al. 2000; Goicoechea et al. 2001; Keyeux et al. 2002; Fuselli et al. 2003; Lewis et al. 2005; Torres et al. 2006; Garcia et al. 2006; Lewis et al. 2007)

prehistoric settlement areas, and prove the existence of migration processes and their influences on culture as well as cultural influence on migration patterns. The Palpa area in southern Peru and the scientific conditions of the Nasca–Palpa project offered the perfect conditions for such investigations. The archaeological evidence shows settlement continuity for this area until now, beginning with the Archaic period (about 3800 BC). In this long period of time the region faced many more or less dramatic cultural changes and the emergence and disappearance of archaeological cultures such as the Paracas and Nasca (Reindel this volume). The new insights into the cultural and ecological history of the southern Peruvian coast that arose from the project at the same time

raised new questions regarding population relationships and population discontinuities or continuities, for instance:

- Was the Paracas tradition in southern Peru represented by a biological uniform population or by solitary local groups sharing cultural traits (Silverman and Proulx 2002)?
- Did the Nasca culture evolve from the Paracas tradition with a continuous population? Or was it introduced to the region by foreign culture-bearers?
- Are there any biological traces of Wari influence in the Palpa region at the end of the Nasca period that justify the assumption of invasion or elite-dominance scenarios as formulated by Allison (1979)?

In addition to those questions that focus on the regional population dynamics in southern Peru the investigations should help to shed light on the peopling of western South America.

As mentioned above there is a constant need for fundamental research, for example, to understand the degradation processes of DNA and to enhance the methods of authentication and contamination prevention. To answer the content-related questions new molecular assays had to be developed. For instance, real-time PCR technology was adapted to the specific requirements of aDNA research in the course of this project. The adoption of this technology and thereby development of new methods for low-copy DNA quantification and inhibition control (Westenthanner et al. in prep) allowed novel insights to differential DNA preservation in human bones (Fehren-Schmitz 2008) and by chromosomal topography. Additionally real-time PCR technology was used to develop new, faster SNP (single nucleotide polymorphism) detection assays for mitochondrial and Y-chromosomal haplogroup determination, allowing high-throughput analysis for aDNA.

10.2 Material and Methods

10.2.1 Molecular Genetic Markers and Analysis Systems

The studies presented here where mainly based on the analysis of mtDNA, and therewith the matrilinear population dynamics. Mitochondrial DNA is a circular double-stranded molecule present in the mitochondria of eukaryotic cells. Each cell contains hundreds to thousands of copies of mtDNA making it much more likely that even after the DNA has undergone degradation processes following death there are more mitochondrial DNA fragments preserved in human skeletal remains than chromosomal DNA. MtDNA is exclusively maternally inherited, lacks recombination, and evolves faster than chromosomal DNA (Pakendorf and Stoneking 2005). These characteristics enable us to trace related maternal lineages nearly unchanged back through time and make it the molecule of choice for phylogenetic and population genetic studies, most notably when analysing aDNA.

To determine the mitochondrial haplotypes we analysed a 388 bp fragment of the mitochondrial HVR I (np16021–16408). A modular analysis system consisting of eight primers generating overlapping PCR products was designed. The modular character of this system allows the amplification of fragments with different sizes: long (434 bp), medium (236–261 bp), and short (157–180 bp). Therewith it is possible to adapt the analysis to the specific DNA degradation grades encountered in different samples. The generated PCR products were further analysed by direct sequencing.

In addition to the determination of the mitochondrial haplogroups by the specific HVR I polymorphisms we analysed four specific polymorphisms of the mitochondrial coding region determining the groups A, B, C, and D (Fig. 10.2). Three of the groups – A, C, and D – are characterised by SNPs (single base transversions or transitions) and group B is characterised through a 9 bp deletion at nucleotide position (np) 8272–8280 of the mitochondrial genome (Merriwether et al. 1995). This twofold determination system for mt-haplogroups was developed to authenticate the results because possible fast-evolving mutational hotspots of the HVR I and miscoding lesions caused by postmortem DNA damage exhibit a high risk of false determinations (Meyer et al. 1999; Willerslev and Cooper 2005; Gilbert et al. 2007). For the analysis of the four coding region polymorphisms a hybridisation probe-based multiplex PCR assay for the real-time PCR was developed. The mitochondrial HybProbe multiplex PCR on the LightCycler 2.0^{TM} (Roche) allows the simultaneous amplification and determination (by melting curves analysis) of all four polymorphisms characterising the

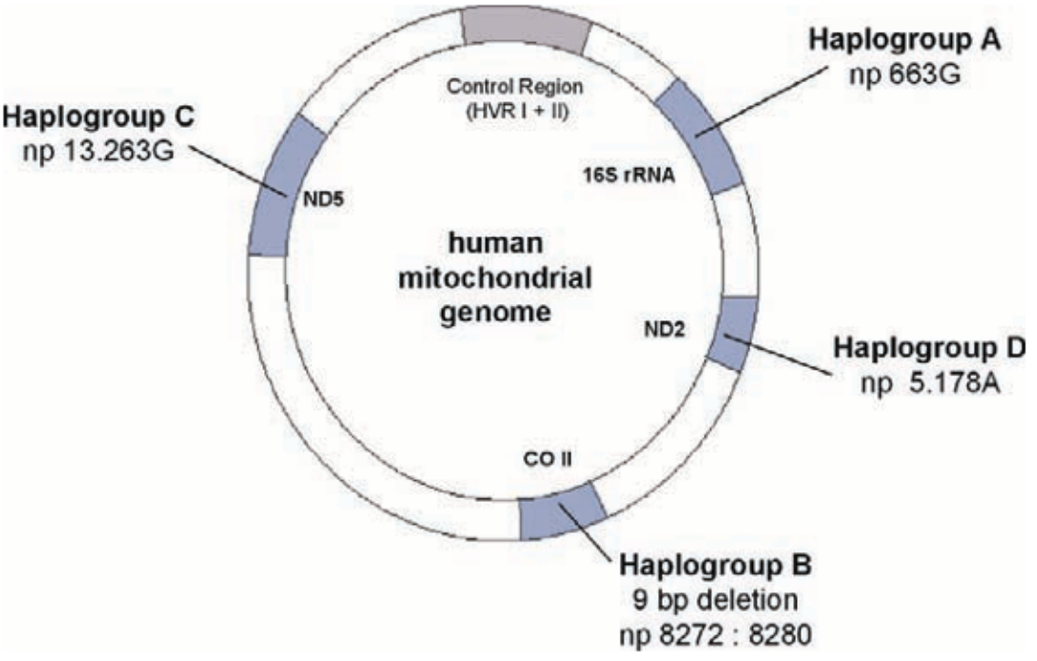

Fig. 10.2 Schematic representation of the human mitochondrial DNA genome with the location of the three base substitutions and the 9 bp deletion determining the Native American haplogroups. For each haplogroup the nucleotide position (e.g., np 663) and realised base substitution (e.g., A) is mentioned. The labels inside the circle specify the respective functional region (genes) of the mitochondrial genome

four Native American mt-haplogroups. Conventional methods used to determine such polymorphisms consist of several analysis steps and therewith are more time-consuming whereas the developed assay is a one-step procedure.

In addition to the mt-haplogroups/-types also investigations on Y-chromosomal haplogroups were made. The Y-haplogroups are also characterised by SNPs (cf. Y-Chromosome Consortium 2002). A HybProbe multiplex assay for the real-time PCR was developed to determine the four most frequently occurring Y-chromosomal haplogroups in Native American populations: C, P, Q, and Q3 (as mentioned above). SNPs analysed were M130 (C>T) for C, M45 (G>A) for P, M242 (C>T) for Q, and M3 (C>T) for haplogroup Q3. All analysis systems were tested on modern DNA from European and South American peoples first before being applied to the aDNA analysis.

For all analysed populations standard genetic diversity indices were calculated (Tajima 1993; Nei 1987). Genetic distances between the populations were calculated on haplogroup and haplotype level. Calculations for the measures were performed using the Arlequin software package (version 3.1, Excoffier and Schneider 2005). The obtained HVR I sequence data were also used to calculate distance-based phylogenetic trees and mean nucleotide distances between populations by the Mega 4.0 software (Tamura et al. 2007).

10.2.2 Sample Material and Sample Preparation

In different field campaigns (2004–2006) bone and teeth samples from 216 skeletonised or mummified human individuals were collected (Fig. 10.3). 172 of these were from different archaeological sites in the Palpa area and 44 individuals were from pre-Columbian burial grounds outside this area: Monte Grande (near the coast to the west of Palpa); Paracas Peninsula (Paracas

Fig. 10.3 Skulls of three human individuals from different archaeological sites of the Palpa area (*left*: Los Molinos; *right*: Pernil Alto) showing the encountered average state of macroscopic preservation. Individuals are largely skeletonised with some soft tissue conservation through mummification

Cavernas 6), and Pacapaccari (Andean highlands to the east of Palpa). The Palpa samples were collected from chronologically varying sites so that it was possible to investigate a timeframe from the late Archaic period (approx. 3800 BC) to the Middle Horizon (650–1000 AD). Sites bearing burials from more than one archaeological phase were preferred. Sampled sites, their chronological classifications, and the number of individuals sampled from them for each chronological period are listed in Table 10.1.

Sample preparation for DNA extraction followed a standardised protocol (Hummel 2003). Bone and teeth fragments were mechanically pulverised and afterwards chemical procedures for decalcification and cellysation of the bone-powder followed. Automated DNA extraction and purification were performed with an EZ1 Biorobot (Qiagen). For each sample two or more extracts were made. This precaution allows an authentication of analysis results by comparison (Hummel 2003).

In addition to the aDNA investigations, mt-haplogroup (cf. Fig. 10.1) and HVR I sequence data of over 4000 Native American individuals from different South American populations were collected from the literature to compare the pre-Columbian Palpa populations with the whole continent. Only a part of the obtained data and comparisons is presented here. For further information concerning the used extraction methods, primer sequences, analysis parameters, and statistic parameters, for example, refer to Fehren-Schmitz (in prep.). In the context of this text it is only possible to present a fractional

Table 10.1 Distribution of individuals sampled (number) tabulated by site and dating

Period / Culture	Phase	Pernil Alto	Mollake Chico	Jauranga	Los Molinos	La Muna	Hanaq Pacha	Monte Grande	Paracas Peninsula	Pacapaccari
LIP								8		16
MH					15		2			
Nasca	Late					7	19			
	Middle	15		21	27			8		
	Early		4							
Paracas	Late			48					12	
	Middle									
	Early	5	10							
Initial Period										
Archaic Period		1								

amount of all generated genetic data, used datasets, population statistics, and other details of the conducted studies.

10.3 Results and Interpretation

10.3.1 Molecular Analysis Results and Data Evaluation

Despite recently formulated hypotheses that the ecological conditions of desert environments allow a maximum preservation time for DNA of approximately 700 years (e.g., Marota et al. 2002) the methods used and developed in the context of this study proved successful in the recovery of DNA from much older bone material stored in desert soils. Overall it was possible to reproducibly determine the mt-haplogoups of 131 individuals and mt-haplotypes (complete 388 bp HVR I sequence) of 105 individuals. Amplification of Y-chromosomal DNA was only successful for six individuals (all Y-haplogroup Q-M3), five from the site Pacapaccari (Andean highlands) and one from Jauranga (Palpa). Generally it can be stated that the grade of DNA preservation found in the individuals of the highland Chullpas proved to be better than in the individuals from desert burials. The stable level of humidity and temperature encountered in the Chullpas can be best compared to storage conditions in caves, which proved to be very good for DNA preservation (Burger et al. 1999). The poorer DNA preservation in the Palpa area may be explained by higher temperature and soil pH-value, but also the chronologically changing environmental conditions (Eitel and Mächtle 2006) and therewith storage conditions of the region.

For population statistics the data obtained from the different archaeological sites were grouped by time period and region (e.g., Paracas–Palpa and Paracas–Paracas Peninsula). For the Nasca period two extra divisions were made based on the socioeconomic character of the sites with which the individuals were associated. Individuals from Los Molinos and La Muña belong to the group Nasca-urban whereas all other individuals from sites such as Jauranga or Hanaq Pacha are grouped as Nasca-rural (Table 10.1).

All successfully analysed individuals belong to one of the four Native American haplogroups A, B, C, and D (see above). The distribution of the mt-haplogroups for the analysed populations is found in Table 10.2. For both Paracas populations there are very high frequencies of haplogroup D followed by haplogroup C with a much lower fequency. This dominancy of D persists into the Nasca time as seen with the Nasca (Palpa-rural) population (Table 10.2). For the urban Nasca population, however, D and C were determined with nearly equal frequencies. Parallel to the decrease of D there is an increase of haplogroup B which emerges first in the Palpa area with the Nasca period. This trend continues with the transition to the Middle Horizon (cf. Table 10.2). The frequency distributions of the Palpa populations differ significantly from the highland population of Pacapaccari. Here B is definitely the dominating group and C the only other

Table 10.2 Mitochondrial haplogroup frequencies and haplotype diversity (HD) for the Analysed pre-columbian populations

Group / Population	n[a]	H[b]	Haplogroup Frequency A	B	C	D	Hd[c]
Paracas (Peninsula)	10 (6)	5	0,00	0,00	0,30	0,70	0,93
Paracas (Palpa)	28 (25)	15	0,07	0,00	0,14	0,79	0,95
Nasca–Rural (Palpa)	37 (30)	26	0,02	0,11	0,22	0,65	0,98
Nasca–Urban (Palpa)	28 (25)	17	0,00	0,18	0,43	0,39	0,97
Middle Horizon (Palpa)	11 (6)	6	0,00	0,27	0,36	0,36	1,00
Pacapaccari (Highlands)	16 (12)	6	0,00	0,69	0,31	0,00	0,86

[a] n = Number of individuals with successful haplogroup determination; the number of individuals with sucessfully determined mt-haplotypes follows in brackets.
[b] H = Number of determined different haplotypes in the population.
[c] Hd = Haplotype diversity (Nei 1987). The value relates to the HVR I sequence data not to the haplogroup data.

detected (Table 10.2). The frequencies of haplogoup D of all pre-Colombian coast populations analysed in the context of this study are much higher than in the recent indigenous Peruvian populations and those of the other northern and southern central Andean regions (Fig. 10.1).

The HVR I sequence data from the 105 successfully typed individuals could be assigned to 57 mitochondrial haplotypes of which 32 were single-haplotypes. Twenty-five haplotypes could be detected in more than one individual. Four of them – all distinct haplotypes different from the founder types – appear synchronous in populations from different archaeological sites, cf. one in the Jauranga (Paracas–Palpa) and the Paracas–Peninsula population. Ten haplotypes persist over more than one time period and appear in different populations from the Palpa sites (cf. Fehren-Schmitz 2008). All analysed populations have a high degree of genetic diversity as shown, for example, in the mitochondrial Haplotype-Diversity (Hd, Table 10.2). Even though there is a diachronic and group specific change in the haplogroup frequencies, there is no increase of overall mitochondrial genetic variability. Other conducted population statistic analyses (not shown here) verify this conclusion and also that the high frequencies of group D cannot be explained in terms of genetic isolation.

Conducted genetic distance calculations based on the HVR I sequence data support the considerations derived from the haplogroup data. Very low distances can be determined between both Paracas period populations and the rural Nasca group. These three populations cluster in a genetic distance-based neighbour joining (NJ) tree (Fig. 10.4). The urban Nasca and Middle Horizon populations exhibit a higher distance to the other three pre-Columbian coast populations but still cluster within the same branch of the tree whereas the recent indigenous populations of Peru (data: Fuselli et al. 2003; Lewis et al. 2005) and the pre-Columbian Andean highland site of Pacapaccari form a distinct branch of the tree (Fig. 10.4).

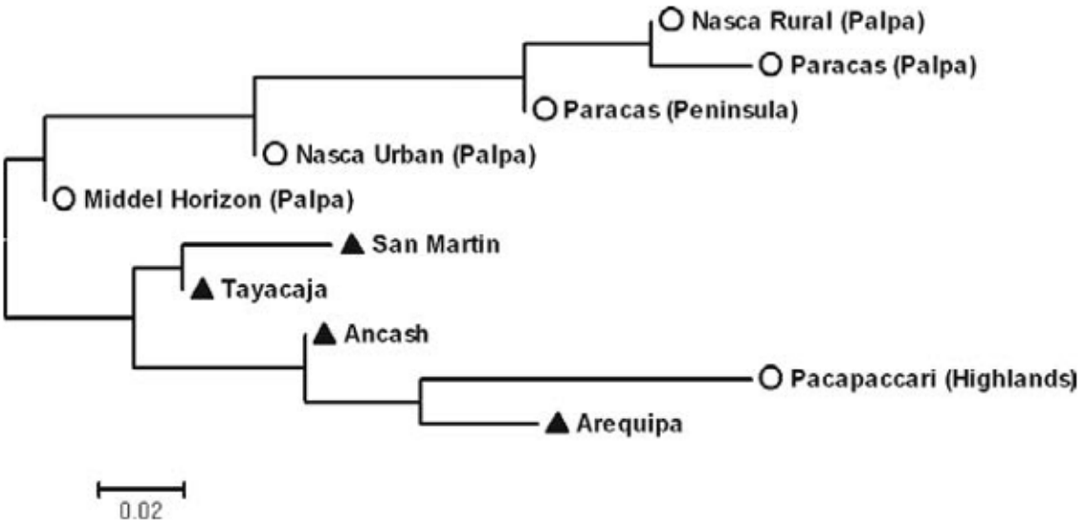

Fig. 10.4 NJ-Tree based on the pairwise F_{ST}-distances of the analysed pre-Columbian populations (*circles*) and four recent Native American populations (*triangles*) from Peru. The calculations are based on HVR I data. The tree is drawn to scale, with branch lengths in the same units as those of the evolutionary distances used to infer the phylogenetic tree

10.3.2 Ancient DNA Data Translated to the Population History of South Peru

Combined with knowledge of the cultural and ecological history the population genetic data can be translated to reconstruct the population dynamic processes of the Palpa region for the investigated timeframe. The genetic similarity of the Paracas populations from the Palpa area and the peninsula, and also the low genetic distance between both allows the conclusion that the Paracas culture of the southern Peruvian coast formed a uniform population. The results also show that there is a high gene flow, thus migration frequency, within the distribution area of the Paracas culture but no significant genetic exchange with the surrounding populations, for example, from the Andean highlands. Distance calculations and distribution patterns also show that there is a constant population in the Palpa area persisting into the Nasca period. These findings combined with archaeological evidence such as parallels in ornaments and the existence of early geoglyphs (Reindel and Gruen 2006) suggest that the Nasca culture of this area evolved from the bearers of the Paracas culture.

Even though the urban and rural Nasca populations exhibit a degree of genetic distance there is no evidence that this results from foreign influences, as it would be expected with an elite dominance migration scenario. This assumption is supported by the fact that individuals from the elite burials of La Muña share mt-haplotypes with the rural populations. The emergence of haplogroup B and the differences between the rural and urban populations suggest that there is a higher amount of genetic exchange with populations from outside the investigated coast area, maybe the highlands. This might be a result of the increase of socioeconomic complexity in the Nasca period which concurrently

would have caused an increase of the migrational pull-factor of this area. A grade of social complexity as is reached in the Nasca culture requires craft and administration specialists (Service 1962). The fact that the genetic population structure changes slightly in the Nasca period, and the urban Nasca population differs from the rural can be best explained by the immigration of foreign specialists into the urban settlements. At the same time these results verify the urban, respectively, central character of this settlements.

There are no significant genetic changes from the Nasca period to the Middle Horizon and therewith no evidence for allochthonous contributions to the Palpa gene pool. Invasion or colonisation scenarios can be rejected as a cause for the demise of the Nasca culture in this area. The decrease of population density in the Late Nasca period and the Middle Horizon contrasted with the constantly high mt-haplotype diversity fits best with scenarios suggesting that the main settlement area of the people shifts eastwards into the Andean valleys as a consequence of climatic aggravations (Eitel and Mächtle 2006).

The pre-Columbian populations of the southern Peruvian coast significantly differ from the recent Peruvian and ancient highland populations although they are very similar to the recent Native American populations of Middle and South Chile (cf. Fig. 10.1; Fehren-Schmitz 2008). Mitochondrial distribution patterns of today's coastal Peru therefore have to be a result of cultural and political processes succeeding the time span investigated in this study. The high frequency of haplogroup B in recent indigenous Peruvian populations suggests that the observed genetic changes are best explained by the expansions of the vast-reaching highland empires, especially the Inca. This assumption is supported by the affinity of the recent Chilean populations to the pre-Columbian Peruvian coastal populations. The maximum southward geographic extension of the Inca empire is congruent with the recent border between populations exhibiting mitochondrial distribution patterns similar to recent Peruvian populations and Chilean populations that exhibit the ancient coastal patterns (Fig. 10.1).

10.4 Future Prospects

The conducted investigations and conclusions show that the use of the archive 'ancient DNA' allows insights into prehistoric population dynamics that could not be achieved by the analysis of archaeological sources or the use of modern DNA alone. Although it was possible to gain novel information about pre-Columbian colonisation and migration processes in western Southern America, especially the southern Peruvian coastal regions, there is still no information about equal processes in the Andean highlands. The only available highland population datasets (this study; Shinoda et al. 2006) date into the Middle Horizon or the Inca period. To reveal the colonisation and migration processes that took place in this second major cultural area of western South America,

studies have to be conducted involving populations dating into the earlier time periods especially those analysed in the present studies.

Furthermore it should be investigated how far the genetic distribution patterns of the populations that settled in the Andean highlands were also affected by terms of selective forces. It is imaginable that the harsh environmental conditions – physiological stressors such as hypoxia (Moran 2000) – of the highlands and therewith the necessary adaptive reactions also had influence on the genetic structures of the populations (Fehren-Schmitz 2008). To answer these questions new genetic markers have to be explored and analysis systems suitable for aDNA analysis have to be developed. As mentioned above, knowledge about the colonisation history of South America is still not satisfying. The presented studies show that one method of resolution for this could be the genetic analysis of more pre-Columbian populations. The analysis of recent native South American populations alone will not solve the problem.

Chapter 11
Humans and Camelids in River Oases of the Ica–Palpa–Nazca Region in Pre-Hispanic Times – Insights from H-C-N-O-S-Sr Isotope Signatures

Peter Horn, Stefan Hölzl, Susanne Rummel, Göran Åberg, Solveig Schiegl, Daniela Biermann, Ulrich Struck and Andreas Rossmann

Abstract Thirty years ago the use of isotope abundance ratios (IR) of bioelements in nutrition studies was a rather young discipline (Krueger and Sullivan 1984). Developed from hydrology, geochemistry, cosmo- and geochronometry isotope studies became a fertile tool also in other fields, and had an especially productive impact on archaeology, respectively, archaeometry (Koch et al. 1994; Buikstra et al. 2005).

The advantage of isotopic parameters is that they are much more insensitive to often unknown influences compared to elemental concentrations or concentration ratios, where one has to deal with ambiguities which arise from differences in chemical properties of the elements. In contrast, IR of elements from various environments (including plants and bodies of animals and humans) are rather predictable or comprehensive after many studies although much remains to be done in this direction. The state of the art in isotope systematics has been presented in several monographs (Kendall and McDonnell 1998; Valley and Cole 2001; Johnson et al. 2004) and in journal articles (Schmidt 2003; Hölzl et al. 2004, and many articles in *Analytical Bioanalytical Chemistry* 2004).

The main objectives of isotope applications in archaeometry are to gain insights into ecosystems and food webs on which once-settling human groups and their animals subsisted, to find out about migrations and relations with trade partners from near and far, and to find hints to reasons why long-lasting socioeconomic evolutions and developments ultimately came to an end after a steep and rapid decline which had been interpreted empirically from archaeological and geomorphological evidence.

S. Hölzl (✉)
Bavarian State Collection for Palaeontology and Geology, Munich, Richard-Wagner Straße 10, 80333, München, Germany
e-mail: s.h@lmu.de

M. Reindel, G.A. Wagner (eds.), *New Technologies for Archaeology*, Natural Science in Archaeology, DOI 10.1007/978-3-540-87438-6_11,
© Springer-Verlag Berlin Heidelberg 2009

11.1 Applications of Isotopes in Archaeology and Palaeoanthropology

The principles of using elements' isotope ratios in these disciplines are that constituent chemical elements from food and beverages – from which hydrogen (H), oxygen (O), carbon (C), nitrogen (N), sulphur (S) and also strontium (Sr) are essential for organisms – enter tissues and carry with them IR which are each specific for a given environment and foodstuff.

With regard to the lithology of rocks from which soils and plant substrates, developed, Sr and S are of use, whereby both elements may also show clear isotopic signals of ocean water in coastal areas. Qualitatively different and mostly independent of the former elements, H and O bear information on climate and weather, distance of a living area from the oceans, its topographic altitude, and geographic latitude. C and N allow insights into the kind of food consumed (plants, freshwater fish, seafood, and whether there were C4-plants such as maize, CAM-plants such as cactuses, or C3-plants such as potatoes in their diets and in the fodder of animals), hence into trophic levels of subsistence, as well as on the prevailing climate and kind of crop cultivation and animal breeding.

When results for human and animal tissues which integrated chemical elements and their IR at different times of life are compared, one gains insights into possible regional provenances and changes of habitats (Horn et al. 1994), and even into times when babies were breast-fed and weaned (Craig 1992).

Amongst human tissues, teeth mirror nutrition in human life from some weeks before birth up to the end of puberty, and hair mirrors that of the last months of life, equal to a growth rate of about a cm/month. Different kinds of bones have (also depending on the age of the individual) biological turnover, or rebuilding, half-lives ($T_{1/2}$) which correspond to overall total remodelling times (τ) from about 2 years (*Crista illiaca*) to 50 years (*cranium*); the relationship between these notations is $\tau = T_{1/2}/\ln 2$.

11.2 Multielement Isotope Analyses (H, C, N, O, S, Sr)

Most of the isotope work performed in the larger region of southern Peru and at many different places on earth, relied on either C- and N-isotopes (Tomczak 2003; Kellner and Schoeninger 2008), on O- and Sr-IR (Knudson and Price 2007), or on Sr-IR alone (Knudson and Buikstra 2007), respectively. Despite the clear evidence that significant contributions to an understanding of the socioeconomic settings for populations under investigation were obtained, even more unequivocal interpretations will be possible by analysing as many isotope parameters as feasible on single or clearly related samples.

Accordingly, we analysed IR of the elements H, C, N, O, S, and Sr on tissues of mummies and animal remains (teeth, hair, and wool in the form of fabrics) from burial sites in the southern Peruvian coastal Atacama desert. The region is situated between Ica, Palpa, and Nasca and the Andean mountain ranges to the east. Archaeological sites are found in or near river oases. The main river which reaches the ocean almost permanently is the Rio Grande with its perennial and smaller ephemeral tributaries. In order to obtain reference values, we also analysed modern and archaeological samples such as plants, phytoliths, foodstuff, raw materials, and tools and some few recent human and animal tissues.

For the first time phytoliths were taken as site-specific spatial integrators for local Sr-isotope signals. Phytoliths are opallike secretions around stomata and between cells of plants which integrate – in addition to other elements – biologically mobile Sr from the soil substrate. By analysing these from different plants growing in former living areas one has a more representative Sr-signal of an area than by analysing single plants; phytoliths are of use whenever one has no local reference tissues (such as snail shells or mouse teeth) available for analysis.

We consider the co-development of analytical tools and instruments (Sect. 11.4) as our main contribution to the aspect of 'new technologies' within the overall research program in that these allow for analyses of higher numbers of samples with rather a variable character, in addition to some further improvements in methodology such as the consideration of hair and wool for determinations of H-IR, which we used for the first time in 2002 on hair of murder victims (unpublished), and in 2003 on mummy hairs (Fehren-Schmitz et al. 2004; Hölzl et al. 2004). A systematic study on the usefulness of hair as a carrier of H-isotopes in archaeological studies was published by Sharp et al. (2003).

This chapter presents an isotopic view of the old ecosystems of river oases which were inhabited from near the Pacific coast (Santa Ana and Monte Grande) to the highlands (Pacapaccari), although most of them at different archaeological periods. We have focused on mummies and items such as food and wool excavated at the localities Jauranga, Los Molinos, Monte Grande, Paracas, and Pacapaccari and covers, whenever hair and tooth samples were both available for analyses, mainly the timespan from Middle Paracas (550 BC) to the end of Wari culture (1000 AD).

After a short description of the applied analytical methods and of their improvements and developments achieved by us in the course of the study, we present the acquired data and interpret them in a general way and give details whenever appropriate (Table 11.1, full data are available on request).

Table 11.1 Mean values and standard deviations of isotopic values from tissues at indicated sites used for diagrams with pooled data

Simple Type, Site, N	δ D(‰)	δ ^{13}C(‰)	δ ^{15}N(‰)	δ ^{34}S (‰)	^{87}Sr/^{86}Sr	δ ^{13}C(‰)	δ ^{18}O(‰)
Wool, all sites, 28	−71±7	−17.3±2	6.8±0.8	4.8±2.3	0.70736±5	–	–
Animal Teeth, all sites, 14	–	–	–	–	0.70669±26	−5.5±2	26.8±1.7
Human Hair, LM A 20, 20	−67±10	−11.3±0.5	8.6±0.9	4.7±1	–	–	–
Hair, LM A 674, 11	−84±4	−15.2±0.6	6.5±0.1	6.3±0.8	–	–	–
Human Teeth, LM A, 16	–	–	–	–	0.70705±30	−6.8±1.7	24.4±0.9
Hair, LM C 34, 14	−74±7	−16.8±0.9	6.0±1.1	4.65±1.3	–	–	–
Teeth, LM C, 10	–	–	–	–	0.70681±32	−7.3±0.8	24.1±1.2
Teeth, LM Nasca, 3	–	–	–	–	0.70715±16	−7.8±0.3	25.2±0.9
Tooth, LM, 1	–	–	–	–	0.70700±3	−6.8±0.1	23.9±0.2
Hair, Mo. Grande 682, 12	−87±4	−10.2±0.4	11.3±0.6	8.3±0.4	–	–	–
Hair, MG 9 Mummies, 9	−83±9	−11.2±1.3	11.0±1.3	7.1±1.3	0.70808±68	–	–
Teeth, MG 9 Mummies, 9	–	–	–	–	0.70772±45	−3.6±1.8	27.1±0.8
Teth, MG, LIP, 6	–	–	–	–	0.70739±33	−7.9±2.7	24.1±0.4
Hair, Pueblo Viejo, 1	−78±2	−13.7±0.9	8.5±1	2.3±0.5	0.70648±3	–	–
Tooth, Pueblo Viejo, 1	–	–	–	–	0.70597±3	−6.3±0.1	24.6±0.2
Teeth, Hanaq Pacha, 6	–	–	–	–	0.70724±32	−7.2±0.9	24.0±1.0
Hair, Puebl, Viejo 1227, 33	−89±4	−12.2±1.3	9.1±0.4	3.4±0.4	–	–	–
Teeth, Jauranga, 26	–	–	–	–	0.70696±26	−9.7±1.4	23.7±0.7
Teeth, Jauranga Nasca, 2/4	–	–	–	–	0.70711±8	−9.5±0.8	22.6±2.5
Teeth, Pinchango Viejo, 4	–	–	–	–	0.70686±40	−10.5±0.2	25.1±0.7
Hair, Par, Huari K. 815, 8	−88±3	−15.2±0.2	14.9±0.7	11.4±0.5	–	–	–
Hair, Paracas, H.K. 816, 7	−98±4	−15.0±0.5	15.1±0.2	12.5±0.5	–	–	–
Hair, Paracas, H.K. 818,5	−87±1	−15.2±0.4	16.0±0.6	12.8±0.3	–	–	–
Teeth, Paracas, H.K. 818, 2	–	–	–	–	0.70722±3	−10.8±0.9	22.6±0.4
Hair, Parac., C. Col. 817, 9	−82±4	−15.2±0.5	15.2±0.5	14.0±0.5	–	–	–
Hair, Par. Cer. Col. 820, 6	−93±3	−16.4±0.3	15.6±0.8	12.8±0.3	–	–	–
Teeth, Paracas, Cave VI, 6	–	–	–	–	0.70754±23	−11.1±0.8	22.9±0.6
Teeth, Pacapaccari, 14	–	–	–	–	0.70659±12	−5.3±0.9	27.3±0.7
Teeth, Sayhua, 4	–	–	–	–	0.70601±2	−4.9±1.9	28.3±1
Teeth, Pernil Alto, 1/7	–	–	–	–	0.70778±3	−9.3±1.1	25.4±2.6

Tables including values for all samples analysed can be provided on request. Analytical uncertainties, STD, of single values for H, C, N, O, S, Sr are ± 2, 0.1, 0.2, 0.2, 0.3, and ± 0.000035, resp.

11.3 Sampling, Sample Selection, and Preparation

After preliminary tests and first analyses on the different kinds of tissues encountered we decided to use hair (animal wool and cotton) and teeth and equally well-preserved remains of plants, tools, and phytoliths. Instead of hair we could have used skin as well. But because this tissue does not allow for time series analyses as do long hair strands (and teeth), we refrained from making much use of it either. Equally, hard tissues of bones proved to be of no value just by the fact that one inevitably needs to analyse several (at least three!) consecutively acid-etched samples in order to, possibly, obtain one single $^{87}Sr/^{86}Sr$ which is equal to that acquired in vivo (Horn et al. 1994; Horn and Müller-Sohnius 1999). Tooth dentine was not analysed for Sr-isotopes in that it is similar to bone. It is, however, used for determinations of C- and O-isotope compositions as it seems to behave conservatively with respect to these. Bone collagen was not well preserved in the bones in too many cases, and nails were hardly ever found. This latter fact is interesting by itself and, most likely, is a result of alterations upon putrefaction soon after death of the individuals).

Recent environmental samples were collected in the region, whereas archaeological samples were either obtained from Peruvian collections or sampled from burial sites and graves together with competent archaeologists. All different kinds of samples were thoroughly ultrasonicated in distilled water in order to remove S- and Sr-containing aerosol precipitates from old and recent seaspray that are ubiquitous even at large distances from the ocean shore and at high altitudes in the Andes. Appropriate cleaning was assumed to be indicated by negative chloride tests (with $AgNO_3$) after washings, which also removed the very fine sulphate particles from this source. Ultrasonication, after pertinent tests, does not bias the results although some fragile wool and plant samples partially disintegrated thereupon and were not analysed.

11.3.1 Hair and Wool

Hair and wool samples were sometimes rather difficult to clean due to adhering limonitic and clayey substances and pieces of grass, seeds, fine wood particles, insects, and the like. After a first raw cleaning by hand, hair strands were brought to the same unidirectional (root-end) lengths of individual hairs, then cut by a kind of hair guillotine with a razor blade into sections of the desired lengths (usually 1 cm), defatted and cleaned again, freeze-dried and ground in a cryogenic steel mill, and weighed out and stored for several days to weeks together with reference casein or keratin before analyses, in order to allow for a correction for exchangeable H (Wassenaar and Hobson 2003). Wool was treated accordingly. Reference material was either casein or, for most of the samples analysed, sheep wool as its chemical composition and structure is more

similar to that of hair. For complex wool samples (fabrics) we differentiated between the discernible kinds of materials and colours: fine or coarse laces, cotton, and rather frequently, interwoven human hairs, whereby the latter were not analysed.

11.3.2 Teeth

Teeth were chosen according to visual inspection and state of preservation and detoriation by 'caries' and indications for coca-chewing. After mechanical cleaning and drilling out deteriorated and stained ('limonitic, cocainic') parts, a given tooth was cut into an enamel and dentine fraction (crown, resp., root section) by use of a thin diamond saw. After drying (6 h at 80°C), the two types of dental tissues were carefully disintegrated in a deep (to prevent undue losses) agate or steel mortar into a coarse powder with grain sizes smaller than approximately 0.4 mm (this is fine enough because at about this nominal particle size brittle, hence relatively fine-grained, enamel and cement already separate well from more ductile and coarser dentine tissue and concentrate in the undersize fraction). The samples were then etched with 0.2 N HCl for 30 min, rinsed with pure water, decanted, and dried repeatedly (etching and rinsing help in washing away particles which are too undersized; amongst those are not only, although predominantly, altered tooth tissues and cement but also secondary or extraneous contaminants).

11.3.2.1 Enamel/Dentine Separation

After the above cleaning steps, we performed heavy liquid separation (pure bromoform, 2.82 g/mL) of the two tissue fractions (Brekhus and Armstrong 1934). Density of enamel is higher than that of bromoform, and that of dentine much lower. The gravity separation is readily done at grain sizes above approximately 10 μm. Whenever one has pure (water- and collagen-poor) enamel, as in our case, its density is >2.89 g/cm^3, that of dentine approximately 2.3 g/cm^3. After this separation is done (with a simple separation device that consists of a separation funnel, an attached plastic tube, and a clamp) the heavy fraction is separated from the lighter one. Suspended particles are discarded or saved for another try at a different liquid density below 2.82 g/cm^3, after free choice by adding ethanol with a low density of about 0.8 g/mL. If the recovery of pure fractions was successful they were ultrasonically washed in ethanol, dried under infrared light and stored.

For the separation of larger numbers the turnover of samples is approximately 20 times that of the conventional technique by manual separation with dentist's tools.

11.3.3 Plants and Phytoliths

Plants were washed, ground to a powder in a cryogenic mill, washed again and freeze dried, and – whenever hydrogen had to be analysed – were treated as described above in the case of hair and wool. Phytolith concentrates were extracted from modern and archaeological plants, dung, and ashes. Thoroughly washed plant material or dung was dried and ashed at 400°C for 2 h, then the ashes dissolved using 3 N HCl and 3 N HNO_3 as 1:1. The acid-insoluble residue was centrifuged from diluted acid and distilled water repeatedly (up to 8 cycles) and comprised a phytolith-enriched fraction. This was suspended in water in a PE beaker and thoroughly stirred and allowed to settle for 60 min and decanted. This procedure was repeated until the water remained clear after 1 h of sedimentation (up to 5 cycles). Whenever miniscule plant fibres remained the concentrate was treated with 30‰ H_2O_2 at 90°C until gas release ceased. This fraction was repeatedly density-separated in a heavy liquid ($[Na_6(H_2W_{12}O_{40})\ H_2O]$, water solution) of density 2.4 g/mL, sonicated, and washed until only grains remained with a density between 2.4–1.3 g/cm^3. Microscopic inspection (under polarised light) showed that phytolith fractions obtained in this way were up to >95‰ (by vol.) clear opal substance; the remaining contaminations were mainly 'black carbon' inclusions.

11.4 Analytical Techniques

11.4.1 $^2H/^1H$, $^{13}C/^{12}C$, $^{15}N/^{14}N$, $^{34}S/^{32}S$

Stable isotopes for which data are presented in this chapter were analysed by means of an instrument combination which, in part, was developed and tested within the frame of this study. Basically an elemental analyser (Vario EL III, Elementar Analysensysteme GmbH, Hanau, Germany), with a water reduction unit and with an automatic carousel for up to 80 samples was coupled to an isotope ratio mass spectrometer (IsoPrime, GV Instruments, Manchester, UK) with an inlet system for four reference gases (N_2, CO_2, H_2, and SO_2). The calibration of the measurement is described in the literature (Sieper et al. 2006). Single sample analyses, including determination of elemental compositions and isotope ratios for the four elements, took 20 min. Results (in delta notation, for nitrogen, carbon, hydrogen, and sulphur relative to AIR, V-PDB, V-SMOW, and CDT) are stated in Table 11.1. Elemental ratios C/N and C/S (not given) for soft tissues are in the conventionally accepted ranges for well or reasonably preserved tissues; those with aberrant values were excluded from further consideration.

11.4.2 $^{13}C/^{12}C$ and $^{18}O/^{16}O$ of Structural Carbonate in Enamel and Dentine

Analyses for these elements' isotopes were performed on 300±100 µg aliquots of samples. These were treated with orthophosphoric acid at 72°C (1.5 h), and the evolved CO_2 flushed into the isotope ratio mass spectrometer with He as carrier gas (the instrument combination used is the Gasbench II and Delta plus, Thermo-Finnigan). Laboratory isotope standards were calibrated against IAEA carbonate standards NBS 18 and NBS 19. Data for structural enamel and dentine apatite–carbonate are given in delta notations for carbon and oxygen relative to V-PDB and V-SMOW, respectively; conservatively assumed uncertainties of results (standard deviations, STD) are indicated in Table 11.1.

Although we do not discuss details concerning differences between $^{13}C/^{12}C$ and $^{18}O/^{16}O$ of enamel and dentine in this chapter, we want to point to the fact that $\delta^{13}C$-values for enamel and dentine are well correlated but systematically higher in enamel overall by 1–2‰, whereas for $\delta^{18}O$ there is no systematic difference discernible between the two tissues. Only careful comparison of these and other parameters considering mixing relationships, too, can show if differences or agreements of values are acquired in vivo or whether secondary diagenetic influences play a role.

11.4.3 $^{87}Sr/^{86}Sr$

Hair, wool, and enamel aliquots from preparative steps (Sect. 11.3) were strongly rinsed and etched under ultrasonic agitation in 2 N HNO_3 (in order to remove outer layers) and ashed; leachates were discarded. Equally, surface-etched teeth were totally dissolved in 6 N HCl and evaporated to dryness and ashed in carefully precleaned quartz glass beakers at 800°C for approximately 2 h, as were the acid-rinsed hair and wool samples.

Ashes were dissolved in concentrated HNO_3, evaporated to dryness and taken up with 6 N HNO_3. Sr was then isolated from other elements such as Ca, Ba, and Rb by ion-chromatography on Eichrom Sr-spec® resin. Due to small resin volume (50 µL) and the small amounts of chemicals required (2 mL of HNO_3 in total), the usage of only extremely clean reagents (water and acid were cleaned by subboiling distillation) and multiply cleaned quartz- and teflon-beakers and the performance of separations under clean-room conditions (class 100 laboratory), total blanks were mostly well below 100 pg Sr (depending on type/amount of samples and decomposition method). In view of Sr contents of 200 ng and more in samples this value is negligible. Phytolith concentrates with typical Sr-conc. of approximately 5–20 µg/g were acid digested in HF plus some drops of $HClO_4$, evaporated, taken up with 6 N HNO_3, and submitted to ion exchange.

Isotope analyses of Sr were performed on a Thermal Ionisation Mass Spectrometer (TIMS, MAT 261.8, Thermo Finnigan). Tungsten-single-filaments were used for the measurements. Any extant Rb was evaporated from the loaded filament by controlled preheating before the isotopic composition of Sr was measured. For quality control and to check for proper operation of the mass spectrometer, a certified reference material ($SrCO_3$, NIST SRM 987) was co-analysed under the same conditions as samples (60 single scans, $^{87}Sr/^{86}Sr$ mean value: 0.710251±0.000023, STD, and $n = 120$). Isotope mass fractionation during analysis was corrected by referencing to an invariant $^{88}Sr/^{86}Sr$ value of 8.37521. The precision of Sr isotope measurements normally is <30 ppm ($2\sigma_m$). Total analytical uncertainty (precision + accuracy) for $^{87}Sr/^{86}Sr$ on natural samples is assumed to be <50 ppm.

This value was confirmed by replicate analyses of (homogenised) tooth samples within the project. Analytical uncertainties thus are smaller by a factor of 10–100 than natural variations even within lithologically very homogeneous areas (Horn et al. 2005). Repeated analyses of similar but nonidentical sample material (e.g., nonhomogenised tooth fractions) also showed that sample inhomogeneity (e.g., due to nonidentified partial alteration) is occasionally the limiting factor for total uncertainties of results (reproducibility is in worst cases ±100 ppm). For deeper insights into best achievable uncertainties of Sr isotope measurements on approved international standards see Müller-Sohnius (2007).

11.5 Interpretation

The mean values and standard deviations of isotopic data are presented in Table 11.1. As a consequence of very different grades of tissue preservation (and different burial traditions through the times), and due to availability of samples from different sites it was not possible to obtain and analyse the very same kinds of tissues from all excavated habitats and cemeteries through the whole time-range of settlements (from the Initial period up to the Late Intermediate period) and for all elements. Therefore, occasionally we had to puzzle out how to arrange for the best comparisons of data from only hair, or hair and teeth, and of those obtained on teeth only; we decided to use mean values from either tissue from given sites. Thereby, we also integrated over hair values which in most cases represented those of segments from pigtails which most likely belonged to one, and only one individual (an assumption which, however, need not be true in every case if one takes into account the proven assemblages of hair strands to mimic longer than naturally grown pigtails (cf 11.5.6)).

11.5.1 Soft Tissues, a Synopsis of $\delta^{15}N$- and $\delta^{13}C$-Values

Figure 11.1 displays $\delta^{15}N$ versus $\delta^{13}C$ for all soft tissues analysed and is aimed at providing an overview of values encountered in a variety of recent and fossil

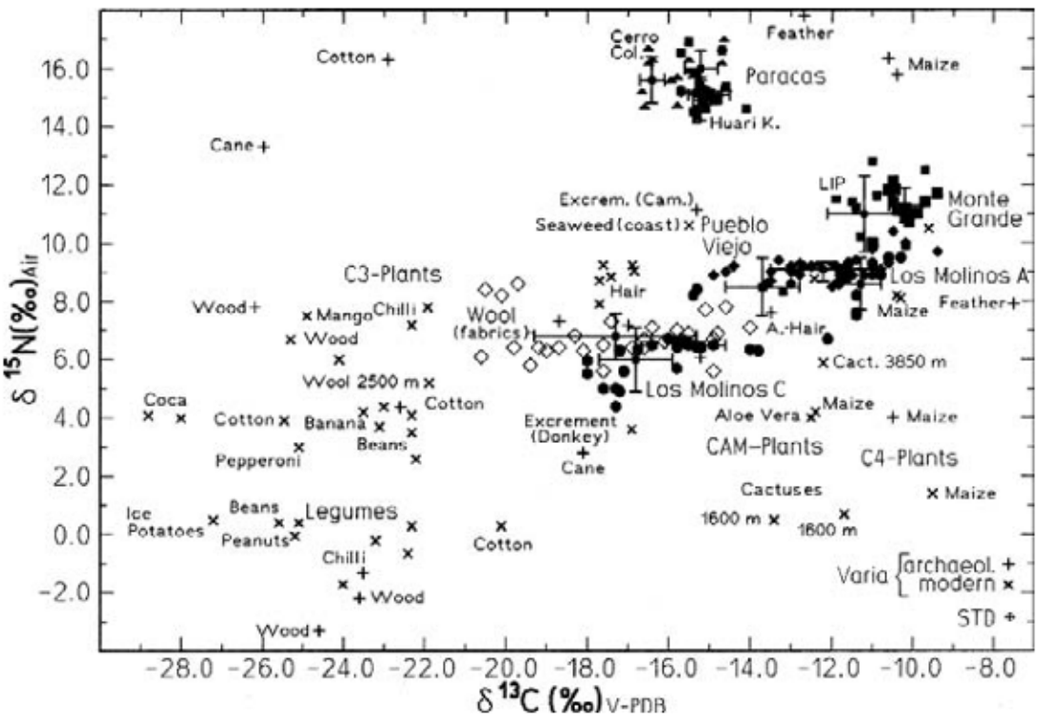

Fig. 11.1 Overall view on $\delta^{15}N$ versus $\delta^{13}C$ single isotopic values (with mean values ± standard deviations, for main sites with archaeological finds) analysed on recent and archaeological hair, wool, food, and materials collected in the project study area. The latter reaches from the Paracas peninsula near Pisco in the north to the city of Nazca in the south, and follows the Ica–Nazca depression between the Andean western slopes and the mountain range of the coastal cordillera; it also comprises the site of Monte Grande some 5 km inland from the Pacific coast within the cordillera. To $\delta^{13}C$ values determined for recent samples 1.5‰ were added to correct for the Suess-effect (global fossil CO_2 effect); this allows for direct comparisons of recent values with archaeological ones. Archaeological hair: black symbols, wool: diamonds. Marine food web plot in the upper right quadrangle of the diagram with $\delta^{15}N$ above about 10‰ and $\delta^{13}C$ above −17‰

plants, foodstuff, wool, and hair in the total study area; we refrain from going into details here and just mention that with regard to $\delta^{13}C$-values we can clearly distinguish among C4-, CAM-, and C3-plants (including legumes that fix atmospheric nitrogen). Relatively high values in hair, at a first sight, we interpret to mirror maize and/or seafood consumption.

From the widely varying $\delta^{15}N$ for hair, however, it is readily evident that the nutritional status of members from the various human groups were rather distinct. Those with values higher than 14‰ (Paracas) had at their disposal the highest share of animal proteins from their food, and those from Los Molinos C, LM C, the lowest, if any at all. The latter must have eaten like persons who nowadays are vegans! From archaeological evidence the inhabitants (presumably those buried there, to be correct) of LM C lived in relatively simple huts made from cane and hay, whereas at Los Molinos A brick and stone buildings were prevalent (Reindel and Isla 2001). Taking the data at face value, the fact that data for wool (camelids, from LM A, LM C, and also from Monte Grande) coincide almost perfectly with those for human hair from LM C implies that the latter must have eaten almost the same as animal feed (plants,

vegetables, CAM-plants, although presumably not C4-grasses), and the others (Pueblo Viejo, LM A, Monte Grande, and those with their remains on Paracas peninsula) subsisted more comfortably or privileged.

Before reasoning about the kind of protein taken up by humans (herbal, animal, terrestrial vs. marine), from LM A, Monte Grande, and from Paracas sites in the next sections, we have a look at nitrogen values of some of the foodstuffs and other plants available in the region. According to archaeological evidence maize was consumed, cotton was used for weavings and cords, and cane as building material and for making baskets. The spread in $\delta^{15}N$ values is very large, and 'normal' values are around -2 to $+6$‰, whereas higher values are best explained by organically fertilising with dung or manure and, hence rather clearly, prove cultivation efforts, especially at sites with high levels of plant $\delta^{15}N$ ('dung effect'). In this context, it has to be mentioned that at the archaeological sites in the valleys of Rio Grande, Rio Palpa, Rio Santa Cruz, and Rio Viscas, where at the valley flanks cultivation terraces with at least remains of shelters were found, the (still remaining) A-horizons on these terraces are sometimes very thick with organic litter (and fragments of pottery and other artefacts) and point to intentional deployment of dung and manure.

A similar (much earlier) observation on archaeological Peruvian plant remains from the coastal desert (that showed $\delta^{15}N$-values of up to 48‰) was interpreted rather differently by DeNiro and Hastorf (1985) in that they ascribed it to diagenetic alterations of unknown character; microbial decomposition and adsorption of particulate soil components upon diagenesis they, however, ruled out. In this chapter we offer the dung effect as a possible explanation (although questions remain!).

From Sect. 11.5.1 we sum up:

1. Human nutritional states or trophic levels were rather different at different/similar sites/times in the region of study. Some, especially those that lived/were buried at Los Molinos A, Pueblo Viejo, Monte Grande, and Paracas subsisted on higher shares of proteins and maize than those buried at LM C (note: maize is a plant very poor in proteins; coca is the richest in herbal proteins).
2. Some humans nourished themselves as did camelids (LM C) and lived in the same environments; animals had maize in their fodder, presumably leaves from this plant, and most likely also CAM-plants.
3. On crop cultivation terraces and at other places indications for very intense organic fertilisation of substrates by manure and plant litter were observed which show up in elevated $\delta^{15}N$ in useful plants from there (such as cotton, cane, and maize). Values can be well above 14‰, a level never found in recent plants from the whole region; we like to call this a "dung effect".
4. Camelids, from which wool was used for web fabrics, were approximately at the same (relative) health level as the humans from LM C (with respect to water and nutritional stress); for none of the wool samples, hence animals, can we deduce a highland provenance. They, by all evidence, were tended near living places of humans.

11.5.2 Soft Tissues, a Synopsis of $\delta^{15}N$- and $\delta^{34}S$-Values

From Fig. 11.2 it should be possible to recognise those individuals or groups who had access to seafood or food grown under the influence of sea spray which both would show elevated $\delta^{34}S$-values up to approximately 20‰ (present-day seawater sulphate = 21.1±0.25‰, Coplen et al. 2003). The situation is not really simple in that plants are typically depleted in ^{34}S by 1.5‰ compared to sulphate sources (soil water, wet and dry deposition; Trust and Fry 1992) and especially because Richards et al. (2003) have shown that animals (horses) fed on C3-plants showed a small trophic level effect of −1‰, whereas those on C4-fodder (low accessible protein contents) of +4‰. The latter effect, however, was explained by these authors through isotope fractionation upon recycling of endogenous body proteins and not in the course of sulphur metabolism from fodder. In that organic sulphur ultimately is derived from assimilatory sulphate reduction which conserves IR of the sulphate source rather well (Canfield 2001), we discuss our data by taking into account an effective and enhanced uncertainty of −1.5/+4‰ = ±3‰ for found $\delta^{34}S$-values.

Even with such an assumed large and quite conservative uncertainty we can ascribe a significant share of food of marine provenance to individuals from Paracas and most likely but to a minor extent also to those buried at Monte Grande although they consumed less seafood. Also because Palaeozoic,

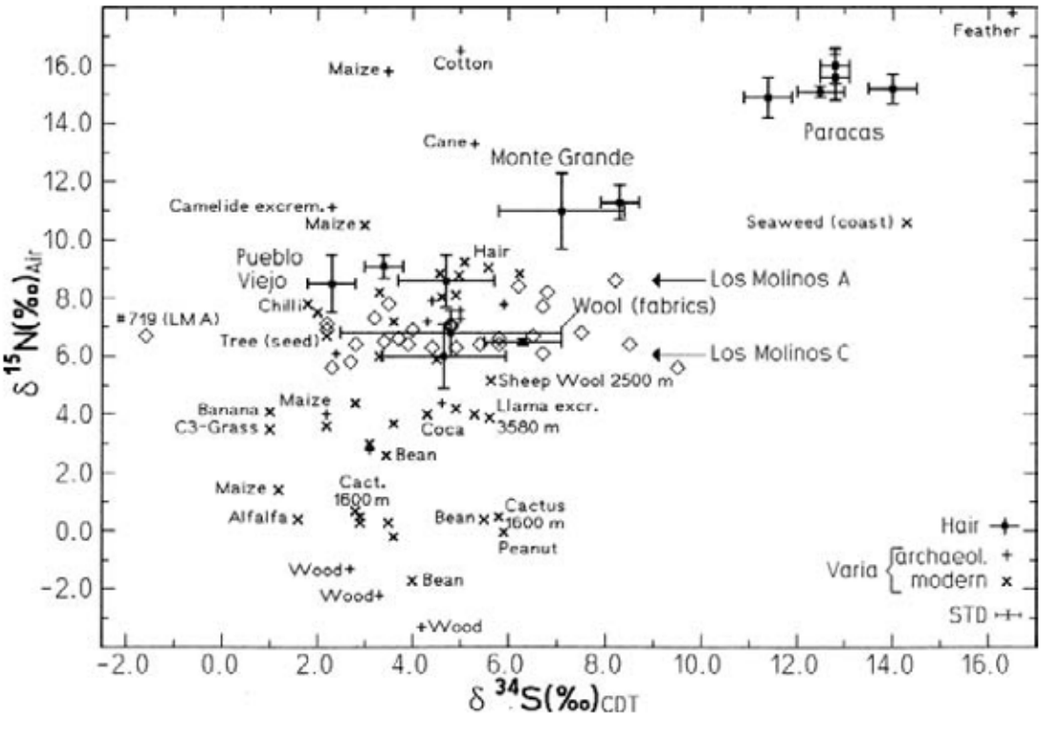

Fig. 11.2 Overall view on mean values (and standard deviations, for $\delta^{15}N$ vs. $\delta^{34}S$) analysed on recent and archaeological hair and wool from various sites, and on recent and archaeological plants and materials. Archaeological hair: black squares, archaeological wool: diamonds. Marine food web plot in the upper right corner of the diagram above approximately 10‰ in $\delta^{15}N$, and 8‰ in $\delta^{34}S$

Mesozoic, and Tertiary marine sediments are found in the studied area (with sulphates that show values from 12 to 22‰ in $\delta^{34}S$) we consider the relatively high values in hair of individuals from Paracas, and to a lesser extent in those from Monte Grande, as markers for presence of marine sulphur; but only because at the same time $\delta^{15}N$- and $\delta^{13}C$-values are high as well. A $\delta^{34}S$ above 7‰ is only a necessary requirement for a possible presence of marine sulphur in the tissue, but this must inevitably be accompanied by high $\delta^{13}C$- and $\delta^{15}N$-values (above approx. −17‰, resp. + 10‰) in order to prove direct uptake of marine sulphur in the sense of a satisfying condition! This restriction has to be considered because also inland one may well encounter food with marine sulphur which stems from widespread (old) marine sediments; in our study these are mixed marine/terrigenic sediments. However, it is unlikely that corresponding high carbon- and nitrogen-isotope values in those sediments are preserved and find their way into the food chain.

From Sect. 11.5.2 we sum up:

1. From the combined consideration of $\delta^{34}S$-, $\delta^{15}N$-, and $\delta^{13}C$-values in hair and wool, we see clear evidence for access to food from marine resources only for burials from the Paracas peninsula, and for a small share of seafood for those buried at Monte Grande (which is only 5 km from the coast). Inhabitants from Los Molinos A had no significant share of food from the ocean, nor of food cultivated onshore and exposed to seaspray.
2. Slight indications for an admixture of marine sulphur in some wool samples can be explained by occasional feeding of animals with seaweed from the coast (as is the case also today).
3. Admixtures of oceanic sulphur in the form of guano or seaweed as fertiliser or dung to substrates of plants are not discernible.

11.5.3 $\delta^{2}H$ of Hair and Wool, $\delta^{13}C$ of Teeth Versus $\delta^{18}O$ of Teeth and the GMWL

In Fig. 11.3 water from La Maquina plots well on the GMWL (Global Meteoric Water line) and its isotopic composition seems to be the result of a normal altitude effect on precipitation, which is also described for northern Chile. The apparent systematic decrease in IR of both hydrogen and oxygen along the GMWL with height is a kind of artefact which results from combining data for summer and winter seasons (Gonfiantini et al. 2001). Without going into details it should be mentioned here that most of the air masses which bring rain (in winter) originate from the Atlantic and are transported by northeast and southeast trade winds, pass the Amazon basin, and ascend the Andes and rain out at convective centres on western mountain slopes. A small fraction of precipitation on the western slopes of the Andes, also in southern Peru, is fed from moisture which originates from the Pacific.

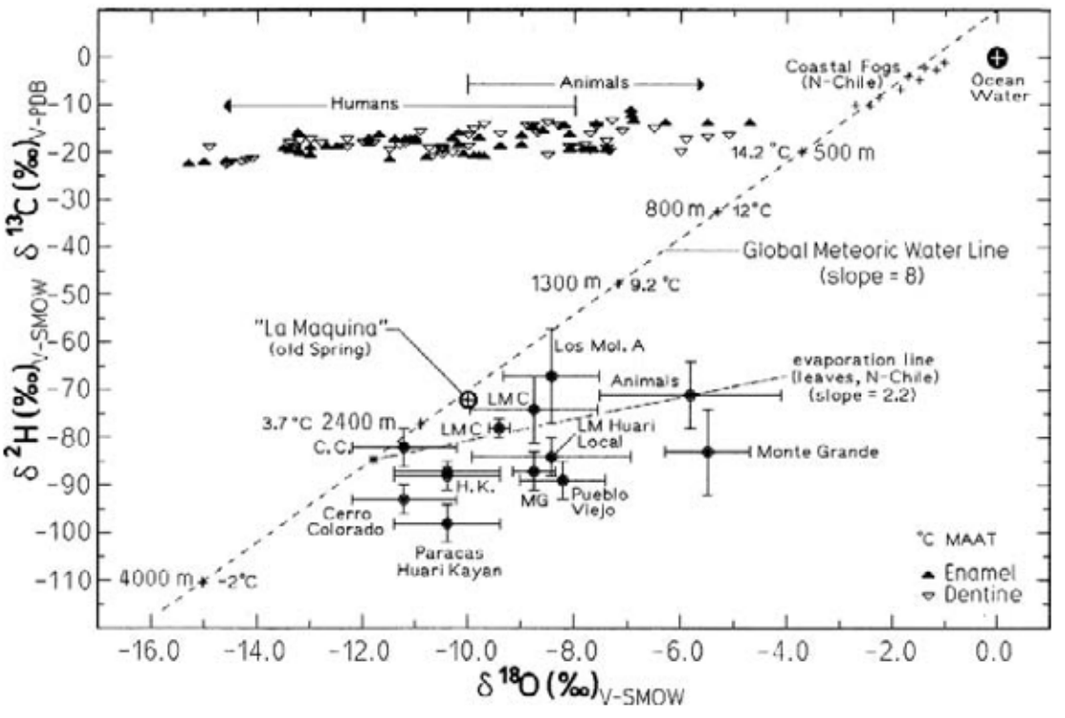

Fig. 11.3 The global meteoric water line (GMWL) and measured δ^2H data for archaeological hair and wool together with derived δ^{18}O data for teeth from the same sites or from the very same individuals according to $(\delta^{18}O_{\text{apatite-phosphate}}-23)/0.9$, which represents ingested water + drinking water according to Kohn and Cerling (2002). In addition to river water the old spring La Maquina probably served as a permanent water source in past times and is still active today. Mean annual air temperatures, MAAT, were calculated from O data of structural carbonate of teeth according to Dansgaard (1964); mean altitudes of water catchments are estimated from general relationships in the Andes (Gonfiantini et al. 2001); data for coastal fogs and the leaves' evaporation line from northern Chile are from Aravena et al. (1989, 1999). Included in the diagram are δ^{13}C-values for enamel and dentine of humans and animals (measured values minus 9.4‰ to represent total diet C)

A straightforward comparison of hydrogen and oxygen isotope ratios in animal and human tissues, which ultimately stem from precipitation certainly is not possible due to complex metabolic pathways (Tuross et al. 2008). However, qualitative or even semi-quantitative assumptions seem to be justified in that the δ^{18}Otissue-ingested water relationship is well established and the fractionation correction for δ^2Htissue-ingested water + drinking water is relatively small (e.g., −17‰ according to Sharp et al. 2003). If we apply no correction and use the values for hair and wool as they were measured we obtain a picture which best matches the evaporation line for leaves and includes the values for water from La Maquina as a definite former water source for humans. This picture is not so unrealistic as all data plot to the right of GMWL and as the fractionation line for leaves passes through the mean values for animals (wool) which grazed on such plants that inevitably suffered evapotranspirative losses of water with increases in δ-values for hydrogen and oxygen.

According to this diagram those groups or individuals for whom the data are farthest off the GMWL (on an evaporation tieline with the same slope as that for leaves) had water (from food and drinking water in proportions of about 75:25, Sharp et al. 2003) in their tissues which underwent evaporation or

evapotranspiration before it was ingested. This is in accordance with the fact that data for animals plot relatively far off the GMWL, as do those for humans buried at Monte Grande, whereas mean values for individuals from Cerro Colorado plot almost on the GMWL and imply no or only little evaporative water losses. Intercepts of individual evaporation lines with the GMWL represent isotopic compositions of water that was actually available. For those from Los Molinos A this could preferably have been water from La Maquina.

Birchall et al. (2005) presented striking empirical evidence for a trophic level effect for hydrogen in collagen-proteins from animals between levels of herbivores and omnivores to those of carnivores of about +90‰. If we assume that at least individuals from LM A had animal meat or fish in their diets occasionally one should expect higher δ^2H-values in hair from this group than the rather insignificant enrichment actually discernible from Fig. 11.3 over those values found for animals, and humans from LM C. We, however, do not recognise such an enrichment in our data which implies that none of the groups had significant shares of meat or fish in their diets (individuals from Paracas have to be excluded from this discussion here in that they had access to very 'cold' isotopically depleted water; but if one assumes that they actually had access to meat, a trophic level effect of +90‰ would lead to unrealistic low values for water at disposal).

δ^{13}C versus δ^{18}O data for dentine and enamel are presented to demonstrate that there is an apparent altitude effect for carbon (Fig. 11.5, Sect. 11.5.5), which, more likely, represents only variable shares of maize or seafood in respective diets.

From Sect. 11.5.3 we sum up:

1. Humans ate no or only little meat and fish according to the lack of evidence of a trophic level effect for hydrogen between animals (wool) and hair, a conclusion which evidently is in contradiction to the summary of Sect. 11.5.1, point 1; therefore, we consider the lacking enrichment of δ^2H a strong argument against consumption of significant amounts of meat. (Paracas burials are excluded from this argumentation in that we do not know from where they originally stem and which water they had at their disposal; we only know that it was very cold and fresh.)
2. Water-use conditions in the region are typical for arid regions with low humidity; nevertheless, animals also had access to fresh water from high lying catchment areas; this points to a favourable water management strategy (at all archaeological periods under consideration).
3. From δ^{18}O- values for animal teeth, we conclude that animals lived with humans at archaeological sites in the lowlands; none of the animals shows highland isotope values in tissues (this confirms Sect. 11.5.1, point 4).

11.5.4 Soft and Hard Tissues: $^{87}Sr/^{86}Sr$- and $\delta^{13}C$-Values

$^{87}Sr/^{86}Sr$-values in tissues and phytoliths from our region are confined to a relatively narrow range and, unfortunately, are not very specific. Values around

the mean found here (0.70713±0.00046, $N = 116$) are found everywhere (in country rocks, soils, plants, hair, wool, and teeth, modern or archaeological) on the western slope of the southern central Andes (Coudrain et al. 2002; Knudson 2004; Knudson and Buikstra 2007; Knudson and Price 2007; Knudson et al. 2004). Lower or higher values are rarely encountered at certain areas with mafic, respectively, silicic rocks exposed (Wipf 2006; Zeil 1983).

A phytolith concentrate from the Pernil Alto site has a value of 0.70918, which is the highest found for all our samples and is assumed to faithfully reflect loess occurrences in the region; by fortuitous coincidence this value is also that of seawater (which in archaeological times was the very same as today).

Despite the narrow range of Sr-values, in Fig. 11.4 values for tissues from the main sites cannot only be discriminated by $\delta^{13}C$- values, but also by Sr-IR. Sites from the Paracas peninsula especially form a distinct group, also those of Pacapaccari (+Sayhua), and of Monte Grande. The values for other sites overlap within standard deviations calculated for all samples from a given site. As in the foregoing figures, teeth values for animals overlap with values for humans and confirm similar nutrition. However, somehow irritating is the very significant difference between wool and animal tooth data, in both $^{87}Sr/^{86}Sr$ and $\delta^{13}C$. This difference implies that teeth of the camelids grew when they lived in an environment other than that when hair grew which was

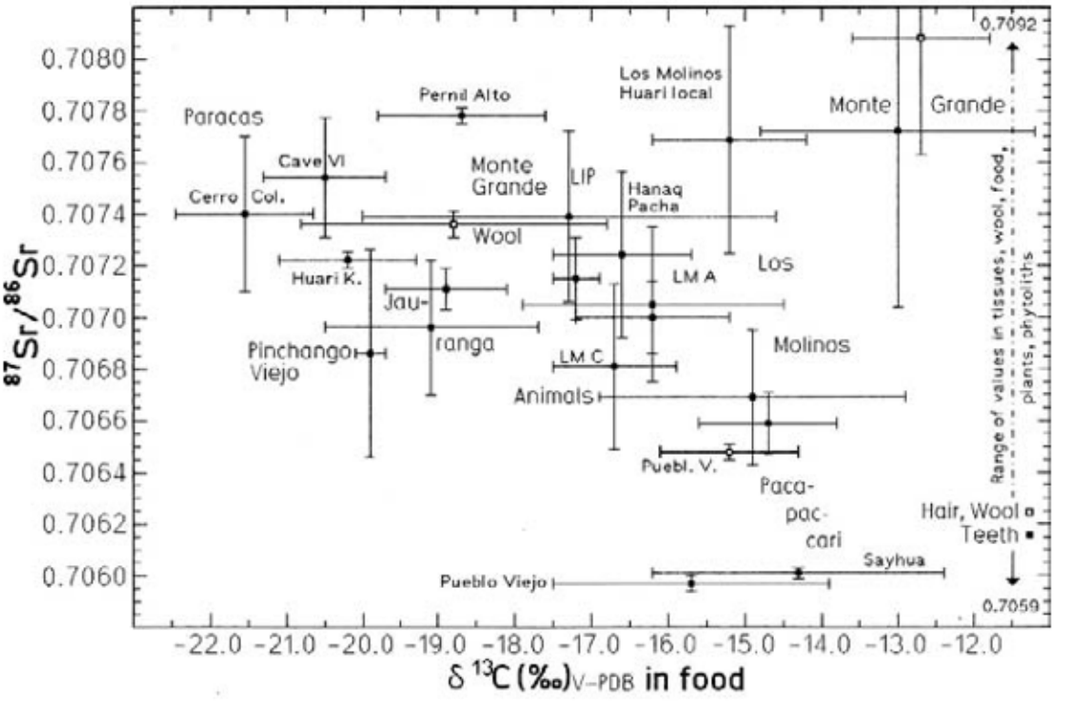

Fig. 11.4 Overall view on mean values (and respective standard deviations, for $^{87}Sr/^{86}Sr$ vs. $\delta^{13}C$) from human teeth and hair, wool, and animal teeth from archaeological sites. Values for $^{87}Sr/^{86}Sr$ are those measured; those for $\delta^{13}C$ on hair and wool are corrected for trophic level effects by subtracting 1.5‰ and those for teeth (structural apatite carbonate) by subtracting 9.4‰ from measured values (Ambrose et al. 1997), hence on both axes represent mean food (fodder) values

used for wool. We want to try to solve this problem when the remainder of available data are discussed in the next section below. There, we also try to solve the apparent contradiction between carbon data for teeth from Pacapaccari and Sayhua (burial sites located at 3500 m, but maize in the diet) and from Paracas (burial sites near the Pacific, but mainly C3-plants in the diet).

Significant differences of $^{87}Sr/^{86}Sr$ in hair values from those in teeth (e.g., from Pueblo Viejo) are clear indications of changes of environments or habitats; concordance of data (as in the case of Monte Grande) points to general sedentariness for the group under study.

If we consider $^{87}Sr/^{86}Sr$ that has, as does S, a well-defined constant value in ocean water of 0.70918 under aspects of two component mixtures with site-specific $^{87}Sr/^{86}Sr$ and 0.70918 as end members, we do not find any hints of an admixture of Sr from seawater to any of the samples analysed (although Sr has a relatively high concentration of 7.6 µg/g in ocean water). Certainly, the reason for this is that in food chains Sr is strongly discriminated against Ca, an effect that is called 'biopurification' (Elias et al. 1982). In transfer of Sr from soil to tissues of omnivores Sr/Ca is decreased to 1/72 of the original value in soil. Therefore, the lacking influence of seawater Sr on that of tissues (which by themselves have high Sr concentrations of about 10 ppm in hair and wool up to 100 mg/ppm or more in teeth, is therefore not astonishing.

From Sect. 11.5.4 we sum up:

1. By considering $^{87}Sr/^{86}Sr$ from hard and soft tissues a parameter is at hand which allows us to differentiate between main archaeological sites within the study area, although the total variance of Sr-values is small.
2. Due to the process of biopurification of Ca from Sr it is unlikely that isotopic signals from occasional ingestion of marine food show up in tissues.
3. Generally low values for $^{87}Sr/^{86}Sr$ in all analysed samples is proof that neither human individuals nor animals lived or grazed in the coastal cordillera where values can be high (well above 0.715 on terrains with granitic rocks and as they are exposed, e.g., near Monte Grande).

11.5.5 $\delta^{18}O$ and $\delta^{13}C$ in Teeth Versus Burial Sites – Two Contradictions

Teeth of individuals who were buried as mummies on the peninsula of Paracas (<700 m a.s.l.) show isotopic signatures in $\delta^{18}O$ and $\delta^{13}C$ (Fig. 11.5) which are indicative of habitats (when their teeth formed till end of puberty) in the highlands, those from Pacapaccari and Sayhua (found at bone and skull places at approx. 3500 m a.s.l.) carry isotope signatures in teeth which point to coastal habitats. Only for individuals from Paracas we could also analyse hair (pigtails), the results of which are in concordance with a coastal habitat and nourishment in all cases, namely five, at times when hair grew (the last 50 months, hence four years, of life as estimated from the longest pigtail with

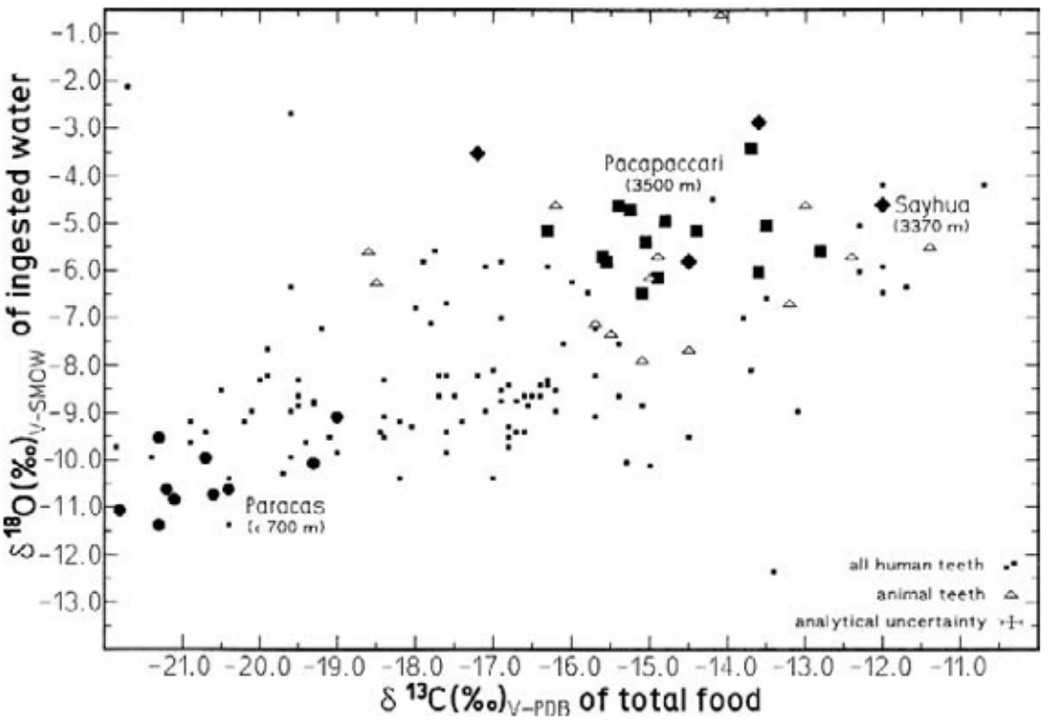

Fig. 11.5 $\delta^{18}O$ versus $\delta^{13}C$ diagram with values for enamel and dentine calculated for ingested water, respectively, total food (see legends to Figs. 11.3 and 11.4). The apparent paradox is that those individuals buried at high altitudes (Pacapaccari and Sayhua) show lifetime values which point to a warm and damp climate, and those buried on Paracas peninsula lived in a cold climate, presumably at height

50 cm of length). This implies a change of habitat at least four years before death (for this individual).

In that water – which was then available for all humans and animals considered here – is rather uniform isotopically (low values for H- and O-IR, Sect. 11.5.3) and clearly stems from high altitudes in the Andes, the very high tooth values for individuals buried at Pacapaccari (and Sayhua) imply that they cannot stem from any of the river oases on the western slopes of the Andes in our study area, not even directly from the coast, because there rivers still have 'cold' (low) isotopic signatures (e.g., at Monte Grande) and where Chilean Mediterranean fog, neblina, or Camanchaca (for data see Fig. 11.3) did not then significantly contribute to water accessible for humans.

As we have only results from tooth analyses from burials at high altitudes at hand (for C, O, and Sr), we cannot discuss further isotopic evidence in order to assign a reliable provenance; to do so we plan to extract enamel-collagen from such teeth in the near future. Until results for this tissue are available we refrain from speculation and just mention that the respective humans, most likely, stem from places far away from their burial site and from outside our study area, perhaps from the Amazon Basin, as we feel that data already available could be appropriate. Sr-isotope values, however, fit those of a mummy from Pueblo Viejo, well within our study area, but do not prove an origin from that region.

For burials from Paracas we assume that they originate from our study area (although far inland/upland), and that they had access to seafood in their last approximately four years of life.

From Sect. 11.5.5 we sum up:

1. Individuals buried on the Paracas peninsula lived there at least four years before death and burial; they grew up in a totally different environment which well might have been located in the highlands of our study area, not ruling out other similar provenances.
2. For individuals buried at sites of Pacapaccari and Sayhua our data (only from teeth) point to a youth in an area very different from any of those within our study area; according to available isotopic arguments they stem from a moist and damp inland area which, however, shows biologically available Sr-values such as those found for the region from Pueblo Viejo (which is, however, not a proof for a provenance from there).

   Significant differences between $^{87}Sr/^{86}Sr$ and small ones of $\delta^{13}C$ of animal teeth and wool have to be interpreted as indications for living areas in youth (up to ages of ca. two years when tooth development ceases) rather different from those at higher ages when they were browsing and grazing around. Whether within the higher values of $\delta^{13}C$ in teeth over that in wool a suckling signal is hidden can only be decided also after $\delta^{15}N$ in tooth collagen is analysed.

11.5.6 Side Results

1. On segments of three 160–186 cm long pigtails (from the Museum of Ica, and archaeological sites at Monte Grande and Pueblo Viejo) we analysed IR for H, C, N, S, and found that there are hiatuses at about 30–40 cm in each (not shown). Together with more convincing observations upon dissections of the objects (G. Horn, priv. comm. 2007), we interpret these combined results and observations as proof for artificial extensions of pigtails at least in these three cases. Time series analyses on pigtails in no case allowed a clear recognition of seasonal fluctuations of values.
2. We can identify by our data only few 'outliers' (from data for groups of humans; see Table 11.1) which we prefer to consider as migrants. In that these are only few by number, we do not discuss this subject further here.
3. At Pernil Alto (the oldest settlement, Initial period, amongst those considered) maize (or seafood) contributed to the diets after C isotope evidence in tooth tissues. In order to verify or disprove this, analyses on soft tissues from teeth (collagen) are in progress.

11.6 Summary and Conclusions

In essence, our results show that humans who once lived in the area of Ica–Palpa–Nazca, behaved very conservatively. They remained at places of birth, with very few exceptions such as those buried at Paracas and Pacapaccari. All in all, one can deduce a steady living, at all time periods, and a subsistence on almost the very same natural resources among which maize played a major role.

In the river oases humans and camelids had access to fresh water from high-altitude catchment areas which is taken as proof for an effective water use management.

The society of Los Molinos was hierarchically structured in that inhabitants of LM C, most likely, have been herdsmen/-women of camelids and nourished themselves as vegans, whereas those from LM A subsisted mainly on maize cultivation and consumption. Only individuals buried at the Paracas peninsula had seafood in their diets, as did those from Monte Grande but in smaller amounts.

In plant cultivation dung in the form of manure and plant litter was used, sometimes excessively; guano and seaweed were not used as dung.

Results obtained in the course of this study are presented here as a framework for ongoing detailed studies on behaviour and provenances of those individuals for which migrations can be inferred, and by taking into account accumulated archaeological and anthropological knowledge from other study groups of the project.

Acknowledgment We thank the organisers of the project in Peru and Germany and colleagues who participated in the multidiscipline consortium study for all the support which we experienced during sampling campaigns in the field, and on occasions of discussing results and problems with interpretations of data. We thank Ewgenija Kuhl from HU, Berlin, for carefully analysing O- and C-isotopic compositions of teeth, Susanne Schlegel from DAI, Bonn is thanked for providing help in sample assignments, and Christine Lehn, Forensic Institute LMU, München for preparing numerous plant and hair samples for H-,C-,N-, S-isotope analyses.

Chapter 12
The Nasca and Their Dear Creatures – Molecular Genetic Analysis of Pre-Columbian Camelid Bones and Textiles

Rebecca Renneberg, Susanne Hummel and Bernd Herrmann

Abstract In the excavation sites of the Palpa valley most of the animal remains are South American camels. By morphological methods the distinction between the four types, the two wild species, vicuña and guanaco, and the two domesticated species, llama and alpaca, is nearly impossible. This study, as part of the subproject 'Palaeogenetics/Human Ecology', was concerned with the molecular genetic species identification and determination of genetic variability of the skeletal remains of camels as well as textile material, and should contribute to clarify the strategy of subsistence as well as possible trade relations with highland populations of the (pre-) historic populations of the Nasca–Palpa region.

Analysis systems for mitochondrial DNA, chromosomal short tandem repeats and phenotypic associated single nucleotide polymorphisms were developed. The results of the mitochondrial DNA were used to determine the specie of every sample.

In bones the portion of llamas and guanacos and in textiles vicuñas and alpacas are dominant. It is assumed that llamas and guanacos were used for daily meat supply or as pack animals in case of the llamas. The predominant use of vicuñas and alpacas seems to have been in textile production. A change of the use over time could be observed. Trade between highland and lowland can be proven for the entire settlement period and it increased at the same time with the occurrence of unstable environmental conditions. As a whole this increasing trade and possible specialization at different settlements are a reference to the existence of stratified societies.

R. Renneberg (✉)
Graduate School Human Development in Landscape, Universitätsklinikum Schleswig-Holstein, Arnold-Heller-Straße 3, 24105 Kiel, Germany
e-mail: rrenneberg@gshdl.uni-kiel.de

M. Reindel, G.A. Wagner (eds.), *New Technologies for Archaeology*, Natural Science in Archaeology, DOI 10.1007/978-3-540-87438-6_12,
© Springer-Verlag Berlin Heidelberg 2009

12.1 Introduction

The domestication of animals and their use as a daily product and part of the subsistence strategy is, next to the invention of agriculture, one of the most important factors for the success of *Homo sapiens*. The husbandry of animals started in the Stone Age with the dog. Later in the Neolithic period, humans began to ensure their protein supply by herding animals that had previously been hunted. One possible cause for this change was the extinction of big mammals through climatic changes in the Late Pleistocene, which destabilized hunting success and forced the hunter-and-gatherer population to find a new way of reliable food supply (Diamond 2002). Another possible cause was that the invention of agriculture opened up the possibility of an increase in human population, which led to a higher demand for animal products (Ingold 1996).

Today's domesticated animals can be divided in two classes: the partners, who are really domesticated and show clear differences compared to the wild species, and the exploited captives, who are characterized by features that are more natural with most of them having a special adaptation to harsh environments (Clutton-Brock 1999). One example of exploited captives is the South American camelids, because the herding strategy is not very strict and human influence is less significant than in other species.

In most cases the domestication process leads to changes in the morphological pattern. These are changes in size, hair structure and colour, tail shape, and changes of physiological patterns such as a loss of seasonality, an earlier onset of maturity, and a retention of juvenile characteristics (Trut 1999). In archaeological contexts, only the change in bone size is visible. Here, the interpretation of whether the human population were herders can be sustained by means of biogeographic and palaeogeographic features of animal remains (Legge 1996) as well as archaeological remains associated with animal husbandry such as corrals. The data collected from skeletal remains can lead to an interpretation of the nutritional pattern of ancient populations. If there are products which could not have been produced locally because the raw material was not available in the area, the assumption of trading relations to nonregional groups is obvious. For common European domesticated animals, morphological investigation has contributed to the reconstruction of domestication history. The place of origin of the domesticated goat, for example, has been revealed through analysis of the morphological changes of bones (Zeder and Hesse 2000).

The determination of species as well as the determination of genetic variability can provide information about when domestication history started and may reveal the ancestor of the analysed population. However, the combination of data from recent populations and the data of ancient specimens always supports a higher resolution of the domestication process (Beja-Pereira et al. 2006). So, the analysis of ancient DNA becomes more and more interesting in the reconstruction of the past.

12.1.1 The South American Camelids

In South America, of the few animals domesticated just one was a large mammal: the New World camelid. There are four South American types of camelids known today: the guanaco and the vicuña as wild types, and the llama and the alpaca as domesticated types. Their natural habitat is in the highlands over 1500 m. Llamas are mainly used as pack animals and as a source of meat whereas alpacas mainly provide wool used in textile production. Other products such as skin for leather production and dung as building or heating material are also used. The vicuña and the guanaco were hunted in (pre-) historic times and were used for protein and wool supply.

The reconstruction of the domestication history of llamas and alpacas is based on the morphological investigation of (pre-) historic material (Yacobaccio 2003) and the analysis of recent animals (Kadwell et al. 2001). The determination as to which of the four types an animal belongs is based on criteria of body height and the corresponding length of their bones. These criteria are not very useful for ancient specimens because it is not known if these phenotypic patterns, which are deduced from a present-day pattern, have changed over the last millennia because of domestication processes or adaptation. By morphological investigation, llamas are accounted for in the archaeological record from around 5000 BC (Yacobaccio 2003) and alpacas from around 2500 BC (Hesse 1982). The place and time of the domestication has not been clarified thus far. However, over the last millennia up to the Spanish invasion a steady increase of camelid skeletal remains in archaeological contexts is observed (Cartajena et al. 2007).

The use of camelids in the lowland is not very well explored. In Chavín de Huántar (N-Peru) the skeletal remains of the South American camelids, mainly bones of the zygopodia and the trunk, prove the import of camelid meat as *char'ki* (Miller and Burger 1995), that is, dried meat packages, which were produced in the highlands and transported to the lowlands, a process called the 'Schlepp-Effect' (Burger 1985). The use of camelid wool has been proven as dating to the Paracas period (around 500 BC; Biermann 2001). Camelids played an important role not just in nutritional contexts, but they were also important in ritual contexts. Therefore, they are often found in ceremonial centres (Silverman and Proulx 2002) or can be identified as ritual objects (Wheeler et al. 1992). Their depiction on stones, ceramics, and textiles is also proof of their significance (e.g., Cartajena et al. 2007).

For the South American camelids no genetic species identification system has been available, and genetic studies on them have shown that phenotype and genotype are not always identical (Stanley et al. 1994). This means that, for example, an animal which looks like an alpaca can show the genotype of a vicuña. On the other hand, there are special genetic signatures referring to only one type, because they are present in the majority of individuals of one type. This is because the South American camelids are able to interbreed and produce

fertile descendants. Therefore, the four types are not reproductively isolated even though they are denominated as being four different species. The cross-breeds make it difficult to distinguish the four types genetically. Therefore, when there is no information about the phenotype, as in archaeological remains, the genetic determination may lead to a false phenotype interpretation. This is important because it means that this study does not determine the appearance and external qualities of an individual: it is just a view on the genetics. However, the view on the genetics gives a more distinct picture of ongoing domestication and breeding processes, because the change in the phenotype of individuals is always based on the change in genetic material.

12.1.2 Camelids in the Nasca Period

In the Nasca period, camelids were the most important meat supply (Silverman and Proulx 2002). The iconography of the Nasca shows hunting as well as herding scenes. There are no indications of local herding but caravansaries are known (Valdez 1988). Morphological investigation for the determination of the species has been carried out only at the archaeological site of Cahuachi (100 BC–500 AD), where the existence of alpacas in the skeletal remains was detected. Therefore, there is no information as to which of the species was primarily used by the Nasca and whether the pattern of usage changed over time. In the Palpa valley camelid remains are present in archaeological contexts of every cultural period (Fig. 12.1). The assumption was that the animals were imported individually into the valley because their natural habitat is in the Andean highland.

The Nasca–Palpa project offered the opportunity to analyse camelid remains from the Paracas culture up to the Late Intermediate period. Therefore, the possibility of comparing and seeing changes in the use of camelids was given. Fine textiles made of wool, cotton, or both were found in the burial contexts.

A species determination of the skeletal camelid remains as well as of the material used for textiles would provide information about the subsistence strategy of the ancient population of the Palpa valley. A change to a higher variability in the camelid remains and a change in the use of domesticated animals would indicate a change in cultural tradition and a change in economic strategies. Comparison of the results for the different archaeological sites could show different usage indicating division of labour and a stratified society. If they primarily used the wild types of the camelids, hunting rather than import could be assumed. The use of the domesticated forms would indicate import rather than hunting. Import and trade are often associated with stratified societies (Service 1962), therefore information about the social organization of the ancient cultures could also be revealed by the analysis of animal remains.

Fig. 12.1 Skeletal remains of a camelid at the excavation site of Jauranga

12.2 Material and Methods

The main aim of this study was to establish an analysis system for species determination based on genetic polymorphisms, which are applicable in the context of ancient DNA. The results were evaluated from different perspectives. The species and the genetic variability were assumed as given. Based on these results the composition of the skeletal material was compared by archaeological provenience and period. An interpretation followed regarding domestication history and phylogenetics, as well as the interpretation as regards the actual use of camelids, their cultural meaning, and the role they played in the subsistence strategy of the ancient human populations.

For species identification, four analysis systems of different genes of the mitochondrial DNA were established. The system development was based on one complete mitochondrial sequence of an alpaca (NC 002504, NCBI).

For the Cytochrome-b (cytb) gene a system based on the analysis of a 273 bp fragment was designed, this fragment being analysed in ancient DNA by the amplification of four short fragments. For the genes NADH-Dehydrogenase Complex 5 (Nd5) and the Cytochrome-Oxidase Complex I (COI) the analysis of fragments of 135 and 121 bp were developed. The fragments of the three genes were sequenced in their entirety and then compared.

For the analysis of the gene 12srRNA a Hyb-Probe-System on the LightCycler (Roche) was designed. This system allows a direct analysis of polymorphisms without sequencing the whole fragment, by the use of DNA-probes, which are specific for one of the possible bases of the analysed polymorphisms. It was developed by first sequencing 802 bp of the 12srRNA-gene in recent material. This analysis revealed the three polymorphic positions 189 (A/G), 193 (C/T), and 247 (A/G). The typical pattern for guanaco in these polymorphisms is ATA, for llamas ACA, and for vicuñas GTG. Only the alpaca shows no clear pattern in these polymorphisms. Based on these results a Hyb-Probe-System was designed and optimized for use in ancient DNA analysis. In the case of the Cytochrome-b, sequences of all four camelid types are available on the NCBI-database. Nevertheless, the variability of the genes Nd5, COI, and 12srRNA were not known in camelid populations until this study.

The four analysis systems were tested on hair and blood material of zoo-camelids. This preparatory study showed a high diversity in the camelids and a high default in the concordance of pheno- and genotype. Therefore, a system of compound interpretation of the results was developed. Haplotypes based on the observed polymorphisms were defined for every system. They were named after the phenotypic species in which the haplotype existed. In comparing the different species-haplotypes in the four systems, a compound species was determined for the analysed individuals (Fig. 12.2). Of the guanacos 85%, of the vicuñas 78%, and of the llamas 83% could be correctly determined. The highest deviation was observed in alpacas where only 66% could be

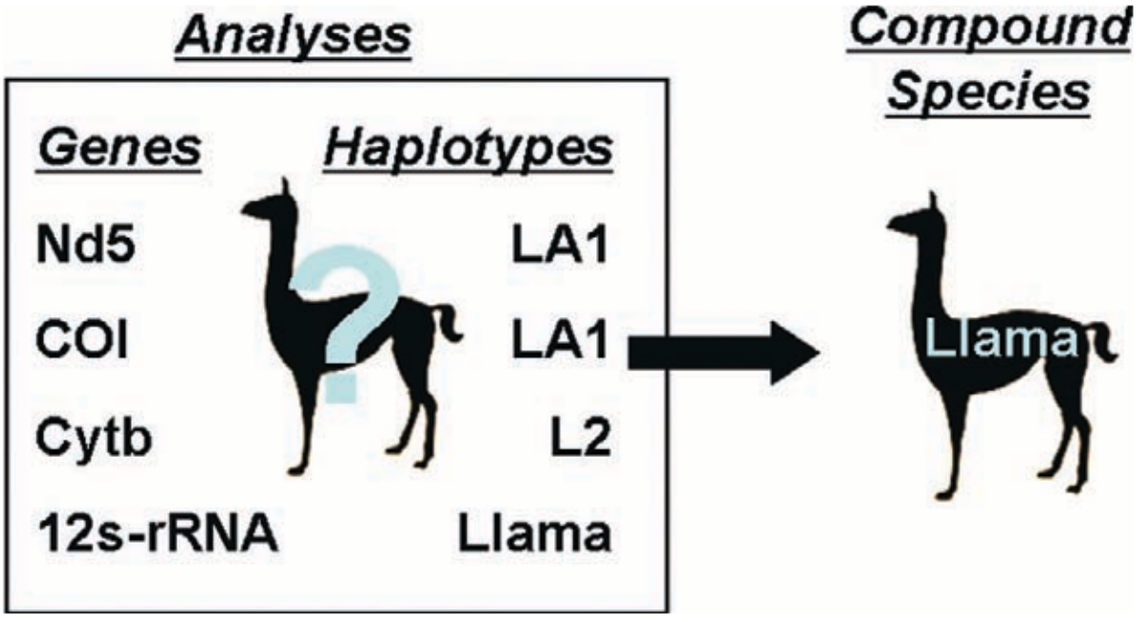

Fig. 12.2 Exemplified determination of the compound species. In the genes Nd5 and COI the observed haplotypes exist in the species llama and alpaca (LA). By addition of the gene haplotypes of cytb (L2) and 12srRNA (llama), which show clear llama haplotypes, the species llama can be assigned to the analysed individual

Fig. 12.3 Vertebra and phalanx of a camelid found in the excavation site of Chillo in a waste disposal site. On the phalanx soft tissue and hair remained

determined correctly. This has to be taken into account when determining the species of ancient remains.

During the 2005 and 2006 campaigns 156 bones and teeth of camelids (Fig. 12.3) as well as 40 textiles were collected. The skeletal sample represents the following times and excavation sites: the Initial phase (1800–800 BC) is represented by four samples from the excavation site Pernil Alto; for Middle Paracas (520–400 BC) there are nine samples from Jauranga and Los Molinos; for Late Paracas (350–200 BC) 20 samples from Pernil Alto and Jauranga; for Early Nasca (80–200 AD) 23 samples from Los Molinos; for Middle Nasca (330–430 AD) 33 samples from Los Molinos, La Muña, and Hanaq Pacha; for Late Nasca (430–650 AD) 17 samples from Montegrande; and for the Late Intermediate period (LIP, 1000–1400 AD) 24 samples were collected from Chillo. For 26 samples, the chronological classification is vague. For the textiles, samples from Early Nasca (11, Los Molinos), Middle Nasca (6, La Muña and Los Molinos), and Late Nasca (14, Montegrande) were collected. Here the chronological classification is vague for another nine samples from Los Molinos.

The extraction of DNA from bones and teeth followed a standardized decalsification-cellysation protocol (Renneberg 2008). Following the rules for authenticating the results in aDNA analysis (Hummel 2003) for every sample, at least two DNA extracts were made.

The extraction of DNA from the textiles was carried out by a lysation protocol (Pfeiffer et al. 2004) followed by DNA purification with the EZ1 Biorobot (Qiagen). For reducing the numbers of possible individuals in the textile DNA-extracts the twines of the textiles were separated by colour and between two and up to five 0.5 cm pieces of the twine were used, thus multi-coloured textiles yielded more than one extract.

For every sample, the analysis of the single genes was repeated atleast twice for every DNA extract to ensure the authenticity of the results (Hummel 2003). The results were interpreted with the compound haplotype method and a species was assigned.

12.3 Results and Interpretation

In the skeletal remains 36 (22%) samples and 14 textiles (19%) showed evaluable results. Overall, the excavation sites from the younger periods (Montegrande, Chillo) clearly showed better results than the older ones (Fig. 12.4).

This may be because the environmental conditions in the Palpa valley changed over time (Eitel and Mächtle 2006), which resulted in different storage conditions for the samples in the soil. For the conservation of DNA a dry, cold, and stable environment is optimal (MacHugh et al. 2000). Perhaps the instability of these conditions in the Palpa valley led to a higher degradation of the DNA. The samples from Montegrande, which were all surface finds, on the other hand, showed that the high doses of UV-light and the high temperature did not affect the DNA as much as postulated in the literature until now.

The genetic variability of the ancient remains showed a higher variability than the recent populations. This may be due to the effect of the Spanish invasion that led to a decrease in the camelid population and lesser breeding interests in camelids caused by the introduction of cattle, sheep, and goats. The genetic distance among the four camelid species is very low, which implies that all four belong to one species and the domesticated ones should be named as races. The data indicate a descent from llama to guanaco and from alpaca to vicuña, but the data also show high crossbreeding among all four, which is also indicative of all four South American camelids belonging to one species. Only between vicuñas and guanacos was no crossbreeding detected, which reflects they did not inhabit the same area and thus naturally did not have any contact.

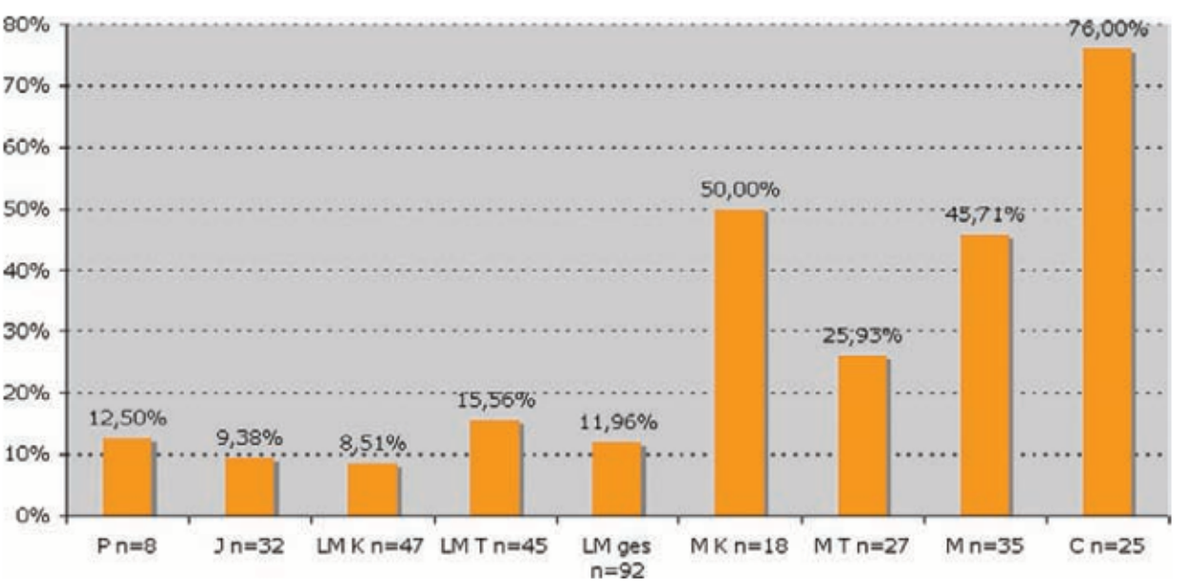

Fig. 12.4 Analysis success for the different excavation sites. P = Pernil Alto, J = Jauranga, LM = Los Molinos, M = Montegrande, C = Chillo, K = bones and teeth, T = textiles, n = number of samples

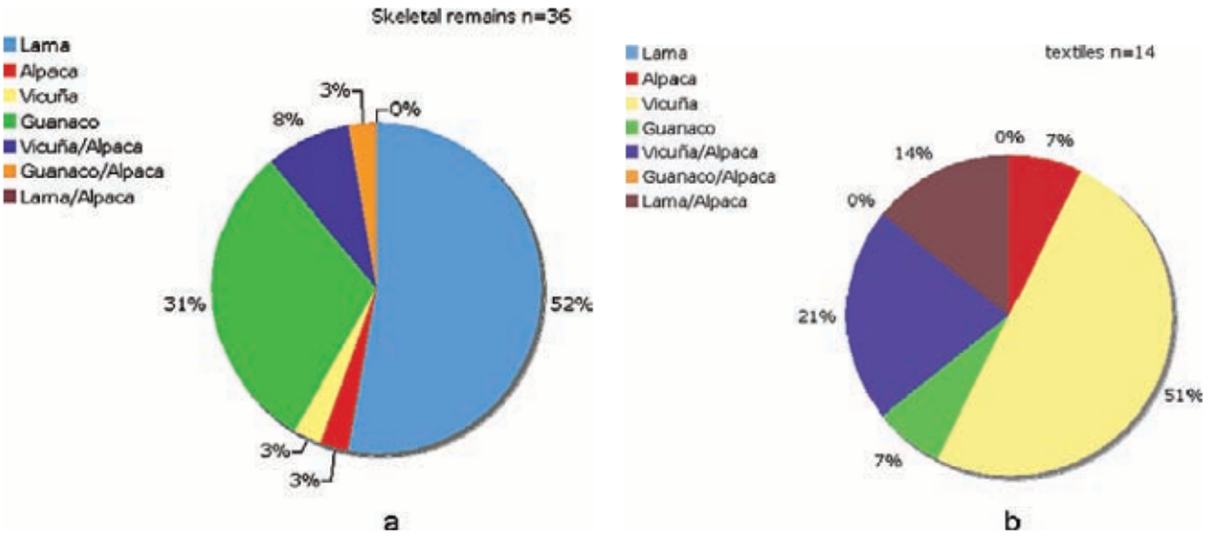

Fig. 12.5 (**a**) Species distribution in the skeletal remains. (**b**) Species distribution in the textiles

For a better readability of the following interpretation, the term species is carried on, even though it is not correct biologically.

The determination of the species showed clear differences in the ratio of animals between the skeletal remains and the textiles. In the skeletal remains the llama is the dominating species (52%) followed by the guanaco (31%). Vicuñas and alpacas are rare and only around 11% of the samples were determined as crosses between alpaca and guanaco or vicuña (Fig. 12.5a). In the textiles, the vicuña is the dominating species followed by alpaca/vicuña and llama/alpaca cross-breedings. Llamas are not present in the textile samples (Fig. 12.5b).

These results show that the wool used in textile production did not originate from the individuals represented in the skeletal remains. Therefore, it can be postulated that the wool was imported and that the animals themselves were never imported into the valley. One textile showed different species for different colours, the red, brown, and black twine all stemmed from individuals with different haplotypes. Maybe this is an indication for the use of different coloured hair in the dyeing process. Furthermore, llama hair seems to never have been used in wool and textile production, whereas guanacos, present in both groups, were used in textile production. Because guanacos are untamed animals it is postulated that the inhabitants of the Palpa valley hunted them or their corpses were imported from highland populations into the valley and were used for protein supply. The llama as a domesticated animal could have been introduced into the valleys as a transport animal and/or for the daily meat supply. The import of guanacos and llamas as *char'ki* can be excluded because every part of the body was represented in the skeletal remains.

The distribution of the camelid species in the different periods and excavation sites shows a clear increase in variability (Fig. 12.6). For the Late Paracas period, the sample is small but it clearly shows that the domesticated forms of the camelids were already used. This means that the domestication of camelids

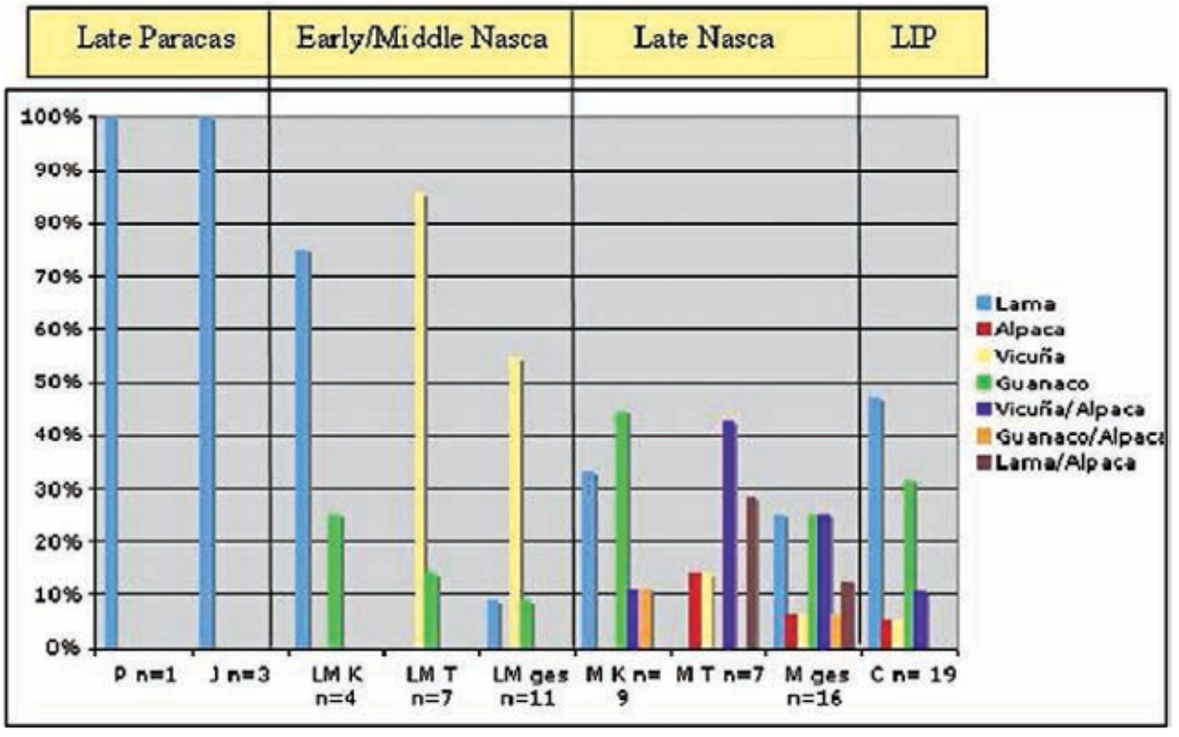

Fig. 12.6 Species distribution in the excavation sites and periods. LIP = Late Intermediate Period, P = Pernil Alto, J = Jauranga, LM = Los Molinos, M = Montegrande, C = Chillo, K = bones and teeth, T = textiles

started earlier than 350 BC; they were already known to the inhabitants of the valley, and their use was not restricted to the highlands. Through the importation of llamas into the valley, trading relationships to highland populations are clearly proven for that time.

During the Early and Middle Nasca period llamas and guanacos are present in the skeletal remains sample. In the textiles, next to guanacos, vicuñas are present. This indicates a trade with wool, the hunting or importing of guanacos, and the importation of llamas. The usage of guanaco and vicuña wool in the fine textiles from burial contexts in Los Molinos by the human inhabitants of the valley also indicates a special care-taking for their deceased and the existence of a system of belief in the afterlife.

In the Late Nasca period the first mixed species types appear in both bone and textile samples. An increase in diversity and the use of wool from domesticated forms indicate an increase in trading relationships. This could be evidence for an increase in population size and an intensified exchange between highland and lowland populations. The high variability in Montegrande may also indicate a division of labour and a specialisation in camelid processing. Excavations in Montegrande might prove this assumption. In the Late Intermediate period, all types of camelids are present in the skeletal remains. This indicates that all types were imported. This may indicate a change in behaviour caused by a renewed settlement of the Palpa valley by settlers

from the highlands bringing their customs with them after the valley had been abandoned during the Middle Horizon.

In addition to the results of the DNA analysis of human remains (Fehren-Schmitz et al. this volume), these results show that the region of the Palpa valley changed in means of settlers and customs over time. This fits well into the picture of the archaeologists and the environmental reconstruction. Moreover, the trading relationships indicate that the Palpa valley populations were stratified and had their own culture and belief system.

12.4 Outlook

This study shows that the genetic analysis of animal remains can support and contribute to the reconstruction of ancient populations. To support these findings animal remains from the highlands of the same time should be analysed, in order to compare the genetic patterns and find out where the original population of the valley animals was located. The area of investigation should be extended into other valleys to pin down where and when the usage of domesticated animals by the inhabitants of the valley started. Moreover, an extension to the highlands would be useful to reveal the domestication history of the South American camelids in general.

The data of this study also show that only little is known about the phylogenetic and genetic variability of the camelids. Further investigations of ancient remains could contribute to reveal these questions. Moreover, this information would help today's farmers in South America to produce higher quality animals and wool by a better crossbreeding program.

Part IV
Archaeochronometry

Chapter 13
Of Layers and Sherds: A Context-Based Relative Chronology of the Nasca Style Pottery from Palpa

Niels Hecht

Abstract The archaeological fieldwork in the Palpa area allowed establishing a relative chronological scheme for the local Nasca-period pottery. This regional sequence defined for the Palpa area shows some remarkable differences from the sequences defined formerly for the adjacent valleys: former approaches dealt with regionally heterogeneous pottery assemblages, often without known context provenience. The chronological ordering relied on stylistic seriation and grave contexts. But when applied to settlement evidence the phases were represented quite unevenly. Most likely the stylistic approach could not sufficiently distinguish regional from chronological differences. Thus, some of the defined phases would be better interpreted as contemporaneous substyles.

The focus has shifted to the regional uniformity of the material to define a local sequence for the Palpa area first. Instead of stylistic arguing, the sequential ordering of the pottery now follows the stratigraphic evidence encountered in our excavations in settlement sites. As a result, four settlement phases could be defined for the Palpa area. These newly defined phases reflect changes in settlement habits better than the former stylistic phases did.

Together with the C14 dates provided by our natural sciences partners a revised and well-established chronological framework for Palpa can be presented here that will serve as a standard and chronological reference for the development of other regional sequences.

13.1 Introduction

For the archaeologist, chronology is a basic tool needed to arrange the finds and features in time. Excavations reveal data from different moments in the past and these data have to be ordered chronologically to see which

N. Hecht (✉)
German Archaeological Institute (DAI), Commission for Archaeology of Non-European Cultures (KAAK), Bonn, Dürenstraße 35-37, 53173, Bonn, Germany
e-mail: nihecht@web.de

M. Reindel, G.A. Wagner (eds.), *New Technologies for Archaeology*, Natural Science in Archaeology, DOI 10.1007/978-3-540-87438-6_13,
© Springer-Verlag Berlin Heidelberg 2009

events were contemporaneous in the past and can therefore be meaningfully interpreted together.

In Peruvian archaeology the definition of archaeological cultures and the relative chronological sequences are based on pottery style. Pottery is the most frequent archaeological find and for the multitude of observable morphological and stylistic traits it is very suitable for classification and sequential ordering. This chapter concerns the Nasca period pottery from Palpa, its classification, and relative chronological ordering. The Nasca style flourished in the valleys of Nasca, Palpa, and Ica between approximately 120 BC and 620 AD (Fig. 1.1 of Chap. 1 this volume). Despite 100 years of research on the Nasca culture and its pottery, the relative chronology is still under discussion (Silverman and Proulx 2002; Proulx 2006). Therefore, the objective of the analysis summarised here is to develop a regional relative sequence for the Nasca pottery from Palpa, based on stratigraphic evidence from settlement contexts.

For the last 60 years natural sciences have provided methods for the numerical dating of archaeological remains (Rowe 1967a,b; Wagner 2007; Kadereit et al. this volume; Unkel and Kromer this volume; Greilich and Wagner this volume). Although numerical chronology now is an important aspect in the interpretation of archaeological remains, the classification and comparison of artefacts and the relative ordering of the finds in time still have to be done by the archaeologist. For this, modern archaeological investigation still resorts to the principles of superposition and association of remains, introduced to archaeology more than 100 years ago (Montelius 1903), now a standard in archaeological fieldwork (Eggert 2001; Harris 1989; Renfrew and Bahn 1996; Rowe 1962a,b). Comparison of artefacts is based on morphological and stylistic description and classification. These steps can be done independently from scientific dating and are the basic preparatory steps in analyzing archaeological data. The ongoing need for relative archaeological dating in the time of improved scientific dating is obvious: through comparison archaeological artefacts and the associated contexts can be put in a relative sequence (earlier – contemporaneous – later). Changes in the morphology and style of artefacts are not random, but they follow a certain developmental pattern. Once having identified this pattern through stratigraphic analysis it serves for the relative dating of culturally and regionally related artefacts.

The numerical age of a given object is calculated through scientific dating. This age is valid only for the analysed object and for the objects found in the same stratigraphic context. Now, archaeological artefact classification and relative chronology provide a method for extending the numerical date to other objects from other contexts by simple comparison.

Thus both methods offer a different but complementary kind of information. The benefits of combining relative and numerical chronologies are mutual. Relative sequences can be related to concrete time spans, an important step in archaeological interpretation. On the other hand, relative chronology and classification maximize the value of scientific dating by transferring the ages calculated for one object to other unrelated objects. Additionally, an

established relative sequence can help to calibrate the scientific dates and improve the methods, by sorting out dates that can hardly fit the context. This strong interdependence was the reason why special attention was paid to the traditional method of archaeological chronological analysis within the Nasca–Palpa project. The improvement of the existing cultural sequence was one major task for the archaeologists cooperating in the project. Although the archaeological methods applied are well established, the results are new, because by the detailed analysis of pottery from the excavations in Palpa we were able to significantly improve the existing chronology for the Palpa region.

13.2 The Research Problem

The study of pottery chronology for the Peruvian south coast goes back to the very beginning of Peruvian archaeology and the work of Max Uhle (1913, 1914). Later, more approaches to a chronological ordering of the Nasca pottery style were undertaken (Gayton and Kroeber 1927; Kroeber 1956). The most influential attempt has been the Dawson Seriation that resulted in the definition of nine consecutive Nasca phases, Nasca 1–9 (Rowe 1960a,b). These formed part of a master sequence for Peruvian archaeology established by John Rowe, Dorothy Menzel, and Lawrence Dawson during the 1950s (Rowe 1967).

When the Archaeological Nasca–Palpa Project started in 1997, the Dawson Seriation had been the sequence used in most Nasca studies. However, the sequence's limitations were revealed when applied to archaeological field data. Some phases of the nine-phase sequence were underrepresented or nearly absent from the archaeological record. Many investigators were aware of this problem, but sufficient data were not available from excavations to test the sequence or to establish independent regional sequences (Browne 1992; Silverman 1993; Silverman 2002; Silverman and Proulx 2002; Proulx 2006; Vaughn 2000). But the fieldwork in Palpa yielded more than enough data to develop an independent regional chronology.

With the objective of establishing a more sound regional chronology for the Palpa area, the method and the database of the existing scheme, the Dawson Seriation, had to be critically reviewed.

The method originally chosen for the chronological ordering of the pottery in the 1950s was the similiary seriation (Rowe 1961). This is a nonquantitative method to arrange artefacts according to their stylistic similarity as observed in a number of single design and shape features. Rowe (1961:324) states that for the elaboration of a chronological sequence this stylistic approach would bring results as valid as the results from stratified contexts, as long as the approach would be cross-checked by grave contexts which serve as units of contemporaneity (Rowe 1962a,b). Thus, the Nasca sequence is principally based on two arguments: style and association. The third possible argument, the stratigraphic

superposition, had been widely neglected due to the scarcity of stratigraphic information at the time. Only few stratigraphic excavation units from Nasca (phases Nasca 1–3, Nasca 8–9; Strong 1957) and others from Ica (phases Nasca 4, 5, and 7, and Nasca 7–9; Proulx 1968: 7; Menzel 1971) were known. Until the work of the Nasca–Palpa project this situation had not changed substantially. The procedure consisted in defining a hypothetical stylistic development line that would be cross-checked by grave associations. However, the advantage of using evidence of vertical stratigraphy for a chronological analysis is that these already imply a sequence, whereas stratigraphically unrelated contexts can be contemporaneous although associated with different artefacts or they can be successive while showing the same artefacts.

These difficulties in the sequential ordering of the style are increased by the fact that the analysis data came from different valleys of the Nasca region (Fig. 1.1 of Chap. 1 this volume). The uniformity of the style has only been assumed (Rowe 1960a,b) but not proven by a thorough comparison of regional sequences. The only regional analysis (Proulx 1968) showed regional differences in the style during phases Nasca 3 and Nasca 4, and for phase Nasca 5 a number of contemporaneous substyles were defined (Blagg 1975), but not regionally analyzed. Considering these findings, the supraregional uniformity of the style is to be doubted.

Thus, within the discussion of Nasca chronology the data from Palpa is important for two reasons: it has stratigraphic information and the regional uniformity is guaranteed. Finally, the scientific dating of some of the contexts links the relative sequence to numerical dates.

13.3 Method

A relative chronology has its foundation in two important aspects of archaeological research: first, during excavation a thorough record of the stratigraphic relationship between contexts has to be guaranteed; second, the pottery encountered has to be classed according to the properties of ware, shape, and design. Finally, during the analysis this information has to be linked. The distribution of ware, shape, and design features will be checked in relation to the stratigraphic position of the context.

13.3.1 Database

Within the Nasca–Palpa project, excavations were conducted in several settlement sites of the Palpa area and numerous additional test pits were documented. During excavation special attention was paid to the stratigraphic relationships between the excavated contexts. All materials were catalogued with reference to their stratigraphic context, so a comprehensive database of

stratigraphically related pottery is now available. For the analysis a total of about 6000 diagnostic pottery fragments were documented, classed, and analysed with reference to their relative stratigraphic position. Complete vessels from grave contexts provide an additional source for this study. Together, they provide a complete sequence of the Nasca occupation in the Palpa area. Data provenience is principally from four major sites, each being characteristic for one part of the Nasca Sequence. These sites are (Fig. 1.1 of Chap. 1 this volume):

- Estaquería (Initial Nasca)
- Los Molinos (Early Nasca)
- La Muña (Middle Nasca)
- Parasmarca (Late Nasca)

13.3.2 Pottery Classification

For a systematic comparison of pottery a classification scheme is needed. As stated above, the project's work started applying the Dawson classification (Reindel et al. 1999; Reindel and Isla 2001). By shape and design most sherds could be classed in one of the nine Dawson phases. The Dawson Seriation is useful as a detailed classification scheme. If we consider the phases as units of style and not necessarily of time we can thereby describe the material using a terminology that makes it comparable to the results of former investigations in the region. However, for an independent chronological analysis we have to abandon this classification scheme. The style/phase units have to be split up to define new phases that better reflect the stratigraphic distribution of material in the archaeological context.

The classification of the Palpa material follows the standards of archaeological pottery classification (Rice 1987; Shepard 1956). Pottery has been classed according to its principal observable characteristics: (1) ware, that is, technological aspects such as firing atmosphere as well as petrographical and chemical properties of the paste; (2) shape; and (3) design.

In the case of the Nasca pottery, the analysis of the ware principally allows a fineware–coarseware distinction. According to the macroscopic analyses of the Palpa material up to now, these classes are chronologically insignificant. A petrographical and chemical analysis of a sample of Nasca pottery from Palpa from all phases is in progress at the Ruhr-Universität Bochum. The chronological relevance of these microscopic and chemical analyses will have to be evaluated in the future. Other componential studies of Nasca pottery did not reveal any chronological differences and have their focus mainly on pottery provenience (Vaughn and Van Gijseghem 2007; Vaughn et al. 2006).

Shape classification follows the morphological characteristics observable in the fragmented pottery as well as the complete vessels. In addition to the general

need for an independent classification a new shape classification is also necessary due to the fact that the established classes had been based mainly on entire vessels. Therefore the classes depend highly on vessel proportions and in some cases only major shape categories had been defined that do not allow finer chronological distinctions (Blasco and Ramos 1980; Gayton and Kroeber 1927; Kroeber 1956; Kroeber and Collier 1998; Proulx 1968; Roark 1965; Wegner 1975).

Thus the classification of shape in the present approach focuses on the most important aspects that can be observed in a large sample of fragmented pottery: the orientation of the rim and upper wall of the vessel, the shape of the rim/upper wall, and the rim diameter. To a smaller degree the shape of the base and the existence of a base angle can be included in the classification where present.

The design of the Nasca pottery from Palpa is more strongly related to the Dawson classification. Complex iconography can best be studied on complete objects. Therefore, when working with fragmented pottery, the observed design features have to be related to an existing classification. Still, the classification can be used independently from the phase definition so that the application of the Dawson classification does not hinder the establishment of an independent chronology. Applying the Dawson approach, design is classified in iconographic themes, components, and features (Rowe 1961). The definition of themes, components, and features is adapted from Dawson as far as possible. New – or still unpublished – traits can be additionally defined wherever necessary.

13.3.3 Stratigraphic Analysis

Stratigraphic analysis is concerned with observing the superposition or association of archaeological contexts and their related objects. A context can be, for example, a cultural layer in a settlement or a grave. Excavations in the Palpa area by the Nasca–Palpa project revealed sufficient contexts in direct stratigraphic relation to attempt a stratigraphic analysis of these.

In the Palpa excavations, the quantity of diagnostic pottery in a single stratigraphic layer varies between about 600 fragments and none. Stratigraphic analysis consists mainly of describing the pottery assemblage (ware, shape, and design) of each context and in comparing it to the stratigraphically related ones. By this, specific changes in the inventory of ware, shape, and design can be correlated with chronological changes as observed in the stratigraphic superposition of building phases in one site, by the abandonment of a site and a later reuse associated with different materials, or by the appearance of different material in another site that can be identified as later by other stratigraphic evidence. A summary of this analysis is presented in the following.

13.4 Stratigraphic Evidences from Palpa

The presentation of data is structured following the four major Nasca settlement phases defined for the Palpa region, each represented in this analysis by settlement contexts from one phase-specific site. The stratigraphic evidence cited in continuation shows that all contexts together reveal a complete uninterrupted sequence of the Nasca culture in Palpa.

13.4.1 Initial Nasca: Estaquería (120 BC–90 AD)

The type site for the Initial Nasca phase in the Palpa area is the Estaquería site in the lower Grande valley (Fig. 1.1 of Chap. 1 this volume). The stratigraphic evidence at this site shows a superposition of up to nine cultural layers and a small but representative sample of about 100 diagnostic fragments was excavated. The analysis of the material shows a characteristic set of wares, shapes, and designs. The characteristics are:

(1) Ware: there is coarseware and fineware, easily distinguishable by the size of inclusions (temper): fineware is nearly untempered or has very small (<0.5 mm) inclusions, whereas coarseware shows a significantly higher quantity of larger inclusions. In the fineware category it is possible to distinguish between reduced blackware and oxidized redware. The chemical composition of these wares is still under analysis.

(2) Shape: Open vessels prevail. Many bowls have characteristic low convex, sometimes slightly incurving walls (Fig. 13.1). Some specimens show walls of medium height that are also slightly incurving (Fig. 13.2c–e). Other bowls have a hemispherical appearance, with convex flaring walls (Fig. 13.2 h–g). There are some closed vessels of a jar shape that might have a neck, but always show a flaring rim (Fig. 13.2a–b).

(3) Decoration is mostly monochrome, sometimes with some simple geometric elements. Variation is present through the application of different decorative techniques. There is a monochrome red engobe painting (Fig. 13.1 k–l) that is either applied to the whole surface or in simple geometric designs (Fig. 13.2f), sometimes over a crème background (Fig. 13.2d). Other techniques are reduced firing (blackware) combined with pattern burnishing (Fig. 13.1a,d–e), negative decoration (Fig. 13.2 h), and finally very few complex incisions with polychrome engobe painting (Fig. 13.2i).

Despite the duration of about 210 years calculated for the Initial Nasca phase (see Unkel and Kromer this volume), the pottery analysed from Estaquería shows no significant changes in the distributional pattern; that is, all wares, shapes, and designs appear throughout the stratigraphy, not permitting any further chronological subdivision. Maybe more stratigraphic evidence for this ceramic complex would be of help.

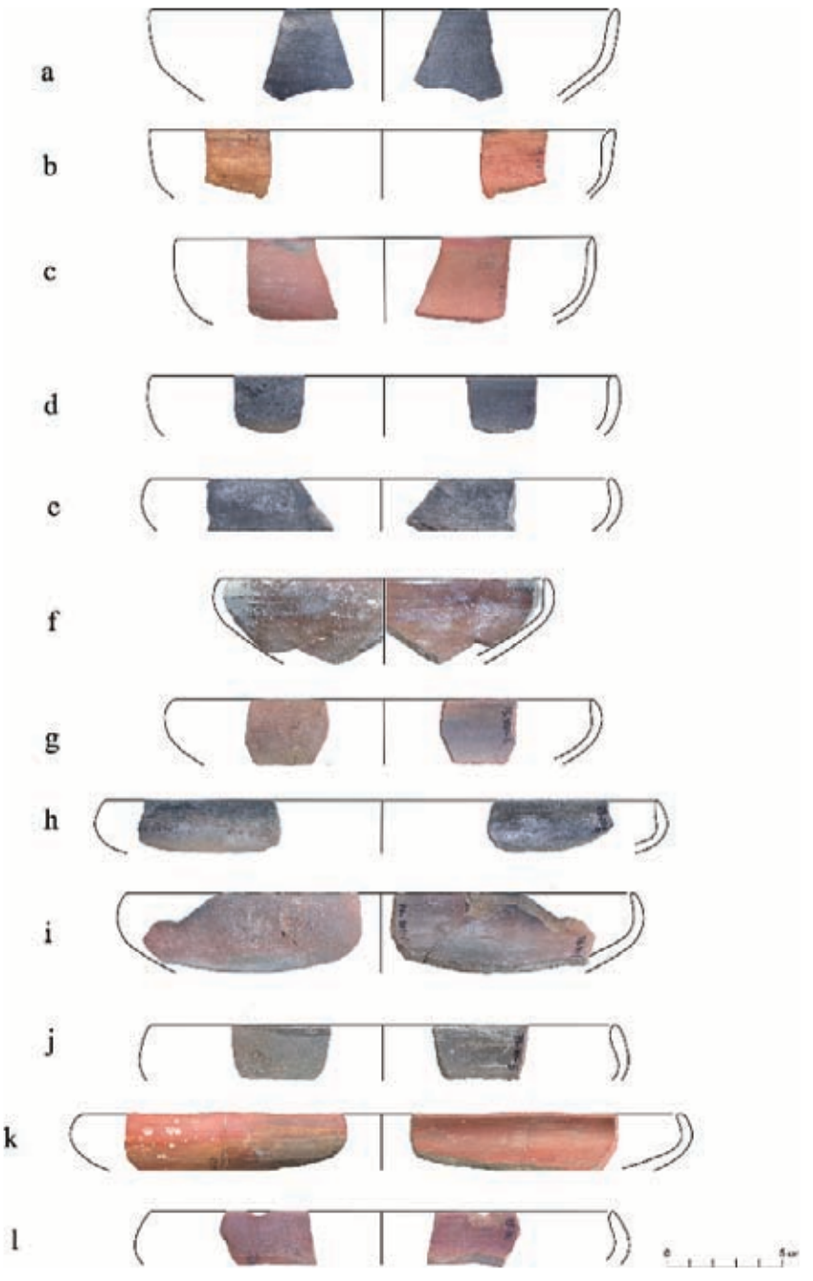

Fig. 13.1 Initial Nasca pottery from Estaquería

However, in the uppermost levels of the Estaquería stratigraphy a different kind of pottery can be observed (Fig. 13.2j). The differences in its style are striking. It has a thick engobe painting in white and black, sometimes also in red. As the evidence from Los Molinos shows, this pottery leads over to the Early Nasca phase.

13.4.2 Early Nasca: Los Molinos (90 AD–325 AD)

For the Early Nasca phase several dense stratigraphies were observed at the Los Molinos site (Fig. 1.1 of Chap. 1 this volume). A total of about 2000 diagnostic pottery fragments from Los Molinos were analysed. There is a greater variety of shapes and designs than in the Initial Nasca contexts from Estaquería. The earliest finds can be linked to the stratigraphy from Estaquería:

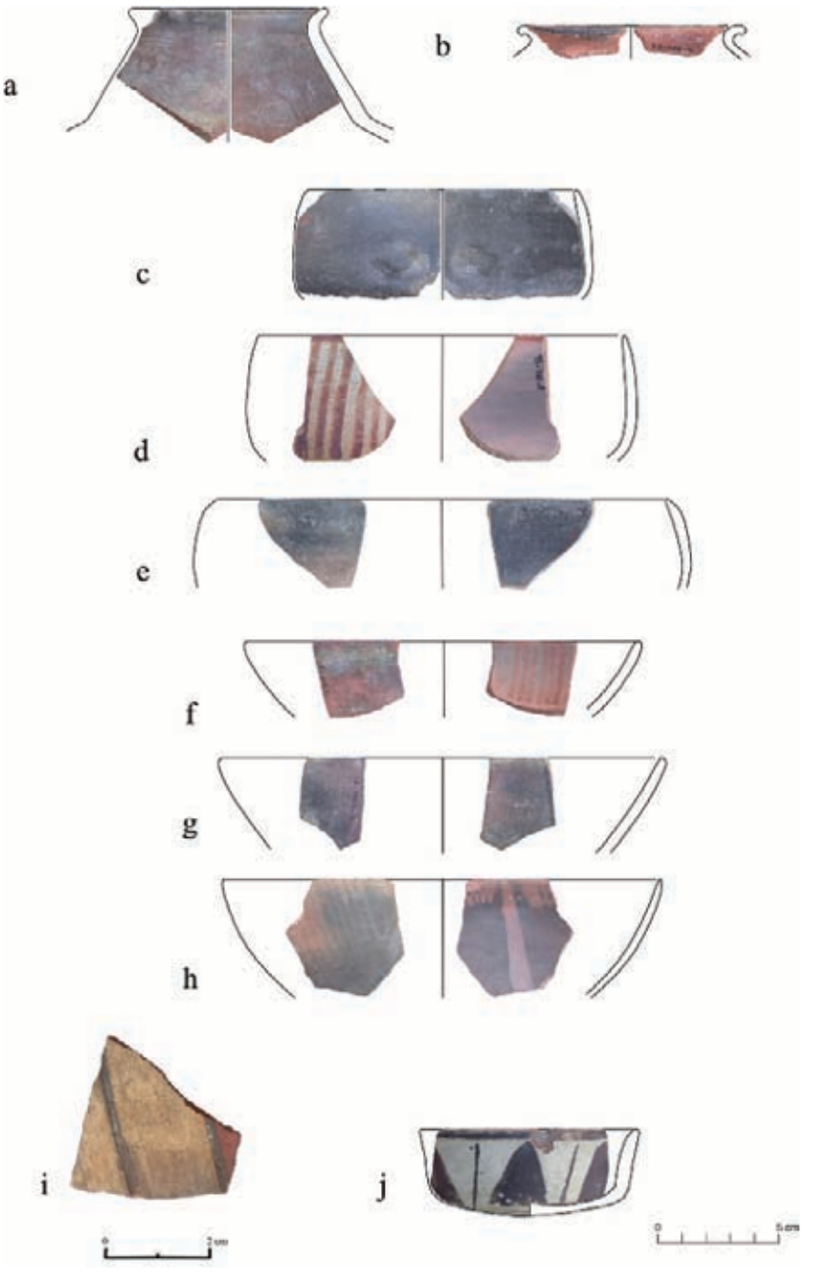

Fig. 13.2 Initial Nasca pottery from Estaquería

In sector A of Los Molinos (Reindel and Isla 2001) a deep and clear stratigraphy of several superposed floors and fillings could be observed. In the lowest level some of the sherds show the same characteristics as those from the uppermost levels of Estaquería, however, the bulk of the characteristic Initial Nasca material from Estaquería is not present in the Los Molinos contexts.

Some of the shapes of this Early Nasca engobe painted pottery can be derived from the Initial Nasca shapes: there are several fragments of bowls with low walls that are straight and vertical or slightly incurving (Fig. 13.3g–i), but the inward slope is not as pronounced as in the case of the Initial Nasca examples. In the lowest level of Los Molinos again two to three colour engobe painted vessels without incision lines can be observed (Fig. 13.3f–i.). Design themes are simple geometric, diamond-, or crescent-shaped. Although in Estaquería this stylistic homogeneous pottery had been found in association

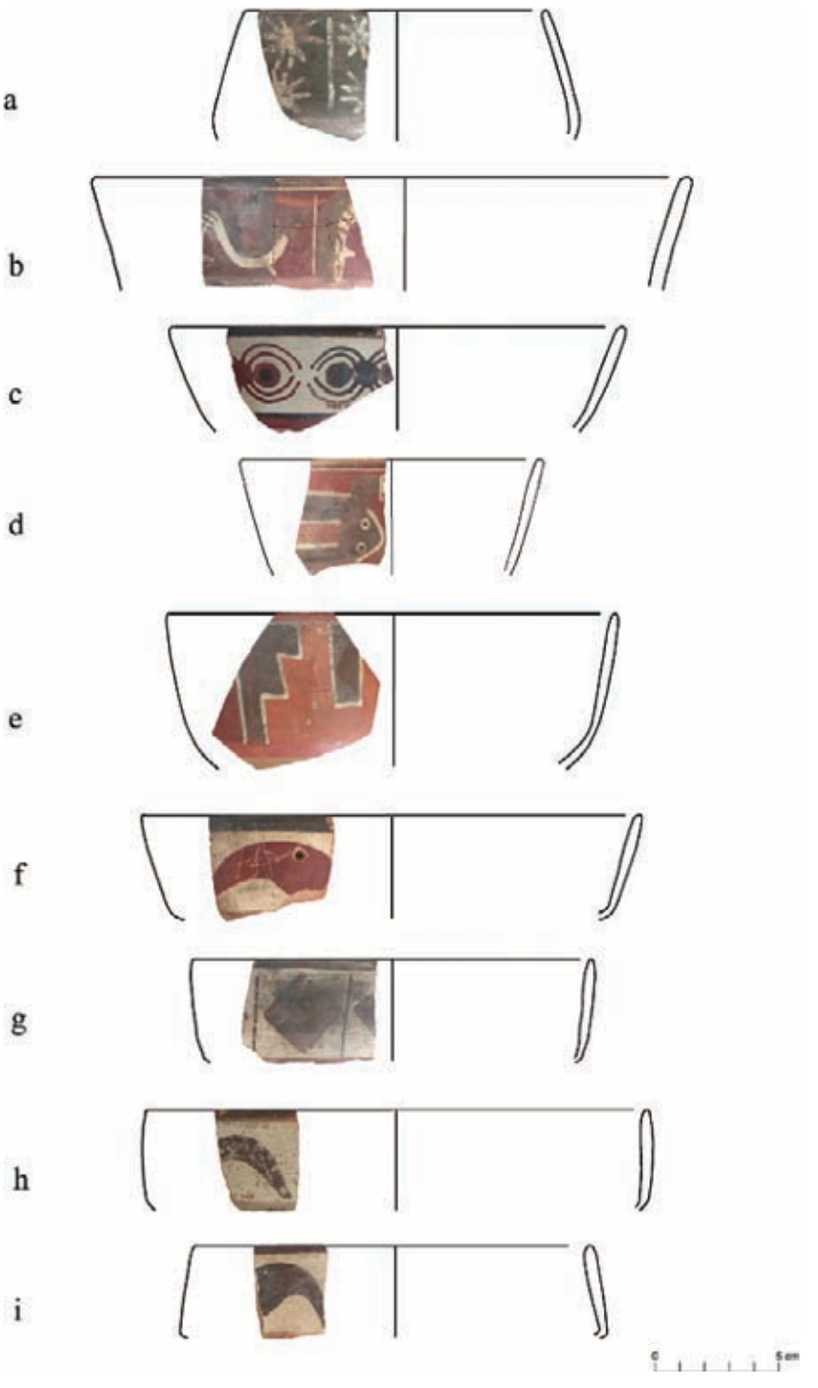

Fig. 13.3 Early Nasca pottery from Los Molinos sector A

with Initial Nasca pottery, it now occurs with some distinct pottery showing the following characteristics.

Early Nasca wares can macroscopically be divided into fineware and coarseware. There are no more variants of the fineware. All fineware pottery shows a characteristic polychrome engobe painting. Differences occur in the quality of execution of design and surface polish.

Early Nasca shapes again consist mainly of open bowl shapes, but the differences are striking. Walls tend to be higher, diameters larger, and the orientation of the wall is now often slightly flaring instead of incurving. Several bowl shapes can be defined according to the orientation of the wall and its height relative to the vessel diameter. There are large bowls with slightly flaring and relatively high walls (Fig. 13.6d–f) and others with more strongly flaring

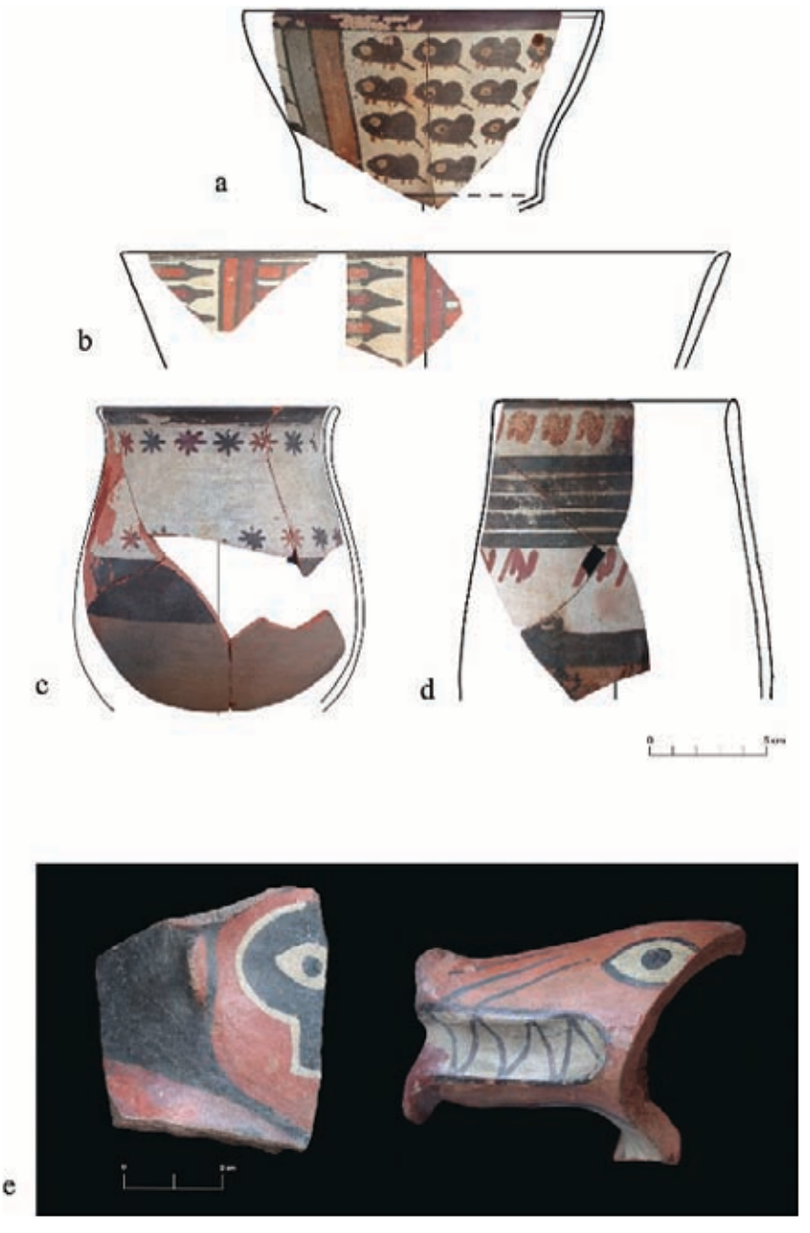

Fig. 13.4 Middle Nasca pottery from Los Molinos sector A

walls (Fig. 13.6a–c). Bowls with relatively low walls can be straight or slightly convex walled with vertical or flaring walls (Figs. 13.5e–j and 13.3b–g); rare examples of incurving walls occur (Fig. 13.3a).

New among the closed vessels category are the bulbous vase (Fig. 13.5a–d) and figure jars (Fig. 13.4e).

The analysis of shape does not provide major chronological differentiation. It seems that higher vessels such as the bulbous vase occur somewhat later in the stratigraphy, but as the other shapes and the iconography continue, a subdivision of the Early Nasca phase would be forced. Vessel proportions form a major argument in the Dawson shape classification (Roark 1965; Proulx 1968; Wegner 1975). However, with fragmented pottery, details of shape such as the exact proportions cannot be observed and the potentials of shape analysis for chronological subdivision are therefore more limited.

The changes in the design as compared to the Initial Nasca pottery are even more striking. Design themes are no longer limited to geometric forms;

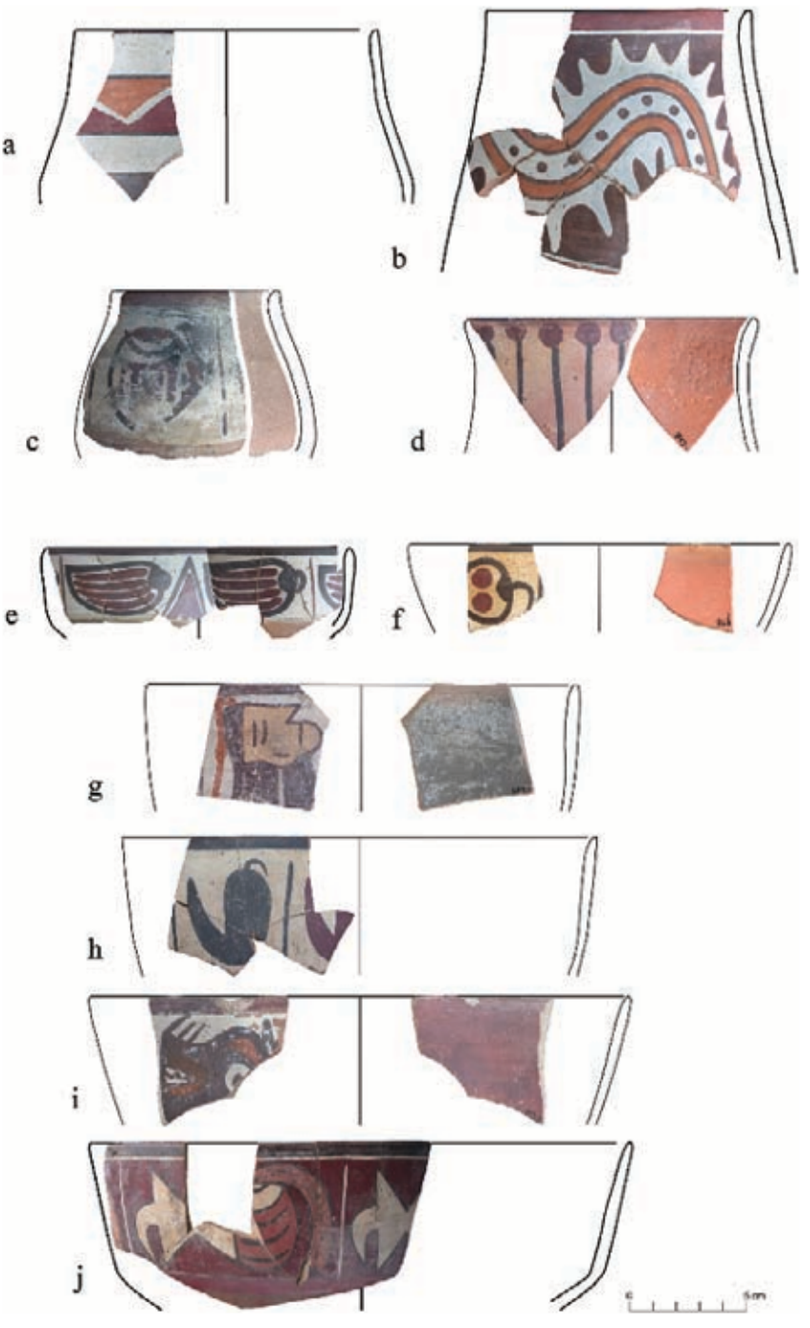

Fig. 13.5 Early Nasca pottery from Los Molinos sector B

there is now a large variety of naturalistic and mythological themes, such as representations of fruits, animals, and complex anthropomorphic figures or separated human heads. The motives are depicted in three or more colours and details are drawn outlined with a characteristic black line.

Comparing the materials from the different settlement sectors of Los Molinos we see differences between the pottery assemblages of sectors A (Fig. 13.3) and B (Figs. 13.5 and 13.6), but these seem to be more related to function than chronology. In sector A small bowl shapes were found with mainly naturalistic and geometric designs, whereas in sector B a significantly higher number of very well elaborated pottery with mythical design themes was observed (Figs. 13.5b and 13.6c–f). However, with the exception of the geometrically decorated bowls from the lowest level in sector A (Fig. 13.3f–i) which seem to constitute an early component of this period, the overall comparison of the materials of the two

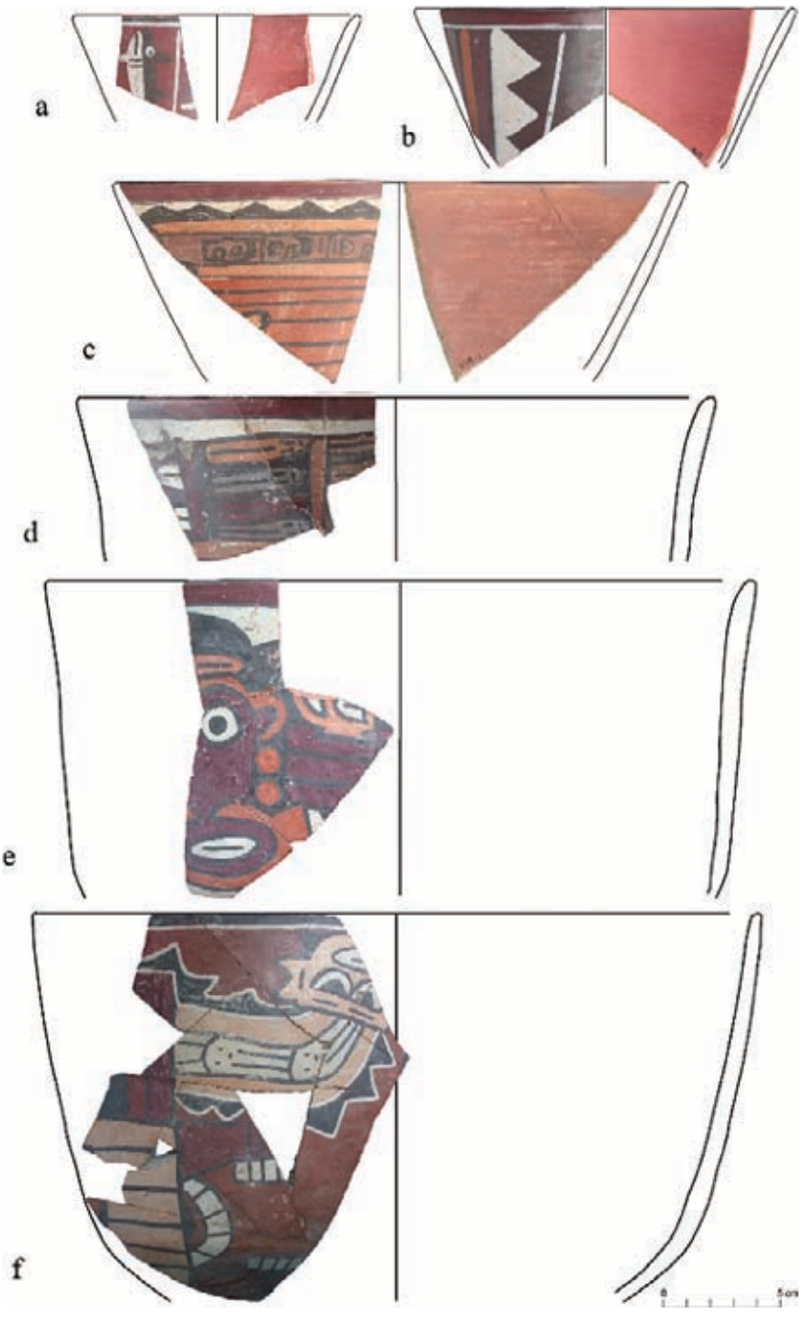

Fig. 13.6 Early Nasca pottery from Los Molinos sector B

adjacent sectors shows that they are contemporaneous. During the Early Nasca phase the introduction of new traits, such as variations in shape, the use of more colours, the addition of new design themes, or the alternation of white, red, and black backgrounds occurs quickly and cannot be traced stratigraphically. Features that occur in the lowest level of one excavation unit can be observed in the uppermost levels of another pit and the reverse. Other designs have a unique occurrence and can therefore not be compared. In addition to these differences in colour scheme and category of design theme the stylistic overall appearance is homogeneous. This stylistic continuity is also reflected in the associated architecture at the site that is used throughout the sequence with only minor changes.

Towards the end of the Early Nasca phase construction activity at Los Molinos ceased. Still, some evidence from the uppermost levels of excavation mark the end of the Early Nasca phase. In some parts of sector A, reduced

settlement activities took place. Minor restorative work on the adobe architecture could be observed in association with some pottery and domestic refuse (Reindel and Isla 2001). The associated material differs from that of the Early Nasca style in many aspects. At Los Molinos we observe the first appearance of Middle Nasca pottery. New shapes such as the bulbous vase and cup bowl shape become more dominant. The decoration also shows some new traces. Some pottery is executed in a hasty way with simple geometric lines, others with more complex designs (Fig. 13.4a–d). Other very clear stratigraphic evidence is provided by some graves that cut the Early Nasca architecture. The pottery associated with the graves is of Middle Nasca style (Reindel and Isla 2001). The main Middle Nasca site excavated in Palpa is La Muña.

13.4.3 Middle Nasca: La Muña (325 AD–440 AD)

The La Muña site (Fig. 1.1 of Chap. 1 this volume) is divided into two central sectors: Sector A with the settlement and Sector B with the characteristic Middle Nasca elite tombs (Reindel and Isla 2001; Isla, this volume). The excavations in the settlement sector revealed a stratigraphy with an extraordinarily high number of associated pottery. This provides a representative sample for the observation of chronological changes in the pottery assemblage. Several test pits as well as area excavations in architectural structures brought about a total of about 2500 diagnostic sherds.

The shapes can be traced back to Early Nasca antecedents. The major shape classes continue into this phase, but with slight changes. Walls of bowls tend to be more flaring than the early Nasca specimens. Formerly slightly concave walls now show a pronounced concavity. The convex bowls are also more pronounced and rounded. The contour of the vessel wall, its concave appearance or flare, is sometimes marked by changes in the thickness of the wall (Figs. 13.8a,c; 13.9e,g; and 13.10c). Early Nasca pottery is widely characterized by a very even thickness that marks the severe character of the style, however, the Middle Nasca shapes show a more cursive elegance.

A significant increase in higher shapes such as vases is observable. Vases are mostly of the bulbous vase shape, although some more cylindrical specimens occur (Figs. 13.7 h, i; 8 l; 13.9a–c; and 13.1-d–e). Another very prominent shape class is the cup bowl, a deep flaring bowl of mostly small diameter, with a characteristic concavity of the wall and a flaring rim (Fig. 13.8a–c and 13.10f,h).

Most of the Middle Nasca designs derive from the Early Nasca phase. However, some themes are new, such as the representation of human beings with sticks (Figs. 13.10b,f). Some themes are very similar to the Early Nasca ones, but are more hastily executed and appear on different vessel shapes. Other designs, such as fruits, have changed noticeably (Figs. 13.7i; 13.8 h,k–l; 13.9e,f; and 13.10a). The interior of the vessels is no longer covered completely with engobe. In some cases a band of red engobe of 2–5 cm is painted on the interior rim.

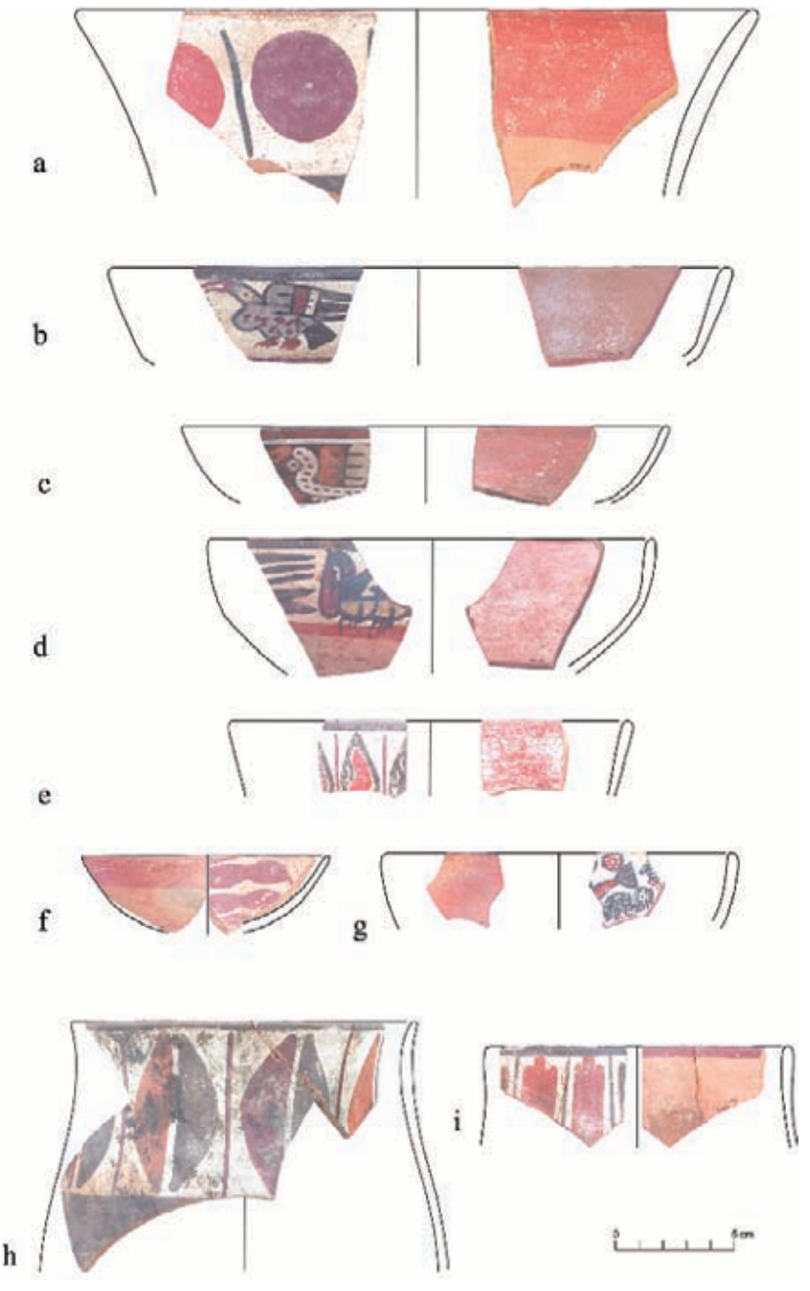

Fig. 13.7 Middle Nasca pottery from La Muña

The colour scheme has changed: buff becomes a common colour, sometimes used as background (Fig. 13.8b,d,f,k). Light backgrounds such as white are now the most common in contrast to the dark black or red backgrounds of the Early Nasca phase. Simple geometric designs, without black outlining, such as those of the early bowls from Los Molinos occur but on other vessel shapes and sometimes with large parts of the vessel surface left undecorated (Fig. 13.7a,h–I; 13.9b; and 13.10g). Some vessels show interior and exterior decoration (Fig. 13.8i–k).

It is possible that the subdivision of this phase on the basis of the stratigraphic evidence is hindered by the overwhelming diversity of the design. Because the pottery is fragmented, even the more frequent themes that occur in several different strata can hardly be compared with each other because the fragments show different parts of the complex themes.

The end of the occupation of the La Muña site is not marked by the existence of a later pottery style in the uppermost levels as observed at Los Molinos at the

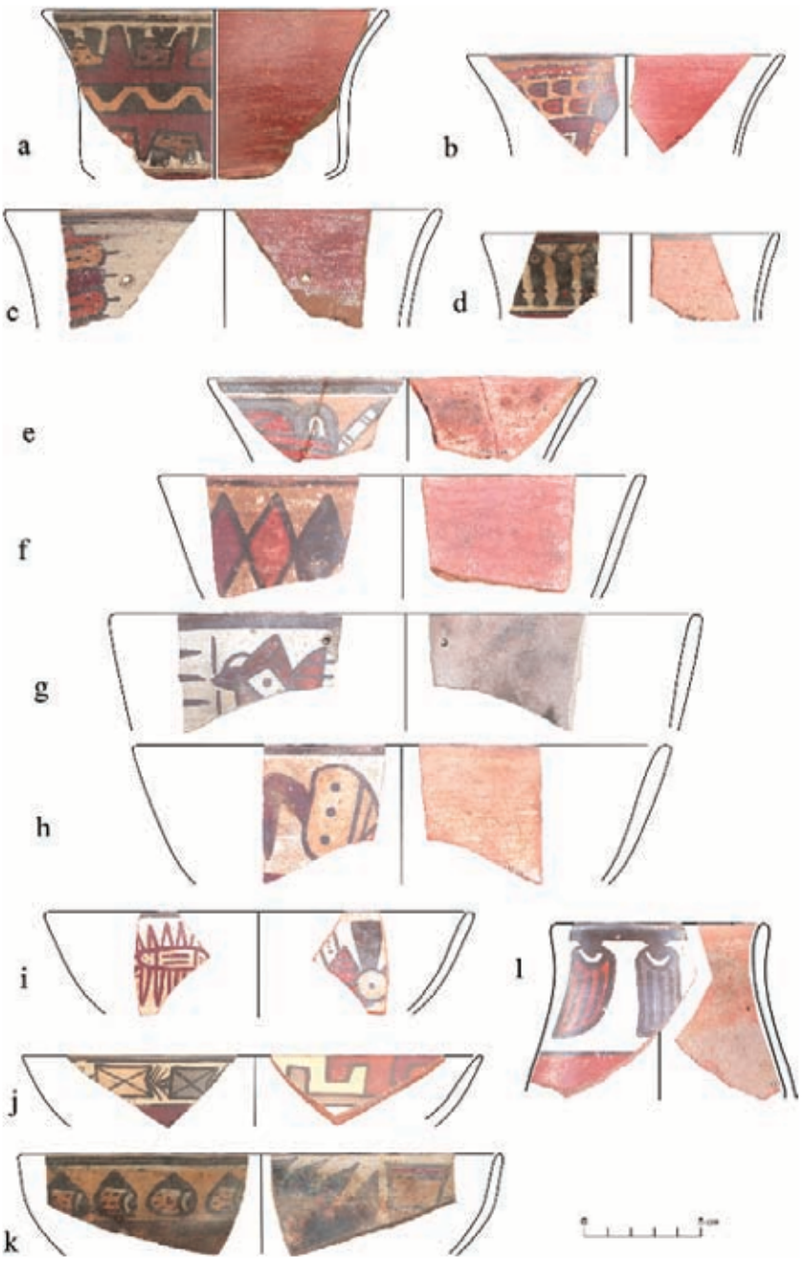

Fig. 13.8 Middle Nasca pottery from La Muña

end of the Early Nasca phase. The site had been left open and the population moved to some other site.

There is weak evidence of later activities at the site. The grave architecture of some of the elite tombs has been the scenario of later rites. The deposition of some Late Nasca vases on the surface of at least two of the elite tombs indicate that the ancestors buried in these graves were worshipped even after the abandonment of the settlement of La Muña (Reindel and Isla 2001:276). The stratigraphic evidence at this site for the superposition of Late Nasca over Middle Nasca is only weak, because stratigraphically these offerings could be contemporaneous to the closure of the grave. But, stylistically the ceramics show traits that have not been observed in any of the excavations at La Muña or any other Middle Nasca context known to date. Stylistically this pottery is without any doubt Late Nasca, as can be seen by comparing it to the pottery assemblage from Parasmarca.

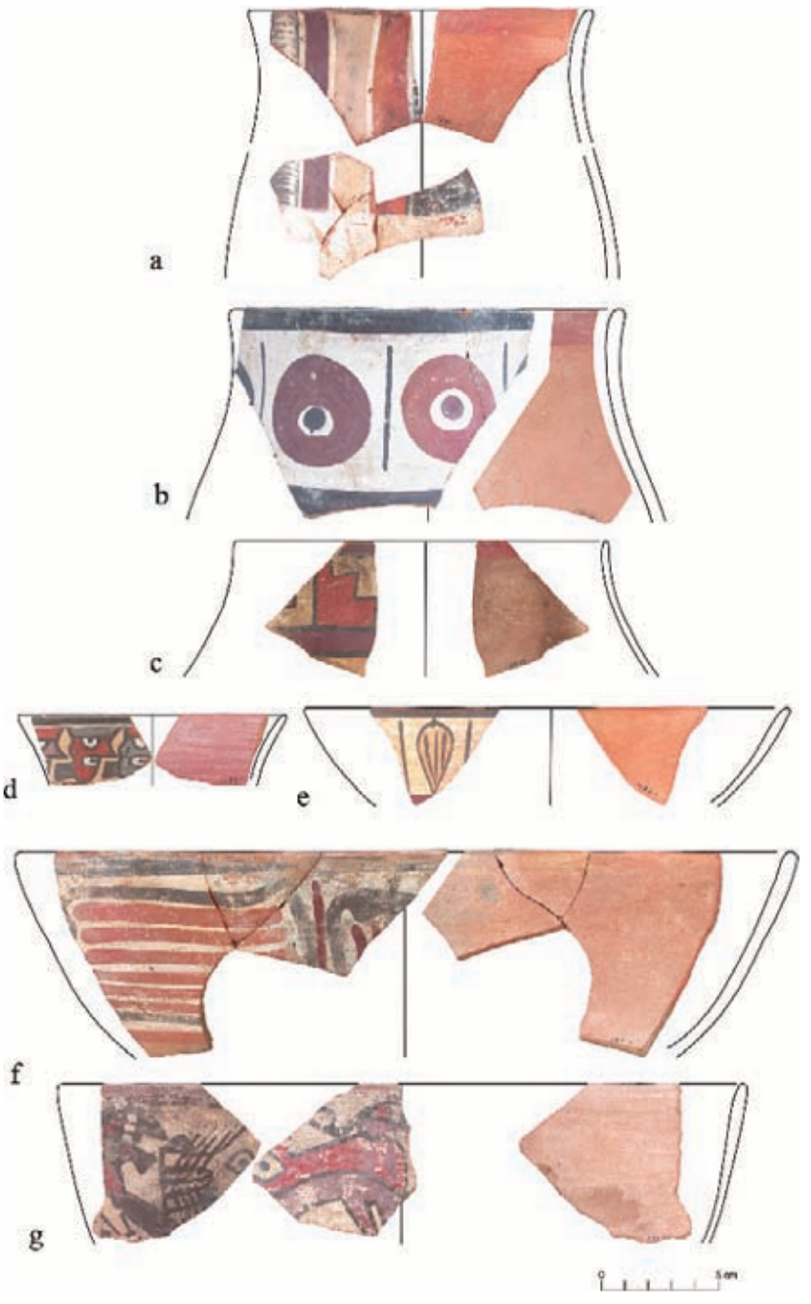

Fig. 13.9 Middle Nasca pottery from La Muña

13.4.4 Late Nasca: Parasmarca (440 AD–620 AD)

At Parasmarca (Fig. 1.1 of Chap. 1 this volume) the principal settlement belongs to a Late Nasca occupation of the site. In the central sector of the site there is some Late Nasca related rectangular stone architecture that was studied by area excavations. From these excavations about 1500 diagnostic pottery fragments have been included in the analysis.

In Late Nasca, the ware distinctions continue to be nonspecific with fineware and coarseware. The shapes of the Late Nasca phase can be seen as a continuation of the middle Nasca trends, but can easily be distinguished: many bowls have characteristically flaring walls with an inclination of up to 50°. As a result the difference between rim diameter and base diameter is increased (Fig. 13.12). Other bowl shapes with slightly convex, vertical, or flaring walls are very

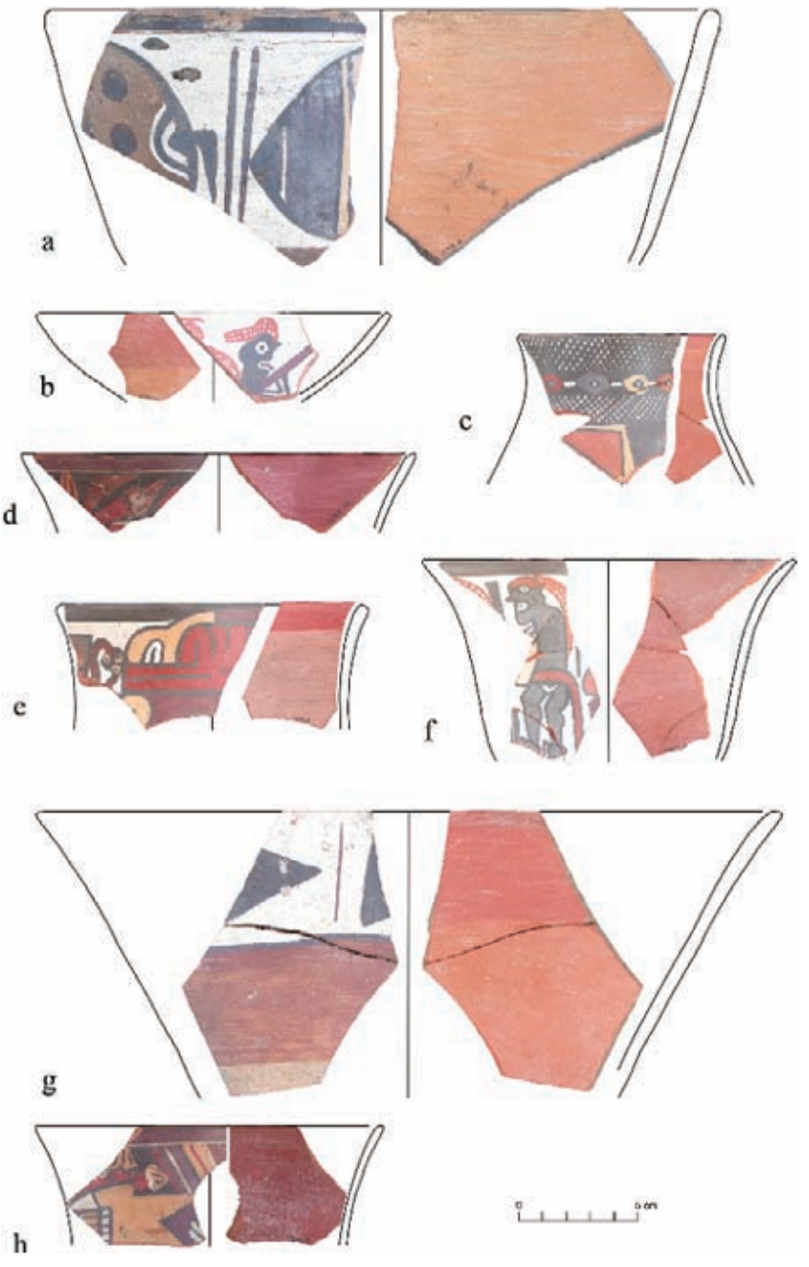

Fig. 13.10 Middle Nasca pottery from La Muña

similar to some Middle Nasca specimens, but bear a phase-specific design (Fig. 13.13c–e). A third category is a flaring bowl with characteristically concave, low to medium high walls, and a pronounced base angle (Fig. 13.11f–h, j). Vases of the Late Nasca phase tend to be taller and more cylindrical than the Middle Nasca vases (Reindel and Isla 2001: 276). However, there are also some incurving vase shapes (Fig. 13.13f–g).

The designs also show some drastic changes. Naturalistic and geometric designs become more stylized and simpler in comparison to Middle Nasca. Naturalistic themes such as animals or fruits are extremely rare now (Fig. 13.12c,g). There is less variation observable. Mythical themes appear more complex, but this is due to stylization and repetition of principal components such as headdress and mouth mask which are represented by volutes and rays (Figs. 13.11c, i; 13.12b; and 13.13d). Human trophy heads are very stylized and sometimes hard to interpret (Figs. 13.11a,j and 13.13a,d,g). Dot fillings of interspaces or wavy lines become a

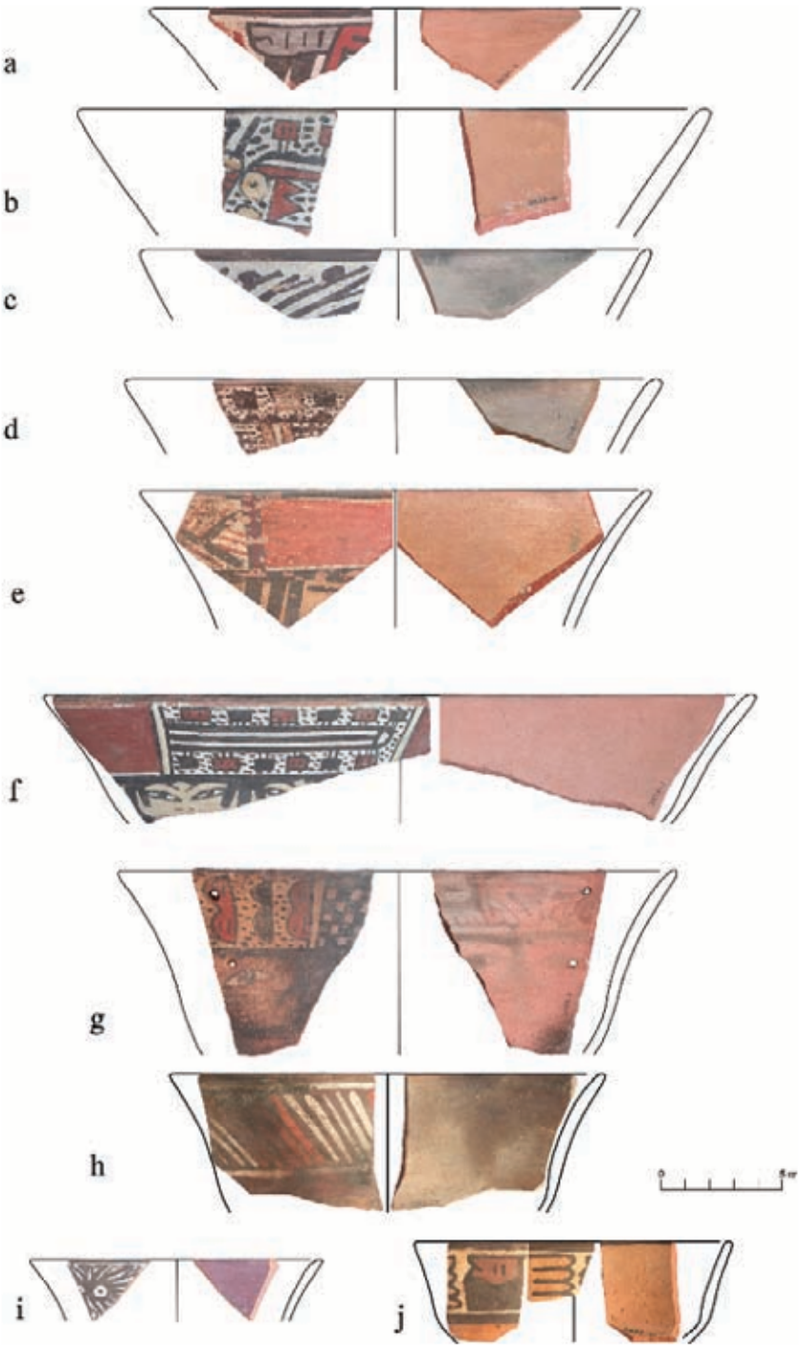

Fig. 13.11 Late Nasca pottery from Parasmarca

frequent feature (Figs. 13.11b,f–g; 13.12a,b,d; and 13.13d,f). Geometric designs consisting of crosses, simple step designs, or wavy lines are very characteristic. The lower part of flaring bowls is frequently decorated with a series of human faces (Figs. 13.11e–g and 13.12 h). In other instances decoration is restricted to the upper part of the vessels. And those shapes with a wide opening may have an inner rim decoration. However, monochrome decoration of the inner wall is limited to a few red or black lines.

A stratigraphic subdivision of the Late Nasca phase is not possible on the basis of the material from Parasmarca. There are stratigraphies showing a superposition of several Late Nasca related occupations, but there are no significant changes observable in shape or design.

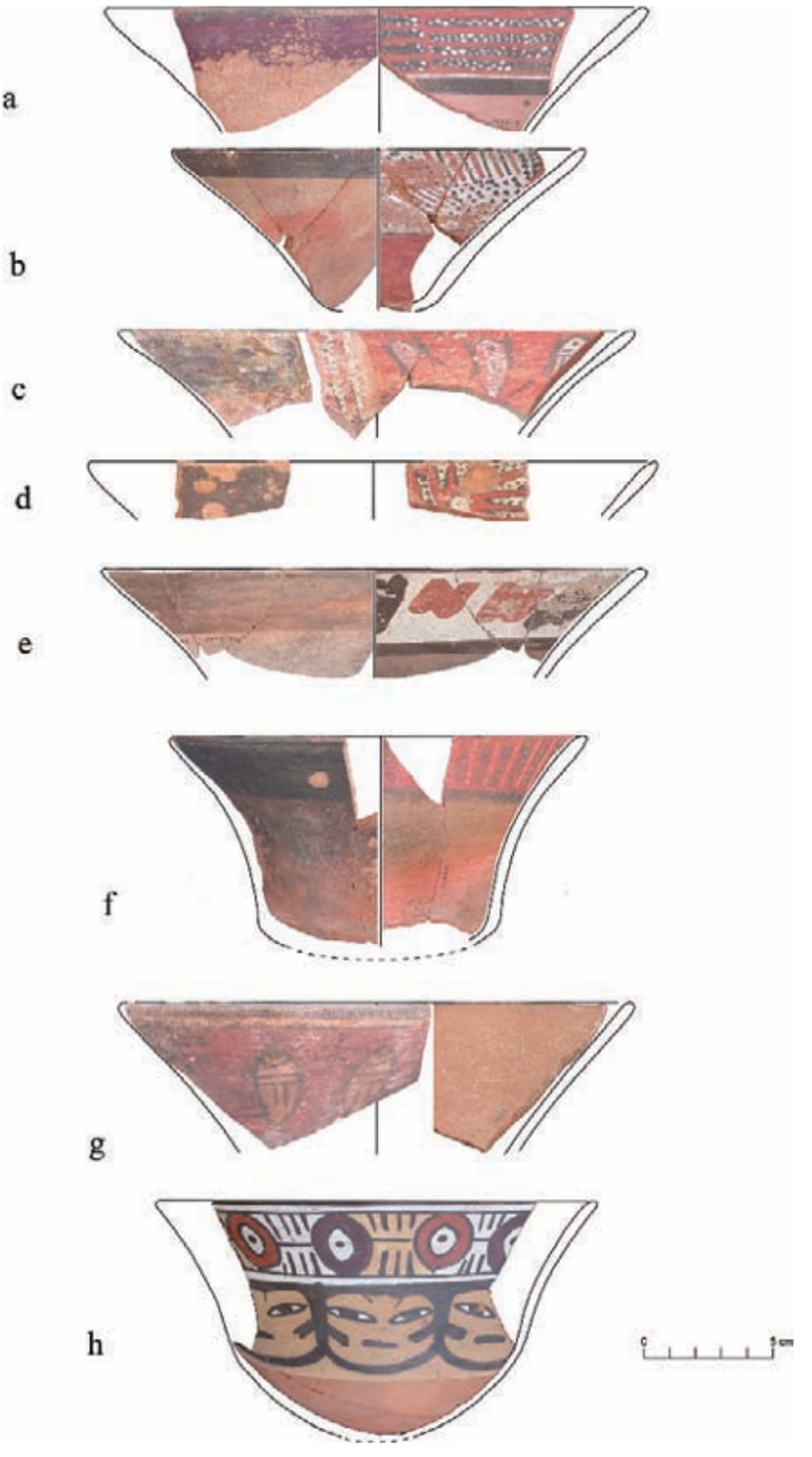

Fig. 13.12 Late Nasca pottery from Parasmarca

For the placement of the Late Nasca phase in the sequence there is a problem with the stratigraphic link between Late Nasca and the presumably preceding Middle Nasca phase. In Parasmarca, the material encountered on the surface of the central sector is mainly Late Nasca, but frequently we also see Middle Nasca and Initial Nasca pottery. This mixture of phases is due to the earlier use of other sectors of the site: sector B comprises a large Initial Nasca settlement, and sector C in the upper part of the site is an erosion fan with geoglyphs associated with Middle Nasca pottery.

In Late Nasca times the people building the architectonical structure of sector A used soil for their construction filling from nearby. Therefore, in

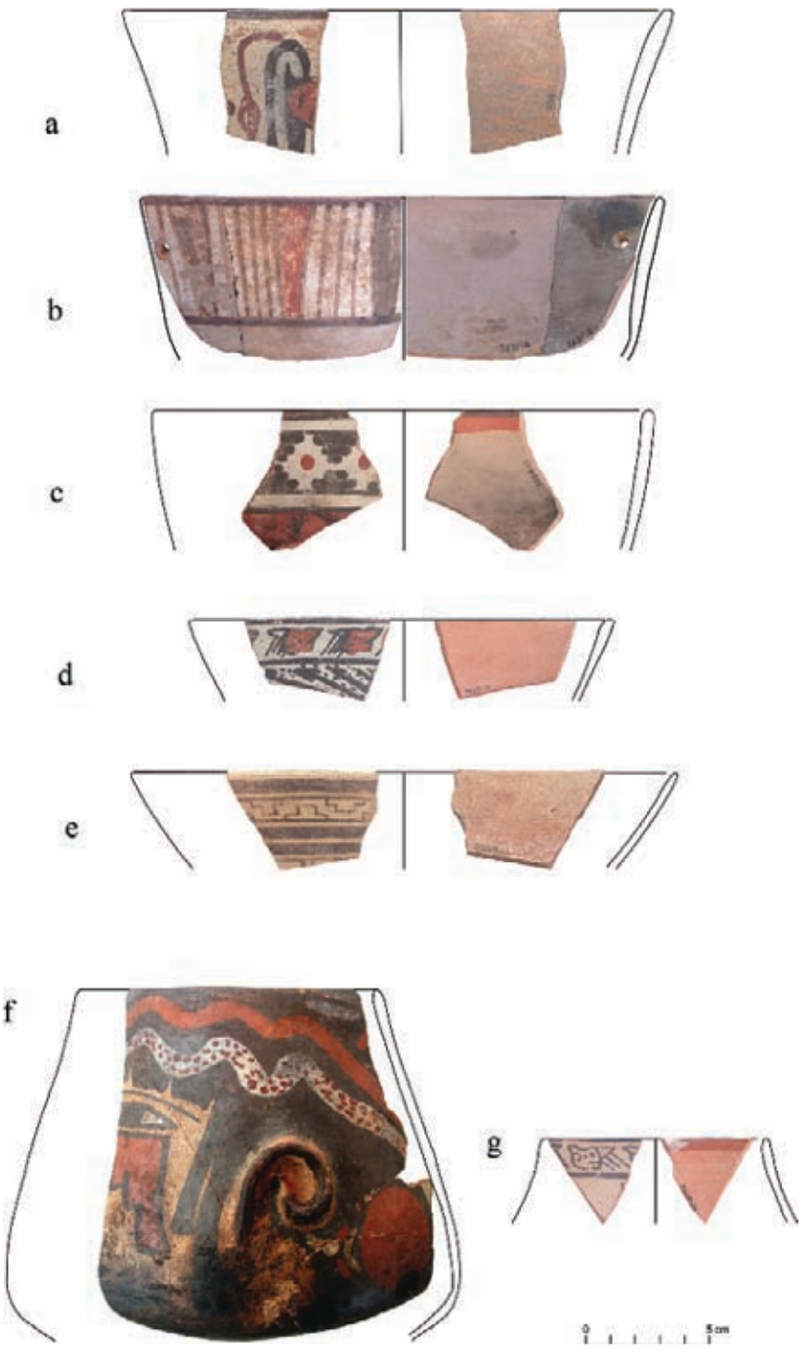

Fig. 13.13 Late Nasca pottery from Parasmarca

some cases pure Late Nasca associated contexts are found beneath fillings with Initial Nasca and Middle Nasca material. Although clear superposition of Late Nasca above Middle Nasca can be cited, sometimes the situation is the reverse. There is no clear evidence of Late Nasca overlaying Middle Nasca or Initial Nasca at the Parasmarca site. In all excavations conducted at the site the principal component was Late Nasca pottery. However, in nearly every trench Middle Nasca and Initial Nasca pottery are included to some degree.

The attribution of the architecture to Late Nasca is based on several arguments: most of the pottery is Late Nasca; the architecture differs considerably from that observed at Estaquería, Los Molinos, and La Muña; and Loro phase graves of the Middle Horizon (see chronological chart) cut the architecture, just as the Middle Nasca graves cut the early Nasca settlement structures of Los Molinos.

One might argue for a contemporaneity of Middle Nasca and Late Nasca pottery. But, at La Muña no Late Nasca fragment has been found thus far. The only Late Nasca finds are the vessels deposited in association with the funeral yard, as cited above. If both styles were contemporaneous, one would expect to find more evidence. In gravelots from Palpa and other valleys of the Nasca region (see Carmichael 1988) no Middle Nasca pottery associated with Late Nasca was observed. Mixing of the earlier phase material in a later context is always possible. However, clear stratigraphic proof is still lacking. As a final argument for Late Nasca being later than Middle Nasca, the C14 dates can be cited: the samples from Parasmarca all date to after 420 AD and therefore are definitely later than the samples from La Muña.

13.5 Discussion

A second step in the analysis is the comparison of the pottery sequence observed in Palpa with materials from other valleys and with the Dawson sequence. For the Initial Nasca pottery from Estaquería the closest resemblance is found in the materials classified as Nasca 1 and Ocucaje 10 by Menzel et al. (1964), and in the pottery types defined by Strong (1957) as Proto-Nazca. There is no material from other valleys published in sufficient detail for comparison. We have only some general descriptions based on materials from Ica and Nasca. It cannot be told from the information available, if some features occur more frequently in Palpa or in other valleys. The polychrome engobe painted incised pottery of the Nasca 1 style may have had its main area of circulation in the Nasca area, as it is very rare in Palpa.

The engobe painted pottery without incision observed in the uppermost levels of Estaquería and in the lowest levels at Los Molinos (Fig. 13.3f–i) corresponds to some of the Nasca 2 pottery defined by Dawson, called Nasca 2 A and B by Silverman (1977). However, the more complex decorated Nasca 2 C pottery could not be observed in Palpa. The Early Nasca pottery from Los Molinos corresponds to Dawson's Nasca 3. Again, finer subdivisions of the Dawson phase, as proposed by Proulx (1968) with his Nasca 3 A–D distinction, cannot be transferred to the fragmented pottery from Los Molinos, nor can a similar subdivision of the Early Nasca phase be seen in the material.

Up to this point of the sequence the results from Palpa are in accordance with the Dawson sequence. The stratigraphic superposition proves the accuracy of the Dawson Seriation in this aspect. However, it should be noted that the Dawson phases are not represented equally in the stratigraphy. Phase Nasca 2 has the character of a short transitional phase, marking the beginning of the early Nasca phase and rarely occurring towards the end of Initial Nasca. A pure Nasca 2 settlement site has not been documented in the Palpa area thus far. In a few instances Nasca 2 pottery is prevalent in small areas of a site. Dawson's phases Nasca 2 and Nasca 3 are closely related by settlement continuity, and

they are separated from the Initial Nasca material. Thus, the context-based sequence better reflects the sociopolitical background of the style phases.

In the uppermost layers of Los Molinos changes in the shape and design repertoire have been observed (Fig. 13.4). This pottery can be compared to Dawson's phases Nasca 4 (Proulx 1968) and Nasca 5 (Roark 1965). Also, the material found in La Muña and in the Middle Nasca graves from Jauranga and Hanaq Pacha corresponds to these two stylistic phases. In Palpa the two phases interpreted by Dawson as successive, occur in association, without any stratigraphic division. The differences in shape and design that mark the phase distinction in the Dawson sequence can be observed in the Palpa materials, but lacking a stratigraphic delimitation both phases were classed together as Middle Nasca. The phases Nasca 4 and Nasca 5 appear to be contemporaneous, as had already been proposed by Dawson on the basis of grave associations (Rowe 1956:147). Later in his analysis, however, he subdivided the two phases.

The Late Nasca Pottery from Parasmarca corresponds to Dawson's Nasca 7 (Wegner 1975, 1976; Kroeber and Collier 1998; Lothrop and Mahler 1957; Proulx 2006). Again, a subdivision of the phase on the basis of the stratigraphic evidence from Palpa is not possible. In an unpublished work, Dorothy Menzel (1957) subdivided Nasca 7 in subphases A–C (Menzel 1971). No comparable differences in style and shape were observed in the Palpa material. As expected, Late Nasca proved to be later than Middle Nasca, apparent from the frequent occurrence of earlier materials in Late Nasca construction fill at Parasmarca. Interestingly, no Nasca 6 pottery could be observed in Palpa. As there is no evidence for an abandonment of the valley after Middle Nasca, it is more probable that the Nasca 6 style represents a regional substyle of the southern Nasca drainage, where it has been documented in several graves (Silverman 1993, Kroeber and Collier 1998). On the basis of grave associations this substyle would be part of the Middle Nasca phase.

13.6 Results

For the Palpa area we can define four major settlement phases, each associated with larger settlement sites. The intensive survey of the Palpa valleys suggests that no major settlement phase has been neglected. Judging from the present data it is not to be expected that sites showing pottery assemblages intermediate between the four phases presented here will be found in the Palpa area.

In terms of the Dawson phase classification Fig. 13.4 this means that there is Nasca 2 associated architecture at Palpa, but this cannot be seen isolated from Nasca 3 settlements. Nasca 4 is present to a certain degree in Nasca 5 contexts, but we have no pure Nasca 4 settlement site that would permit speaking of a proper phase. Nasca 6 was not observed and it is not expected that future investigations will reveal pure Nasca 6 settlement sites as intermediate between the Nasca 5 and Nasca 7 occupation of the valley. Also, there is no evidence that would suggest a hiatus in the valley occupation during one of the phases.

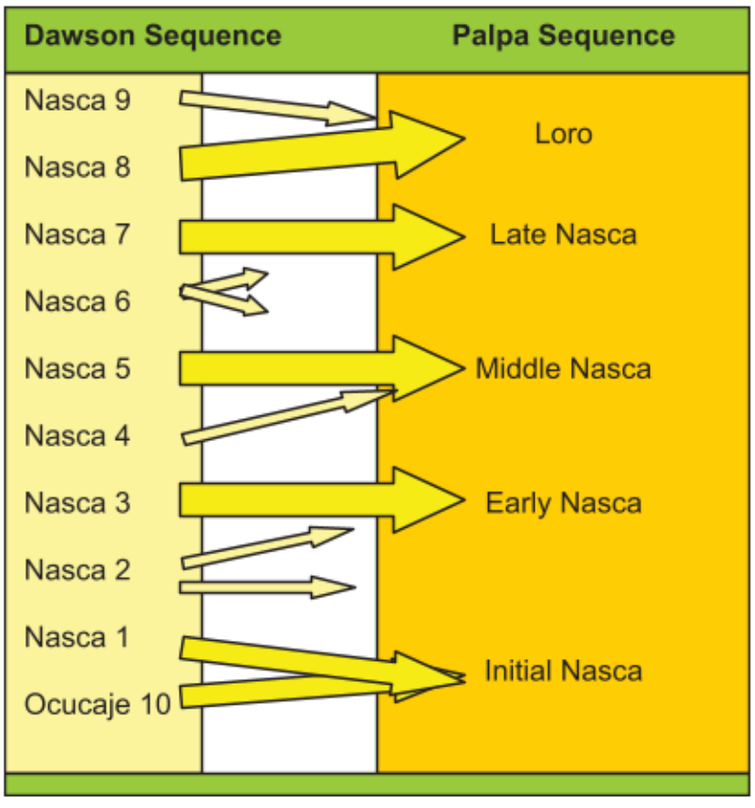

Fig. 13.14 Comparative scheme of the Palpa sequence and Dawson sequence (Archaeological Project Palpa)

The continuous settlement history of the Palpa area cannot be adequately described using Dawson's seven-phase sequence. In this case the reduction of the sequence to four phases means a refinement of the chronology, because it corresponds better to the sociopolitical changes that can be observed by changes in settlement sites, architecture, funeral patterns, iconography, or regional distribution of these aspects.

When we combine the relative sequence with numerical data obtained during the project, for each settlement phase a definite time span can be given, without the need to leave gaps (for Dawson's phase 6) or arrange the numerical data in the case of two contemporaneous phases (Nasca 4/5). In the case of Nasca 2, that surely constitutes an early component of the Early Nasca phase, specific scientific dating of pure Nasca 2 contexts might help for a further refinement of the sequence. The results of the scientific and archaeological chronological analysis are merged and illustrated in the project's chronological chart where the newly defined relative cultural periods are combined with the latest numerical data (Fig. 1.2 of Chap. 1 this volume).

Chapter 14
The Clock in the Corn Cob: On the Development of a Chronology of the Paracas and Nasca Period Based on Radiocarbon Dating

Ingmar Unkel and Bernd Kromer

Abstract The people of the Paracas and Nasca cultures, who created the world-famous geoglyphs, lived in the desert of the south coast of Peru approximately between 800 cal BC and 630 cal AD. The archaeological chronology of these cultures thus far was based almost exclusively on a sequence of seriated ceramic styles. The numeric dating of some of the style phases was supported only by few radiocarbon dates. Here we present the first numeric chronology of the Paracas and Nasca culture based on ^{14}C-dating of approximately 120 organic samples from settlement and tomb relics, as well as on material derived from geoglyph sites in the Nasca/Palpa region (South Peru). It is thus far the largest detailed numeric chronology for pre-Columbian times in all of South America. The main focus has been on the Nasca settlement centers near Palpa, Los Molinos, and La Muña, the Paracas site of Jauranga and the Initial period site of Pernil Alto. Most of the ^{14}C-samples have been dated at the AMS facilities at the ETH Zürich (Switzerland) and at the Lund University (Sweden). The targets were produced in the new graphitization line at the Heidelberg ^{14}C-laboratory (Germany), which was designed and developed during the NTG-project.

14.1 Introduction

Pottery is a quite durable cultural product and in most prehistoric cultures shows a marked chronological sensitivity. Therefore, ceramics are widely used among archaeologists to arrange ancient cultures spatially and temporally (Eggert 2001). Since the dawn of archaeological ceramic analyses it was not only used as a source of cultural information, but also as a tool to create a

I. Unkel (✉)
Department of Physics, Nuclear Physics, Lund University, Professorsgatan 1, 22100 Lund, Sweden
e-mail: ingmar.unkel@geol.lu.se

M. Reindel, G.A. Wagner (eds.), *New Technologies for Archaeology*, Natural Science in Archaeology, DOI 10.1007/978-3-540-87438-6_14,
© Springer-Verlag Berlin Heidelberg 2009

relative chronology of archaeological complexes, especially at the beginning of the twentieth century when radiometric dating methods were still lacking.

An initial approach to the question of the age of the Paracas and Nasca cultures was made in the 1960s when the first detailed ceramic chronologies for the south coast of Peru were established (Menzel et al. 1964; Rowe 1960a,b). But in the course of archaeological investigations during the last decades these relative chronologies have shown several problems and a number of new questions have arisen (Wetter 2005). For example, are the ceramic phases that form the basis of the chronology in the correct order? How long does a single style phase last? Do certain style elements perhaps co-exist rather than follow one another? Silverman and Proulx (2002) mention that, for example, regional differences in ceramic style elements may be misinterpreted as chronological stages.

In 1964 Menzel, Rowe, and Dawson published a chronology of the Paracas culture with ten style-phases named 'Ocucaje', which was based mainly on ceramics from the Ica valley and the Paracas peninsula. The last phase of this Paracas chronology, Ocucaje 10, incorporates style elements similar to the first phase of the Nasca chronology, Nasca 1; thus this transitional period is referred to as Proto Nasca or Initial Nasca (Lambers 2004; Reindel et al. 1999).

The Ocucaje sequence was established on the background of a huge number of sample materials in museums and private collections mostly lacking information on archaeological contexts. Only few scientific excavations of Paracas sites have been conducted on the south coast of Peru, and several relative chronologies with different phase designations co-exist (Reindel and Isla Cuadrado 2001; Wetter 2005).

The ceramic chronology of the Nasca period faces the same problem as that of the Paracas time, because much of the pottery, building the basis of the classification, comes from looted contexts and lacks stratigraphic information. The first descriptions of the Nasca ceramics and attempts at a relative chronology were published by Joyce (1912) and Uhle (1914).

During the last century a number of archaeologists worked on a systematic chronology of the Nasca time based on the ceramic analysis with respect to decoration style, iconography, and vessel type (Silverman and Proulx 2002). Lawrence Dawson developed a style chronology of nine phases which is still in use today. However, Dawson never published his investigations himself. A summary of the style sequence was published by Rowe (1960a,b).

The existing attempts at a numerical chronology of the Paracas culture have been discussed controversially (Velarde 1997). The date of the onset of the so-called Early Horizon varies up to 900 years depending on the author (Paul 1991). This conflict is based on ^{14}C-data which are either derived from less distinctive archaeological complexes or belong to locations such as Chavín de Huantar that are far away from the centers of the Paracas culture and are parallelised by stylistic comparison (Burger 1981). In trying to fix the end of the Paracas period and the start of the Nasca period, meaning the onset of the Early

Intermediate period, the archaeological opinions vary less, but they still differ up to 200 years (Silverman 1991).

14.2 Archaeological Context

The archaeological framework of the ^{14}C-chronology of the Paracas and Nasca period presented here is given by excavations conducted under the guidance of Markus Reindel (Deutsches Archäologisches Institut, DAI-KAAK, Bonn) and Johny Isla Cuadrado (Instituto Andino de Estudios Arqueológicos, INDEA, Lima) in the region of Palpa since 1996. The main focus has been on the Nasca period settlement centers near Palpa, Los Molinos, and La Muña, the Paracas location of Jauranga, and the Initial period site of Pernil Alto. The context of the approximately 120 ^{14}C samples used to build up the numerical chronology is described in detail in the publication of Unkel (2006) and in the excavation reports of Reindel, Isla Cuadrado, and colleagues, for example, cited by Unkel (2006).

14.3 Method

For a sound numerical ^{14}C-chronology of the Paracas and Nasca periods a large number of datable organic samples are required. Quite often, however, there is only little material available, either because the archaeological objects which are to be dated are too precious, such as the textiles of the Paracas period, or because the objects contain only little organic matter such as adobe or soil samples. In this situation the application of AMS (Accelerator Mass Spectrometer) measurements for ^{14}C dating has a large advantage over the conventional counter-techniques, because with AMS samples in the range of milli- or even micrograms can be measured compared to the gram-size samples required for conventional dating.

When arriving in the laboratory all samples need to be chemically pretreated to remove different kinds of contamination which might have penetrated the sample since deposition. For charcoal, wood, and corn samples we use the well-established AAA method (Acid–Alkali–Acid) as described by De Jong et al. (1986). The samples are kept in 4% HCl (hydrochloric acid) for an hour at 80°C to remove carbonate contamination, then left in cold 4% NaOH (sodium hydroxide) over night (ca. 17 h) to remove humic acids; afterwards the acid step is repeated before the sample is rinsed with demineralised water to pH 7. After drying 3–10 mg of the material are combusted to CO_2 at 900°C for 3 h in a sealed quartz-glass tube together with 200 mg of CuO (copper oxide, oxygen source) and 100 mg of silver wool (to remove sulphur).

For the AMS measurement the sample CO_2 needs to be transformed into graphite. A basic method to graphitise ^{14}C-samples was described in the 1980s

(Vogel et al. 1984) and was improved and modified by the facilities of each ^{14}C-laboratory since then. During the NTG-project a graphitisation line for the Heidelberg ^{14}C-laboratory was built and the process was optimised with the help of the samples from Palpa/Nasca. The main goals when setting up the line were (1) a high throughput of samples which was achieved by installing six parallel reaction chambers; (2) an automation of the process as far as possible to monitor the graphitisation online with control software; and (3) a constant quality of the final graphite targets and a low ^{14}C-background (low contamination with modern carbon). For details on the Heidelberg graphitisation line see Unkel (2006).

At the beginning of the project a single-lined prototype of a graphitisation line was built which was used to test the influence of the reactor design and of different catalyst materials on the reaction rate. Iron and cobalt in different grain sizes were examined as catalysts. As cobalt-based graphite targets were preferably run at the AMS facility at the ETH Zürich, one of our collaboration partners, we decided to use cobalt for our samples instead of the more widely used iron catalysts. The various test runs showed that the longer reaction time using cobalt (usually 5–6 h) is not related to slower diffusion processes due to a certain reactor design, as was assumed, but only depends on the type of catalyst material. We also found that the ideal reaction temperature for cobalt is around 625°C which is notably higher than the temperature for iron (575°C). Temperatures higher than 625°C did not accelerate the reaction process.

The graphitisation line designed after the prototype consists of six parallel reaction chambers and can be run by a single person. The software Hamster (Heidelberg AMS Target genERating system), which was programmed by the authors especially for this line, controls the valves and monitors pressure and temperature during the reactions. Running the graphitisation line via a computer terminal is far clearer and simpler than the manual procedures of a conventional line. However, we decided to design the system as only semi-automated to have the possibility to act manually on problematic samples. Depending on the type of catalyst used for the reaction, about 15–30 samples per week can be graphitised with this setup.

The AMS measurement of the ^{14}C background has yielded a mean value of 0.50 pmC (percent modern carbon) which is equivalent to 42,500 years. This shows that with this line background values can be achieved which are very close to the background level of the accelerator itself. This was one of the main goals at the beginning of the project.

Most of the ^{14}C-samples used in the chronology have been measured at the AMS facilities at the ETH Zürich (Switzerland) and at the Lund University (Sweden). ^{14}C measurements on dendro-dated tree rings show that the atmospheric ^{14}C concentration varies with time (de Vries 1958). As nearly all ^{14}C on earth is produced in the atmosphere from where it enters the carbon cycle, these variations influence the ^{14}C content of all organic matter. Because the fluctuations of the atmospheric ^{14}C content are not regular, ^{14}C-dating requires

calibration (Suess 1965), which is performed with the help of a calibration curve and specialised software tools.

All ^{14}C samples presented here were calibrated with respect to the IntCal04 curve (Reimer et al. 2004) and corrected for an offset of the southern hemisphere of 41 ± 14 years (McCormac et al. 2002). The calibration curve for the southern hemisphere, SHCal04 (McCormac et al. 2004), suggests a correction of 55–58 years with a statistical error between ± 7.9 years (up to 1000 BP) and ± 25 years (around 11,000 BP). However, for SHCal04 the southern hemisphere is defined as the part of the globe south of the Innertropical Convergence Zone (ITCZ). As Peru is located within the range of the ITCZ (our research area is located at 14°30′S) but an offset compared to the northern hemisphere can be expected, we here apply the minor correction of 41 ± 14 years according to McCormac et al. (2002). For calibration we used the software OxCal, version 4 (Bronk Ramsey 2001).

Although already applied in several fields of archaeology, Bayesian statistics have only rarely been used in the investigation of the pre-Columbian cultures of South Peru (Görsdorf and Reindel 2002; Michczynski et al. 2003). However, for building a coherent ^{14}C-chronology this special statistical approach is mandatory (Buck and Millard 2004). The fundamental idea of the Bayesian theorem is the probability of certain assumptions, events, or datasets under the condition of some prior or a priori information (Bayes 1763). This information can simply be the stratigraphic position of two samples or can be extended to the affiliation of a group of samples to a certain phase. In the case of the Paracas–Nasca chronology this would be the attribution of each sample to a certain ceramic phase, based on the excavation context and the association of organic sample material with ceramic findings.

A first approach to building a Nasca chronology based on Bayesian statistics was performed by Görsdorf and Reindel (2002) with 12 samples from well-documented excavations in Los Molinos and La Muña. They calibrated their samples with OxCal 3.5 (Bronk Ramsey 1995) based on the IntCal98 calibration curve (Stuiver et al. 1998). In two aspects of the calibration we slightly differ from the previous approach of Görsdorf and Reindel (2002). (1) They applied a southern hemisphere correction of -24 ± 3 ^{14}C-years based on Stuiver et al. (1998), whereas we used a correction of -41 ± 14 ^{14}C-years with respect to McCormac et al. (2002). (2) They do not use statistical boundaries for their chronology model, neither for defining single phases nor for separating two phases which can be distinguished archaeologically. However, using boundaries is strongly recommended by Bronk Ramsey (2001) as modelled time spans without boundaries tend to spread disproportionately.

Both Görsdorf and Reindel (2002) and we use the *sum*-function of the OxCal syntax (Bronk Ramsey 2001) for adding probability distributions of single samples to arrive at the best estimate for the chronological distribution of each Paracas and Nasca phase to be determined. It is important to note that the 2σ-range for a *sum* distribution gives an estimate for the period in which 95.4% of the events took place and not the period in which one can be sure with

95.4% probability that all of the events took place (Bronk Ramsey 2001). Due to this difference it is possible that single samples, which were previously included in the statistical model of a Paracas or Nasca phase, finally end up outside the calculated phase after running the model (for further considerations on outliers see Buck and Millard 2004).

As the algorithm used in OxCal 4 (Bronk Ramsey 2008) to calculate the chronology is slightly different from the one incorporated in OxCal 3.8, which we used previously (Unkel 2006; Unkel et al. 2007b), the accuracy of the calculated periods has improved. Note that we therefore decided to present here the 2σ (95.4%) probability ranges for the phases of the Paracas–Nasca chronology instead of the 1σ (68.2%) ranges, which are normally used for presenting ^{14}C data.

14.4 Results and Discussion

A first extensive numeric chronology of the Paracas and Nasca period based on approximately 100 ^{14}C samples from the Palpa area was published in 2007 by Unkel et al. Here we present an enhanced chronology based on additional samples, including to some extent the Initial period and the Middle Horizon.

There are 15 ^{14}C-samples from the Initial period, the period preceding Paracas, which are included in the chronology model (Fig. 14.1). All these samples were excavated in Pernil Alto. Due to the archaeological context they are all ascribed to the final phase of the Initial period. The end of this epoch is well defined by seven dates of the last period of use of the site, but we do not yet have information about the beginning and the duration of the Initial period (for details see Unkel 2006). So far, the samples of the Initial period can be perfectly used as the lower boundary of the Paracas chronology.

The Early Paracas phase is represented by only four samples from the sites of Mollake Chico and Pernil Alto (Fig. 14.2). So we have a first estimate of the time range of this phase, ranging from approximately 800 to 525 cal BC. However, more samples, especially from the transition between the Initial period and Early Paracas, are necessary to narrow the error margins. Eight samples are available from the Middle Paracas which were all excavated in Jauranga (Fig. 14.2). They yield an age range for this phase from 570 to 360 cal BC, but more samples are desirable to achieve a sound statistical basis.

Twenty-three samples build a strong backbone for the Late Paracas phase (Fig. 14.3), appointing this phase between 385 and 280 cal BC. Up to now all of these ^{14}C-samples were excavated in Jauranga. The Initial Nasca phase is represented by five samples (Fig. 14.3), all derived from a single archaeological complex at Estaquería. Based on these few samples the transition between Paracas and Initial Nasca could not yet be modelled sufficiently (Fig. 14.7). There is still a not well-defined time gap between 280 cal BC

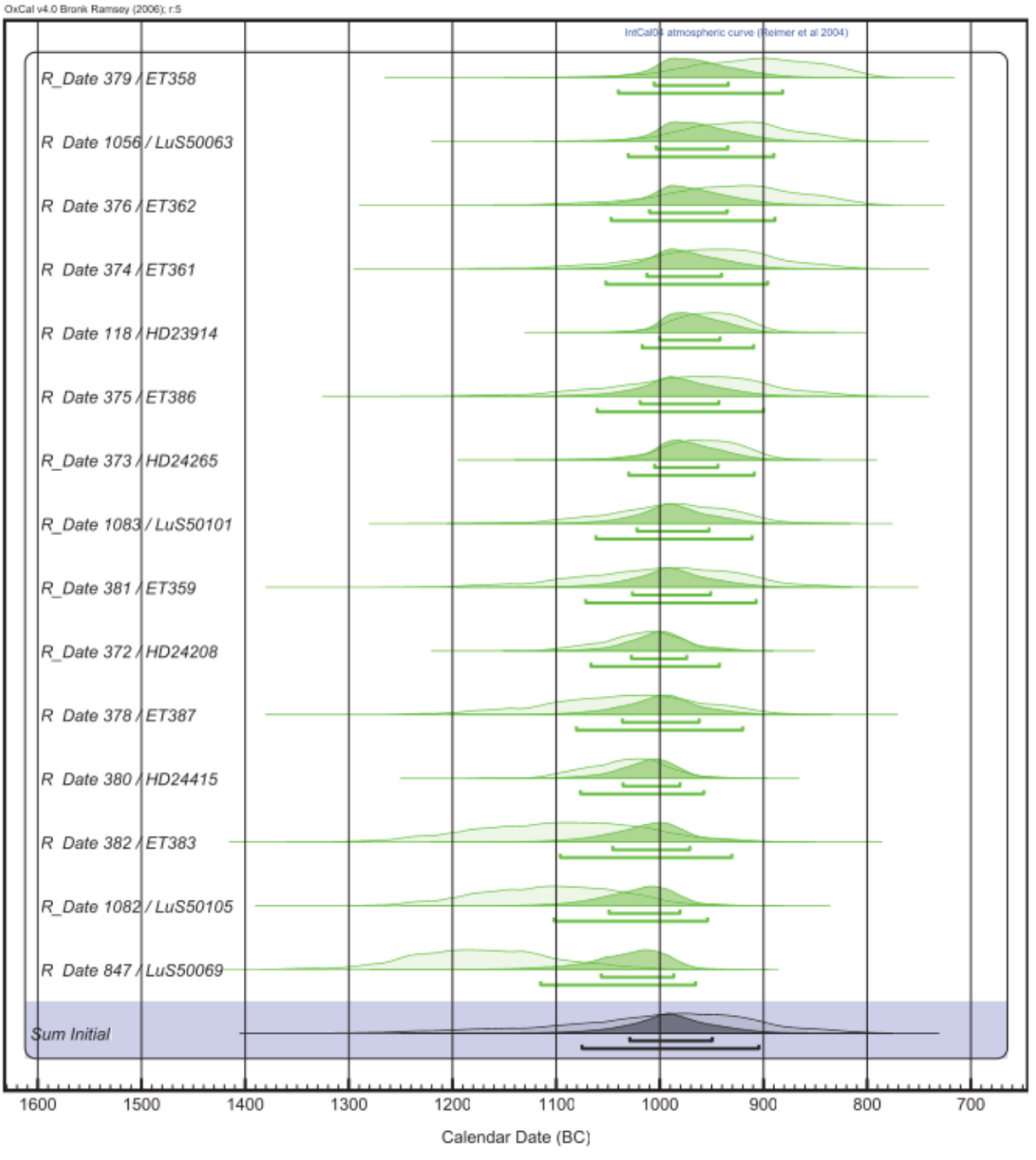

Fig. 14.1 The ^{14}C data of the 15 samples from the Initial period which were excavated in Pernil Alto. All dates were calibrated with OxCal4 with respect to IntCal04 (Reimer et al. 2004), including a southern hemisphere correction of 41 ± 14 years (McCormac et al. 2002)

(upper 2σ-boundary of the Late Paracas phase) and 120 cal BC (lower 2σ-boundary of the Initial Nasca phase) which needs to be closed by ^{14}C-samples from future excavations. Three samples from Los Molinos, which Görsdorf and Reindel (2002) used for a first approach to the Early Nasca phase, were also included in our Paracas–Nasca chronology model (analysis numbers ERL-*, Fig. 14.4). The transition between the Initial Nasca and Early Nasca phases could be determined well to 90 cal AD within the 2σ uncertainty margins.

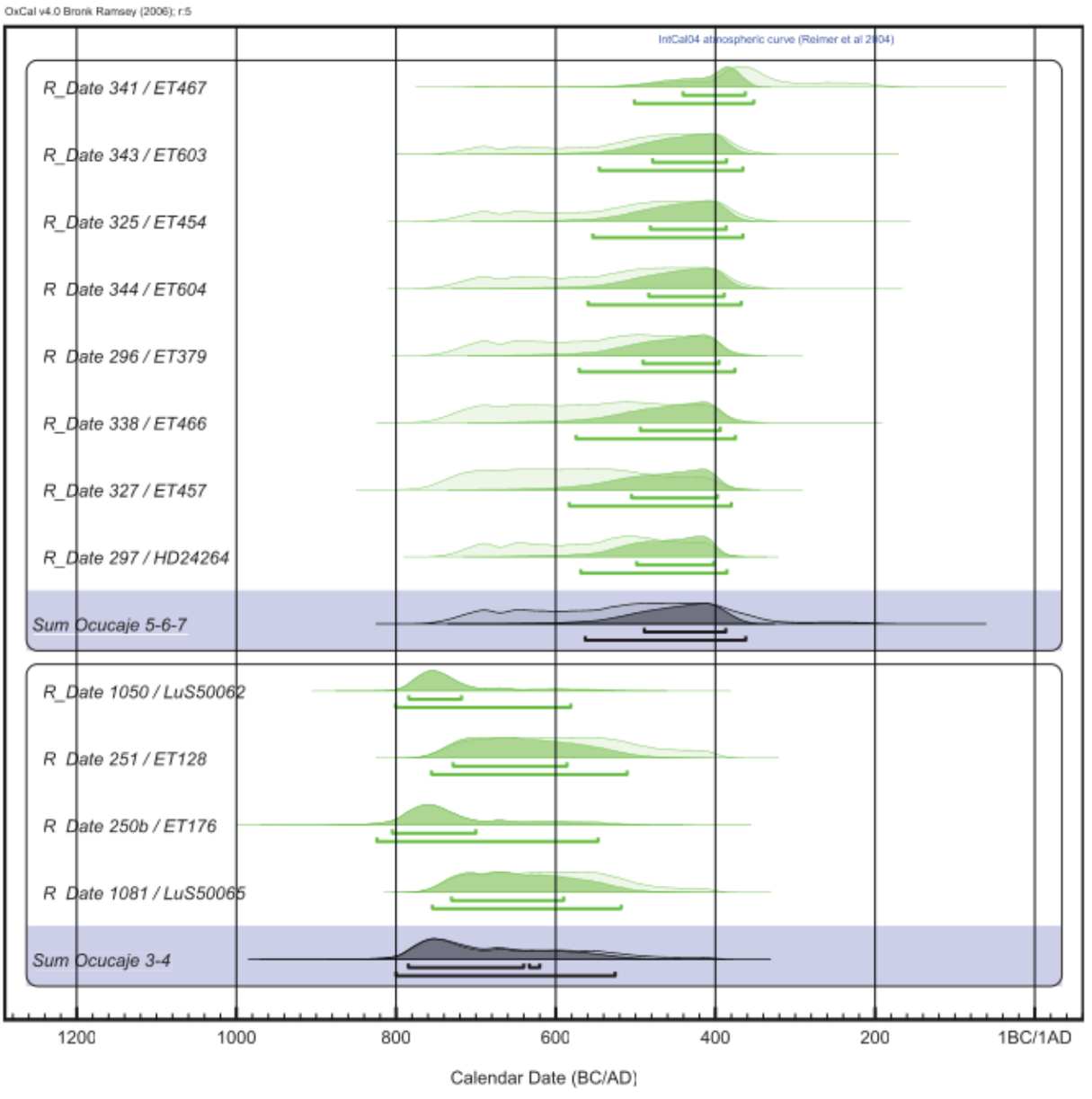

Fig. 14.2 The ^{14}C data of the 12 samples from the Early and Middle Paracas phases which were excavated in Pernil Alto, Jauranga, and Mollake Chico. All dates were calibrated with OxCal4 with respect to IntCal04 (Reimer et al. 2004), including a southern hemisphere correction of 41 ± 14 years (McCormac et al. 2002)

The Middle Nasca phase is very well dated (Fig. 14.4), based on 10 ^{14}C-samples from different excavation contexts defining the time span between 325 and 440 cal AD (2σ). The definition of the lower boundary of the Middle Nasca phase especially has improved considerably since our previous chronology (Unkel et al. 2007b). Five ^{14}C-samples, two of them dated twice in two independent analyses (samples 90 and 139, Fig. 14.5), were used to determine the Late Nasca phase. Based on the style of the associated pottery in the archaeological context all samples were ascribed to the Nasca 7 ceramic phase. Thus far there are no ^{14}C-samples available from the Nasca 6 phase. Within the 2σ uncertainty limits there is no time gap left between Nasca 4/5 and Nasca 7 as it was described

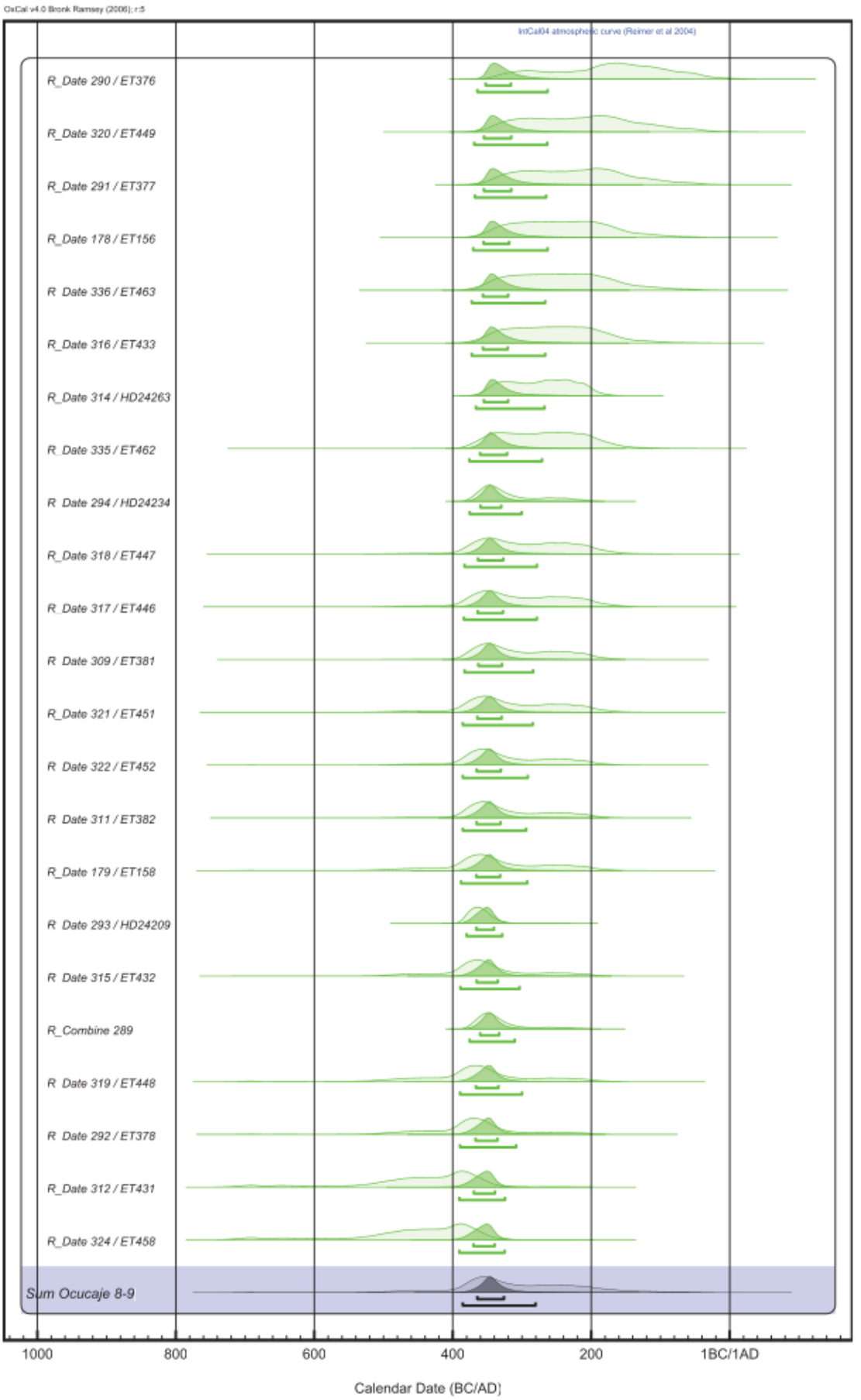

Fig. 14.3 The ^{14}C data of the 23 samples from the Late Paracas phase which were excavated in Jauranga and Pinchango Viejo. All dates were calibrated with OxCal4 with respect to IntCal04 (Reimer et al. 2004), including a southern hemisphere correction of 41 ± 14 years (McCormac et al. 2002)

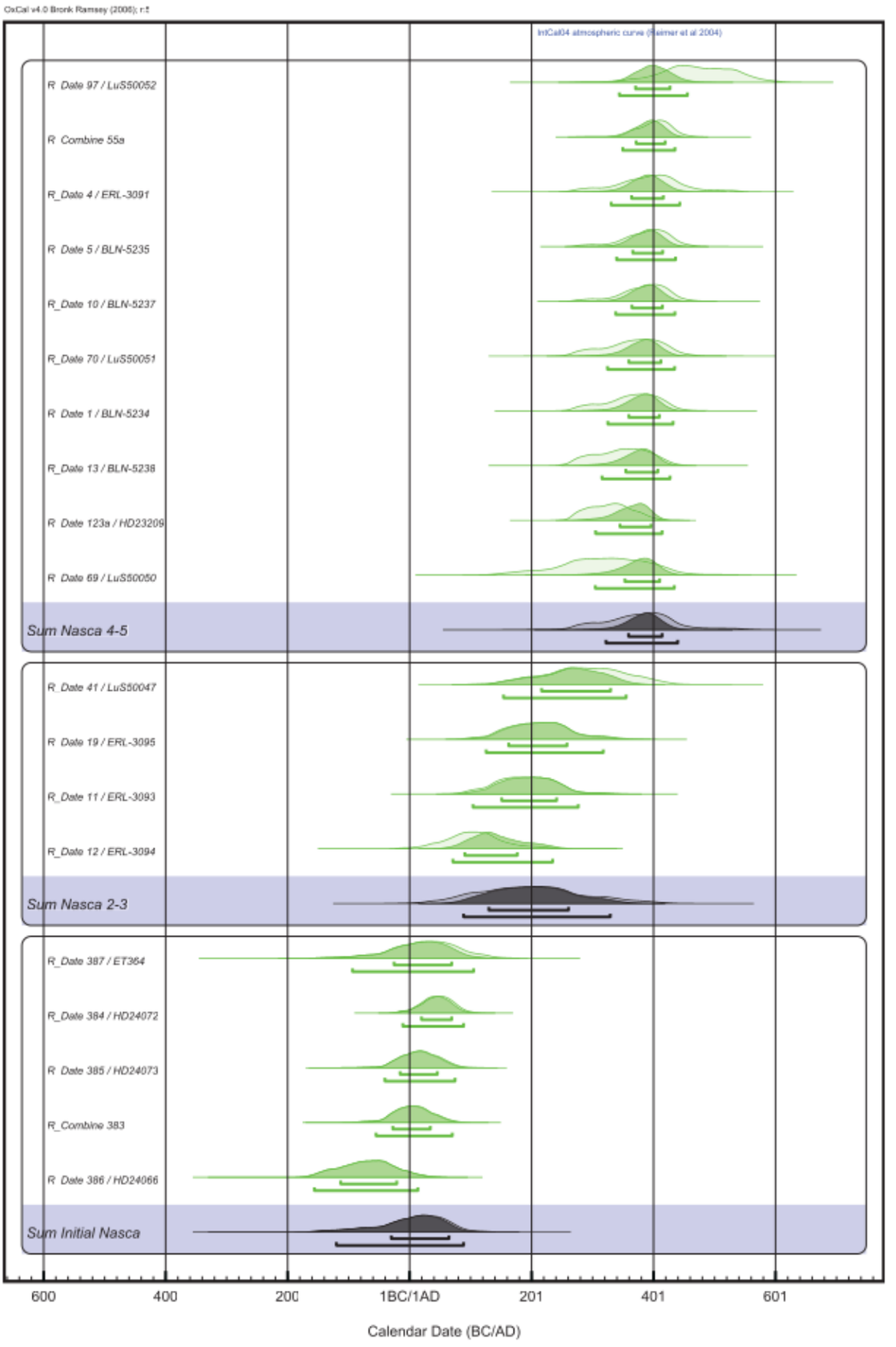

Fig. 14.4 The ^{14}C data of the 19 samples from the three phases Initial Nasca, Early, and Middle Nasca. The samples were excavated in several sites around Palpa (Estaquería, Los Molinos, La Muña, Jauranga, and Hanaq Pacha). All dates were calibrated with OxCal4 with respect to IntCal04 (Reimer et al. 2004), including a southern hemisphere correction of 41 ± 14 years (McCormac et al. 2002)

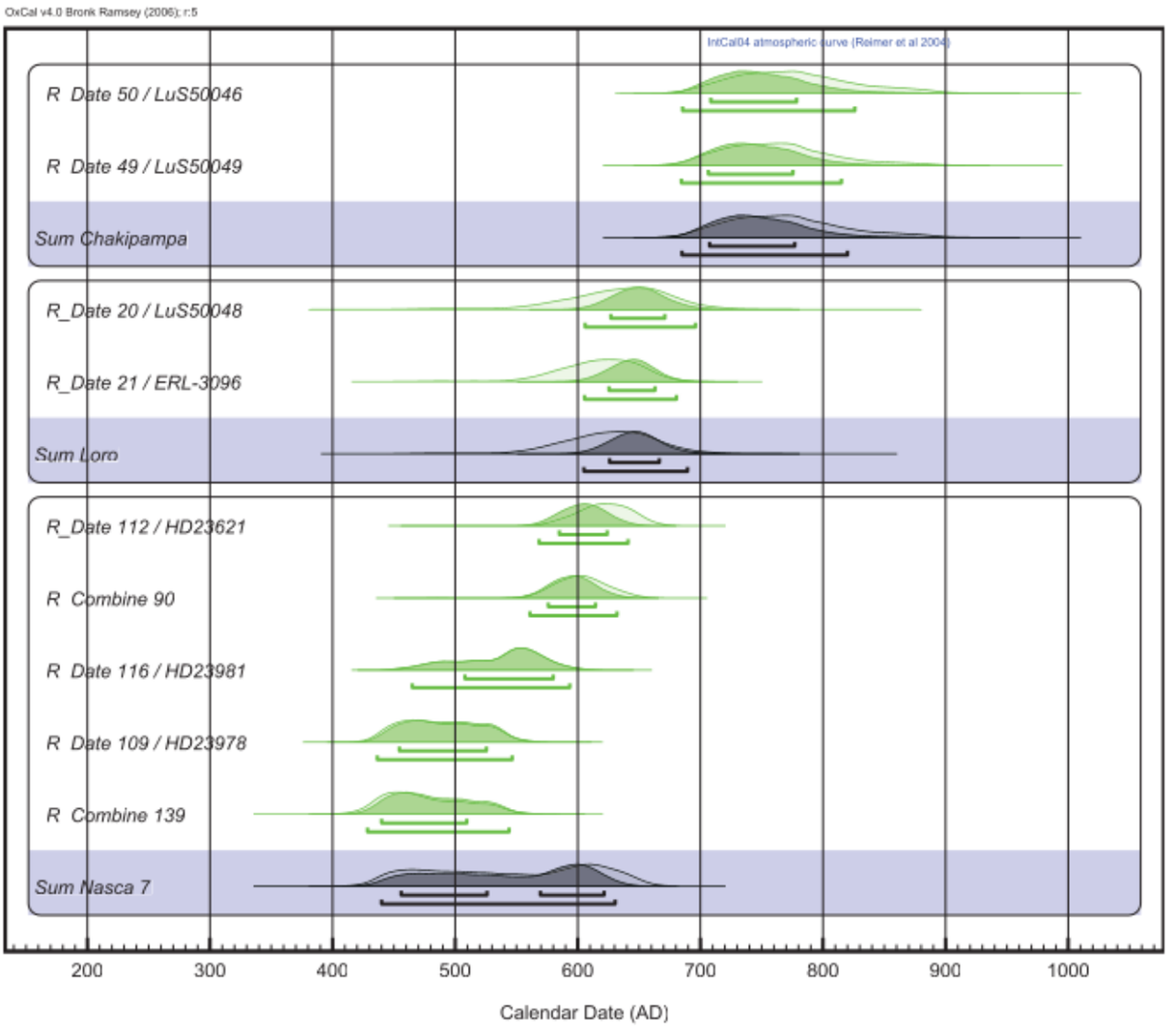

Fig. 14.5 The ^{14}C data of the nine samples from the Late Nasca phase and the Middle Horizon period which were excavated in Los Molinos and Parasmarca. All dates were calibrated with OxCal4 with respect to IntCal04 (Reimer et al. 2004), including a southern hemisphere correction of 41 ± 14 years (McCormac et al. 2002)

previously (Unkel et al. 2007b). Further archaeological investigations on the Nasca pottery will show if the definition of a Nasca 6 phase is still justified. The end of the Nasca period in our chronology is defined by two samples from the Loro phase at the beginning of the Middle Horizon to the time between 605 and 630 cal AD (Fig. 14.5). Two more samples from the Middle Horizon, which were ascribed to the Chakipampa phase due to their archaeological context, were dated to the time between 690 and 820 cal AD. Thus far they mark the end of a more or less continuous archaeological record in the Palpa area since the late Initial period, but further investigations are on their way (Figs. 14.6 and 14.7).

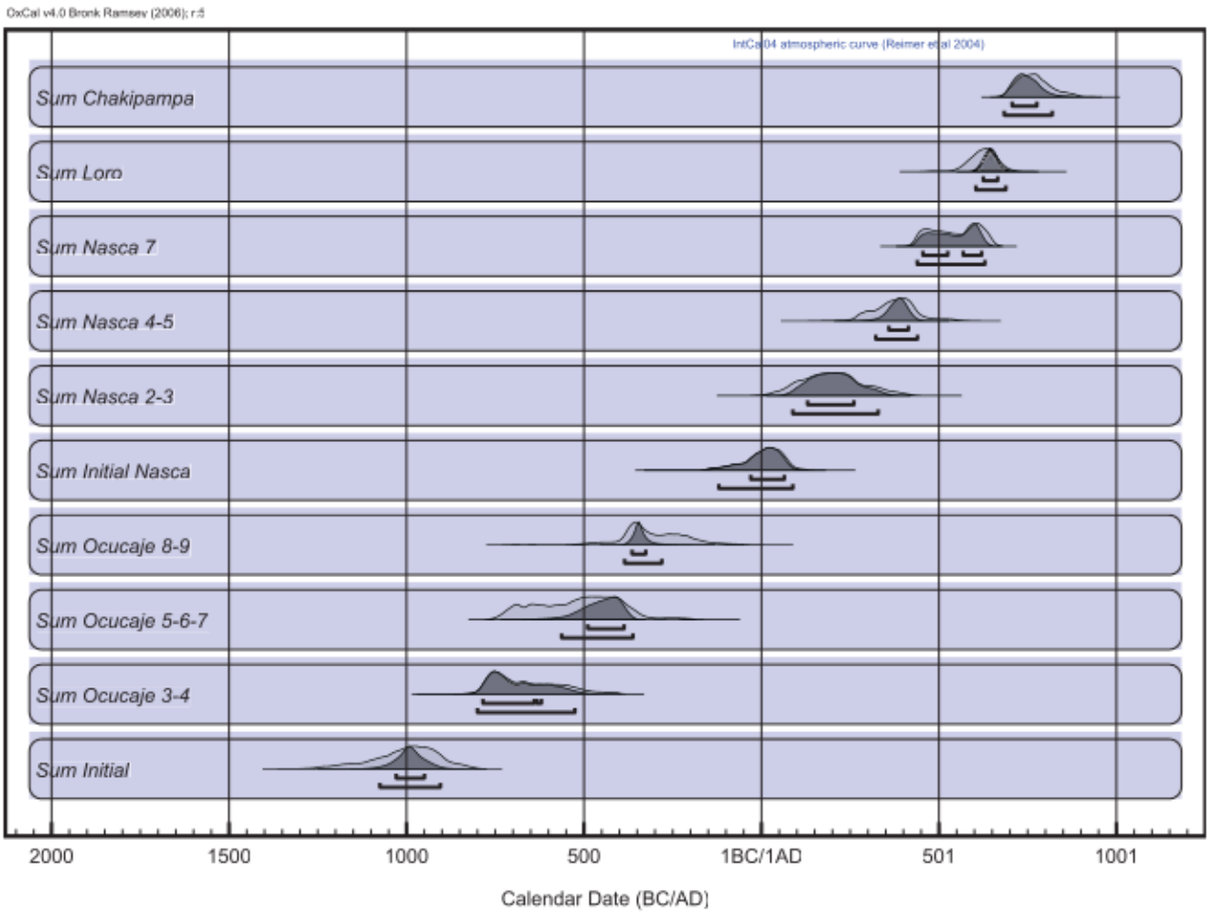

Fig. 14.6 Summary of the statistical distribution of the single phases as calculated with the software OxCal 4 (Bronk Ramsey 2001; 2008)

14.5 Conclusions

Around 120 ^{14}C-analyses give for the first time a solid numerical framework for the ceramic-derived periods of the pre-Columbian Paracas and Nasca cultures at the South Peruvian coast. The chronology model, which was developed during the NTG project (Unkel 2006) and which was refined and extended with the data presented here, can easily integrate new ^{14}C data from ongoing work and it can be adapted to new archaeological findings due to its open structure based on the Bayesian statistics of OxCal. The relative ceramic chronology of the Paracas (Wetter 2005) and Nasca (Reindel et al. 1999) was confirmed by our numerical data. Hence, we can now ascribe the Paracas period to the time between 800 and 280 cal BC and the Nasca period to the time between 90 and 630 cal AD, with a transitional Initial Nasca period in between.

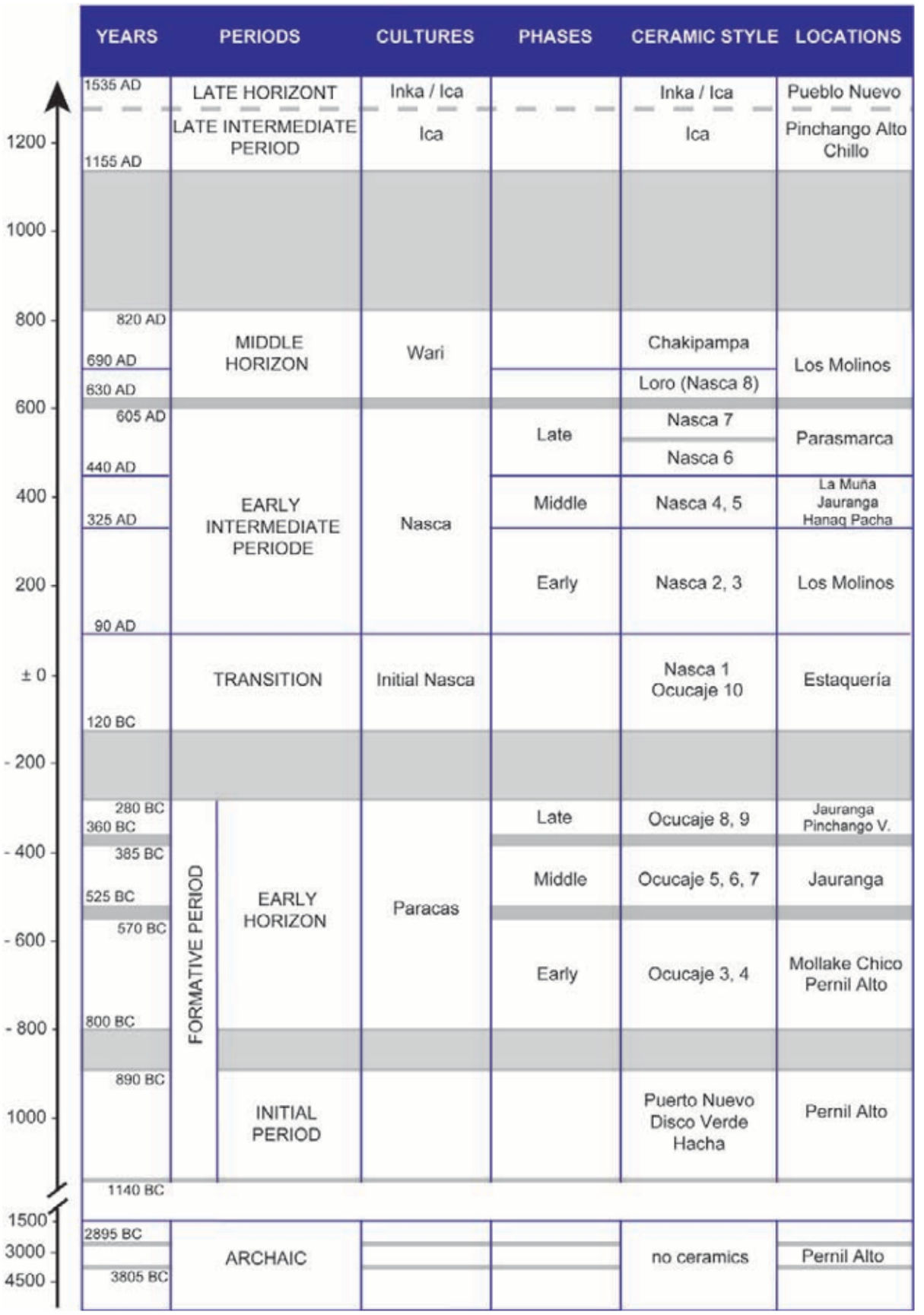

Fig. 14.7 Chronology of the Paracas and Nasca periods on the South Peruvian coast based on approximately 120 ^{14}C dated samples, which were derived from excavations yielding pottery in the Palpa region. Grey areas in the table mark transition zones between the single phases with an upper and a lower boundary. The pre-Paracas and post-Nasca periods were not examined in detail in this work and are therefore shown mainly for the temporal and cultural context

Acknowledgments For the AMS-^{14}C measurements we would like to express our sincere thanks to Georges Bonani, Irka Hajdas, Martin Suter, and Lukas Wacker (PSI/ETH Zürich, Switzerland) and to Göran Skog (Lund University, Sweden). We especially thank Heike Otten, Peter Siegle, and Angelika Wetter from the KAAK (Bonn, Germany) for their extraordinary help in supplying us with the archaeological contexts of the samples.

Chapter 15
Cold Light from the Sediments of a Hot Desert: How Luminescence Dating Sheds Light on the Landscape Development of the Northeastern Atacama

Annette Kadereit, Steffen Greilich, Clemens Woda and Günther A. Wagner

Abstract Optically stimulated luminescence (OSL) dating is essential to establish a chronometry for the reconstruction of the history of the landscape development in the Palpa-Nasca region. To achieve this, we apply both traditional techniques based on the preparation of disturbed samples and a novel, spatially resolved HR-OSL technique used for samples with their original mineral-grain structure (Greilich and Wagner, this volume). The new technique offers a great potential to access new types of sediment archives relevant to geomorphological and geoarchaeological studies.

15.1 Introduction

Mineral grains, such as common quartz and feldspar, are nonconductive solid-state bodies which contain crystal-lattice impurities. Considering their widespread occurrence at the earth's surface, this makes them ideal natural dosimeters. Through the impact of environmental radiation, *cold light* is generated inside the crystal lattice and stored, thus recording the time period, the minerals have been shielded from any external light influence. To put it another way: the quartz and feldspar grains store the time information as to when sediments were last exposed to (day)light. Therefore, many geological and geomorphological events are datable: surface processes of erosion and transportation, such as, for example, wind blowing sand and dust over a desert plain or rivers reworking sediments, which usually involve daylight exposure, are followed by processes of sediment deposition, such as dune and loess-cover accumulation or sandbar formation, which lead to the covering of the previously light-exposed mineral grains. The sediments of dunes and river sandbars as well as many other geomorphic forms are the archives geosciences

A. Kadereit (✉)
Luminescence Laboratory, Institute of Geography, University of Heidelberg, Im Neuenheimer Feld 348, 69120 Heidelberg, Germany
e-mail: annette.kadereit@geog.uni-heidelberg.de

M. Reindel, G.A. Wagner (eds.), *New Technologies for Archaeology*, Natural Science in Archaeology, DOI 10.1007/978-3-540-87438-6_15,
© Springer-Verlag Berlin Heidelberg 2009

use to reconstruct the history of a landscape. Luminescence dating is a tool to date the geoarchives and to establish a chronometric framework for the history of landscape development.

15.2 Methods

Unlike radiocarbon dating (Unkel and Kromer, this volume), the luminescence technique directly dates the sediments by measuring the cold-light emission from the quartz and feldspar mineral grains. The term *cold light* denotes luminescence (fluorescence, phosphorescence), which is emitted as radiating deactivation during the transition from an excited to the ground state and which is not blackbody radiation. Luminescence dating is based on a two-step process. (1) Excitation within the sedimentary archive is caused by ionizing radiation resulting from the decay of natural radionuclides such as ^{40}K and ^{87}Rb as well as from entire decay chains of the radioactive mother nuclides ^{235}U, ^{238}U, and ^{232}Th (Fig. 15.1). The released electrons and corresponding electron holes are caught at crystal defects (luminescence traps and centres), where they are stored over geologically relevant time scales. The longer the time span of excitation lasts, the more electrons are captured in the traps. The crystal is loaded like a battery. (2) Deactivation occurs when an energy supply from outside releases the electrons from the traps, which then recombine at hole centres, partly by radiating a measurable cold light (luminescence). The battery is discharged once again. As the strength of the light-emission correlates with the number of displaced electrons (battery charge), the last time of light exposure of a mineral grain may be determined by measuring the intensity of its latent luminescence signal. In the luminescence dating laboratory, intentional energy supply may be induced by optical stimulation, the method being called optically stimulated luminescence dating or OSL-dating. Basically, the process of radiating deactivation is the same, both in nature, when the mineral grain is exposed to daylight during the event to be dated, and in the laboratory, when the luminescence signal is deliberately read out for dating purposes. As the

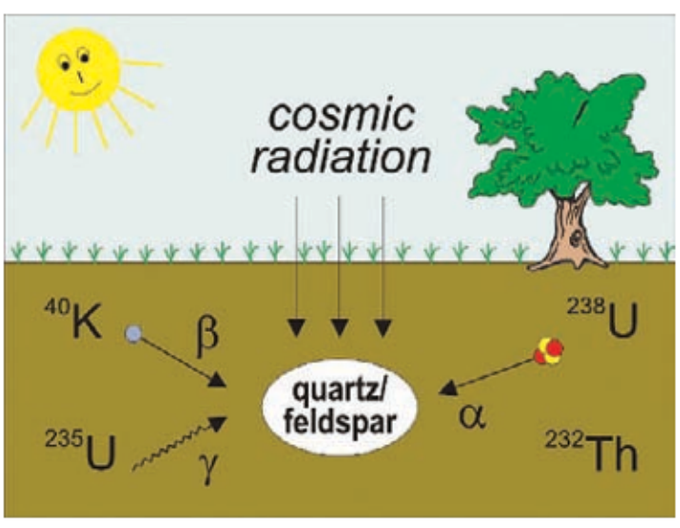

Fig. 15.1 Ionizing radiation from natural sources of radioactivity in a sediment archive

energy supply always discharges the battery, luminescence dating determines the last time of light exposure, even for sediments that have been reworked repeatedly during several cycles of erosion and accumulation. If, however, bleaching is incomplete, that is, the battery has not been completely discharged, the size of a newly grown latent luminescence signal will not correspond to the dose deposited in the mineral grain by ionizing radiation since the dating event, but the signal will overestimate its amount, resulting in age overestimation.

When in luminescence dating quartz and feldspar are used as natural dosimeters, apart from the dose represented by the latent luminescence signal also the dose-rate, that is, the dose per unit time, must be determined in order to calculate an age:

$$\text{age[ka]} = \text{dose[Gy]}/\text{dose rate[Gy/ka]},$$

whereby ka = 1000 years and Gy = Joule per kilogram.

15.3 Luminescence Dating of Sediments

Sediment dating with luminescence techniques usually implies the preparation of mineral separates with well-defined grain-size fractions: either fine-grain (here: 4–11 μm) or coarse-grain (here: 125–212 μm). The reason is the effective range of the ionizing radiation within a sediment body, which is ~20 μm for α-radiation, ~2 mm for β-radiation, and ~30 cm for γ-radiation. Fine-grain material is completely penetrated by all three types of radiation. Coarse-grain material is big enough to eliminate the outer rim of a grain reached by external α-radiation (e.g., by etching in hydrofluoric acid), but still small enough for calculable dose deposition by external β-radiation and, of course, γ-radiation.

Usually, OSL-dating is carried out on commercially available luminescence readers, which allow automated dose measurements (including optical stimulation, irradiation, and preheat; see below) of up to 48 aliquots (subsamples) in one go. The luminescence readers are equipped with a photomultiplier tube which detects the bulk signal of a subsample. As photomultipliers cannot discriminate the luminescence signals from different grains of an aliquot, it does not matter that disturbed samples are measured, which are the outcome of traditional sample preparation (see below). Disturbed-sample measurement versus undisturbed-sample measurement and undiscriminating bulk-signal detection versus spatially resolved luminescence-signal measurements are the principal differences between the traditional proceeding and a novel technique newly developed within the BMBF project network for the dating of archaeological structures (Greilich and Wagner, this volume). In the present contribution, we show the great potential of the new technique to access also natural sediment archives in order to promote the reconstruction of landscape development.

Until measuring, samples have to be handled very carefully to avoid any light contamination, which would delete (or reduce) the latent luminescence signal. Most samples were taken in light-tight steel cylinders (Ø 6 cm) and the outer light-influenced rim was removed in the dark luminescence laboratory (~1 cm). At the locality of La Muña the wall of an excavated trench was cleaned and sampling positions were prepared during daytime, whereas samples were taken at night under red light (8 LEDs: 660 nm, 20 μW/cm^2) by collecting light-unaffected material in light-tight black bags. In the laboratory, samples are handled under extremely subdued red (Siemens LS5421-Q diodes covered by Hoya R62 glass filter) or green light (Nichia NSPG-500 diodes covered by 3 mm OG515 glass filter; only feldspar-containing fine grains).

15.3.1 Sample Preparation – The Traditional Way

Coarse grain (125–212 μm) is gained by wet sieving. Organic material and carbonate content are eliminated by repeated addition of hydrogen peroxide (10 and 30%) and acetic acid (20%). Quartz is derived by heavy-mineral separation in lithium polytungstate (densities ≥2.63 and ≤2.74 g/cm^3). The α-rim is etched off in hydrofluoric acid (40%), while occasionally stirring the fluid. To remove any residual fluorine compounds, the etched quartz separates are washed in HCl (10%) and demineralised H_2O. By sieving with a 90 mesh, a monomineral 90–170 μm fraction is gained for OSL dating. A restricted number of grains (here: 200–500) are mounted on steel cups (Ø~10 mm) using silicon spray for adhesion. The idea behind these so-called 'small' aliquots with a limited number of grains is that insufficiently bleached sediments may be recognised (Olley et al. 1998). If one takes respectively small subsamples (aliquots) from a badly bleached sediment, a scatter in dose values and ages is expected, with aliquots containing many insufficiently bleached grains delivering higher ages overestimating the dating event and aliquots with (mostly) well-bleached grains yielding (almost) correct ages (Fig. 15.2).

Grain-size enrichment of polymineral fine grains was done with a water-cooled centrifuge. Fine-grain aliquots were prepared by pipetting ~1.8 mg of the 4–11 μm fraction onto aluminium plates (Ø~10 mm). After drying, the polymineral fine grains stick adhesively to the plates. As only feldspar but not quartz is stimulated by infrared, the feldspar component of polymineral fine grains may be selectively analyzed applying infrared stimulated luminescence (IRSL).

15.3.2 OSL Measurements – The Conventional Technique

For OSL dating the luminescence signal of a natural sample is compared to the strength of luminescence signals produced by the ionizing radiation of calibrated

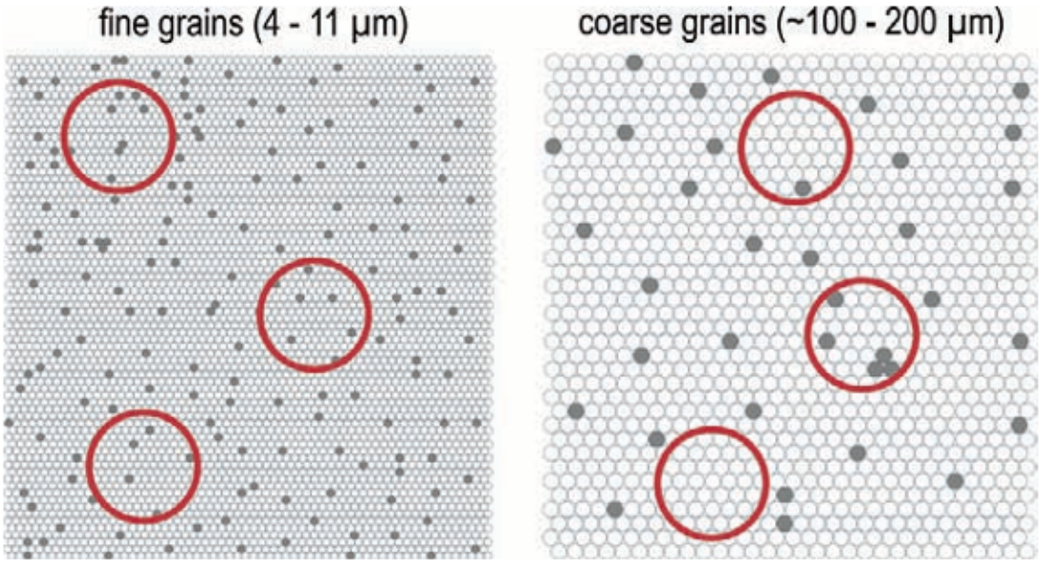

Fig. 15.2 Aliquots from insufficiently bleached coarse grains (*right*) and fine grains (*left*). Insufficiently bleached grains have a gray colour, well-bleached grains possess a white filling. From coarse grains, small aliquots (*red circles*) may be prepared. If the mixing with insufficiently bleached grains is not too high, the different aliquots show a scatter in dose and age. Aliquots with the lowest ages are supposed to give the least overestimated, and therefore probably the correct ages. The number of grains per fine grain aliquot (several tens of thousands of grains) cannot be reduced effectively enough (few tens to few hundreds), to allow the same procedures as with coarse-grain analyses. Aliquots will always contain plenty of insufficiently bleached grains homogenizing the measuring results so that no scatter will be visible

laboratory sources for α-irradiation (here: ^{241}Am-sources, Littlemore Alpha Irradiation Facility Type 721: ~4.2 Gy/min), and for β-irradiation (here: ^{90}Sr/^{90}Y-sources, Risø DA15: ~5.1 Gy/min and Littlemore Automatic beta irradiation facility Type 733: ~9.2 Gy/min). Natural samples may be irradiated either additionally to their natural latent luminescence signal (additive technique, Fig. 15.3a) or – if the natural signal is artificially bleached – the luminescence signal may be regenerated from zero by laboratory irradiation (regenerative technique, Fig. 15.3b). A model function (most often a saturating exponential), describing the relation between the dose and the luminescence signal, is then fitted to the dataset. From this function the dose that generates an artificial luminescence signal which is equal in size to the natural luminescence signal of the sample is derived (equivalent dose, D_E) (Fig. 15.3). Effective dose deposition of β-radiation is equal to that of γ-radiation. As the effect of α-radiation is approximately only one tenth of the former two types of radiation, so-called a-values (sensitivity ratio of α-radiation compared to β- or γ-radiation) have to be determined for fine grains, by establishing and comparing growth curves both by α- and β-irradiation.

We applied the additive technique to polymineral fine grains, using a multiple-aliquot protocol, which means that for each dose point several aliquots were used (Fig. 15.3a). After laboratory irradiation samples were stored at room temperature in the dark for at least one month. Prior to IR-stimulation for 60 s at room temperature, samples were preheated for 120 s at 220°C to empty any electrons from shallow unstable traps. We filtered the blue feldspar emission

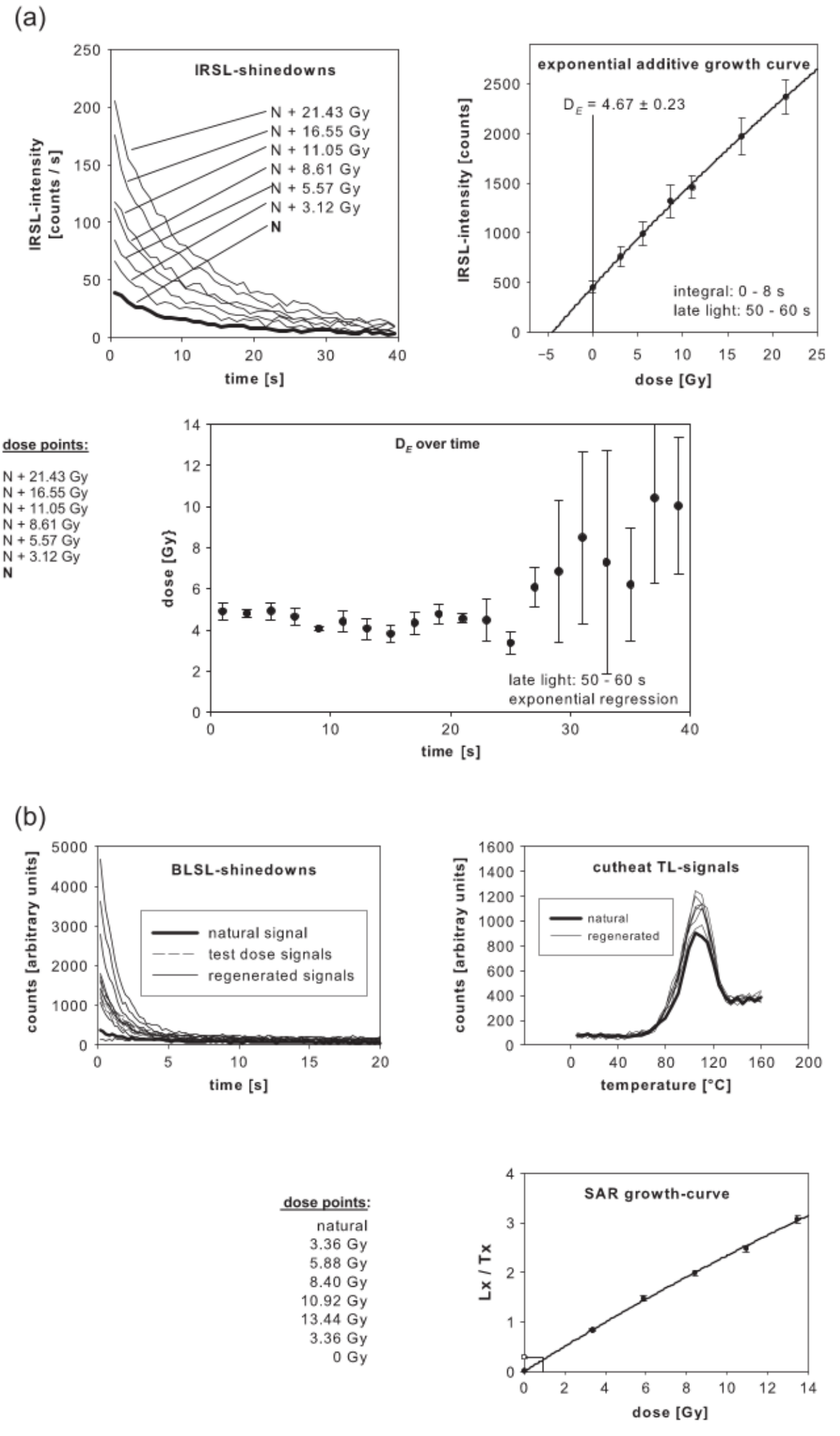

Fig. 15.3 (Continued)

(410 nm) with a set of Schott glass filters (BG39, BG3, BG39, OG400, 3 mm each; Krbetschek et al. 1996). The technique is an infrared-stimulated luminescence (blue detection) multiple-aliquot additive (IRSL-blue MAA) protocol. From each sample a set of aliquots was shelved for an additional two months after irradiation (total storage time: three months or more) to check if the blue feldspar IRSL is a stable signal, which fully stores a gained dose over time, or if anomalous signal fading (Wintle 1973) is detected, which would mean that a sample supplies only minimum ages. For D_E-determination an early integral of 0–8 s to 0–24 s was selected, and the integral 50–60 s was chosen for late-light subtraction (Aitken and Xie 1992).

The regenerative technique was used for coarse-grain quartz, applying the single-aliquot regenerative (SAR) protocol of Murray and Wintle (2000) (Fig. 15.3b). Single aliquot (SA) means that all measurements are carried out on one aliquot (here 'small aliquots'; see above), starting with the readout of the natural signal, and then building up the growth curve with regenerated dose points, including a zero dose point as well as a twice administered and measured regeneration dose point to check for accuracy. As bleaching (regeneration) leads to sensitivity changes of a sample, with SAR measurements these have to be corrected by intercalated normalisation doses (or test doses) that are administered after each dose point, starting with a first normalisation dose after the natural dose, which then is the basis of normalisation for all the following regeneration dose points. Thus, the SAR growth curve (Fig. 15.3b) is a fitting model corrected for sensitivity changes occurring during the OSL measurement procedures.

In the present study, optical stimulation was carried out with blue light (BLSL) for 20 s at 125°C. Preheat prior to BLSL was 10 s at 260°C, and cutheat (i.e., preheat during normalisation measurement subcycles) was 10 s at 260°C (La Muña) or 10 s at 160°C (other samples). The UV-quartz emission was detected through a set of three filters U340 (Hoya, 3 mm each). For D_E-determination the early interval 0–0.2 s (La Muña) or 0–0.4 s (other samples) was considered, and the late interval 16–20 s was used for late-light subtraction. The technique is a quartz coarse grain BLSL-UV 'small aliquot' SAR protocol. For further details of the applied protocols see Unkel et al. (2007).

OSL measurements were conducted on two luminescence readers. Fine grains were measured on a Risø TL/OSL DA12 (24 sample positions) equipped with a ring of TEMT484 diodes (emission at 880 Δ 80 nm; strength ~40 mW/cm^2) for IRSL applications and a photomultiplier tube EMI9235. Quartz coarse grains were measured on a Risø TL/OSL DA15 (48 sample positions),

Fig. 15.3 (Continued) (**a**) Example of IRSL fine-grain dating with a multiple aliquot additive (MAA) protocol. MAA protocol applied to polymineral fine grains of debris-flow sample HDS-967 from La Muña. The D_E-value ~4.7 Gy give an age of ~1.1 ka. Comparison with BLSL- and ^{14}C-ages gives evidence of age-overestimation. (**b**) Example of BLSL quartz coarse-grain dating with a single aliquot regeneration (SAR) protocol. BLSL SAR protocol applied to fluvial sample HDS-1333 from Huayuri

equipped with a ring of NISHIA NSPB-500 LEDs (470 Δ 20 nm) plus a Schott GG-420 edge filter for BLSL measurements and a photomultiplier tube EMI9235QA. Both photomultipliers have a detection maximum in the blue range.

15.3.3 A Novel Way of OSL Sample Preparation and Measurement

Traditional ways of luminescence measurements do not allow the dating of larger grain-size fractions such as pebbles and boulders, which makes various kinds of sediment archives inaccessible for OSL dating. Furthermore, it could be beneficial – especially for possibly heterogeneously (insufficiently) bleached sandy sediments – to preserve and measure the undisturbed structure of a sample. This would allow evaluating whether mineral grains delivering low doses were actually better bleached at the dating event, or whether in postdepositional time they rather yielded lower doses due to microscale dose-rate heterogeneities of the sedimentary environment. Therefore we scrutinised the potential of a novel spatially resolved luminescence technique for the dating of sediment archives. The new technique was developed with the financial support of the BMBF priority programme NTG (for details see Greilich and Wagner, this volume).

The new technique provides high-resolution detection of the luminescence signal of a subsample by means of a liquid-nitrogen cooled CCD camera chip (Princeton Optics) with a maximum resolution of 25 × 25 μm per pixel, thus discriminating up to ~5600 pixels of an aliquot ~10 mm in diameter, instead of collecting one single bulk signal of a subsample by means of a photomultiplier tube. In the present chapter we transferred and extended the novel technique from archaeological stone objects (such as the Palpa–Nasca geoglyphs) to geomorphic archives of the Palpa–Nasca area. This we did in two different ways: by sampling stones and boulders big enough to take drilling cores from (Ø 8 mm), and by sampling sandy material, which prior to drilling 8 mm cores was cast into epoxy resin.

Field-sampling of the sandy sediment occurred in the usual way with light-tight steel cylinders. Resination of the sediments was done using standard procedures by a commercial laboratory producing thin-sections of soils and sediments (Laboratory Thomas Beckmann, Schwülper-Lagesbüttel, Germany).

Adequate boulders, possibly with well-developed feldspar blasts and little to no weathering patina, may be selected during daytime from natural, but additionally cut-back and cleaned exposures or from artificially cut profile walls. The visibly exposed parts of the boulder surfaces are best sprayed with black colour in order to clearly mark the light-influenced surface parts, before the stone is collected at night-time, possibly with a torch with an adequate light-emission wavelenth (see above) and is tightly wrapped in aluminium foil and sealed in black plastic bags. This way, the blackened parts of the boulders may be avoided during drill-hole sampling later in the laboratory and only the rear, light-shielded sides are considered for OSL dating.

At the locality of Jaime we wanted to date stones contained in fine-grained loessic material. As the stones were too small to preserve a large enough surface that was not light-influenced, when the stones are selected individually from a profile-wall, we collected five rather big steel cylinders (Ø~10 cm, ~12 cm long) of the loessic material in order to gain as many of the incorporated stones as possible.

We gained drilling cores using a water-cooled diamond-studded drill bit. Drilling cores from stones, of which the surface side was used for OSL measurements, were usually ≤1 cm in length, whereas drilling cores of hardened sediments, from which unbleached material of the interior had to be gained, were 2.5–3 cm in length. The short drilling cores from the stones were ground from the back side to a thickness of ~2 mm. From the longer sediment cores two or three pieces, each ~5 mm in length, were broken off and ground to a thickness of ~2 mm. Grinding occurred only from one side, and the other side with the undamaged sediment grains was taken as an internal sediment surface for luminescence dating. Aliquots were placed and fixed in the sample holders as described by Greilich (2004) with their natural, that is, unground sides facing upwards for OSL analyses.

D_E-determination is based on an IRSL SAR protocol. As with the presently available LasLUM-reader (for technical details see Greilich and Wagner, this volume) only OSL readout is possible, irradiation is carried out at an external $^{90}Sr/^{90}Y$ β-source (ELSEC Automatic Irradiator System Type 9022: ~3.6 Gy/min), and preheat and cutheat procedures are performed in an external oven for 150 s at 260°C. After heating and prior to OSL readout, the sample is cooled for 300 s at ~16°C on a water-cooled metal plate. Stimulation of the feldspar component occurs with an IR-laser diode (837 nm; ~15 mW/cm^2 at the sample).

For IRSL dating we used the relatively bright yellow feldspar emission. Detection of the ~560 nm emission occurred through a set of Schott glass filters of GG475 and BG39, each 3 mm thick (Greilich 2004). For detection of the luminescence signal on the CCD camera chip we used a resolution of 100 μm (bins of 4 × 4 pixels). IR stimulation was done over 900 s, and data collection occurred in 15 consecutive frames of 60 s each. Data analysis was done with the program *AgesGalore* (Greilich et al. 2006). The HR-OSL measurements delivered spatially resolved images of the yellow feldspar IRSL signal (see Fig. 15.11, right). Feldspar grains adequate for D_E-determination are recognised as clusters of adjacent pixels with comparatively bright IRSL signals, which may be denoted as regions of interest (ROIs). The first frame (1–60 s) of such ROIs was used for D_E-determination, whereas the last frame (841–900 s) was considered for late-light subtraction (Aitken and Xie 1992).

The SAR protocol was applied with usually five regeneration dose points bracketing the natural signal, before repeating the lowest dose to test the recycling ratio and finally measuring a zero-dose point (see Fig. 15.11, left). Depending on the strength of the luminescence signal and the expected palaeodose of a sample, test doses of ~1.8, 6, or 18 Gy were administered, which is mostly <50% of the measured palaeodose (Table 15.1).

Table 15.1 Determination of palaeodoses, recycling ratios, and fading ratios

Sample	Aliquot	Test Dose		ROIs			D_E	Recycling Ratio	Fading	
	[#]	Absolut [Gy]	% of Natural in ROI [%]	ROI [#]	Counts per Area	Areas in ROI	[Gy]	[Δ]	Fading ratio [Δ]	Storage [Days]
Jaime-1 HDS-1473a	1	1.8	48.7	ROI-1	>200	14	3.70± 0.14	1.11± 0.25	0.83± 0.19	46
Jaime-1 HDS-1473a	1	1.8	132.1	ROI-2	>200	6	1.36± 0.08	1.17± 0.05	0.61± 0.05	46
Jaime-2 HDS-1473b	1	6	16.5	ROI-1	>1000	32	36.32 ± 0.45	1.00 ± 0.11	0.61 ± 0.04	40
Jaime-2 HDS-1473b	1	6	16.0	ROI-2	>1000	5	37.44 ± 1.24	1.03 ± 0.07	0.65 ± 0.02	40
Jaime-4 HDS-1473c	1	6	20.6	ROI-1	>4000	12	29.06 ± 0.29	1.14 ± 0.05	0.90 ± 0.01	39
Jaime-4 HDS-1473c	1	6	23.3	ROI-2	>4000	9	25.78 ± 0.26	1.19 ± 0.04	0.91 ± 0.02	39
Jaime-4 HDS-1473c	1	6	22.6	ROI-3	>4000	30	26.57 ± 0.15	1.15 ± 0.04	0.85 ± 0.04	39
Jaime-7 HDS-1475a	1	6	21.5	ROI-1	>260	[5]	27.85 ± 1.31	1.18 ± 0.21	0.23 ± 0.07	38
Jaime-9 HDS-1475b	1	6	43.3	ROI-1	>220	51	13.87 ± 0.48	1.13 ± 0.29	– –	33
Jaime-10 HDS-1476a	1	18	58.6	ROI-1	>6000	100	30.73 ± 0.04	1.10 ± 0.02	0.79 ± 0.03	25
Jaime-10 HDS-1476a	1	18	46.9	ROI-2	>6000	8	38.39 ± 0.23	1.07 ± 0.03	0.78 ± 0.01	25
Jaime-10 HDS-1476a	1	18	61.0	ROI-3	>6000	14	29.51 ± 0.12	1.11 ± 0.02	0.83 ± 0.01	25
Jaime-10 HDS-1476a	1	18	68.5	ROI-4	>6000	4	26.27 ± 0.24	1.07 ± 0.02	0.83 ± 0.01	25
Jaime-10 HDS-1476a	1	18	62.9	ROI-5	>6000	6	28.63 ± 0.16	1.10 ± 0.01	0.86 ± 0.01	25
Huyaco HDS-1478a	1	18	51.7	ROI-1	>500	34	34.80 ± 0.43	1.06 ± 0.12	1.03 ± 0.05	32
Huyaco HDS-1478a	1	18	49.7	ROI-2	>500	12	36.20 ± 0.82	1.06 ± 0.08	1.08 ± 0.05	32
Huyaco HDS-1478a	1	18	50.7	ROI-1	>400	59	35.51 ± 0.37	1.07 ± 0.11	1.05 ± 0.07	32
Huyaco HDS-1478a	1	18	47.9	ROI-2	>400	22	37.57 ± 0.68	1.08 ± 0.11	1.08 ± 0.05	32
Huyaco HDS-1478a	1	18	44.9	ROI-3	>400	15	40.12 ± 1.10	1.05 ± 0.10	1.13 ± 0.07	32
Huyaco HDS-1478a	1	18	51.3	ROI-4	>400	7	35.07 ± 1.23	0.58 ± 0.27	1.08 ± 0.04	32
Huyaco HDS-1478a	1	18	44.1	ROI-5	>400	15	40.81 ± 1.11	1.12 ± 0.12	1.06 ± 0.07	32
Huyaco HDS-1478a	1	18	43.1	ROI-6	>400	8	41.76 ± 2.07	1.15 ± 0.15	1.18 ± 0.03	32
Huyaco HDS-1478a	2	18	39.3	ROI-1	>400	20	45.75 ± 0.98	1.10 ± 0.09	0.96 ± 0.09	31

Table 15.1 (continued)

Sample	Aliquot	Test Dose		ROIs			D_E	Recycling Ratio	Fading	
	[#]	Absolut [Gy]	% of Natural in ROI [%]	ROI [#]	Counts per Area	Areas in ROI	[Gy]	[Δ]	Fading ratio [Δ]	Storage [Days]
Huyaco HDS-1478a	2	18	45.4	ROI-2	>400	13	39.67 ± 0.95	1.13 ± 0.16	0.98 ± 0.06	31
Huyaco HDS-1478a	4	18	45.2	ROI-1	>350	10	39.86 ± 1.32	1.05 ± 0.10	1.09 ± 0.09	26
Huyaco HDS-1478a	4	18	46.1	ROI-2	>350	6	39.04 ± 1.59	1.07 ± 0.07	1.03 ± 0.10	26
Huyaco HDS-1478a	4	18	52.4	ROI-3	>350	8	34.34 ± 1.26	1.16 ± 0.08	1.07 ± 0.05	26
Huyaco HDS-1478a	4	18	50.9	ROI-4	>350	8	35.35 ± 1.40	1.13 ± 0.10	1.11 ± 0.39	26
Fundo/OSL-6 HDS-1472	1	6	216.2	ROI-1	>250	12	2.78 ± 0.13	1.20 ± 0.16	0.85 ± 0.08	24
Fundo/OSL-6 HDS-1472	1	6	125.2	ROI-2	>250	28	4.79 ± 0.09	1.38 ± 0.24	0.34 ± 0.04	24

After finishing the prompt SAR measurements, the sample was administered the highest or second highest regeneration dose a second time, preheated and afterwards cooled in the usual way, and then stored for 3–6 weeks at room temperature in the dark for a test on possible anomalous fading of the feldspar signal. Prior to the delayed IRSL readout the stored sample was cooled again for 300 s at ~16°C and the cycle was accomplished with another test dose subcycle.

15.3.4 Dose-Rate Determination

For conventional sediment samples, dose-rate determination was carried out on the possibly light-influenced marginal material of the OSL samples and/or on additionally collected material from around the OSL sample position applying α- and β-counting and low-level γ-spectrometry (for details see Kadereit 2002).

Dose-rate calculation for the new dating technique follows the five-component model of Greilich and Wagner, this volume; see Fig. 16.8. Unless stated otherwise, dose-rate determination of the sediments embedding the dated stones is usually based on low-level γ-spectrometry. Concerning the dose rate of the dated stones, assumptions are made as listed in Table 15.2, which are partly based on analogues from representative stones of the area (Greilich et al. 2005). In case of the Jaime stone samples (Jaime-1, -2, -4, -7, and -8) potassium estimation is based on SEM-EDX measurements of a greater part of the surface of stone sample Jaime-10 (HDS-1476c). For closer analyses and OSL-age estimation of feldspar grains emitting a strong yellow luminescence signal (ROIs), analyses of chemical elements and especially potassium contents, important for evaluation of the internal β-dose-rate of a feldspar grain, were carried out for five selected aliquots by SEM-EDX (see Table 15.3: Jaime-1 aliquot-1, Jaime-10 aliquot-1, Huayco aliquot-1, Huayco aliquot-4, and Fundo/OSL-6 aliquot-1). The contribution of the cosmic component was calculated after Prescott and Hutton (1988, 1994) both for conventionally and for innovatively analyzed samples.

15.4 Chronometric Framework for the Landscape Development of the Northeastern Atacama

A detailed description of the history of landscape development in the Nasca–Palpa region is provided by Eitel and Mächtle (this volume). Here we present the results of the OSL dating of four different types of sediment archives we achieved by means of both the traditional and the novel luminescence dating techniques.

Table 15.2 Analyzed and assumed data for dose-rate determination

Sample	Depth b.g.l. [m]	Stone				Surrounding Sediment[1)]		
		Thickness [cm]	K [Weight-%]	U [μg/g]	Th [μg/g]	K [Weight-%]	U [μg/g]	Th [μg/g]
Jaime-1,- 2,-4 HDS-1473a/b/c	0.25	~0.75	[2)] 3.67 ± 0.50	[4)] 2.89 ± 0.09	10.29 ± 0.21	2.26 ± 0.09	3.40 ± 0.11	11.27 ± 0.34
Jaime-7,-8 HDS-1475a/b	0.25	~0.75	[2)] 3.67 ± 0.50	[4)] 2.89 ± 0.09	10.29 ± 0.21	2.27 ± 0.09	3.62 ± 0.11	11.59 ± 0.35
Jaime-10 HDS-1476c	0.25	~0.75	[2)] 3.67 ± 0.50	[4)] 2.89 ± 0.09	10.29 ± 0.21	2.49 ± 0.15	4.14 ± 0.17	12.54 ± 0.50
Huyaco HDS-1478a	0.45	~5.00	[3)] 3.25 ± 0.47	[5)] 3.37 ± 0.11	14.03 ± 0.27	0.70 ± 0.03	1.96 ± 0.08	5.33 ± 0.21
Fundo / OSL-6 HDS-1472	0.85	–	–	–	–	2.06 ± 0.10	2.70 ± 0.12	13.73 ± 0.49

[1)] Potassium, uranium, and thorium contents of surrounding sediments from low-level gamma spectrometry; preliminary results from measurements after less than four weeks of storage of the sealed sample.
[2)] Analyzed with SEM-EDX on ~ 4 mm^2 area of stone surface of sample Jaime-10 / HDS-1476c.
[3)] Weighted mean from two dioritic samples of the area (CL38AS1 and CL40AS1) (cf. Table 6 in Greilich et al. 2005).
[4)] After representative granitic sample from the area 12/4AS1 (cf. Table 6 in Greilich et al. 2005).
[5)] After representative dioritic sample from the area CL28 (cf. Table 6 in Greilich et al. 2005).

Table 15.3 OSL ages

Sample	Aliquot	ROIs	Cts/ Area	Diameter	D_E	ROIs SEM-EDX Spectrum[2)]	K[1)]	Effective Dose rate	Age
	[#]	[#]		[μm]	[Gy]	[#]	[Weight-%]	[Gy/ka]	[ka]
Jaime-1 HDS-1473a	1	ROI-1	>200	400	3.70 ± 0.14	[a]spec-2	min 0.22	3.77 ± 0.31	0.98 ± 0.09
						[a]spec-3	max 13.91	4.52 ± 0.31	0.82 ± 0.06
						[a]spec-4	0.73		
Jaime-1 HDS-1473a	1	ROI-2	>200	250	1.36 ± 0.08	[p]spec-8	2.94		
						[p]spec-9	min 0.91	3.91 ± 0.31	0.35 ± 0.03
						[a]spec-11	max 5.20	4.06 ± 0.23	0.34 ± 0.03
Jaime-10 HDS-1476a	1	ROI-1	>6000	1000	30.73 ± 0.04	[a]spec-1	0.84		
						[a]spec-2	0.61		
							mean 0.73	3.75 ± 0.40	8.21 ± 0.87
Jaime-10 HDS-1476a	1	ROI-2	>6000	300	38.39 ± 0.23	[a]spec-4	2.31	4.19 ± 0.34	9.16 ± 0.75
Jaime-10 HDS-1476a	1	ROI-3	>6000	400	29.51 ± 0.12	[a]spec-6	1.64	4.11 ± 0.34	7.18 ± 0.59
Jaime-10 HDS-1476a	1	ROI-4	>6000	200	26.27 ± 0.24	[a]spec-6	1.64	4.25 ± 0.36	6.18 ± 0.53
Jaime-10 HDS-1476a	1	ROI-5	>6000	300	28.63 ± 0.16	[a]spec-5	0.49	4.12 ± 0.35	6.96 ± 0.58
Huyaco HDS-1478a	1	ROI-1	>500	800	34.80 ± 0.43	[a]spec-2	0.40	2.71 ± 0.29	12.87 ± 1.36
Huyaco HDS-1478a	1	ROI-2	>500	350	36.20 ± 0.82	[a]spec-6	1.73	3.00 ± 0.26	12.07 ± 1.08
Huyaco HDS-1478a	1	ROI-1	>400	800	35.51 ± 0.37	[a]spec-2	0.40	2.71 ± 0.29	13.13 ± 1.39
Huyaco HDS-1478a	1	ROI-2	>400	350	37.57 ± 0.68	[a]spec-6	1.73	3.00 ± 0.26	12.52 ± 1.11
Huyaco	1	ROI-3	>400	450	40.12 ± 1.10	[a]spec-5	11.37	3.56 ± 0.27	11.29 ± 0.90

Table 15.3 (continued)

Sample	Aliquot	ROIs	Cts/ Area	Diameter	D_E	ROIs SEM-EDX Spectrum[2)]	K[1)]	Effective Dose rate	Age
	[#]	[#]		[μm]	[Gy]	[#]	[Weight-%]	[Gy/ka]	[ka]
HDS-1478a Huyaco	1	ROI-4	>400	250	35.07 ± 1.23	[p]spec-3	1.08		
HDS-1478a						[a]spec-4	0.76		
							mean 0.92	3.03 ± 0.26	11.59 ± 1.06
Huyaco HDS-1478a	1	ROI-5	>400	500	40.81 ± 1.11	[a]spec-7	9.89	3.51 ± 0.27	11.64 ± 0.94
Huyaco HDS-1478a	1	ROI-6	>400	400	41.76 ± 2.07	[a]spec-8	1.57	2.97 ± 0.26	14.06 ± 1.41
Huyaco HDS-1478a	4	ROI-1	>350	300	39.86 ± 1.32	[p]spec-4	0.56	2.98 ± 0.26	13.40 ± 1.23
Huyaco HDS-1478a	4	ROI-2	>350	300	39.04 ± 1.59	[a]spec-3	0.25	2.97 ± 0.26	13.17 ± 1.25
Huyaco HDS-1478a	4	ROI-3	>350	300	34.34 ± 1.26	[a]spec-2	2.04	3.04 ± 0.26	11.30 ± 1.05
Huyaco HDS-1478a	4	ROI-4	>350	300	35.35 ± 1.40	[a]spec-1	2.90	3.08 ± 0.26	11.50 ± 1.06
Fundo/ OSL-6	1	ROI-1	>250	600	2.78 ± 0.13	[p]spec-1	0.47		
HDS-1472						[a]spec-2	0.72		
						[a]spec-7	0.58		
							mean 0.59	3.53 ± 0.30	0.79 ± 0.08
Fundo/ OSL-6	1	ROI-2	>250	400	4.79 ± 0.09	[p]spec-3	0.00		
HDS-1472						[a]spec-4	0.04		
							mean 0.02	3.58 ± 0.29	1.34 ± 0.11

[1)] SEM-EDX, error for K ± 0.5 weight% for rough unpolished surfaces (personal communication by Dr. Hans-Peter Meyer, Mineralogisch-Petrologisches Institut, University of Heidelberg).

[2)] [a]spec-# = SEM-EDX spectrum data collected from area, [p]spec-# SEM-EDX spectrum data collected from point.

15.4.1 The State-of-the-Art Techniques

15.4.1.1 Holocene Loess Coverings

The eastern margin of the northern Atacama desert is characterised by widespread covers of loess, which is a fine-grained, silty, aeolian sediment. The desert dust was deposited during more humid times of the past, when nowadays hyperarid parts of the coastal desert were regularly influenced by moisture supplied by monsoon rain intruding on the Nasca–Palpa area from the Amazon basin via the high Altiplano and the western Cordillera. A then denser vegetation cover combed the dust from the air associated with the southerly winds blowing over the bare desert area. The Bolivian High is a steering element transporting moisture on its northern rim westward over the Andean crest. The dynamic high-pressure cell is most intense at times when the South American summer monsoon (SASM) is well developed and then leads to above-average moisture transport from its source area over the Atlantic Ocean to the Andean region.

Nowadays, this condition occurs during high index, respectively, cold phases (La Niña phases) of the El-Niño–Southern-Oscillation (ENSO). La Niña-like ENSO high index/cold phases of strengthened South American Summer Monsoon (SASM) imply an enhanced moisture advection from the Atlantic ocean, increased convection and rain-water recycling in the Amazon basin area, the evolution of a strong and southerly displaced Bolivian High, the advective assistance of higher-tropospheric zonal easterly winds, and thus more moisture transport from the continental source area to the area of the eastern Atacama desert margin (e.g. Garreaud et al. 2003, Zhou & Lau 1998). Principally, the modern day scenario of mechanisms must have also worked in the past (Vuille 1999). At times, when ENSO is weakly developed (El Niño phase) the Bolivian High is barely formed, which means that less moisture transport from the Atlantic source region combines with less possibly moisture-transporting easterlies into the study area. However, during the basically drier periods, El Niño-driven rainfall events may cause runoff and landslide events, which apart from northern Peru may affect coastal regions in southern Peru south of the Nasca–Palpa area. We think that the moister periods at the eastern desert margin were periods of on average more La Niña-like conditions. To get an idea when today's hyperarid northern Atacama experienced moister conditions at its eastern margin, loess deposits were analysed by OSL dating techniques. The dominantly silty sediments were dated applying an IR-stimulated MAA protocol to the blue emission from the feldspar component of extracted polymineral fine grains.

Sixteen samples from 14 localities have been analysed (Fig. 15.4). At two locations the thickness of the cover bed allowed us to take two samples, one above the other (HDS-1359/60, HDS-1363/64). In both cases the upper sample yielded ages ~4.2 ka, whereas the samples from the base gave dates ~9.8 ka. In Fig. 15.5 the IRSL ages are presented as a cumulative probability distribution. It seems that during the Holocene, humid periods of loess accumulation around 9.9, 7.3, 4.2, and perhaps 2.7 ka (only one sample) alternated with drought periods of no loess sedimentation around 8.6, 5.3, and 3.2 ka. These findings are consistent with

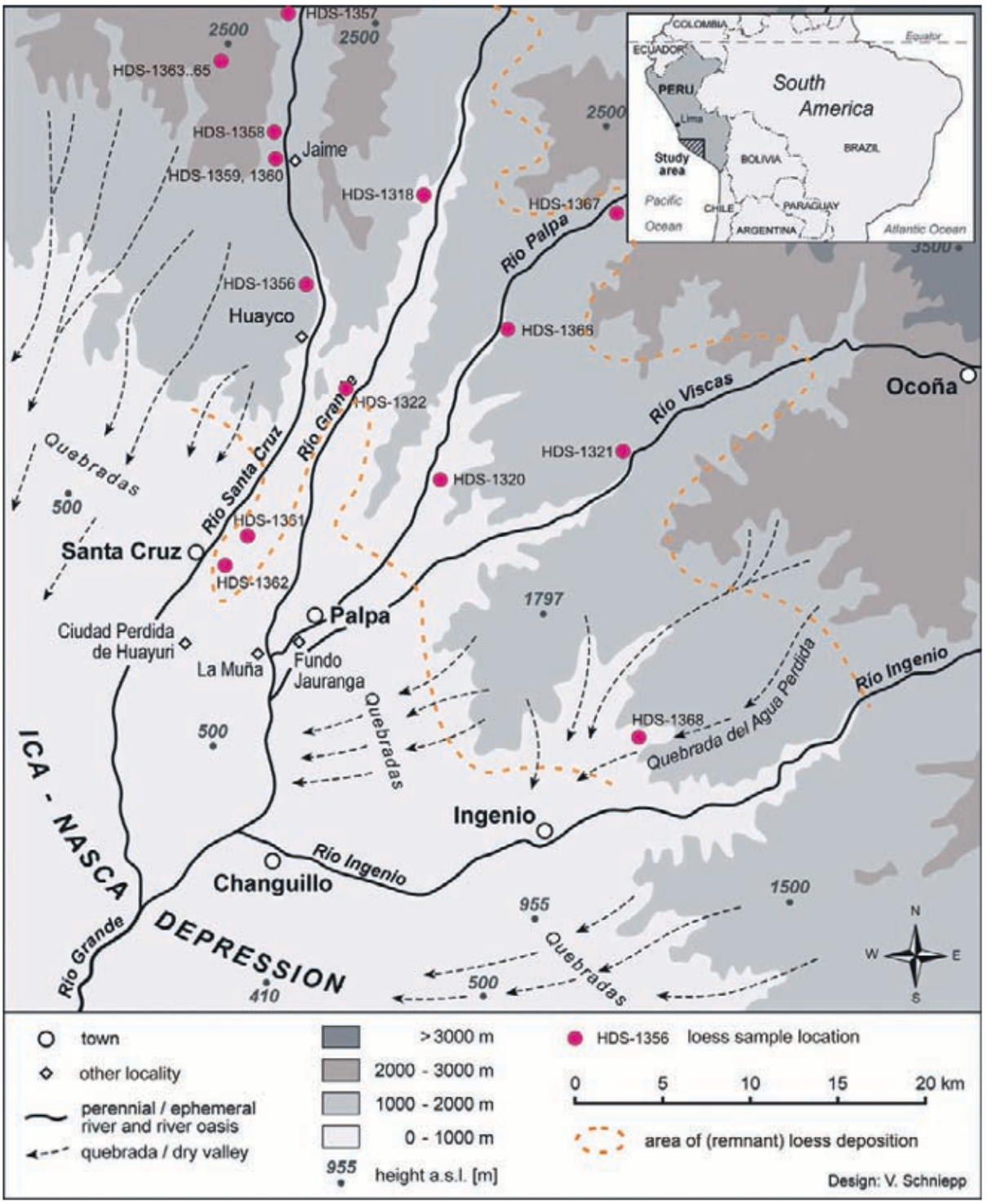

Fig. 15.4 The Nasca–Palpa study area with sampling sites Jaime, Huayco, and Fundo Jauranga and with sampling sites for loess dating (after Eitel et al. 2005)

observations of shifts of the eastern desert margin farther south in Chile (22–23 °S), where changes of SASM have been derived from ^{14}C-dated midden analysed for their content of pollen from grass and herbaceous species (Latorre et al. 2003).

Interestingly, in the middle to younger Holocene intervals of apparently increased SASM influence (La Niña-like situation) alternate with periods of El Niño-borne debris flow (huayco) deposits in southern Peru. Debris flow dating was performed using ^{14}C-dating on terrestrial material (mostly intercalated between huayco units). The youngest historical huaycos date after 3.5 ka

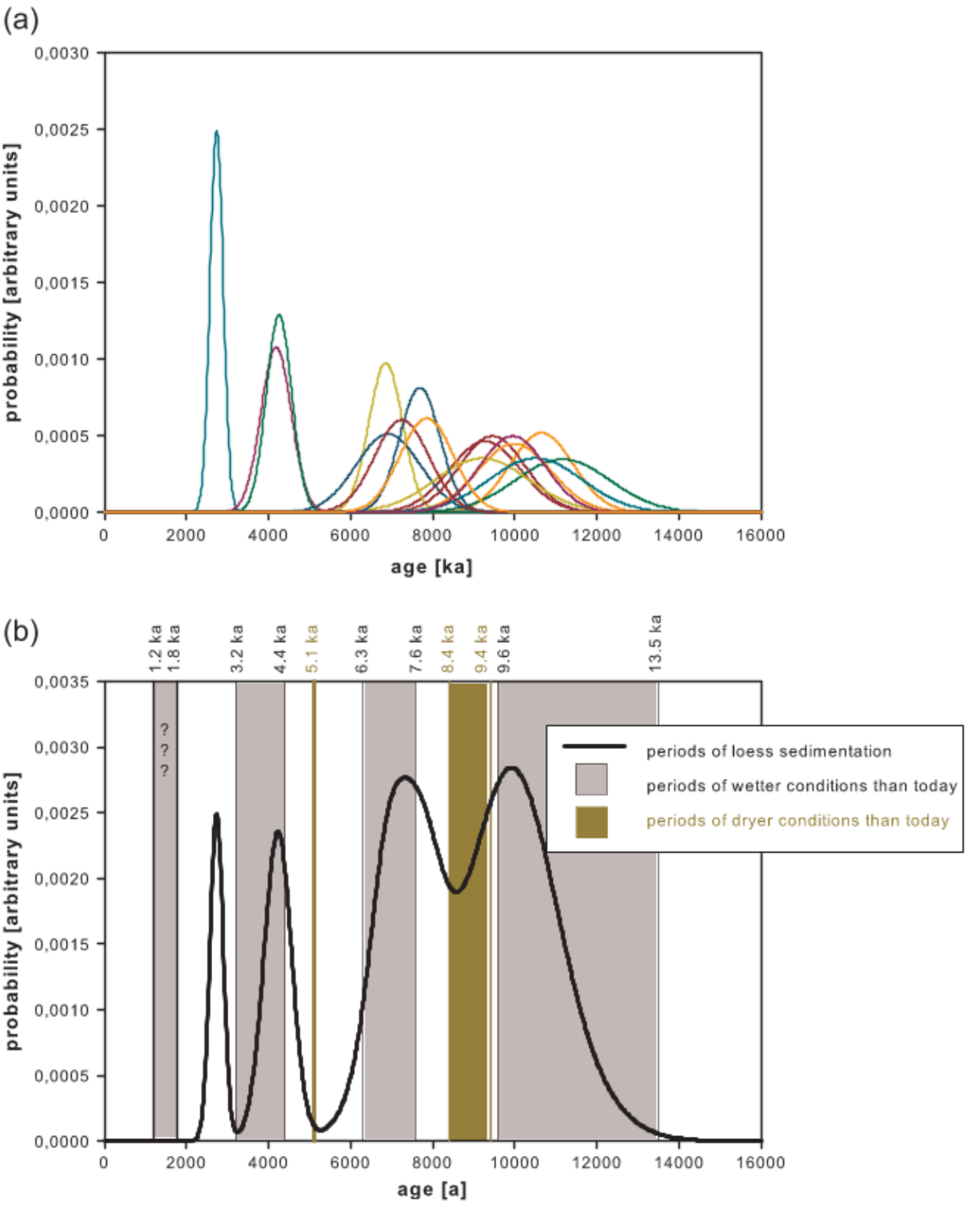

Fig. 15.5 IRSL fine-grain ages of the blue emission of 16 loess samples. (**a**) Probability distribution of individual samples; (**b**) summed probability distribution and periods of drier and wetter conditions than today as derived by Latorre et al. (2003) from pollen analyses of ^{14}C-dated midden from the eastern margin of the Atacama desert 22–23°S

at Quebrada Los Burros, after ~3.8 ka at Punta el Abogado, and between ~3.0 and ~4.2 ka at Quebrada Jara, which all might correspond to the dry period ~3.2 ka. The next older deposits date between ~6.3 and 5.0 ka at Quebrada Los Burros and ~5.1 ka at Quebrada Tacahuay, which all correspond to the dry period ~5.3 ka. The next older deposits date at ~8.7 ka at Tucahuay and between ~8.5 and ~9.4 ka at Los Burros, respectively, which could suit the

dryer period ~8.6 ka (all huayco data are calibrated ^{14}C-ages from Fontugne et al. 1999, Keefer et al. 1998, 2003, Keefer and Mosley 2004, and Ortlieb and Vargas 2003; Fig. 15.5). Thus the moister periods marked by loess deposition are in cycle with the expansion of the grassland area but anticyclical with probably El Niño-driven debris flow deposits. Therefore loess deposition seems to be favourable during La Niña-like climate conditions.

15.4.1.2 Fluvial Deposits of the Little Ice Age Period

In the Palpa–Nasca area two types of fluvial sediment archives denote former periods of increased geomorphic activity:

(1) River terraces along the allochthonous rivers that originate from the high Andes and provide fertile river oases amid the desert region which they cross on their way to the Atlantic coast. River terraces are partly made up of reworked loess material, washed off the slopes at times when the climate became drier so that sporadic rainfall could hit the bare ground and remobilise the silty, easily erodible material. The river terraces partly contain much coarser, that is, sandy and/or pebbly material. The changes in grain size indicate either variation in the intensity of runoff events and hence flow competence or they denote lateral shifting of the riverbed with deposition of coarser material at the bottom of the channel bed and fine material in more distal floodplain areas. Downstream Palpa, nearby the Fundo Jauranga, the Rio Palpa exhibits prominent terrace remains ~1–2, ~3, and ~5 m above the present-day thalweg, pointing to respective periods of sediment accumulation and subsequent fluvial incision (Fig. 15.6). At other places, terraces may show no further subdivision, like the Rio Santa Cruz at Huayuri, which exhibits only one terrace-level at ~3 m above the thalweg (Fig. 15.7). At several locations, samples were taken from fluvial terrace deposits for BLSL coarse-grain quartz dating applying the SAR protocol to small aliquots. The results of the dose determination indicate insufficient bleaching of the fluvial

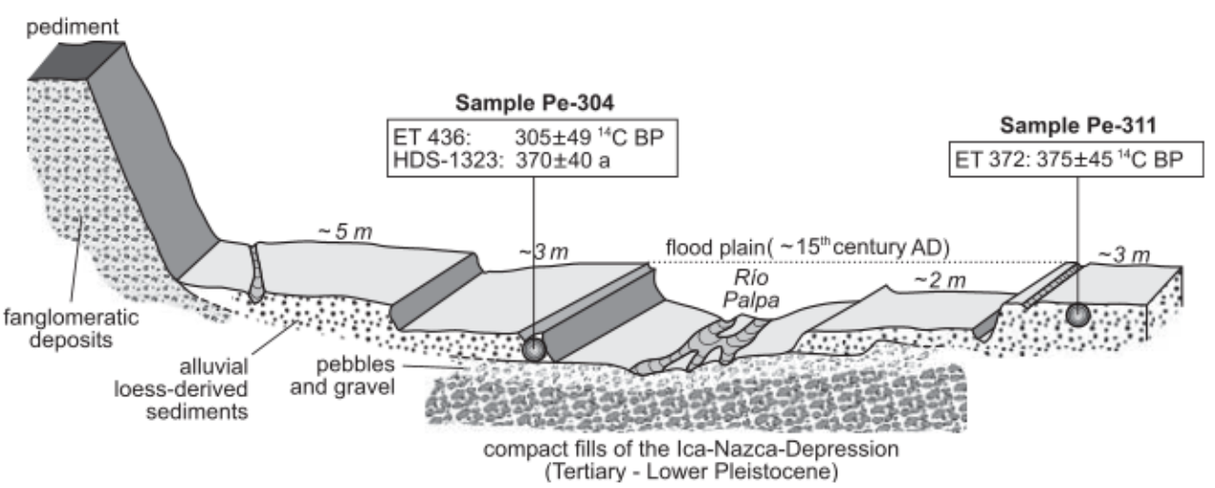

Fig. 15.6 Generalised cross-section through the Rio Palpa terraces north of Jauranga. Sediments of the ~3m terrace above todays' thalweg were deposited during the Little Ice Age (after Unkel et al. 2007)

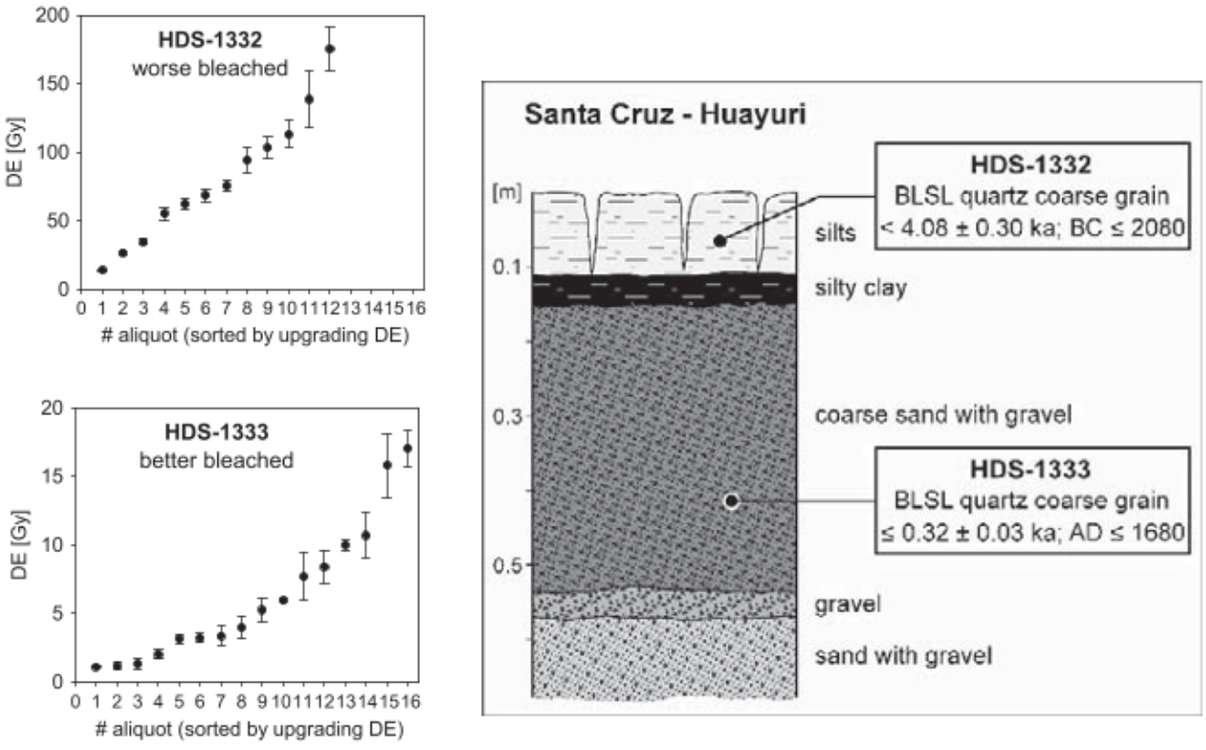

Fig. 15.7 Dating results of fluvial samples at the locality of Huayuri using small aliquots and a BLSL coarse-grain quartz protocol. The large scatter in DE-values (*left*) shows that the sediment is insufficiently bleached. If DE-values are sorted in upgrading order, sample HDS-1332 exhibits a steep decline, whereas the lower values of sample HDS-1333 seem to indicate a better bleaching by bottoming out on a plateau. The maximum ages (*right*) were calculated from the lowest DE-value for sample HDS-1332 and from the three lowest DE-values of sample HDS-1333. The age younger than 1680 AD of the apparently better bleached sample points to the Little Ice Age period as a time of major fluvial activity (after Unkel et al. 2007)

sediments (Fig. 15.7, left), which means that only maximum ages can be calculated. Yet, supported by the results of accompanying ^{14}C-datings, the dates indicate a period of major fluvial activity during the Little Ice Age (LIA). At that time ~1400–1700 AD, the riverbed must have been ~3 m above its present level, as may be deduced from the gravely components in the terrace sediments. The period of geomorphic activity coincides with a period of ice aggradation on the Quelccaya glacier, which is caused by an intensification of the SASM and leads to increased influence of the eastern monsoon at the eastern margin of the Atacama desert.

(2) Fluvial cones at the outlet of quebradas, which are autochthonous dry valleys with much smaller catchments confined to the arid footzone of the western cordillera. One of the prominent fluvial cones at the outlet of the zero-order basins in the Andean footzone lies ~5 km southwest of Palpa at the archaeological site of La Muña on the western part of the valley bottom of the Rio Grande and across from the mouth of the Rio Palpa (Fig. 15.3). A 2 m high profile cut into the sediment cone (Fig. 15.8) reveals on top of finer grained sandy-silty Rio Grande flood deposits a sequence of coarser debris-flow layers and finer sandy layers from the tributary, that are intercalated by organic-rich layers.

Three samples were taken for BLSL dating of small aliquots of the coarse-grain quartz component. Again, variation in dose-values points to insufficient

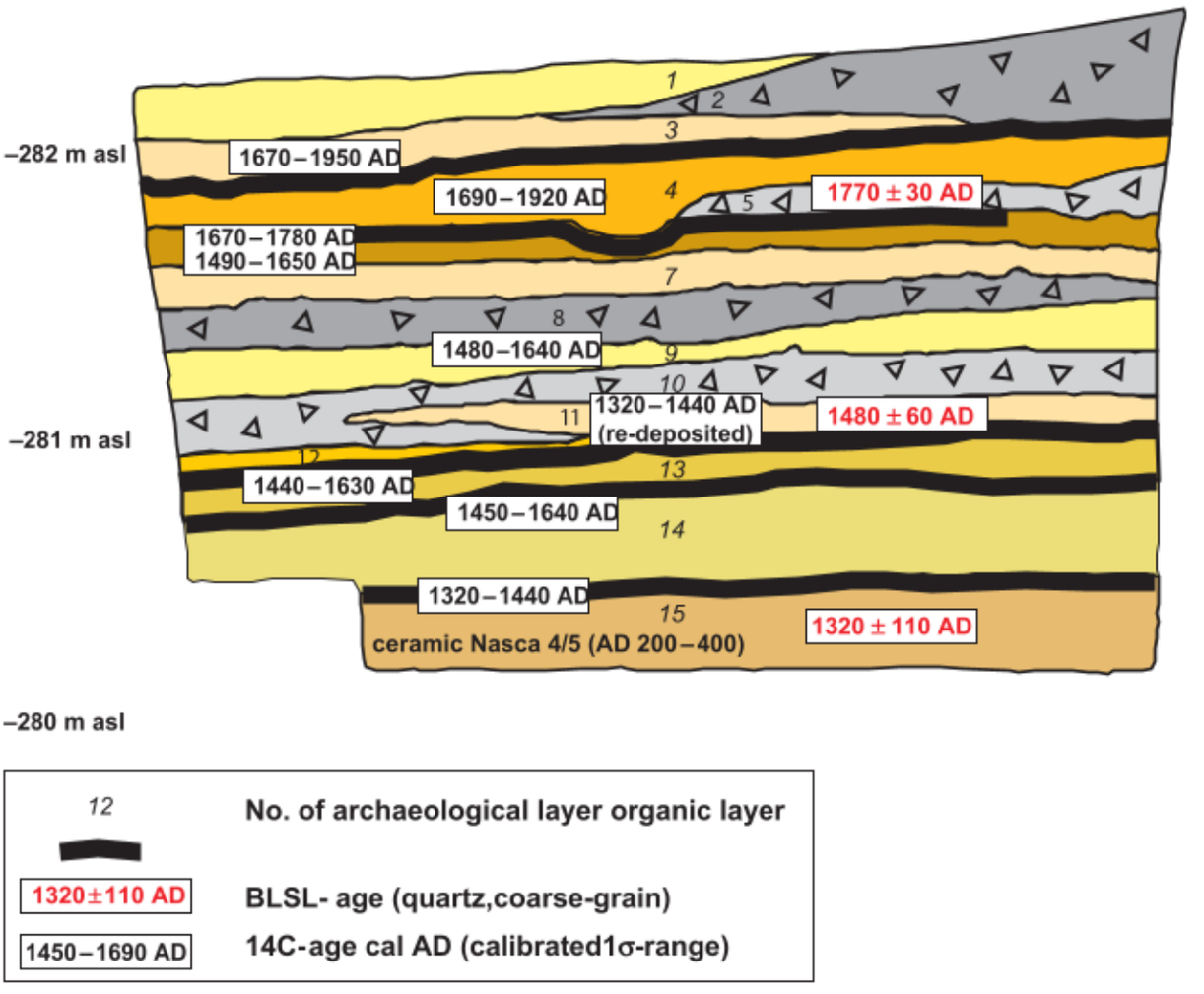

Fig. 15.8 Profile through the debris-flow deposits at the ancient settlement of La Muña. The debris-flow cone is situated at the outlet of the quebrada onto the alluvial plain of the Rio Grande. The basal sandy layers <281 m a.s.l. are alluvial sediments deposited by the ephemeral allogenetic Rio Grande, and the coarser debris-flow deposits >281 m were deposited by storm runoff resulting from the autochthonous catchment of the dry valley. ^{14}C-dating of the organic rich layers and BLSL-dating of quartz coarse grains show that sediment reworking occurred in the geomorphologically active Little Ice Age 1390–1710 AD (after Unkel et al. 2007)

bleaching allowing only maximum-age calculation. Yet again, the ages are in agreement with the results from the ^{14}C-dating of the organic-rich layers. The results show that the more humid conditions during the LIA ~1330~1770 AD did not only affect the allochthonous rivers reaching far into the high Andes but also the quebrada catchments farther to the west. Here the environmental and geomorphic effects of the LIA, including the mobilisation of debris flows probably by sporadic convectional rainfall in a period of generally increasing aridisation, apparently promoted the end of the Late Intermediate period culture (~1300–1430 AD at the locality of Chillo, Unkel 2006) in the area.

15.4.2 The Novel High-Resolution Technique

Prior to HR-OSL dating, IRSL emission spectra were measured on representative aliquots of all samples investigated, using the high-sensitivity TL/OSL

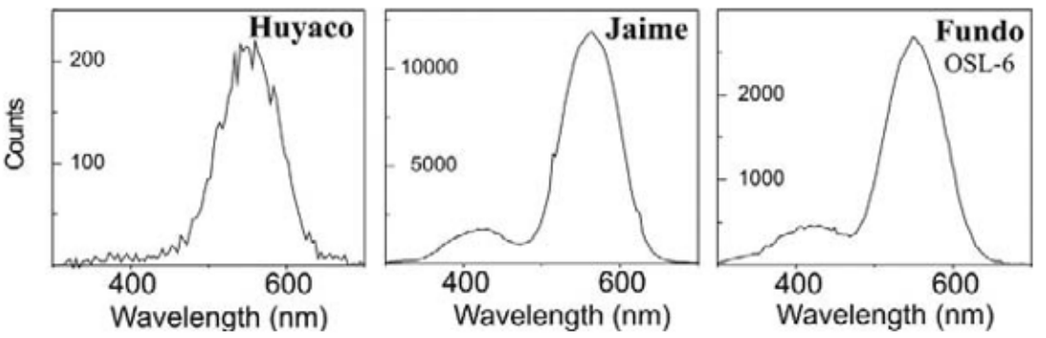

Fig. 15.9 Feldspar IRSL-spectra from stone surfaces (Huayco and Jaime) and resined fluvial sands (Fundo). All samples show a comparatively strong yellow (~560 nm) luminescence signal and only little blue emission (~410 nm)

emission spectrometer described in Rieser (1999). All samples possess a pronounced yellow (~560 nm) emission (Fig. 15.9). Therefore in every case HR-OSL dating was done by applying the IRSL-SAR protocol to the yellow feldspar emission, in the way described above.

15.4.2.1 Huayco Deposits at the Transition from Late- to Post-Glacial Times

Alluvial fans and debris flows (huaycos) made up from coarse sediments such as pebbles and boulders often fill the mouths of the (presently) dry valleys (quebradas) at the Andean foot. The deposits are attributed to major El Niño events, which involve moisture uptake from the Pacific in the west and lead to heavy rainfall in coastal areas of southern Peru. However, the hypothesis that they may have had catastrophic effects on pre-Columbian people and may have promoted the fall of the Nasca culture (200 BC–800 AD; Grodzicki 1994) must be rejected, as superposed Nasca geoglyphs cross the quebradas (Eitel et al. 2005).

From a huayco deposit in the lower Santa Cruz valley we sampled a dark coloured, dioritic boulder (Ø~20–25 cm, ~5 cm thick) with small whitish porphyric feldspar components (Fig. 15.10). The covered, lightproof back-side of the boulder was used for HR-OSL analyses. Larger areas of the huayco surface are covered by remains of houses, likely from the Late Intermediate period (personal communication M. Reindel), indicating a minimum age for the underlying sediments.

Twelve analyzed ROIs from three measured huayco aliquots yielded D_E-values of 34.3–45.8 Gy (Fig. 15.11, Table 15.3). For the ten ROIs, for which we determined the internal potassium content, the ages range between 11.3 and 14 ka, but are equal within error ranges. In contrast to all other ROIs from the other samples none of the huayco ROIs gives an indication of anomalous signal loss during the storage period of 26–32 days. The OSL ages support the hypothesis that huayco deposition preceded the time of the Nasca culture. According to the gained OSL ages it is possible that huayco activity preceded loess accumulation, probably in the wet latest-Pleistocene Tauca period (14,000–10,500 BP, uncalibrated ^{14}C-ages according to Argollo and Mourguiart 2000).

Fig. 15.10 Artificial exposure in a huayco deposit in the lower Rio Santa Cruz valley. A ~5 cm thick, and ~20–25 cm long dioritic boulder with whitish feldspar blasts and little surface-weathering and desert varnish at a depth of ~75 cm below ground level was selected for HR-OSL dating

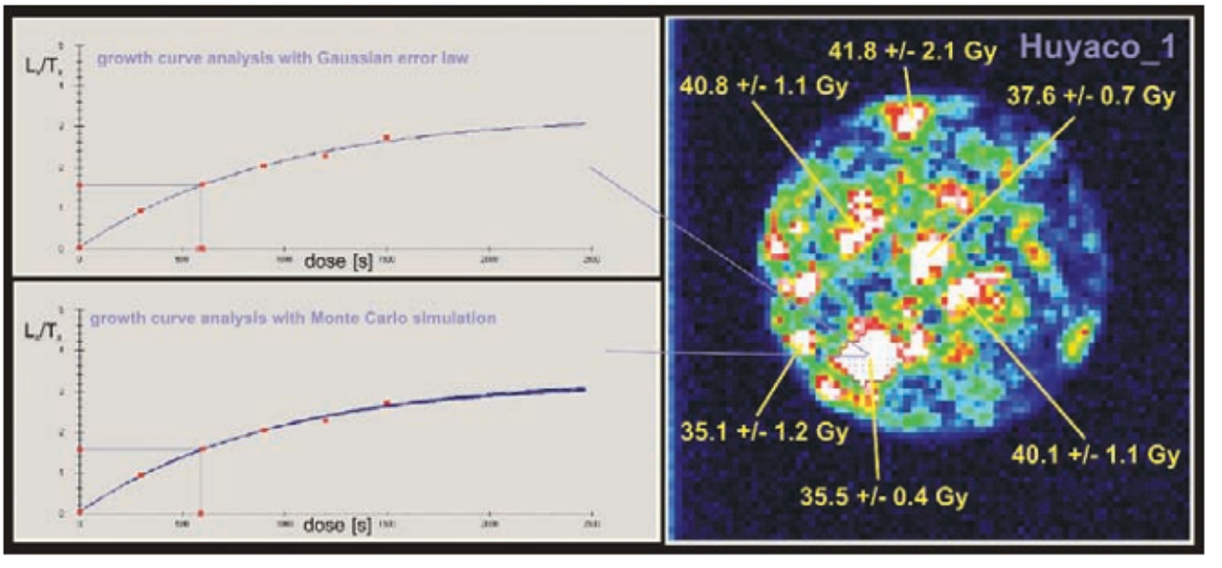

Fig. 15.11 HR-OSL D_E-determination for one aliquot (82 × 82 areas, each area 100 μm side length) of the sampled boulder (cf. Fig. 15.10). Luminescence intensities are presented in false colours. Low intensities are represented by dark colours (*black* and *dark blue* denoting background noise), and the regions of interest delivering the brightest luminescence signal have a white filling

15.4.2.2 Irrigation Channel from a Late-Holocene Semi-Arid Period

At Jaime in the Rio Santa Cruz valley, people had built a canal to collect water for irrigation from small tributaries that are nowadays completely dry (Eitel et al. 2005). The erection of such hydroengineering works in the archaeological past would have only made sense during more humid times, as, for example, the Late Intermediate period, when east monsoon rainfall must have reached the area more or less regularly each year. We attempted OSL dating on the material of the manmade heaped-up downhill sidewall of the irrigation channel.

The sediment is mainly made up of the fine-grained loess covering the slopes widely. Occasionally it contains pieces of granitic stones from the underlying desert stone pavement.

We tried dating on both, fine grains and incorporated stone fragments (usually only ~2 cm in diameter and <1 cm thick) (HDS-1473–HDS-1477), but were not successful with HR-OSL analyses on hardened fine grains. Dose-recovery tests, which are tests to reproduce a laboratory dose with the same protocol also used for OSL dating, produced unsatisfactory results (Fig. 15.12, left). This is unlike dose-recovery tests for granitic stone surfaces with much bigger feldspar grains and a stronger luminescence signal, which reproduce the administered dose well (Fig. 15.12, right). We suspect that not yet understood optical effects at the rim of grains, dominant in fine-grain material, might be the reason (Greilich and Wagner 2006).

Further HR-OSL analyses were focused on stones contained in the sampling cylinders. For six aliquots from eight samples (i.e., different stones, each from a different sampling cylinder) measured with the IRSL-SAR protocol, intensities of the yellow feldspar luminescence were high enough for dating (samples Jaime-1, -2, -4, -7, -9, and -10 in Table 15.1). Palaeodoses in the range of ~25.8–38.4 Gy were found for the brightest areas (ROIs) from five aliquots with >260 cts/area/first 60 s (dim sample Jaime-7) up to >6000 cts/area/first 60 s (very bright sample Jaime-10). Assuming a dose-rate of ~4.1 Gy/ka (weighted mean of ROIs from Jaime samples analysed by SEM-EDX; see Table 15.3) gives ages between 6.3 and 9.4 ka.

Apparently, the stones were not (sufficiently) bleached during the channel construction but preserved much of what presumably is the palaeodose

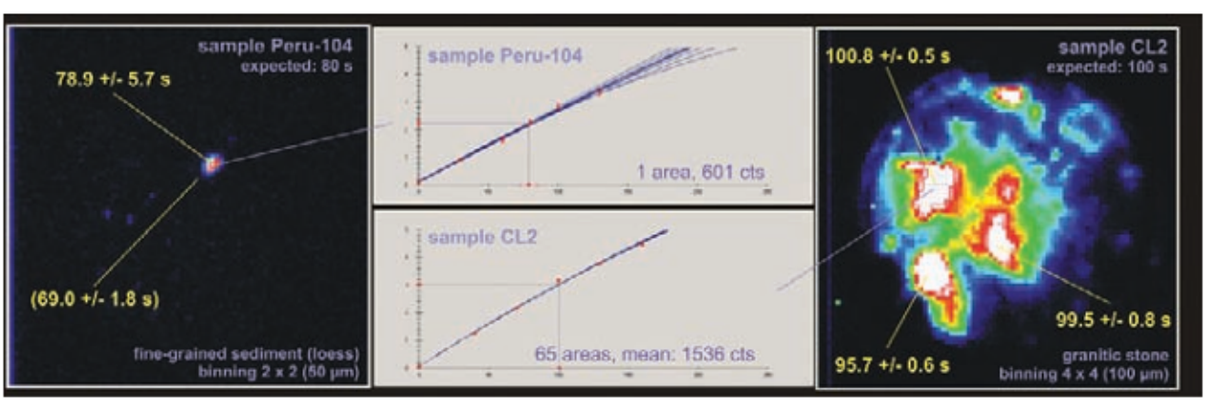

Fig. 15.12 Dose-recovery tests for resin-hardened loess (*left*, sample Peru-104) and granitic stone surface (*right*, CL2 from Cerro Llipato). In the false-colour graphics low intensities of the luminescence signal are represented by dark colours (*black*, *dark blue*: background noise), whereas bright shining ROIs show a white colouring. Fine grains and high resolution (50 µm) do not lead to satisfactory results (*left*). Although a generally bad signal-to-noise-ratio allows analysing only a few areas at all, the administered laboratory dose is retrieved reliably only for one, that is, the brightest area; otherwise it is underestimated due to the high impact of rim effects. However, dose-recovery of large feldspar grains measured with lower resolution (100 µm) provides good results recovering the laboratory dose (right). The given laboratory doses are 4.8 Gy (resp., 80 s irradiation time) for the loess and 6.0 Gy (resp., 100 s) for the granite

corresponding to the covering of the desert pavement by the loess deposition. As, however, all samples from Jaime show significant anomalous fading after a period of 25–46 days of storage, they provide only minimum ages. Although the aliquots from stone Jaime-9 seem much better bleached (OSL age of ~3.4 ka), sample Jaime-1 yields significantly younger ages for the two analysable ROIs of ~0.9 and ~0.35 ka. Assuming that the whole piece of stone had been homogeneously bleached, the older age seems to be more reliable, as this ROI-1 shows considerable less anomalous fading (0.8±0.2) than ROI-2 (0.6±0.1) (Table 15.1).

As irrigation activities in the more humid period of 1000–1400 AD are probable, it is not unlikely that this ROI provides an OSL age related to the historical construction of the earthwork. For a sound dating, of course a statistically significant number of stones and ROIs have to be analyzed. Yet, the results show that the HR-OSL dating technique provides plausible, that is, interpretable, ages and a tool to meet new challenges in OSL dating. Similar to a minimum-age model applied to a D_E-distribution gained from single grain dating (Galbraith et al. 1999) HR-OSL dating may be used to retrieve the best bleached stones or parts of stones, as recognised from age distributions of a suite of ROIs. As with all other samples, the Jaime samples exhibit good recycling ratios for the lowest above-zero SAR regeneration dose point (Table 15.1).

15.4.2.3 The Little Ice Age Period in the Fluvial Deposits at Yunama

From an open cut into sediments of the 5 m terrace of the Rio Palpa/Rio Viscas at the Fundo Jauranga (Fig. 2.6 in Eitel and Mächtle, this volume) we took a sample of sandy pebbly material for a HR-OSL dating attempt of insufficiently bleached alluvial deposits (sample Fundo, OSL-6, HDS-1472). In its lower part the profile contains Nasca artefacts (personal communication M. Reindel). We measured one aliquot of the resin-hardened sediment (Fig. 15.13). The two ROIs analysed from that one aliquot gave OSL ages of ~0.8 and ~1.3 ka (Table 15.3).

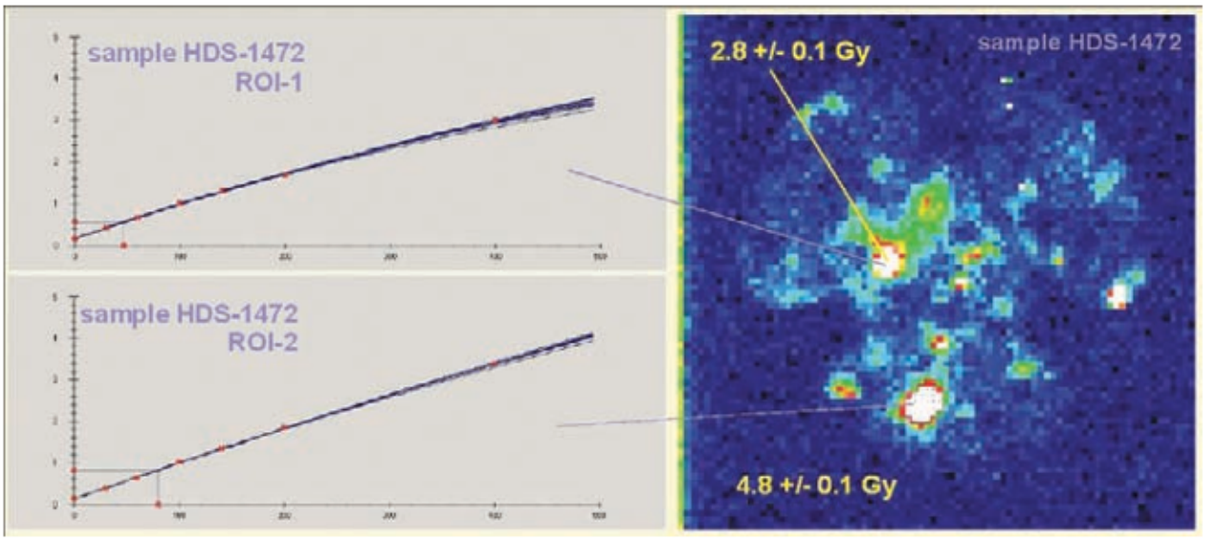

Fig. 15.13 HR-OSL DE determination for two ROIs of one aliquot from sample Fundo cored from an epoxy resin-embedded alluvial sand

The younger OSL age from ROI-1 seems more reliable for two reasons. First, it is likely that in the fluvial environment this grain was better bleached; second, it shows a much less pronounced fading ratio of only 0.9±0.1 as compared to 0.3±0.04 (Table 15.1). Within errors the age is in agreement with the other OSL ages and independent ^{14}C-ages gained for the prominent river terraces of the area, which apparently were deposited in a period of major fluvial activity during the Little Ice Age.

Again, as with the analyses of the irrigation channel at Jaime, this is only a preliminary dating attempt. Yet again, the results are plausible and principally show the great potential the novel HR-OSL dating technique bears even for the analysis of primarily unconsolidated sediments. ROI-by-ROI (i.e., grain-by-grain) analysis becomes especially interesting for insufficiently (differentially) bleached sediments allowing us to distinguish between badly and better bleached grains.

Acknowledgments Loess samples were collected during two field campaigns in 2002 by G.A.W., together with Bernhard Eitel and in 2004 by Bernhard Eitel. Sampling at La Muña was done by Irmtrud Wagner and Markus Reindel. Susanne Lindauer helped with the sample preparation.

Chapter 16
Light Thrown on History – The Dating of Stone Surfaces at the Geoglyphs of Palpa Using Optically Stimulated Luminescence

Steffen Greilich and Günther A. Wagner

Abstract A foremost goal of the Nasca–Palpa project was the development of a method allowing the numeric dating of the renowned geoglyphs. Hitherto, the various types of geoglyphs had been dated solely by the principles of superposition and archaeological style. Due to the almost total lack of organic materials, radiocarbon dating is not applicable in this case. Because the geoglyphs were constructed by moving away stones of the desert pavement and depositing them at the geoglyph rim, it seemed near at hand to adapt the OSL sediment technique for dating the last exposure of the stones to daylight. A new high resolution OSL (HR-OSL) technique was successfully developed, using the quartz and feldspar grains within in their original stone surfaces. In this way, the last light exposure of the lower, dark surface and thus the last movement of the stones was dated. The HR-OSL ages of granitoid stones sampled on different types of geoglyphs are in good agreement with archaeological and geomorphological reasoning. Our sampling procedure left no visible traces on the geoglyphs.

16.1 Introduction

The geoglyphs of Palpa presented a superb testbed for the development and the application of a novel luminescence method for dating stone surfaces. This method is based on bleaching the latent optically stimulated luminescence (OSL) signal in feldspar and quartz grains at granitoid rock surfaces during the exposure to daylight. When the surfaces are shielded from light after the bleaching, the latent OSL signal builds up again, such that its intensity provides an age for the event of this last light exposure.

S. Greilich (✉)
Radiation Research Department, Risø National Laboratory for Sustainable Energy, Technical University of Denmark, Frederiksborgvej 399, 4000 Roskilde, Denmark
e-mail: Steffen.Greilich@risoe.dk

M. Reindel, G.A. Wagner (eds.), *New Technologies for Archaeology*, Natural Science in Archaeology, DOI 10.1007/978-3-540-87438-6_16,
© Springer-Verlag Berlin Heidelberg 2009

Fig. 16.1 The process of geoglyph construction becomes apparent in the image of a site that has been left half-finished. Desert pavement stones are first piled up into smaller units and later transferred to a wall (on the *right*)

In the case of the Palpa geoglyphs, this event can be their construction when the dark brown stones of the desert pavement were moved to uncover the underlying pale silt (Fig. 16.1). Stones carried aside were laid upside-down; from thereon covered surfaces have been shielded from further light exposure, provided the stones stayed there in situ since then.

The last light exposure event can also be any reworking or eventual destruction of the stone structure, in which surfaces were exposed to light again. In addition, in the case of large granitic boulders in the Ica–Nasca depression, the latent OSL signal can represent the sedimentary deposition in pediment deposits.

Technically, our novel approach utilized a high spatial resolution detection technique (HR-OSL) for the OSL from minerals that are left in their original petrologic context, that is, without any mineral separation. This method allowed direct access to gradients at the surface as opposed to more conventional methods used in luminescence dating of sediments (Greilich and Wagner 2006).

16.2 Luminescence Dating of Rock Surfaces

The fact that the exposure to daylight bleaches latent luminescence signals of mineral grains was first reported by Wintle and Huntley (1980). Since then, the phenomenon has been widely used for dating sediments whose quartz and feldspar constituents had been sufficiently light exposed during sedimentary transportation. Variation in mineral type and grain size yields differences in luminescence properties and dose-rate. This is tackled by physical separation

of the loose grain sediments measuring a subfraction of the original sample containing grains of similar properties and dose-rate. For a more detailed description of luminescence sediment dating, see Kadereit et al. (this volume).

Analogously, it should be possible to determine the age when the surface of a stony object had been exposed to daylight before it became ultimately shielded from light. There have been several attempts to employ this unique potential of luminescence dating. Liritzis (1994) proposed to use thermoluminescence (TL) to date the construction of a megalithic limestone building. Studies were undertaken to determine the ages of the Apollo Temple at Delphi and of limestone pyramids in Greece (Liritzis et al. 1997; Theocaris et al. 1997). Scraping off the uppermost part from the bleached surface provided the necessary conservation of spatial information with depth (i.e., staying within the bleached surface). The applied methodology was, however, partly hampered by the fact that in calcite – even after extended exposure to sunlight – a significant residual TL signal is left (Liritzis and Galloway 1999).

In sediment dating, this problem of unbleachable luminescence signals was earlier overcome by the use of optically stimulated luminescence (OSL) instead of TL (Huntley et al. 1985). It seems, therefore, only consequent also to employ OSL dating to stone surfaces. Early attempts to determine the burial age of quartzite pebbles by this approach were reported by Huntley and Richards (1997); a recent study using OSL was done by Vafiadou et al. (2007). Habermann et al. (2000) showed that granitoid stone samples satisfy all the requirements for OSL dating, that is, appropriate dose-response and long-term stability, and that the light penetration depth is sufficient for resetting the OSL signal at the surface.

Granitoid rocks (e.g., granite, granodiorite, quartzdiorite, diorite, quartz porphyry, dacite, and andesite) contain quartz and feldspars, i.e. K-feldspar and plagioclase. During the past, most of these rocks were recurrently used as building stones, which is favourable for the wide application of surface dating. Granitoid rocks are also abundant around Palpa. However, scraping off the uppermost layer in a controlled manner as for limestone (to overcome depth gradients) is difficult due to their hardness. In addition, granitoid rocks exhibit additional gradients in luminescence in the surface plane compared to calcite due to small-scale variations in dose-rate. Habermann et al. (2000) established that the feldspar component could be exclusively simulated using infrared light, however, also feldspars exhibit a wide range of dose-rate values due to their highly variable potassium content. The infinite matrix dose-rate of plagioclase (0% K, 0.8 mGy/a-solely from U and Th) is about 20 times less than that of sanidine (14% K, 15 mGy/a). Calculations using a simplified polymineral surface model show that incorrect ages may result when the OSL contributions of feldspars are averaged (Greilich 2004). Naturally, this problem is aggravated when blue or green stimulation instead of infrared light is employed as this also stimulates other minerals.

This led to an all-optical approach of separating luminescence signals from a surface while leaving the grains physically in their context; it was achieved by shrinking the spot size of a single luminescence measurement to a scale of a few tens of micrometers. To then perform a sufficiently large number of such

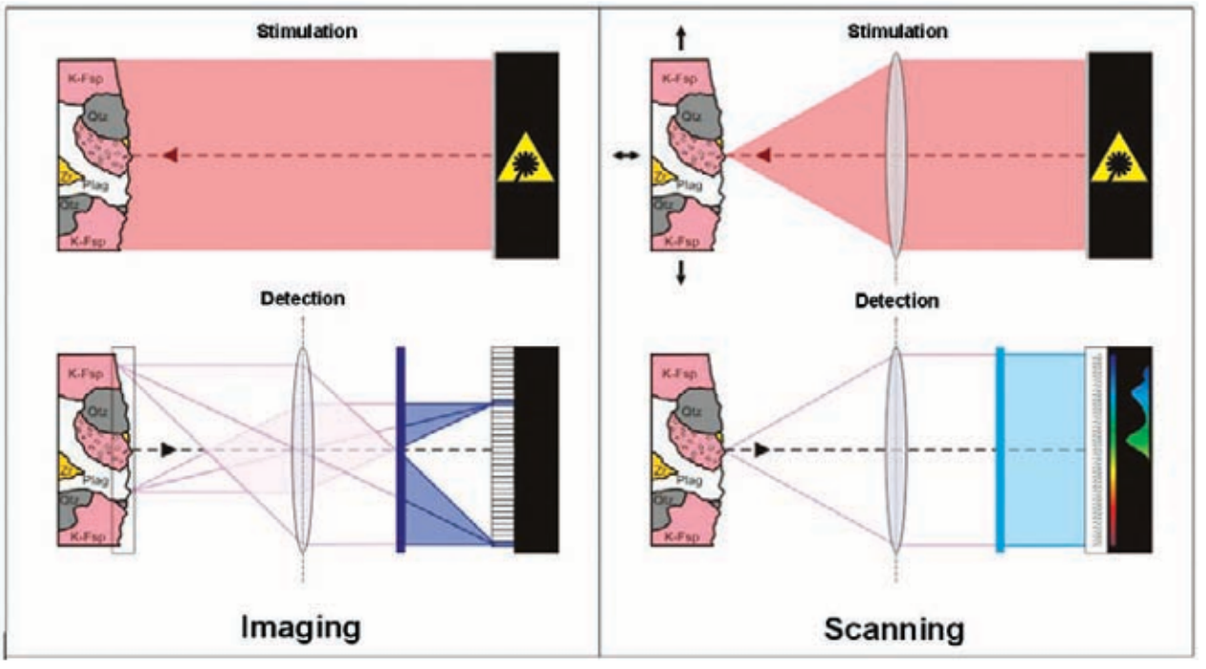

Fig. 16.2 High-resolution luminescence data from intact samples can be recorded either by using the spatial information from a detector (*left*) or from a small-spot stimulation (*right*)

measurements across a surface, basically two techniques can be used (Fig. 16.2), either to stimulate the entire sample and image the signal distribution onto a detector providing spatial resolution (imaging), or to subsequently stimulate a confined part of the sample only (e.g., by a focussed laser beam) and compose the recorded signals to a pseudo-image afterwards (scanning). Both approaches have been utilized in low-light luminescence studies (for references see Greilich et al. 2002); with the availability of highly sensitive CCD chips and confocal microscopy, their application for dating become feasible (Duller et al. 1997).

When the measurement spot is reduced so that gradients become negligible the age equation can be individually applied to each or to clusters ('regions of interest') of the many measurement spots at the surface. This also requires spatially resolved dose-rate determination at grain level, which can be achieved by techniques such as a scanning electron microscope with microprobe (SEM-EDX, mainly for K content) and fission-track mapping (U and Th contents).

Dose-rate assessment for spatially resolved dating has to be performed on a similar scale to equivalent-dose evaluation, which is probably the most challenging task. Up to now, little has been known about the microdosimetry in natural samples. For our experiments, a simple geometrical model was employed. It computes the annual dose-rate for a region of interest (Greilich et al. 2005). It is a simplified approach to a surface grain surrounded by up to three media, for example, at a granite–sediment interface or within a building structure (stone–mortar–stone). The spatial distribution of potassium is assessed by SEM-EDX. For uranium and thorium, the use of fission tracks has been proposed (Wagner et al. 2005).

16.3 Technical Developments

Imaging technique: The first of our HR-OSL devices is based on imaging the OSL-signal at the surface onto a liquid nitrogen cooled, 1100 × 330 pixel CCD chip. Green (532 nm, Nd:YVO_4, 100 mW) and IR (830 nm, diode, 150 mW) lasers are employed for stimulation (Fig. 16.3). This setup is capable of recording OSL at a surface with a spatial resolution down to 25 μm. Using a regenerative protocol, the successful evaluation of laboratory beta-doses previously applied to granitic surfaces was shown (Greilich et al. 2002). However, this imaging technique does not discriminate OSL signals from different depths z. Heterogeneities in depth with respect to the mineralogical parameters – although unknown – can be reasonably inferred from data obtained at the x-, y-surface plane. z-gradients and their influence on the dating results, however, need careful consideration (Greilich et al. 2005). Generally, one should preferably use the opaque mineral component of a surface for dating.

The imaging technique allows the fast parallel recording of up to several 10^4 detection areas. The resolution needs to be adjusted to find the appropriate

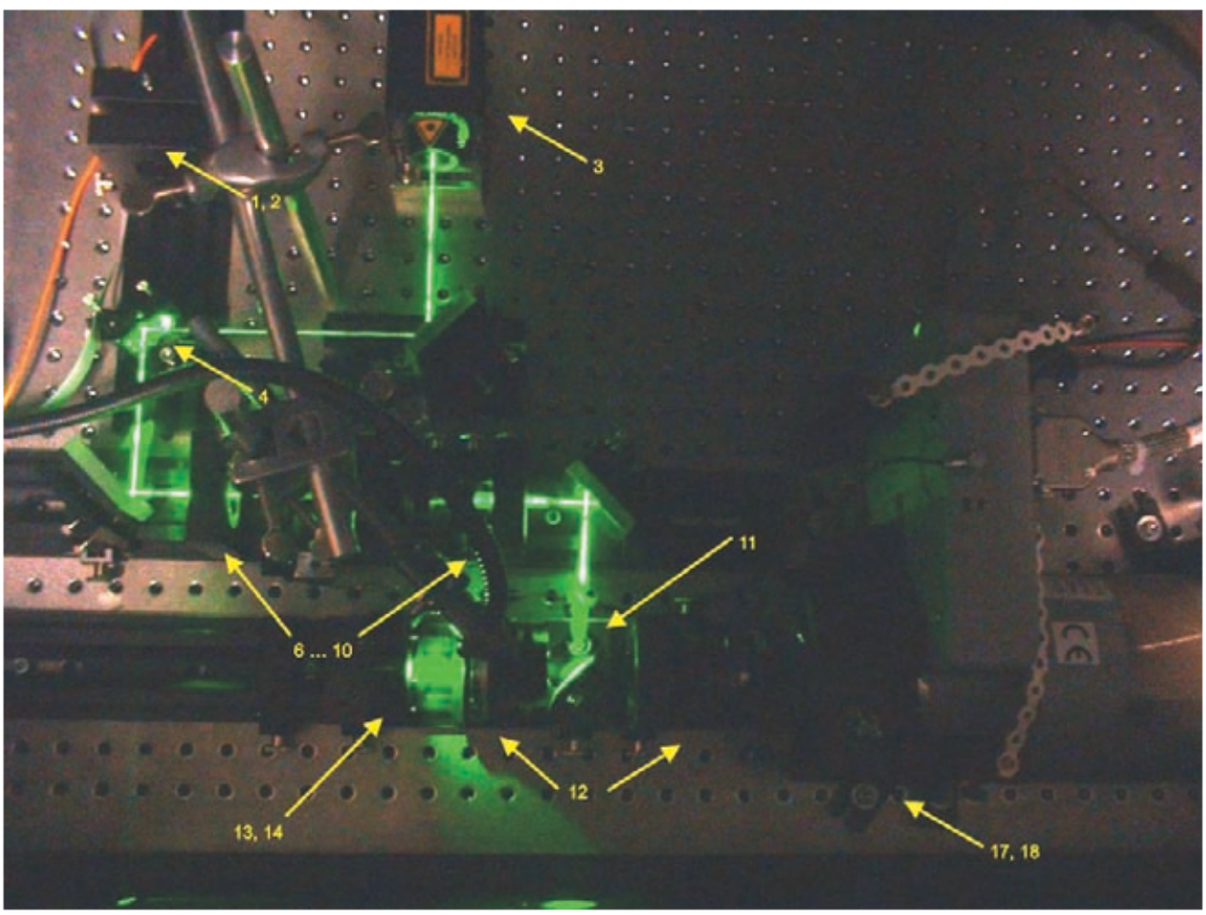

Fig. 16.3 The LasLUM I HR-OSL reader. The light from either a green or IR laser (1–3) is guided by a setup of lenses and mirrors (4–11) onto the sample (13–14). The resulting luminescence light is recorded by a liquid nitrogen cooled CCD camera (17–18) through two 35 mm lenses (12)

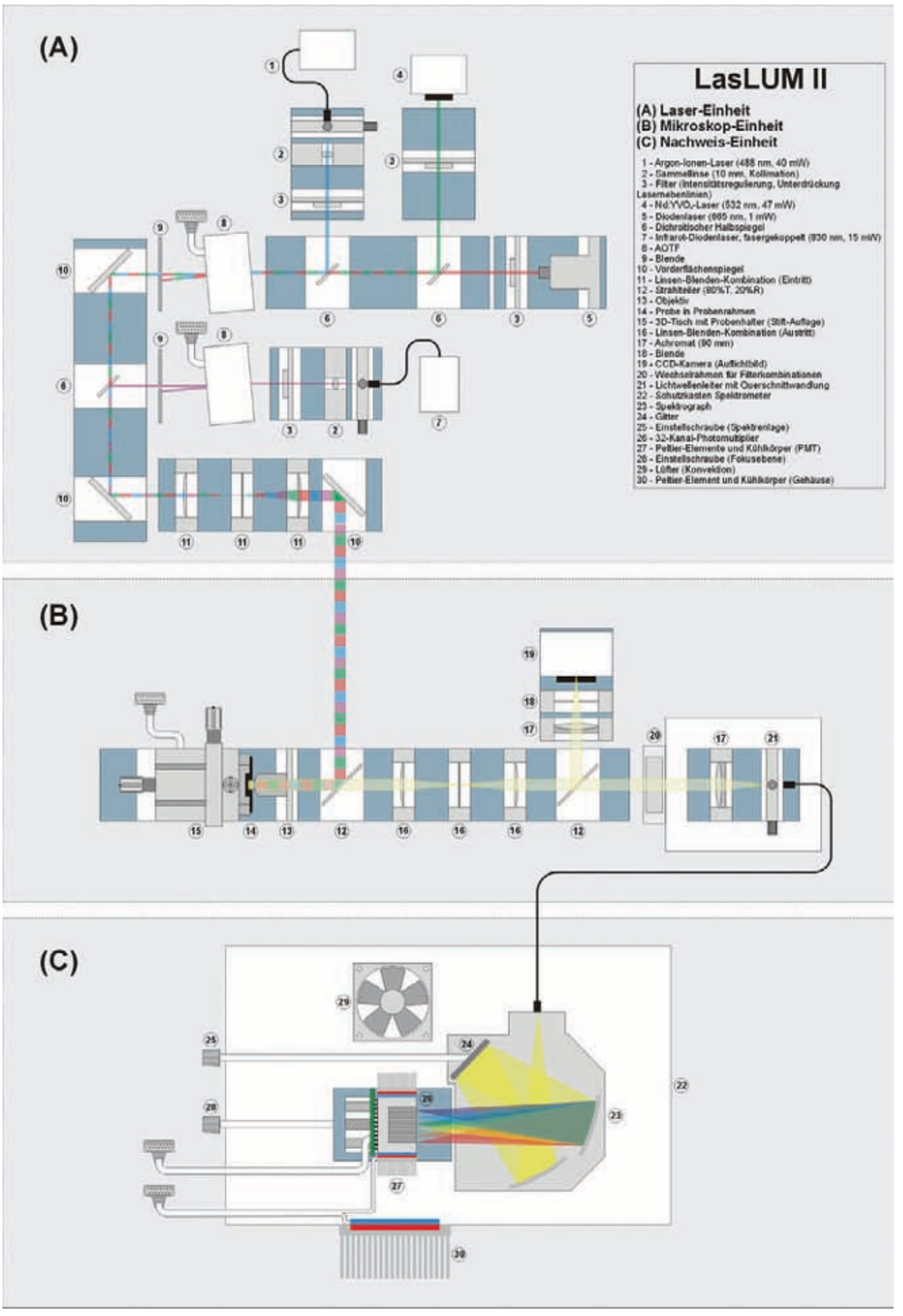

Fig. 16.4 The LasLUM II/III HR-OSL. Part (**B**) is based on a fluorescence microscope with the output from a suite of four lasers (**A**, intensity controlled by acousto-optical filters) coupled into it. As opposed to LasLUM I, a narrow beam is scanned across the surface by moving the sample stage and both the luminescence intensity and spectrum can be analysed in a spectrometer (**C**)

signal-to-noise ratio for the sample's sensitivity. For granitoid samples, approximately 6500 areas, each 100 × 100 μm in size, can be achieved in most cases. Due to the large amount of recorded data, common software programs for luminescence dose-evaluation might be inconvenient to use. More particularly, they are not able to benefit from the spatial information provided by the HR-OSL images and they are not designed for the special requirements of CCD data. A dedicated software program ('AgesGalore') allows us to compute an equivalent dose for each area of measurement as well as the presentation and analysis of spatial and frequency distributions and radial or x–y plots (i.e., plotting one quantity vs. another, e.g. equivalent doses vs. sensitivity; Greilich et al. 2006).

Scanning technique: A second OSL device was built around a commercial fluorescence microscope. Customization included a new external laser unit, low-light detection suitable for luminescence, and a microscope stage (moveable in three dimensions) which is used for focusing and scanning the fixed laser across the surface (Greilich 2004). This setup allows better control of the depth gradients and spectral information of the luminescence signal (Fig. 16.4).

16.4 Procedures for Rock Surface Samples

The sampling at the Nasca geoglyphs was undertaken in the darkness at night (Fig. 16.5), and was preceded by the selection of individual stones by daylight. The selection criteria were: (1) petrology (rich in quartz and feldspars), (2) desert-varnish (as little patination as possible), and (3) the firm contact of the stone within the ground. For sampling, the stones were lifted out of the ground at night (even moonlight was avoided). Three to four drill-cores were taken from the light-shielded bottom surface of the stones by drilling short cores (8 mm in diameter and approx. 1 cm in length) with water cooling (Fig. 16.6). The cores were wrapped in light-tight aluminium foil and opaque plastic bags and transported to the laboratory. The only illumination that was tolerated during the sampling were two headlamps with red LEDs. After drilling, the stones were put back into their original position without any visible disturbance of the site occurring. In the dark laboratory, the drill-cores were cut into slices of 2 mm thickness by a water-cooled diamond saw. The uppermost slice of the drill-core representing the stone surface was used for the luminescence measurements.

Spatially resolved equivalent doses were obtained by the MASS (multiple areas single section) protocol, an adapted regenerative single-aliquot protocol (Greilich et al. 2005). For calculating ages, equivalent doses were averaged within clusters at the surface where the dose-rate can be considered homogeneous (Fig. 16.7).

To assess the dose-rate of such a cluster or 'region of interest' (ROI), the five-component model was employed (Greilich et al. 2005). It considers contributions

Fig. 16.5 Preparation for core-drilling at night. The tent is an additional protection against the bright moonlight

within the ROI, from up to three surrounding media and from cosmic radiation. Quantitative analysis of the K (and thus the radioactive ^{40}K) was carried out using scanning electron microscopy. Bulk K, U, and Th contents were analysed with low-level gamma spectrometry on pulverized sample material (Fig. 16.8).

Fig. 16.6 Water-cooled drilling into a stone which has been turned upside-down. The template hinders the drill from slipping across the surface. (Image: I. Unkel)

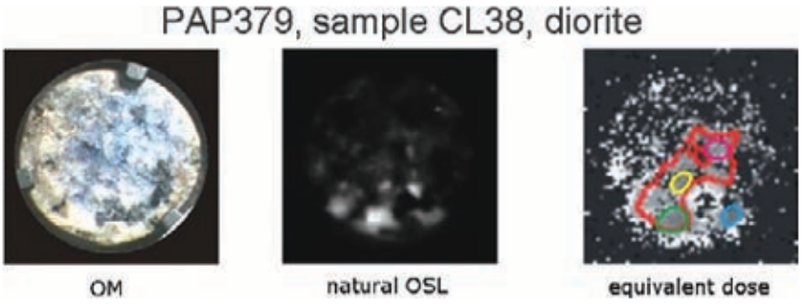

Fig. 16.7 Example of an MASS measurement. Four ROIs are defined in the right image (*yellow*, *green*, *blue*, and *violet*)

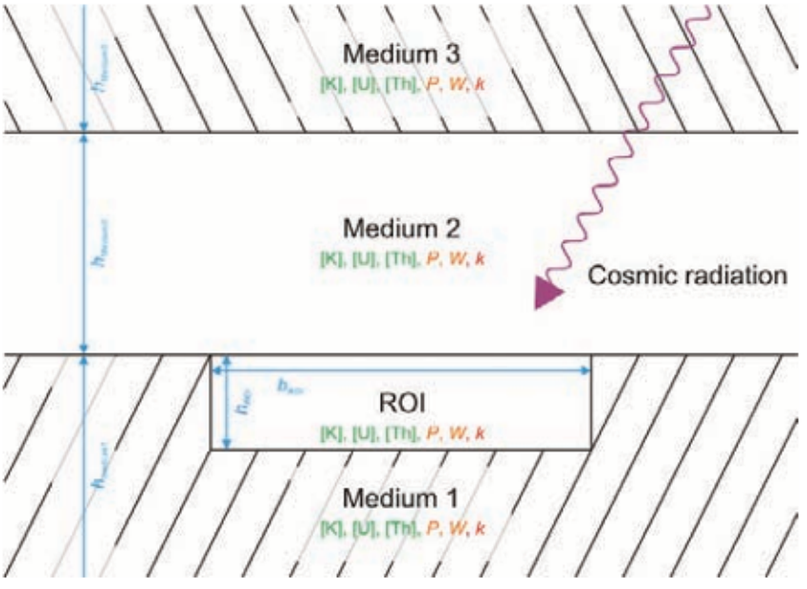

Fig. 16.8 Dose-rate model with simplified geometry as employed for surface dating. For the ROI and up to three media (e.g., a stone and underlying sediment or two stones with mortar in between), the uranium, thorium, and potassium content, porosity P, water content W, and alpha efficiency k are considered

16.5 Results for Geoglyph Samples

During four campaigns in 2002, 2003, 2004, and 2005 we collected and analysed 87 drill cores from 64 geoglyph stones at eight sites, namely:

- PAP-51 (PV67A-270) Geoglyphs at Cresta de Sacramento (2002)
- PAP-51 (PV67A-270) Stone platform at Cresta de Sacramento (2002)
- PAP-379 (PP01-036) Pampa de Llipata (2003)
- PAP-283 (PV67B-56/57) Cerro Carapo (2004)
- PAP-376 (PP01-032) 'Goddess of Fertility' (2004)
- Rio Palpa valley (2005)
- PAP-265 (PV66-133) Pernil Alto (2005)
- PAP-368 (PP01-042) 'Royal Family' (2005)

First measurements showed that the method could reproduce the stratification of two overlying geoglyph lines and reveal by a 'zero-age' a recent excavation previously unknown to the author but confirmed later (Greilich et al. 2005; Fig. 16.9). Although the variation in the results was at that time attributed to the uncertainties of the method in an early stage, more extensive data collection at the Pampa de San Ignatio confirmed the relatively widespread age variation

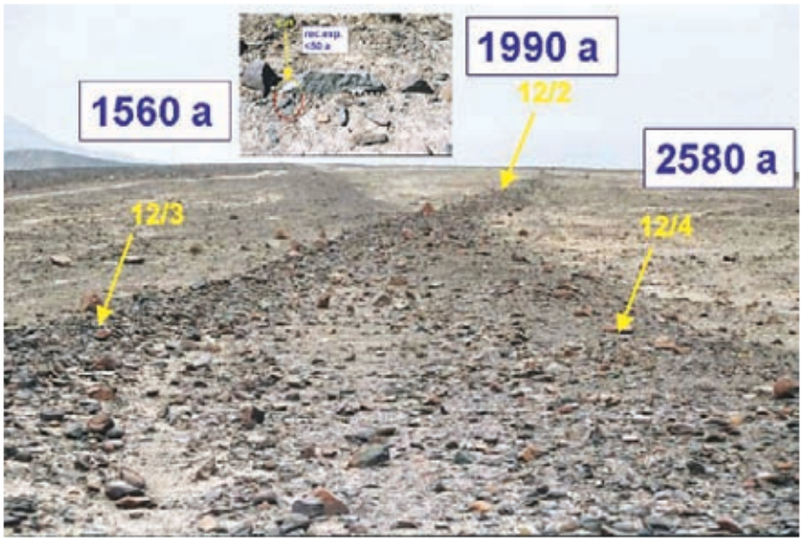

Fig. 16.9 Surface ages at Cresta de Sacramento

(Greilich and Wagner 2006; Fig. 16.10). With better knowledge on the uncertainty budget, three age groups could be identified:

(i) Very young ages from samples that had been recently exposed
(ii) Ages of the last exposure to light related to activities during the periods of the Paracas, Nasca, and Wari cultures
(iii) Geological burial ages for two fanglomeratic boulders (see Fig. 16.10 inset)

We could not, however, find in every case a clear relation between the stone (sub-)structure the sample was taken from and the age and conclude that reworking affected the surface ages to a larger extent than previously thought. This is

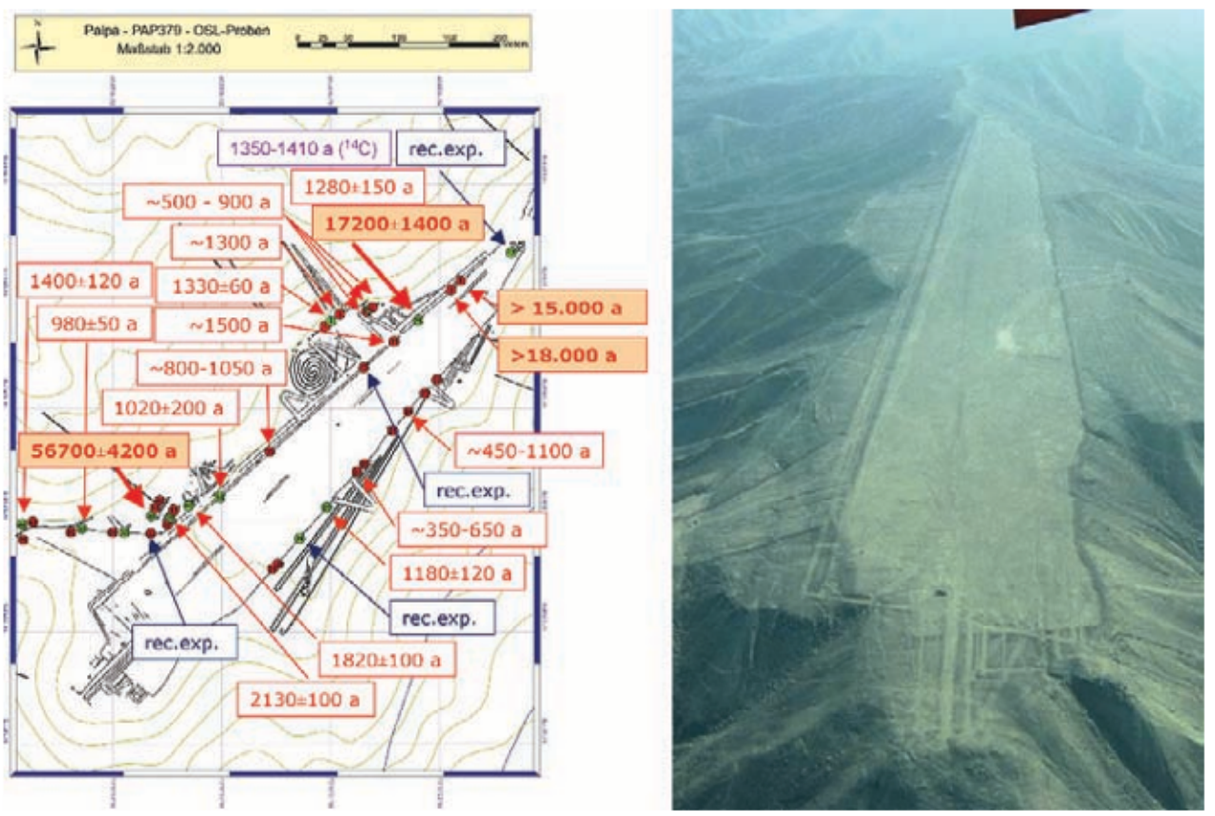

Fig. 16.10 Surface ages at geoglyph PAP-379. (Pampa de Llipata, Aerial image: I. Unkel.)

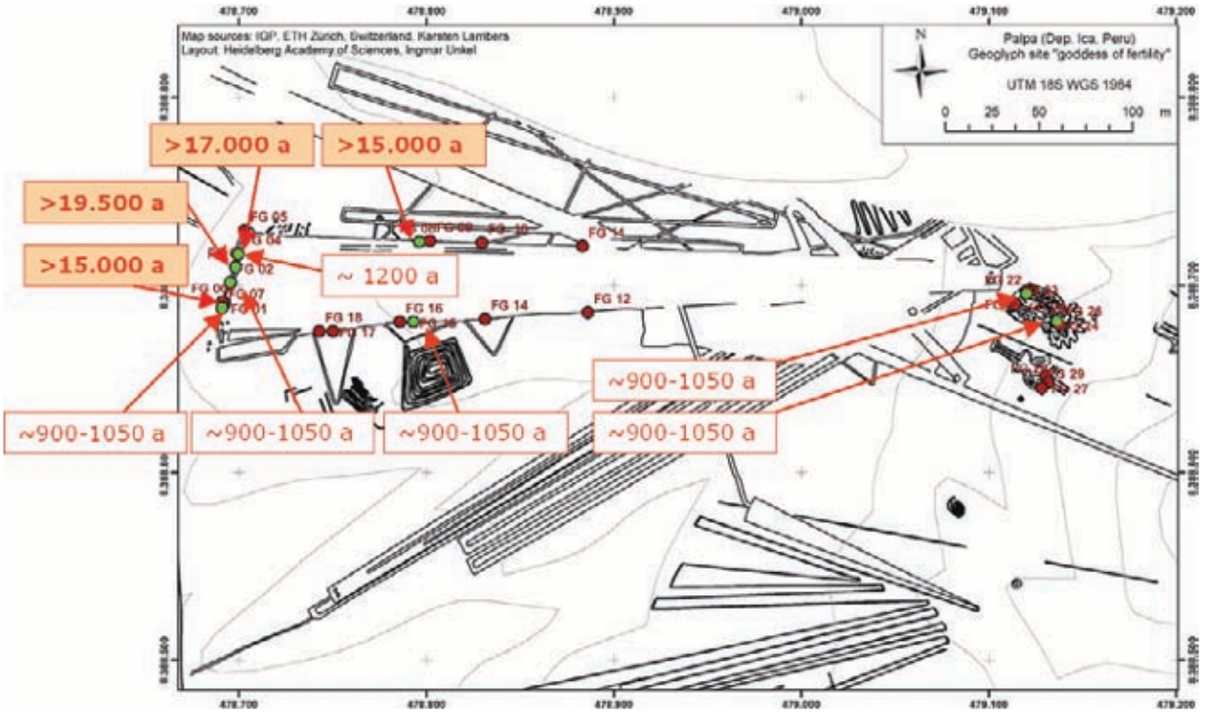

Fig. 16.11 Surface ages at geoglyph, 'Goddess of Fertility'

supported by the findings at the 'Goddess of Fertility' and 'Cerro Carapo', where for the first, no significant difference were identified between figurative human-like geoglyphs and abstract geoglyphs where the latter are believed to be younger (Fig. 16.11; Table 16.1). Instead, a remarkable accumulation of ages around 1000

Table 16.1 Equivalent doses and age results for samples

Sample	Dose/Gy	Age/a	Sample	Dose/Gy	Age/a
FG01BS1	>60	>15.000	CC02BS1	<0.2	<50
FG02A1S1	>78	>19.500	CC03AS1	3.6–4.2	900–1050
FG02A2S1	4.8 ± 1.7	1200 ± 400 a	CC05AS1	3.6–4.2	900–1050
FG02B1S1	>90	>22.500	CC06CS1	~8.1	~2000
FG02B2S1	3.6–4.2	900–1050	CC07BS1	3.6–4.2	900–1050
FG03AS1	4.8	1200	CC08AS1	1.8–2.4	450–600
FG04BS1	>69	>17.000	CC09AS1	1.8–2.4	450–600
FG08AS1	>72	>18.000	CC10AS1	3.6–4.2	450–600
FG08BS1	>60	>15.000	PT01CS1	>48	>12.000
FG15AS1	3.6–4.2	900–1050	PT02CS1	0.6–1.8	150–450
FG17AS1	3.6–3.9	900–1000	PT06BS1	>21	>5.200
FG20AS1	3.6–4.2	900–1050	PA03AS1	3.6–4.2	900–1050
FG26AS1	3.6–4.2	900–1050	PA03BS1	~4.2	~1050
			PA04CS1	~3.6	~900
			RF01AS1	>72	>18.000
			RF02AS1	>72	>18.000
			RF03AS1	~6.0	~1500
			RF05AS1	6.0–6.6	1.500–1.650

Sites 'Goddess of Fertility' (FG), Cerro Carapo (CC), Rio Palpa valley (PT), Pernil Alto (PA), and Royal Family (RF), showing a remarkable grouping. Here, the range of single equivalent doses in the ROIs is reported and a common dose-rate of 4 mGy/a is assumed.

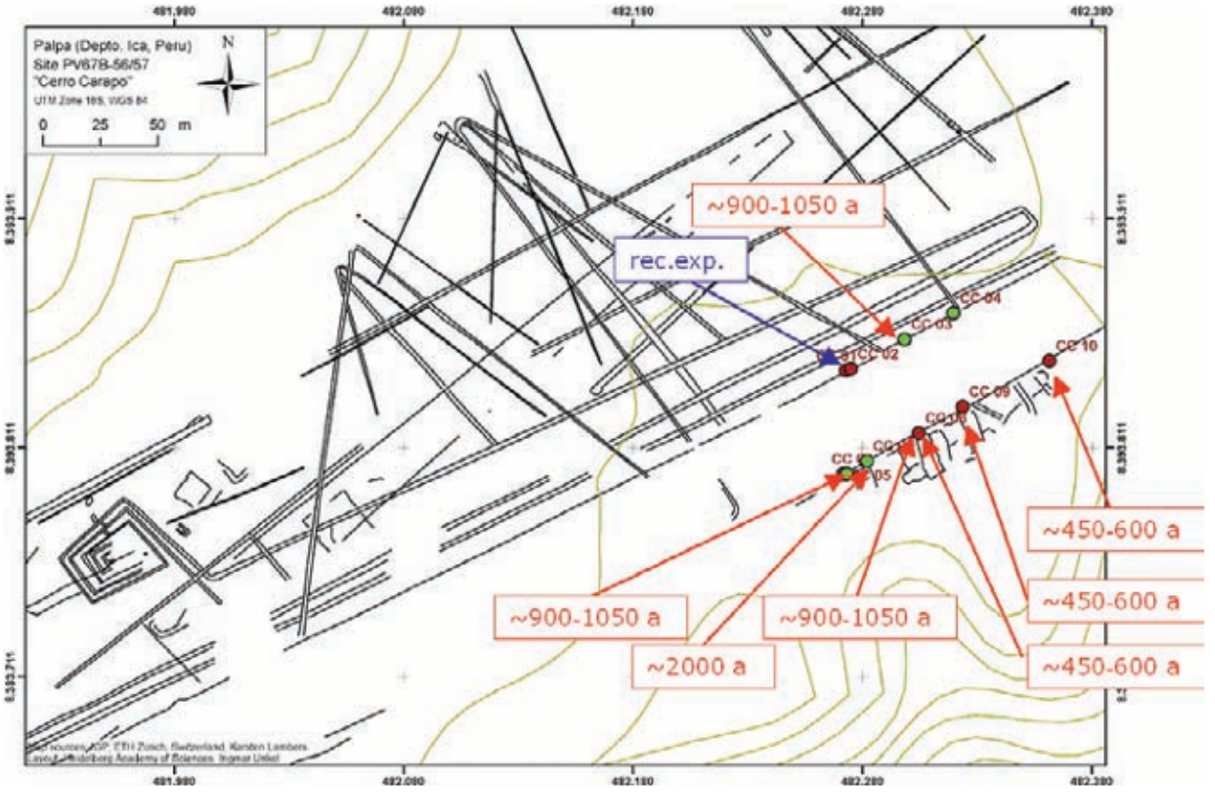

Fig. 16.12 Surface ages at Cerro Carapo

a was found – almost outside the chronology established during the Nasca–Palpa project (Unkel and Kromer, this volume) – at the 'Goddess of Fertility', Cerro Carapo (Fig. 16.12), and Pernil Alto. Furthermore, a considerable number of samples exhibited geological ages although coming from small stones that were easy to carry as opposed to the large boulders at PAP379. A possible conclusion is that they were not moved during daylight which seems puzzling. The influence of later reworking can also be clearly identified at the southwestern edge of Cerro Carapo where stones were used to build houses adjacent to the geoglyph.

16.6 Conclusion

Luminescence dating of granitoid stone surfaces is feasible and gives reliable results. The OSL ages date the events when the surfaces had been exposed for the last time to daylight. During the building of geoglyphs the light exposure was sufficient for resetting the OSL signals in the minerals at the stone surface. The cases for which the OSL ages disagree with archaeological evidence can be readily explained. Although the analytical uncertainties of rock surface dating are still considerable, they are in principle understood and can be improved.

The age range of our approach of surface dating covers about the last 100,000 years, which is the same as the conventional OSL dating. Furthermore, luminescence dating of rock surfaces has – apart from architectural history and

archaeology – also a unique potential for geomorphology as shown here and by Kadereit et al. (this volume). There is potential for HR-OSL also in other fields of luminescence dating. Initial data of coarse-grained sediments are also presented by Kadereit et al. (this volume); further applications are the in situ dating of 'supergrains' to extend the age range of OSL dating, isochrone dating for small surface finds of pottery, better authenticity tests, and slag dating. We also believe that challenging, non-standard luminescence dating applications, including rock surfaces (Woda 2007), can benefit from studying the properties of their samples in detail with HR-OSL and thus tailoring a dedicated procedure for the use of conventional OSL equipment.

Part V
Geomatics

Chapter 17
Virtual Archaeology – New Methods of Image-Based 3D Modeling

Armin Gruen

Abstract The latest developments in sensors and data processing technology have strongly influenced many disciplines and have led in many cases to completely novel ways as to how the respective work is conducted, with new possibilities for improved data acquisition, handling, and analysis. Archaeology and cultural heritage are definitely among those fields that have drawn many advantages from this situation. Advanced 3D modeling of landscapes, sites, single architectures, statues, findings, and artifacts have given the experts in the field and office new tools in their hands for better analysis and interpretation of processes, developments, and relations.

This chapter, after a brief review of currently available sensor technology and an introduction into the photogrammetric data acquisition and processing procedures, shows how this technology works and what kind of products can be generated. We touch upon the use of satellite, aerial, and terrestrial images, but also address laser scanning and structured light systems. The use of different imaging sensors in the case of the recording of large sites is shown, presenting results from our Bamiyan, Afghanistan project. With our project Tucume, Peru, we demonstrate how we can go back in time with image-based techniques. With different examples of terrestrial applications we indicate the wide variety of available sensors.

17.1 Introduction

This contribution aims at demonstrating how the digitization and virtualization of archaeology and cultural heritage can take advantage of some of the latest technologies. We limit ourselves to image-based techniques. That is, we look at

A. Gruen (✉)
ETH Zurich, Institute of Geodesy and Photogrammetry, ETH Hönggerberg
HIL D 43.2, 8093 Zurich, Switzerland
e-mail: agruen@geod.baug.ethz.ch

M. Reindel, G.A. Wagner (eds.), *New Technologies for Archaeology*,
Natural Science in Archaeology, DOI 10.1007/978-3-540-87438-6_17,
© Springer-Verlag Berlin Heidelberg 2009

procedures that are capable of turning images into 3D or even 4D models and can record dynamic processes as well (Gruen 2008).

Images may come from a wide range of different sensors and platforms. Earth-observing satellite platforms carry increasingly high-resolution imaging sensors with stereo capabilities. Digital aerial cameras of various types collect images at an unprecedented speed and amount. For instance, Pictometry currently collects oblique aerial images with eleven aircraft and as many five-camera systems over 900 European towns. This will result in 1.1 GB of imagery for every sqkm at a resolution of 12–15 cm and a positioning accuracy of 50 cm.

Still video cameras and camcorders are nowadays available in great numbers and can, after calibration, also be used for photogrammetric purposes. In Japan alone 43.5 million 3G phones were sold in 2006. GPS capabilities were available for 45 out of 98 models for self- and remote location tasks and almost all included digital cameras. We have lately investigated the suitability of using mobile phones in photogrammetry (Gruen and Akca 2007), showing the great potential of these devices.

For quite some time imaging techniques have no longer been restricted to the use of photographic cameras or even to the visible part of the electromagnetic spectrum. Photogrammetry and remote sensing are defined as image-based modeling techniques, which allow for the extraction of both geometrical and semantic information from images. Efficient (accurate, reliable, and fast) processes of transforming raw image data into value-added 3D model information are nowadays of utmost importance for the creation of geospatial databases.

On the technology side we have now at our disposal a vast array of relevant and efficient data acquisition tools: high-resolution satellite images; large-format digital aerial cameras; hyperspectral sensors with several hundreds of channels; interferometric radar from space, aerial, and lately even from terrestrial platforms; laser scanners of aerial and terrestrial type, partially with integrated cameras; model helicopters and airplanes with off-the-shelf digital cameras; panoramic cameras; and a large number of diverse consumer-type still video cameras, camcorders, and even mobile phone cameras. These are augmented by structured light systems and GPS/IMU systems for precise navigation and positioning.

Automated and semi-automated algorithms allow us to process the data more efficiently than ever before and Spatial Information System (SIS) technology provides for data administration, analysis, and other functions of interest. Finally, visualization and animation software are also becoming affordable at better functionality and lower cost. This sets the scene for a totally new evaluation of the tools and techniques for use in archaeology and cultural heritage recording and modeling.

We have conducted in the past a number of projects of large-site modeling, that have shown the potential, but also the limitations, of some of these new technologies. These can be consulted on our homepage www.photogrammetry.ethz.ch under PROJECTS. Two of them, the Bamiyan and the Tucume projects, are

briefly described in this chapter, because they represent very special cases of 3D modeling. We also report here about our experiences which we gained with the automated processing of terrestrial still video images for bas-relief modeling and with the use of a structured light system and of a laser scanner for the modeling of statues.

17.2 Object Recording and Modeling in Cultural Heritage Documentation

In photogrammetric recording and modeling, we distiguish the following components in data handling: acquisition, processing, administration, analysis, and representation. Figure 17.1 shows the data and information processing pipeline, as it is usually used in order to turn images into models.

Data acquisition: Whereas in the old days we only had one type of sensor available—the photographic camera—we nowadays have a great variety of different devices: CCD and CMOS still video cameras of various geometrical, spectral, and radiometric resolutions, camcorders, linear array cameras of various types (among these three-line scanners and panoramic cameras), laser scanners, X-ray and electronic imaging devices, microwave and ultrasound sensors, GPS/INS, videotheodolites, and so on. Several aspects have led to new concepts in data acquisition: the ease of image taking, the possibilities for fast image processing, and the need for real texture mapping. Although traditionally the art of photogrammetry consisted in taking and processing as few images as possible, very often from a fixed stereobase, we nowadays experience a paradigm shift towards the collection of large numbers of images (image sequences), taken from all possible directions, in order to facilitate automated processing and good photorealistic texture mapping. Also the combination of different sensors (e.g., images and laser scans) is a viable means to support automated processing.

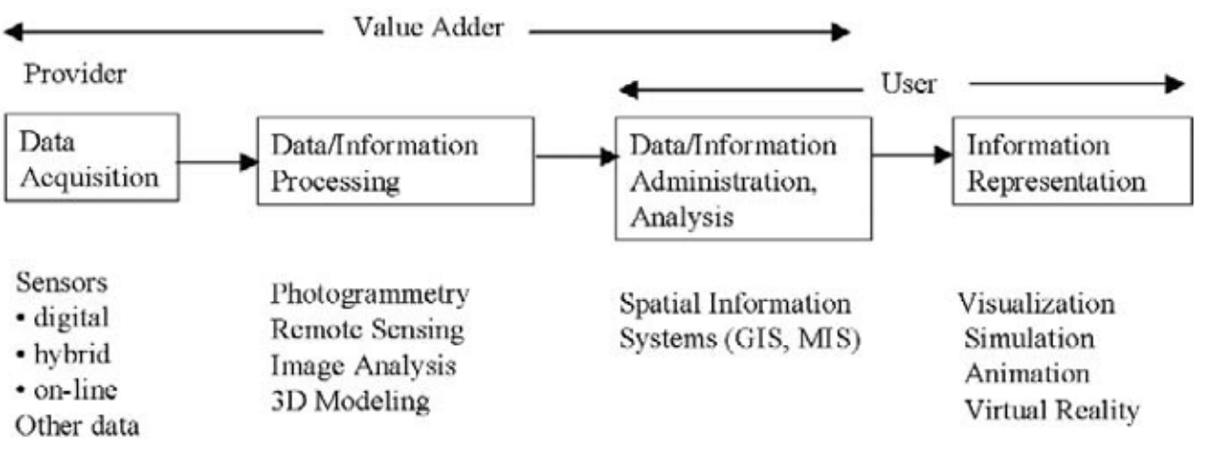

Fig. 17.1 Data and information pipeline, as used in photogrammetry

Data processing: The increased power of computers and the availability of application software allows for much faster processing of the data and for new kinds of products. Also, with digital photogrammetry the costs of systems are reduced drastically. The automation of processing is the key topic in research and development today. However, one has to note that fully automatic processing procedures are still in a state of infancy. The related results are mostly not reliable enough and require a large amount of postediting. One can observe very often that results generated by automated methods by far do not match the requirements of the user of cultural heritage data. Therefore semi-automated processing techniques have lately found much interest and offer a way out of the existing dilemma.

Data administration and analysis: The use of spatial information systems (SIS) has opened new venues for the storage and administration and also for the analysis of data. The database functions of SIS allow for the storage of consistent, nonredundant data, both for geometric and attribute information. This way up-to-date vector and raster data can be combined with information from archaeological records. Database functionality also provides for analysis functions that would otherwise have to be implemented with much effort. Some SIS also include 3D visualization modules, which are very important in cultural heritage applications.

Data representation: Traditionally the results of processing were presented as graphical plots (maps and plans) or in the form of lists and tables. Nowadays 3D visualization products are standard. A great amount of commercial software is available for this purpose, but in most cases with severe limitations. The key parameters to be observed here are true 3D modeling, real-time capability, quality of rendering, and size of datasets. There is no package available yet that would satisfy all requirements simultaneously in a reasonable way. Beyond pure visualization, techniques from virtual reality, augmented reality, simulation, and animation are also very useful for cultural heritage applications.

Photogrammetry and remote sensing are image-based techniques for the extraction of metric and semantic information from images. Originally terrestrial photogrammetry, aerial photogrammetry, and satellite remote sensing developed along separate lines, both in terms of types of sensors used and processing methodology and tools. Today, within an almost totally digital environment, we see a strong trend towards convergence. This opens the path for a much more cost-efficient use of a variety of different sensor data and processing tools.

As opposed to photogrammetry, which is strongly geometry oriented, remote sensing is looking more into the radiometric properties of images, in order to extract useful information in particular for landuse applications. However, the steady increase of the geometrical resolution of satellite images puts the 3D modeling issues also there on the top of the priority list. Figure 17.2 shows the workflow of the photogrammetric/remote sensing process for 3D model generation.

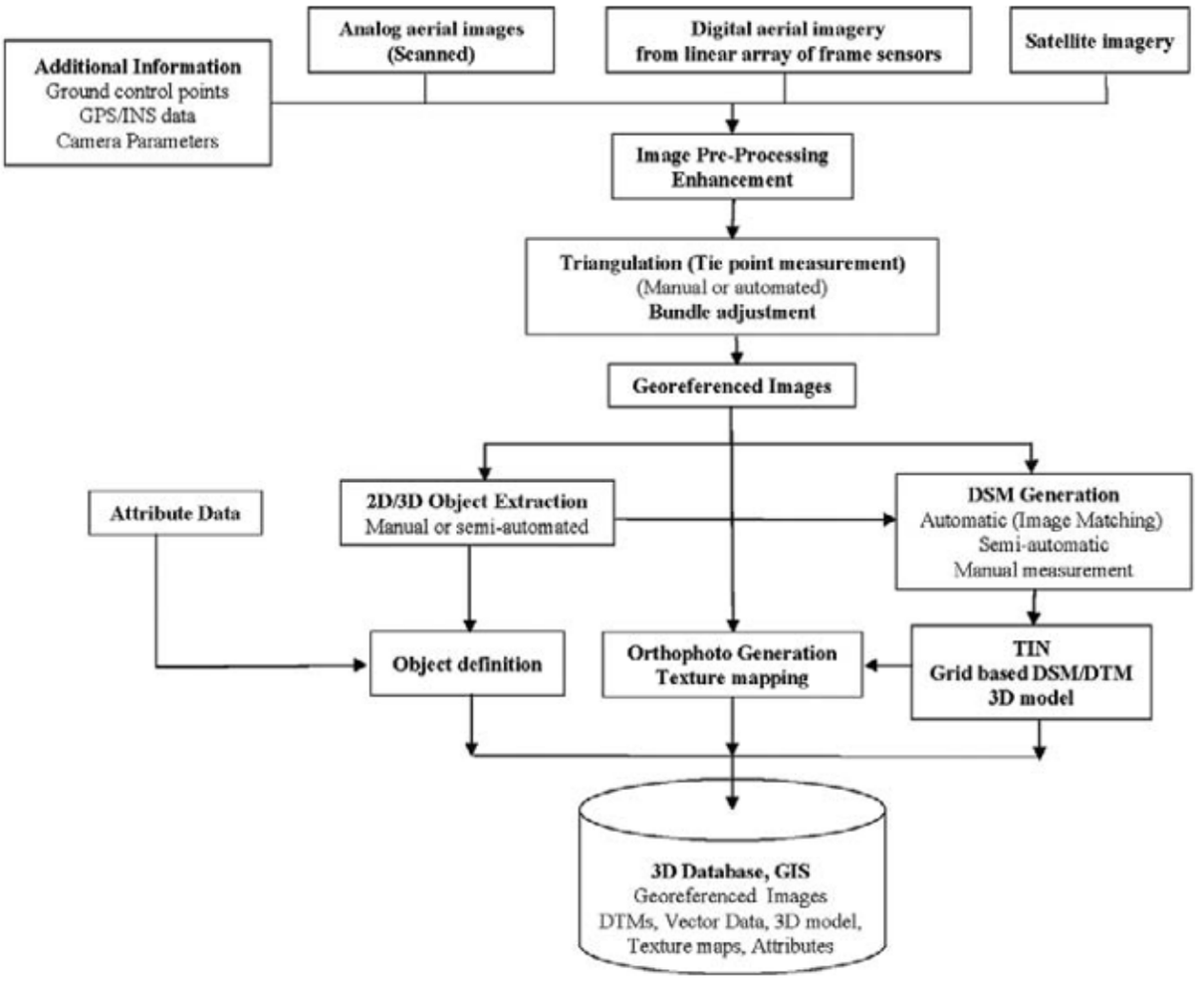

Fig. 17.2 Workflow and products of the photogrammetric/remote sensing process for 3D model generation

17.3 Relevant Satellite Sensors and New Aerial Digital Cameras

The development and increased availability of high-resolution, multispectral and stereo-capable satellite sensors and of a new generation of digital large-format aerial cameras is very crucial for the efficient modeling of large sites. Table 17.1 shows an overview of high-resolution satellite sensors (including medium-resolution ASTER because of its good availablity and low costs), which might be useful in cultural heritage applications. There is a great variety of image products available in terms of geometrical resolution (footprint), spectral resolution (number of spectral channels), and costs. All images of Table 17.1 are acquired with digital sensors, using linear array CCD camera technology. For precise processing this requires a particular sensor model and the related special software (see Chap. 17.4).

The latest satellite sensor WorldView-1 provides images with 0.5 m spatial resolution in panchromatic stereo mode, a 1.7 day revisit period, and collects up to 750,000 million sqkm of images per day. This takes satellite imagery into the domain of medium-resolution aerial images and provides for exciting new application opportunities.

Table 17.1 Main characteristics of high and medium resolution pushbroom sensors carried on satellites

Sensor	# Cameras	Focal Length (mm)	Stereo	Incidence Angles (°)	Channels	Ground Resolution (m)	Swath Width (km)	#Pixels/ Line	Providers
Quickbird	1	8800	L[1]	up to ±30	PAN RGB, NIR	0.6 2.4	16	27000	Digitalglobe http://www.digitalglobe.com
IKONOS-2	1	10000	L[1]	up to ±60	PAN RGB, NIR	1 4	11	13500	GeoEye http://www.geoeye.com
Orbview-3	1	2820	L[1]	up to ±45	PAN RGB, NIR	1 4	8	8000	GeoEye http://www.geoeye.com
EROS-A1	1	3500	L/C[1]	up to ±45	PAN	1.8	14	7800	ImageSat Int. http://www.imagesatintl.com
ALOS-PRISM	3	2000	L	0 ±24	PAN	2.5	70 35	28000 14000	RESTEC, Japan http://www.restec.or.jp
SPOT-5/HRG	2	1082	C	up to ±27	PAN RG, NIR	5 (2.5)[2] 10	60	24000 6000	SpotImage http://www.spotimage.com
SPOT-5/HRS	2	580	L	±20	PAN	10	120	12000	Spotimage http://www.spotimage.com
ASTER-VNIR	2	329	L	0 0, –27	RG NIR	15	60	5000	LP DAAC (NASA)

L = along-track; C = across-track, PAN = panchromatic, NIR = Near infrared.
[1] One-lens sensor with ability to rotate up to a certain off-nadir angle.
[2] Supermode.

There are and have been a number of film-based photographic satellite cameras in use (Jacobsen et al. 1999). This includes the U.S. Corona satellite (2–3 m footprint, B/W, stereo, US$ 24 for a scanned image). The availability of images and the costs can be checked through a number of image providers over the Internet (Table 17.1).

Aerial photogrammetry is nowadays also going fully digital. Large-format digital aerial cameras are offered by a number of manufacturers since the year 2000 and these cameras have found their way into many projects. We have actually witnessed a worldwide replacement of the traditional film-based aerial cameras by this new generation of digital cameras. There are currently six different digital aerial large-format cameras on the market. We define 'large-format' as having more than 10,000 pixels in at least one image format direction.

In addition, there are many consumer-type still video cameras available, some of them with up to a 12 Mpixel image format, or even semi-professional ones with up to 39 Mpixel, which are also used on aerial platforms, but none of them will even closely match the format of these professional photogrammetric cameras.

17.4 New Methods for Digital Photogrammetric Processing

The new generation of sensors has a number of particular properties that require new approaches in processing, if the inherent accuracy and data processing potentials are to be used. Images from CCD sensors do have a much larger dynamic range than film-based images, so there is more detailed radiometric information present in those images. This is important in particular in areas of shadows and areas close to saturation. Linear array sensors do have almost parallel projection in the flight direction, which leads to fewer occlusions and gives better orthoimage products. Linear array imagery, if acquired in multi-image mode (e.g., by three-line scanners or multiline scanners), has 100% overlap for all strip images over the same area. This delivers better precision and reliability of results. Finally, linear array imaging systems use GPS/IMU sensors for position and attitude determination of the imaging sensor, which can be used advantageously at different stages of the processing chain (Fig. 17.2). Taking into consideration these facts and other parameters and constraints, we have developed some new methods and the related software packages for high-accuracy processing of aerial and satellite linear array images.

In recent years we have done a number of experiments and tests with different types of sensors with respect to georeferencing (orientation), measurement accuracy (point positioning), Digital Surface Model (DSM) determination, and orthoimage generation (Gruen and Zhang 2003a; Gruen et al. 2003;

Zhang and Gruen 2004; Kocaman et al. 2006, 2007; Poli et al. 2004; Gruen and Zhang 2003b; Eisenbeiss et al. 2004; Gruen et al. 2005; Gruen et al. 2007; Gruen and Wolff 2007). These investigations have shown that with the proper methodology and software one can achieve extraordinary results. Both with aerial and satellite images we can get a georeferencing accuracy of better than one pixel. In automated DSM generation we can achieve a height accuracy of one to five pixels, depending on factors such as surface roughness (flat and smooth or mountaineous), land-use parameters (forest, desert, urban areas), local texture (sand, snow), time and month of image taking, image quality, and so on. Accurate DSM/DTM data are not only an important product in their own right but are also necessary for the derivation of good quality orthoimages and textured models.

17.5 Status of Automated Processing

The automation of photogrammetric processing is obviously an important factor when it comes to efficiency and costs of data processing. The success of automation in image analysis depends on many factors and is a hot topic in research. Progress is slow and the acceptance of results depends on the quality specifications of the user. Also, the image scale plays an important role in automation. Potentially, the smaller the scale is, the more successful automation will be. Therefore it is a bit difficult to make firm statements that would be valid in all cases. However, in general one can state that

- Orientation/georeferencing can be done partially automatically.
- DSM generation can be done automatically, but may need substantial postediting.
- Orthoimage generation is a fully automatic process.
- Object extraction and modeling are possible in semi-automated mode at best.

For the 3D modeling of buildings and other manmade objects we have developed and tested a methodology called CyberCity Modeler (CC-Modeler). This is a semi-automated technique, where the operator manually measures a weakly structured point cloud in the stereomodel, which describes the key points of an object. The software then turns this point cloud automatically into a structured 3D model, which is compatible with CAD, visualization, and GIS software. Texture can be added to the geometry to generate a hybrid model. A DTM can also be integrated. An example using CyberCity Modeler for 3D modeling of terrain and buildings in an archaeological application was conducted for the pre-Hispanic site of Xochicalco, Mexico, where an urban center was reconstructed from two aerial images (Gruen and Wang 2002; Fig. 17.3).

Fig. 17.3 Partially textured 3D model of Xochicalco, derived semi-automatically from a stereo pair of aerial images using CyberCity Modeler

17.5.1 Automated Model Generation in Close-Range Photogrammetry

Fully automated model generation from images is a hard and basically still unsolved problem. Image matching is generally defined as the establishment of correspondences between two or more images to reconstruct surfaces in 3D. In order to determine these correspondences, the image primitives to be matched must be defined. Afterwards a similarity measure is computed and evaluated between primitive pairs or multiple sets. Then the 3D point cloud can be generated. The main reason for the problems in image matching is the difficulty in finding unique matches. There may exist multiple possible matches or no match at all, because of partly or fully occluded features or changes in appearance from image to image due to light and geometric variations. We have developed image-matching techniques through several stages (Gruen 1985; Gruen and Baltsavias 1988; Baltsavias 1991; Zhang and Gruen 2004: Zhang 2005: Remondino and Zhang 2006).

The latest approach essentially consists of three components: the image preprocessing, the multiple primitive multi-image (MPM) matching, and the refined matching procedure. A TIN (Triangular Irregular Network) form DSM is reconstructed from the matched features by using the constrained Delauney triangulation method. This TIN in turn is used in the subsequent pyramid level for the derivation of approximations and adaptive computation of some matching parameters. Finally and optionally, least squares matching methods can be used to achieve more precise results for all matched features and for the identification of some false matches. For more details on image matching

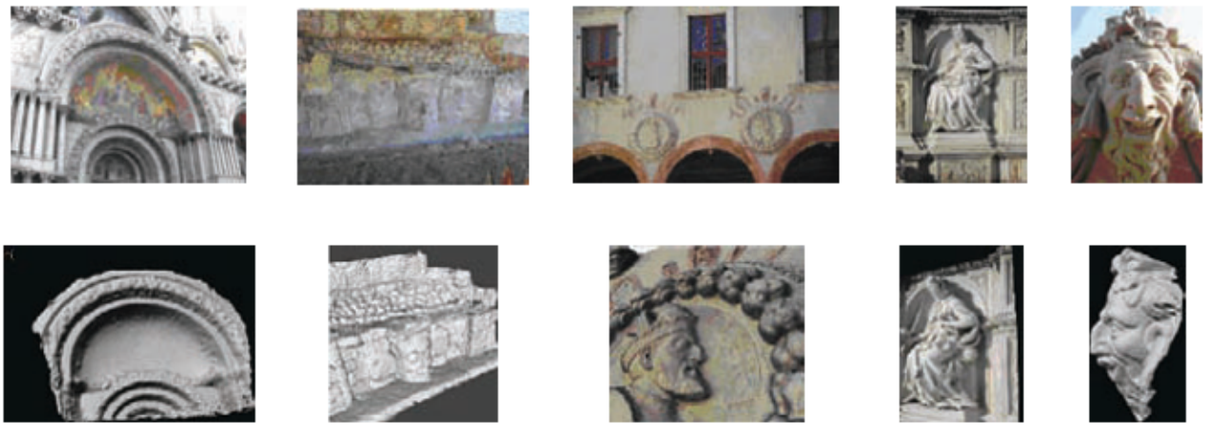

Fig. 17.4 Typical cultural heritage objects requiring detailed and accurate 3D models for documentation, conservation, analysis, restoration, or manufacturing of replicas. *Upper row*: images; *lower row*: 3D models, generated automatically by image matching. (From Remondino et al. 2008)

of close-range images see Remondino et al. (2008), Zhang and Gruen (2004), and Zhang (2005). Figure 17.4 shows some examples of automated image matching.

17.5.2 Object Scanning with Structured Light Systems

A structured light system is an active stereo vision method. The key feature of the system is the replacement of one of the cameras by an active light source, which illuminates the object with a known pattern. This solves the correspondence problem in a direct way. Many variants of the active light source exist (Beraldin 2004; Blais 2004).

Topometrical high-definition 3D scanners, optimized for the requirements of arts and cultural heritage, allow the 3D digitization of art objects and paintings with high resolution and accuracy. Also, the texture and/or color of the object can be recorded, offering a one-to-one correspondence of 3D coordinates and color information. Topometrical scanners are based on the principal of optical triangulation using structured light: a special projection unit projects a known pattern of light onto the object. A digital camera records the image of the object together with the projected pattern.

State-of-the-art systems (e.g., Breuckmann optoTOP-HE, optoTOP-SE, triTOS) use special projection patterns with a combined graycode/phase-shift technique, which guarantees an unambiguous determination of the recorded 3D data with highest accuracy. The time for a single scan takes about one second for a 1.4 Mpixel camera and a few seconds for high-definition cameras with 4–8 Mpixel.

17.6 Terrain Modeling/Natural Heritage Site Generation

The terrain is a key element in all georelated applications and investigations. Therefore 3D modeling of terrain is an ever-relevant issue. The status of terrain modeling varies worldwide very much. Although there already exist worldwide

Digital Surface Models (DSMs), for example, SRTM-based. They show the terrain only in 2.5D representation, have many gaps, and are partially very inaccurate. The need for more detailed modeling is obvious in many applications. Mapping efforts are underway in many countries. Sometimes LiDAR is used, giving an accuracy of 0.5 m in open terrain and 1.5 m in vegetation-covered terrain. In larger projects satellite stereo images are combined with aerial images in order to generate new DSMs over vast areas.

Such efforts can only be successful if the required data can be generated in an automated or at least semi-automated way. Although image matching has a long history of research and development, the problem is not fully solved yet. New methods for image matching, as implemented for instance in our software SAT-PP (Gruen and Zhang 2003b; Zhang 2005; Zhang and Gruen 2004), have led to some progress and deliver much better results than the current commercial packages.

Sometimes DSMs may be derived from already existing analog images and maps (Gruen and Murai 2002). Certain studies may require the analysis of changes occurring over time. Image-based techniques allow us to go back in time and process existing older images. This has been done with the archaeological site of Tucume, Peru, where a 3D model was produced from aerial images from the year 1949 (see Chap. 17.8.1 and Figure 17.5). Sometimes

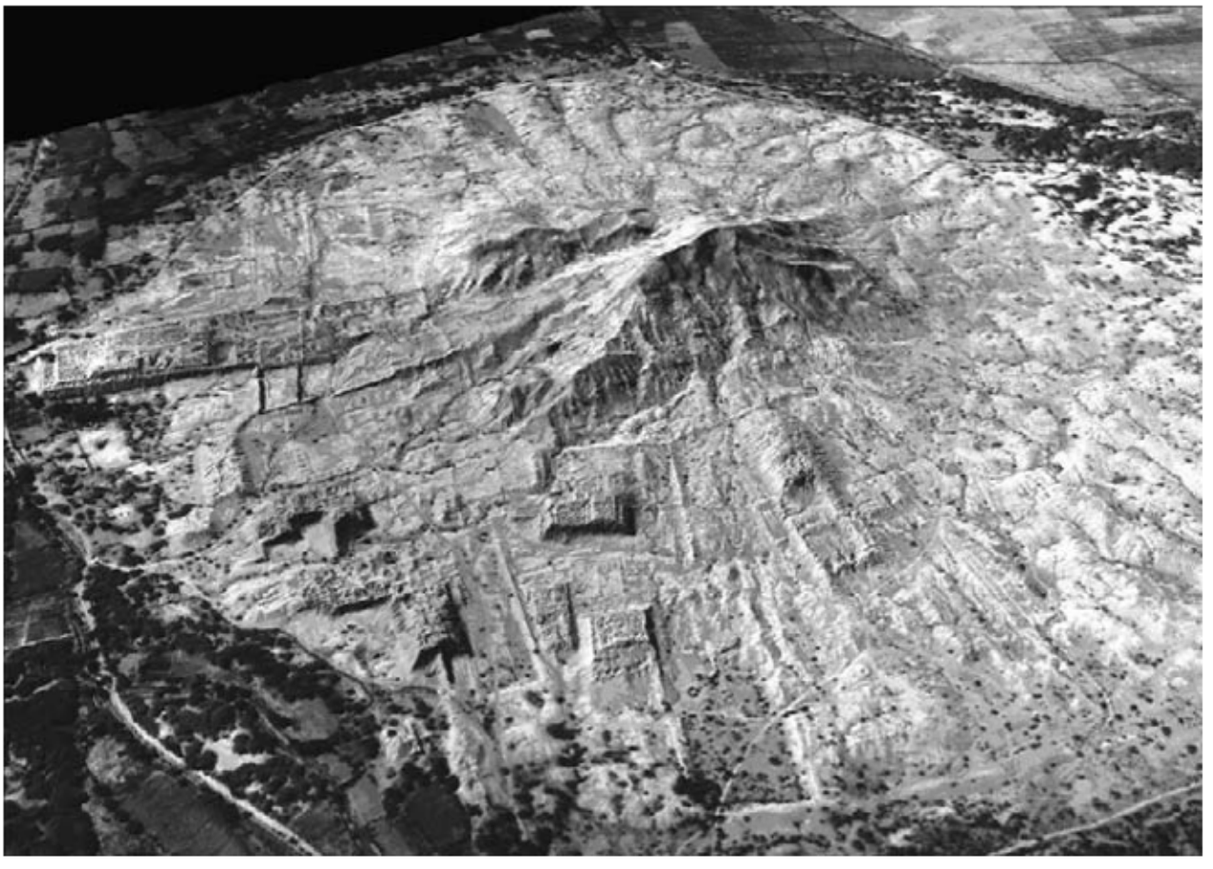

Fig. 17.5 View of the 3D model of the Tucume adobe complex. Overlaid is the texture from 1949 aerial images. To the left is Huaca Larga, a huge adobe building of 545 m base length, with an Inka stone building on top

images from different platforms, sensors, and times may have to be combined in 3D modeling, as in the case of our Bamiyan project in Afghanistan (Gruen et al. 2004a,b, 2005, Chap. 17.8.2).

17.7 Visualization of 3D Models

Visualization of 3D models is an essential function. A model that cannot be seen at all or can only be seen with great time delay is losing much of its value. Software packages for terrain visualization are abundantly available (http://www.Tec.army.mil/TD/tvd/survey/survey_toc.html).

Although the conceptional aspects of computer graphics algorithms are quite straightforward, it is always the implementation and the quality of the key components of the computer platform that define the performance. Geovisualization packages are complex software systems, with strong dependencies on the hardware as well. In order to represent an efficient system, all components have to perform well individually, but also their interaction must be solved in an acceptable manner.

When analyzing visualization software a major consideration is whether interactive or even real-time performance is required. The fascination of real-time performance is intriguing enough so that most users, once they have been exposed to it, will not want to do without it. Also, for many analysis applications, real-time performance is just a must for the sake of economy and efficiency of operation.

One can classify visualization software on the basis of its real-time performance, given a certain computer configuration. In this context one can distinguish high-end, middle-class, and low-end systems (e.g., Skyline, http://www.skylinesoft.com; IMAGINE VirtualGIS, http://www.erdas.com/software/ProductModules.asp; and Cosmo Player, http://cai.com/cosmo; in this order). Although low-end software is increasingly available as freeware over the Internet, the other levels of quality can only be reached by paying, in parts dearly, for the software. In Gruen and Roditakis (2003) we have reported our experiences with commercial visualization packages. None of them, when used in interactive mode, showed really satisfying performance.

Although very many terrain visualization packages are available worldwide, there is still the need for development of more efficient software, combining ease of use with speed and quality of rendering for large and very large datasets. However, one must note that much progress has been achieved in the past few years. Yet, the interested user of such packages is strongly advised to check the performance beforehand by using his or her typical datasets. Certain packages may perform quite well when only 2.5D terrain data are used, however, they may exhibit problems with truly 3D data, especially if vertical building faces are textured.

17.8 Examples

In recent years we have modeled a number of large natural and cultural heritage sites that can be consulted on our homepage www.photogrammetry.ethz.ch under PROJECTS. In the following we report the results and experiences gained with the projects Tucume (Sauerbier et al. 2004) and Bamiyan (Gruen et al. 2004a,b, 2005). We also show two typical examples of terrestrial sensor applications: a structured light system (Weary Herakles, Museum Antalya, Turkey) and a laser scanner (Escher statue, Zurich, Switzerland).

17.8.1 Tucume, Peru: 3D Reconstruction of an Adobe Architecture Using Old Imagery

In the region of Tucume in northern Peru, in the department of Lambayeque, the so-called "Pyramids of Tucume" represent a unique example of adobe architecture built during different periods of pre-Hispanic cultures. Most of the buildings were constructed during the Late Intermediate period (1000–1400 AD) and later also used by the Incas until the arrival of the Spaniards in 1532. From the Cerro La Raya, a characteristic hill in the center of the site, 26 adobe buildings are visible, the largest one, Huaca Larga, with a base length of 545 m, 110 m in width, and 21 m in height.

As the adobe structures are heavily affected by wind erosion and the occasional El Niño rains, the architecture should be modeled as well as possible in an unaffected state. For this reason, aerial imagery from the years 1949 and 1983 were acquired from the Peruvian SAN (Servicio Aerofotográfico Nacional, Lima), which show the adobe complex in two different states. As no control points existed for the 1949 images, two maps and the 1983 imagery had to be used for the orientation. The orientation of the 1983 images was accomplished on an analytical plotter WILD S9, whereas for the orientation of the 1949 images, both the analytical plotter and a digital photogrammetric workstation Virtuozo 3.1 were used. The photogrammetric products derived from the oriented 1949 images are a manually measured DTM, an automatically generated DSM, an orthomosaic and a photorealistic 3D model (Sauerbier et al. 2004). The hybrid model was visualized with the software packages Skyline Terra Builder/Explorer Pro (Fig. 17.5) and ERDAS Imagine Virtual GIS. The 3D model now can serve archaeologists and other scientists as a means for documentation, analysis, and presentation of the cultural heritage site of Tucume in a state of preservation as of 1949.

17.8.2 Bamiyan, Afghanistan: 3D Modeling of Natural and Cultural Heritage with Multiple Sensors

The Bamiyan region, situated about 200 km northwest of Kabul in Afghanistan, is one of the most famous Buddhist monument sites worldwide. Global attention

was attracted to Bamiyan when the Taliban regime destroyed the large standing Buddha statues in March 2001. Our main goals of the Bamiyan project were:

- Terrain modeling of the entire Bamiyan area from satellite images for the generation of virtual flights over the UNESCO Cultural Heritage site
- Modeling of the rock cliff from which the Buddhas were carved
- 3D computer reconstruction of the two lost Buddha statues and the remapping of the frescos of the niches
- 3D modeling of the two empty niches where the Buddha statues once stood
- Documentation of the Cultural Heritage area with a topographic, tourist, and cultural information system.

The project is an excellent example of image-based modeling, using many types of images, with different spatial resolutions (Table 17.2). It shows the capabilities and achievements of the photogrammetric modeling techniques and combines large-site landscape modeling with highly detailed modeling of objects by terrestrial images.

Photogrammetric processing was used by our group for different purposes: 3D reconstruction of the Great Buddha statue (Gruen et al. 2004a), 3D modeling of the rock façade (Gruen et al. 2006), and generation of a high-resolution mosaic of the destroyed fresco in the Great Buddha's niche (Remondino and Niederoest 2004), all from terrestrial close-range images (old metric photographs, Internet images, semi-metric images, still video images, and small format tourist images), and the generation of a digital terrain model of the Bamiyan valley and its surroundings from SPOT-5 and IKONOS satellite imagery using SAT-PP (Gruen et al. 2004b). The DTM was generated automatically from SPOT-5 stereo images for an area of 49 × 38 sq km. For texture mapping we used one of the B/W SPOT-5 images, but also a MS (multispectral) IKONOS mosaic for a smaller area of 12 × 18 km^2, containing the rock façade, the village of Bamiyan, and its surroundings (Fig. 17.6).

For the reconstruction and modeling of the Bamiyan cliff, a series of terrestrial images acquired with an analog Rollei 6006 camera was used. The images were digitized at 20 μm resolution and then oriented with a photogrammetric

Table 17.2 Multiresolution data (Geometry and Images) used in the bamiyan project

Source of Data	Year	Image resolution (μm)	Geometry resolution (m)	Texture resolution (m)
SPOT-5 HRG [a]	2003	–	20	2.5
IKONOS [a]	2001	–	5	1
Rollei [b]	2003	20	1	0.5
Sony [b]	2003	4	0.5	0.1
TAF, Kostka [b]	1970	10	0.05	0.01
Frescos, tourist small format[b]	60s & 70s	20	N.A.	0.002

[a]Satellite images.
[b]Terrestrial images.

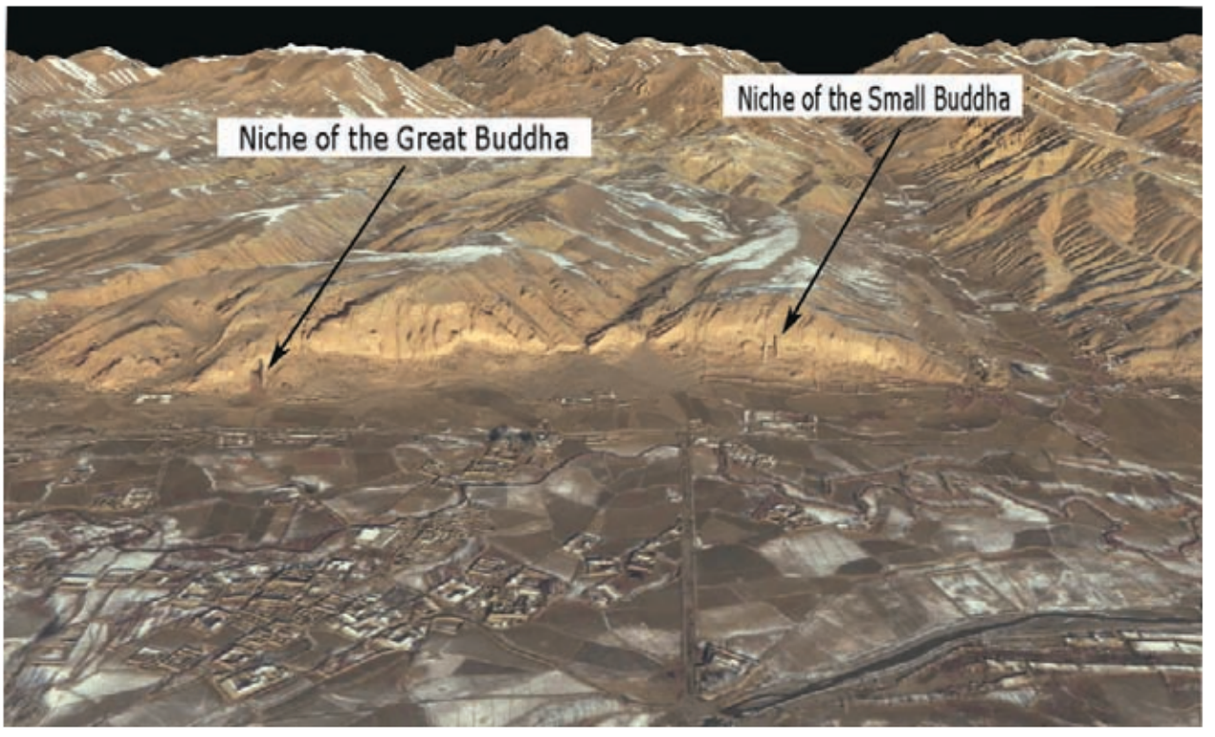

Fig. 17.6 View of the 3D hybrid model, textured with an IKONOS orthoimage mosaic, showing the rock cliff with the now empty niches of the Buddhas

bundle-adjustment. Then manual measurements were performed on stereo-pairs in order to get all the small details that an automated procedure would smooth out. The recovered point cloud was triangulated, edited, and finally textured.

The 3D computer reconstruction of the Great Buddha statue was performed with different image datasets and using different algorithms (Gruen et al. 2004a). Various 3D computer models of different quality, mostly based on automated image measurements were produced. However, in most of the cases, the reconstructed 3D model did not contain essential small features, such as the folds of the robe and some important edges of the niche. Therefore, for the generation of a complete and detailed 3D model, manual photogrammetric measurements were indispensable. They were performed along horizontal profiles at 20 cm interval on three metric images, acquired in 1970 by Professors Kostka and Graz and scanned at 10 μm resolution. The final 3D model of the Great Buddha (Fig. 17.7, right) was used for the generation of different physical models.

The modeling of the empty Buddha niches was performed using five digital images for each niche, acquired with a Sony Cybershot F707 during our field campaign in August 2003. After the image orientation, three stereo models were set up and points were manually measured along horizontal profiles, and the main edges were measured as breaklines. Thus a point cloud of about 12,000 points was generated for the Great Buddha niche. The final textured 3D model is displayed in Fig. 17.7, left.

Fig. 17.7 Textured models of the Great Buddha of Bamiyan (*right*) and its currently empty niche (*left*)

17.8.3 The "Weary Herakles," Antalya, Turkey: Object Scanning with Structured Light Systems

The "Weary Herakles" is a marble Herakles statue dating to the second century AD. The lower part is on display in the Antalya Museum in Turkey (Fig. 17.8). The upper half is currently to be found at the Boston Museum of Fine Arts (MFA).

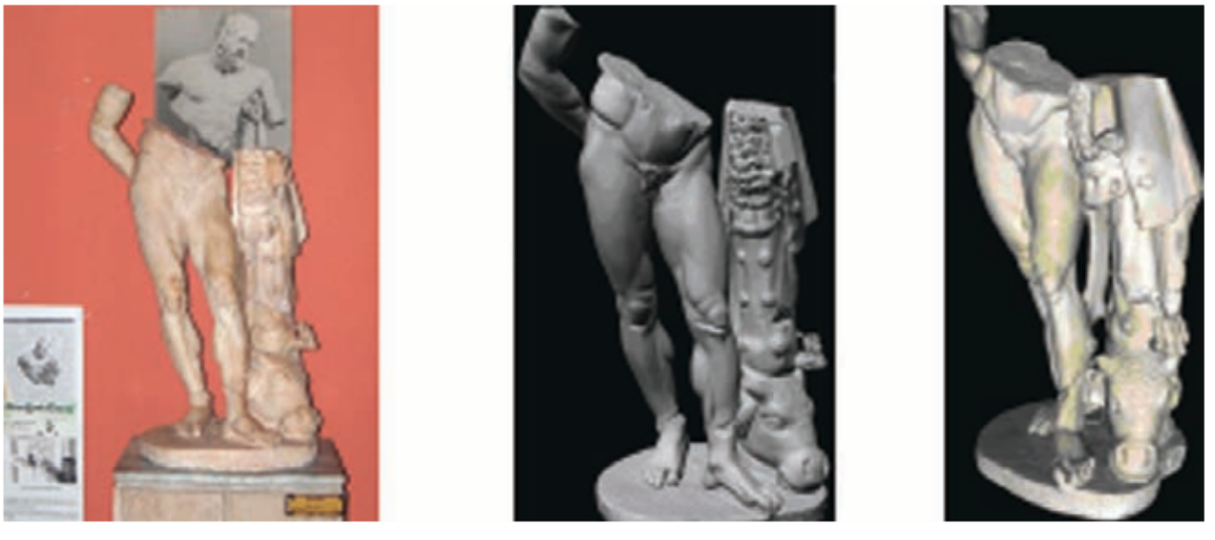

Fig. 17.8 "Weary Herakles" in the Antalya Museum, Turkey (*left*); frontal view of the grey shaded (*central*) and texture mapped model (*right*)

Because both parts are separated geographically, our aim was to record and model both the lower and the upper part and bring these partial models together in the computer, so that at least there the complete statue could be seen, appreciated, and analyzed. The digitization of the lower part of the statue could be realized in the Antalya Museum with a Breuckmann optoTOP-HE structured light system, but access to the Boston Museum was denied.

The scanning campaign was completed in one and a half days of work. The statue is around 1.1 m in height. The whole object was covered with 56 scans on the first day. The remaining 11 scans of the second day were for filling the data holes and occlusion areas. A total of 83.75 million points were acquired in 67 scan files. The pairwise co-registration of the point clouds was done by use of an in-house developed method, called Least Squares 3D Surface Matching (LS3D) (Gruen and Akca 2005).

After the registration step, all scan files were merged and imported into Geomagic Studio^{TM} 6 (Raindrop Geomagic Inc.). The dataset was cropped to include only the area of interest (AOI), concluding with 33.9 million points. A low-level noise reduction was applied. The number of points was further reduced to 9.0 million by applying a subsampling procedure based on curvature information. Some holes on the triangulated surface resulting from inner concave parts were interactively filled by use of the corresponding functions of Geomagic Studio.

Separately taken images, with a 4 Megapixel CCD Leica Digilux 1 camera, were used for the texture mapping. The visualization of the final model was done with the IMView module of PolyWorks^{TM} (InnovMetric Software Inc., version 9.0.2). The textured model was visualized with the viewer of VCLab's Tool (Fig. 17.8).

17.8.4 The Alfred Escher Statue, Zurich, Switzerland: 3D Modeling by Laser Scanning

In Zurich a monument of Alfred Escher, Swiss politician, promoter of the Gotthard Tunnel, railroad entrepreneur, and founder of Credit Suisse as well as of ETH Zurich, is located in front of the main railway station and is approximately 5 m in height. The goal of the project was the generation of a 3D computer model for the production of ten physical replicas of the Escher monument for an exhibition.

The digitization was done with a Faro LS880 HE80 laser scanner, placed on a cherry picker. In total 36 scans were acquired during two half-nights of on-site work. The dataset contains approximately 4.4 million points with an average point spacing of 5–10 mm. For the co-registration of the point clouds our in-house developed algorithms and software of 3D least squares surface matching was used (Akca 2007; Akca and Gruen 2007).

Fig. 17.9 Alfred Escher statue: (*left*) the final 3D computer model, derived from 36 laserscans; (*right*) a physical replica (the missing parts were attached later) at scale 1:2

At the first step, 3–5 tie points per point cloud were interactively measured. Initial approximations were calculated by use of the tie point coordinates in a chained 3D similarity transformation. The final iteration of the adjustment used 20.4 million surface correspondences. After the co-registration step, all point clouds were merged, filtered for noise reduction, subsampled, and triangulated for surface generation.

The 3D modeling operations were carried out using Geomagic Studio 9. Note that no editing has been done on the final model of Fig. 17.9, except for the cropping of the area of interest. An edited version of the 3D model was used for the replica production. Ten replicas were produced at a scale 1:2 (Fig. 17.9).

17.9 Conclusions

In the past years image-based modeling techniques such as digital photogrammetry and remote sensing have opened many new areas of applications.

With the recent expansion of photogrammetry's data acquisition tools (sensors) and processing techniques we see many more novel applications emerging. The generation of reality-based data for virtual environments, animation, video gaming, and the like constitutes a huge potential for future work. The pressing need for georelated modeling of our 3D environment (3D city and terrain modeling) from aerial and high-resolution satellite images and laser scanners will have a tremendous impact in archaeology and cultural heritage in the near future.

With the new generation of high-resolution satellite sensors with stereo capabilities the issue of 3D modeling is gaining much more prominence. Therefore, photogrammetric techniques are also becoming more important in satellite image applications. On the other hand, radiometric analyses are also attaining more attention in photogrammetry. We observe that the originally different techniques in remote sensing and photogrammetry are converging today strongly.

We have shown here how high-resolution satellite, aerial, and terrestrial images can be used in order to generate hybrid 3D models for archaeological and natural and cultural heritage applications with photogrammetric techniques. The digital nature of many of those images and the progress in automatic photogrammetric processing allows for very efficient procedures and for new kinds of results. Among the many various projects that we have conducted we have reported here about the large sites of Xochicalco/Mexico, Tucume/Peru, and Bamiyan/Afghanistan, where aerial and satellite images were used as the primary data source.

Active sensors such as structured light systems are well suited for the recording of smaller objects as they are represented by statues and excavation artifacts. They are largely independent of ambient light, accurate, and deliver results quickly and in a robust manner. Active sensing with coded structured light systems is a mature technology and allows high-resolution documentation of cultural heritage objects.

Raw data acquisition with laser scanning in the form of point clouds is very fast, but heavy user interaction is needed in the editing steps, for example, for filling the data holes, deleting blunders, and so on. Texture mapping is another issue that is not yet fully supported by existing software.

All these presented technologies, together with spatial information systems, visualization, and animation software are still in a dynamic state of development, with even better application prospects for the near future.

Acknowledgments I would like to thank my cooperators Dr. Devrim Akca, Henri Eisenbeiss, Dr. Daniela Poli, Dr. Fabio Remondino, Martin Sauerbier, and Dr. Zhang Li for their very valuable contributions to this chapter.

Chapter 18
Virtual Flight Over the Nasca Lines – Automated Generation of a Photorealistically Textured 3D Model of the Pampa de Nasca

Martin Sauerbier

Abstract In this chapter, the generation of a textured 3D model of the Pampa de Nasca by means of digital photogrammetry is described. The whole workflow, from image acquisition, image orientation, generation of a Digital Terrain Model (DTM), and an orthomosaic as well as the 3D visualisation of these photogrammetric products is presented and discussed. Furthermore, limitations and problematic factors influencing the quality of automatically derived DTMs and commercial as well as an in-house developed software for DTM generation were evaluated within this project.

18.1 Photogrammetry

The work described in the following sections was focused on photogrammetric methods for widely automated generation of Digital Terrain Models (DTM), Digital Surface Models (DSM), and orthoimages, images which are georeferenced and rectified with respect to a coordinate system as used in maps. Photogrammetry, one discipline in geomatics among others, is the science of the reconstruction of positions and shapes of objects based on images. Generally, any arbitrary images can be deployed for photogrammetric processing, nevertheless, in this chapter the author concentrates on aerial images acquired with metric cameras of high geometric stability.

Examples of other types of images suitable for photogrammetric processing are given in this volume (see Gruen, Eisenbeiss, Fux et al.). Aerial images nowadays are mainly used for the purposes of DTM and orthoimage generation and 3D measurement of objects, for example, for 3D city models or for Geographic Information Systems (GIS). Within the frame of the Nasca–Palpa project, aerial images and the photogrammetric products which can be derived, served as

M. Sauerbier (✉)
ETH Zurich, Institute of Geodesy and Photogrammetry, ETH Hönggerberg HIL D 43.2, 8093 Zurich, Switzerland
e-mail: martin.sauerbier@geod.baug.ethz.ch

M. Reindel, G.A. Wagner (eds.), *New Technologies for Archaeology*, Natural Science in Archaeology, DOI 10.1007/978-3-540-87438-6_18,
© Springer-Verlag Berlin Heidelberg 2009

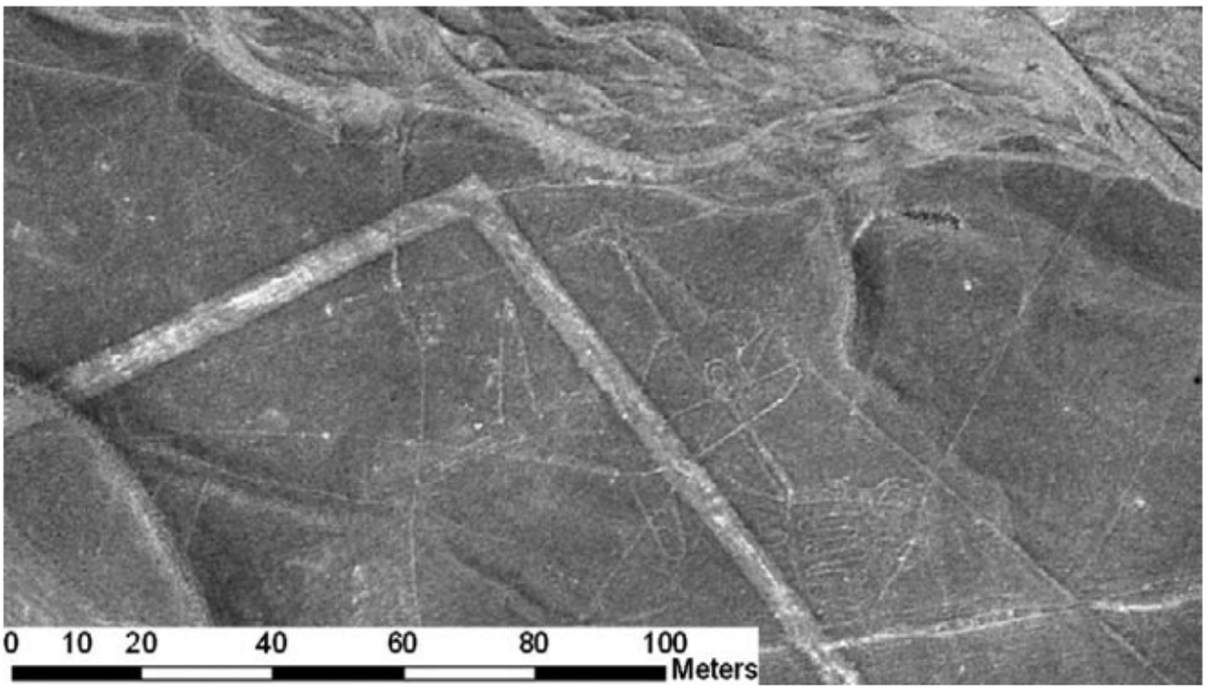

Fig. 18.1 Geoglyphs in the southern part of the Pampa de Nasca. In the center, one can recognise a whale. Furthermore, various linear geoglyphs are visible

valuable means for various tasks. The main application was the 3D documentation and recording of the geoglyphs of the Palpa and Nasca region, which was and still is being conducted based on DTM and orthoimages (Sauerbier and Lambers, 2004). Figures 18.1 and 18.2 show selected geoglyphs as they are displayed in the textured 3D model of the Pampa de Nasca which was generated within this project.

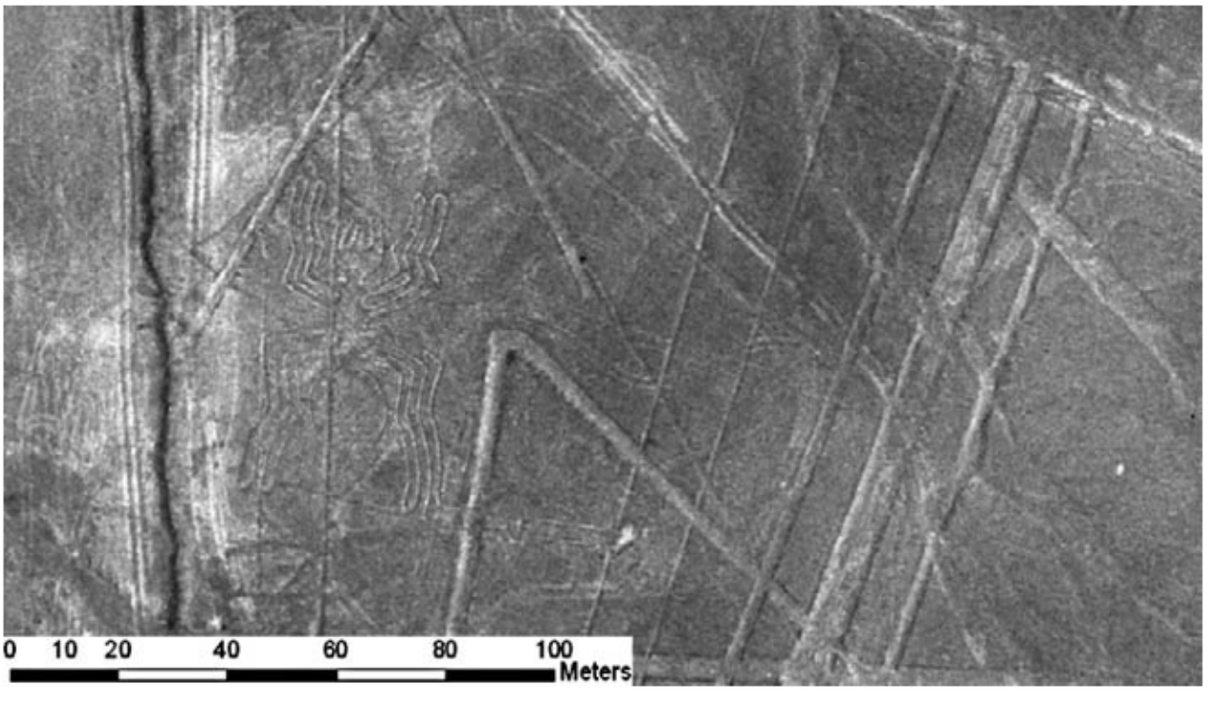

Fig. 18.2 Geoglyphs in the northern part of the Pampa de Nasca. Note the spider figure on the left and various linear geoglyphs. Moreover, traces from cars which caused damage to geoglyphs can be identified

18.2 Research Topic

Currently, research in photogrammetry mainly concentrates on the automation of the processing steps from image acquisition, image orientation, DTM, and orthoimage generation and object extraction. Automation for some parts of the photogrammetric processing pipeline was achieved in the last two decades. This especially applies to image acquisition using modern navigation units, powerful data storage devices, and computer-assisted flight planning during the photo flight as well as to the generation of orthoimages. These two technologies today are already in use for commercial purposes. Although automation approaches for image orientation and DTM generation also exist, both still lack in terms of accuracy caused by certain effects. The same applies to object extraction.

Aiming for the generation of a 3D model, the image orientation and DTM generation steps were of importance in our case. For geoglyph extraction it was clear from the beginning that manual measurements would be required (Sauerbier and Lambers, 2004). The two mentioned steps share a common problem: both are based on the extraction of points in one image which then have to be assigned to the identical points, so-called homologous points, in the stereoscopically overlapping images. This procedure generally is denoted as image matching. Various approaches for image matching exist; in the majority of cases they are classified as feature-based, area-based, and object-based matching methods. Basically, matching techniques work with two or more images.

In the case of image orientation, matching is applied for automated measurement of tie points, which connect the images of one block together. For this purpose, a comparably low number of tie points are sufficient for a stable relative orientation of the images with respect to each other as long as the point distribution covers the images evenly. For DTM generation, one aims for a preferably high density of matched points over the whole image in order to accurately represent the earth's surface in as much detail as possible.

Automation for these point measurement tasks is aimed at for two reasons: automatic measurements under good conditions can exceed human measurements in terms of accuracy, and on the other hand processing speed can be increased drastically. The latter of course applies only if marginal manual editing of the automatically obtained results is required. Problems in image matching which can lead to a significant amount of editing effort – and these affect image orientation as well as DTM generation – occur mainly for the following reasons (Gruen and Zhang, 2002):

1. Little or no texture
2. Distinct object discontinuities
3. Local object patch is not a planar face in sufficient approximation
4. Repetitive objects
5. Occlusions

6. Moving objects
7. Multilayered and transparent objects
8. Radiometric artefacts
9. Reduction from DSM to DTM

Although factor 8 depends on image quality and 9 on the applied method for object removal, 1–7 are object-dependent. For the specific case of the Pampa de Nasca, keeping in mind the arid character of the landscape, 1 and 4 especially apply. Furthermore, the available aerial images also feature low image quality caused during film developing. Issues 5–7 can be considered negligible for the Nasca case. Due to these facts, the Pampa de Nasca can serve as a suitable test area for the evaluation of different matching approaches.

18.3 Methods

18.3.1 Image Acquisition

In 1998, a photo flight was conducted over the Pampa de Nasca and the region around the modern town of Palpa, covering the two largest agglomerations of geoglyphs known in South America. Three blocks of B/W images were obtained from this flight: one block covering the Cresta de Sacramento to the northwest of Palpa consisting of 135 images, one block of 168 images covering the San Ignacio area, and one block of 401 images covering the Pampa de Nasca.

All blocks feature an along track and across track overlap of 60%, the two firstly mentioned blocks additionally share an overlap of 20% for the last and first strip, respectively (Gruen and Brossard 1997). Therefore, all derived photogrammetric products could be merged without a gap. The images were acquired on analog film using a ZEISS RMK A15/23 camera with a camera constant of 152.994 mm. During the flight, additional kinematic GPS measurements were conducted which yielded the UTM coordinates of the perspective centers of each image.

Figure 18.3 shows the image blocks, overlaid on a Landsat TM satellite image showing the Peruvian south coast. Additional control points were measured and signalised on the Pampa de Nasca and around Palpa using differential GPS, which later were used to orient the images in the UTM Zone 18 South coordinate system with WGS-84 as horizontal and vertical datum, the coordinate system in which all project-related spatial data as well as the current Peruvian maps are available. Furthermore, natural ground control points were measured on the Pampa de Nasca in 2003. The images were digitised using a photogrammetric scanner Vexcel Ultrascan 5000 with a resolution of 15 m, according to a footprint of 15 cm in object space.

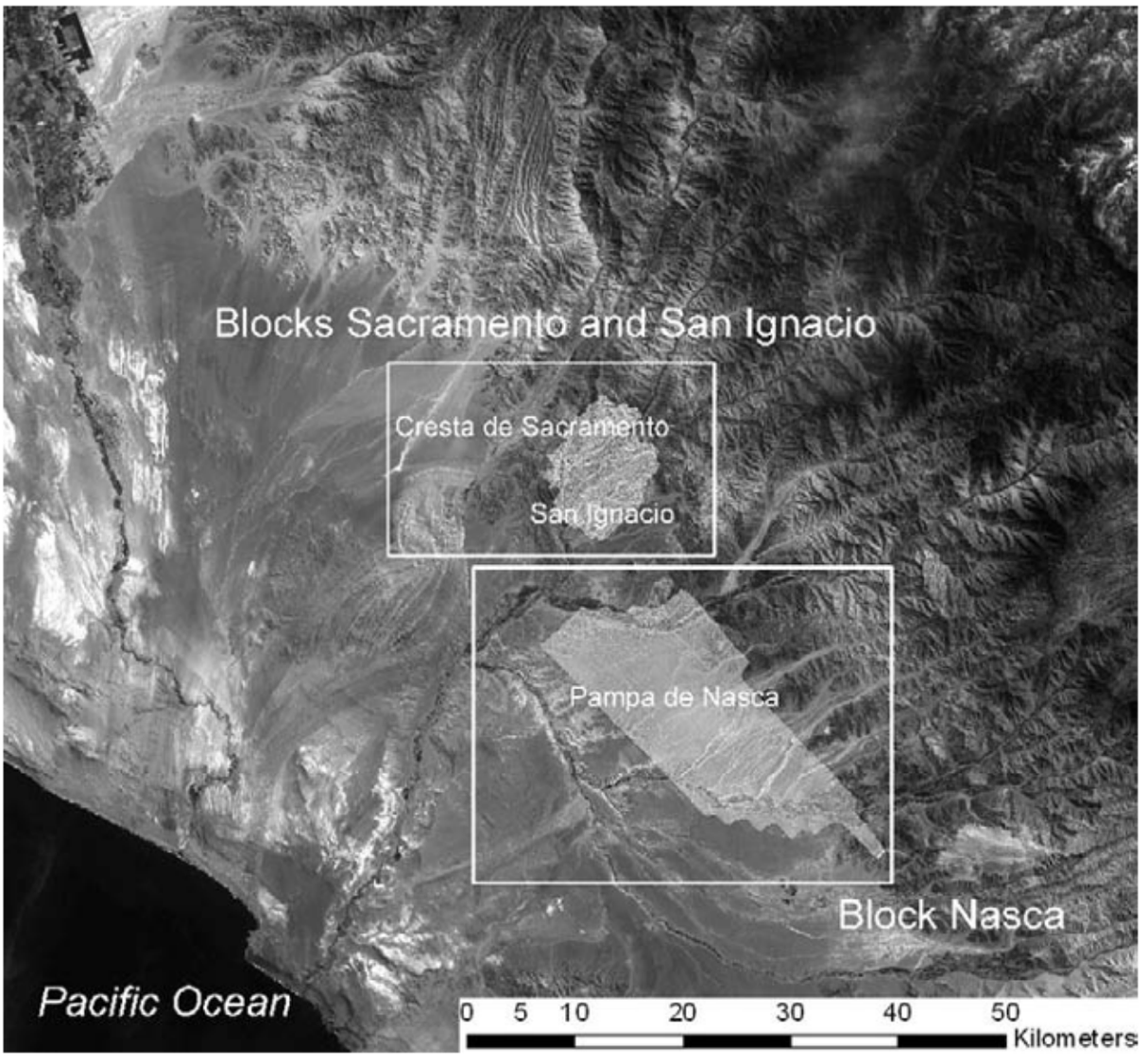

Fig. 18.3 Overview of the Nasca and Palpa aerial image blocks

18.3.2 Image Orientation

The first two blocks were processed manually on an analytical plotter (Lambers 2006), however, for the Nasca block we aimed for an automated processing. For the purpose of image orientation, the commercial photogrammetric software Z/I Image Station 2002, Virtuozo 3.1/3.3 (Supresoft Inc.), and Leica Photogrammetry Suite (LPS) were tested using two subblocks of the Nasca block (Sauerbier, 2004). One consisted of the first two image strips, covering the western part of the Pampa de Nasca and parts of the Río Grande valley; the other one consisted of images from the northern part of the Pampa, featuring images with low quality and low texture.

Finally, LPS was selected for tie point measurement with ORIMA for bundle adjustment. In LPS, the workflow started with the project setup. Camera constant, coordinates of the principal point, lens distortion values, and the fiducial coordinates known from the calibration protocol had to be imported. Furthermore, the UTM coordinate system was selected and the control point coordinates were imported.

For the purpose of fast image display, for example, for zooming and panning, as well as for the image-matching procedures, image pyramids with different levels of resolution were generated. Then the fiducials were measured automatically in order to reconstruct the acquisition geometry inside the camera, the so-called interior orientation. Possible distortions of the film due to storage can be corrected by affine transformation of the measured fiducial coordinates to the fiducial coordinates known from the camera calibration.

In LPS, manual fiducial measurement had to be performed for the first image which subsequently served as a template to automatically identify the fiducials in the following images and measure them using template matching with the centroid operator in order to obtain subpixel accuracy. After successful interior orientation, tie point measurement could be conducted.

Due to the available kinematic GPS measurements, which provided the coordinates of each perspective center, the flight direction could be calculated approximately for each strip. With the known flight direction at hand, no initial manual tie points were required and automatic tie point measurement by means of image matching could be started immediately.

For consideration of the factors influencing the image matching, matching parameters had to be adapted to the terrain characteristics. In LPS, the following parameters can be adjusted to the terrain characteristics; the according values finally set were obtained from tests using differing parameter values.

- The size of the search window, set to 35×35 pixels.
- The size of the correlation window, set to 9×9 pixels.
- The size of the window used for least squares matching, set to 21×21 pixels.
- The feature point density, set varying according to the individual texture of each stereo model. This parameter influences the number of tie points measured at each Gruber position.
- The limit for the correlation coefficient, set to 0.85.
- The value for initial accuracy.

The deployed matching algorithm of LPS is a combination of feature- and area-based approaches. By means of a coarse-to-fine approach through the image pyramids, tie points are being generated as follows. Area-based matching by cross-correlation is performed, and then refined by least squares matching. Additionally, a feature-based algorithm detects and matches interest points by cross-correlation. Finally, an error detection procedure is performed to eliminate gross errors.

For the Nasca block, following the described procedure, 6699 points were measured automatically, from which 1030 were detected and eliminated as blunders in the subsequent bundle adjustment in ORIMA, according to 15.4% of the automatically measured points. This amount of blunders is notably higher than experienced with matching results from more cooperative terrain.

The error-prone mismatches occurred mostly in areas with no texture and in the block center, where image quality turned out to be exceptionally low. Additionally, manual measurements had to be conducted in the mountainous

Table 18.1 Number of tie points measured according to the number of intersecting rays

Rays	2	3	4	5	6	7	8	9
Points	3071	1522	1174	680	199	41	10	2
Rate (%)	45.84	22.72	17.53	10.15	2.97	0.61	0.15	0.03

Source: Sauerbier (2006).

areas in the northeastern part of the Pampa de Nasca. Another reason for mismatches is the low redundancy inasmuch as LPS made only poor use of the manifold stereo overlap (Table 18.1).

After removal of the blunders, bundle adjustment yielded a global accuracy of the image measurements of $\sigma_0 = 6.4$ µm, which is according to 6.4 cm in object space for an image scale of 1:10.000. The mean RMS error in the ground control points was computed to 5.8 cm in the x-, 5.7 cm in the y- and 11.8 cm in the z-direction. The obtained accuracies for image orientation were regarded as sufficient for the following DTM and orthoimage generation and coincide with the theoretically achievable accuracy.

18.4 DTM and Orthoimage Generation

For DTM generation, various commercial photogrammetric software as well as the in-house software SAT-PP were evaluated. In order to compare the obtained results from the different software packages meaningfully, the aforementioned orientation values were imported into the respective software.

Tests were conducted using various matching parameter configurations in order to achieve the optimal result in any software. Again, the results were affected by the general factors with an impact on image matching mentioned above. Furthermore, software-specific characteristics turned out to influence the results significantly.

Details on the matching algorithms for DTM generation of the commercial software can be found in the respective manuals or literature for Leica Photogrammetry Suite 9.1 (Wang et al. 2004), Z/I Image Station 2002 (Z/I Imaging Corporation 2002), VirtuoZo 3.1/3.3 (Supresoft 2002), and SocetSet 5.3.0 (BAE Systems National Security Solutions Inc. 2006) and are not described here. The ETH Zurich in-house software SAT-PP can be distinguished from all investigated commercial systems mainly due to two features:

- Multistereoscopic overlap can be exploited by means of multi-image matching, therefore a higher reliability of the matching results can be expected.
- Multiple primitive matching allows matching not only of interest points, but also 3D edges and grid points. Therefore, breaklines can be modelled more accurately and continuously and matching results are obtained in low-textured areas.

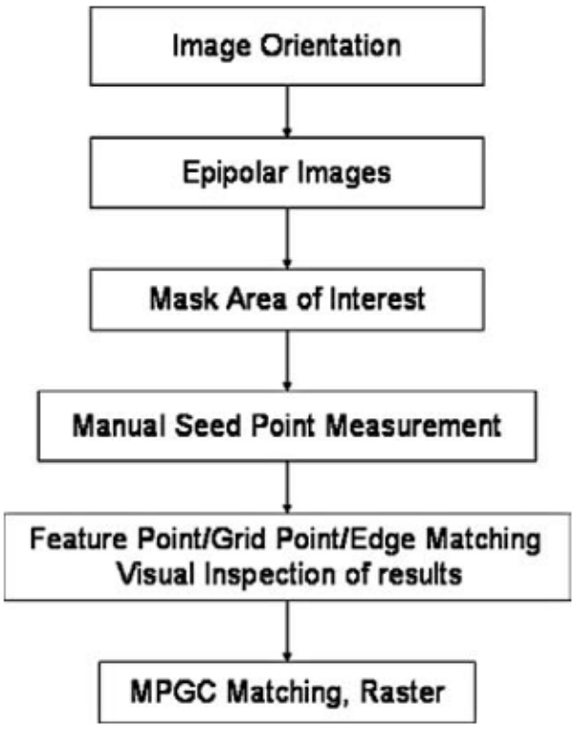

Fig. 18.4 Workflow for DTM generation in SAT-PP. (Sauerbier, 2006, based on Zhang, 2005)

The workflow of automated image matching in SAT-PP from a user's point of view is shown in Fig. 18.4.

In contrast to the mentioned software packages, instead of pairwise matching, SAT-PP uses all available images which cover an area of interest (Zhang 2005). Additionally, it makes use of a coarse-to-fine hierarchical matching process, trying to extract and match grid points, feature points, and edges.

The workflow for DTM generation in SAT-PP requires a certain amount of manual interaction and measurement. Given that imported and oriented images are at hand, one first has to generate epipolar images for stereo viewing. It has to be mentioned here that during image import the Wallis filter is applied in order to enhance image contrast locally in the images.

In the next step, it is required to measure at least five various well-distributed seed points manually; depending on image quality, texture, and topography the number has to be increased. Furthermore, a matching mask has to be defined which determines the area inside the stereo model for which the DSM will be generated. Although the software offers the option to generate the mask automatically, first tests have shown that a manual definition should be preferred in order to avoid the fiducial marks and image frame causing problems during the matching procedure.

After seed point measurement and mask definition, image matching can be initiated. In the investigated version of SAT-PP no option exists that would allow the user to influence matching parameters except the choice of the mesh size of the resulting DTM. Figure 18.5 shows the three types of primitives matched using SAT-PP for a subset of an image from the Nasca block. Grid point matching results are displayed in three different colors according to their reliability: red means unreliable, yellow means medium, and green means reliable.

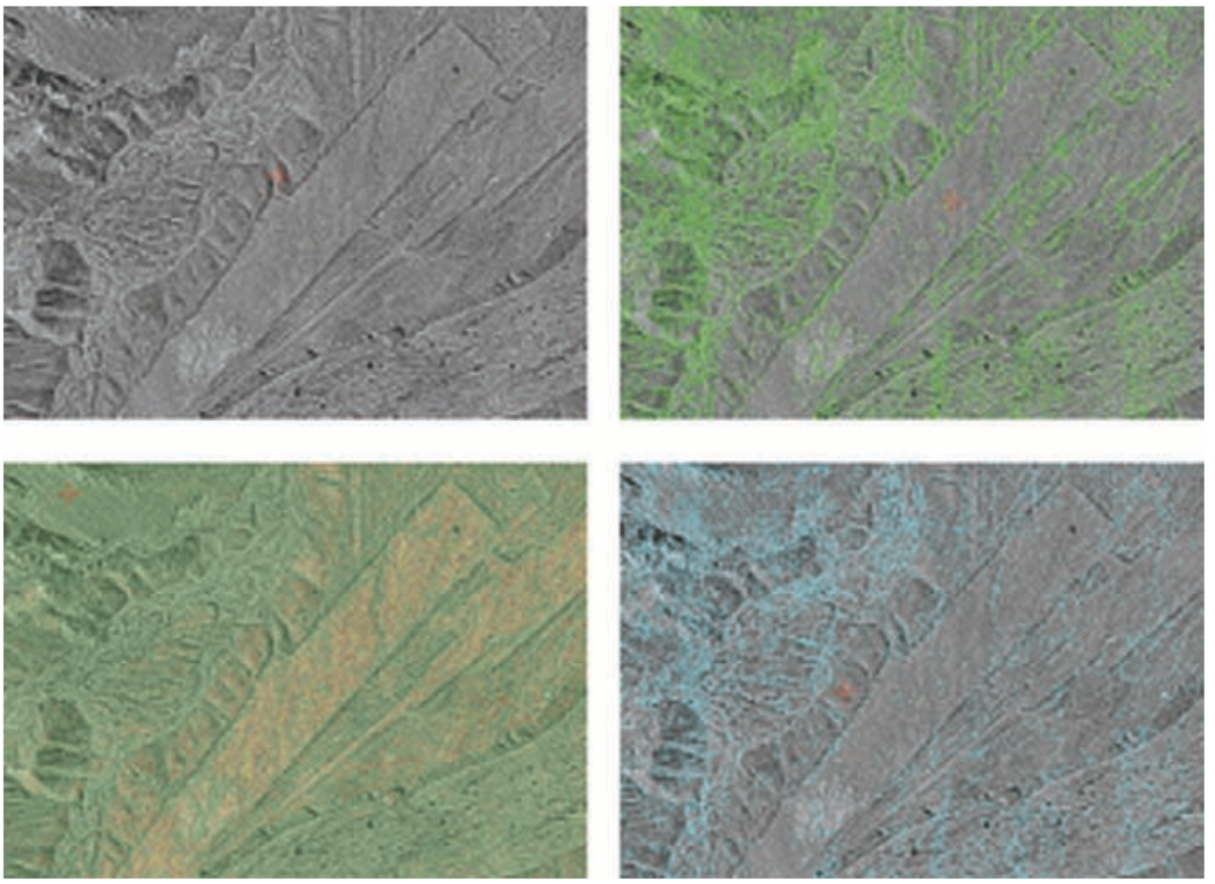

Fig. 18.5 Multiple primitive matching: (**a**) aerial image after Wallis filtering; (**b**) overlaid with matched interest points; (**c**) overlaid with matched grid points; (**d**) overlaid with matched 3D edges

For accuracy assessment, manual DTM measurements were conducted on an analytical plotter WILD S9 in profile measurement mode with approximately 20 m point distance and additional breakline measurements which then were interpolated to a regular grid with 5 m mesh size using our inhouse software DTMZ. The reference models were compared to the results obtained from the commercial products by means of the 3D modelling software Geomagic.

The Euclidean distance served as a measure for deviation of the DSMs obtained from SAT-PP according to the reference models due to its capability of assessing spatial differences in the *x*-, *y*-, and *z*-coordinate directions, not only in height. Table 18.2 shows the results from the conducted comparison between SAT-PP and a manually measured reference dataset. Detailed results of comparisons of results from commercial software were described in Sauerbier (2004).

Table 18.2 Comparison of results obtained from SAT-PP for five stereo models from the nasca block

Model	1	2	3	4	5
Maximal positive deviation [m]	10.44	39.64	9.13	5.01	6.22
Maximal negative deviation [m]	–8.31	−44.61	−11.67	−5.00	−9.79
Average Euclidean distance [m]	0.00	0.00	−0.49	0.00	0.02
RMS Error [m]	0.97	1.20	2.00	0.11	0.98

Source: Modified from Sauerbier (2006).

From the obtained results, one can clearly conclude that SAT-PP yields the most accurate results for all stereo models. For each stereo model, the best result was obtained using SAT-PP compared to all other investigated commercial products. Nevertheless, one can conclude that all matchers, including SAT-PP, show problems in the same areas, the steep slopes of quebradas and the mountainous areas in the northeast part of the Pampa de Nasca. However, the magnitude of error is the smallest for the DTMs generated with SAT-PP. Figure 18.6 gives an impression of the topography of the most problematic area: the largest deviations occurred at the quebrada slopes, a fact that applies to all investigated software packages.

A further topic to be addressed is computing time, which due to the complex image-matching approach is considerably higher using SAT-PP than using the investigated commercial products which perform pairwise matching only. As an example, it has to be stated that the processing of one image strip from the Nasca block took one week, whereas using Socet Set the whole block could be processed in two days.

The accuracy of the generated DTM is essential for the accuracy of orthoimages derived from the aerial images. Height errors in the DTM produce planimetric errors in the resulting orthoimage. Blunders particularly cause significant errors, but also systematic errors, such as a bias, affect the orthoimage systematically and subsequently all further measurements conducted in the error-prone orthoimage.

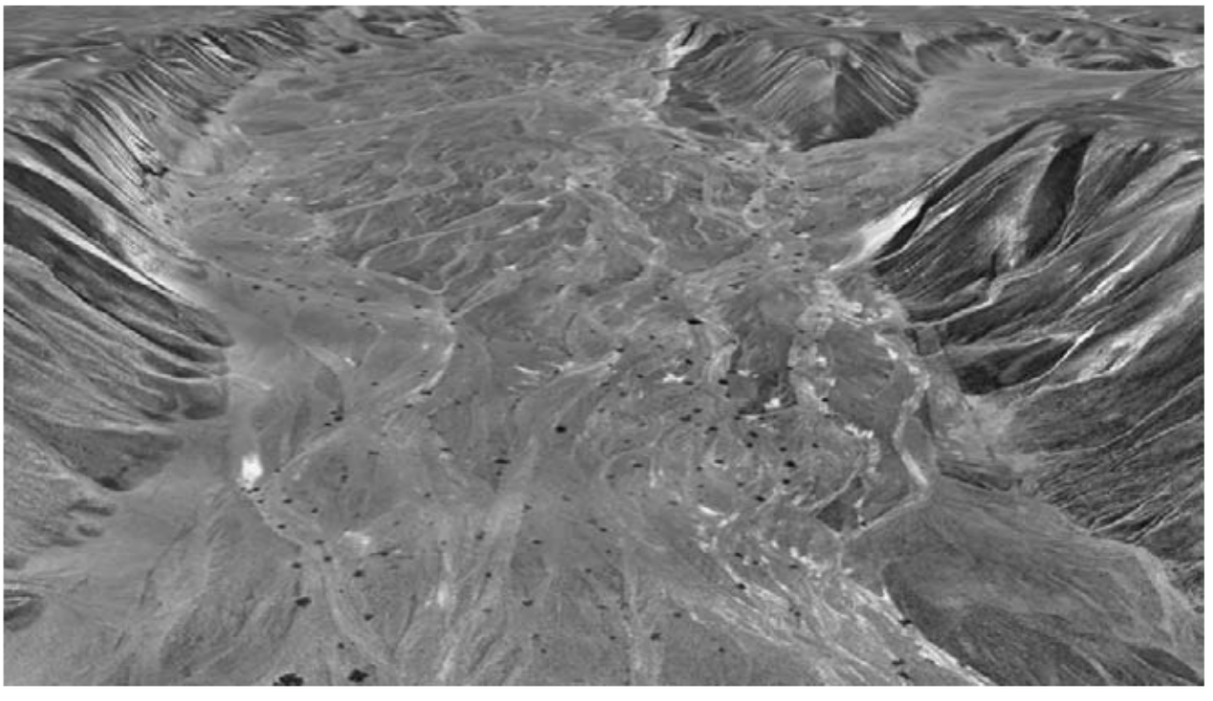

Fig. 18.6 3D view of the area covered by stereo model 2. The largest deviations occurred on the slopes of the quebrada. The underlying DTM is exaggerated by a factor of 2. (Software: Skyline Terra Explorer)

18.5 Results

The above-described photogrammetric processing of the aerial images of the Nasca and Palpa areas yielded highly accurate, large area datasets which now serve as a basis for geoglyph mapping, GIS-based analyses, and 3D visualisation. Nevertheless, for various tasks, further data were generated in order to enhance the available DTMs and orthoimages spatially or in terms of geometric resolution (see Eisenbeiss this volume). As in this contribution the focus is on large-scale objects and large areas; the respective data are listed in Table 18.3 with a brief description of how they were generated and their resolution.

Table 18.3 Overview of photogrammetric products generated within the nasca project from aerial and satellite imagery

Dataset	Resolution [m]	Method of Generation
DTM Palpa	2	Analytically from aerial images 1:7000
Orthoimage Palpa	0.25	Based on DTM Palpa, aerial images 1:7000, using SocetSet 4.4.1
Geoglyph vector Data Palpa	N/A	Analytically from aerial images 1:7000 (Palpa)
DTM Nasca	5	Automatically from aerial images 1:10,000 using SAT-PP
Orthoimage Nasca	0.15	Based on DTM Nasca, aerial images 1:10,000, using SocetSet 5.4.0
ASTER DTM	30	Automatically from ASTER satellite images using ERDAS Imagine LPS 9.1
ASTER orthoimage	15	Based on ASTER DTM and ASTER imagery using ERDAS Imagine LPS 9.1

18.6 Visualisation

In addition to geoglyph mapping using the DTM and orthoimage in a GIS environment, these data also allow for high-quality visualisations due to their high resolution. Static views on the 3D model can be produced by means of visualisation software such as ERDAS IMAGINE Virtual GIS 9.2, showing a subset of the data with the original resolution in the visible foreground, whereas in the background resolution is reduced using different Levels of Detail (LoD) (Sauerbier and Lambers 2003).

A more challenging task is the real-time visualisation of a large terrain dataset with high-resolution image texture, such as that produced for the Nasca block and earlier conducted for the Palpa block.

Whereas the Palpa block consists of an amount of data of 2.3 GB for image texture and approximately 400 megabytes for the DTM, the Nasca block exceeds these values by a factor of ten in terms of image texture. The computation time for

the generation of the Skyline model required one day on a standard PC with 1 GB of RAM and a 1.8 GHz CPU.

For real-time visualisation, the software packages Skyline Terra Builder version 1 and Terra Explorer Pro (Skylinesoft) version 5 were used. Although the Terra Builder was used to set up the 3D model by determining the model boundaries, determination of the stratigraphy of the layers, and processing the data to achieve the final textured 3D model, the Terra Explorer Pro provided the navigation functionality and a wide range of options for the customisation of the visualisation in terms of navigation, quality, and graphical user interface.

The data are stored in the proprietary MPT format and only can be viewed by means of the Terra Explorer. The advantage of this software package is the streaming technology that loads only the visible parts of the terrain into the graphics memory successively while the user navigates through the 3D model. If enough memory is available, neighboring areas are also stored in the graphics memory for smooth movement through the terrain.

Additionally, a LoD technique is implemented, which divides the visualised data into two to seven different levels of detail. Nevertheless, borders between these levels are considerably visible, therefore the quality of visualisation is partly decreased by this effect. Compared with older versions of Terra Explorer, the actual version 5 preserves a notably higher resolution of the visualised texture; in the case of the Palpa and Nasca blocks, no loss of detail compared to the unprocessed orthoimages could be observed (Fig. 18.7). Using the Terra Explorer software, the user can either navigate through the 3D model interactively in real-time, or record a flyover to a video file in different formats which can be viewed on a standard PC without the need to provide the underlying data to the user.

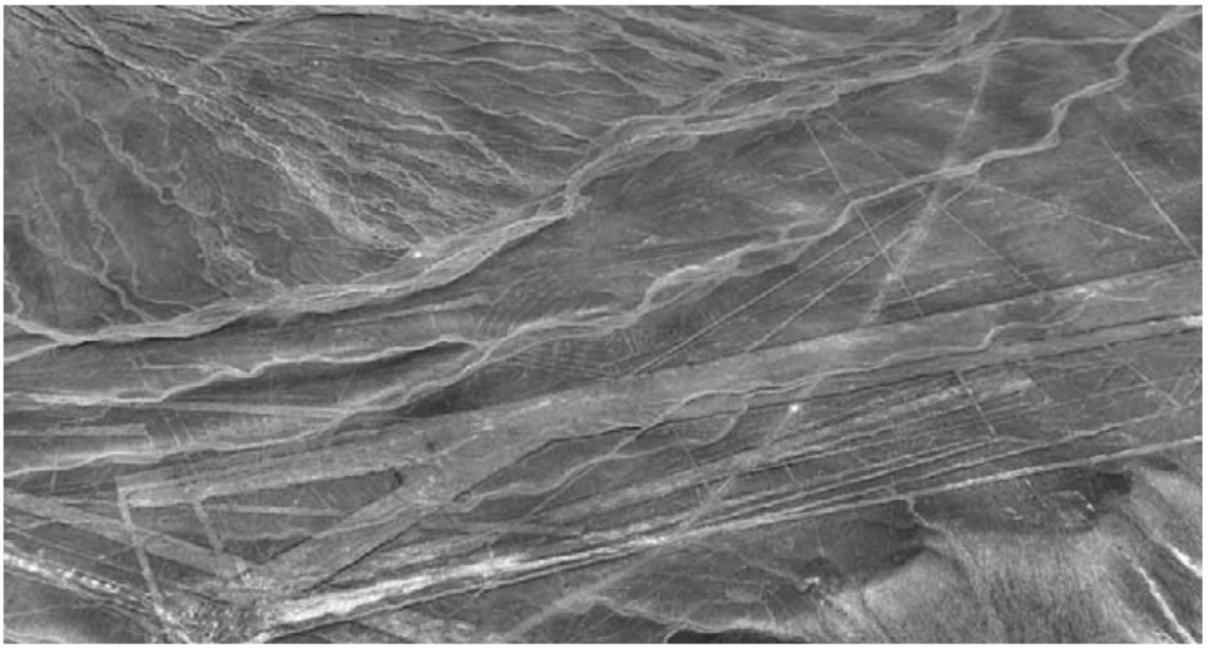

Fig. 18.7 3D view of a geoglyph complex – mainly linear and trapezoidal geoglyphs – on the Pampa de Nasca from north generated with Skyline Terra Explorer

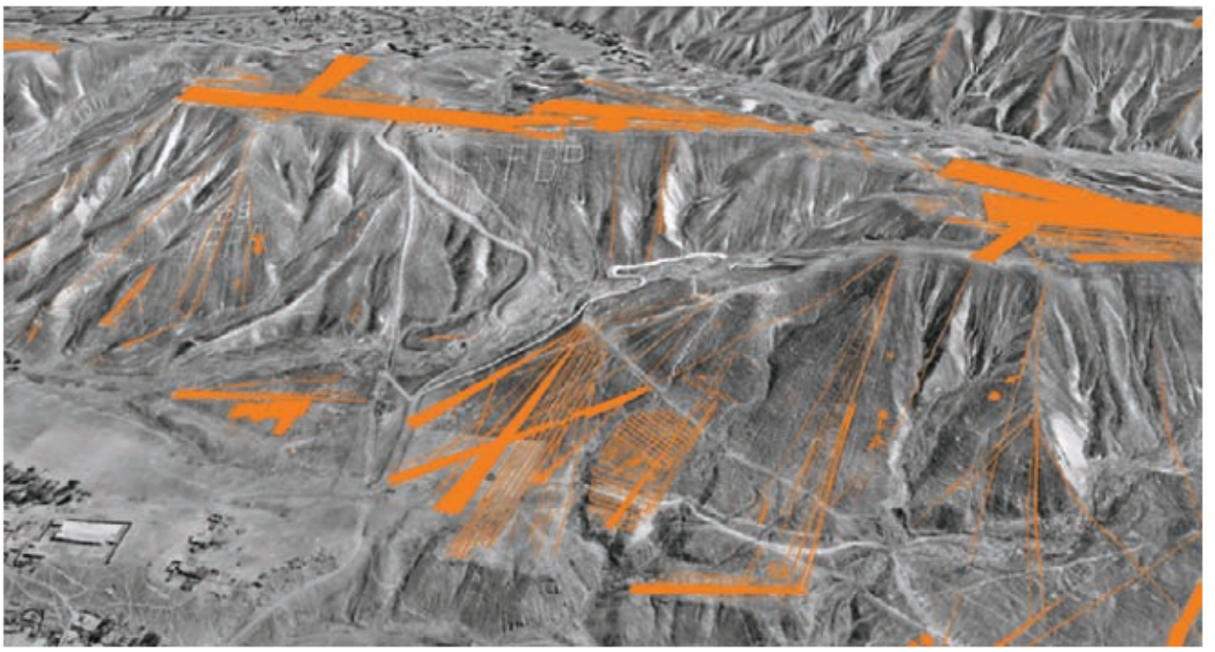

Fig. 18.8 Geoglyph vector data from the Palpa area overlaid on the respective DTM and orthomosaic

A further option allows for the overlay of 3D vector data on the textured terrain. Figure 18.8 shows a view on the textured 3D model of the Palpa area with the mapped geoglyphs draped over the DTM and orthomosaic.

18.7 Conclusions and Outlook

The SAT-PP matching algorithm clearly yielded the best results for DTM generation. Nevertheless, an improvement of DTM accuracy for low-textured areas and poor image quality cases can be obtained by enhancements on the sensor side. One option would be the combination of aerial images with aerial laser scanning, which is not affected that significantly by the texture of the terrain surface as are image-based measurement techniques.

A future alternative can be expected from high-resolution Synthetic Aperture Radar (SAR) interferometry, because first results obtained from TerraSAR-X, a satellite operated by the German Aerospace Center (DLR) and in orbit since 2007, are promising.

Despite the remaining problems, the obtained DTM and orthoimage are well suited for the original purpose, geoglyph mapping, in terms of resolution and accuracy. Image data with such high resolution actually is the only efficient data source for 3D recording of the Nasca geoglyphs due to their size, extent, and spatial distribution. Photogrammetry can be concluded as the ideal method for the documentation and modelling of large archaeological objects as it provides the operator with image data that can be interpreted intuitively and effectively once the images are oriented. The available data now can serve as an accurate

basis for analysis and interpretation of the geoglyphs in the Nasca region with respect to the surrounding topography and be visualised in high quality and real-time.

Recently, providers of commercial photogrammetric software started to implement matching algorithms with multi-image matching capability and edge matching, such as the new module NGATE (Next Generation Automatic Terrain Extraction) in Socet Set 5.4.0 (BAE Systems) which seem to yield results of similar quality as with SAT-PP. Nevertheless, this should be an issue for future investigations as well as the improvement of processing time in SAT-PP, which is currently under development by means of implementation of a grid computing procedure.

Acknowledgments The author thanks the German Research Foundation (DFG) for the opportunity to take part in this interdisciplinary project and the Swiss-Liechtenstein Foundation for Archaeological Research Abroad (SLSA) for funding the photoflights and field campaigns in 1997/98. Further thanks go to Natalia Vassilieva and Sebastian Sussmann for their valuable contributions during photogrammetric image processing.

Chapter 19
Context Matters: GIS-Based Spatial Analysis of the Nasca Geoglyphs of Palpa

Karsten Lambers and Martin Sauerbier

Abstract In this chapter we report on the GIS-based analysis of the Nasca geoglyphs of Palpa, Peru, undertaken in the course of the Nasca–Palpa Archaeological Project. We focus here on the analysis of spatial relationships between the geoglyphs and the surrounding landscape in terms of visibility and orientation. Our motivation for this contextual analysis was to gain a better understanding of the function and meaning of the geoglyphs by virtually assuming the viewpoints of the people who conceived, built, and used the geoglyphs between approximately 400 BC and 800 AD. In this sense our study of geoglyph visibility and orientation is a contribution to current attempts to incorporate cultural variables into the quantitative environment of GIS, thereby rendering GIS a more useful instrument for archaeological research. This approach required the development of new GIS tools tailored to the specific needs of archaeological analysis. The results of our study indicate that the geoglyphs can be understood as stages for public rites performed by social groups, whereas the incorporation of the surrounding landscape through visual links was apparently not a major concern.

19.1 GIS Applications in Archaeology: Chances and Limitations

Geographical information systems (GIS) have become a widespread tool in archaeological research due to their manifold capabilities in terms of data capture, management, analysis, and visualisation (Wheatley and Gillings 2002; Conolly and Lake 2006). Because of their origin in cartography and geography, GIS are especially well suited for archaeological investigations at a regional scale, be they more traditional studies of settlement patterns or recent approaches to landscape archaeology. However, as GIS were not originally

K. Lambers (✉)
University of Konstanz, Zukunftskolleg, Department of Computer Science,
P.O. Box 697, 78457 Konstanz, Germany
e-mail: karsten.lambers@uni-konstanz.de

M. Reindel, G.A. Wagner (eds.), *New Technologies for Archaeology*,
Natural Science in Archaeology, DOI 10.1007/978-3-540-87438-6_19,
© Springer-Verlag Berlin Heidelberg 2009

conceived for archaeological applications, their usability in archaeology is affected by certain conceptual limitations. The most important constraint results from the fact that GIS are designed to handle measurable data that can easily be quantified and expressed by either of the two standard data formats of GIS, vector and raster data, whereas other kinds of information are difficult to process and analyse. Due to this requirement, data describing the current environment that can be obtained through a variety of methods and sensors are the most readily available information to be used for GIS-based analyses. This includes, for example, topographical data (digital elevation models), environmental data (hydrological, geological, botanical data), cadastral and administrative data (borders, real estate ownership), and economic data (land and resource use).

Archaeological information, on the other hand, often differs considerably from the kinds of data mentioned above. It is impossible to record archaeological data with the degree of reliability, completeness, and accuracy of common environmental or cadastral datasets. For example, archaeological sites and features tend to be wholly or partially destroyed, considerably altered, or buried, such that a complete inventory of the material remains of a given society under study is impossible to achieve. Archaeological data furthermore describe material remains of past societies that in most cases experienced a quite different environment from the one modelled by modern geodata, inasmuch as climatic conditions, land use, population density, and other parameters have often changed considerably since the time period under study. This leads to a general problem of archaeological GIS applications, namely that datasets that are ultimately incompatible in terms of their quality and time reference are commonly related to each other and analysed in conjunction. A careful, case-specific consideration of which aspects of available environmental and archaeological data actually represent the situation at the time under study is required to mitigate this problem.

A related major problem of using GIS in archaeological research concerns the existence of many parameters operational in the cultural development of a society over time that are not easy to capture and translate into GIS-compatible data. Such parameters refer to qualitative information that is difficult to measure, quantify, or georeference. This includes the significance or value of areas and places – for example, areas of high or low prestige, sacred places, or places of remembrance – as well as the often unmarked boundaries of political, ethnic, religious, or linguistic spheres. Although spatially reflected, parameters such as these are often ambiguous, ephemeral, or contested.

They are therefore difficult to model in the abstract, quantitative, Cartesian framework provided by GIS. Rather, they correspond to cultural, social, and qualitative concepts of space that today are often subsumed under the term 'landscape' (for a comprehensive discussion see Anschuetz et al. (2001) and Gramsch (2003); cp. Palang and Fry (2003)). In this conceptual framework, the environment provides the spatial framework for many different landscapes that depend on subjective, individual, situational, and a variety of other perspectives

that may be difficult to model in GIS. This has led to serious concerns about the usefulness of GIS in archaeological research: 'Given [the] apparent incompatibility between recent theoretical perspectives on landscape and space, and the nature of GIS, is the latter really a suitable environment for the interpretative analysis of archaeological data?' (Witcher 1999:15).

As a contribution to this debate, we focus here on the analysis of the visibility and orientation of archaeological features, in this case the Nasca geoglyphs of Palpa described in the following section. Over the past decade, visibility and observation have been extensively studied in archaeological GIS applications by using viewshed analysis for elevation-dependent visibility studies and visualisation and virtual reality for reconstructing possible observations (see discussion in Wheatley and Gillings (2000) and Lake and Woodman (2003)). In visibility analysis, variables of the physical environment such as terrain elevation and Euclidean distance serve as spatial proxies to study cognitive and other phenomena that are not directly measurable, such as perception (Whitley 2004). Such studies start from a middle ground between 'the applied scientism of processual archaeology and the attempted humanism of post-processual approaches' in landscape archaeology (Lock and Harris 2006:43). Addressing the concerns raised above, visibility analysis is thus a pragmatic attempt to indirectly approach qualitative cultural phenomena within the quantitative and Cartesian framework of GIS (cp. Verhagen et al. 2007). Specifically, it allows us to reconstruct how archaeological features may have been perceived by people moving through the study area, and how they might have been spatially related to cultural and natural components of their surrounding environment. In the case of the Nasca geoglyphs of Palpa, this evidence is hoped to provide clues on the function and meaning of the geoglyphs.

19.2 Studying the Visibility and Orientation of the Nasca Geoglyphs in Palpa

The object of our GIS-based spatial analysis was the geoglyphs of Palpa, in the northern part of the Río Grande basin, where a long-term multidisciplinary research project to investigate the cultural and environmental history of the Nasca region has been conducted since 1997 (Reindel and Wagner this volume). The pampas of Nasca farther to the south between Río Ingenio and Río Nasca, where the best-known concentration of geoglyphs is located, have recently been included in our study area, and the topography of this area has been recorded with advanced methods of digital photogrammetry (Sauerbier this volume). However, although intended for the future, a GIS-based archaeological study of the geoglyphs on the pampas of Nasca has not yet been undertaken and is thus not covered here.

Built approximately between 400 BC and 800 AD, the geoglyphs cover the stony desert surface of the hills and pampas between the fertile river oases of the

Río Grande basin at the foot of the Andes (Kern and Reiche 1974; Aveni 1990; 2000a,b). Although biomorphic figures are today the best-known geoglyphs, they are by far outnumbered by geometric shapes such as lines, trapezoids, and spirals, many of which overlap, converge, or are grouped into huge complexes that often emerged over several centuries (Fig. 19.1). The origin of the geoglyph phenomenon can be traced back to the petroglyph tradition of the Paracas culture of the Early Horizon (800 to 200 BC), however, the vast majority of geoglyphs that are visible today were made during the Nasca culture of the Early Intermediate period (200 BC–650 AD; Lambers 2006b).

Through the geoglyphs, the ancient inhabitants of the Río Grande basin marked and transformed the desert landscape in a unique and spectacular way that can still be appreciated today. Whatever their specific meaning, the geoglyphs clearly integrated the vast and uninhabitable desert plains into the cultural domain of the valley-based society (Silverman 1990: 451). In spite of the wide variety of available literature on the origin and function of the geoglyphs, archaeological investigations have been surprisingly sparse (see review in Aveni 1990). The principal objective of our investigation of the Palpa geoglyphs was therefore to learn more about the geoglyphs through a thorough field study of the geoglyphs and their associated features and artefacts (Reindel et al. 2003). To this end, we started with a comprehensive digital mapping of the geoglyphs (Sauerbier and Lambers 2003, 2004) that

Fig. 19.1 A trapezoid and several linear geoglyphs on a spur overlooking the Río Grande valley westwards (site PV66-122). A range of hills is visible in the background. (Photo: K. Lambers)

enabled the first GIS-based spatial analysis of the geoglyphs in their natural and cultural context.

Archaeological fieldwork on geoglyph sites in Palpa revealed ample traces of ancient activity on and around geoglyphs such as placement of ceramic vessels and other offerings along geoglyph borders, frequent walking over linear geoglyphs, and a variety of acts associated with stone platforms and wooden posts erected on trapezoidal geoglyphs (Lambers 2006b; Reindel et al. 2006). The background of these activities can to a certain degree be inferred from the archaeological evidence. Although offerings such as *Spondylus* shells, crawfish, and field crops strongly hint at a cult revolving around concepts of water, irrigation, and fertility, rites performed on geoglyph sites had at the same time probably an important social dimension concerning the groups involved, as discussed below.

Furthermore, evidence from unfinished geoglyphs indicates that the construction and remodelling of geoglyphs and geoglyph sites was a continuous process that was arguably never regarded as finished. This process apparently involved large parts of the ancient population and had a meaning in its own right, being likely as important as the actual use of the geoglyphs for other forms of group activity, with which it was closely interwoven. Thus, whatever their intended meaning, the archaeological evidence clearly indicates that geoglyphs served as locations for continuous, structured, and varied group activity.

This archaeological finding is in stark contrast to today's perception of the geoglyphs. Modern visitors to the Nasca region tend to get the impression that geoglyphs are only visible from the air. This false notion perpetuated through popular media is fostered by modern patterns of movement through the region that are very distinct from ancient ones. Today, visitors to Nasca spend their time mainly in one of the valleys without ever entering the pampas. To see the geoglyphs, they board small airplanes that offer spectacular views of the pampas from above. Due to this remote perspective, geoglyphs are today often seen and interpreted as images or pictures largely devoid of any context. Labellings of well-known biomorphic geoglyphs such as Monkey, Spider, or Lizard are hardly disputable due to their distinct shape, however, popular names of geometric geoglyphs such as Yarn and Needle, Sundial, or Paddle Wheel (Kern and Reiche 1974; Aveni 2000a) show that these geoglyphs are often understood as images of real-life objects as well. This modern perspective was not shared by the people who conceived, built, and used the geoglyphs.

A ground-based perspective is therefore a better approach to learn more about the geoglyphs. A close-up view may reveal the size, composition, and construction details of a geoglyph, showing, for example, that many geoglyphs are less straight or clear-cut than they seem from above, and often incorporate elements dating from different time periods. A ground-based perspective also reveals how geoglyphs appear in their topographic setting. This is important, as the landscape in which the geoglyphs are situated may have been incorporated into geoglyph complexes by means of visual links or other kinds of spatial relationships. An investigation of such a possible spatial order may thus

reveal, in addition to findings from archaeological fieldwork, important clues to understanding the function and meaning of the geoglyphs.

GIS provide tools to simulate such perspectives in a computer environment. For our investigation of the visibility and orientation of the Nasca geoglyphs of Palpa we took into account the issues concerning GIS applications in archaeology mentioned in the previous section. We regard visibility (encompassing vision and observation) as a constitutive yet insufficient element of perception (cp. Witcher 1999:14 and Wheatley and Gillings 2000: 3f), thus allowing us to approach perspectives of the people who conceived, built, and used the geoglyphs in order to learn more about their function and meaning. We developed new tools for the calculation of geoglyph orientation, and adapted and enhanced proven methods such as cumulative viewshed calculation (Wheatley 1995; Lake et al. 1998) for visibility analysis. We are aware that advanced methods and concepts such as Higuchi viewsheds (Wheatley and Gillings 2000) and visual affordance and prominence (Llobera 1996, 2001, 2003) might be fruitful approaches to further explore the geoglyphs in the future.

For our investigations in the Palpa region we relied heavily on the results of recent investigations into the geomorphology and paleoclimate of the study area (Eitel and Mächtle this volume) in order to determine which elements of the present-day landscape reflected in the geodata available for our study were representative of the time when the geoglyphs were built and used. Considering the setting of the geoglyphs on desert plains surrounded by river valleys, a coastal cordillera to the west, and the Andes to the east, an investigation of two different perspectives seemed worthwhile: the view of the geoglyphs, and the reverse view from the geoglyphs on the surrounding landscape. This bidirectional visibility study was aimed to detect possible recurrent patterns of spatial relationships between archaeological features and the surrounding landscape.

19.2.1 The View from Outside: Visibility of the Geoglyphs

In Late Paracas and Nasca times, the desert between the fertile river valleys was well integrated into the daily life of the ancient society. People left their settlements in the valleys on a regular basis, ascending the sandy slopes that led up to the flat plains, crossing plateaus and dry valleys in order to spend time at geoglyph sites for all kinds of group activity (Aveni 1990; Reinhard 1996; Lambers 2006b). People thus frequently assumed viewpoints that today are largely abandoned. From many of these vantage points, the geoglyphs, the groups of people gathering upon them, and the rites performed on them, were an important visual element of the landscape. In this sense, it seems possible that this activity taking place on geoglyph sites was meant to be seen by others. Although the sociopolitical organisation of Nasca society is still a matter of debate, it may have been organised in large clanlike groups (Lambers 2006b: 119ff). These groups may have been associated with major geoglyph complexes,

which they developed over time and used for group rituals. In this hypothetical scenario, rites performed on geoglyph sites may have served to raise awareness of group identitiy among group members as well as observers. This would have required good visibility of geoglyph sites.

In order to test the hypothesis that geoglyphs were deliberately placed in locations that afforded good visibility, we decided to compare the visibility of points on geoglyph sites to the visibility of points randomly distributed over the terrain. If the visibility of the geoglyph points were significantly better, this would support our hypothesis. While the details of this study have been presented elsewhere (Lambers and Sauerbier 2006, 2008), in this section we focus on the general outline of our investigation and summarise its main results.

The situation in Palpa provides quite favourable conditions for GIS-based visibility studies, as several factors often cited as questioning the results of such simulations are of limited relevance here. Most importantly, geomorphological change that occurred since Nasca times has been minimal, at least concerning the desert portion of the landscape, as indicated by recent geoarchaeological research (Eitel et al. 2005; Mächtle et al. 2006; Mächtle 2007; Eitel and Mächtle this volume). This means that digital terrain models (DTMs) modelling the current state of the topography can be regarded as largely representative of the conditions in Nasca times at least with respect to the pampas and surrounding mountains. Furthermore, vegetation cover (Llobera 2007) does not pose a problem in a desert environment. Vegetation cover is, and used to be, present in varying density on the flood plain, however, it may only marginally, if at all, have obstructed intervisibility between the pampas and the surrounding mountains, as both are situated on higher elevations.

The question of discernability of cultural features over large distances (Ogburn 2006) is more difficult to answer. As shallow surface markings, geoglyphs may not have been visible beyond a certain distance, which is confirmed by our experience from eight months of fieldwork on geoglyph sites around Palpa, even though geoglyph outlines and their colour contrast to the surrounding desert surface must have been much clearer in Nasca times. However, considering the ample evidence of group activity on geoglyph sites, it is highly likely that it was not the geoglyphs themselves, but rather people interacting upon and moving over them that were at the focus of attention in ancient times. We know from our own experience that single persons in the desert are distinguishable as moving dark spots over a distance of several kilometres, even across the wide flood plain of the Palpa and Viscas rivers. Groups of people must have been visible even more clearly. Therefore, discernability limitations over large distances are again not a major problem affecting the study of geoglyph visibility.

For our investigation we had at our disposal a DTM of the study area generated from aerial and satellite images with 30 m resolution and an accuracy of 18.7 m with respect to a manually measured DTM derived purely from aerial images (Sauerbier and Lambers 2003; Sauerbier et al. 2006). The DTM was large enough to avoid edge effects when calculating visibility. We defined every centre point of a DTM cell intersected by a geoglyph as a geoglyph point,

resulting in 2067 geoglyph points. We then determined visibility values for each of these points by calculating lines of sight (LoS) between each DTM cell and each geoglyph point, taking into account observer's height, earth curvature, and refraction. The resulting values indicated for each geoglyph point from how many DTM cells it was visible.

In order to assess these values, we calculated a second sample of 2067 points in Matlab that were randomly distributed over our study area. For these random points we calculated visibility values by the same method as for the geoglyph points. By doing so, we obtained a reference dataset to which we compared the visibility values of the geoglyph points. Applying the two-sample Kolmogorov–Smirnov goodness-of-fit test, we were able to determine that the visibility of the geoglyph points differed significantly from the visibility of the random points (Fig. 19.2). The corresponding chart in our detailed report on this study (Lambers and Sauerbier 2008, Fig. 8) shows miscalculated values, even though the values given in the text are correct. We thank Jens Andresen and Irmela Herzog for kindly pointing out this mistake to us, and correct the chart here (Fig. 19.2).

A direct comparison of the visibility values showed that a majority of geoglyph points reached much higher values than the random points (Lambers and Sauerbier 2008; Fig. 7). At the same time, our study showed that the variable visibility was largely independent of other spatial variables, such as slope degree and elevation. This allowed us to conclude that visibility had had an effect on the choice of place for geoglyphs in that locations that were well visible from the surrounding landscape were preferred. This result clearly supports our hypthesis that rites performed by social groups on geoglyphs were meant to be seen, thus allowing glimpses into the social dynamics of ancient Nasca society.

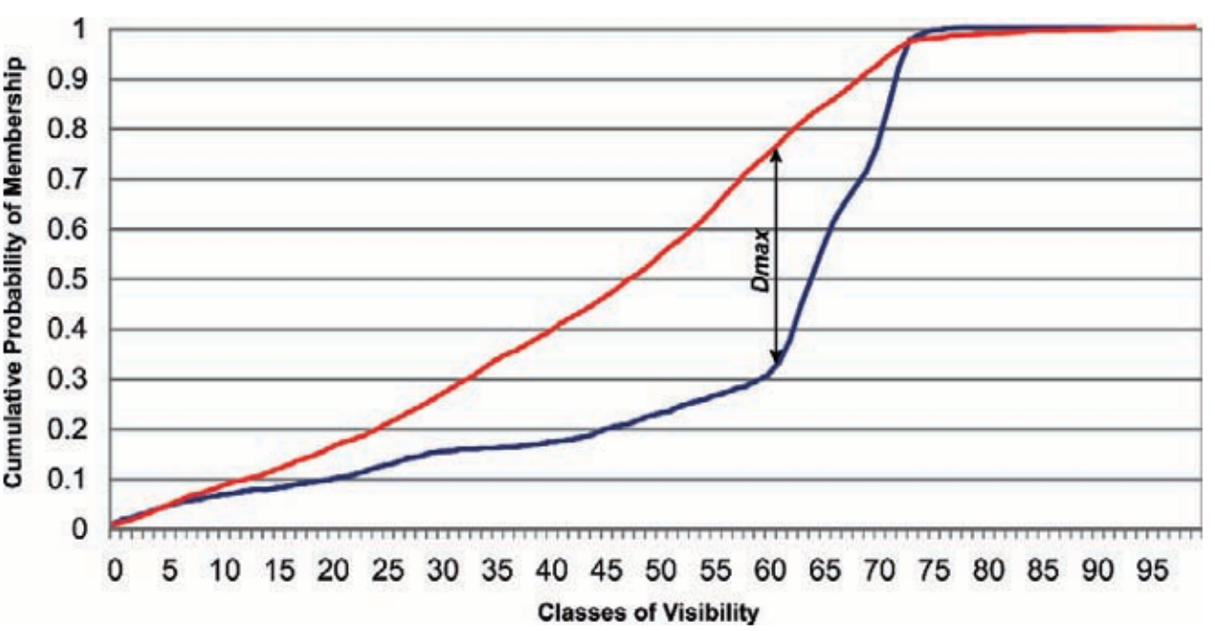

Fig. 19.2 Cumulative probability of membership in visibility classes of points on geoglyphs (*blue line*) versus random points (*red line*). *Dmax* indicates the maximum difference between both curves. (For further detail see Lambers and Sauerbier 2008)

19.2.2 The View from Within: Orientation of the Geoglyphs

From our study of perspectives of the geoglyphs we turned to a study of perspectives from the geoglyphs, the results of which are presented in detail in this section. While apparently meant to be observed by others, rites performed on geoglyph sites at the same time afforded the participants manifold views of the surrounding landscape. As geoglyphs visually marked and structured the desert surface, and often assumed geometric shapes with predominant straight elements such as borders or axes of trapezoids, straight sections of lines, and so on, these straight elements may have served as visual pointers to certain natural or cultural features of the surrounding landscape.

Geoglyph orientation has up to now usually been discussed in terms of astronomical alignments of geoglyphs with the position of celestial bodies (Hawkins 1974; Aveni 1990; Reiche 1993; Teichert 2007). As the astronomical hypothesis had been extensively tested and failed to provide a plausible explanation for the majority of known geoglyphs, we decided to focus our investigation of geoglyph orientation in Palpa on other possible targets closer by. According to well-documented Andean traditions, mountains may have been regarded in the Nasca region as seats of deities and sources of water (Rostworowski 1993; Reinhard 1996). Because many offerings placed along geoglyphs and on stone platforms indicate a concern for water, a link between geoglyphs and mountain veneration seemed possible. Visually dominant straight sections of certain geoglyphs may thus have directed the views of people gathering upon them to certain mountains. Another observation hints in this direction as well. The well-documented line centres on the pampas, from which straight lines radiate out or in which they converge, respectively, tend to be located on elevated terrain such as low hills or rock outcrops (Aveni 1990; Reiche 1993). This supports the idea of linear geoglyphs pointing towards terrain peaks. That way, lines would visually incorporate elements of the surrounding landscape into the rites performed on geoglyph sites.

In order to test this hypothesis, we first needed to determine the orientation axes of the Palpa geoglyphs. These were calculated on the basis of the digital documentation of geoglyph outlines (Sauerbier and Lambers 2004) that had resulted in two sets of 3D vector data: polylines mapping the preserved borders of geoglyphs usually marked by heaped stones, and polygons covering the most likely original cleared area of a given geoglyph, defined by combining and complementing the polylines. On the basis of these polygons, we first calculated the area and the centre of gravity of each geoglyph based on Gauss' theorem, and then derived the azimuth of the principal axes by means of a principal axis transformation:

$$A_{Geoglyph} = \frac{1}{2}\sum_{i=1}^{n}(x_i y_{i+1} - x_{i+1} y_i),$$

where $A_{Geoglyph}$ is the area of a polygon, n the number of vertices, and x, y the vertex coordinates. With the static moments S_x and S_y in the x- and y-direction:

$$S_x = \frac{1}{6}\sum_{i=1}^{n}(x_i y_{i+1} - x_{i+1} y_i)(y_{i+1} + y_i)$$

and

$$S_y = \frac{1}{6}\sum_{i=1}^{n}(x_i y_{i+1} - x_{i+1} y_i)(x_{i+1} + x_i),$$

we obtained the coordinates of the centre of gravity X_{CG} and Y_{CG} as

$$X_{CG} = \frac{S_y}{A_{Geoglyph}} \quad \text{and} \quad Y_{CG} = \frac{S_x}{A_{Geoglyph}}.$$

In a next step, we calculated the moments of inertia I_{uu}, I_{vv}, and I_{uv} in the principal axis coordinate system:

$$I_{\alpha\beta} = \int_A \rho(\overrightarrow{r})(r^2 \partial_{\alpha\beta} - x_\alpha x_\beta) dA$$

with

$$\partial_{\alpha\beta} = \begin{cases} 1 : \alpha = \beta \\ 0 : else \end{cases}, \quad \alpha = u, v, \quad \beta = u, v \quad \text{and} \quad r_i = \sqrt{x_i^2 + y_i^2}.$$

We then derived the azimuth of each principal axis with respect to the UTM Zone 18 S system:

$$\alpha = \frac{1}{2}\arctan\left(\frac{2I_{uv}}{I_{vv} - I_{uu}}\right).$$

Although the method that we used theoretically allows the axis of orientation to be determined for all kinds and shapes of geoglyphs, we limited our calculation to those geoglyphs that actually feature visually dominant straight sections, such as straight and meandering lines, rectangles, and trapezoids (Fig. 19.3), whereas all biomorphic figures, spirals, and the like were not considered. This way, 421 geoglyphs out of a total of 639 defined geoglyphs were considered, slightly more than in our first attempt (Lambers 2006b:116f, Fig. 45).

Compared to previous attempts to determine geoglyph orientation by field measurements, our approach has the advantage of factoring in all the irregularities featured by many geoglyphs which are reflected in the detailed geoglyph

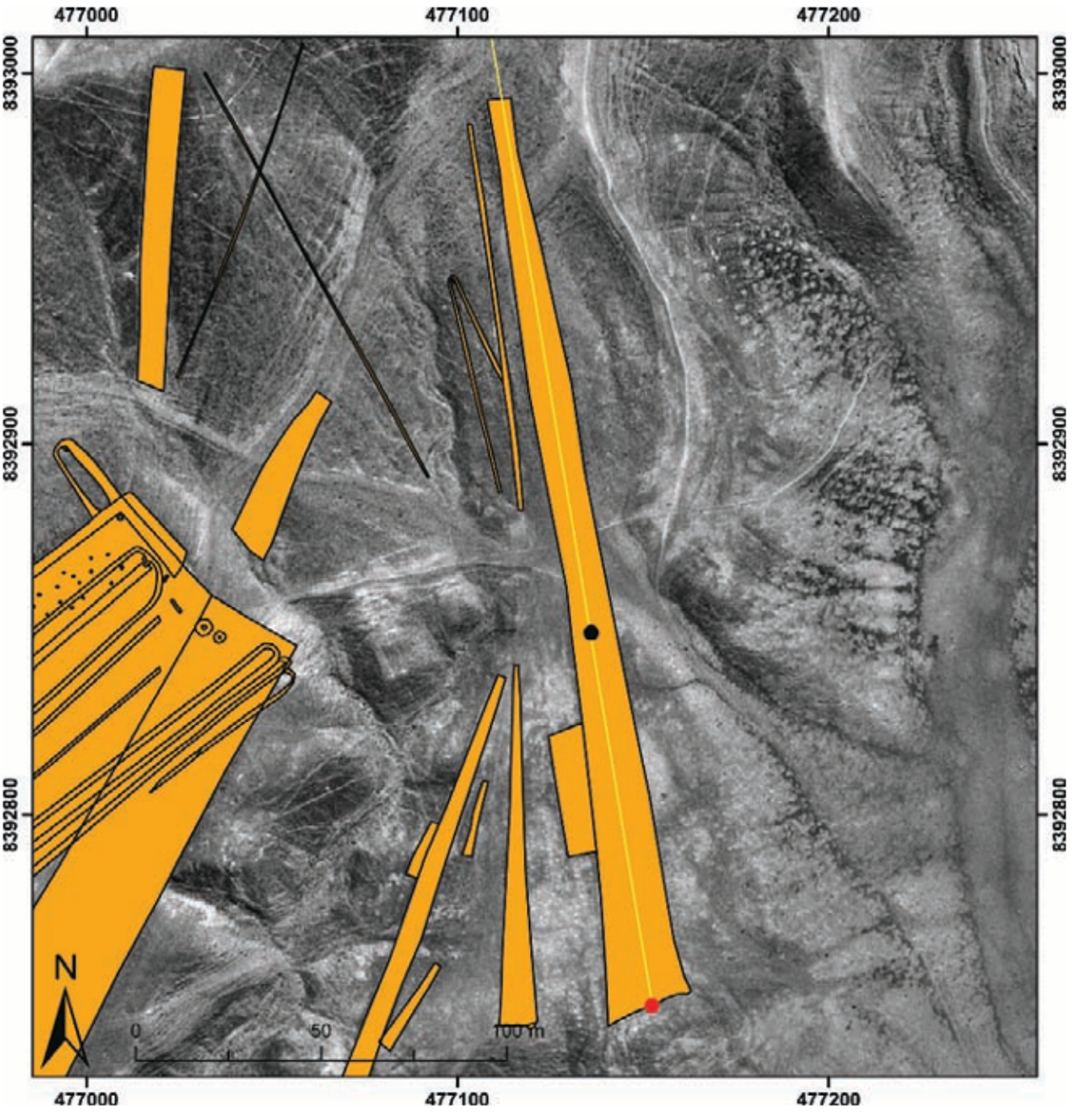

Fig. 19.3 Example of a geoglyph represented by a polygon from which the centre of gravity (*black dot*) and then the axis of orientation (*yellow line*) were calculated. The far intersection of the axis with the polygon border as seen from the peak (*red dot*) serves as observer's point for LoS calculation (cp. Figs. 19.5 and 19.6.) (Coordinates: UTM 18 S, WGS 84)

mapping. Furthermore, for all geoglyphs considered here, the axis of orientation calculated by means of a principal axis transformation runs through the centre of gravity of the geoglyph, as opposed to field measurements that may, for instance, indicate the orientation of one of the two nonparallel borders of a trapezoid instead.

Once the orientations had been established, we needed to test if the corresponding axes intersected mountain peaks, for which we determined local maxima in the terrain elevation of our study area. For this purpose we used the same digital terrain model of the Palpa area described in the previous section. We used an algorithm implemented in the Landserf 2.2 software

(www.landserf.org) to detect local maxima of terrain elevation in the DTM (Wood 1996: Chap. 5). This algorithm identifies peaks in a raster DTM based on the height differences of each cell with respect to its surrounding neighbour cells. A peak requires a local convexity of the terrain, therefore the necessary and sufficient conditions for a peak can be formulated mathematically by using the first- and second-order derivatives as follows.

$$\frac{\partial z}{\partial x} = 0, \quad \frac{\partial z}{\partial y} = 0, \quad \frac{\partial^2 z}{\partial x^2} > 0, \quad \text{and} \quad \frac{\partial^2 z}{\partial y^2} > 0.$$

The size of the window used to search for local maxima can be varied according to the terrain characteristics. In our case, we defined a search window size of 7×7 cells, although calculations with 5×5 and 9×9 cells yielded exactly the same results. A second parameter required for peak detection is the minimum height difference within the search window required to accept a DTM cell as a peak. We decided to set this value to 20 m in order to detect only significant peaks.

With these parameters, the calculation yielded 116 local maxima for the whole area covered by the DTM (Fig. 19.4). However, 43 out of these were not visible from any of the geoglyphs, as we determined by calculating a multiple viewshed using the geoglyph points described in the previous section as observers' points. Only 73 local maxima were located within the area covered by this viewshed and were thus further considered in our calculation. A review of these 73 points showed that the algorithm had quite reliably identified peaks of mountains, hills, and spurs that we knew from our fieldwork to be visually prominent in our study area.

In the following step we tested which axes of orientation calculated for the geoglyphs intersected these local maxima. In order to account for inaccuracies inherent in the geoglyph mapping as well as in the calculation of both the axes of orientation and the local maxima, a given axis of orientation was regarded as intersecting a local maximum if it passed the actual point within a threshold distance of

$$\Delta d = \mathrm{d}_{\mathrm{Geoglyph-Peak}} * \sin(\alpha) + 20\ \mathrm{m} \ \text{ with } \ \alpha = \arcsin(0.15\mathrm{m}/L_{\mathrm{Geoglyph}}),$$

where 0.15 m is the accuracy of the photogrammetric measurement of the geoglyph border points, 20 m the estimated accuracy of the DTM, and L_{Geoglyph} the length of the orientation axis segment intersecting the geoglyph. The threshold distance Δd therefore varies for each possible geoglyph/peak combination, factoring in the accuracy of both the geoglyph mapping and the underlying DTM.

This calculation resulted in 28 orientation axes intersecting a local maximum (Fig. 19.5). Although 50 local maxima were not intersected at all, 19 were intersected by one axis of orientation each, 3 local maxima by two axes each, and one peak even by three axes.

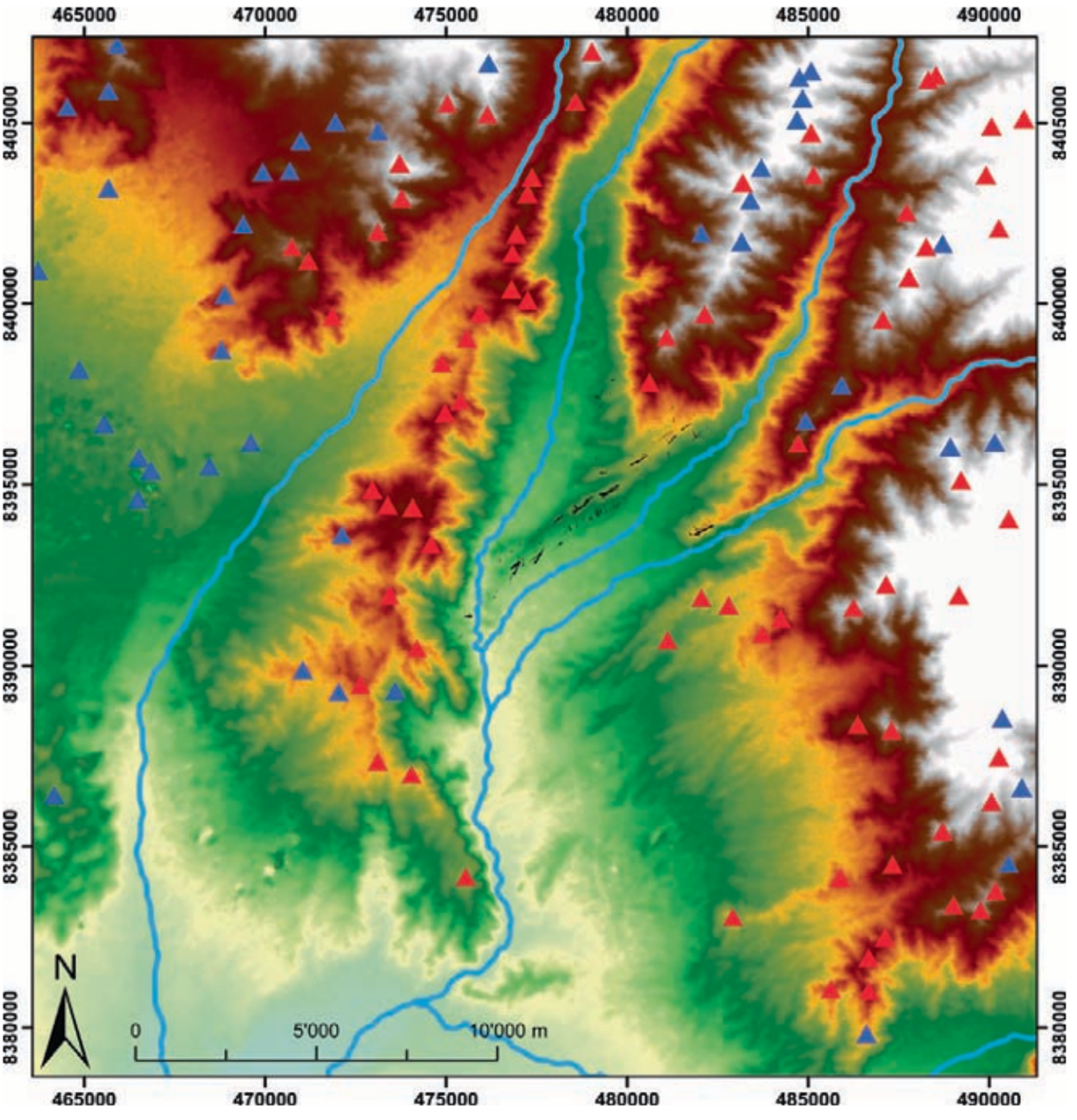

Fig. 19.4 Digital terrain model covering the study area around Palpa. Geoglyphs are shown in black near the centre of the map. Peaks determined in Landserf that are visible from the geoglyphs are shown as red triangles, whereas blue triangles represent peaks outside the area covered by the multiple viewshed. (Coordinates: UTM 18 S, WGS 84)

However, these results could not be taken at face value. As the intersections of axes of orientation and local maxima were calculated in 2D space, possible terrain obstacles blocking the view between both features in 3D space were not considered and had to be factored in in a next step. We therefore calculated lines of sight along the 28 axes using our own software which was adapted to single line of sight calculation (Lambers and Sauerbier 2006). The programme considers earth curvature and refraction. For each axis we defined its intersection with the far end of the respective geoglyph as seen from the peak as the observer's point in order to simulate a view of an observer along the geoglyph towards the horizon. Furthermore, to achieve more realistic results, we

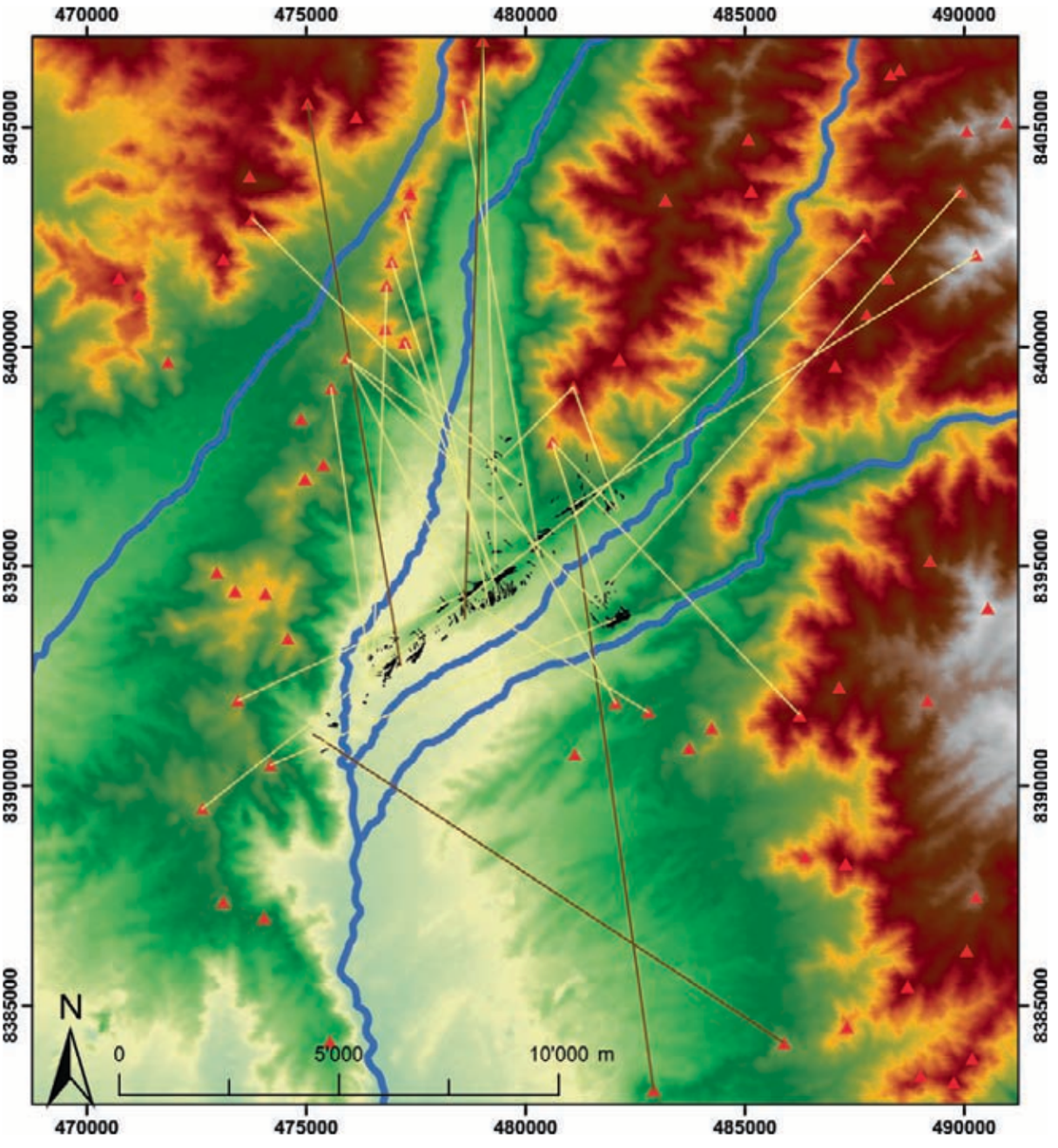

Fig. 19.5 Axes of orientation intersecting mountain peaks. Lines in bright yellow indicate continuous lines of sight, whereas dark green lines break off shortly before reaching the peak but are still regarded as indicating visibility according to the conditions formulated by us (cp. Fig. 19.6). (Coordinates: UTM 18 S, WGS 84)

considered that lines of sight between geoglyph and peaks needed not necessarily end exactly at the respective peak, but might end shortly before reaching that point. This is because when viewing a hill or mountain from the valley, one often gets the visual impression of seeing its peak, even though the actual highest point might be hidden behind the uppermost portion of the slope. In order to model this, we regarded visibility to be given even if the line of sight were blocked by the DTM below the actual peak, the condition being that the remaining distance to the peak must be covered by ascending terrain (Fig. 19.6).

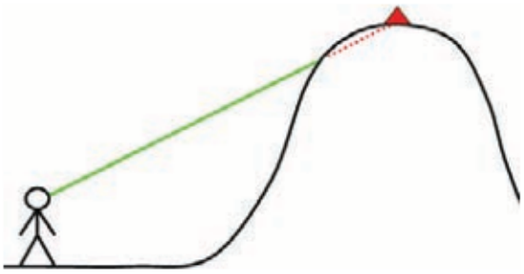

Fig. 19.6 Example of a LoS (*green line*) not reaching the actual mountain top (*red triangle*) but stopping shortly before. In this case, because the remaining distance to the mountain top is covered by ascending terrain, the mountain peak is assumed to be visible regardless (cp. Fig. 19.5)

This calculation yielded the following results. Out of the 28 axes of orientation that intersect peaks, continuous lines of sight between geoglyphs and peaks exist in 24 cases. In the remaining 4 cases, the lines of sight end shortly before reaching the peak, with the remaining distance covered by ascending terrain, meaning that visibility was given as well according to our conditions (Figs. 19.5 and 19.6). The preliminary numbers given above were thus confirmed.

In sum, 28 geoglyphs out of the partial sample of 421 geoglyphs with straight sections considered in this study, and out of a total sample of 639 geoglyphs can be regarded as being oriented towards mountain peaks. This corresponds to 6.7% of the partial sample and 4.4% of the total sample, respectively.

19.3 Discussion: Geoglyph Visibility and Orientation

The question underlying our spatial investigation of the Palpa geoglyphs was in which way a consideration of the surrounding landscape can contribute to an understanding of the geoglyphs. Only in GIS could this kind of contextual analysis be undertaken in a systematic way.

Concerning geoglyph visibility, we extended proven methods of cumulative viewshed calculation to determine if the variable visibility had an impact on the location of the geoglyphs. The results of our study indicate that this was indeed the case. Places with good visibility were apparently preferred for the construction of geoglyphs over places with low visibility, even though the latter were not completely avoided. This allows us to interpret the abundant traces of group activity recorded on geoglyph sites in the framework of rites performed to be seen by others. Geoglyphs can thus be understood as stages rather than images. On these stages social groups acted and interacted, and spectators in the valleys and on other geoglyph sites were able to watch and observe. This visual interaction may have played a role in the differentiation of social groups within Nasca society. This finding does not in itself provide an explanation of the geoglyphs or the acts performed on them, however, it allows important clues about the social context of geoglyph-related activities.

The material remains of the activities performed on geoglyphs provide hints as to the ideas and concepts that motivated these acts. Objects such as *Spondylus* shells, crawfish, and field crops placed on stone platforms indicate a strong concern for water, irrigation, and fertility. The assumption that mountains may have been regarded as sources of water led us to explore the orientation of geoglyphs towards this type of prominent landscape feature. Although parts of this analysis could be performed in standard GIS software such as ArcGIS, we had to develop additional tools for the specific requirements of our analysis, namely for the calculation of the axes of orientation of the geoglyphs and their intersection with mountain peaks. The question was whether prominent landscape features such as mountain peaks were visually integrated into the geoglyph scenery by linear geoglyphs pointing towards them.

Although less clear than the visibility study, the results of our orientation study do allow us a preliminary answer to this question. The fact that only about 4–7% of the geoglyphs of Palpa (depending on the initial sample) are apparently oriented towards mountain peaks clearly shows that such orientations were not a major concern to the people who built the geoglyphs. In fact, the numbers are quite low, considering that the pampas on which the Palpa geoglyphs are located are surrounded by ranges of mountains and hills on three sides (to the north, east, and west). Clearly, orientation towards mountain peaks was not a major ordering principle during geoglyph construction. This conclusion is supported by the observation that the above-mentioned 28 geoglyphs do not include any of the visually predominant geoglyphs of the study area, that is, the large trapezoids and the wide straight lines on the flat plateaus. Rather, most of the 28 geoglyphs are minor elements of large complexes in which the more prominent geoglyphs are apparently not oriented towards mountain peaks.

In spite of these rather clear findings, the fact that 4 out of 23 peaks are intersected by more than one axis of orientation, one of them even by three axes, leaves the possibility open that some geoglyphs were indeed deliberately oriented towards specific mountain tops. We do not know if the corresponding mountains show any special features, for example, archaeological remains on their peaks such as those recorded on Cerro Blanco in the Nasca valley (Reinhard 1996). But even without such features these mountains may once have had a special meaning now concealed to us. This requires further investigation before definite conclusions can be drawn.

In sum, although a small number of geoglyphs may have been deliberately oriented towards mountain peaks, such an orientation cannnot be regarded as a major ordering principle underlying geoglyph placement and construction. In this regard our conclusions are remarkably similar to those of archaeoastronomical studies of the Nasca geoglyphs: although there are indications that some astronomical alignments may have existed, the majority of geoglyph orientations cannot be explained in this way (Aveni 1990). The analogy goes even further. Just as the negative results of archaeoastronomical studies do not mean that astronomy was not important in Nasca society, the negative results of our

study do not imply that mountain worship did not exist. We can only show that, if it existed, it did not become manifest in consistent spatial relationships between geoglyphs and mountains. It should be noted in this context that our workflow of calculations can also be used for an archaeoastronomical study of the Palpa geoglyphs, which was not a part of our project.

A general conclusion from our spatial study is that the landscape played an important role in the conceptual framework of the geoglyph phenomenon. In the majority of cases, the locations where geoglyphs were placed were carefully chosen such that the acts to be performed on them would be well visible. People on other geoglyph sites, but also down in the valleys, were this way integrated into the activity on the geoglyphs. Visual links to other landscape features, on the other hand, may have been less important, although this requires further studies. The landscape was apparently perceived as a whole, not divided into fertile valleys and barren desert as today. To consider this spatial context is as important when trying to interpret the geoglyphs as the temporal and cultural context.

19.4 Conclusions: GIS Applications in Archaeology

Apart from answering questions about geoglyph function and meaning, our study of geoglyph visibility and orientation also illustrates some of the chances and limitations of GIS applications in archaeology.

As mentioned above, GIS was not originally designed for archaeological applications. In our project this became apparent at many stages. Although software packages such as ArcGIS provide a powerful toolbox for a wide variety of analyses, many of the requirements resulting from our research problem were not met by them. In the study described here, standard tools for LoS calculation were not sufficient for our purposes, and tools for the calculation of the centre of gravity of the geoglyphs and the axis of orientation running through them had to be newly developed. There are still very few ready-made GIS models and methods available for archaeological investigations. Thus, archaeological GIS applications have to confront many practical problems.

A more general problem stems from the fact that the digital data analysed in GIS are always a simplification of the real world. There are many potential sources of error in the long process of measurements and calculations that led to the results of our study. These range from the accuracy and resolution of the DTM to the accuracy of the geoglyph mapping, the identification of mountain peaks, and finally the various methods of calculation. An unfavourable accumulation of these errors may lead to false results. This is indeed the case for at least one of the 28 axes of orientation that is supposed to hint at a mountain peak which, as we know for certain from our fieldwork, is in fact not visible from the corresponding geoglyph. Such discrepancies between the real world

and its virtual representation modelled in GIS are common but rarely considered in detail. We do not regard this problem as questioning our overall results, but we do not want it to go unmentioned either.

In spite of these issues, we were able to use GIS to shed light on important spatial relationships between the geoglyphs and the landscape in which they are situated. We used spatial proxies such as terrain elevation, Euclidian distance, azimuth angles, and the like to investigate the ways in which the landscape of Palpa was seen and perceived by the people who built and used the geoglyphs. GIS allowed us to address this question, which had so far been discussed mainly in impressionistic terms, in a systematic way and to draw well-founded conclusions concerning the cultural and social context of the geoglyphs. In this regard our study answers the concerns raised in the first section about the general usability of GIS in archaeological research. In our view the capabilities of GIS to spatially analyse archaeological features, thereby contributing to their interpretation, are far from exhausted.

Nevertheless, the further one explores the potential of GIS to address archaeological research problems, the clearer become its conceptual limitations. All GIS-based studies have to be undertaken within the narrow confines of the concept of physical Cartesian space and the need to quantify and georeference all information. To deal with qualitative, subjective, fragmented, or ambiguous information concerning cultural, social, and ideological aspects of the history of ancient societies within these conceptual limitations clearly remains a challenge. In this sense, GIS should not be regarded as a panacea for archaeological research, but rather as a powerful tool to systematically test carefully formulated hypotheses regarding spatial aspects of cultural history.

Chapter 20
A Model Helicopter Over Pinchango Alto – Comparison of Terrestrial Laser Scanning and Aerial Photogrammetry

Henri Eisenbeiss

Abstract Two novel methods, which were applied for the recording of the site Pinchango Alto, LIP (Late Intermediate period; 1400 AD), are presented. After describing the archaeological site, the utilized technologies, terrestrial laser scanning, and photogrammetric processing of mini-UAV (unmanned aerial vehicle) imagery are illustrated, compared to traditional surveying methods, and research requirements for the documentation are discussed. Hence, the combined application of these technologies, the established workflow and the resulting products, which allowed a fast yet accurate recording of the site and its stone architecture, are presented and analyzed.

20.1 Introduction

How to get an autonomous flying model helicopter and a laser scanner to Pinchango (Peru)? Here we describe this challenging task.

We start by focusing on two novel recording techniques for the documentation of archaeological sites. In our work we evaluated the techniques using the site Pinchango as a unique pilot study of a Late Intermediate period (LIP, AD 1000–1400) site within the framework of the Nasca–Palpa Archaeological Project.

Recently, Denise Kupferschmidt (KAAK) measured the structure of the settlement Pinchango Bajo using the existing aerial orthoimage (Fig. 20.1 and Kupferschmidt 2008). In the following section, this method and the established methods by Zwicker (2000) are compared to the capabilities of the new techniques employed for the documentation of archaeological settlement structures.

H. Eisenbeiss (✉)
ETH Zurich, Institute of Geodesy and Photogrammetry, ETH Zurich HIL D 52.4, 8093 Zurich, Switzerland
e-mail: henri.eisenbeiss@geod.baug.ethz.ch

M. Reindel, G.A. Wagner (eds.), *New Technologies for Archaeology*, Natural Science in Archaeology, DOI 10.1007/978-3-540-87438-6_20,
© Springer-Verlag Berlin Heidelberg 2009

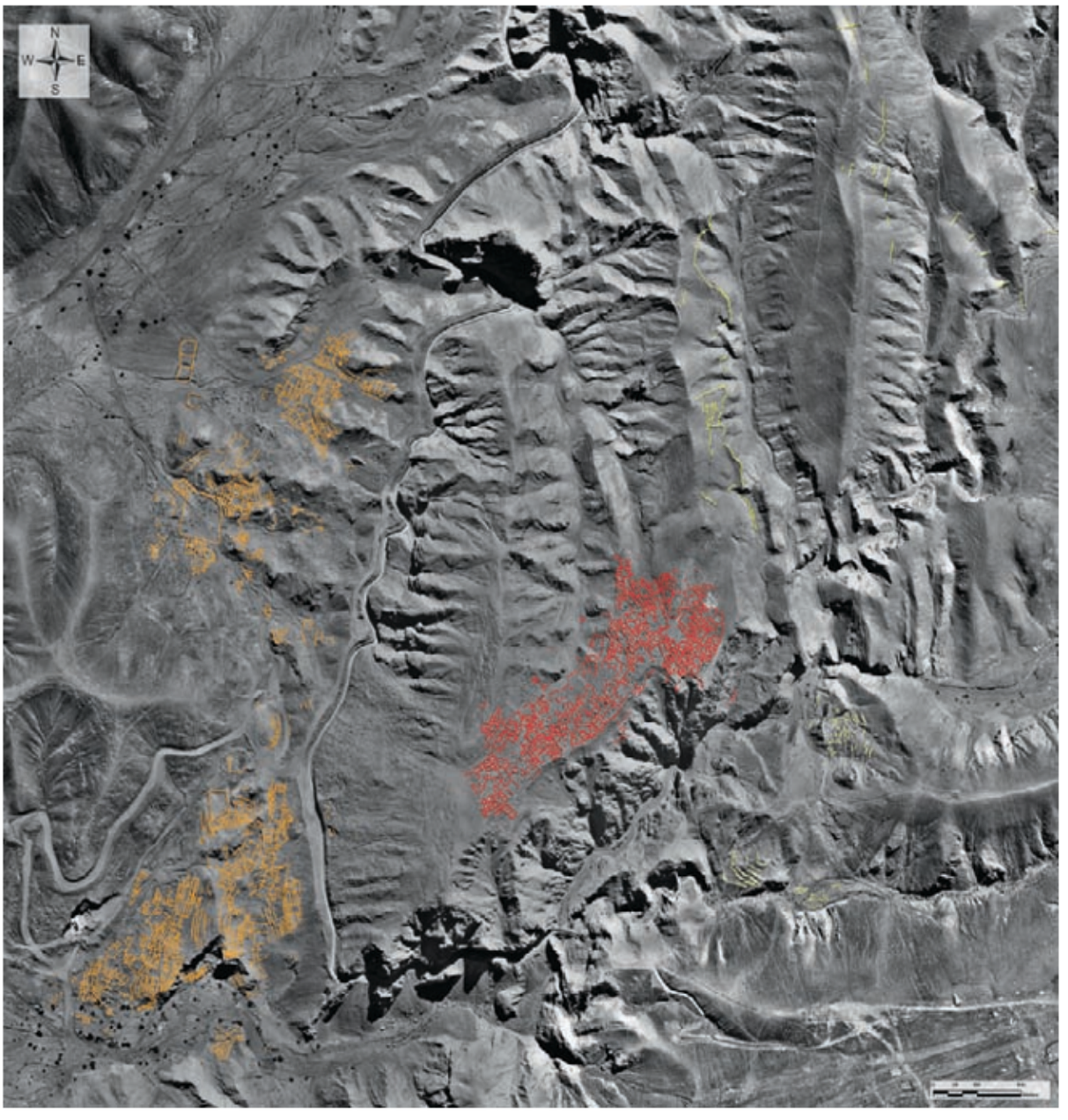

Fig. 20.1 A cut-out of the orthoimage from aerial images which shows the entire Pinchango site (14_3002700 S, 75_1100300 W). The orange shading indicates Pinchango Bajo, and the *red shading* indicates Pinchango Alto. The *yellow lines* show the defensive walls of the settlement and small settlement structures, which also belong to Pinchango

20.1.1 Pinchango

Pinchango is located in the Palpa region submontane of the Cerro Pinchango. The site is surrounded by the Rio Grande and Palpa valleys at the horizontal spur of the Cresta de Sacramento. Pinchango is subdivided into a lower and an upper part (Bajo and Alto, respectively), as shown in Fig. 20.1. Both parts form the largest and also one of the best preserved sites from the LIP in the Palpa region. Our investigation on recording techniques for the documentation of archaeological sites concentrates mainly on Pinchango Alto. However, at this

point both parts are introduced, because Pinchango Alto (PV66-137) and Pinchango Bajo (southern part PV66-136 and northern part PV66-138) form the site Pinchango. In the following it is explained how the local measurements of both sites were integrated into one database. The size of the region is approximately 20 ha. The upper part is situated about 150 m above the valley floor and 490 m.a.s.l., whereas the lower part extends along the northwestern slope towards the Rio Grande valley.

It is extremely difficult to access the Pinchango Alto site. The access from the north is only possible along a steep trail leading over a ridge. At the same part of the site a large number of defensive walls are found. To the south and east, the hilltop site is flanked by a deep gorge. The only direct access to Pinchango Alto is from the northwest via Pinchango Bajo. Unfortunately, a modern irrigation channel now cuts through the whole length of the site, and the alleged access path no longer exists. The preserved wall height is about 40–70 cm but can reach a maximum of 1.5 m (Fig. 20.2). The walls structure the site in small and large rooms, open squares, and narrow paths, which are laterally bordered by long slabs. In the central part of Pinchango Alto a series of holes were burrowed into the ground and underlying bedrock in ancient times. In addition, close to the holes grinding stones and accumulations of mica pebbles are located. The discovery of grinding stones and the holes, which look like short mine shafts, have led to the assumption that the settlement was a mining and mineral processing centre (Reindel et al. 2002; Reindel 2005). However, the holes may also have served as storage of other goods (Stöllner and Reindel 2007); this has to be investigated in upcoming archaeological excavations.

Fig. 20.2 Pinchango Alto, looking from the southwest to the northeast

20.1.2 Previous Work at Pinchango

The earliest aerial images were taken in 1944 over the area of Sacramento, which also include the Pinchango area (Lambers 2006). Some 40 years later, Johnson did a number of experiments with balloon photogrammetry and medium format images taken from a sporting airplane in the Nasca area. The balloon experiments were not successful, as the system was susceptible to winds. Moreover, in higher altitudes it turned out to be increasingly difficult to position the camera accurately if a series of overlapping photographs was required and the balloon did not have enough lift to reach the desired altitude above the terrain. This was almost certainly due to impure hydrogen (Johnson et al. 1990).

In 1999, in the framework of a diploma thesis at ETH Zurich (Zwicker 2000) the first photogrammetric and geodetic observation for the archaeological documentation of the site Pinchango Alto and the surrounding area was accomplished (Reindel and Isla 1999 and Fig. 20.1). At this time, the structure of the site was surveyed by using two methods, which were established in the last decades. For the first method a tachymeter TC 600 (Leica) was used. Therefore, for the definition of the coordinate system four fix points were established. Using these points, the terrain and the walls were recorded using tachymetric survey with an accuracy for the tachymetric measurements of 2 cm in planimetry and 3 cm in height. However, the accuracy of the measurements of the walls in height was approximately 20 cm, because the structure of the walls varies significantly from one stone to the next.

In the second method the site was mapped using an analytical plotter by manual measurements in analog aerial images. The average image scale was intended to be 1:5000 (Gruen 1999). Finally, the aerial images were acquired in 1998 in the framework of the geoglyph survey (Lambers 2006) with a scale of 1:7000. Because the aerial images covered a larger area than Pinchango Alto, it was also possible to map the defensive walls. The accuracy for the manual measurements of the walls was 10–20 cm. The photogrammetric measurements of the contour lines were done in the framework of the Palpa DSM (Sauerbier and Lambers 2003, hereafter aerial-DSM (digital surface model)), whereas the measurements of the settlement structure were done by Zwicker (2000). The aptitude of both methods varied significantly inside the site. The contour lines produced from the terrestrial measurements showed high accuracy, but they could cover only a limited part of the area of interest. In contrast, the photogrammetric measurements could cover the complete area, but the accuracy of the measurements was insufficient. However, finally for the general plan the photogrammetric data were used.

For the analysis of the mapping of the settlement structure the area was separated into the area with the best preserved walls and the area with the most damaged parts of the site. Comparing the terrestrial and photogrammetric measurements for the well-preserved part, both methods are

equivalent, whereas for the demolished part the destroyed structures were not identifiable in the aerial images. Nevertheless, the surrounding defensive walls have been only measured in the aerial images, due to time constraints in the thesis work. Finally, the terrestrial measured walls were combined with the photogrammetric measurements of the contour lines and the far-flung defensive walls. These results allowed the analysis of the settlement structure of Pinchango Alto, including agglutinated rooms, enclosures, corridors, and several large plazas (Fig. 20.1). Using the experiences from 1999, the archaeologists involved in the Nasca–Palpa project searched for new technologies which would allow a more detailed and accurate data acquisition.

20.1.3 A Challenge for New Technologies

Why was Pinchango Alto again in the focus of the archaeologists? Because of its state of preservation and size, Pinchango Alto is well suited for the analysis of a typical LIP site in detail. In addition, due to the demand to do the surveying of the sites in a rather short time, the archaeologists were looking for documentation techniques which fulfill the given time frame. Furthermore, the surveying techniques needed to be easy to use, easily transportable, have simple handling, be able to handle big datasets, and the costs for the techniques should fulfill the usually limited budgets of archaeological field campaigns.

In archaeology it is common practice for the documentation to be based on classical surveying techniques such as single point measurements using tachymetry, leveling, or tape measurements. These methods are accurate, but for the recording of larger sites such as Pinchango Alto, they are quite time-consuming. Furthermore, the methods just allow producing coordinates, which are used for maps or to put distance measurements in archaeological sketches. Therefore, a high-resolution, flexible, and mobile recording system was needed to document the terrain and the architecture of the site. The recording of the site was also planned to show the potential of novel surveying techniques in archaeological research in terms of detail, efficiency, and accuracy.

Finally, considering the general characteristics of LIP sites in the region of Palpa and Nasca, and Pinchango Alto in particular, three goals and levels for the intended investigation of the LIP in the Palpa region were defined: (1) a spatial analysis of the site in its topographical context focusing on accessibility, visibility, and defensibility; (2) a functional study of the internal structure of the site; and (3) an example for the documentation of LIP stone architecture and masonry. Such a multilevel investigation required 3D models of the site and its surroundings at various levels of resolution (Lambers et al. 2007).

20.2 Technologies and Research Requirements

20.2.1 Mini UAVs

'UAVs (unmanned aerial vehicles) are to be understood as uninhabited and reusable motorized aerial vehicles' (van Blyenburg 1999). These vehicles are remotely controlled, semi-autonomous, autonomous, or have a combination of these capabilities. The term UAV is used commonly in the computer science, robotics, and artificial intelligence community. Supplementary, in the literature also synonyms such as remotely piloted vehicle (RPV), remotely operated aircraft (ROA), and unmanned vehicle systems (UVS) can be found. The definition of UAVs encompasses among others fixed and rotary wing UAVs, lighter-than-air UAVs, and lethal aerial vehicles (van Blyenburg 1999).

However, for our investigation a model helicopter was selected. Model helicopters are clearly defined by the Unmanned Vehicle Systems International Association as micro, mini, close, short, and medium range UAVs depending on their size, endurance, range, and flying altitude (UVS International 2008).

Model helicopters, in contrast to standard airplanes, are able to operate closer to the object. In addition, model helicopters are highly flexible in navigation in comparison to fixed wing UAVs (Bendea et al. 2007) and, in contrast to microdrones (Nebiker et al. 2007), more stable against environmental conditions such as wind. The developments of model helicopters and comparable autonomous vehicles are primarily driven by the artificial intelligence community (AAAI 2008) and have been used mainly in the past for military applications with increasing use in the civilian sector.

In the past, model helicopters were already used in photogrammetric applications. However, at that time the model helicopters were controlled manually via radio link. In 1980, Wester-Ebbinghaus first used a model helicopter for photogrammetric documentation of a monorail in Wuppertal (Germany) by using a medium format camera. The flight was completely manually controlled by the pilot, and the navigator monitored the altitude and activated the camera shutter via radio link (Wester-Ebbinghaus 1980). Twenty years later Zischinsky et al. (2000) used images taken from a model helicopter partly for the generation of a 3D-model of an historical mill. The small format amateur camera mounted on the helicopter took mainly images of roofs and the courtyard.

Nowadays, these new technologies allow low-cost navigation systems to be integrated in model helicopters, enabling them to fly autonomously. These kinds of autonomous flying model helicopters fit into the class of mini-UAV systems (van Blyenburg 1999, Eisenbeiss 2004). Mini-UAVs are highly maneuverable, due to the possibility for hovering, change of flight direction around the center of rotation, as well as the capability for turning the mounted camera in the horizontal and vertical directions. However, due to the difficulty of keeping the ideal position and attitude, the vibration of the helicopter, and the manual planning of image acquisition points, model helicopters have not

been used successfully in the past for measurements, precise modeling, and mapping of objects (Eisenbeiss 2004). Latest developments integrate GPS/ INS (Global Positioning System/ Inertial Navigation System) together with a stabilization platform for the camera. Because of the small size and the low payload, the selection of the installed hardware is mostly limited to low-cost navigation systems with low precision. However, the combination of GPS/INS sensors with image data for navigation allows for more precise and reliable results. Furthermore, the integration of GPS/INS and image data in a real-time triangulation method will drastically reduce time and cost for postprocessing.

Mini-UAVs have been used recently for civilian applications such as 3D city modeling (Wang et al. 2004) and a medieval castle in Sarnen (Pueschel et al. 2008), in forestry (Horcher and Visser 2004), in agriculture (Herwitz et al. 2004, Rovira-Más et al. 2005, Eisenbeiss 2006, Reidelstuerz et al. 2007, Eisenbeiss 2008, Rovira-Más et al. 2008), and for the documentation of rockslides (Eisenbeiss 2008).

The above-mentioned examples of using mini-UAVs in photogrammetry have already shown the great potential of the technology. However, these studies have also pointed out that for precise documentation of specific sites, a guarantee of a complete coverage and a stable flight is essential. Therefore, the position of the system has to be controlled and stabilized. In 2002, a mini-UAV (Yamaha RMAX) was used in photogrammetric flights over two test sites in Sweden, to analyze the accuracy of the GPS/INS for the photogrammetric purposes in manual and autonomous flying modes. The results show that the stability of the camera mounting, the vibrations caused by the main rotors, and the GPS/INS accuracy are the most important factors of mini-UAVs. Furthermore, using the autonomous flying mode the helicopter could follow the predefined path also under wind conditions (Eisenbeiss 2003).

In 2003, during the planning phase of the Pinchango Alto field work, the mini-UAV system Copter 1b from Surveycopter (Fig. 20.3 and Table 20.1) was selected for the documentation campaign in 2004. The Copter 1b holds the flight control system wePilot1000 from weControl, which allows for the stabilization of the platform and for an autonomous flight following a predefined flight path for image acquisition. The flight control system features the following main characteristics: an altitude stabilization and velocity control, position and RC transmitter sticks interpreted as velocity commands, integrated GPS/INS system, altimeter, magnetometer, payload intensive flight controller, built-in data logger and telemetry capability, programmable hardware for rapid customization, and an embedded computer system. Furthermore, the system consists of a ground control station (a laptop with monitoring software (weGCS)), a Canon D60 still-video camera, communication links, power supply, video link (incl. video camera) as visual control for monitoring image overlap, and transport equipment.

Nowadays, mini-UAVs are stabilized and work with an onboard computer determining their position and orientation in real-time. Using this technology, a goal of this project was the automation of the complete photogrammetric

Fig. 20.3 *Top* image shows the selected mini-UAV system, whereas the *bottom* image illustrates the chosen terrestrial laser scanner RIEGL LMS 420 at Pinchango

Table 20.1 Main features of the mini-UAV System from Surveycopter Copter 1b and the Riegl Laser Scanner LMS-Z420i

Mini-UAV-System Copter 1b		Laser Scanner LMS-Z420i	
Length	2 m	Main dimension	463 × 210 mm
Rotor diameter	1.8 m	Weight	16 kg
Maximum takeoff weight	15 kg	Power supply	12–28 V DC
Payload capacity	5 kg	Measurement range	Up to 1000 m
Flight endurance	Max. 45 min	Minimum range	2 m
Altitude	1500 m	Measurement rate	11000 pts/sec
Range	5 km	Beam divergence	0.25 mrad

workflow for the documentation of archaeological sites, starting from the flight planning, autonomous flight of the mini-UAV, and the data processing. Therefore, a specific flight planning tool for mini-UAVs, which would allow the image acquisition in a specific position and a defined configuration, had to be developed. In addition, the stability and the reliability of the autonomous flight and the adaptation of the flight control system to the needs for photogrammetric flights had to be utilized.

A further objective of our work was the high reliability, precision, and resolution of the photogrammetric products such as elevation models, orthoimage, and textured 3D models by using a mini-UAV and a terrestrial laser scanner as data acquisition platforms. Therefore a workflow had to be developed that would allow the processing and combination of the data. In particular, the focus was on the workflow for the orientation and automated generation of elevation models of amateur still-video images taken from mini-UAVs.

20.2.2 Terrestrial Laser Scanning

Laser scanners are active measurement systems that can generate point clouds with 3D-coordinates for each point and intensity images. Depending on the observation platform, laser scanners are classified into airborne or terrestrial laser scanners. Because airborne laser scanners need a precise GPS/INS system onboard the airplane or helicopter, the complete system is quite expensive in comparison to a terrestrial laser scanner. Based on the financial limitations as mentioned above and the limited availableness of airborne laser scanners in Peru, the focus of this study was on terrestrial laser scanning.

Over the past years a wide variety of terrestrial laser scanner systems has been developed for surveying tasks. The terrestrial laser scanner system is normally equipped with a still-video camera. These systems are so-called combined systems, where the camera is integrated or adapted to the system (Kersten et al. 2006; Wendt 2007). For the integrated system, the camera is set up into the chassis of the scanner, whereas for the adapted system the camera is

mounted outside the chassis. The integrated system has the advantage that both sensors are protected and the calibration of the individual sensors, as well as the supply of the systems is stable over a longer period. Main disadvantages of these systems are that the camera and the lens cannot be adjusted for individual applications. Furthermore, these systems have a limited field of view of the camera, which limits the access to the complete image. These disadvantages and advantages are also a feature of adapted systems. Therefore the adapted systems are more flexible and can be individually modified based on the specific task. However, after varying the system the relation between the scanner and camera of the adapted systems has to be calibrated.

A comprehensive overview of terrestrial laser scanners with still-video cameras is given in Kersten et al. (2006) and Lemmens (2007). Kersten et al. describe the state-of-the-art of laser scanner systems and available postprocessing software packages for 3D-point clouds are explained.

Based on the systems existing on the market in 2004, the Riegl laser scanner LMS-Z420i was the most appropriate one (Fig. 20.3, Table 20.1). The LMS-Z420i system, a combined laser scanner system, has a long scanning range of 1000 m, is robust, allows working in an extreme environment such as the Atacama desert, and the adapted camera allows the combination of several lenses (Gaisecker 2006); all of which fulfilled our requirements for the documentation of the archaeological site Pinchango Alto. The main characteristics of the laser scanner are listed in Table 20.1 and Gaisecker (2006).

The site Pinchango Alto laser is a good example of large volume data and a high number of scan positions. Moreover, due to the topography of the site and relatively large incident angles of the signal paths, large occlusions occurred in the laser point clouds. This is a difficult case for the surface registration problem. Therefore, a 3D surface registration method had to be developed that also allows the registration of the single scans without using reflectors.

The above-described research topics enable spatial analysis on the regional and on the site level, however, the unique documentation of LIP stone architecture and masonry requires the highest possible resolution. Thus, a method had to be developed that allows error detection, surface reconstruction, and texture mapping with image and range data acquired with the Riegl LMS Z420i laser scanner.

20.3 Methodical Contribution

20.3.1 Field Work Preparations

Before going to Peru, the existing data of Pinchango had been evaluated for the planning of the field work. With the existing aerial orthoimage (Fig. 20.1) the dimension of the settlement was determined. The complexity of the settlement could be appraised from a video, which was recorded during the field work of

1999. Based on these evaluations, one week of field work for laser scanning was estimated. Moreover, the aerial-DSM and the orthoimage were used for the flight planning of the mini-UAV flight. From prior fieldwork experiences with UAVs in Sweden (Eisenbeiss 2003) the attended time for the mini-UAV flight, including system checks and flight tests in the field, was assumed to be one week as well.

Based on the separation between the area with the best preserved walls and the area with the most damaged parts of the site from the survey campaign in 1999, the site was divided into the same classes (A and B, respectively) for the laser scan positions density of the field work in 2004. The area A was covered with factor five more than the number of scan positions for area B. Therefore, it was possible to guarantee both high-resolution scan- and image-information on every single wall and to have only minor areas without data acquired (Gaisecker 2006).

The flight planning was done in the office in Zürich using the existing orthoimage and elevation model of the area. The image scale was defined to 1:4′000 to obtain an average image resolution of 3 cm with the still-video camera Canon D60 (Lens: EF14mm f/2.8L USM) implemented on the model helicopter. With a flying height of 56 m, an image format of 15 by 22 m on the ground and an image overlap along and across track of 75%, starting from one corner of the site, the acquisition points were calculated. The flying speed between the image points was set to 2 m/s. Finally, the predefined image coordinates and the flying speed were saved into the flight mission file. This planning prior to field work was done with a flight planning tool developed for standard photogrammetric flights for UAV platforms (Eisenbeiss 2004).

20.3.2 Field Work

After arriving in Peru the laser scanner was brought to Palpa and the field work started according to schedule. Unfortunately, the time allocated for field work with the model helicopter was reduced to two days, as the release of the model helicopter from the customs authorities took almost one week. For the laser scanning all the field work was carried out within five days. Area A was scanned from 47 scan positions, and the remaining part B was scanned from 13 scan positions (Fig. 20.4). For the registration of the scan data using RiscanPro and also for the orientation of the helicopter image data 80 signalized control points (Fig. 20.4) were put into the site and measured with differential GPS with a 3D accuracy of 2 cm in the horizontal and 3 cm in the vertical direction after net-adjustment. For this purpose, retroreflecting cylinders were combined with circular white cardboard discs. Whereas the reflectors were clearly marked in the laser scan point clouds, the cardboard discs were easily discernable in the aerial images. The combined control points were affixed to stones with a special glue that was easily removable without traces. Because the differential GPS

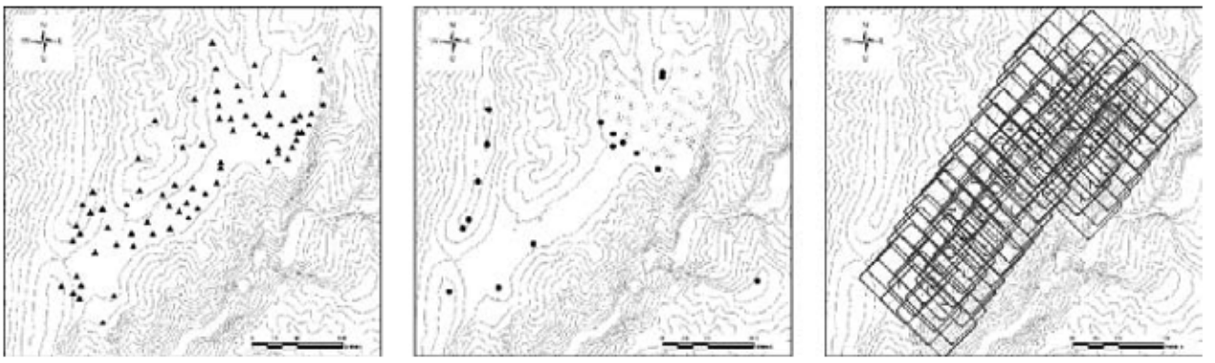

Fig. 20.4 Left: Distribution of ground control points over Pinchango Alto; middle: distribution of scan positions for the eastern respectively area a (*circles*) and western (*dots*) part of the site; right: distribution of image coverage of UAV images

measurements of the control points were done on the first two days, the laser data could already be registered during the data acquisition stage (see Eisenbeiss et al. 2007). Thus, immediately after completion of field work a first result for a registered point cloud, which consists of approximately 270 million single point measurements and 420 digital terrestrial images was available (Table 20.2).

Table 20.2 Overview of original data and derived products of the pinchango site

Product/Source	Type	Specifications	
		Resolution or Footprint	Amount
Original Data			
Laser scanner (raw data)	Point cloud	1–35 cm	~270 million points
Terrestrial images	Digital Image	Depending on distance to object	427
UAV aerial images	Digital Image	~3 cm	85
Aerial images	Analog Image	~10 cm	4
Digital Elevation Models			
LS3D-DSM	Raster	5 cm	~14.8 million points
UAV-DSM	Raster	10 cm	~4.7 million points
Aerial-DSM	Raster	2 m	~ 1.6 million points
Orthoimages			
DSMs + UAV images	Orthoimage	3 cm	2
Aerial images	Orthoimage	25 cm	1
Textured 3D Models			
Produced with Maya	Video	10/20 cm (Orthoimage/DSM)	1
Visualised using ArcScene	Real-time navigation	3/10 cm (Orthoimage/DSM)	1
Produced with Blender	Real-time navigation	1–5/5 cm (Texture/3D-model)	2 selected areas
Produced with Skyline	Real-time navigation	3/20 cm (Orthoimage/DSM) 25 cm/2 m (Orthoimage/DSM)	1

After finishing the field work with the laser scanner, the helicopter was brought to Palpa and the remaining time for field work was used for image acquisition using the model helicopter. The helicopter flight was navigated both by an operator and a pilot. Although takeoff and landing were controlled by the pilot due to the difficult terrain on the site, the actual flight mission was then controlled by the operator via the flight ground control station. During the flight the operator sent navigation commands to the helicopter to fly to the individual image acquisition points on the predefined flight path. The compliance of the flight trajectory was controlled via the weGCS software (weControl), and the interface enabled the control of parameters such as position, altitude, speed, and the like.

During one flight 1–2 image strips could be captured, after which the helicopter had to land to refill gasoline and to recharge the batteries. Therefore, on the first day only 5 out of 8 predefined strips could be flown, acquiring a total of 85 images (Fig. 20.4, Table 20.2). On the morning of the second day, dusted petrol and sand in the engine caused the helicopter to crash before reaching its normal flight height of 56 m. Due to time constraints it was not possible to repair and relaunch the damaged system. However, 95% of the site had already been covered on the first day by images suitable for stereoscopic postprocessing. This was thanks to the precisely predefined flight path, the GPS/INS-based stabilizer, and the considerable overlap between the image strips (Eisenbeiss et al. 2005). The complete image acquisition with the model helicopter, less the time for recharging batteries and flight tests on-site, was done in 50 min.

20.3.3 Processing of the Mini-UAV Images

Three different software systems were employed for photogrammetric image processing: the commercial software package LPS (Leica Photogrammetry Suite, Leica Geosystems) and the in-house software packages BUN (Bundle adjustment software) and SAT-PP (ETH Zurich).

LPS offers the functionality required to accomplish the complete photogrammetric working process from project definition and interior orientation to measurement of tie points (either in manual or automated mode), manual measurement of control points, bundle adjustment, and finally to DSM generation and orthoimage production, whereas the BUN software allows a more sophisticated aerial triangulation and comprises a robust algorithm for error detection during data processing.

The automatic measurement of tie points in LPS turned out to be time-consuming and error prone, as LPS is designed for the standard aerial case, implying the use of calibrated aerial cameras. In Pinchango Alto we used instead an uncalibrated still-video camera with a wide-angle lens. These special conditions, in combination with considerably varying terrain elevation not accounted for by the software, change of light conditions, and strong shadows

in the images, caused the automatic tie point measurement tool to produce a lot of blunders. Therefore we decided to initially measure a few points manually and then to run the automatic tie point measurement tool. This procedure still yielded a lot of errors in mountainous areas. These were removed using LPS and BUN, with BUN detecting more errors than LPS. Finally, using BUN for bundle adjustment with self-calibration of selected parameters following Brown's model (without share factor and parameters for tangential distortion), an RMSE value of 1/3 pixel (1 cm in object space) was achieved (Eisenbeiss et al. 2005).

For DSM generation from the helicopter images we used the software package SAT-PP. The software was initially developed for the processing of satellite images and later adapted to be capable to handle still-video camera and aerial images. Following the workflow of automated image-matching in SAT-PP (Sauerbier this volume: Fig. 18.4), an interpolated regular DSM (hereafter UAV-DSM) from the matching results with a resolution of 10 cm was derived (Table 20.2). The combination of the multiple primitive matching and the large overlap of 75% in and across flight direction, allowed the generation of a highly detailed DSM out of the still-video image data (Fig. 20.5).

Using the image orientation data and the produced UAV-DSM an ortho-image of the whole site with a ground resolution of 3 cm was generated using LPS. Finally, for 3D visualisation we used the orthoimage and the UAV-DSM. In order to generate a virtual flight through the model we employed Maya (Autodesk; Lambers et al. 2007).

20.3.4 Processing of the Laser Data

Using the Riegl RiSCANPRO software the laser data can be postprocessed in numerous ways. The optimum choice depends strongly on the application

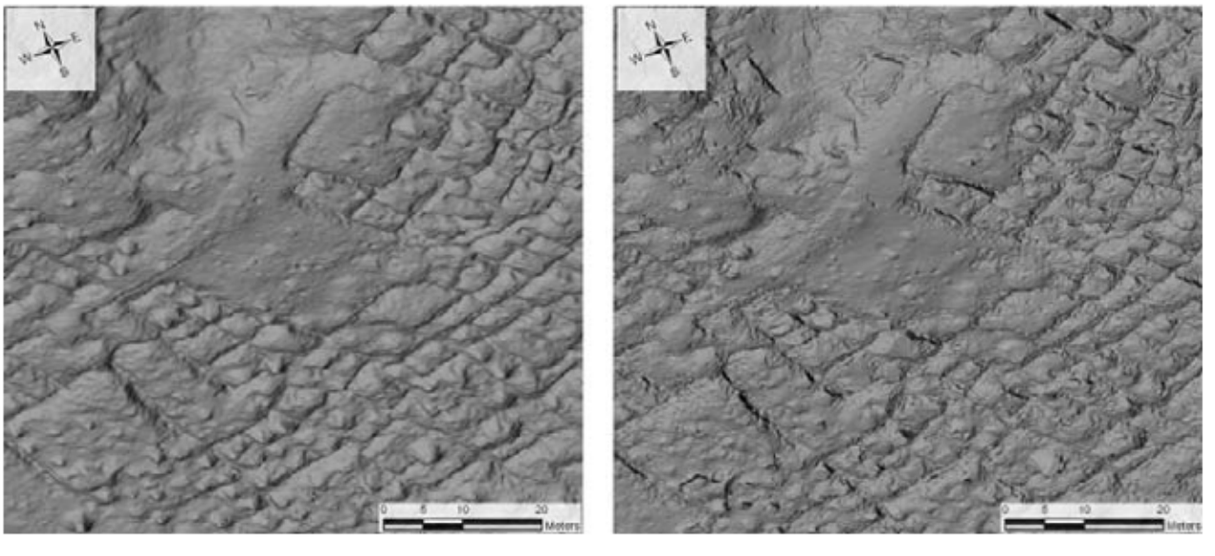

Fig. 20.5 Detail view of the center part of Pinchango Alto. Left: SATPP-DSM, Right: LS3D-DSM

and/or the requirements of the end-user. One of the possible output products is a triangulated 3D model, which can be used for automatically extracting contour lines and profiles, and to perform volume calculations.

In our project, as mentioned above, the registration of the single scans with RISCANPRO to one point cloud was done during the field work with the control points. Although the internal registration accuracy of the scan data was about ±1 cm, the accuracy for the global registration using control points was about ±5 cm. The final registered laser point cloud was reduced from a total number of 270 million points by means of a point decimation algorithm implemented in the Riegl software and outliers were detected manually and semi-automatically, again using RiSCANPRO. Finally, for area A of Pinchango Alto the resolution was set to 10 cm. This part of the model covers an area of approximately 100 × 100 m and consists of 1.5 million points and around 3 million triangles generated in Polyworks using a 2.5D Delauney triangulation. For the whole area of Pinchango Alto (200 × 300 m), a model with a mesh size of 20 cm consisting of 0.5 million points was generated. The result of the triangulation is a waterproofed digital surface model (hereafter RiSCANPRO DSM) that allows volume and section calculation (Lambers et al. 2007).

In contrast to the software provided by Riegl, we applied our in-house surface matching algorithm LS3D for the registration of the point clouds. This software allows the registration of the single scans without using control points. The matching process was performed with an average sigma naught value around 1.0 cm, which is consistent with the reported accuracy potential of the LMS-Z420i scanner. After registration the point cloud was georeferenced with 48 well-distributed ground control points (GCPs) to the LS3D-DSM (Fig. 20.6, Table 20.2). The GCPs were identified on the intensity image of the scans, and a posteriori sigma naught of the adjustment was 4.1 cm, which is comparable with the accuracy of the GCP measurements (Akca 2007).

Before doing the modeling of the surface the point cloud has to be analyzed for outliers. Therefore, an outlier detection algorithm for laser point clouds was developed by Sotoodeh (2006). This developed method is founded on a density-based algorithm. In the laser scan data mainly single and small cluster outliers are detected, such as people, GPS, bags, and boxes.

For the surface modeling the commercial software package Geomagic Studio 6 (Geomagic, Inc.) and an in-house method based on the most advanced sculpturing method using proximity graphs (Lambers et al. 2007; Sotoodeh et al. 2008) were selected. For the surface reconstruction of the whole site Geomagic was used, and the in-house method was applied with higher point density for single walls and rooms of the settlement. Using Geomagic the number of points was reduced to 14.8 million point using the "grid sampling" function with a 5 cm grid size. The final surface wrapping was done with a medium-level noise reduction option. Due to data unavailability some holes occurred on the meshed surface. These holes are mainly the result of occlusions of walls and the invisibility of the "mine shaft" entrances. The holes were filled with the "Fill Holes" function of the software. After the editing the final model

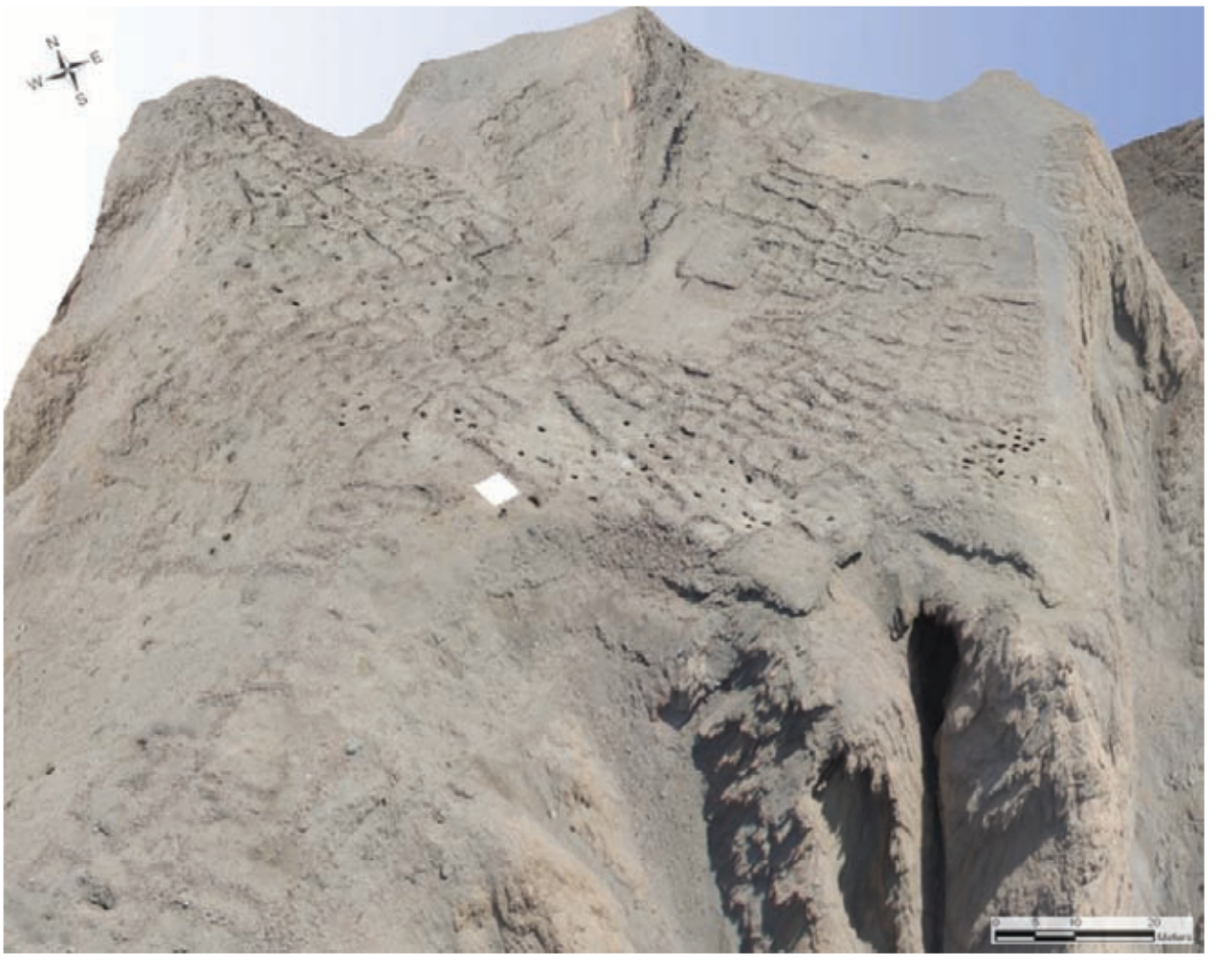

Fig. 20.6 The LS3D-DSM overlaid with the corespondence orthoimage showing the central part of Pinchango Alto

contained 5.8 million triangles. For detailed surface reconstruction of single walls using our method, we selected a wall in area A, where the scan point density was much higher than in the overall area. Although there are some holes in this model, due to undersampling, the object is completely modeled in terms of coverage in the areas that fulfilled the minimum sampling distance criteria. Most of the process was accomplished with only minimal user interaction. In addition, no threshold parameter or predefined values were required.

20.3.5 Combined Data

After the processing of the helicopter images and laser data we then needed to texture the reconstructed surface models and to combine the available data into one dataset.

Skyline (Terra Explorer) allowed us to combine the UAV-DSM and the orthoimage and to navigate in near real-time through the textured 3D model (Fig. 20.8). Furthermore, thanks to the automatic registration of the terrestrial image data within the scan data, the triangulated mesh could be textured with

Fig. 20.7 Textured 3D model of a single wall showing a sample of plotted stones forming the walls

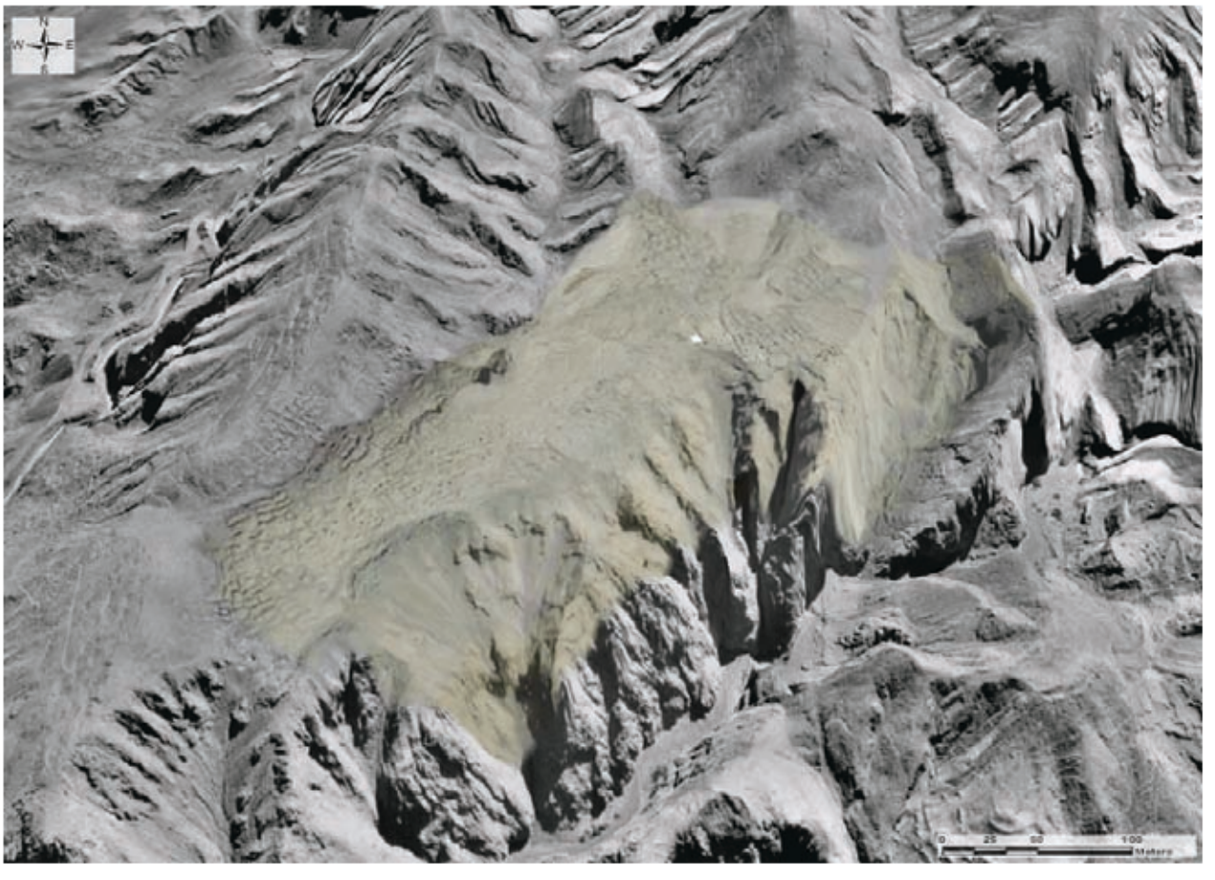

Fig. 20.8 Textured 3D model of Pinchango Alto showing the 3 cm UAV-orthoimage draped over the SAT-DSM with 20 cm resolution. The surrounding areas are presented by the aerial-DSM (2 m resolution) overlaid with the aerial orthoimage (25 cm). (Skyline, Terra Explorer; Sauerbier, this volume)

the high-resolution image information. Therefore, using the laser point cloud and the terrestrial images characteristic bricks from a wall were measured and visualized in the point cloud, the terrestrial images with RiSCANPRO, and in a CAD-program at once (Gaisecker 2006). For the selected wall in area A also in-house software for automated texture mapping was applied (Hanusch 2008).

This software calculated the visible parts of the model for every image. For each vertex of the mesh, we calculated the image coordinates. For visualization of the textured model, the open source software Blender was used (Blender 2008; Fig. 20.7).

The derived surface model from laser data was also used for the orthoimage generation and texture mapping of the model helicopter images. Furthermore, the generated surface models from laser data and model helicopter images were also inserted into the 3D model of the surroundings of Pinchango Alto generated from aerial images, thus enabling reliable studies of the visibility and accessibility of the site in a GIS environment. Figure 20.8 shows a combined textured 3D model for this purpose comprising the UAV-DSM that covers Pinchango Alto and the aerial-DSM.

20.4 Results

The application of two highly versatile recording systems, the laser scanner and the UAV, allowed the LIP site of Pinchango Alto to be documented in high resolution and accuracy in basically five days of laser scanning and 50 minutes flight time of the UAV. The acquired and processed data of Pinchango Alto are a good starting point for a detailed architectural, structural, and functional study of a typical large LIP site in the region of Palpa and Nasca. Table 20.2 illustrates the available datasets for the archaeological interpretations: the oriented UAV and terrestrial images, the original laser point cloud, the produced DSMs, orthoimages, and texture 3D-models with different resolutions.

For archaeological analysis, the UAV image data is of advantage, because the image data can be used for the automated generation of elevation models and for manual measurements in stereo viewing mode. For the definition of walls, rooms, forecourts, and so on, the stereo images provide valuable information for interpretation by archaeologists. On the other hand, the laser-DSM can be used for interpretation of the architecture of single walls and rooms due to the high point density.

In that the resolution of the laser is higher than in the UAV-DSM, single structures such as stones can be seen in the LS3D-DSM (Fig. 20.5). However, errors were contained in both datasets. The comparison between the LS3D- and the UAV-DSM shows a mean difference of less than one centimeter with a standard deviation of 6 cm (Eisenbeiss and Zhang 2006). The differences occurred mainly where the topography changes suddenly, for example, walls elongated along the flight direction, at the border areas of the settlement, and inside the holes (Fig. 20.9). For the UAV-DSM, the main difficulties were on walls and structures with vertical surfaces, which were not covered in different image strips. The laser could not acquire points in the holes, therefore the UAV-DSM fits better in these areas (see Fig. 20.5).

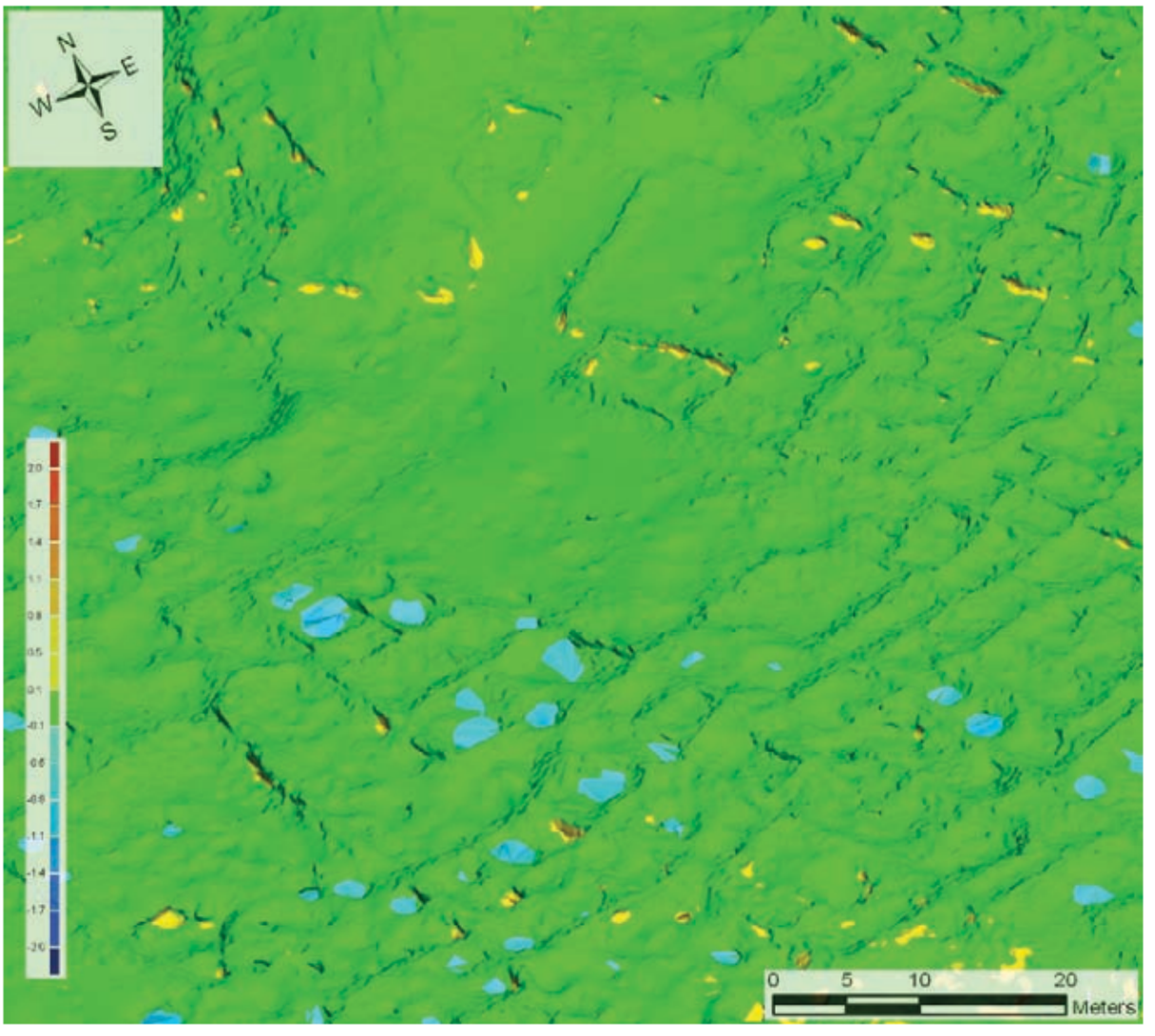

Fig. 20.9 Discrepancy map of 3D distances of UAV-DSM and LS3D-DSM after registration

The UAV- and the laser-DSM showed more detail and have higher accuracy in comparison to manual measurements (Eisenbeiss and Zhang 2006) and to the photogrammetric and geodetic measurements accomplished in the field campaign in 1999 (Zwicker 2000). Furthermore, traditional measurement methods are more time-consuming for data acquisition and processing with respect to the proposed methods. Therefore, the new methods will be established in the near future and can be expected to replace the traditional documentation techniques for comparable applications.

The 3D models resulting from the combination of photogrammetry and laser scanning offer many opportunities for future archaeological investigations of the site of Pinchango Alto in particular and the Late Intermediate period in the Palpa region in general that go well beyond previous studies of prehistoric architecture in southern Peru (Lambers et al. 2007).

In order to enable GIS-based studies of the site's context, the high resolution 3D-model was integrated into the textured aerial-DSM (Fig. 20.8). This combined 3D-model allows, for example, the calculation of access pathways from different directions. It is expected to reveal from which valley the site was most

accessible and whether a direct access from Pinchango Bajo existed. Also in the line of the question of defensibility, visibility studies taking into account reconstructed wall height may reveal if the site was visible from the valley floors.

Finally, according to our experience for future projects, it would be more suitable to use a laser scanner and a camera mounted on a mini-UAV, because more viewing directions are possible from an airborne platform, for example, nadir or oblique. Using the advantages of both techniques, combined approaches will yield more precise elevation models. The laser scanner creates high dense point clouds in areas with low texture, whereas image data is advantageous for edge measurement and texture mapping.

Acknowledgments The author thanks Prof. Armin Gruen, Dr. Karsten Lambers, and Martin Sauerbier, who were involved in the planning, organization and field work phases of the project. In addition, the author thanks our pilot Daniel Kraettli and the companies Helimap, Riegl, and weControl for supporting the project with manpower and measurement instruments.

Chapter 21
Perspectives and Contrasts: Documentation and Interpretation of the Petroglyphs of Chichictara, Using Terrestrial Laser Scanning and Image-Based 3D Modeling

Peter Fux, Martin Sauerbier, Thomas Kersten, Maren Lindstaedt and Henri Eisenbeiss

Abstract In this chapter we present our research activities at the petroglyph site of Chichictara near Palpa. Along with the discussion about the documentation methodology including terrestrial laser scanning and photogrammetry we here present the Geographic Information System (GIS) that we intend to use as a tool for archaeological interpretation of the site and its components. Furthermore, we focus on the question of the added value of the adoption of new documentation technologies concerning archaeological interpretation. We are confident that through such adoption new perspectives regarding both the interpretation of the original social meaning of the petroglyph site and the iconography of its pictures are revealed. The adoption of new technologies sheds new light on the archaeological interpretation of the petroglyphs of Chichictara.

21.1 The Project's Perspective

If not in theory, then certainly in the practice of archaeology one traditionally likes to separate documentation and interpretation of findings, a principle which seems especially true in the case of recent rock-art research. In terms of adoption of new technologies, the focus is usually set on accuracy of the documentation, whereas discussion about the possible added value of the adoption with regard to interpretation—notably inquiries into the once social meaning of the specific place and especially iconography—is often missed. Cognizant that rock-art in general represents a class of cultural heritage especially exposed to destruction, in particular because of its fixed position in the landscape, the goal of realistic documentation is certainly justified. The evaluation of an accurate documentation method is therefore one aim of the

P. Fux (✉)
Museum Rietberg Zürich, Gablerstrasse 15, 8002 Zürich, Switzerland
e-mail: peter.fux@zuerich.ch

M. Reindel, G.A. Wagner (eds.), *New Technologies for Archaeology*, Natural Science in Archaeology, DOI 10.1007/978-3-540-87438-6_21,
© Springer-Verlag Berlin Heidelberg 2009

Fig. 21.1 Zoomorphic petroglyphs on rock 20, sector 2

Chichictara project presented here. Furthermore, the project aims to exemplify in which regard the adoption of new technologies leads to insights into the original social meaning of the petroglyph site of Chichictara and even affords new perspectives for iconographic studies.

Although in the Nasca–Palpa region many petroglyph sites have been well known to archaeologists for a long time (the site of Chichictara, e.g., was mentioned by several authors (Orefici 1983, Núñez 1986, Hostnig 2003)), none have been archaeologically analyzed in further detail. Indeed, Matos Avalos (1987) did an excellent job, taking into account his limited resources, in recording the entire site of Chichictara, and Nieves (2007) is to be lauded for her comprehensive documentation of rock-art sites in the Nasca–Palpa region. However, a satisfying interpretation of the social meaning of a specific site and its figures has not yet been conducted. Thus, this is the aim of our Chichictara project.

Along the eastern slope of the lower valley of the Palpa River there are several concentrations of petroglyphs within a range of about 2.5 km Fig. 21.1. The largest of them is Chichictara, situated 11 km to the northeast of Palpa at an altitude of around 550 meters above sea level (see Figs. 21.2 and 21.9). It is the largest petroglyph site in the Nasca–Palpa region. Approximately 150 sculptured rocks are covered with anthropomorphic, zoomorphic, and geometric figures or with depictions of activities such as hunting (Fig. 21.5). On the basis of iconographic similarities with datable archaeological findings, for example, textiles or ceramics, most of these petroglyphs can be dated to the Paracas

Fig. 21.2 A panoramic view of the lower Palpa valley. The Chichictara side valley at the eastern slope is framed in red

period (800–200 BC; see Fux et al. in press). The rocks are mostly located on the bottom of the Chichictara valley and on its rocky slopes.

Because we strongly advance the view that rock-art in general has to be regarded as "an intentional and meaning afflicted human assertion," which corresponds to Geertz's (1973) appreciation of the term *symbol*, we opt for a consideration of rock-art as symbols. Whereas the term *symbol* has to be understood in an open and general sense—it comprises letters, words, texts, images, diagrams, maps, models, and more (see, e.g., Goodman 1976)—the discussion concerning the comprehension of symbols is a delicate issue. However, in general it seems to be clear that for an appropriate understanding of any assertion, be it within the range of language or even art, the consideration of further contextual information, for example, gestures, attitudes, and attendant circumstances, is indispensable (e.g., Langer 1942).

At this point, skepticism regarding the ability to understand symbols from ancient societies and cultures is common (see, e.g., Layton 2001: 316). The most skeptical view conceivable is presumably the one of the relativists: they argue that there are different ways of organizing experience and systems of categories that give form to the data of sensation. There are different points of view from which individuals, cultures, or periods survey the passing scene. Such ways of organizing experience are called *conceptual schemes* (Davidson 1974), and potentially we may not be able to understand assertions belonging to a foreign conceptual scheme (see, e.g., Whorf's (1956) comments on the impossibility to "calibrate" the language of the Hopi with English) because reality itself was relative to a scheme. Note at this point that understanding of an assertion means the ability to translate it into our own language, or, in other words, to find an explanation within our own conceptual scheme. The relativist's demur seems especially appropriate to symbols from ancient societies and cultures.

However, Davidson (1974) pointed out that even the postulation of disjunctive conceptual schemes in which assertions are made is only valid by the assumption of a common coordinate system in which these different conceptual schemes could be plotted, whereas, at the same time, the existence of such a common coordinate system falsifies the claim of dramatic incomparability. Obviously, we face a dualism of scheme and content, of organizing system and something waiting to be organized. Inquiries into this dubious something waiting to be organized are commonly seen as the business of (empirical)

science per se, inasmuch as universal explanations for any human assertion can be expected. Science, we are told, differs from softer discourse in having contact with the real as a touchstone of truth. As true believers in science, one expects to detect the coordinate system in which different conceptual schemes can be plotted by means of empirical disciplines. In other words, there is widespread confidence that scientific inquiries into this underlying coordinate system will allow rational explanation of any cultural behavior, which itself may be, and is occasionally expected to be, thoroughly irrational (see, e.g., Langer 1942).

Hence, in rock-art research too, the request for universal, and therefore "scientific," explanations is well established: Approaches such as neuroscientific studies that Whitley regards as providing "a key to unlocking the mind and emotions of prehistoric shamans and other creators of rock art" (Whitley 1998: 32), or unified explanations of how the human being responds to his environment (see, e.g., Swartz's "Unified Space Model" in Swartz and Hurlbutt 1994) may be cited as examples.

By contrast, mainly due to dissatisfaction with dogmatically generalized explications, we follow Davidson's comment that the postulation of an underlying coordinate system is nothing but dogmatism (see Davidson's so-called "Third Dogma of Empiricism" in Davidson 1974), by giving up the aim to discover a general empirical content of rock-art. Dropping the image of science as a touchstone of truth means to dispose of both the hope for unified explanations of meaning or function of rock-art and the fear of potential incomprehensibility.

What we propose is to search for latent structures of a frame of action related to a given rock-art site. As in the case of any assertion—be it a spoken word or sentence, a scientific symbol, literature, or a piece of art—understanding of rock-art is only possible by taking into account contextual information of many kinds. This point was impressively pointed out by Wallace (1986) and furthermore illustrated with the example of the decipherment of Minoan scripts, called Linear B: many latent structures of action and life form, which certainly cannot be reduced to pure evidence, were considered. To give an example, assuming that one would have found the Linear B plates not within palace structures but in a temple or in any kind of sacral context, the translation of Linear B would be completely different from the current state of knowledge. In such a context the plates would have been understood as notes or texts of ritual chants rather than accounting records. Only by means of the conception of the social structure, life form, frame of action, and specific needs of the society that produced these Linear B plates, did a translation and comprehension become possible. Because there are no grave inconsistencies apparent within the dense mesh of argumentation, we seem to be comfortable with our understanding of Linear B. Hence, the understanding of intentional and meaning-afflicted human assertions, and therefore of rock-art as well, is always possible. Our satisfaction with an offered translation or explanation of any assertion depends much more on our empathy with its producer than on scientific provability and dogmatism (see, e.g., Geertz 1995). And that is as objective as can be.

In order to obtain as much contextual information about the petroglyph site of Chichictara as possible, we opted for the following methodology. To capture the natural environment the petroglyph site of Chichictara was recorded in 3D using terrestrial laser scanning (Fig. 21.3). Then, each rock with petroglyphs was documented and modeled in 3D by means of photogrammetric image processing. From these models 3D vector graphics for iconographic studies can be extracted (see Fig. 21.13). The goal of the project was the integration of each particular rock-model with its petroglyphs in high resolution into the Digital Terrain Model (DTM) of Chichictara (Fig. 21.4). Additionally, the integration of the whole Chichictara model into a second Digital Surface Model (DSM) derived from ASTER satellite imagery, which covers the Palpa region with its river valleys, is planned. Finally, the aim is to integrate the entire combined terrain model into a GIS database containing spatial and archaeological information, collected during ten years of multidisciplinary research activities (see Reindel, this volume). The presented approach allows a comprehensive analysis of the petroglyph site Chichictara as a whole and its single components.

In the following the field work conducted in 2006 and the ongoing work are summarized and the first results of the archaeological interpretation are presented.

21.2 Putting the Landscape in Perspective: Terrestrial Laser Scanning

The planned digital terrain model for the Chichictara valley needed to suit the integration of photogrammetric 3D models of the rocks. Because investigations on generation of DTMs by means of terrestrial laser scanning were conducted successfully in 2004 with the capture of a Saxon ring embankment (Hönniger and Kersten 2005), we decided on terrestrial laser scanning in order to model the Chichictara valley. The dimensions of the valley are approximately 250 m in length, 130 m in width, and 70 m in height. A terrestrial laser scanner MENSI GS 200 from Trimble with a wavelength of 532 nm and an optimum range of 200 m, but with somewhat longer range capacity in reality, was used due to its long measurement range. The instrument works according to the time-of-flight principle and measures between 1000 and 2000 points per second. In order to guarantee power supply for the computer and scanner during the fieldwork, we used a gasoline-driven generator with a power of 1 kW.

The data acquisition in Chichictara was completed during six days of fieldwork by using 13 scan positions. We distributed 14 spherical tie points in the terrain for the registration of the individual point clouds derived from each scan position. The coordinates of the spheres were determined using a Leica TCA 700 total station in a local coordinate system. We achieved a mean standard deviation of 6 mm after network adjustment for the 3D coordinates. By means

Fig. 21.3 Fieldwork with the laser scanner: The laptop is protected against dust and sunlight by a cardboard box

of the GPS measurements we transformed the resulting local network to the Universal Transverse Mercator (UTM) system, in which the spatial data of the Nasca–Palpa project are available. The absolute accuracy of the transformation of the DTM to the UTM system can be regarded as 0.3 m.

For the terrain scans we chose a resolution of 15 cm at a distance of 100 m, so that for each scan position, even at distances greater than 100 m, a point density of at least 50 cm could be obtained. In addition, for certain petroglyphs we collected scans at a high resolution of 3 mm at a distance of 10 m, aiming for

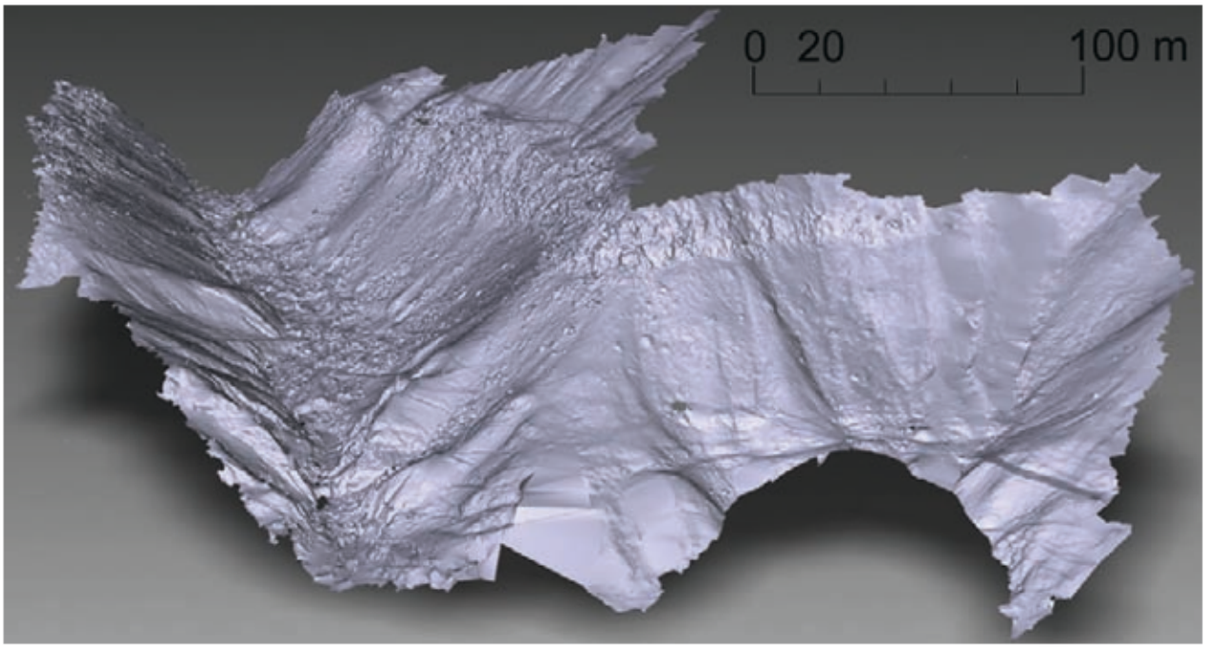

Fig. 21.4 The digital terrain model of the Chichictara valley derived from terrestrial laser scanning

exemplary comparison with the photogrammetrically derived 3D models. In total, 27 million points were measured, resulting in 512 MB of data.

21.3 Utilizing Contrasts: Photogrammetric 3D Modeling of the Rocks

Documentation of petroglyphs and other types of rock-art was conducted in the past by various means, from hand-drawn sketches to photos to images rectified using control points or surface models, mostly in 2D. In recent years, with the emergence of terrestrial laser scanners and their wide application, and with developments in digital photogrammetry, these two techniques have also been applied to record rock-art, extending the documentation to three dimensions (see, e.g., Barnett et al. 2005; Chandler et al. 2007; Díaz-Andreu et al. 2006; Jones 2007). Currently, even structured light systems, providing very high accuracy under controlled conditions, have been successfully applied to rock-art digitization (Landon and Brent Seales 2006). Nevertheless, the results obtained in an on-site experiment compare to the accuracy achievable by means of multi-image photogrammetric processing.

Especially for petroglyphs, 3D documentation can provide added value. Depth information, if acquired at sufficient accuracy, can contribute to investigations into the construction technique of the petroglyphs (see Fig. 21.7). In addition, in some cases worn or damaged structures might become visible in the modeled geometry. As already mentioned, a further important aspect of 3D petroglyph documentation is the issue of preservation. Environmental and human impact threatens most of the unique rock-art sites. The consequences can be observed in Chichictara as well. Therefore, a 3D recording at least allows for a digital preservation of the objects and research on them even after possible destruction. Due to the advantage of digital cameras compared to other mentioned documentation instruments in terms of manageability (this point is of particular interest in a rocky, sandy, and steep environment such as Chichictara) we decided to apply photogrammetry in order to document the rocks with petroglyphs.

21.3.1 Image Acquisition

The photogrammetric image acquisition was conducted during a field campaign from the end of August to the middle of October 2006 (Sauerbier et al. 2007, Fux 2007, Fux et al. in press). The goal was to obtain a 3D documentation, textured photorealistically, as a basis for 3D vectorization of the petroglyph drawings using image-based and geometric information. For this purpose we used a Canon EOS 10D digital still-video camera with single lens reflection optics and with an image format of 3072 by 2048 pixels. All 66 rocks covered with petroglyphs were documented. These were situated either

on single rocks on the valley floor or on vertical rock facades in the upper part of the valley. Because some of the petroglyphs are located in groups, on rocks as well as on the facade, image blocks contain one or more rocks with petroglyphs and typically consist of 20–80 images. For the image acquisition we used two types of configurations: whereas the single rocks were photographed with a radial network of acquisition points, the rock facade parts were acquired using approximately horizontal and parallel viewing directions.

During image acquisition, we affixed carton targets on the rocks to ensure the availability of well-defined tie points for image orientation. Furthermore, in each image block at least three points were measured using differential GPS with Trimble GeoExplorer XT instruments, which allow for rough positioning of the rock in the superior UTM coordinate system. The positioning accuracy of the GPS measurements was limited to 0.3 m in differential mode. However, due to partial occlusions of the horizon caused by the topography even this accuracy could not be achieved. Additional scale bars placed in the images ensured that the generated 3D models could later be transformed to the correct scaled size. This was necessary due to the lack of control points. Considering the chosen configuration for image acquisition in terms of image scale, base length, and object distance as well as the camera parameters, an accuracy of the measured points of approximately $s_{X,Y} = 0.8$ mm in X and Y (planimetric with respect to the sensor chip) and $s_Z = 2$ mm in Z (optical axis) can be expected for most of the rocks. In some cases, it was not possible to achieve an optimal configuration due to the neighboring topography, therefore the expected accuracies were not achieved for all rock models.

21.3.2 Image Orientation

For both the orientation of the image blocks in an arbitrary 3D coordinate system and for the manual tie point measurement and bundle adjustment including the scaling we used the photogrammetric close-range software PhotoModeler, versions 5 and 6. In addition to the well-defined target points mentioned above, natural points on the rock were also measured and used for orientation. By means of a bundle adjustment with self-calibration, the following parameters were determined, resulting in oriented images, which serve as a prerequisite for the subsequent modeling procedure.

- Coordinates of the perspective centers X, Y, Z for each image
- Three angles ω, φ, κ representing the spatial rotation of each image
- Corrections for the camera constant c and the principal point coordinates x_H, y_H
- Correction parameters for the lens distortion

For the completed image blocks, standard deviations of the image coordinates of $\sigma_{xy} = 0.9 - 3.2$ pixels were achieved as precisions for the image measurements for 60 of the 66 image blocks.

21.3.3 3D Modeling of Rocks and Petroglyphs

Image-based 3D models of objects such as the petroglyphs and basic rocks can be generated using two approaches. One can manually measure the required features—points, lines, and surfaces—in the oriented images. On the other hand, automatic surface extraction can be performed. The first approach is a straightforward standard method. Error sources mainly result from orientation precision and the human operator's measurement skills. With the software PhotoModeler 3D points, lines, and surfaces can be measured quite comfortably in the relevant images. The generated 3D models including the texture information were exported to different 3D data formats to enable visualization using different software on various platforms. We mainly used the formats VRML 1.0, OFF, and OBJ (Wavefront Technologies) and the programs Vrmlview (Systems in Motion) and MeshLab (CNR) for visualization and editing purposes (Fig. 21.5). The advantage of both programs is the multiplatform design, which allows us to run them on PCs as well as on Apple computers, which was an important issue in this project.

In order to investigate the applicability of automated surface generation, we applied the ETH Zürich in-house software SAT-PP (SATellite Precision Processing), which was enhanced by a sensor model for close-range applications. SAT-PP is capable of generating, in comparison to manual measurements, highly dense 3D point clouds using a complex image-matching technique (Zhang 2005). Basically, the matching routine goes from coarse to fine through the generated image pyramids. It tries to match three different types of features in two or more images: interest points, grid points, and edges (see Zhang 2005). Matching of these features overcomes some of the weaknesses of matching algorithms implemented thus far in existing commercial photogrammetric software packages:

Fig. 21.5 Photogrammetrically derived 3D model of rock 33, sector 2. Depicted is a hunting scene: the person on the lower right holds a blowtube and aims at an animal, probably an armadillo. On the upper left, a bird is depicted

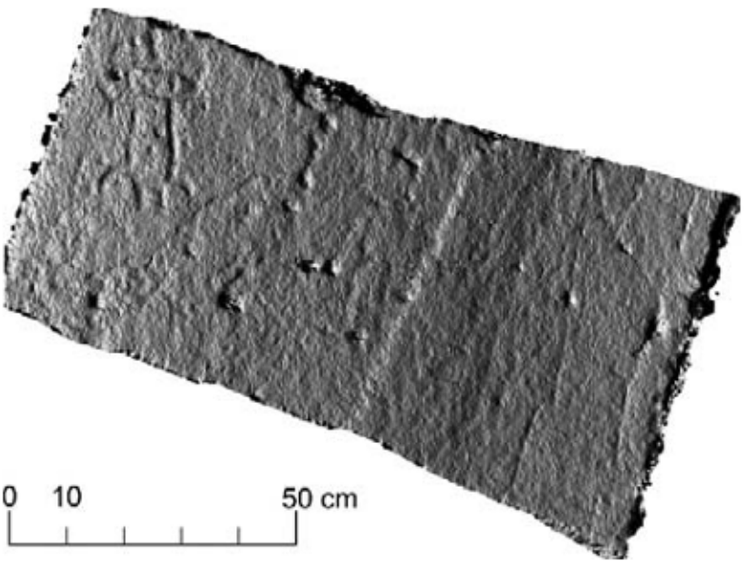

Fig. 21.6 3D Surface model of rock 33, sector 2 (see Fig. 21.5), derived using image matching with SAT-PP

- Grid point matching improves the results in areas with low texture information.
- Interest point matching measures well-defined points and ensures high accuracy at least in areas where significant points can be detected.
- Edge matching improves the modeling of edges that define the shape of an object. Smoothing effects therefore can be minimized in order to preserve edges.

The result obtained with SAT-PP clearly shows that it was even possible to model the geometry of the petroglyph carvings based on images (Fig. 21.6). Due to the fact that automatic processing was not considered in image acquisition planning, image matching did not yield results for all rocks. Nevertheless, on the basis of the results from the surface modeling of some selected petroglyphs we are convinced that the method bears huge potential regarding analysis of worn and damaged structures, because in some cases they might become visible in the model geometry or in radiometry (compare Fig. 21.5 with Figs. 21.6 and 21.7). SAT-PP is also suitable for orthoimage generation in order to texture the surface model.

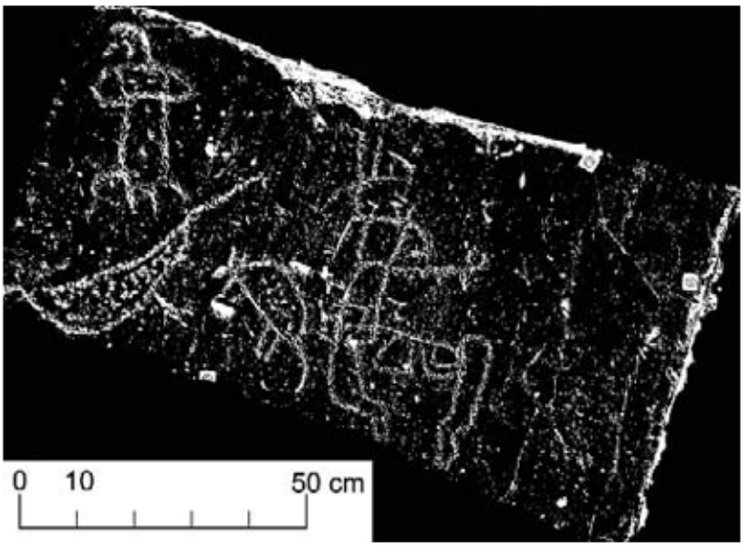

Fig. 21.7 The binary image of rock 33 clearly makes the petroglyphs and their construction technique (pecking) visible

Finally, based on the oriented images, we digitized the petroglyphs manually in 3D using PhotoModeler. PhotoModeler provides various geometric primitives for 3D modeling, such as points, lines, triangles, and the like. In our case, we used lines and curves to digitize the petroglyphs. The resulting 3D vectors were exported to the VRML format as an integrated model with the textured rock and as standalone 3D vectors (see Fig. 21.13).

21.3.4 Transformation of the 3D Models to the UTM System

A common analysis in a GIS environment can only be accomplished if all spatial data are available in a common coordinate system. For this reason, we aimed for a transformation of the rock models as well as of the laser scan DTM into the UTM Zone 18 S system, with WGS-84 as horizontal and vertical data (Fig. 21.8). Although the laser scan DTM could be transformed based on the GPS coordinates of registration control points, which additionally were measured using a tachymeter and refined by network adjustment, the rock models had to be transformed by means of the 3D modeling software Geomagic 9 (Raindrop Geomagic Inc.). For this purpose, based on the rock coordinates obtained from the network adjustment, a rectangular part from the laser scan point cloud with 3 × 3 m extent was segmented using a C program. This

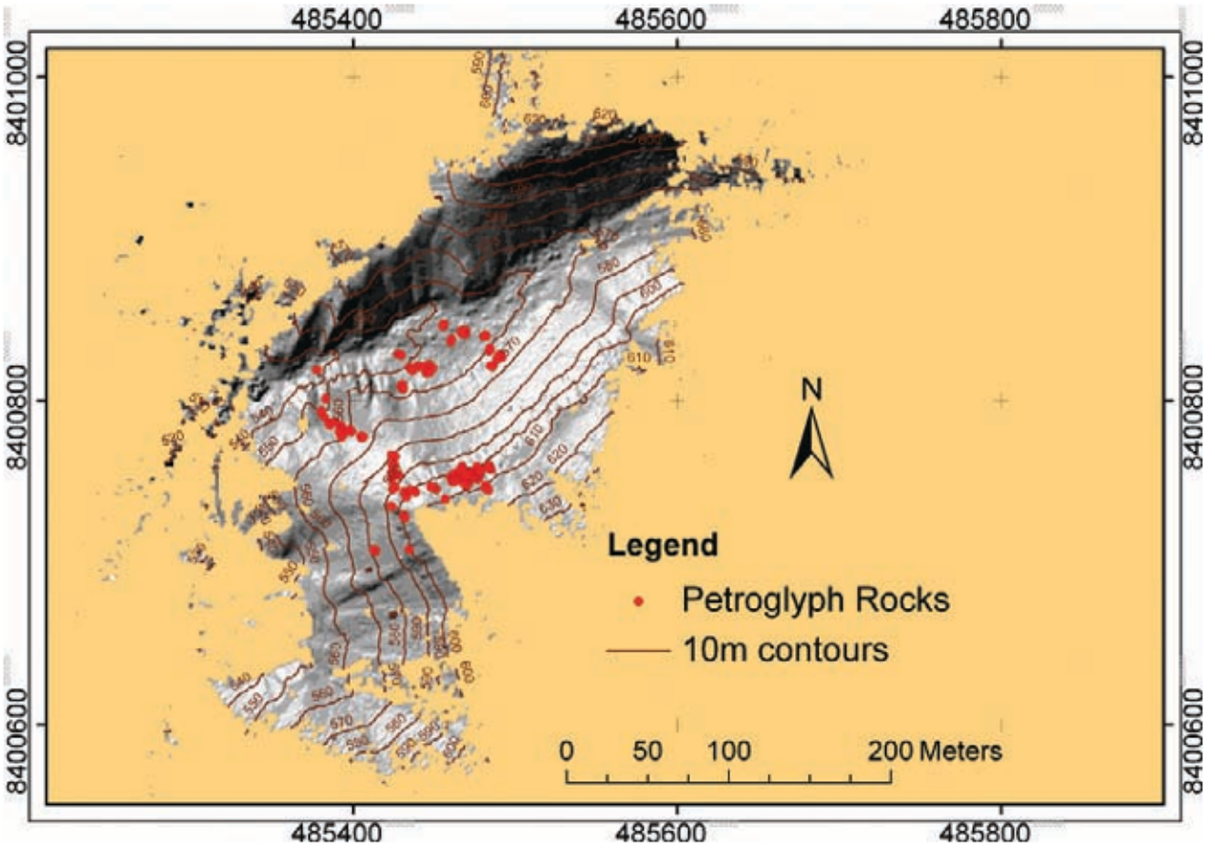

Fig. 21.8 The digital terrain model of the Chichictara valley in the UTM coordinate system. The rocks with petroglyphs are marked as red points

preserved the original resolution and was loaded in Geomagic together with the photogrammetrically derived rock model.

Using the manual registration functionality, the laser scan subset was set as a reference, which means that the coordinates were fixed during the registration procedure, and common points were manually measured in both datasets. Based on three or more common, manually measured points, the coordinates of the rock model were transformed into UTM coordinates using the implemented ICP algorithm. In case of the rock models, not only the geometry, but also the texture coordinates which connect each triangle that describes parts of the rock surface by a triangular patch from the source image, had to be transformed into UTM in order not to lose the texture. This requirement was ensured by the VRML data structure. The triangles are connected to the point coordinates via their point ID, such that a transformation does not affect the relation of the patches to the texture sources.

Because the DTM derived from terrestrial laser scanning and the 3D rock models were available in the UTM system, they could in turn be integrated in a DSM generated from ASTER images, which has a mesh size of 30 m. The ASTER DSM covers a large region from the modern city of Ica in the northwest to Laramate in the northeast and the Pacific coastline at Monte Grande and therefore serves as a basis for large area investigations. The accuracy of the ASTER DSM can be assumed to be approximately 20 m in the plain areas, according to a comparison with a DTM derived from aerial images. The accuracy is 2–5 times worse in the mountainous areas according to our experiences with other satellite sensors.

21.4 Capturing Contextual Information: 3D GIS Database

In addition to spatial data, further information was acquired describing the characteristics of the petroglyphs. In order to be able to store these data in a structured way and to make them accessible for attribute queries and spatial analyses, a conceptual data model using the Unified Modeling Language (UML) was defined and implemented in an Oracle 10 g database management system. Unique identifiers enable the exact connection of a petroglyph object to the relevant 3D model and its position in UTM coordinates. Furthermore, concepts realized in 3D data formats such as VRML or X3D, were also modeled and implemented in the database. This procedure has two main advantages. The 3D data can be stored inside the database and allow for queries on parts of the geometry, and the storage is independent of data formats; an export to arbitrary 3D formats can be accomplished via conversion programs. For current ASCII-based 3D formats such as VRML, X3D, KML, or COLLADA, converters can be developed in PL/SQL with comparably low effort. The simultaneous high-resolution real-time visualization of the combined datasets including texture is still an unresolved issue at present.

21.4.1 GIS-Based Analysis

The integrated multiresolution 3D data served as a basis for a first analysis conducted in order to investigate a possible relation of petroglyph sites with routes connecting the coastal region in the vicinity of Nasca and Palpa with the highlands (compare Jensen 2003). The modern settlement Laramate, located upwards of the Palpa valley with respect to Chichictara, served as a target point for a first analysis. The goal was to determine routes towards the Andes that pedestrians would most likely choose for traveling from the coast to the highlands and vice versa. For this purpose, a cost surface was generated based on the ASTER DSM representing the walking speed for crossing each cell of the DSM. An empirically determined function of slope degree was implemented to calculate the cost surface according to the following formula (Tobler 1993),

$$v = 6^{*} \exp(-3.5^{*} abs(S + 0.05)),$$

where v means the walking speed in kilometers per hour and S the slope in radians.

In Fig. 21.9, the light grey and white values display cells that can be crossed comparatively quickly, whereas dark cells require more effort and can only be

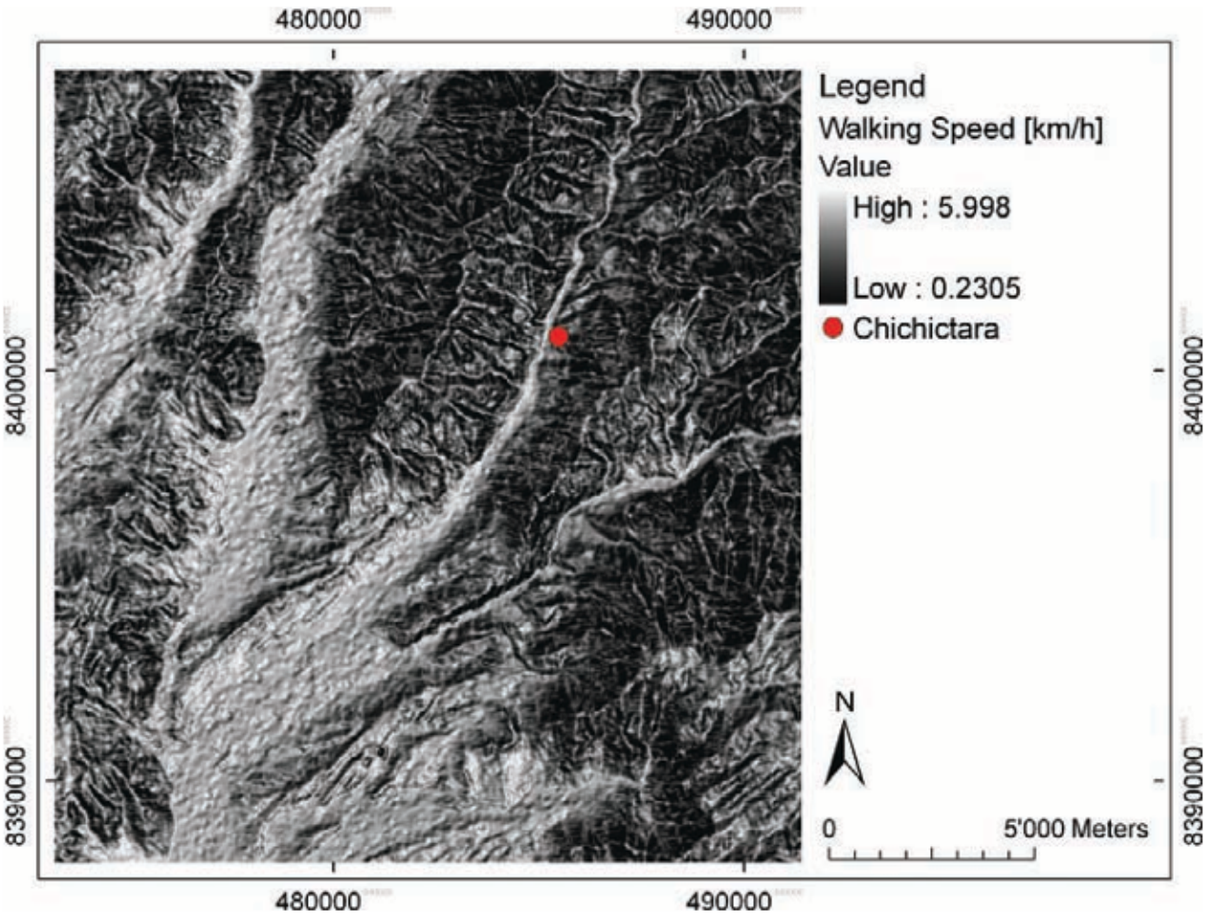

Fig. 21.9 The walking speed raster derived from the ASTER DSM. Chichictara is marked by the red point. Note the comparably high walking speeds on the mountain ridges in the northern part

crossed more slowly. Even from visual inspection, one can deduce that two types of topographic features are suitable for walking. One option is to travel along the river valleys, and the other option is to follow the mountain ridges. Taking into account the vegetation on the fertile valley ground, the second possibility was more likely to be chosen. Taken as a cost surface, cost analyses for travel routes and least cost path calculations can be performed to investigate possible connections between different regions. Nevertheless, for this purpose the area of investigation has to be enhanced significantly (see below).

21.5 New Perspectives for Archaeological Interpretation

As mentioned initially, two issues are matters of particular interest to the Chichictara project. First, due to the exposure of the petroglyphs to destruction, mainly by uncontrolled visitors, the goal of accurate documentation is certainly a target. For this reason, sector 2 (according to the division of the site into four sectors by Matos Avalos (1987)), which is the most frequently visited part, was chosen for detailed documentation in 3D. The digital terrain model of the Chichictara valley with the integrated rock models in high resolution, in combination with the GIS database containing among other information vector graphics describing each petroglyph, represents the optimum documentation in terms of modeling (Fig. 21.13). Furthermore, our successful application of the software SAT-PP to model carved rock surfaces in 3D demonstrates the capability of extracting barely visible petroglyphs by simply using a handy and inconspicuous calibrated digital camera in the field.

Secondly, the added value of the adoption of new technologies regarding interpretation—notably inquiries into the original social meaning of the specific place and iconography—should be discussed on the basis of our investigations at Chichictara:

We are convinced that mainly the decision to model the Chichictara valley in digital 3D put the landscape into the center of our attention as an integral part of the petroglyph studies. Indeed, Chippindale and Nash (2004), for example, already pointed out the high importance of the landscape for rock-art studies. However, in the case of Chichictara it was the change of perspective, obtained by the application of new documentation technologies, that evoked further contextual insights. As in the case of the decipherment of Linear B, information about a frame of action and life form, mainly derived from latent structures, is a key for understanding.

First of all, our discovery of an ancient footpath originating from the nearby ridge and entering the slope of the Palpa valley exactly at Chichictara is illuminative (Fig. 21.10). Furthermore, in the highlands at an altitude of 3200 m a.s.l. another petroglyph site with similar iconography, Letrayoc, was found by T. Stöllner (Ruhr-Universität Bochum, Germany). This site is located where the footpath leaves the ridge in the vicinity of a water source (see Fig. 21.10). The distance between Chichictara and Letrayoc is around 30 km, which is, in consideration of the altitude difference of around 2600 m, within a day's walking

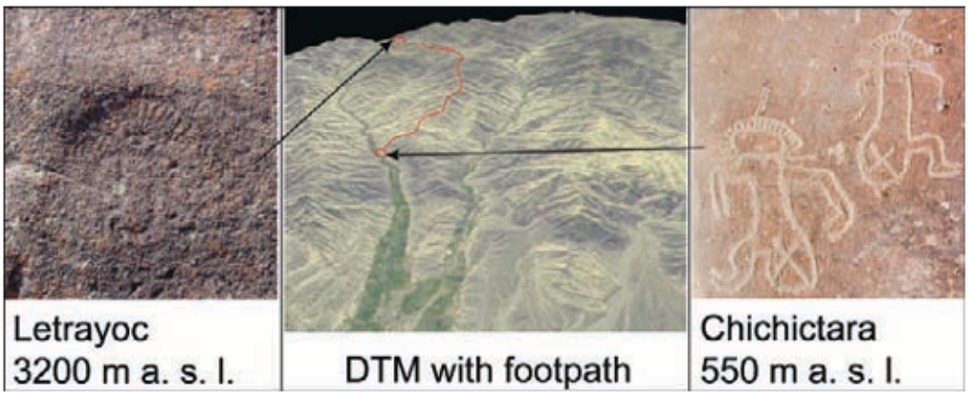

Fig. 21.10 The center image shows the footpath between Chichictara and Letrayoc, mapped in the textured 3D model derived from ASTER satellite imagery. The left and right images show petroglyphs of similar type found at the two sites Letrayoc and Chichictara

distance. It is reasonable to contemplate Chichictara in the context of this footpath and the availability of water, because Chichictara is just by the Rio Palpa.

This thesis is supported by the discovery of further petroglyphs of a similar type at the rock shelter of Coyungo, a few kilometers from the estuary mouth of the Rio Grande and after its confluence with the Rio Palpa (see furthermore Fux 2007). Numerous shell artifacts occurred within archaeological contexts near Chichictara that dated to the Paracas period (e.g., Jauranga, Mollake Chico; Reindel and Isla 2004) thus a connection between the adjacent plain of Palpa and the coast is clearly documented. Therefore, one could postulate the continuation of the above-mentioned footpath between Letrayoc and Chichictara to the Pacific coast (near Monte Grande?), passing the site of Coyungo.

In addition, there is an apparent pattern of Andean people moving up and down the mountains, crossing multiple ecological zones (Murra 1972; Moseley 1992: 25–51). The exploitation of many different ecological zones, in combination with cultural interactions and material exchange, can be seen, among other reasons, as an adaptation to extreme topographic and climatic situations and as a reduction of a substantial risk. This circumstance is in line with many archaeological findings: obsidian artifacts, found, for example, in the graveyard of Jauranga (Reindel and Isla 2004), near Palpa (350 m a.s.l.), dated to the Paracas period (800–200 BC) are evidence of interaction between people from the highlands and the coastal lowlands, because obsidian exclusively occurs in the highlands, predominantly near Huanca Sancos (Fux 2007; Silverman and Proulx 2002: 65–66). Vice versa, Paracas-style ceramic findings in the highlands are further evidence for interaction (Hohmann 2006: 44).

On the basis of this contextual information we propose to regard the petroglyph site of Chichictara within the frame of interecozonal interaction. Most probably, Chichictara, just as the other mentioned petroglyph sites Letrayoc and Coyungo, served as a resting place for caravans (with camelids as pack animals? Note camelid depictions, e.g., Rock 44, Fig. 21.12) on the way between different ecological (and cultural) zones, or as their handover place. Regarding the section between Chichictara and Letrayoc this thesis is furthermore supported by the cost surface analysis described above (Fig. 21.9).

At this point it is worth mentioning that there is a good reason to ascend or descend the easily walkable ridge exactly at Chichictara. Here, the steep run-of-hill scree is covered with loess, and therefore exceptionally walkable. Nieves' (2007: 162–169) conclusion that the petroglyphs within the Nasca–Palpa area differ from valley to valley in style seems to support our interpretation. Interaction (mainly regarding goods and material exchange) makes much sense between different ecological and climatic zones, but little between parallel and ecologically similar river valleys. Thus, latent structures of interaction (e.g., similarity in the style of petroglyphs) are expected in the west–east direction along the river valleys. Additionally, it seems plausible that the above-mentioned petroglyph sites had the following social function in common with geoglyphs dated to the Paracas period, for example, El Mirador near Llipata (see Fux 2007: 190). The figured landscape, whose original absence of especially striking structures is characteristic, allows a conversation about areas, places, and stretches of way. Analogous social functions are stated for geoglyphs of the Atacama Desert in Northern Chile (Briones 2006).

We now show in which regard the proposed frame of action will enable new perspectives for iconographic studies. Against the background of the footpath and its use by caravans carrying goods and materials between different ecological zones, one presumably is inclined to expect (with reference to the cultural affiliation) well-established symbols as petroglyphs at sites such as Chichictara. Indeed, the petroglyphs of Chichictara's sector 2 contain figures that are said to be typical for the coastal Paracas culture (800–200 BC; see, e.g., Silverman and Proulx 2002: 142; Proulx 2006: 88/89 and 94), such as the so-called two-headed Serpentine Creature (rock number 47, according to the numbering of Matos Avalos (1987), Fig. 21.13) or feline depictions (e.g., rock 44, Fig. 21.12). Furthermore, there are figures that make long-distance cultural connections apparent, such as the Chavin Head (rock 6), pointing to northern Peru, or depictions of monkeys (e.g., rock 12, Fig. 21.11), pointing to the rainforest on

Fig. 21.11 The petroglyph on rock 12 shows a monkey

Fig. 21.12 View of the 3D model of rock 44, which shows among others a feline and a camelid on the upper left

the eastern slope of the Andes. Depictions of camelids (e.g., rock 44, Fig. 21.12) illustrate the connection with the highlands (see Horn et al., this volume).

Because a connection between the plain of Palpa and the coast is clearly documented, the proposal of Wickler and Seibt (1998: 15–25) to regard the so-called two-headed Serpentine Creature (Fig. 21.13), as depicted on rock 47, as a derivation of a marine bristle worm is strengthened. Presumably the bristle worm's periodic appearance near the water surface attracts fish and indicates favorable conditions for fishing. Alleged Serpentine Creatures regularly occur on textiles and ceramics in close relation with representations of human beings

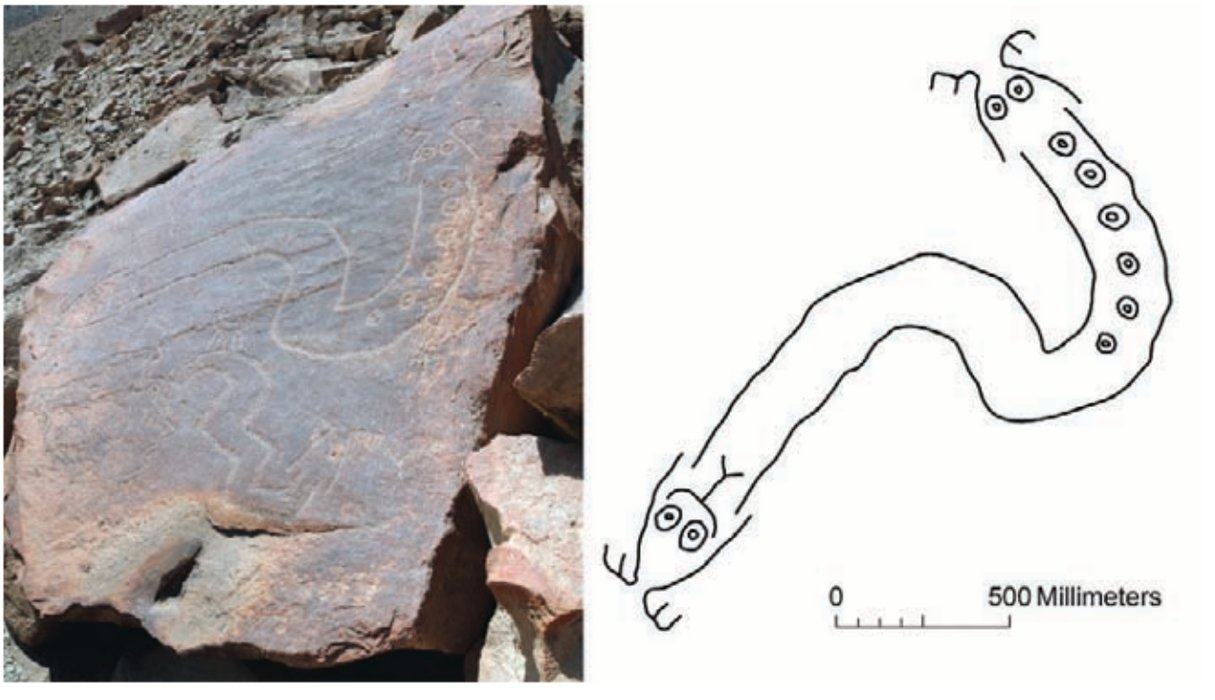

Fig. 21.13 Left: Rock 47 with several "Serpentine Creatures." Right: Result of the 3D digitalization of a "two-headed Serpentine Creature" depiction on rock 47

during the Paracas (800–200 BC) and Nasca periods (200 BC–650 AD), and could therefore be interpreted as a symbol of the dependency of humans on these animals, which bring them food, or, because of the bristle worm's periodic appearance, as an indicator of time.

Second, monkey depictions (e.g., rock 12, Fig. 21.11) should be regarded as indicating cultural contact with the rainforest. Moseley's above-mentioned argument for the high importance of interecozonal interaction for Andean people (see Reindel, this volume) even becomes apparent in the petroglyph figures themselves. A good deal of further archaeological indications, such as parrot feather findings in Paracas and Nasca contexts and monkey depictions on ceramics and in the form of geoglyphs, clearly support this claim (see, e.g., Proulx 2006). At Chichictara we seem to face the footsteps from the coast area to the highlands and even towards the rainforest and vice versa. Against the background of this circumstance one should put into perspective long-distance cultural connections across multiple ecological zones while analyzing the iconography of both the coastal Paracas and Nasca cultures.

Indeed, the figure on rock 44 (Fig. 21.12), as with feline depictions on ceramics and textiles from the Paracas culture in general, looks similar to a small feline (with ruffled fur?) known as the pampas cat (*Felis colocolo*; see, e.g., Proulx 2006: 88/89), which is an identification further strengthened by climatological evidence, inasmuch as a clearly less arid climate and a pampas vegetation are postulated for the Paracas period (see Eitel, this volume). However, there is another question of whether the figure named the *Mythical Spotted Cat*, which we know from ceramics and textiles dated to the subsequent Nasca culture, is a direct development from the feline depictions of the preceding Paracas culture (see Proulx 2006: 88/89).

It is remarkable that this figure is—as pointed out by Wolfe (1981)—mainly represented in close relation to crops and fruits, frequently holding them in its forepaws, which is generally seen as supporting Seler's (1923: 174) widely accepted interpretation of this creature as standing for a "bringer of food" within the Nasca culture. Mainly by reason of the difficulty of relating felines meaningfully to crops and fruits (not to mention the action of bringing) and the above-argued cultural contact with the rainforest in the Paracas period (a pattern that certainly was still effective during the Nasca period), the question about the relation of this figure to a raccoon (see Wickler and Seibt 1998: 34/35), instead of a feline, seems not to be digressive, inasmuch as raccoons are still present in the Amazon Basin (see Pearson and Beletsky 2002: 441) and furthermore well known for holding crops and fruits in their hands. However, the *Mythical Spotted Cat* was rather identified as a "remover of food" within the Nasca culture.

Based on all of the evidence, we are convinced that, taking into account a multitude of multifaceted contextual information, the petroglyph site of Chichictara should be regarded within the herein-exposed frame of action of cultural interaction by means of caravans, carrying goods and materials between different ecological zones. It is this postulated frame of action, which

opens up the understanding of the petroglyphs of Chichictara, just as the form of life and the needs within a Minoan palace structure enabled the decipherment of Linear B. Because of the contemplation of Chichictara and Letrayoc in the context of the footpath on the ridge, in addition to further described indicative archaeological findings (see Reindel, this volume), the postulated interaction between the highlands and the plain of Palpa, and even the coast, is conclusively documented. As illustrated, the cultural contacts between these zones are reflected in the petroglyph figures themselves. Furthermore, we postulate that mainly on the basis of the petroglyph's iconography, and supported by a good deal of other indications, these interecozonal cultural contacts should be regarded as expanding as far as the rainforest. The investigation of this issue certainly is a desideratum.

We are confident that our explanation has shown that by means of the adoption of new technologies for the documentation of the petroglyph site Chichictara new perspectives regarding both the interpretation of the prior social meaning of the petroglyph site and iconography of its pictures are opened up. The adoption of new technologies brings a new edge to the archaeological interpretation of the petroglyphs of Chichictara.

Acknowledgments The authors thank the Swiss-Liechtenstein Foundation for Archaeological Research Abroad (SLSA) for funding this project and J. Isla Cuadrado, M. Reindel, A. Gruen, and P. Della Casa for their support regarding the field campaign. Furthermore, we thank J. Peterhans, M. Belkaïd, N. Vassilieva, M. Schmid, and T. Graeger for their contributions to photogrammetric data processing.

Chapter 22
Pottery Plotted by Laser – 3D Acquisition for Documentation and Analysis of Symmetry of Ancient Ceramics

Hubert Mara

Abstract Due to increasing demand of archaeologists for accurate and fast documentation of ceramics, we provide an automated system for acquisition and documentation of sherds. This is done by 3D-acquistion using structured light and by estimation of the profile line using the axis of rotation. As ceramics manufactured in South America are not supposed to be manufactured on rotational plates, we conducted experiments together with the German Archaeological Institute (DAI) to apply and adapt our system on freehand manufactured Nasca ceramics. The experiments including a comparison between manual and automated drawings of profile lines were done in-situ at the excavations in Palpa, Peru. To gather a ground truth about the vessels the sherds belong to, we acquired 102 complete vessels with well-known archaeological context. The symmetry of these vessels was analyzed and experiments for automated profile estimation were used to cross-validate existing classification rules. We could show how to assist archaeological work by estimation of profile lines and additional quality features based on the symmetry of the acquired vessels. Furthermore we show how the use of 3D-scanners can be used by estimation of unwrapped surfaces and virtual restoration of decorations of the painted Nasca fine-ware (30–40% of the findings). Therefore we can show that the documentation can be done in a fraction of time compared to manual documentation. We also show how the high resolution 3D-acquisiton can be used to answer archaeological questions about ancient manufacturing techniques of ceramics.

H. Mara (✉)
Vienna University of Technology, Institute of Computer Aided Automation, Pattern Recognition and Image Processing Group, Favoritenstrasse 9/183-2, 1040 Vienna, Austria
e-mail: mara@prip.tuwien.ac.at

M. Reindel, G.A. Wagner (eds.), *New Technologies for Archaeology*, Natural Science in Archaeology, DOI 10.1007/978-3-540-87438-6_22,
© Springer-Verlag Berlin Heidelberg 2009

22.1 Introduction

Documentation of ceramics is a main task in archaeology, because ceramics are the most common findings, used and produced in large numbers by humans for several thousands of years. Archaeologists use analysis of ceramics on a daily basis to reveal information about the age, trading relations, advancements in technology, art, politics, religion, and many other details of ancient cultures.

Therefore we are developing an automated system for ceramics documentation to help archaeologists document their finds in an efficient and accurate way, which can be used for further (computerized) research. The basis of documentation of ceramics is a manually drawn vertical intersection, which is called the profile line (Leute 1987). Figure 22.1 shows a sample for Nasca vessels and a manually drawn profile line.

The profile line is the longest elongation around, or cross-section through, the wall of a ceramic defined by the rotational axis (also called axis of symmetry). The term rotational axis relates to the fact that rotational wheels (plates) have been used for thousands of years for manufacturing ceramics. This assumption could be made for our previous work in interdisciplinary projects with archaeologists working in Europe and the Mediterranean area (Kampel and Sablatnig 1999, Cosmas et al. 2001). We showed that orientation of ceramics for automated estimation of profiles of 3D-models can be done for complete objects as well as for fragments (Mara 2006). In the case of Nasca and other South American ceramics this assumption is under discussion as the concept of wheels was not used prior to the Spanish conquest in the sixteenth century. An opposing opinion is the computer tomography (CT) survey by

(a) (b)

Fig. 22.1 (**a**) Photograph and (**b**) manual drawing of vessel 2801-V3 and its twin found near Palpa

Hoffmann-Schimpf and Tellenbach (2004). Therefore the NTG-project was our opportunity to evaluate our methods on objects that look symmetrical, but may not be at all. On the other hand we could conduct experiments for estimation of multiple profile lines at random positions of unbroken ceramics, which have shown notable deviations (>1 mm) leading to quality criteria for classification and determination of manufacturing techniques, which is another important question for archaeology. This question is of even more interest for the region of South America where, unlike the Mediterranean area, no written sources about vanished civilizations are known to exist.

A further important research question is the so-called relative chronology, which is based on the assumption that artistic style and therefore the shape of the profile line changes continuously over time. The final constraint for our work was performance as ceramics are found in tens of thousands at virtually every excavation and manual drawings require a lot of time, skill, and man-power of experts. This is especially important for the vast number of Nasca ceramics having painted surfaces, which are typically documented as unwrapped drawings.

First we describe the acquisition process of ceramics, followed by the description of the symmetry analysis including results of synthetic and real ceramics for archaeological documentation by profile lines. Furthermore we show the use of the symmetry for automatically unwrapping painted surfaces.

22.2 Acquisition

The challenging tasks of developing a documentation system for archaeology are to build a system which is accurate, portable, inexpensive, radiation-free, easy-to-use, and robust for all kinds of climate and range from desert to jungle to arctic. This means several technologies such as computer tomography and other laboratory equipment are often not suitable for the daily work of archaeologists, especially not for ceramics. As photography has already proven its reliability for archaeology, we chose to use the principle of structured light (DePiero and Trivedi 1996, Liska 1999) requiring a camera and a light-source for 3D acquisition.

For recent work we use 3D scanners from the Konica-Minolta Vivid (Mara 2003; Mara and Hecht 2006) product range, because of their resolution (<0.1 mm), as they meet the requirements given by archaeologists for their documentation. Figure 22.2 shows the setup of our 3D scanner from recent experiments at the excavations in the Valley of Palpa, Peru (Reindel and Isla Cuadrado 2001). Figure 22.2a shows the triangulation principle (Mara 2003) using a laser (bottom) and a camera (top) having a well-known distance and orientation. In addition the turntable is used to get a complete 3D-model of the ceramic. The number of 3D-scans depends on the complexity of the ceramic and

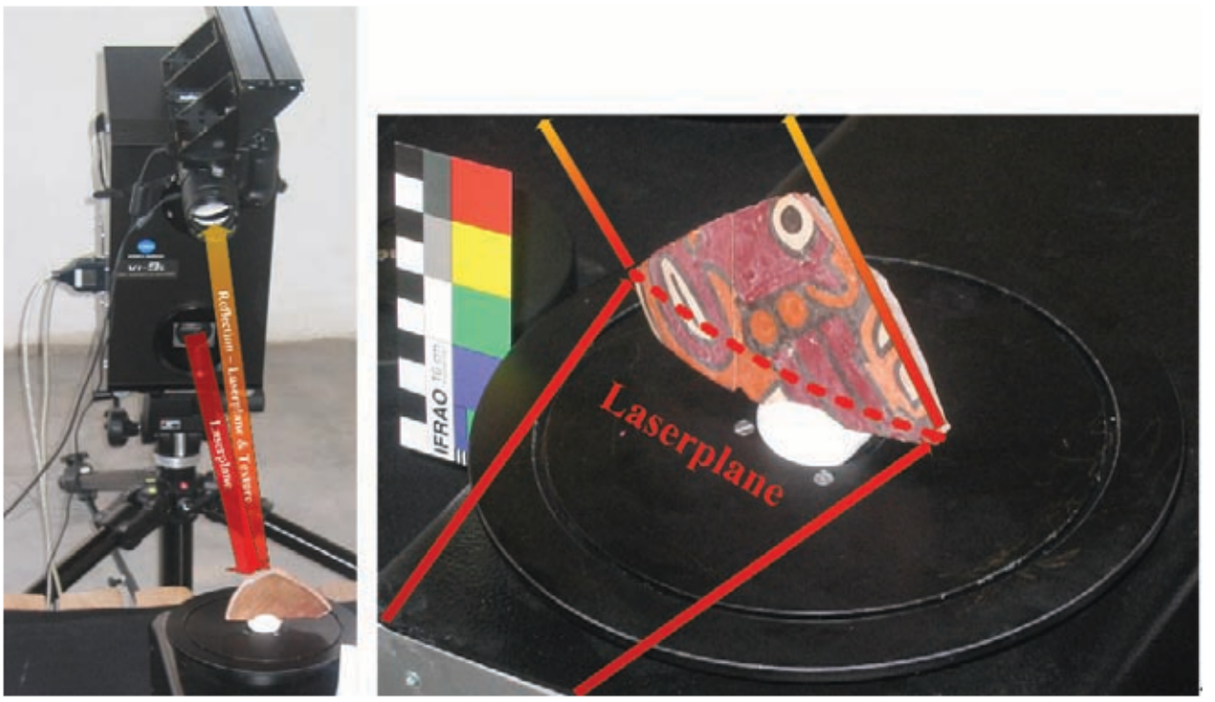

Fig. 22.2 (**a**) Konica-Minolta Vi-9i 3D-scanner projecting a plane of laser-light (*bottom arrow*) on to a sherd, while cameras (*top*) acquire the projection of the laser and the color of the painted surface as well. Having a well-known distance and orientation of the plane of laser light and the field of view of the camera, the distance (*range*) can be estimated. (**b**) Detail of this setup showing a sherd mounted with plasticine on the turntable, which is used for controlled acquisition of all sides of an object

it typically ranges from two scans for sherds up to eight scans for vessels. The 3D scans are registered using Tosovic (2002) to reassemble a complete 3D model.

After the registration, noise from dust and other objects such as holding devices (e.g., clamps or plasticine) is removed from the 3D model. Then the orientation is estimated based on the assumption that ceramics are rotationally symmetric objects (Mara 2003). The principle of our orientation method is fitting of circle templates (Gander et al. 1994) similar to manual orientation using the rills on the inside of a sherd or matching caliber. In comparison to the computerized but manual method of (Melero et al. 2003) our orientation method can be used fully and semi-automatic (Lettner et al. 2006). Furthermore our system is capable of storing the 3D model and further archaeological information (e.g., description, photographs, etc.) in a database. For solving the puzzling problems of other, typically industrially manufactured, rotational objects, methods such as those by Pottmann et al. (1998), Willis (2004), and Orriols (2004) can be applied. Having an oriented 3D model, a vertical cross-section is estimated using the point of maximum height of the 3D model. This cross-section is the so-called profile line, which concludes the traditional

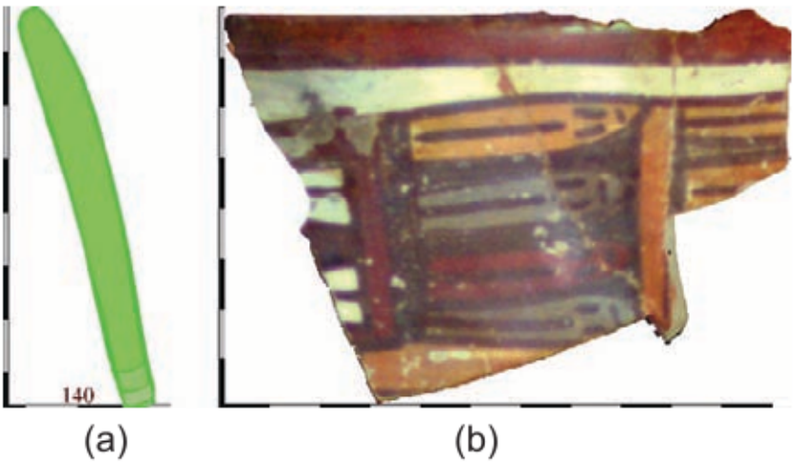

Fig. 22.3 (**a**) Automatically estimated profile lines(s); (**b**) front view of the Nasca sherd 824-157

archaeological documentation. Figure 22.3a shows a result for an automatically estimated profile line, where the longest profile line at the maximum height and two more neighboring profile lines at ~1 cm distance along the circumference of the sherd are shown. As the correct axis of symmetry was found these profile lines overlap and a deviation can only be seen at the bottom due to the fracture. Figure 22.3b shows the front view of the oriented sherd.

As already mentioned, our method was originally designed on an assumption which is not assured for South America. Therefore the rate of successfully oriented sherds changed from >90% for ceramics in and around Europe (Mara and Hecht 2006) to ~70% for Nasca ceramics. It has also to be noted that for half of the oriented Nasca ceramics the automated method as well as manual orientation return a range of possible angles (e.g., +/–10°) for orientations instead of a single angle. Even for the remaining 30% of incorrectly oriented fragments we get overlapping neighboring profile lines as for the correct ones, which means Nasca ceramics have only a plane of symmetry instead an axis of symmetry, which confirms the common archaeological opinion of the nonexistence of rotational wheels. Figure 22.4a,b shows examples of neighboring profile lines of the same vessel type as shown in Fig. 22.4c for profiles within a valid range of orientation angles and an invalid still having a correct overall diameter and shape.

As the existence of a pottery wheel in ancient Peru can be ruled out, another feasible possibility known in archaeology is the use of some kind of slow rotating pottery plates. This would also explain the g results of our work, the evidence presented in Carmichael and Rowe (1986), and the opposing results of Hoffman-Schimpf and Tellenbach (2004) and Wieczorek and Tellenbach and Tellenbach (2002). For the applicability of our method on Nasca ceramics we can conclude that we can find the plane of symmetry having overlapping profiles, which means we can automatically estimate an overall diameter as well as a correct shape of the profile line, and only the orientation has to be adjusted manually or by using an expert system as a future addition.

Fig. 22.4 Profile lines of sherds (**a**) 824-4b and (**b**) 824-4 in comparison to (**c**) the same vessel type; (**a**) is within a valid range of orientation angles and (**b**) invalid, but still having a correct overall diameter (120 mm) and shape

22.3 Symmetry Analysis

Inasmuch as rather simple two-dimensional profile lines, as shown before, do not reflect any information about the manufacturing quality leading to the manufacturing technique, we decided to enhance our system by giving the archaeologists a tool to gather further information about the acquired 3D model.

Therefore we had to investigate the question of manufacturing technique and quality of the symmetry of Nasca vessels to determine these variations. In general technological advancement is determined by archaeologists between ceramics that have been produced either on slow rotational plates or fast-turning pottery wheels. As we use structured light as our 3D acquisition method, we cannot make assumptions about the internal structure of a ceramic as did Wieczorek and Tellenbach (2002), but we can estimate the surface with a high resolution (0.1 mm). Therefore we can analyze the symmetry and estimate features such as deviation of real surfaces with respect to a perfectly symmetrical surface. Such features can help archaeologists to decide about the technological advancements of ancient cultures.

As archaeologists are also excavating burial places where unbroken ceramics or complete sets of sherds are found, we present a method to determine the manufacturing process of ceramics, which reveals information about the technological advancement of an ancient culture. Furthermore this method can be applied, but is not limited, to unbroken or reconstructed vessels.

To begin our investigation and answer questions about the manufacturing process of ceramics, we chose to use two modern pots that were manufactured in a traditional way. Therefore these data can be interpreted as mixture between

synthetic and real data, because we used real objects. However, unlike real archaeological fragments, we know how they were produced.

Furthermore we decided to use the method for finding the orientation of a sherd (Mara and Kampel 2003). We began with the profile line, which can be estimated in a similar way as in the case of sherds. The difference is that for complete vessels the bottom plane can be used for orientation, because it is the counterpart for the rotational plate, which defines the (orthogonal) axis of rotation.

We estimated multiple profile lines, which can be overlaid by transforming them into the same coordinate system, where the y-axis equals the rotational axis. By this means the distance between profile lines can be estimated. Figure 22.5 shows for two different vessels of similar shape the longest profile line and multiple profile lines combined with the side view, as archaeologists show such vessels in their documentation. In the case of the multiple profile lines, we have estimated that the distance between the profile lines differs and therefore these pots and their profile lines are unique. The maximum distance between two profile lines of the first pot was 9.8 mm, whereas for the second pot it was 21.2 mm.

In the multiple profile lines shown in Fig. 22.6b,d, the distance between profile lines, measured parallel to the y-axis, is not equal. If the profile lines were parallel, this would mean that the pots had an elliptic (horizontal) cross-section. As it appears, the asymmetry is more complex. Therefore, we chose to analyze the pots slice-by-slice along the rotational axis which is presumed orthogonal to the bottom plane.

Figure 22.6a,c shows horizontal intersections that have been applied with a distance of 10 mm along the rotational axis. The distance of 10 mm corresponds to the manufacturing process, which has left traces in the form of rills as seen along the right-hand sides of Fig. 22.5b,d. These rills are spaced 10 mm apart, which corresponds to the width of the finger or tool used to "grow" the pot

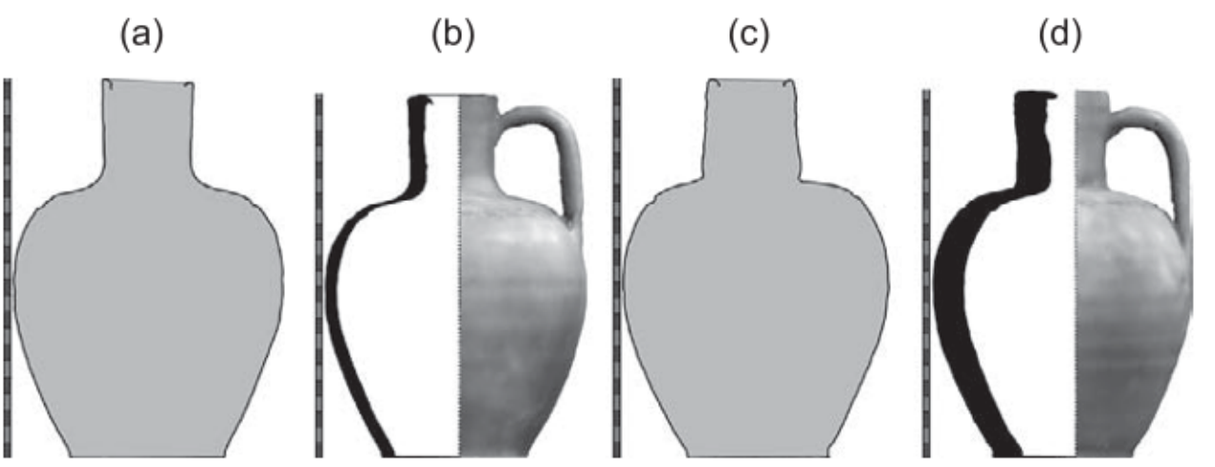

Fig. 22.5 (**a**),(**c**) Longest profile lines and (**b**),(**d**) multiple profile lines of modern ceramics, manufactured in the traditional way, which are supposed to be identical

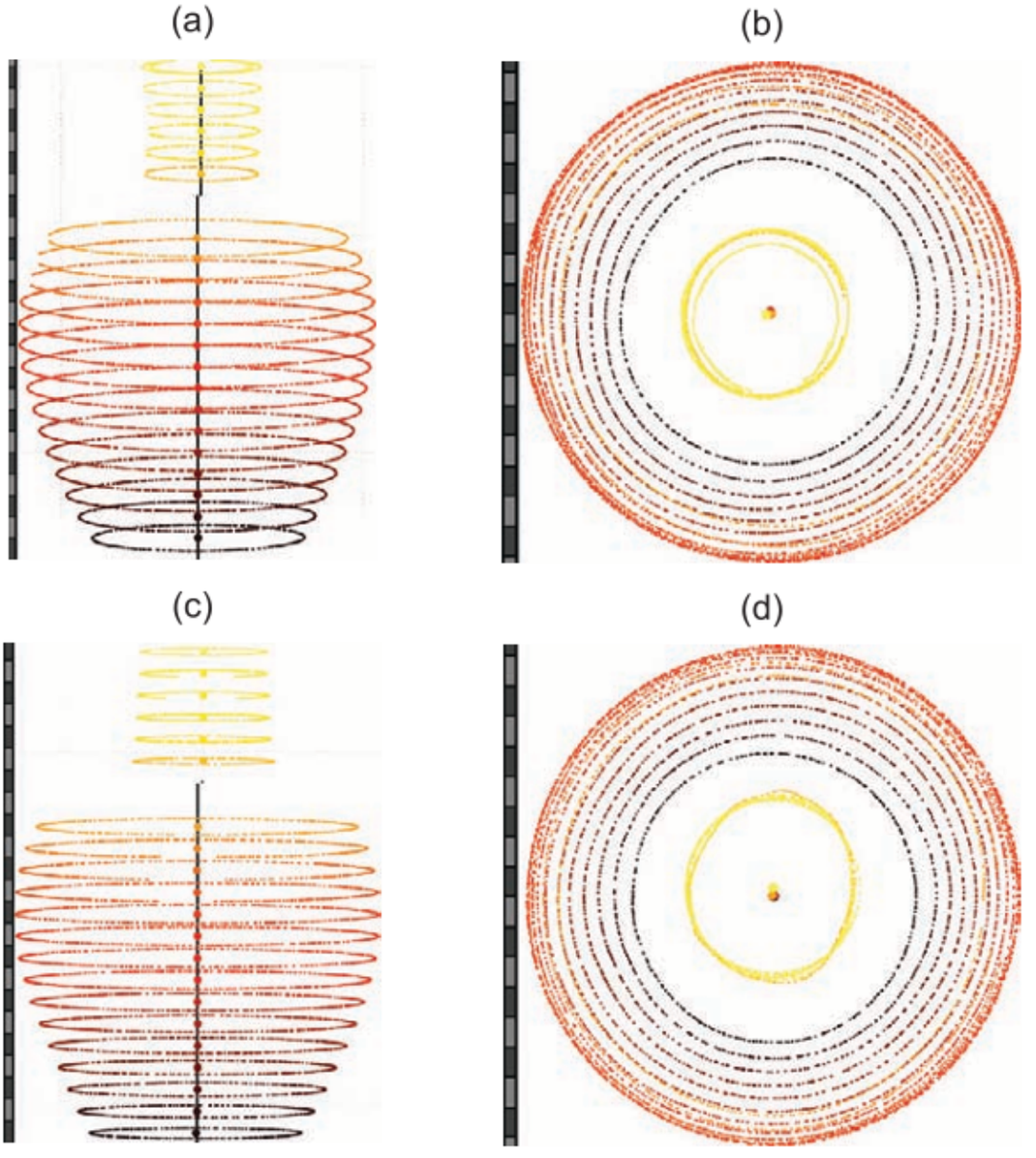

Fig. 22.6 (**a**),(**c**) Side-view and (**b**),(**d**) top-view of the horizontal cross-sections; the level of color-scale corresponds to the height. The axis of rotation for the lower and upper part is shown as a black line, defined by the centers of the concentric circles (shown as dots)

along the axis of the rotational plate. The intersections at 160 and 170 mm in height have been discarded, as they intersect the "shoulder" of the pot with a very low angle ($<<5^\circ$), resulting in an intersection having a nonrepresentative, random curvature.

Dividing ceramics into sections by characteristic points (such as the shoulder) is carried out by archaeologists for classification. Therefore we chose to analyze the object segmented into a lower and an upper part. This means we have two fragments where axis estimation can be applied, as for sherds (fragments). The estimation of the axis is shown in Fig. 22.6b,d. The numeric results for the axis are that they have a minimum distance of 4 mm towards each other and to the axis defined by the bottom plane. Furthermore the angles between the axes differ between 5° and 7°.

Using the rotational axis of the lower and upper fragments, we repeated the estimation of the profile lines, which are shown in Fig. 22.5. The maximum distance between the profile lines is 7 mm for the upper and 2 mm for the lower part. Therefore the first conclusion is that the upper and lower parts do have a different axis of rotation, which means that these parts have been produced separately and combined after separation from the rotational plate.

We can conclude that, based on the different deviation of the multiple profile lines, the upper part is of lesser quality than the lower part. This leads to the conclusion that these parts may have been made by potters with different experience and/or on a slower rotational plate. The deviation in the upper part of up to 7 mm compared to less than 2 mm of the lower part shows that a faster turning rotational plate has been used and that more experience was required for manufacturing the upper part.

From the differing angle between the axis of rotation based on the bottom plane compared to the axis of rotation of the upper and lower fragments, we can conclude that either the bottom has been reworked or the pot was contorted before being fired in the oven.

Even correcting the axis for the parts of the object, the horizontal intersections are not perfectly circular. The horizontal intersections are elliptic. Therefore we estimated the direction of the major and minor axes of the ellipses. We estimated that the minor axis has the same direction as the orientation of the handle. This means that the symmetry of the pots was broken when the handle was attached and the pots were still wet. Figure 22.7 shows the pots intersected

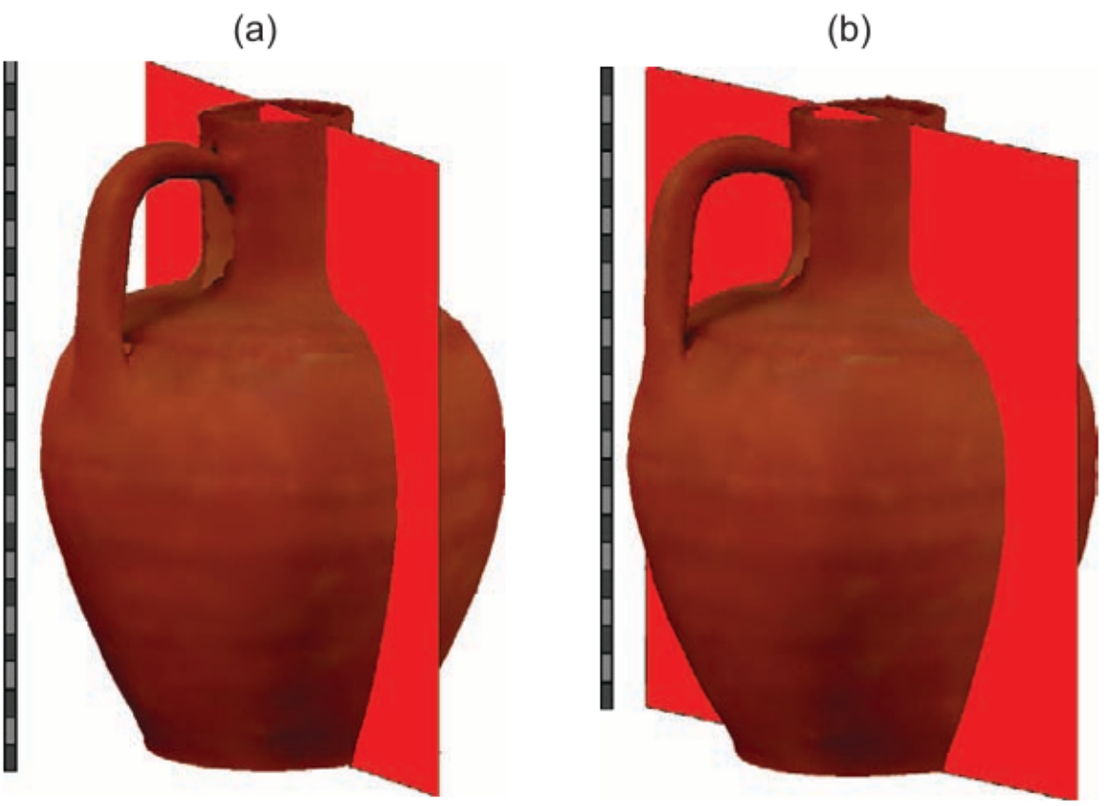

Fig. 22.7 Planes of symmetry of the (**a**) first and (**b**) second object

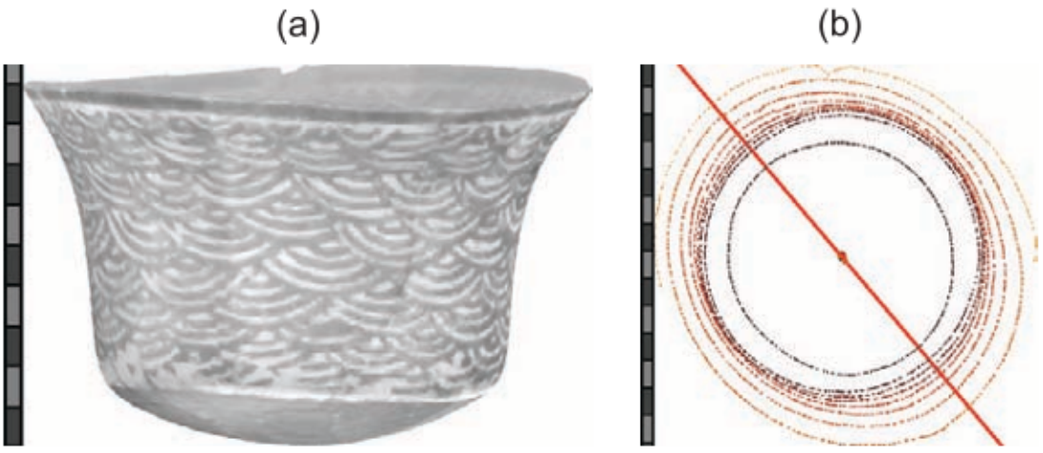

Fig. 22.8 (**a**) Frontview and (**b**) Topview of the horizontal intersection with plane of symmetry of vessel 2827-V1 found in the Valley of Palpa, Peru

by a plane, and defined by the center of gravity of the pot and the direction of the major axis of the ellipses. The angle between the minor axis and the handle of the pot was 7° and 14° for the second pot. Furthermore, Fig. 22.8 shows an example from the excavations in the valley of Palpa, Peru.

We additionally conclude that the ellipses fitted (Gander et al. 1994) to the horizontal cross-sections can be used as an additional feature. Therefore the distance between the foci of the ellipse is estimated. Ceramics with a distance converging towards zero (circular cross-sections) are of higher quality.

The proposed method has also been tested on 17 real vessels of the Nasca period (Carmichael and Rowe 1986), which were found in the valley of Palpa, Peru (Mara; Reindel001). By this means we could separate these vessels into three classes determined by the symmetry. The vessels (60%) of two of these three classes were not produced on rotational plates. This additional classification helps to answer the question about the manufacturing technique and the use of rotational plates in South America. This classification by quality is also used by archaeologists of the German Institute for Archaeology (DAI, Bonn) to refine their classification schemes.

22.4 Unwrapping and Enhancing Surface Painting

A further archaeological task for documentation is manually unwrapping and drawing of painted ceramics. Using the rotational axis we can generate an unwrapped image of painted ceramics. Figure 22.9 shows the unwrapped cylinder and the manual unwrapped drawing of vessel 2801-V3. Additionally image-processing methods were applied to enhance the contrast as well as line-detection algorithms as proposed by Kammerer et al. (2005).

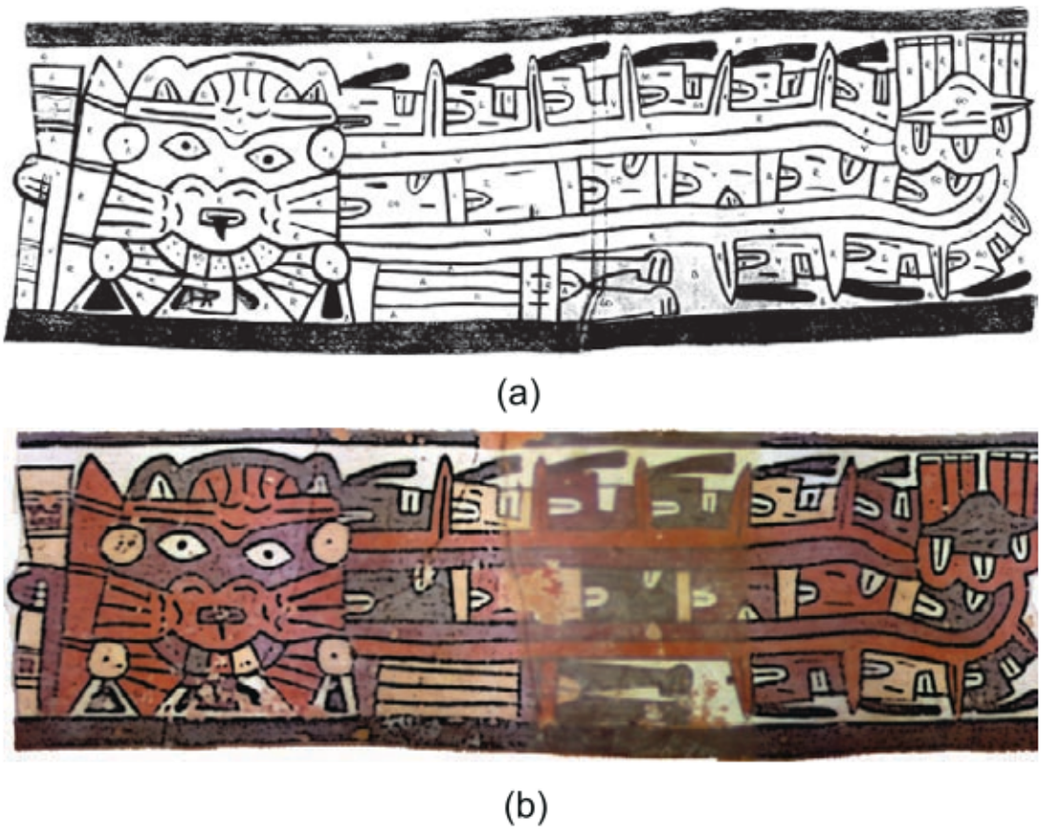

Fig. 22.9 Comparison of (**a**) manual drawing and (**b**) automatically unwrapped drawings with (*left* and *right*) and without (*center-right*) with postprocessing

Generally surfaces of ceramics can be unwrapped only with distortion; we estimated three different images of unwrapped vessels. An example for an extreme case, closely reassembling a sphere, is shown in Fig. 22.10. The first image is an unwrapping of a parallel projected texture. The third image is an unwrapping of the surface by stretching into a plane. The image in between is a combination of the first and the third images. The combination can be weighted towards the cylindrical unwrapping and vice versa, so that archaeologists can choose the most suitable image for documentation.

22.5 Summary and Outlook

Summarizing the presented work, we can conclude that symmetry analysis can and will be used to estimate quality features of Nasca ceramics and related ceramics for classification and archaeometry (Leute 1987). Furthermore it can be used to approximate a ground truth and therefore to estimate possible variations of the orientation of the profile line for manual drawings and automatically estimated profile lines. For the automated profiles however, we can estimate the expected error of ceramics which might not have been manufactured on rotational plates. Finally we can conclude that symmetry analysis can

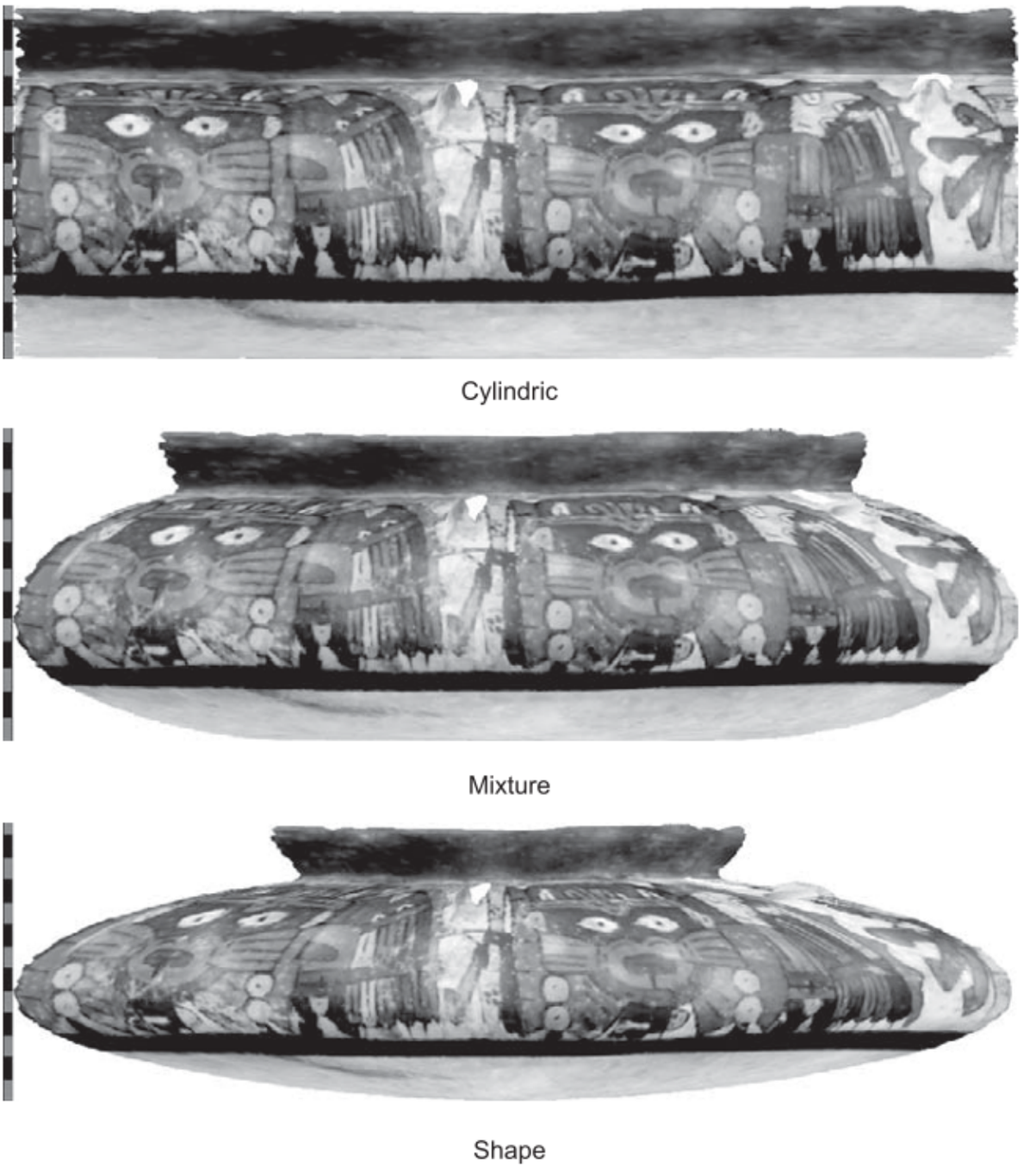

Fig. 22.10 Unwrappings of vessel 2801-V2, which closely reassembles a sphere, that cannot be unwrapped without any distortion, therefore we show three different estimations of the planar image of the object's surface

reveal detailed information about the manufacturing process, such as quality requirements and production steps of ancient ceramics. Future work will also include an automated ordering using shape-matching methods to establish a relative chronology.

Part VI
Archaeometallurgy

Chapter 23
Gold in Southern Peru? Perspectives of Research into Mining Archaeology

Thomas Stöllner

Abstract In contrast to the northern Peruvian coast or the altiplano the southern coastal area never played an important role in the discussion of gold metallurgy. This is partly due to the fact that research thus far never focused on the metallurgical relicts of traditional southern cultures such as the Paracas, Nazca, or Ica/Chincha. A reason for this neglect might be the fact that gold did not play the same prominent role in burial customs as it did in the more northern Moche area for instance. But now, first provenance studies provide evidence for local gold use. This chapter deals with the potentials of further research and provides interesting results of mining gathered from the ethnographical record. Some of the presumptions discussed before are also evaluated. There is now good reason to start with systematic surveying of ore deposits of the Nazca–Ocoña ore-formation. However, a wider frame of economical archaeological studies needs to be chosen if the level and importance of mineral deposits is to be understood.

23.1 On Our Knowledge About Pre-Columbian Peruvian Metal Exploitation

Although much research has been done on Andean metallurgy which – especially highlighted by precious metalwork – was always in the focus of archaeological research, only little knowledge has been gained about the primary stages of metal exploitation, especially in pre-Inka periods. Nowadays it seems that there was a certain concentration on gold metallurgy right from the beginning. Even Spanish chroniclers such as Cieza de Leon (1553) and Garcilaso de la Vega (1609) or Girolamo Benzoni (1572) have reported the

T. Stöllner (✉)
Deutsches Bergbau-Museum Bochum, Forschungsstelle Archäologie und Materialwissenschaften, Fachbereich Montanarchäologie, Herner Straße 45, 44787 Bochum, Germany
e-mail: thomas.stoellner@bergbaumuseum.de

M. Reindel, G.A. Wagner (eds.), *New Technologies for Archaeology*, Natural Science in Archaeology, DOI 10.1007/978-3-540-87438-6_23,
© Springer-Verlag Berlin Heidelberg 2009

abundance of gold in rivers where it could be won easily. So did Garcilaso when he wrote "...Gold is collected in Peru everywhere although it is more frequent in some regions. It can be found at the surface and in rivers and torrents, whereto it is transported by rainwater. There it is extracted by washing from sand and earth...." (Garcilaso de la Vega 1609). There still is restricted knowledge concerning direct field evidence of primary production steps. In Peru basic steps have been carried out first by Root (1949) followed later by a survey of Lechtman (1976): it was possible to define three regions in which autonomous metallurgical concepts could be observed (Fig. 23.1).

In contrast to the Old World, the oldest pre-Columbian metallurgy was based on gold, especially in South America (Lechtman 1979; Rovira 1987). The oldest findings have been reported from Waywaka north of Cuzco which date to the beginning of the second millenium BC, that is, 1890–1640 cal BC (Grossman 1972): some golden plates, an anvil stone, and some stone hammers

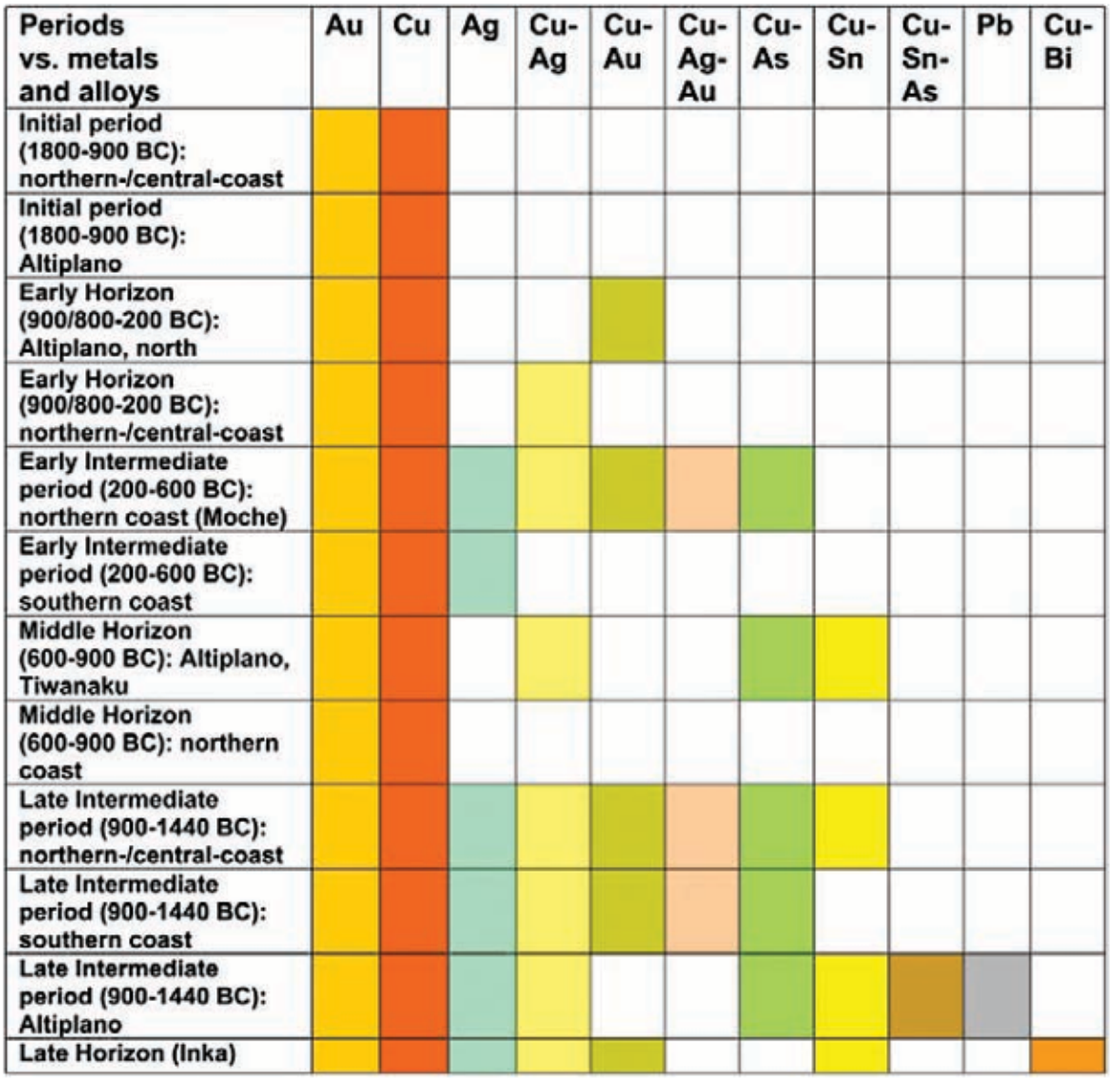

Fig. 23.1 Development of central Andean metallurgy according to regions and cultural stages on the basis of alloys

can be assigned to a simple cold-working technique; younger evidence has been detected from the so-called Initial period from Central Peru as well: The ceremonial centre of Mina Perdida at the Lurin Valley has produced very pure copper (perhaps native copper) and some very thin follies of gold (Burger and Gordon 1998). It certainly belongs to the end of the second millenium BC according to the ^{14}C-dates (1410–1090 cal BC). Since the first millennium BC metals have been used regularly. It is probable that the northern Peruvian Chavín culture seemingly has produced metals on a larger basis, but there are still only comparatively few metal objects. This scarcity of metals also can be observed on the Peruvian southern coast in the context of the Paracas culture (Uhle 1913; Tello 1959; Tello and Mejía Xesspe 1979).

This situation changed completely during the Early Intermediate period (200 BC–AD 600) when different regional cultures emerged at the arid coastal regions: northern Peru can still be described as a centre of precious metals working whereas the southern region, especially the Altiplano between Bolivia, northern Argentina, Chile, and Peru was dominated by copper working. These regional differences certainly can be deduced from some variation in the composition of the ore deposits that contained high portions of cassiterite in the surrounding of Lake Titicaca, where tin-bronzes appeared for the first time before they became commonly used later on in the Inka period (Lechtman 2007). It is also likely that the different metallurgical traditions of North and South Peru were initiated during the Early Intermediate period. Despite the rarity of well-documented complexes the Moche culture of northern Peru (Lambayeque valley) has produced early examples for the typical Andean metallurgical tradition that is based on a binary or ternary alloy system of gold, silver, and copper. Especially the famous grave furniture of the "lord" of Sipán (AD 300) has produced a large variety of alloys and metals that obviously have been used to express symbolic and cosmologic meanings: gold and silver alloys represented a certain ideological duality (Alva 2001; Lechtman 2007). For the Moche culture (200 BC–AD 800) the deliberate usage of arsenic bronzes has been discussed for a couple of years (Lechtman 1979). These alloys, however, dominated the whole Andean metallurgy, especially from the Middle Horizon on and in large quantity also during the Late Intermediate period (Mayer 1986, 1992, 1994, 1998).

In general the northern coastal area can be considered an area much better investigated than the southern coast or even the Altiplano (Rovira 1990; Lechtman 1997; 2003). Well-documented metals from the Nasca and Palpa valleys are rarely reported; most of the materials came from clandestine excavations and thus are not secured. Therefore our knowledge is based on the older excavations, for example, of Julio C. Tello or Max Uhle in the necropolis of Ica or Nasca (Fig. 23.2).

In the Lambayeque valley in northern Peru a characteristic production ensemble has been discovered and investigated. The sites of Batán Grande can be considered as one of the best-known metallurgical ensembles of South

Fig. 23.2 Copper and copper alloy artefacts from the southern Peruvian coast. (After Mayer 1998)

America. It consists of mines at the Cerro Blanco and a mining settlement that delivered evidence for beneficiation and smelting. Both sites were interconnected by a track way that certainly had been used for ore transport and people's access to the mining field (Shimada et al. 1982; Shimada and Merkel 1991). A neighbouring Chimú settlement has produced a large quantity of bronzes, most of them alloyed with arsenic. Not less than 100 kg of bronzes have been discovered. According to Shimada's investigations copper has been smelted in Huaca del Pueblo (Batán Grande). The technological concept is based on simple pit furnaces with linear working ditches in front of them. It seems likely that arsenical bronzes were manufactured finally into tool-shaped ingots (Mayer 1998) before they were traded to other areas. Northern Peru has delivered a large quantity of distinct metal types. It is obvious that centres such

as Batán Grande were directly linked with such metal series during the Late Intermediate period (Chimú).

Another development can be noted in the southern parts of the Altiplano among Peru, Bolivia, and northwestern Argentina: González (1979) has concluded an extension of bronze metallurgy from northwestern Argentina towards the north from about 1000 AD onwards. Especially tin-bronze was used in northwest Argentina. But it never reached the importance of the ternary copper–arsenic–nickel alloys which were so successful during the Middle Horizon in the Tiwanaku culture of the Altiplano and on the north coast of Peru. Recent studies carried out by Lechtman and Macfarlane (Lechtman 1997, 2003; Lechtman and Macfarlane 2005, 2006) made clear that metallurgical centres such as San Pedro de Atacama (Lautaro Núñez 1999), Tiwanaku, or the Wari centre of Pikillacta have been supplied mainly by regional copper. This certainly has some consequences for our models in material exchange between the different cultural areas of the central Andes. Centres of metallurgy have developed their own technological traditions especially around the Titicaca lake and in northern Chile. Likewise this could be expected for the southern coastal areas of Peru as well: a gold metallurgy that was comparatively traditional and developed on a low level during the Paracas and the Nasca periods (Lothrop 1937; Root 1949). Natural gold alloys are dominant in regional metal assemblages.

A considerable increase of metal production only is notable beginning with the Ica phases (Late Intermediate period). The metallurgy of the south coast, especially of the Nasca period, remains enigmatic up to now. Although some slag-sites and remnants of copper metallurgy are known (Lechtman 1976), the smelting of complex sulphides or poly–metal copper ores could be expected even before the end of the Nasca culture (around 600 AD), but this certainly needs more detailed field work for a confirmation: only at a few sites have archaeological investigations been carried out such as in the Ica valley and the Paracas peninsula (Uhle 1913; Tello 1959; Tello, Mejía Xesspe 1979) and the Palpa region (Reindel 2004).

Considering pre-Columbian metal production, the gold objects have been intensively discussed. The focus was centred on technological aspects, and more recently also on the question of provenance. On the other hand, the primary production of gold and metals could be traced only with difficulty (Noack and Thiemer-Sachse 1991; Weisgerber 2006). In fact there are serious shortcomings regarding the investigation of primary production. This is due to the methods of winning of gold, that has been carried out as panning of alluvial sediments in most cases. It seems that mining of primary resources was of minor importance. But this is just a hypothesis at the moment.

In conclusion it is obvious that the southern coastal part of Peru, together with northern Chile and the southern Altiplano, can be seen as an independent metallurgical focus of the central Andean area. There is very little knowledge about metallurgical processes, however, especially before the late Ica/Chincha

period, when the number of metal objects increased in general. This certainly contradicts the situation on the northern coast, where metals have appeared in high quality and quantity since the Moche period.

23.2 Perspectives in Southern Peru

Important perspectives of mining archaeology and archaeometallurgy can be shown for southern Peru, especially for the Palpa and Nasca region. In this area a microregion has been investigated under several aspects including the climatic, geomorphological, and settlement history. Diachronic aspects not only help to reconstruct a historical development, they also bring us closer to ancient strategies using landscapes and resources (Reindel and Isla 1999; Reindel 2004; Eitel et al. 2005). The ecological impact of climate certainly played a decisive role in the procurement of raw materials and in subsistence strategy. Water supply especially was a problem both under very dry climatic conditions and under high population density, as we can conclude from the evidence regarding the Late Intermediate period in the Palpa valleys.

It is interesting to consider the gold items found in Paracas and Nasca graveyards dating as early as the Early Horizon: few gold findings have been reported from scientific excavations (Root 1949). Undoubtedly gold objects normally were made of sheet-gold often decorated by embossing. As joining techniques, welding and most likely soldering were known. Casting was still unknown and this is one major difference from the metallurgy of northern Peru that was innovative during this time, that is, Moche and Vicús cultures (Schlosser et al. this volume).

Although the state of research is insufficient, there are southern Peruvian gold objects that allow some conclusions. Seemingly there was an increase in gold usage in general since the Early Intermediate Horizon, especially during the later Nasca culture: the objects became more elaborate and more massive in weight. This coincides with the appearance of gold in funeral contexts: small items and sheet-gold covered by textiles in mummy bundles are known from the earlier stage, such as Mollake Chico (Isla and Reindel 2006a,b). In the Early Nasca period the elite burials of Ica and Palpa, especially La Muña, exemplify the social transformation to a seemingly stratified society. Therefore it is not surprising that the trace element studies carried out by Schlosser and Pernicka on Paracas and Nasca gold objects indicate the usage of northern coastal gold but also of material from the south. It is a hypothesis at the moment, but it seems that regional gold was used only on a smaller scale at the beginning (Fig. 23.3). So it is self-evident to conclude an increase of metal production especially in the Nasca but even more in the following Middle Horizon or in the Late Intermediate period, when metal use did generally increase in the southern coastal area. Following such a scenario it was not unlikely to think of a mining

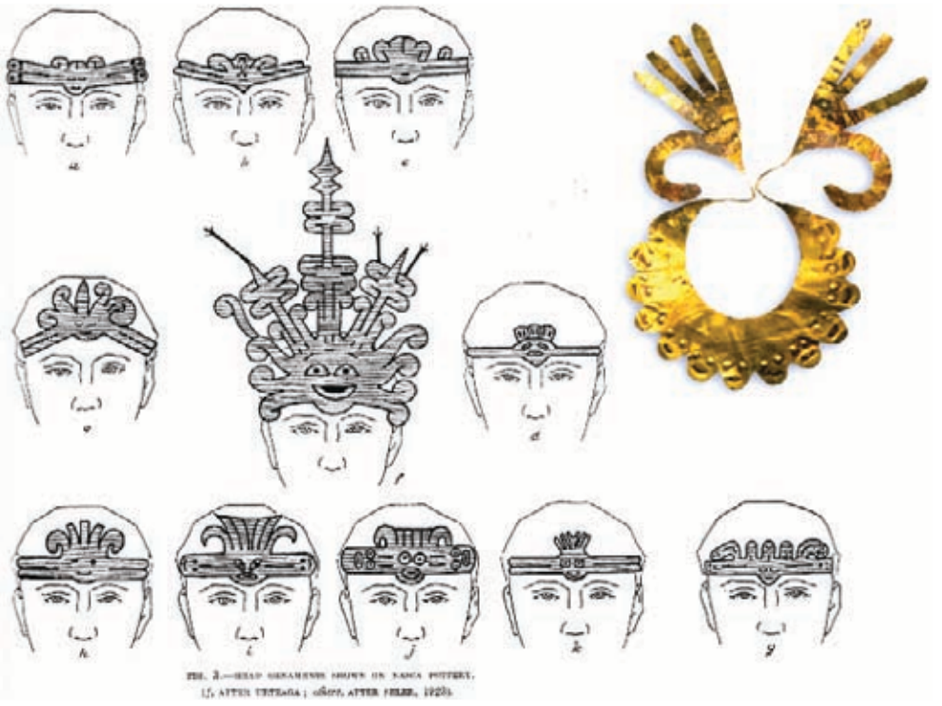

Fig. 23.3 Golden ornaments of the Nasca culture as found (so-called "mouth-mask") or indicated by pottery decorations. (After Lothrop 1937)

background when interpreting the settlement of Pinchango Alto which was occupied during the Late Intermediate period (1000–1450 AD) and located on an elevated ridge far away from actual water sources (Reindel 2005; Fig. 23.4).

Pinchango Alto is situated in a region of gold-bearing quartz veins, something that might have influenced the above interpretation. One argument was the occurrence of large milling stones (Spanish: *batanes*) that can be found in large quantities in Pinchango Alto and in the neighbouring settlement of Los Batanes (Fig. 23.5). Their purpose is not quite clear yet. They might have been used for fine-grinding of grains or minerals. At the moment it remains a

Fig. 23.4 One of the cellar pits furnished by a wall-lining at the settlement of Pinchango Alto, Late Intermediate period, 1200–1400 AD. (Photo: DBM, Th. Stöllner)

Fig. 23.5 The settlement of Los Batanes. Dry stone walls are enclosing the pitshaped "cellars"; on top large grinding stones (*batanes*) can be observed. (Photo: DBM, Th. Stöllner)

hypothesis whether they have been used for gold-bearing sands. Testing of sediments in shaftlike cellars – thought to be for the exploitation of alluvial gold-bearing sediments – have brought no indication yet. Perhaps the multitude of holes at the site can be interpreted as storage pits located beneath the houses of these settlements, keeping in mind that the settlements of Pinchango Alto and Los Batanes certainly had to be supplied from outside.

During the second half of the Late Intermediate period several hundred people must have settled there at the fringes of the fertile agricultural grounds in the valleys. Recent investigations of the Nasca–Palpa project have proved a considerable population growth and expansion of settlements during that time (see Reindel this volume). This certainly also increased the demand on metals and other mineral resources. Root (1949) mentioned this generally for southern Peru: "Some time about 1200 A.D., fairly large quantities of gold, silver, and copper became available to the inhabitants of the southern coast. . . . The source of this new spirit may have been the middle coast in the region of Lima."

In addition to gold we may consider colored stones and semi-precious stones, such as malachite, sodalith, or turquoise that could have been sought from such locations in the vicinity. Turquoise itself is extremely interesting as we can suppose deposits both in southern and northern Peru (Ruppert 1982). Artefacts of turquoise and even a source recently have been identified during the archaeological investigations in the Palpa area (U. Glasmacher, pers. comm.). It seems not unlikely to find a major source of turquoise in the area of southern Peru.

Considering again the possible gold exploitation we may start with the gold items of the Nasca chamber burial of La Muña (Reindel and Isla 2001; Isla this volume; Schlosser et al. this volume): Trace-element studies now prove the usage of regional gold sources of the Nasca–Ocoña formation. Even today gold is exploited by small-scale mining, the *mineros artesanales* (Schulz 2007; Stöllner and Reindel 2007). But there was no evidence for ancient mining. On

the invitation of Johny Isla and Markus Reindel the German Mining Museum Bochum started with a one-week survey in Spring 2006 to evaluate the regional potential for further research of pre-Columbian mining and raw material exploitation in southern Peru (Stöllner and Reindel 2007).

23.3 Mining Sites in the Palpa Region – Results of a First Evaluation

Considering the metal resources in southern Peru the main formations with gold or copper-bearing mineralisation are the "Batolito de la Costa" and the "Complejo Bella Union". The metal deposits consist of epithermal or hydrothermal veins oriented parallel to the western cordillera in most cases (Fig. 23.6). Host rocks are either Jurassic or Cretaceous volcanic or sedimentary–volcanic rocks. The copper deposits regularly also contain a smaller amount of noble metals, lead and zinc. Also native gold–silver fine disseminated in hydrothermal quartz veins are found: the whole metal ore district is designated as the Nasca–Ocoña belt.

We began a first visit of several days to clarify potential mining activities and also evaluate presumptions made by the archaeological research thus far. One of the research questions was whether mining and raw material procurement were the main reason for locating settlements in high elevations at considerable distance from the main settlement areas. As mentioned above, to date we have found no clear indication and prefer an interpretation based on general developments in settlement history of the region. High-altitude settlements such as Pinchango Alto and Los Batanes may also indicate a necessity for a settlement ground when intensive usage of valley grounds did not allow further extension of settlements there. Their well-protected position nevertheless may also indicate a need for fortification and defence.

Our first survey included sulphidic copper deposits in the neighbourhood, so it is not unlikely that such deposits had access from these settlements. There are abundant traces of old workings in different copper veins stretching alongside the Rio Grande valley and easily workable at the exposed slopes to the east. Even at the north of Los Batanes a polymetallic deposit is known that were mined in the second half of the twentieth century (Mina Pinchango). The main hydrothermal mineralisation stretches from northwest to southeast, thus crossing the mountain ridge. What can be seen today is just the modern mining that has started in the upper parts of the deposit which is presumably rich in malachite and iron oxides. An ore sample of the oxidic zone was analysed. It can be characterised as polymetallic with a clear copper content with 10–20% Cu. Regular mining with at least two working levels has been opened by following the vein in deeper parts. Whether the deposit was used in

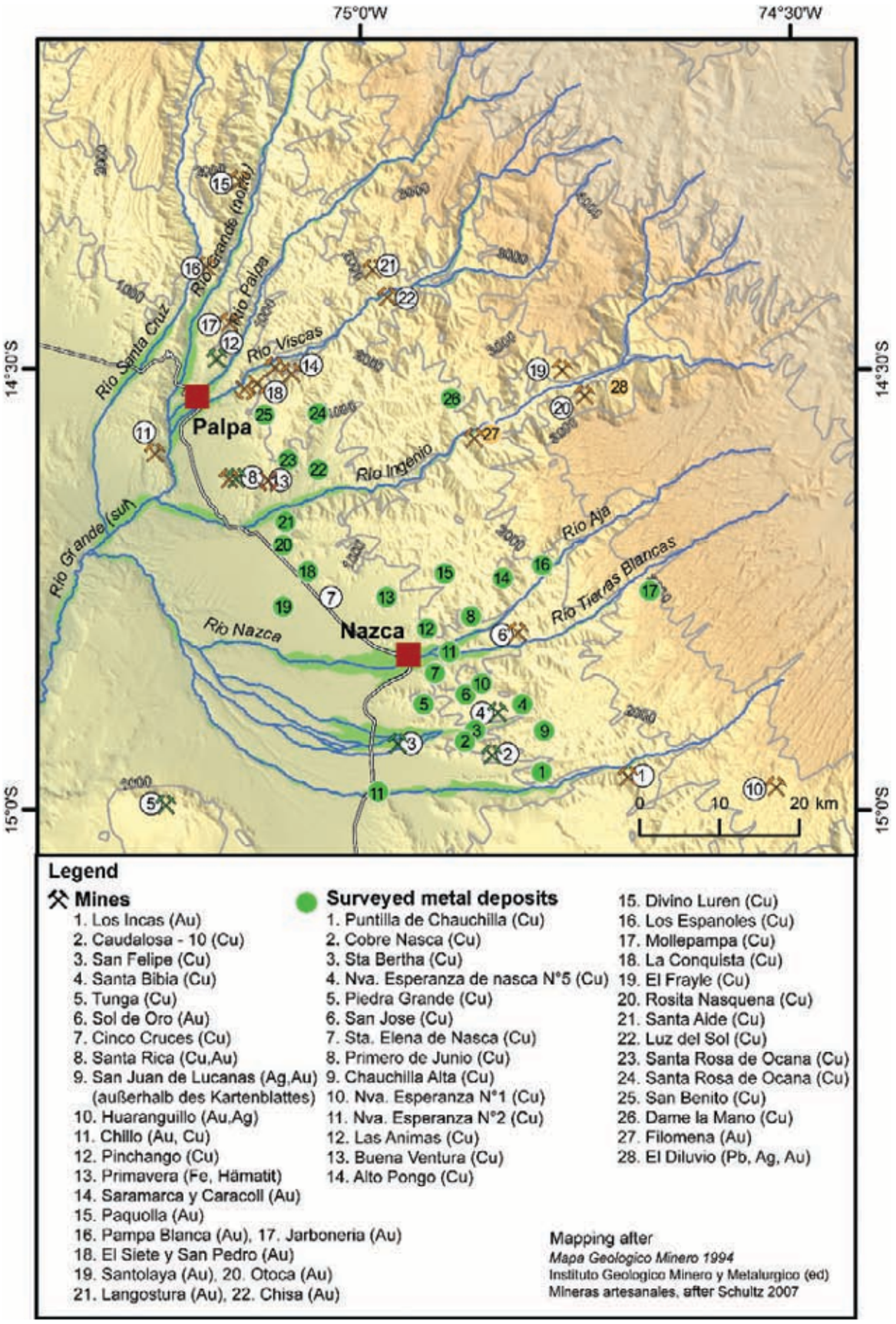

Fig. 23.6 The copper and gold deposits in the surroundings of Palpa and Nasca and their prehistoric and recent use. (Mapped after Montoya et al. 1994; Schulz 2007; Stöllner and Reindel 2007)

Fig. 23.7 The copper–gold mines near Chillo at the western slope above the Rio Grande valley; the outcrop of the mineralisation can be seen by the slightly declining entrances in front of huts of the *mineros artesanales*. (Photo: DBM, Th. Stöllner)

pre-Columbian periods is quite unproven yet. No traces have been found but they may have been destroyed by later mining.

This is also true for the ore deposits that were visited at the western slopes of the Rio Grande Valley near Chillo (Cerro Chillo and Cerro Muña; Fig. 23.7). These deposits are rich in pyrite and sulphides in the lower parts but also have quartz veins with gold and iron content in the upper parts. The deposits have recently been exploited by gleaning the older already exploited mining caverns and tunnels. Families are mining still-profitable smaller veinlets and even sulphidic parts of the deposits as they still contain certain amounts of gold. The complex ores nowadays are transported to the Rio Grande valley where centralized *plantas* treat them by cyanide leaching and mechanical beneficiation. As in Mina Pinchango there are also traces of copper oxides and carbonates in the upper part of the deposit so we can take them also into consideration when discussing the provenance of early copper in the southern coastal area.

The regional usage of copper is not beyond any reason: according to the older analyses of Root (1949) and Rovira (1990) obviously copper was used only seldom. Metals generally were dominated by natural gold and silver alloys and copper–gold tumbagas. Despite the abundance of copper–arsenic bronzes on the northern coast there only are few on the southern coast of Peru. Up to the Middle Horizon and even to the Late Intermediate period it is surprising how few bronzes were recorded.

The dominating metals of the southern coast are also gold or natural gold–silver alloys. Therefore the question has to be raised of whether these metals have been extracted from regional ore deposits. The Nasca–Ocoña formation, however, does cover several gold ore deposits of which Saramarca in the Viscas valley and Tulín in the neighbouring Ingenio valley are the most known and profitable ones. They are presently the target of small-scale mining

(Schulz 2007; Stöllner and Reindel 2007). *Mineros artesanales* are most interesting as they provide insight into production techniques of manual labour operations on small-scale mining. The winning and mining process can be compared with pre-Columbian operations regarding the different steps and even the conditions of work.

The mineralisation is embedded in Mesozoic andesites and granites. Gold occurs as native gold in quartz veins and is easily recognisable either in small nuggets (Fig. 23.8) or embedded in brownish hydro-oxides. Miners have told us they would normally win 5 g for each hauling vessel which they call a *lata* (filling weight about 25 kg). Such a concentration is absolutely on top of what can be expected when calculating an average of 200 g/t (Schultz 2007). One sample that we have collected at one of the mines rendered 8–16% of gold in a mechanically concentrated ore. According to previous investigations and a recently analysed sample the deposit is characterised by a considerable amount of silver that varies around 3:1 (Au:Ag; sample DBM 4326/06). If we look at commercially exploited mines such as the Mina Sol de Oro or the Mina Los Incas farther in the south, we have a gold relation of 1–6 g/t of mined material. The last example

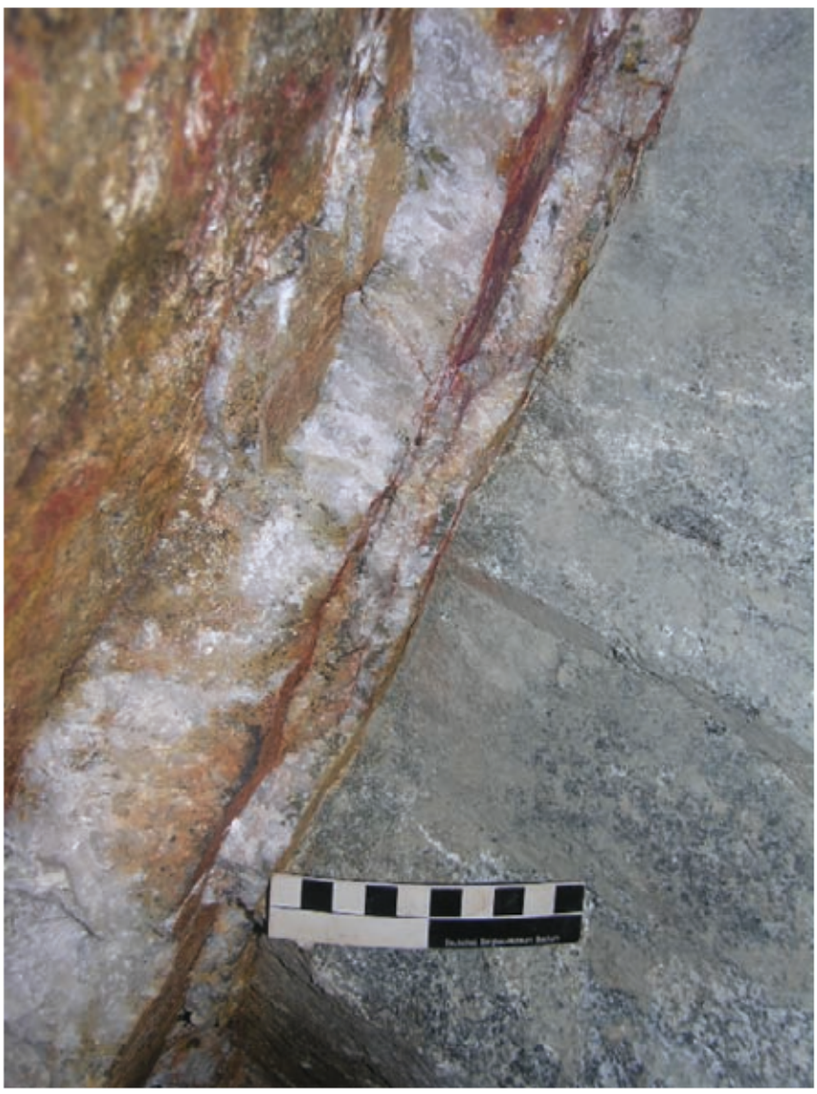

Fig. 23.8 A quartz vein with native gold (visible in the uppermost part of the lode) inside a mine near Saramarca in the Uscita Valley (quebrada of the Viscas valley). (Photo: DBM, Th. Stöllner)

Fig. 23.9 Saramarca in the Viscas valley: a *quimbalete* that has been sharpened at its bottom before getting reused. (Photo: DBM, Th. Stöllner)

certainly refers to a commercially extracted mine where the exploitation technique is less selective than the hand-worked mines from which we are reporting (Kuramoto 2001; Montoya et al. 1994). The selective exploitation especially easily explains the high production values that have been reported from the conquest period when an annual production of 1000 kg was not a rarity at all (Bargalló 1955).

The gold-bearing quartz sand is finally processed at a central location in the valley where traditional *quimbaletes* (Fig. 23.9) are used to mill the sand with water in order to concentrate the gold-bearing mixture. Finally mercury is added to produce pellets in order to win the gold by amalgamation. This technique, although it can be considered as traditional processing, is certainly not older than the conquest period. There is evidence for pre-Columbian cinnabar mines in the Andean region (Huancavelica: Salazar 1991; Burger and Matos 2002), but we have neither evidence for large milling plants with the use of quimbaletes nor there is any analytical evidence for mercury in gold thus far (Lechtman 1976; Rovira 1990). Cinnabar has been used as a dyeing pigment for the body and textiles. Garcilaso de la Vega, for instance, has reported that red cinnabar powder ("ichma") was allowed to be used for cosmetic purpose only by high-ranked women of royal families (Garcilaso de la Vega 1609).

Alluvial gold has not been reported thus far from the Nasca–Ocoña formation. The high dynamics of the river streams in that area prevented alluvial sedimentation since the Late Pleistocene. Older river terraces and alluvial fans could deliver such deposits. But to date no such deposit has been discovered and thus we have to conclude that even pre-Columbian gold mining was based on primary deposits. As Schlosser et al. (this volume) prove the usage of regional deposits it is highly likely that deposits such as in Saramarca and Tulin have been extracted in pre-Columbian times. It still has to be tested if sherd

assemblages, reported recently from that area, really belong to old mining sites (Schulz 2007). It is, however, important to note that the neighbouring Ingenio valley recently has produced the evidence for a pre-Columbian hematite mine. Although some of the opinions according to the dating and interpretation of the artefacts from that feature provoke contradiction, it is a first secure verification of a local mining tradition (Vaughn et al. 2007).

All of the small metal ore deposits are situated in Cretaceous rocks; often there are pyroclastic dacites and andesites, which are pervaded by younger, volcanic intrusive rocks of the upper Cretaceous (often also andesites and granites). This volcanism presumably has responsibility for the metallogenesis of many of the small ore deposits of the region. It can be observed easily by ore deposit mapping how dense copper and gold formations are interconnected or neighboured (Fig. 23.6). This is also true for the lead–silver deposits which occur more seldom than copper and gold ones (Montoya et al. 1994). Most of the occurrences having economic value can be found in those layers. It is obvious that they have been used in pre-Columbian times, as they are easily accessible from the river valleys. More geochemical data of metals and ore is certainly needed to establish such an assumption and understand their importance for the southern coastal cultural history in detail.

23.4 Conclusion and Future Prospect

Our short field survey could not generate direct evidence for ancient exploitation of copper and gold in the Palpa region. But it is clear by geochemical analyses carried out by Schlosser et al. (this volume) that regional metal resources certainly have been used at least during the Paracas and Nasca periods. This is not astonishing considering that the character of the regional gold deposits makes it highly likely that primary gold deposits have been extracted. Therefore one has a clear future prospect for doing systematic mining archaeology in this region, not only to find this evidence but also to understand the social and economic setting of such exploitation within the rather conservative coastal cultures of southern Peru. Similar to the river–oasis system of Ica we should expect at least for the Late Intermediate period a larger production of metals for a broader use in armory and agriculture. Lechtman (1976) was able to list a mining site as well as some pre-Hispanic smelting areas for the southern coast. But we are still lacking scientific and systematic research in cemeteries that may produce the data concerning the metallurgy in the region. Studies rendered by mining archaeology and raw material studies yield an important contribution to the social and economic history. The approach of mining archaeology may be especially productive in a well-defined settlement territory being investigated in such an exemplary way as in the Nasca–Palpa project. It may generally be asked if raw materials, especially metal, held a central role or if

they were just one of many products of this region that perhaps had been used only locally. Such a complex topic can only be followed in the future with the help of detailed provenance studies as well as intensive fieldwork.

Acknowledgments Many thanks to Dr. Markus Reindel of the KAAK (DAI) in Bonn and Johny Isla Cuadrado, Lima, who enabled the travel to Peru and helped us in manifold ways during our stay in Palpa, as well as Prof. Dr. Günther Wagner, Heidelberg, who familiarised us with the research questions and results of the regional geoarchaeology. We are grateful to the German Research Foundation (Dr. Dietrich Hahn, Frau Wera Bodemüller, project 444 PER-18/1/06) and the KAAK Bonn for financial support. During the stay in Peru we tragically lost our colleague Dr. Jan Cierny in the field by a cerebral apoplexy (see T. Stöllner, Dr. Jan Cierny verstorben. *Der Anschnitt* 58/3, 2006: 149–151).

Many thanks to Dr. Michael Prange, DBM, for analyzing and discussing the results of Mina Pinchango and to Pablo Segura, who skilfully processed sand and gravel from several sites to test the occurrence of gold.

Chapter 24
Fingerprints in Gold

Sandra Schlosser, Robert Kovacs, Ernst Pernicka, Detlef Günther and Michael Tellenbach

Abstract According to present knowledge the general use of metallurgy began with the production of gold ornaments that flourished in the Chavín culture of northern Peru in the first half of the first millennium B.C. In the same period metal began to be worked in the Paracas culture on the Peruvian south coast. In order to determine the provenance of the gold, 169 archaeological finds (including looted objects) of the Chavín, Paracas and Nasca cultures and 68 gold deposits were sampled in Peru to perform elemental analysis using LA-ICP-MS. This technique has already been applied for gold provenance studies, but the methodology was further developed involving liquid calibration and solid calibration using new solid gold reference materials. First results show a clear difference between north Peruvian gold objects generally very rich in platinum metals and objects from the south coast with low PGE concentrations. In both cultures, Paracas and Nasca, at least two gold types could be identified, of which the most frequent one seems to represent the local gold available in the Ica-Nasca region. Moreover, the presence of north Peruvian gold is attested in a Paracas gold sheet and a late Nasca head ornament that are chemically similar to objects from the north coast, e.g. from sites such as Morro Eten or Virú. Furthermore new results on alloying with copper and surface gilding at this early stage of metallurgy in south Peru were obtained.

24.1 Introduction

The search for the provenance of archäological materials, especially of ceramics or metals, has long played an important role in archaeological investigations worldwide (Wilson and Pollard 2001). Trace element patterns have been

S. Schlosser (✉)
Curt-Engelhorn-Zentrum Archaeometrie (CEZA) Mannheim, An-Institut der Universität Tübingen, D6, 3, 68159 Mannheim, Germany
e-mail: sandra.schlosser@cez-archaeometrie.de

M. Reindel, G.A. Wagner (eds.), *New Technologies for Archaeology*, Natural Science in Archaeology, DOI 10.1007/978-3-540-87438-6_24,
© Springer-Verlag Berlin Heidelberg 2009

successfully applied to link artefacts with workshops (e.g. for pottery) or natural occurrences of the raw materials (e.g. obsidian). In metal artefacts the trace element patterns are usually more difficult to interpret, because they can be substantially changed during the production process. However, combined with another geochemical fingerprint, for example the isotope ratios of lead, it has become possible to relate copper artefacts to certain ore deposits (Pernicka 1999). At first sight, gold artefacts should be traceable, as gold mostly occurs as a metal in nature. Thus, it could be assumed that the difference in element composition between an ore deposit and a finished artefact is rather low. This, however, is not the case for two reasons. In most cases gold is melted for the fabrication of an artefact, because alluvial gold usually occurs in small grains. It has been shown that this process removes elements that are often significant markers of an ore deposit (e.g. tellurium; Hauptmann et al. 1995). Furthermore, natural gold is rather pure and – with the exception of silver – the concentrations of trace elements are low. Therefore, sensitive analytical techniques are required for trace and ultratrace element analysis. Low sample consumption and minimum sample destruction are further prerequisites for precious gold objects.

Until now, the majority of analyses of prehistoric gold artefacts, running into several thousands, have been performed using atomic emission spectroscopy (Hartmann 1970, 1982). The results have shown that the artefacts can be grouped according to their silver, copper, and platinum concentration. Moreover these groups show significant distributions in time and space. However, the discrimination power between different groups was low and it seemed desirable to obtain a more detailed fingerprint for discrimination. With the introduction of ICP-MS (inductively coupled plasma mass spectrometry) a more sensitive method has become available for the analysis of gold and coupled to laser ablation (LA) quasi-non-destructive direct solid analysis has become available for a wide variety of solid materials (Günther and Hattendorf 2005).

Atmospheric pressure inductively coupled plasmas have been effectively used in atomic emission (AES) and mass spectrometry (MS) for multielement analysis of traces. Advantages of ICP-MS such as high sensitivity, low detection limits, isotopic information, wide linear dynamic range, robustness, and computer-based data processing have made ICP-MS the most widespread and powerful technique which has been and is successfully utilised for trace, ultratrace, and isotope analysis in manifold applications (Date and Jarvis 1989; Houk 1994; Barnes 1996). Laser ablation (LA) sampling has become one of the most versatile solid sampling techniques for ICP-MS (Günther and Hattendorf 2005). The major advantages of LA-ICP-MS are the low efforts for sample preparation, no contamination of the samples from solvents and acids, less interferences owing to the absence of solvents, available elemental and isotopic information, low backgrounds, low detection limits, high sensitivity, and fast data acquisition.

Current limitations of the technique can be attributed to the lack of solid standard reference materials, elemental fractionation (Fryer et al. 1995; Longerich et al. 1996a) and matrix effects (Kroslakova and Günther 2007). However, with improved understanding of the fundamental characteristics of LA-ICP-MS, a variety of strategies for precise and accurate quantitative analyses has been developed and further improved the technique (Halicz and Günther 2004). When performing laser ablation on a solid sample, sufficient energy in the form of a focused or imaged laser beam is directed onto the sample, which is placed within an ablation cell. Material from the surface is ablated and the resulting aerosol, which consists of solid particles, is transported into the plasma by means of a carrier gas (He, Ar) via a transport tube. In the atmospheric pressure plasma the solid aerosol particles are vaporised, atomised, and ionised owing to the high temperature. The generated ions are then transferred through the interface to the mass analyser, which operates at high vacuum. After the mass per charge separation the ions are detected by an electron multiplier, which transforms ions to signals that are recorded by the instrument software.

A large number of successful studies performed in many fields of applications show the interest in LA-ICP-MS (Günther and Hattendorf 2005; Durrant 1999; Günther et al. 1999). The great potential of this technique owing to the high spatial resolution sampling (LA) and the high sensitivity (ICP-MS) has been demonstrated on gold samples (Watling et al. 1994), which proved the concept of trace element fingerprinting and has been applied in many archaeological studies (Taylor et al. 1995; Gondonneau et al. 1996; Outridge et al. 1998). The limitations in quantification have been reported to be linked to the lack of homogeneous solid standard reference materials. Therefore, solution calibration of LA-ICP-MS has been extensively studied and reported to be an alternative calibration method (Günther et al. 1997; Leach et al. 1999; Pickhardt et al. 2000; Halicz and Günther 2004). Solution calibration of LA-ICP-MS has also been reported for analysis of Au–Ag–Cu alloy-based Celtic gold coins (Bendall 2003). However, difficulties concerning the stability of elements in the calibration solutions over time and the limits in the linear dynamic range for gold have been discussed (Bendall 2003).

The aim of this study focused on the development of a method for the determination of major, minor, and trace elements in gold artefacts using LA-ICP-MS. Therefore, two different calibration strategies using liquid calibration and solid reference materials were tested and compared. Furthermore, quantitative analysis of gold objects was carried out and focused on the investigation of early metallurgy in Peru, which is characterised by a high fraction of gold artefacts. Because Peru is rich in gold deposits of various genetic types that may be differentiated by their trace element patterns, this seemed to be a suitable region for a thorough archaeometallurgical study on the provenance of ancient gold.

24.2 Nasca and Early Metallurgy in the Central Andes – Archaeological Introduction

The metallurgy at Nasca cannot be examined without taking into consideration the whole cultural and technological development in the central Andes. With the words of the eminent americanist Alfred Kroeber: 'I should observe first that I regard all native Peruvian civilisation as a unit – a larger historical whole, a major areal culture with time depth.' (Kroeber 1944) Studying Nasca metallurgy as an isolated phenomenon would be just as meaningless, for example, as to deal with Elamitic metallurgy without considering the overall development in Mesopotamia. The central Andean area is, in spite of being subdivided into over 70 valley oases (Rowe 1960a,b), countless mountain valleys and basins, as well as Puna plains, a uniform cultural area which is tightly interconnected. This is especially evident when one considers the cultural development within the three different culture areas: the central and south-central Andes from the 'Circum Titicaca' region to northern Peru, the northern Andes with Ecuador up to the frontier of Colombia, and the south Andean culture area including Chile to the Maulé river and northwest Argentina on the other (Lumbreras 1981).

Common to all these areas is their integration into Tahuantinsuyu, the realm of the Incas. However, in the preceding periods it is extremely difficult to correlate the cultural development of these cultural areas, because there is no corresponding evidence. For example, there has hardly been any cultural import identified in Ecuador which can definitely be attributed to the central Andean area of pre-Inca times.

On the other hand, interregional contacts are evident in the central and south-central Andean regions. We all know the principal deity of the Tiahuanaco culture which can be seen at the famous sun-gate of the eponymic eighth century site (Ponce Sangines 1980). We also know that representations of this god already appear on large textiles, probably wall hangings, such as those found at Carhua in the Ica Valley (Cordy-Collins 1966). The typological relation of these representations with the relief-carving on the so-called Raimondi stela from Chavín de Huántar, the deity with the staffs, is obvious (Rowe 1967a,b). Vessels from Huari–Tiahuanaco times found at Conchopata, Huari, Ayacucho (Cook 1987), and in Pacheco, Nasca show representations of the same deity (Menzel 1964, 1968). These and countless other iconographic examples overwhelmingly prove transregional contacts and cultural uniformity of the central Andean traditions up to the innermost part of culture, the religious sphere. The individual valley oases are only components of a larger unit. This must not be overlooked when we deal with the analysis of the development of settlement patterns, technologies, division of labor, and so on in a valley oasis, because any component would remain unintelligible without the general context.

The peculiar conformity of the central Andean historical region with its varied natural areas has been a preoccupation of investigators for a long time:

Pulgar Vidal distinguished eight climatic zones (Pulgar Vidal 1946), Tosi later defined ten living areas (Tosi 1960), and Carl Troll even defined twelve different landscapes (Troll 1931). Already Eduard Seler had described the varied cultural expressions of the central Andes as '*Kulturgemeinschaft*' (cultural community, Seler 1912). Valid even now is Wendell Bennett's characterisation of the 'Peruvian Co-Tradition', a concept he brought up in 1948 (Bennett 1948): the diachronic unity of a civilisation with common traits with certain cultivated plants and techniques of agriculture, a homogeneous dress code, specialised techniques of craft and trade, a common corpus of motives, massive as well as monumental architecture for sacred and public purposes, organisation of collective work within the framework of supraregional administrative and political units, ancestor worship and marked burial orientation (Bennett (1948) calls it 'necrotropic orientation'), supraregional pilgrim centers, and scenes of oracles. Furthermore, he mentions the overall parallel cultural development and the regional horizon styles.

Bennett refers to the fact that the clearly marked natural pockets conducive to settlement which comprise an area of roughly 2000 km^2 are sufficiently separated from one another to allow for individual developments and still located closely enough in order not to fall through the meshes of the interconnecting system. Finally, he shows the clearly defined natural borders of the 'Peruvian Co-Tradition' which he established. This tradition corresponds in the north with the climatic frontier which is reinforced by areas inappropriate for settlements in the mountains between the Cajamarca basin and Loja as well as on the coast between the Piura oasis and the subtropical coastal areas of Manabí and Guayas. In the east the highlands give way to the Amazon lowlands which also constitute a clear climatic frontier. In the south a wide desert belt from the Atacama to Poopo forms a border to the south Andean area of northwestern Argentina and Chile.

To understand the development of metallurgy in a valley oasis such as Nasca is only possible against the background of the Peruvian co-tradition thus defined corresponding to the central Andean region as a whole. Our general picture of the development of Peruvian metallurgy has not changed substantially since the résumés of William C. Root for the south coast of Peru and Samuel K. Lothrop for the north coast (Root 1949; Lothrop 1951). Based on their analysis André Emerich compiled an overall view of Andean metallurgy in the sixties (Emmerich 1965). In the northern part of the central Andes the manufacture of gold emerges in the early first millennium BC without known antecedents. It concerns a relatively simple gold metallurgy: the gold was worked to sheets which in turn were cut and, according to demand, provided with chasing decoration or fashioned with surface reliefs by champlevé or embossing techniques. To this has to be added soldering as well as working silver, apparently unprocessed silver, in late Chavín times. In this way hollow figures or pearls could be assembled from two hammered components, however, they could not be gilded nor silver-plated, neither founded in open

or closed forms, nor was it possible to produce alloys or to smelt metals such as copper, tin, or lead.

In the succeeding period, the so-called Early Intermediate Period in the first half of the first millennium BC, a complex form of metallurgy emerges spreading over the whole area from Piura in the north to the Lima area of the central coast of Peru and comprising nearly all those techniques and metallurgical knowledge which were prevalent among the ancient cultures of Peru before the advent of the Spaniards: gold–copper–silver alloys, casting in closed forms, and two-mold casting as well as a whole range of different techniques of depletion gilding and silver-plating, electrochemical replacement, fusion gilding, and foil gilding. Only bronze alloys had not yet emerged in this highly developed metallurgy complex.

In fact, as far as the Nasca culture is concerned, we are facing a peculiar situation: from the actually published evidence it must be concluded that during the Early Intermediate, all these new techniques were completely unknown in the Nasca valley; in the Nasca style there appear almost only gold-sheet products: forehead and mouth masks, nose pendants, feathers, belts, cut-out figures for application to textiles, and hollow pearls made from two hammered halfspheres. Technique and material are identical to those found at Chavín from the first millennium BC. An explanation could be that the metallurgy of Nasca is completely rooted in the Paracas tradition which in turn is identical with that of Chavín, inasmuch as Paracas is related to the Chavín tradition not only in metallurgy. It follows that the connection between Nasca and the Chavín tradition of the central Andean region must be studied intensively, the more so because examples of gold metallurgy have also been found in some connection with the Chavín tradition in the intermediate area between the northern central Andes and the region of the Paracas–Nasca tradition.

The view on these far-reaching connections is also called for because the Peruvian co-tradition also comprises a completely different metallurgical tradition which, for various reasons, should be in closer connection with the traditions of the Nasca valley. This tradition originated in the southern highlands around Lake Titicaca and was spread over a large area in the southern Andes. Supposedly, during the later second millennium BC – that is, already before the emergence of gold metallurgy in Chavín – there grew up in this area a complex copper metallurgy (Ponce Sangines 1970) radiating even to the area of the central Peruvian coast where corresponding finds have been made. Thus, Thomas Patterson, for instance, has made a remarkable discovery at the Early Horizon period site of Malpaso in the Lurín valley which dates from the early first millennium BC: a pearl made from a copper–silver alloy with a metal ratio of 41–45%. This must imply a deliberate alloy because natural silver contains only 18% copper at the most (Lechtman 1978). The surface of the pearl reveals enrichment in silver. Another collection of even cast copper findings was also discovered at Tablada de Lurín on the central coast of Peru: associated organic material has been dated by ^{14}C-dates of to the first millenium BC (Lechtman 1978).

The apparent lack of copper metallurgy at Nasca is remarkable for various reasons, for this metallurgy originated in the southern highlands. First, it is to be remembered that the southern highlands are actually located not only geographically but also culturally much closer to Nasca than the northern central Andes. Especially here in the south of the central Andes there are traditionally close connections between the highlands and the coast. Those connections should really be much more influential than contacts along the coast in a northern and a southern direction, for they are a principal requirement for the procurement of foodstuffs as shown by John Murra in his classical paper about the vertical integration of the '*pisos ecológicos*'. After all, one of the classical examples for this is the exclaves of the Colla tribe of the Lupaca on the shores of Lake Titicaca who, in order to grow cotton and corn in the coastal valleys south of Nasca (Moquegua, Llabaya, Sama, and Arica) maintained exclaves even during colonial times (Polo de Ondegardo 1571).

The wide-ranging examination of metallurgy and thus the origin of the gold of Nasca will shed light on the cultural development there in the context of the central Andean culture. The question is, which role Nasca plays. Is Nasca a dynamic centre of new techniques, a centre in the interaction of the copper metallurgy of the southern highlands and the gold metallurgy of the great valley oases and the highland basins of the north? How can the contrast between the apparently archaic Nasca gold-sheet metallurgy and the contemporary highly developed metallurgy of the central coast be explained? Has Nasca preserved an archaic technology of the Chavín period for gold working over hundreds of years, for the manufacturing of artefacts in the style of Nasca, without a relevant cultural exchange between the highlands in the south and the neighboring oases of the central coast further to the north?

Such questions are decisive for the understanding of Nasca and its role and importance in the cultural development in the central Andes. If we want to answer them, it will first be necessary to clarify whether Nasca really was as closely connected with the Chavín tradition as to be assumed at first glance. This is only possible with archaeometric methods that allow the extraction of information unavailable to the naked eye, for example, concerning the provenance of the gold.

24.3 Paracas and Nasca Metallurgy

In the Paracas culture of the first millennium BC metal is often found in mummy bundles where it was placed in different layers of the textiles as offering. All objects are small and very thin gold sheets (usually 0.04–0.06 mm) of simple shape, often crudely cut and of reddish colour owing to the typical patina formation in a desert environment (Frantz and Schorsch 1990). The technology was simple and the decoration technique is limited to soft embossing (Carcedo 1998). Early analyses (Root 1949; Marshall 1964) indicated that two

gold types, a silver-rich (approx. 20%) and a silver-poor (up to 5%), are present. Native copper was available and alloys containing up to 30% copper (estimated from specific gravity and microstructure; Marshall 1964) have been produced. This probably led to a contamination with copper, that is, low contents below 5% without any effect on colour or melting temperature, in some objects. Natural gold rarely contains more than 0.5% copper (Boyle 1979), which suggests that copper was added to gold either intentionally or derives from copper and gold in the same workshop, for example, a crucible used for melting copper could have been reused for gold (Vavelidis and Andreou 2008). For the addition of silver there is no indication yet.

The metallurgy of the Nasca culture is relatively simple compared to the contemporary cultures in the north (Vicús and Moche), where metal became one of the most important media for cultural expression. Generally, there are few Nasca gold objects known from archaeological excavations. Most of them derive from looted graves enhancing the risk that fakes are included. The most common type of gold ornament is the nose ornament or mouth mask with side appendices in the form of serpents or hummingbirds, often also represented in paintings on Nasca pottery.

In continuity of the Paracas traditions, objects were made solely of sheet metal, while casting was still absent. The sheet metal is thicker than in Paracas objects, the pieces are larger, and the decoration technique consists of more elaborate embossings. Bonding techniques have not been studied in detail yet, although it is assumed that soldering and/or welding was known, but only applied for a few smaller and exceptional objects composed of more parts (e.g., Nasca warrior, Fig. 24.1). The bonding technique applied to assemble the Nasca warrior has not been investigated yet. It has been proposed that either welding or soldering was used for two similar Nasca miniature trophy heads (Ica valley; Lechtman 1988). Typological analogies can be found in the contemporary Moche culture in north Peru (Donnan 1992), where similar small warrior figurines were cast in the lost wax technique.

Since the Paracas period, the use of copper seems to have increased, as Root (1949) found up to 10% and Marshall (1964) estimated up to 40% copper in Nasca objects from secure contexts. The division of gold artefacts into a silver-poor and silver-rich group (Root 1949) is still the case. Recent finds from La Muña in the Palpa valley (Reindel et al. 2002) indicate that the variety of the applied metals has increased: a necklace mainly consisting of turquoise and stone beads not contained four gold beads, but also six ones made of silver.

The metallurgical practices of the Paracas and Nasca cultures do not imply an extensive technological exchange with other regions, which would suggest that the material used was also of local or regional origin. In the coastal gold–quartz veins of the Nasca–Ica region many small-scale gold mines are in operation that contribute substantially to the Peruvian annual gold production (Schulz 2007). However, evidence for early mining has not been found up to now.

Fig. 24.1 Nasca warrior figurine (EbN15027). Height 5 cm. (Museum zu Allerheiligen Schaffhausen, Ebnöther Collection)

24.4 A Pilot Study on the Origin of Ancient Peruvian Gold

24.4.1 Collection of Gold Artefacts and Deposits for Investigation

This study is part of a larger project on the origin of the earliest Peruvian gold finds, which is the subject of a dissertation. The focus is on the earliest and technologically simplest gold artefacts from Peru, mainly deriving from the Chavín, Cupisnique or Paracas and Nasca cultures (Table 24.1). In this period it can safely be assumed that alloying, recycling and mixing were not practised or at least important for our purpose, because these objects were separated from a possible metal cycle very early. This is important, because mixing would adversely affect the trace element fingerprint of the gold. Some objects of the Frías, Virú, and Moche cultures have also been included in the study. The artefacts which are being analysed derive mainly from archaeological excavations, but also from unknown origin. In the latter case the objects are assigned to certain cultures only typologically. Unfortunately, there are few artefacts available from secure contexts for comparison.

Although the initial plan was to loan objects for analysis, it was decided to analyse small samples (scalpel scrapings or cuts of about 1 mg) in most cases for two reasons. First, the open bottom ablation cell (Arrowsmith and Hughes

Table 24.1 Chronology of the Peruvian Archaeological Cultures Mentioned in the Text

Time	Period	Culture	
		South Coast	North
700 AD	Early Intermediate	Nasca	Moche
100 AD	Transition	Initial Nasca	Frías, Vicús, Virú
200 BC	Formative: Early	Paracas	Cupisnique
850 BC	Horizon		Chavín

1988) placed directly on the artefacts has to be mounted applying certain pressure, which is considered to cause stress on fragile objects. Second, the substantial administrative and financial effort for loan and transport of the Peruvian objects turned out to be prohibitive. A total of 169 samples from objects deriving mainly from the Cajamarca, Lambayeque, Nasca, and Paracas regions (Fig. 24.2) were collected.

Considering the size of the study area (present day Peru) and the occurrence of gold deposits of various scale, the intention was to collect deposit samples from the largest and most important gold regions (placers, vein type deposits) where natural gold was accessible to prehistoric man. This was accomplished mainly by collecting samples in the field, moreover, some samples were also obtained from mineralogical collections. A total of 68 samples of native gold were collected from places indicated in Fig. 24.2.

24.4.2 Analysed Objects and Samples

The analyses were carried out in two laboratories. At LAC (ETH Zurich) artefacts from one of the largest collections worldwide of Chavín gold objects were determined. The Ebnöther Collection, a private collection donated to the town museum of Schaffhausen, Museum zu Allerheiligen Schaffhausen, Switzerland (Ebnöther 1999) owns 36 objects that include crowns, pectorals, ear plugs, nose ornaments, and finger rings, which can typologically be assigned without doubt to the Chavín and Cupisnique styles. The numerous nose ornaments part of the Ebnöther Collection could be assigned by W. Alva to a site called Cerro Corbacho, Zaña valley, north Peru (Alva 1992). Alva (1986) had performed intensive research following the traces of grave looters and documenting the provenance of pieces published in the United States and Europe.

According to the size of the ablation cells (up to 6 cm in diameter) applied, 24 objects from the Ebnöther collection were analysed. Among them, a remarkable masterpiece of the Nasca metallurgy, the warrior figurine (EbN15027) shown in Fig. 24.1, consisting of 37 individual parts (of which 35 remain today) was also investigated. Furthermore, three geological gold samples from the Petersen Collection, Pontificia Universidad Catolica del Peru, Lima, were determined.

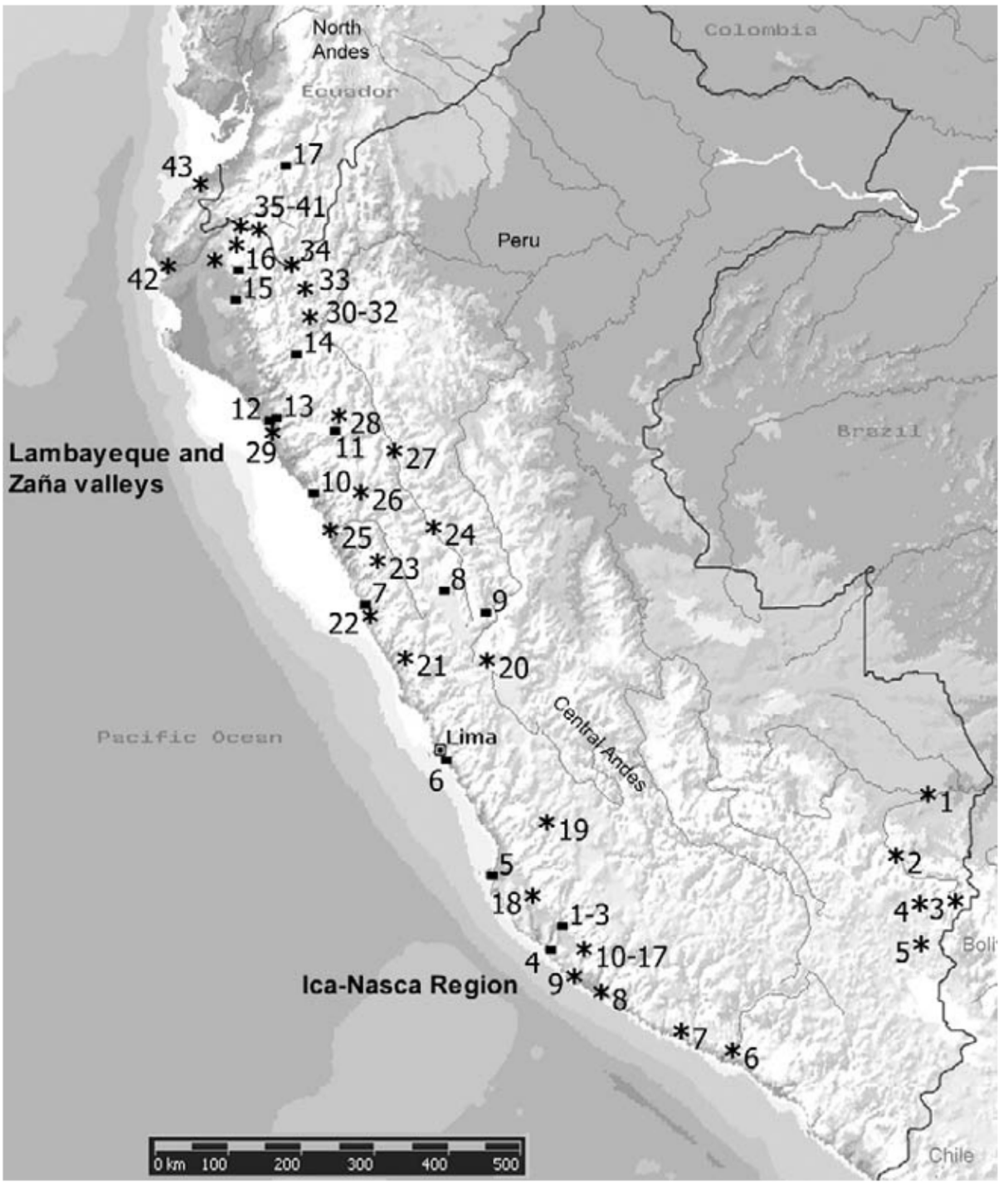

Fig. 24.2 Map showing the sampled archaeological sites (dots) and gold deposits (stars, from placers = 'Rio', others are occurrences of different genetic types). 1 – La Muña, 2 – Wayurí, 3 – Palpa; 4 – Montegrande; 5 – Paracas-Peninsula, 6 – Tablada de Lurín, 7 – Huarmey, 8 – Chavín de Huántar, 9 – Kotosh, 10 – Virú valley, 11 – Kuntur Wasi, 12 – Morro de Eten, 13 – Sipán, 14 – La Granja, 15 – Huaca Macanche, 16 – Cerro Ladrillo Blanco, Frías, 17 – Putushio, Ecuador.

1 – Rio Madre de Dios, 2 – Rio Inambari, 3 – Mina Anonieta, Inambari valley, 4 – Mina Santo Domingo, Limbani valley, 5 – Minas Ananea, 6 – Camaná valley, 7 – Rio Ocoña, 8 – Mina San Francisco 5, Chala valley, 9 – Mina Jaquí, Yauca valley, 10 – Mina Pallarniyocc, Acarí valley, 11 – Mina Otoca, Ingenio valley, 12 – Mina Caracol, Viscas valley, 13 – Mina Langostura, Viscas valley, 14 – Mina Chisa, Viscas valley, 15 – Minas La Muña, Rio Grande valley, 16 – Minas Chillo, Rio Grande valley, 17 – Rio Grande, 18 – Minas Pueblo Nuevo, Ica, 19 – Minas San Genaro, Huancavelica, 20 Minas Cerro de Pasco, 21 – Quebrada

The samples from Paracas and Nasca objects from the Museo Nacional de Antropología, Arqueología e Historia, Lima were analysed at CEZA, Mannheim. To obtain a first glimpse of samples from north Peru, samples from the Virú valley, Morro de Eten, and from Frías were investigated. In addition, gold deposits from four gold–quartz veins in the Ica–Nasca region (Viscas and Acarí valley) were analysed.

24.5 Experimental Part

24.5.1 Experimental Setup

At LAC (ETH Zurich) analyses of the gold artefacts were carried out using a solid-state Nd:YAG laser operating at 266 nm (LSX-500, CETAC Technologies, Omaha, NE, USA) coupled to an ELAN 6100 DRC+ and an ELAN DRC II quadrupole ICP-MS instrument (Perkin Elmer Sciex, Canada). At CEZA, Mannheim the analyses were carried out using a solid-state Nd:YAG laser operating at 213 nm (Microprobe II Laser Ablation System, integrated with LUV213 Laser, New Wave Research, USA) coupled to an XSeriesII quadrupole ICP-MS (Thermo Electron Corporation) with collision cell technology (CCT).

During analysis a 2% nitric acid blank was nebulised into the plasma to maintain stable wet plasma conditions. The laser-generated aerosol and the aerosol produced by the liquid sample introduction system (PFA nebuliser, 100 µl min^{-1}uptake rate, cyclonic spray chamber) were mixed using a glass Y-piece in front of the injector of the ICP. Prior to the analysis the ICP-MS was always optimised in terms of gas flows and RF power. Optimisation criteria were low background count rates, high sensitivity, low oxide, and doubly charged ion formation (based on $ThO^+/Th^+ < 8\%$ for the ablation of a glass standard reference material NIST 610). The operating conditions for the ICP-MS instruments and the laser ablation systems are summarised in Table 24.2.

Fig. 24.2 (continued) Orcon-Pacaybamba, 22 – Minas Pampa Matacaballo, Huarmey, 23 – Minas Pierina, 24 – Rio Marañón, Chuquibamba, 25 – Rio Santa, Pueblo Viejo, 26 – Rio Chuquicara or Rio Tablachaca, 27 – Minas Pataz, 28 – Minas Cajamarca, 29 – Morro de Eten, 30 – Rio Marañón, Bellavista, 31 – Rio Chinchipe, Guayaba, 32 – Rio Tamborapa, 33 – Rio Chinchipe, Zurunde, 34 – Rio Machete, Carmen de la Frontera, 35 – Quebrada Joras-Hualcarumi, 36 – Minas Cerro Sapillica, 37 – Minas Cerro Servilleta, 38 – Minas Cochescorral, 39 – Rio Macará, Hornillos, 40 – Mina Tambogrande, Piura, 41 – Rio Chira, Miramar, 42 – Rio Tumbes, Rica Playa

Table 24.2 Operating Conditions for ICP-MS and Laser Ablation Systems

ICP-MS	LAC ETH Zurich	LAC ETH Zurich	CEZA Mannheim
Instrument	PE ELAN 6100 DRC+	PE ELAN DRC II	Thermo XSeriesII
Nebuliser gas flow	0.6 L min^{-1}	0.7 L min^{-1}	0.69–0.7 L min^{-1}
Auxiliary gas flow	0.75 L min^{-1}	0.8 L min^{-1}	0.7 L min^{-1}
Plasma gas flow	17.5 L min^{-1}	17.5 L min^{-1}	13.0 L min^{-1}
Collision gas	–	–	6.0 mL min^{-1} H_2–He mixture (8% H_2, 92% He)
RF power	1350 W	1400 W	1200 W
Lens setting	Auto lens on	Auto lens on	L1 -1200; L2 -85.5; L3 -79.2; D1 -51.8; D2 -140; DA -65.1 V
Biases	–	–	slightly KED: Pole Bias -12.9, Hexapole Bias -13.0
Detector mode	Dual (pulse and analog counting mode)	Dual	Dual
Dwell time	10 ms	10 ms	10 ms
Scan mode	Peak hopping	Peak hopping	Peak hopping
Carrier gas flow	1.2 L min^{-1} He	1.0 L min^{-1} He	1.1 L min^{-1} He
Laser Ablation			
Laser ablation system	LSX-500, Nd:YAG, 266 nm		Microprobe II with LUV213, 213 nm
Pulse length	4 ns		4 ns
Ablation frequency	4 Hz		4 Hz
Spot size	50 µm		50 µm
Laser fluence	13 J cm^{-2}		24-30 J cm^{-2}

During measurements the Ag and Au signals were recorded in custom resolution mode to reduce the high signal intensities (Heinrich et al. 2003). Depending on the thickness of the samples, ablation was carried out in single-hole drilling or in line ablation mode (Table 24.3). For signal acquisition almost 50 isotopes were monitored and recorded to investigate the influence of potential matrix interferences (oxide, argid formation). The data acquisition started with the measurement of 30 s of the blank followed by a 40–60 s signal acquisition from a single crater ablation with preablation of approximately 5 s to eliminate surface contamination. Preablation was performed on all samples from objects but not on those of native gold, because of the limited thickness of the grains. The data reduction and the signal integration for the measurements obtained at LAC were carried out using the standard procedure described by Longerich et al. (1996b). At CEZA, Mannheim, the data evaluation was performed using the Plasmalab software (Thermo).

Table 24.3 Laser Operating Conditions for Line and Spot Ablation Mode used at the CEZA, Mannheim

	Preablation		Ablation	
	Line	Spot	Line	Spot
Duration	40–60 s	3 s	40–60 s	50 s
Length	500–900 μm	–	500–900 μm	–
Spot size	75 μm	75 μm	50 μm	50 μm
Energy (%)	40	40	100	100

For ^{111}Cd, ^{115}In, ^{125}Te correction factors were applied owing to interferences. The obtained results were then exported to Microsoft Excel and normalised to 100%.

24.5.2 Reagents, Calibration Solutions, and Solid Reference Materials

For this study two calibration methods were tested and compared. The matrix-matched solid calibration for the analysis of the gold artefacts was carried out using gold reference materials (NA1 and NA2), produced by Norddeutsche Affinerie AG, Hamburg, Germany. Because the composition of NA1 and NA2 was solely based on the analysis performed by the manufacturer, they were treated as samples and further validated. Most of the element concentration values were confirmed using solution and solid calibration (FAU7: NIST 8053, 8054, 8055, and FAU10: NIST 8062, 8063, 8064) techniques. Therefore the concentration protocol provided by the manufacturer was applied for the calculations.

The solution calibration was carried out using multielement calibration solutions. For the analyses performed at LAC (ETH Zurich) a blank solution of 2% nitric acid was prepared from subboiled nitric acid and ultra-high-purity water (Millipore). The liquid standard solutions were prepared from single-element solutions (MERCK, CPI International). Two solutions were prepared taking the chemical compatibility of the elements into account. The first solution contained those elements which were dissolved in nitric acid in the stock solution (Ag, As, Bi, Cd, Co, Cr, Cu, Fe, Ga, Hg, Mn, Mo, Ni, Pb, Pd, Se, Sn, Ti, Tl, U, V, W, and Zn). The second solution contained those elements which were dissolved in hydrochloric acid in the stock solution (Au, Cu, Ir, Pt, Rh, Ru, Sb, and Te). The concentration of Au, Ag, and Cu which were considered to be major elements in the gold samples was set to 1 μg g^{-1}. The concentration of the other (trace) elements was set to 100 ng g^{-1}. The dilution of the single-element solutions was performed with 2% nitric acid. The two solutions were used to avoid precipitation (e.g. AgCl) and new

solutions were prepared daily to overcome loss due to adsorption on the container walls (e.g. PGE, Sn, Sb).

At CEZA, Mannheim, three solutions were used: solutions 1 (V, Cr, Mn, Fe, Co, Ni, Cu, Zn, Ga, As, Se, Ag, Cd, In, Au, Tl, Pb, Bi, U) and 2 (Ti, V, Cr, Mn, Fe, Co, Ni, Cu, Zn, As, Se, Mo, Cd, Sb, Tl, Pb) were prepared from the ICP Multi Element Standard (MES) XVI and XXI (MERCK), diluted in nitric acid. To MES XXI, 1 ppm Ag was added, and 1 ppm Cu was added to all three solutions. The third solution (Cu, Rh, Pd, Sn, Te, W, Re, Ir, Pt, Au) was prepared from single-element standards by first preparing a stock solution in 7% HCl, which was always freshly diluted with nitric acid to 5% aqua regia, containing 1 $\mu g\ g^{-1}$ Cu and Au. The concentrations of the other elements were set to 50 $ng\ g^{-1}$ in all three solutions.

24.6 Results and Discussion

24.6.1 Applicability of Solution Calibration

The data acquisition sequence consisted of liquid standard solutions and solid reference material (NA2) twice prior to and after the analysis of the artefacts. The acquired signals of the major elements for many of the gold artefacts were mostly stable. However, spikes were often observed in the signals of trace elements. The calculation of the concentrations was performed using the 100% normalisation procedure (Leach and Hieftje 2000). As an example, a comparison between the two calibration strategies (liquid calibration and solid calibration using NA2: 5.45% Ag, 94.55% Au) for a selected gold object is shown in Table 24.4. The differences between the two calibration strategies were in the order of 10% for most of the elements. However, significant deviations were observed for Pt (approx. 40% overestimation) and Pb (approx. 30% underestimation) when using solid calibration (NA2). For both elements, the concentrations in the NA2 solid gold reference material as provided by the manufacturer were not confirmed. When calibration was performed using FAU7 and FAU10 gold standard reference materials as external standards against NA2, the deviation in the obtained concentrations were within 3% for both elements. However, this value was approximately 25% lower and 10% higher for Pt and Pb, respectively, in comparison to the concentration values stated by the manufacturer. This indicates that the obtained deviations are not caused by the solution calibration performed. Copper as a major element also showed approximately 10% deviation between the two calibration strategies. Further validation of the NA gold reference materials is needed and planned to perform more accurate analysis when using these solid gold reference materials. Liquid calibration was found to be applicable for the analysis of solid gold samples with LA-ICP-MS.

Table 24.4 Determined Element Concentrations ($n = 3$) for a Round Bead (EbN15032) Using Liquid and Solid Calibration (NA2)

		Cu wt%	Ag wt%	Au wt%	Ti ppm	Cr ppm	Mn ppm	Fe ppm	Co ppm	Ni ppm	Zn ppm
Liquid Calibration											
Seam	Average	3.1	24.37	72.4	*	*	3.62	182	*	*	26†
	SD	*0.5*	*0.16*	*0.7*	–	–	*0.25*	*22*	–	–	–
Hemisph. A	Average	3.20	24.0	72.7	1.1†	*	3.5	110	0.3†	*	24.4
	SD	*0.16*	*0.7*	*0.6*	–	–	*2.5*	*50*	–	–	*2.2*
Hemisph. B	Average	3.09	24.17	72.58	1.7†	*	3.5	130	0.137	*	17
	SD	*0.18*	*0.13*	*0.17*	–	–	*1.3*	*60*	*0.018*	–	*3*
Solid Calibration (NA2)											
Seam	Average	2.8	24.8	72.2	*	*	3.8	158	*	*	31.4
	SD	*0.3*	*0.4*	*0.8*	–	–	*0.3*	*20*	–	–	*0.6*
Hemisph. A	Average	2.77	23.7	73.4	*	*	3.6	100	0.3†	*	28
	SD	*0.17*	*0.7*	*0.7*	–	–	*2.5*	*50*	–	–	*3*
Hemisph. B	Average	2.59	23.11	74.22	*	*	3.3	100	0.125	*	21
	SD	*0.15*	*0.23*	*0.20*	–	–	*1.2*	*50*	*0.016*	–	*4*

Table 24.4 (continued)

		Cu wt%	Ag wt%	Au wt%	Ti ppm	Cr ppm	Mn ppm	Fe ppm	Co ppm	Ni ppm	Zn ppm
		As ppm	Se ppm	Pd ppm	Cd ppm	Sn ppm	Sb ppm	Te ppm	Pt ppm	Pb ppm	Bi ppm
Liquid Calibration											
Seam	Average	*	*	30	*	2.00	5.1	*	860	6.6	1.45
	SD	–	–	*4*	–	*0.22*	*0.7*	–	*170*	*2.1*	*0.09*
Hemisph. A	Average	*	*	31	0.3†	2.04	7.10	1.6†	910	6	1.8
	SD	–	–	*5*	–	*0.24*	*1.45*	–	*110*	*3*	*0.4*
Hemisph. B	Average	*	*	30	0.27	1.96	6.0	0.8†	820	10	1.60
	SD	–	–	*4*	*0.17*	*0.21*	*0.6*	–	*160*	*8*	*0.21*
Solid Calibration (NA2)											
Seam	Average	*	*	34	*	1.33	4.8	*	1270	4.6	1.11
	SD	–	–	*5*	–	*0.16*	*0.7*	–	*240*	*1.5*	*0.06*
Hemisph. A	Average	*	*	34	0.2†	1.31	6.36	1.5†	1300	4.3	1.4
	SD	–	–	*5*	–	*0.17*	*1.31*	–	*140*	*1.9*	*0.3*
Hemisph. B	Average	*	*	32	0.20	1.22	5.2	0.7†	1130	7	1.15
	SD	–	–	*4*	*0.13*	*0.14*	*0.5*	–	*230*	*5*	*0.16*

Sampling positions: seam and two hemispheres (three spots each).
* Values under limits of detection.
† Only one value was higher than the limits of detection.

24.6.2 Paracas and Nasca

The classification into a silver-rich (Ag/Au 0.5–0.7) and a silver-poor group (Ag/Au 0.04–0.3) in Paracas and Nasca objects reported earlier (Root 1949) could be confirmed for both cultures (Table 24.5). Only two sheet metal fragments (from Mejía Xesspe's excavation in Mollake in 1957; MA-080924 and MA-080963) contain slightly more silver than gold, which does not necessarily imply that it is an alloy, as both metals can be found in any relation in nature. Gold containing less than 10% silver (Ag/Au <0.1) has so far only been observed in Paracas and Nasca objects, but not in samples from the north.

Figure 24.3 shows a systematic compositional difference between the native gold samples and the Nasca and Paracas artefacts. Such a systematic difference in copper content was also observed for Bronze Age artefacts and natural gold in Europe (Schmiderer 2008).

In this case copper seems to have been added in substantial amounts of up to 26%. Therefore, the suggestion by Marshall (1964) that alloying was also practised in the Nasca culture could be confirmed at least in two cases: two axe-shaped adornments (Fig. 24.4) from Mejía Xesspe's excavation in Mollake (each belonging to a pair) contain 19 and 26% copper (MA-080940, MA-080939).

In this context it is interesting that the surfaces of both objects are yellowish and not reddish as the composition would suggest. This means that the surfaces were treated in a certain way to yield a golden appearance, a technological detail which has thus far not been observed in the Nasca culture. Which of the known pre-Columbian gilding techniques (depletion, fusion, electrochemical replacement, or foil gilding; see Carcedo 1998 for a summary) was used has yet to be investigated. As the samples are still available, polished sections will be prepared to examine the superficial gold layer in detail.

Four objects containing between 33 and 37% copper could be identified as fake and these were therefore not considered any further. There is no indication that such high copper content is preferentially found in gold with high silver content. This could be explained by an attempt to alter the colour of the alloy that becomes pale the more silver is present. It is not impossible that copper was added to increase the amount of metal altogether.

The second group of artefacts contains 2–10% copper. There is none with low copper concentration as in native gold. As suggested in the introduction, such low copper content could be present due to contamination in the workshop. However, it is also possible that even the low concentrations were intentionally achieved. The reason could be the substantial hardening effect of copper addition to a gold–silver alloy. Ancient gold artefacts need not always contain copper as was shown for objects from Central America where very low copper contents were observed besides gold–copper alloys (Schlosser 2004).

Another technological aspect of Nasca metallurgy concerns joining. The joints of the small warrior figurine (EbN15027) show a slightly higher copper concentration than the base metal. This indicates that a technique using copper

Table 24.5 Composition of Objects from the Paracas and Nasca Culture and some objects from north peru, Determined by LA-ICP-MS

Number	Object	Site/Analysed Part	Context	Culture/Style	Cu wt%	Ag wt%	Au wt%
MA-072992	Triangular ornamental sheet with steps	Cerro Ladrillo Blanco, Frías	Looted tomb	Frías	4	16	80
MA-080924	Sheet metal fragment	Mollake, Palpa valley	Mummy	Paracas/ Nasca	4	49	47
MA-080925	Sheet metal fragment	Nasca valley	Mummy	Paracas/ Nasca	7	3	91
MA-080926	Sheet metal fragment	Nasca valley	Mummy	Paracas/ Nasca	8	4	89
MA-080927	Sheet metal fragment	Montegrande	Survey	LIP	3	36	62
MA-080928	Sheet metal fragment	Montegrande	Survey	LIP	6	20	74
MA-080929	Fish-shaped bead	Wayurí, Santa Cruz valley	Tomb	Nasca	4	15	81
MA-080930	Head ornament	–	–	Paracas	3	6	92
MA-080931	Bird-shaped feather	–	–	Nasca	3	21	76
MA-080932	Head ornament	–	–	Nasca	6	17	77
MA-080933	Nose ornament	–	–	Nasca	6	13	81
MA-080936	Small tubular bead	Morro de Eten, Lambayeque	Tomb	Cupisnique	2	40	57
MA-080939	Axe-shaped adornment	Mollake, Palpa valley	Mummy	Nasca	19	11	69
MA-080940	Axe-shaped adornment with embossed figure	Mollake, Palpa valley	Mummy	Nasca 5	26	8	64
MA-080941	Trapezoidal sheet	Virú valley	Tomb	Virú	3	33	64
MA-080942	Birdlike ornament	–	–	“Nasca”	33	6	59
MA-080943	Birdlike ornament	–	–	“Nasca”	37	6	59
MA-080944	Birdlike ornament	–	–	“Nasca”	33	6	61
MA-080945	Birdlike ornament	–	–	“Nasca”	34	6	60
MA-080946	Tongue-shaped pendant	Virú valley	Tomb	Virú	2	30	68
MA-080947	Tongue-shaped pendant	Virú valley	Tomb	Virú	2	27	70

Table 24.5 (continued)

Number	Object	Site/Analysed Part	Context	Culture/Style	Cu wt%	Ag wt%	Au wt%
MA-080948	Tongue-shaped pendant	Virú valley	Tomb	Virú	2	26	72
MA-080949	Ornamental disc 2	–	–	Paracas/ Nasca	3	39	57
MA-080950	Ornamental disc 1	–	–	Paracas/ Nasca	2	40	59
MA-080951	Small disc 2	Nasca region	Mummy	Nasca	7	18	76
MA-080952	Small disc 1	Nasca region	Mummy	Nasca	6	18	76
MA-080953	Sheet metal fragment	Paracas-Peninsula	Mummy	Paracas	3	33	66
MA-080954	Sheet metal fragment	Paracas-Peninsula	Mummy	Paracas	10	4	86
MA-080956	Sheet metal fragment	Paracas-Peninsula	Mummy	Paracas	5	6	90
MA-080957	Sheet metal fragment	Paracas-Peninsula	Mummy	Paracas	5	6	89
MA-080963	Sheet metal fragment	Mollake, Palpa valley	Mummy	Paracas/ Nasca	5	49	46
EbN15027	Warrior figurine	Body	–	Nasca	6	11	83
EbN15027	Warrior figurine	Seam	–	Nasca	9	12	80

Parts of objects with significantly different composition are listed separately.
LIP = Late Intermediate Period.

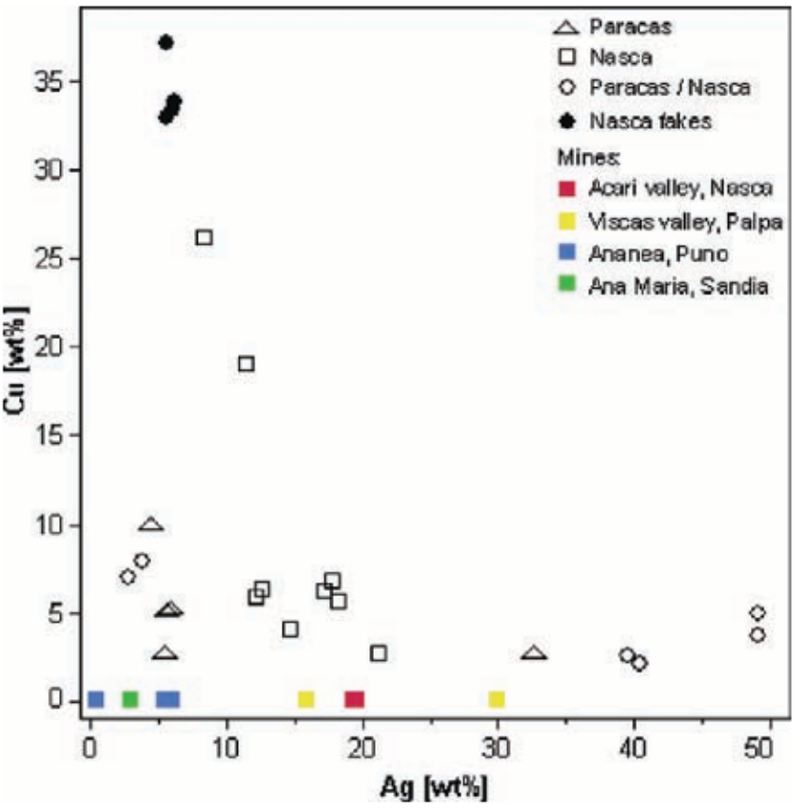

Fig. 24.3 Cu–Ag scatterplot for Paracas and Nasca samples (black and white symbols) in comparison to deposits (coloured squares)

Fig. 24.4 Axe-shaped adornment with embossed design (MA-080940, Orig. nr. M-3493, MNAAHP)

salts and some kind of glue (granulation/protobrazing; Griffin 1986) may have been used but no solder. In the Paracas objects the highest copper concentration found is 10% (MA-080954), which makes it difficult to decide whether it is an intentional alloy.

24.6.2.1 Gold Types Present in the Paracas and Nasca Cultures

The initial assumption that any alloying with copper would affect the trace element pattern of gold in a way that makes it unusable for this study requires a more differentiated view. The trace element pattern in gold with substantial amounts of copper was not different from gold containing only few percent copper. Even elements that are associated with copper, such as As, Ni, Pb or Sb, show no relation to the copper concentration in the Paracas and Nasca samples. Therefore it may be assumed that native or very pure copper was added to the gold, which did not affect its trace element fingerprint. This agrees with the observation made by Marshall (1964) that native copper was used in the Paracas period. Considering the abundance of copper in the so-called copper belt in the southern Andes it is not surprising that in ancient times native copper was available.

Figure 24.5 shows the Pt–Pd scatterplot also including the north Peruvian samples. A correlation between Pd and Pt can be seen, with the gold from the north having far higher concentrations than most of the southern samples. The latter split up into gold with low Pt and Pd, two objects with high-correlating Pt and Pd grouping with the northern samples, gold with high Pd and low Pt, and gold with Pd and Pt in almost equal concentration (the four fake objects).

For cluster and discriminant analysis the trace elements Ni, As, Rh, Pd, Sn, Sb, Os, Ir, Pt, Pb and Bi were selected. Cluster analysis was performed hierarchically using Ward's minimum variance method without standardisation to the standard deviations. The method applied for discriminant analysis was linear, using a common covariance matrix. Figure 24.6 shows a detail of the nine resulting clusters. Most of the southern samples are grouped into two clusters (not regarding the fake objects, cluster 4): Cluster 1 is generally characterised by very low concentrations of all trace elements, whereas cluster 5 shows higher Pt and Pb values. Paracas and Nasca objects are found in both groups, as well as silver-poor and silver-rich gold.

Four southern samples could not be assigned to these groups: one Paracas sample (MA-080957) due to very high Ni and the Nasca sample from Wayurí (MA-080929, cluster 6) due to high As and Sn contents. The two remaining samples group well with objects from the Virú valley, containing high platinum group element (PGE) concentrations, in this case Pt, Pd, Rh, Os and Ir.

This indicates that northern type gold is present in the Paracas and Nasca cultures. The respective objects are a sheet metal fragment found in a mummy bundle from the Paracas Peninsula (MA-080953) and a feather or pin for a headdress in bird shape (MA-080931) in late Nasca style.

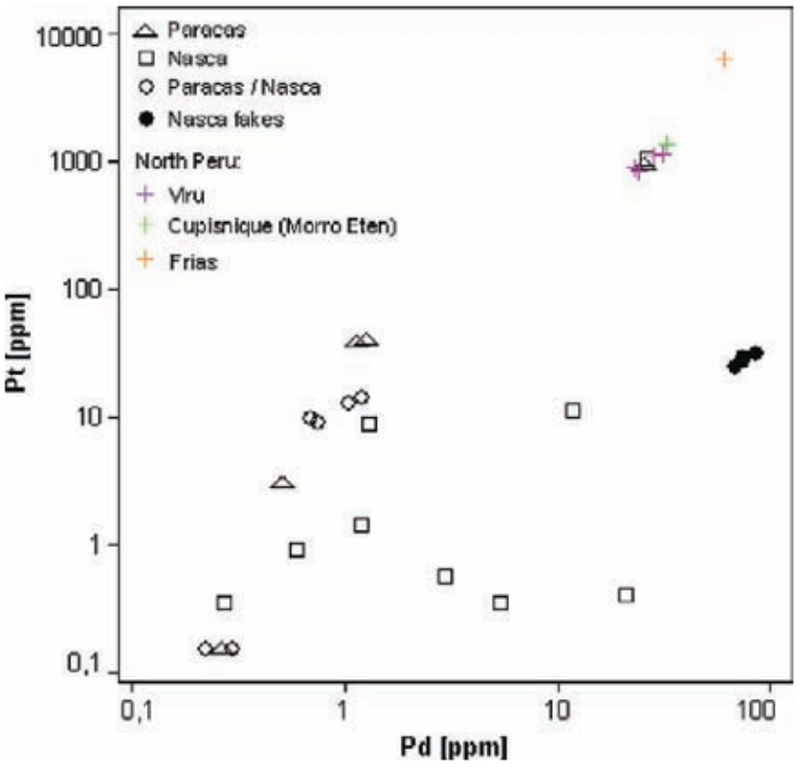

Fig. 24.5 Pt–Pd scatterplot for the Paracas and Nasca samples (black and white symbols) including the north Peruvian samples (coloured crosses) from Virú, Frías, and Morro Eten

24.6.2.2 Comparison with Local Gold Deposits

As shown in previous studies (Hauptmann et al. 1995; Schmiderer 2008), non-volatile elements, which are not affected by melting can be considered for comparison between artefacts and native gold. These comprise Ag, Rh, Pd, Pt, Ir, Ge, Ni, Os, Ru and Cu, although the latter is not useful because of the

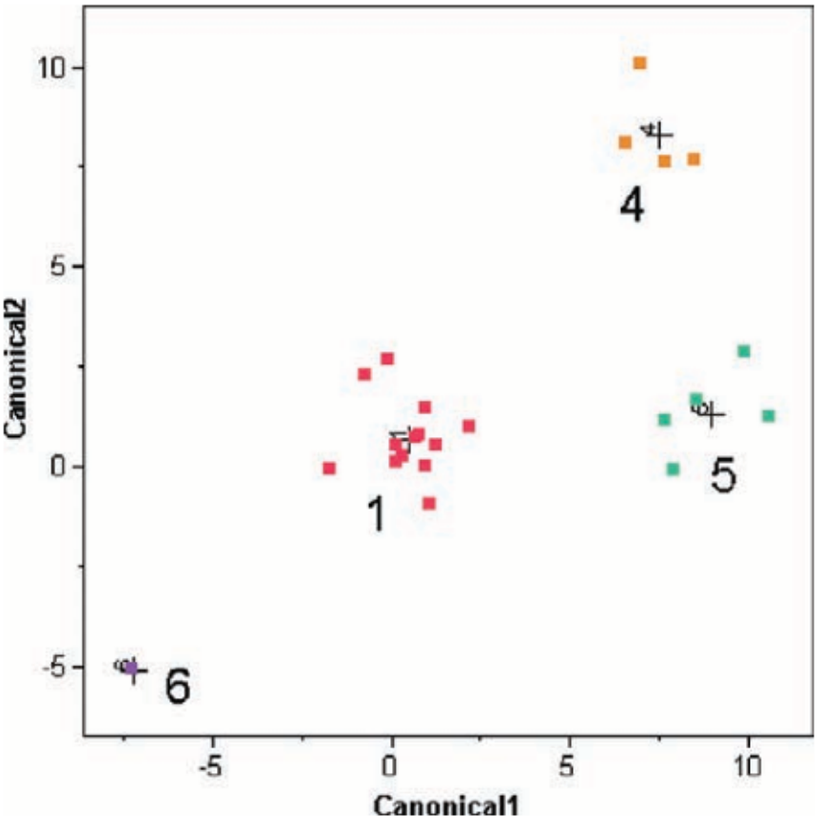

Fig. 24.6 Clusters generated by discriminant analysis of the Paracas and Nasca samples (the north Peruvian samples are not shown for reasons of space due to very large distances). Clusters 1 and 5: Paracas and Nasca objects; Cluster 6: Nasca object from Wayurí; Cluster 4: fake objects

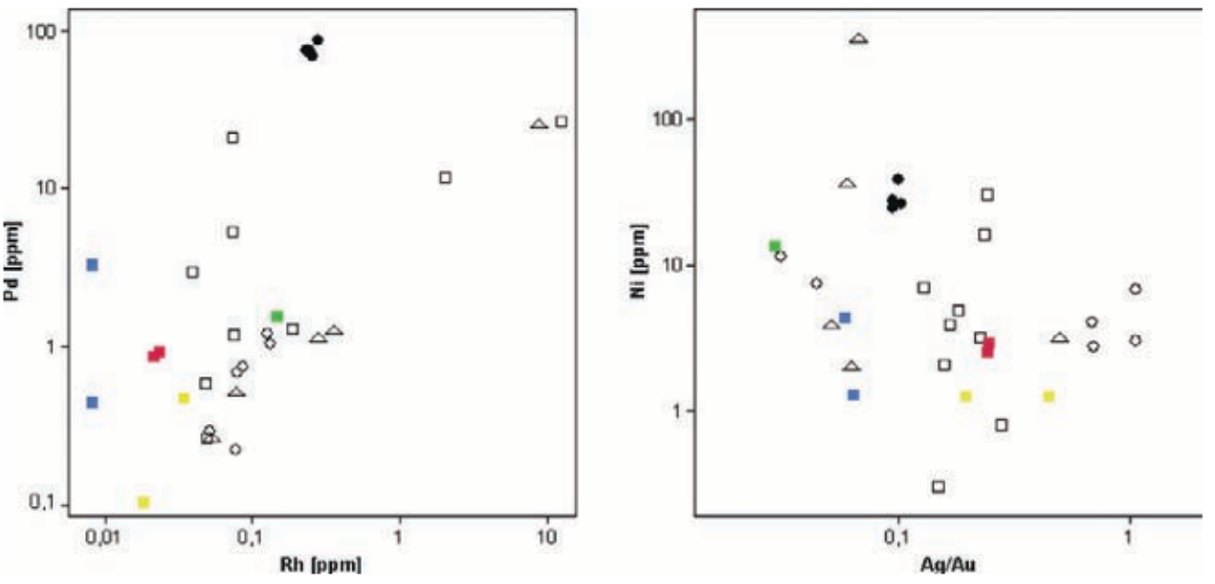

Fig. 24.7 Pd–Rh and Ni–Ag/Au scatterplots for the Paracas and Nasca samples compared to the deposits. See Fig. 24.3 for the legend

contamination or alloying with copper. The analysed samples from four mines (see Fig. 24.3) from the Viscas and Acarí valleys do not provide enough data for statistical analysis, but scatterplots such as Pd–Pt, Pd–Rh or, interestingly, also the Ni–Ag–Au ratio seem to suggest that local gold occurrences were exploited (Fig. 24.7). The local quartz–gold veins have very low PGE concentrations (Pt <1 ppm), as expected for this type of deposit, and are located at the extreme end of the scatter field formed by the objects. The Ni–Ag/Au graph shows that the local deposits group with the silver-rich objects. For further statistics the Ag/Au ratio will also have to be considered.

24.6.2.3 Fake Objects

An interesting outcome of this study is the identification of fake objects. Although the artefacts sampled, especially those without known context, were selected very carefully, it seems that in one case fakes were detected. The suspected fakes are seven equal bird- or butterfly-shaped adornments (Emerich 1992) in supposedly early Nasca style, of which four have been analysed so far.

The following points lead to the conclusion. (1) The style seems to be a misinterpretation of similar objects (also without context but with clear Nasca traits) and therefore the objects cannot be assigned to any known culture in Peru. (2) The obtained signal for mercury was extremely high on both surfaces, which could indicate that mercury was employed in the production process as practised today. (3) The alloy has the highest copper content among all samples. (4) In any statistical analysis the four samples form a group well separated from all other samples (see Fig. 24.6).

24.6.3 Chavín

Compared with the southern samples, these objects have higher silver content (Table 24.6), ranging between 12.5 and 43% (Ag/Au 0.15–0.8). The copper content varies between 1 and 4.5%, also indicating certain contamination. Although at first sight the analysed objects form a homogeneous group, objects composed of more parts (nose ornaments) were sometimes combined from different gold varieties. For example, on the nose ornament with a flying shaman figure (Eb15-052.03) the colour difference between pendant and suspension ring was even visible to the naked eye. A more detailed question concerned the technique used to join the hemispheres of seven analysed beads, as almost nothing is known of Formative metallurgical bonding techniques (Carcedo 1998). It was found that the copper content was not significantly higher at the seam, which indicates that sweat welding (local melting at the edges without adding copper) was used.

Cluster and discriminant analysis were performed using Ir, Rh, Pb, Bi contents and the Pt–Pd ratio. Hierarchical cluster analysis using Ward's minimum variance method with standardisation and linear discriminant analysis using a common covariance matrix were applied. The result showed that the Ebnöther objects form a rather homogeneous group with generally high concentrations of Pt, Pd, Rh and Ir, comparable to the north Peruvian samples in Section 24.6.2.1. However, a few objects are different: the only large object which was analysed (the cruciform pectoral with two hands, EbN15020) and a small round bead (Eb15853C) have higher Pt–Pd ratios and lower Rh, Pd and Pt concentrations than the other objects. Another bead (Eb15853D), not composed of two halves but rolled from one rectangular sheet, contains significantly more lead than all other objects. In the case of the beads, it is expected that they are not of equal composition, as the necklaces were arranged by the huaqueros or dealers who sold the looted objects.

Three more objects are not part of the main group, due to higher Ir and Rh concentrations: a finger ring with feline head design (Eb15044), the pendant of the flying shaman nose ornament, and a suspension ring of another nose ornament (EbN15016). All these objects are without context. Therefore, it would not be wise to draw conclusions from the data until the samples of Formative objects from secure contexts are analysed.

24.7 Conclusions and Perspectives

The analyses of gold matrix-based objects were successfully performed using LA-ICP-MS using solution nebulisation and matrix-matched calibration techniques. The results provided by the different types of calibration were compared and showed agreement for most elements. Therefore both calibration approaches have been found to be applicable for determination of trace,

Table 24.6 Composition of Objects from Chavín Culture Determined by LA-ICP-MS

Number	Object	Site/Analysed Part	Context	Culture/ Style	Cu wt%	Ag wt%	Au wt%
Eb15-027.01A	Bead	Mean seam		Chavín	3	23	74
Eb15-027.01A	Bead	Mean hemispheres		Chavín	2	24	74
Eb15-027.01B	Bead	Mean		Chavín	2	20	77
Eb15-027.01C	Bead	Mean		Chavín	3	27	70
Eb15044	Finger ring with feline head	Mean		Chavín	2	26	72
Eb15-052.03	Nose ornament (flying shaman)	Figure + conn. ring		Chavín	2	18	80
Eb15-052.03	Nose ornament (flying shaman)	Mean suspension ring		Chavín	3	26	71
Eb15-052.04	Nose ornament (bird)	Mean		Chavín	2	16	82
Eb15-052.05	Nose ornament (jaguar)	Mean jaguar		Chavín	1	30	70
Eb15-052.05	Nose ornament (jaguar)	Mean suspension ring		Chavín	2	18	80
Eb15-052.05	Nose ornament (jaguar)	Mean connecting ring		Chavín	1	13	86
Eb15853B	Bead	Mean		Chavín	2	19	79
Eb15853C	Bead	Mean		Chavín	4	26	69
Eb15853D	Bead	Mean		Chavín	4	13	83
EbN15010.01	Finger ring	Mean		Chavín	4	35	61
EbN15010.02	Finger ring	Mean		Chavín	3	24	73
EbN15010.03	Finger ring	Mean		Chavín	3	24	74
EbN15014	Nose ornament (wire serpents)	Mean		Chavín	4	40	56
EbN15015	Nose ornament (green stone, fish)	Mean suspension ring		Chavín	3	35	62
EbN15015	Nose ornament (green stone, fish)	Mean connecting ring		Chavín	3	23	74
EbN15016	Nose ornament (green stone)	Mean connecting ring		Chavín	3	28	69
EbN15016	Nose ornament (green stone)	Mean suspension ring		Chavín	2	22	75
EbN15017	Nose ornament (green stone)	Mean suspension ring		Chavín	4	32	64

Table 24.6 (continued)

Number	Object	Site/Analysed Part	Context	Culture/ Style	Cu wt%	Ag wt%	Au wt%
EbN15020	Pectoral with hands	Mean		Chavín	2	26	72
EbN15032	Big round bead	Mean		Chavín	3	24	73
EbN15036	Nose ring	Mean		Chavín	3	34	64
EbN15038	Nose ornament (small gold disc)	Mean suspension + connecting ring		Chavín	3	30	67
EbN15038	Nose ornament (small gold disc)	Mean disc		Chavín	4	25	71
EbN15039	Nose ornament (stone and gold pendant)	Gold pendant, round top		Chavín	2	32	66
EbN15039	Nose ornament (stone and gold pendant)	Mean of 3 parts above		Chavín	3	43	54
EbN15039	Nose ornament (with stone and gold pendant)	Mean gold pendant, conical part		Chavín	2	30	67
EbN15040	Nose ornament (spondylus)	Mean		Chavín	2	16	82

Parts of objects with significantly different composition are listed separately.

minor and major elements in gold samples. Because the NA2 gold reference material showed an appropriate distribution of elements within the sample, it was most suitable for quantification of the gold objects. Moreover, its composition (~1000 μg g^{-1} Cu, 5.45% Ag, 94.5% Au) was closely matrix-matched to the unknown samples, which leads to most precise and accurate results.

First results obtained from analysis of gold artefacts from Peru already indicate that trace element analysis opens up another dimension in the evaluation of archaeological finds as well as of objects without secure context. It could be demonstrated that in the Nasca region and culture local gold sources but also northern type gold was used. Consequently, its connections to other regions may have to be reconsidered.

Because the analyses are still in progress, especially of the northern Formative gold from archaeological excavations (e.g., from sites as Kuntur Wasi, Chavín de Huántar and Kotosh), the final result will provide more detailed insights. For example, three finger rings from the Ebnöther Collection are stylistically and technically identical to a ring found in a Paracas tomb in Mollake Chico (Isla and Reindel 2006a,b) in the Palpa valley, which makes the comparison of their trace element patterns interesting. Furthermore, the new samples from La Muña objects are expected to shed more light on the sample from Wayurí, which could not be grouped with the rest of the objects. The corresponding archaeological sites are very close to each other and the style and technique of the beads in fish shape are practically identical.

More contextualised objects would be necessary to allow more detailed investigation of the raw material used in different phases of the Nasca or also Paracas cultures. It would be interesting to investigate if the use of northern gold is limited to certain phases.

Regarding the provenance of the raw material, first results already show the potential of LA-ICP-MS. More analyses are also in progress, including microprobe and SEM of native gold.

Part VII
Summary

Chapter 25
Life at the Edge of the Desert – Archaeological Reconstruction of the Settlement History in the Valleys of Palpa, Peru

Markus Reindel

Abstract Within the framework of the Research Project for the Development of New Scientific Methods and Technologies in Archaeological Research, the settlement history of the Nasca–Palpa area was investigated by an interdisciplinary project. This chapter provides an overview of the results in the form of a hypothetical reconstruction of 5000 years of pre-Hispanic cultural history. Earliest traces of settlements and graves in the Palpa valleys date to the Archaic period (approx. 3800 BC). The region then was settled more intensively in times of favourable climatic conditions during the Initial period (1500–800 BC). During Paracas times (800–200 BC) the region slowly became densely populated and during the Nasca period (200 BC–600 AD) the area experienced a cultural florescence followed by a sudden demise triggered by a phase of extreme aridity. After being populated only sparsely during the Middle Horizon (600–1000 AD), a rise in humidity led to another peak in settlement density during the Late Intermediate period (1000–1400 AD). The Inca (1475–1532 AD) established administrative posts in the region which again experienced a decline in production due to the onset of another arid phase just before the arrival of the Europeans.

25.1 Introduction

During the investigations of the Nasca–Palpa Archaeological Project, a multitude of data was assembled concerning the complex cultural history of a region on the southern Peruvian coast and its natural environment. Many questions were answered through the diversified interdisciplinary work which could not have been resolved with the methods of archaeology alone. Where the previously available methods were not sufficient, new technologies and methods were developed or

M. Reindel (✉)
German Archaeological Institute (DAI), Commission for Archaeology of Non-European Cultures (KAAK), Dürenstraße 35-37, 53173 Bonn, Germany
e-mail: reindel@kaak.dainst.de

M. Reindel, G.A. Wagner (eds.), *New Technologies for Archaeology*, Natural Science in Archaeology, DOI 10.1007/978-3-540-87438-6_25,
© Springer-Verlag Berlin Heidelberg 2009

available technologies adapted to the special circumstances and needs. The development of new methods and technologies, now available for archaeological investigations in the New and Old World, was the focus of the research project funded by the German Federal Ministry for Education and Research (BMBF).

The research objective of reconstructing the cultural history of the Nasca–Palpa region presented an ideal frame for the development of methods in the numerous disciplines participating in the project. The starting point for the archaeological investigations of the Nasca–Palpa area was the study of the Nasca culture (200 BC–600 AD), about whose characteristics, antecedents, and successors little was known at the beginning of our research. Early on in the course of excavations in Nasca period settlements and the documentation of geoglyphs clear evidence of the earlier Paracas culture (800–200 BC) emerged; later on even settlement structures dating to the precursory Initial period (1500–800 BC) were found, from which the Paracas developed directly. Meanwhile, the oldest finds date to the Middle Archaic (5000–3000 BC), so the pre-Hispanic settlement history in the area of Palpa can now be traced back over more than 5000 years with only minor gaps.

In connection with the development of new methods in the natural and engineering sciences within the interdisciplinary project cooperation, new results concerning the history of climate and landscape necessitated a closer investigation of the later settlement epochs in the Nasca–Palpa region (Middle Horizon, 600–1000 AD; Late Intermediate period, 1000–1400 AD; Late Horizon, 1400–1532 AD). The history of landscape and culture was supplemented ideally by results from isotope and paleogenetic research. Geophysical research helped in finding new sites. The data from the chronometry projects (^{14}C and OSL) put the historical succession on solid numerical foundations. Archaeometallurgic investigations provided results for an important group of materials in the development of the cultures in the Nasca–Palpa area.

In the course of the project, earlier settlement horizons were successively investigated starting from later cultural strata. Through systematic excavations existing gaps in the settlement history were gradually closed. Now, at the end of the project it is possible to present a hypothetical reconstruction of the cultural history of the Nasca–Palpa region from a historical point of view, that is, from the earliest to the latest pre-Hispanic finds. For every period finds and features can be cited from either survey or excavations.

25.2 The Archaic Period

The Archaic period in the central Andean area is defined as the time from the first settling of the American continent to the beginning of the use of pottery around 1800 BC. According to Kaulicke (1994) this long time interval can be divided into an Early (7600–5000 BC), Middle (5000–3000 BC), Late (3000–2000 BC), and Final Archaic (2000–1500 BC). This relatively unspecific

subdivision shows that the current state of research into the Archaic in South America is still fragmentary. Thus far the only site in the Nasca area with clear features dating to the Middle Archaic has been La Esmeralda (Isla 1990). From earlier surface inspections other sites were known to lie at Santa Ana (Engel 1963; 1987) and San Nicolás, south of the estuary of the Río Grande (Strong 1957). In addition, some datings in the lower strata of a test excavation in the upper Nasca valley point to an archaic settlement (Vaughn and Linares 2006).

In Palpa, graves and settlement features were documented at the site of Pernil Alto (Fig. 25.1). This site occupies a dry slope along the right edge of the Rio

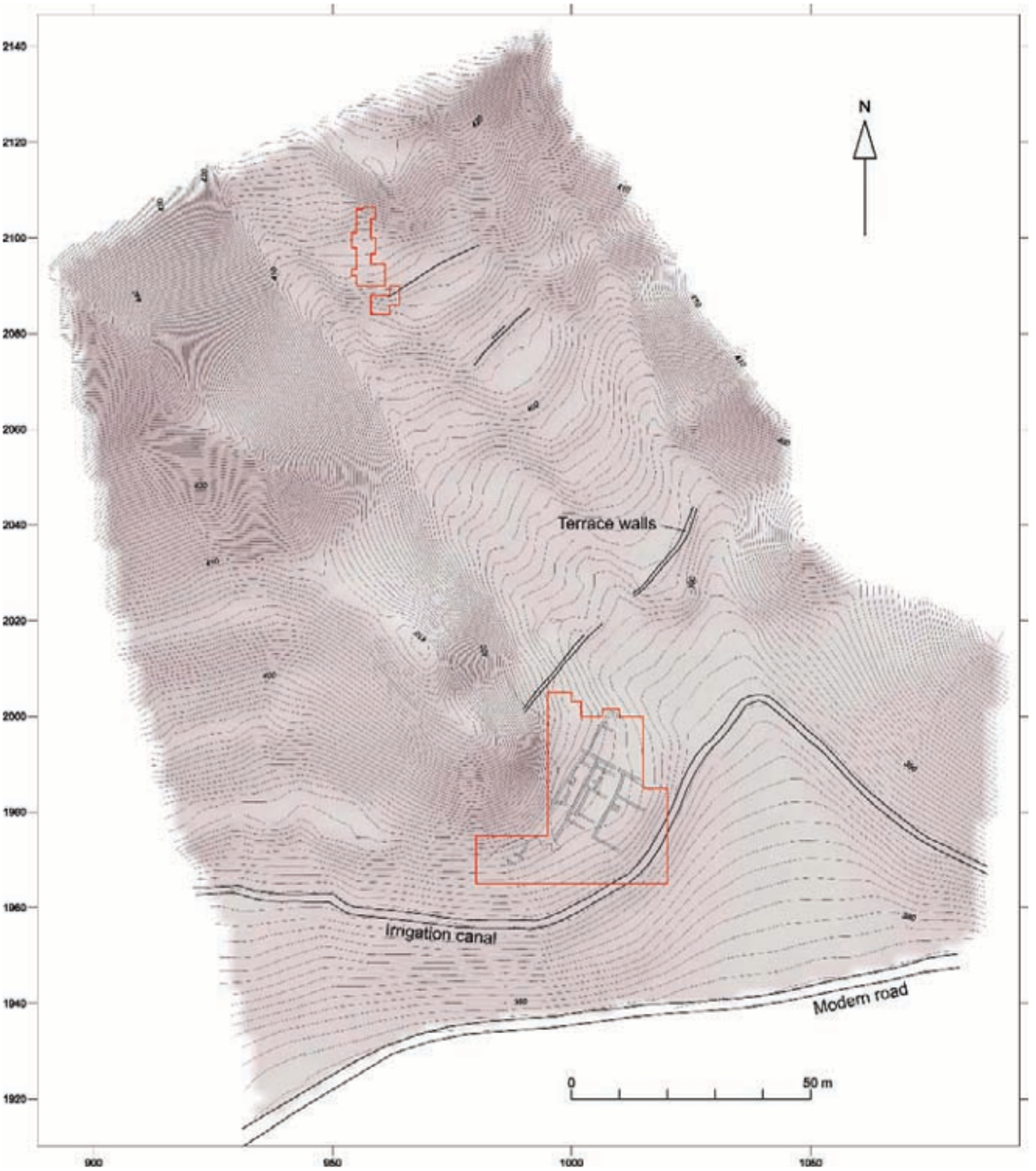

Fig. 25.1 Site map of Pernil Alto with excavation areas (in *red*). A sequence of Archaic, Initial Period, and Early Paracas occupations was found at the foot of the rocky hill and in the nearby quebrada

Grande valley, approximately 6 km to the northwest of the modern settlement of Palpa at an altitude of 390 m a.s.l. and about 10 m above the irrigated valley floor. In Pernil Alto a sequence of settlement strata could be documented running from the Middle Archaic through the Initial period into the Early Paracas phase with some later intruding Nasca graves.

At the margin and below the Initial period constructions (Fig. 25.3) a total of eight graves were found that date into the Middle Archaic (see Isla this volume). The best preserved grave was found on the northern border of the excavation. A man had been laid into a shallow pit in a prone position with irregularly placed limbs (Fig. 25.2). Around the pit were found grinding stones, shell artefacts, bone tools, fragments of gourd vessels, a projectile point of obsidian, and antlers. Remnants of a net were preserved around his head and remains of textiles made of plant fibers were found on his body. The corpse had been covered with leaves and logs. Radiocarbon dates of these organic materials yielded a ^{14}C age between 3800 and 3380 cal BC (LuS-50103, LuS-50070, 3640–3380, 1σ).

Two additional archaic burials were interred at the bottom of large pits with a diameter of approximately 3 m. The bodies had been wrapped in reed mats, but had no offerings. One of the burials yielded ^{14}C ages between 3500 and 3110 cal BC (LuS-50102, Hd-26688, 1σ); carbon remnants from one of the pits were dated to 3020–2890 cal BC (LuS-50068, 1σ). In some places parts of floors, postholes, and hearths were observable, so it can be assumed with confidence that the pits represent the sunken areas of pit houses comparable to those

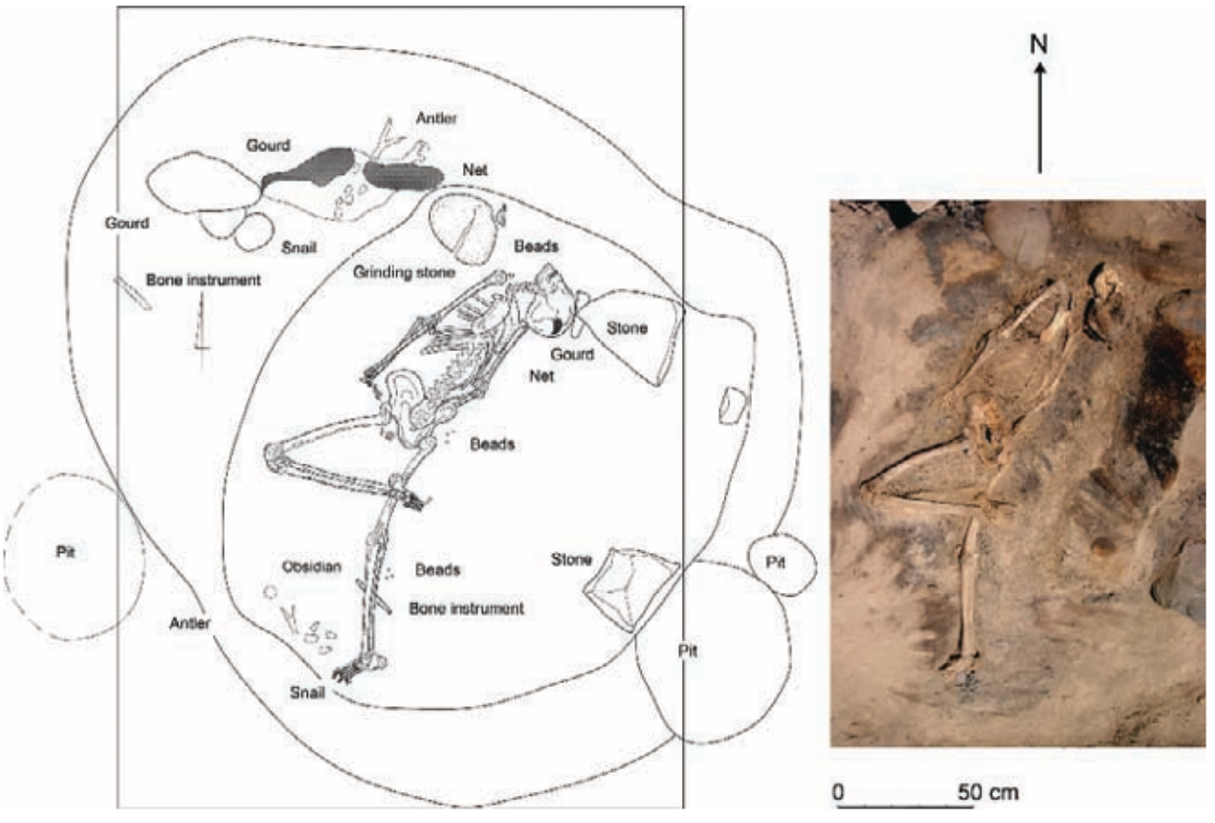

Fig. 25.2 Pernil Alto. Funerary context of the Middle Archaic period (ca. 3800 BC) with several grave offerings

observed in Paloma and Chilca on the central Peruvian coast (Donnan 1964; Engel 1966, 1980, 1987, 1988; Quilter 1989). Such structures belong to the oldest forms of dwellings of sedentary communities in the Andean area.

Judging from the reconstructed paleoclimatic development (Eitel and Mächtle this volume), first tendencies of an aridisation process must have occurred during the Middle Archaic period causing the inhabitants to settle more and more frequently in the flood plains where water was more easily available. The finds of antlers from deer, no longer found today on the coast, point to hunting still playing a certain role in the probably steppelike landscape of the Middle Archaic. At the same time the grinding stones substantiate the processing of vegetable foodstuffs, which probably were not yet domesticated. Typically, cotton is also still absent from the burials; the interred bodies were instead wrapped in reed mats. Shells as offerings show that the action range for food procurement at least reached as far as the marine coast. It can be presumed that the dead of Pernil Alto belonged to the first sedentary people permanently populating the valleys of Palpa, living in pit houses at least temporarily.

25.3 The Initial Period (1500–800 BC)

The Initial period in the central Andean area is defined as the time span from the first introduction of pottery to the spread of the Chavín style along the southern Peruvian coast (Rowe 1962). This definition is afflicted with uncertainties because the use of pottery started at different times in different regions (Bischof 1998, 2000). Still, the term Initial period is used here for the time being because it was coined on the south coast and in the absence of a better definition is the one suited best to describe the time between the preceramic cultures and the well-defined Paracas culture.

The Initial period on the southern Peruvian coast was first defined on the basis of surface finds and limited excavations at the sites of Disco Verde, Erizo and Mastodonte in the Ica valley, and the Hacha site in the Acarí valley (Engel 1991; Lanning 1960; García and Pinilla 1995; Rowe 1963, 1967a,b; Robinson 1994). Although the former sites have not been published in detail, the excavations in Hacha brought to light the remnants of buildings and a limited pottery inventory (Robinson 1994; Ridell and Valdez 1987). Vessels with a cubic body and ring base were identified as characteristic forms of the simple pottery. Decorative elements were limited to simple incisions, especially circles with points, and negative painting.

Ceramics with these characteristics were found in large quantities in Pernil Alto in the Rio Grande valley. Also an extensive complex of adobe structures was encountered that was exposed completely in the course of work of the Nasca–Palpa project at the base of a rocky foothill of the adjacent mountains

Fig. 25.3 Pernil Alto. Panoramic view of the excavations in the Initial period settlement (1300–800 BC)

(Fig. 25.3). The architectural features allowed the identification of four major construction phases as well as a resettlement after the abandonment of the site.

On an artificial terrace, supported on three sides by massive adobe brick walls, several rooms were constructed that were arranged to roughly circumscribe a central court or room. This room constellation was largely maintained throughout the growth of the settlement, with extensions and superstructures added on all sides in the course of time. After the discontinuation following the fourth building phase a thick fill was added, which in turn was covered with a floor, and posts were set but no walls were erected this time. The numerous ^{14}C dates narrow down the time of occupation of Pernil Alto to between the thirteenth and tenth centuries BC (Unkel 2006).

Numerous signs of domestic and specialised crafts production, depots, hearths, workshops, and the like were found in the buildings. The features are an unequivocal sign of a permanent sedentary lifestyle apparently based on agriculture. Craft production points to a certain social stratification. However, graves dating to the Initial period have not been found thus far.

With the excavations in Pernil Alto an Initial period settlement complex was excavated completely and documented together with its rich assembly of finds for the first time on the south coast of Peru. Apart from the already mentioned formal criteria of the pottery, the cubic bodies, the circular foot rings, and the neckless jars, some very typical characteristics, especially in the form of decoration and design elements, could be observed that were continued in the subsequent Paracas period. Thus, the Initial period can be considered the substrate from which the Paracas culture later evolved.

25.4 The Early Paracas Phase (800–550 BC)

The Paracas culture was identified for the first time by Julio C. Tello on the peninsula of the same name in the Pisco valley (Tello 1959; Tello and Mejía 1979). Several settlement remains and graves from different periods were excavated

there. For a better temporal division of the central Andean chronological framework, J.H. Rowe later chose the Ica valley for developing a style chronology on the basis of surface finds, grave inventories, and museum collections. For the Paracas period a chronology was presented consisting of ten phases, although the earliest phases (1, 2, 3) could neither be substantiated with enough sample vessels nor be detected in archaeological contexts in later excavations (Menzel et al. 1964). Graves from the Early Paracas phase were documented for the first time in the excavation at the sites Pernil Alto and Mollake Chico.

A double interment was found in Pernil Alto which was inserted into the last occupational layer of the Initial period settlement, a fill covered by a floor with posts (see above). Two extended bodies had been buried in a dorsal position with two ceramic vessels as offerings. The ceramic vessels' style conforms to the Ocucaje 3 style as described by Menzel et al. (1964). This was the first time this style could be documented in a stratigraphic context above Initial period settlement features and, thus, its relative chronological position fixed. The ^{14}C dates show the Early Paracas phase to have lasted from 800 to 550 cal BC (Unkel 2006; Unkel and Kromer this volume; Siegle 2007).

Other finds and features of the Early Paracas phase were obtained in Pernil Alto from the quebrada bordering the site to the northeast (Isla this volume). Limited excavations in this area yielded parts of spacious terraces as well as graves dating to this time with ^{14}C dates of 760–510 cal BC (LuS-50065, 1 σ).

Another rich burial from the Early Paracas period was documented in Mollake Chico. Although the grave had already been partially looted before, the inventory of the plundered grave could be reassembled entirely, more material be retrieved, and the context documented through further excavations (Isla and Reindel 2006a). Mollake Chico is situated in the lower Palpa valley in a small arroyo next to the valley border. On the surface settlement remnants, graves, and pottery from the Nasca period were observable. In several test excavations only minimal remnants of further Paracas features could be documented. But the grave structure and the lower part of the fill were encountered to be in a good condition still. The grave measured 1.8 $\times$ 2.5 m and was framed with upright slabs that were 60 cm high. The grave offerings consisted of nine complete or nearly complete pottery vessels and fragments that can be assigned to the Ocucaje 3 style in the classification of Menzel et al. (1964; Fig. 25.4). Furthermore, numerous beads with incised decoration, spindle whorls, obsidian arrowheads, bone objects, and other offerings were found.

The grave contained bones from at least 17 individuals, many showing signs of cremation, but none were found in their original anatomic position (Tomasto this volume). Everything points to a secondary burial of the individuals and the burial ceremony was somehow connected to the application of fire. Burials of this kind from the Paracas culture were documented for the first time in the context of the Nasca–Palpa project.

The finds of Early Paracas burials in two places in the valleys of Palpa show that the Paracas culture was deeply anchored there from its very beginnings. This contradicts earlier assumptions that the Paracas culture had been imported

Fig. 25.4 Ceramic vessels of the Early Paracas phase (800–550 BC) from the funerary context excavated at Mollake Chico

into the Nasca region only in the later phases from more northerly regions around Ica, Pisco, and Chincha and even then being only scarcely present (Silverman 1994, 1996). The new findings show that the Paracas in the area of Nasca evolved from Initial period precursors and were present prominently from the earliest phases; perhaps one of their centres of development even lay in the valleys of Palpa.

25.5 The Middle Paracas Phase (550–370 BC)

The earliest settlement sites from the Archaic, the Initial period, and the Early Paracas phase were identified in only a few places during the surface survey. This was partly due to earlier settlement phases being covered by later ones, making them hard to identify on the surface. On the other hand it seems that the density of settlements in these periods effectively was still very low.

This seems to have changed in the Middle Paracas phase. During the first archaeological explorations in the Palpa valley by T. Mejía Xesspe numerous sites belonging to the time of the Paracas were already recorded (Mejía 1972, 1976). Although it is unclear to which phase exactly the mentioned sites from Mejía belong, it is to be assumed that he identified many Late Paracas sites in addition to some from Middle Paracas.

During the excavations undertaken by the Nasca–Palpa project at the site of Jauranga, settlement remnants and graves from the Middle and Late Paracas phases were documented (Fig. 25.5). Jauranga lies in the middle Palpa valley, approximately 3 km west of Palpa and only about 200 m south of the riverbed of the Palpa river. Through its position on the valley floor Jauranga differs markedly from most of the other sites documented in the course of the project, because those are normally situated along the arid valley borders beyond the arable farmland. Sites on the valley floor are barely identifiable due to the intense sedimentation of the rivers. Even grave robbers normally do not search on the valley floor, so that finds and features in Jauranga were encountered undisturbed.

Fig. 25.5 One of the excavation units at Jauranga, with structural remains and graves from the Middle and Late Paracas phases (550–200 BC)

The site of Jauranga was identified when the farmer O. Tijero found Paracas pottery fragments during construction work on his property. Initially, the Nasca–Palpa project planted two test pits at the spot in 1997, which yielded a sequence of Middle to Late Paracas settlement strata (Isla et al. 2003). In 2003 extensive geophysical surveys and test excavations were made showing many other places on the valley floor in the vicinity of Jauranga to contain the remnants of human activities during the Paracas phase. The excavation in Jauranga then was enlarged substantially.

Jauranga is situated on a slight elevation within the arable land. During excavation three settlement phases were identified. The earliest settlement phase stems from Middle Paracas and its duration was verified through numerous ^{14}C dates (Unkel 2006; Unkel and Kromer this volume). The buildings were constructed using irregular pancake-shaped mud bricks that were assembled to form 30 to 40 cm thick walls. The construction material was taken from nearby clay-pits which had been identified during the geophysical prospection and could be ascertained as to having been the source of the material used in Jauranga through material analysis (Wetter 2005). The walls of the buildings were consolidated at the base with stream-lined cobbles from the nearby river. The excavated settlement remains were composed of several rooms and platforms, partially on slightly different levels.

During the excavations at Jauranga 80 graves were found, 49 of which dated to the Paracas period. The earliest of those stemmed from the Middle Paracas

phase, but the largest part dated to the Late Paracas phase. As a general rule, the dead were buried in a stretched dorsal position with ceramic offerings (Isla this volume).

The classification of the ceramic material from the graves as well as the settlement contexts (Wetter 2005), their stratigraphic analysis, and their dating through numerous ^{14}C dates, for the first time allowed the chronological ordering of the Paracas phase on the basis of stratified settlement and grave contexts alone. As a result the classification from Menzel et al. (1964) based on the stylistic seriation of pottery was proven valid by and large. The ceramic styles Ocucaje 5, 6, and 7 could thereby be assigned to the Middle Paracas phase.

25.6 The Late Paracas Phase (370–200 BC)

During intensive surface surveys, 118 settlements of the Late Paracas phase were identified. It is quite obvious that a massive colonisation of the Palpa valleys occurred at this time. Whether the population increase can be attributed solely to local developments or if people moved in from other areas cannot be resolved definitely at the moment. A further manifestation of cultural activities at this time are the numerous geoglyphs found on the slopes around Palpa (Lambers this volume). Mostly they portray anthropomorphic or zoomorphic motifs between 10 and 30 m in height visible from the valley floor. Similar motifs are found in petroglyphs situated in comparable locations. Because petroglyphs without doubt emanate from an older tradition, it can be assumed that geoglyphs in the Middle or Late Paracas phase resulted from the transfer of motifs from the medium stone to the surface of the dry slopes.

The settlements of the Late Paracas period occupy a large part of the middle valleys. The large plain at the confluence of the Grande, Palpa, and Viscas rivers is relatively sparsely populated, contrary to later periods in which this plain was a sought agricultural area. The concentration of settlements at places along and near the valley border with good access to water as well as the construction of settlements on the valley floor could indicate that Paracas settlements were founded in the immediate vicinity of agricultural land and that irrigation systems still played no important role because humidity from the nearby river was used for agriculture. According to the palaeoclimatic reconstructions (Eitel and Mächtle this volume) a long-term aridisation process should already have been perceptible at this time but sufficient water may still have been available in the rivers for farming.

The major part of the burials from Jauranga dated to the Late Paracas phase and showed similar traits to those from the Middle Paracas phase. In the excavation area some elaborate graves were also documented that had been buried in a platform in four chambers with adobe walls and had up to 17 ceramic offerings (Isla this volume). In addition, objects such as shells, obsidian

artefacts, numerous llama bones, and even whole llama skeletons were given as offerings, which might be taken as evidence of far-reaching trade relations during this time. Locally restricted signs of cremation could be observed on some of the buried. This points to a typical burial ritual of the Paracas period,

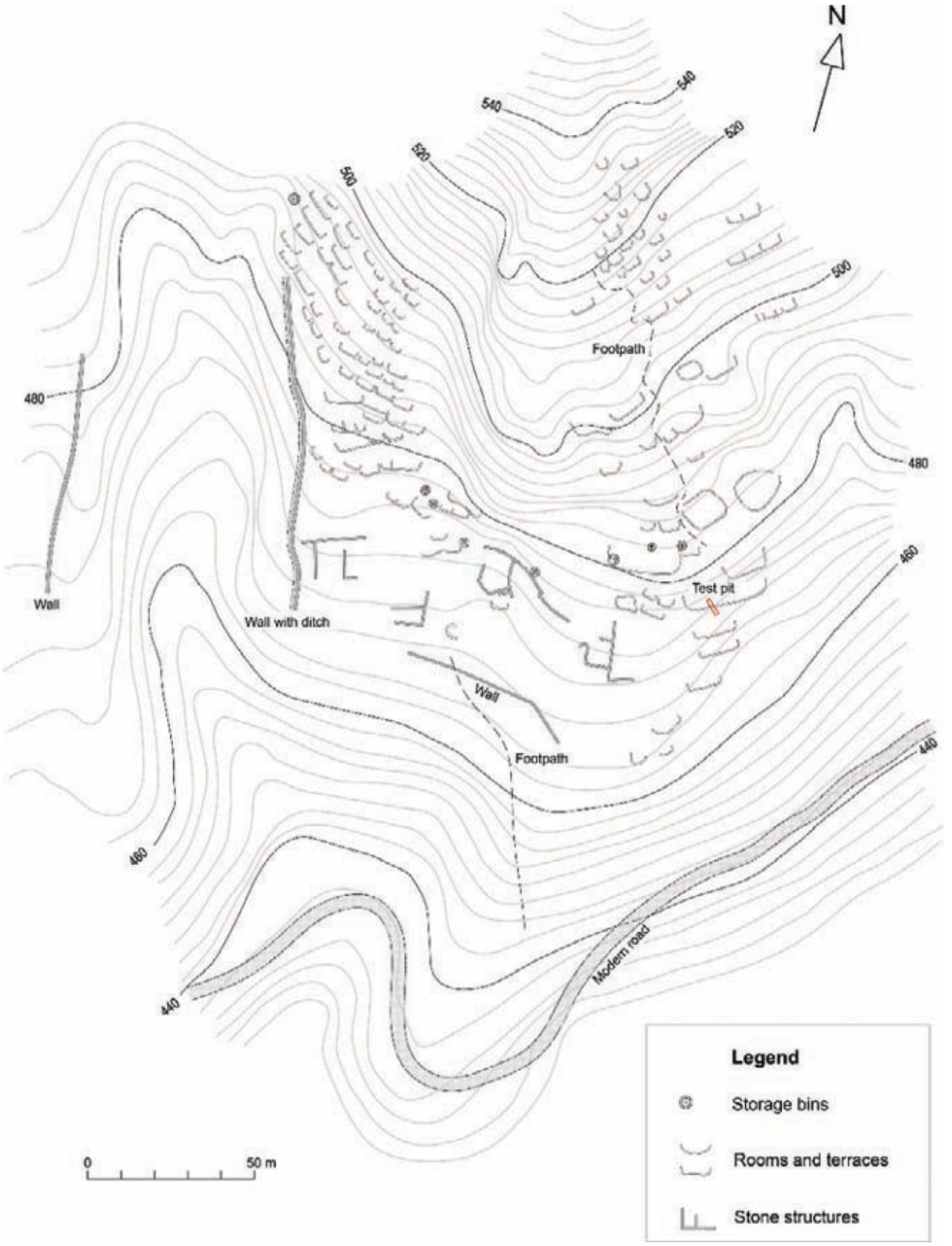

Fig. 25.6 Site map of Pinchango Viejo, a typical settlement of the Late Paracas phase (370–200 BC), with defensive walls, house terraces, and storage devices. Test excavation is marked in red

which had already been observed in the skeletal material from Mollake Chico (see above).

Another characteristic Late Paracas settlement is the site Pinchango Viejo. It lies on the right margin of the middle Palpa valley. Numerous terraces stretch across the slopes and plateaus between two deeply engraved dry ravines (Fig. 25.6). Possible accesses to the south are sealed off with long walls. Another wall, still standing up to a height of 3 m, bars access from the side of the slope. The strategic position at a certain height above the valley floor and defensive features are a typical trait of Late Paracas settlements in contrast to settlements of the later Nasca period which are normally dispersed regularly and openly along the valley border (Reindel et al. 1999; Reindel and Isla 2006a,b).

Test excavations in Pinchango Viejo on both sides of one of the terrace walls yielded settlement strata and two burials. In contrast to the burials in Jauranga these were crouched inhumations. Undecorated pottery vessels were found as offerings, but the excavation context also yielded diagnostic Ocucaje 8 pottery fragments (Late Paracas phase; Reindel et al. 1999).

25.7 The Initial Nasca Phase (120 BC–90 AD)

During the transition from the Paracas to the Nasca culture a gradual change took place in settlement patterns, the ceramic technology, and the textile craft. The border between the Paracas and Nasca phases is drawn using a technological criterion, the transition from the postfiring application of pigments on the pottery, common during the Paracas period, to engobe painting fixed on the pottery through firing, in the Nasca period. Typical traits of this pottery of the so-called Proto Nasca phase, which is characterised by the ceramic styles Nasca 1 and Nasca 2 (Rowe 1960a,b), are naturalistic motifs of the continuing Nasca tradition outlined with incised lines with the incisions being a reminiscence of the earlier Paracas decoration technique. Because the term Proto Nasca coined by Uhle (1913) could be confusing in the light of newer investigations and Nasca 1 and 2 only describe ceramic phases, the Nasca–Palpa project opted for the term Initial Nasca phase for the cultural characterization of this time period.

Pottery fragments with these traits, however, are very rarely encountered in settlements and graves. In fact, more often simple, cream-coloured or darkly fired vessels with characteristic forms, in particular shallow bowls with strongly incurving rims are found (N. Hecht this volume). This pottery shows many similarities with the still poorly described Topará ceramics with their origin supposedly in the Topará valley farther to the north (Wallace 1986; Peters 1997).

Initial Nasca settlements are found in large quantities in the entire area of investigation. With 250 sites they make up the group with the largest single number of sites of any of the settlement epochs defined here. Although only

very limited excavations were undertaken at the site Estaquería, the analysis of the features and ^{14}C dates in conjunction with the preceding Late Paracas phase and the subsequent Early Nasca phase allow for a good temporal placement of the Initial Nasca phase to between 120 cal BC and 90 cal AD (Unkel 2006).

One of the largest Initial Nasca settlements is Carapo where hundreds of residential terraces stretch across the entire height of a hillslope at the confluence of the Palpa and Viscas rivers. It is conspicuous that no central structures or clearly monumental or planned building complexes can be identified. Only in one place some slight differences in the size of the terrace complexes can be detected.

This is also true for the Estaquería site where, however, another construction trait was observed which can be interpreted as the creation of central or monumental structures: natural hills were levelled and rectangular shapes aimed for in the process, so that topographic forms were generated evocative of monumental architecture. These beginnings could have found their succession in the later practice of the Early Nasca culture of using natural formations as a basis for monumental superstructures, such as, for example, those clearly visible in Cahuachi (Silverman 1985, 1993; Orefici 1993).

The test excavations in Estaquería showed that structures on the terraces were simple ones made of *quincha* walls (wattle and daub), some with a stone foundation. All in all the Initial Nasca period presents itself as a very dynamic settlement epoch with an enormous population increase in which the foundations for the subsequent bloom of the Early Nasca phase were laid. With the results of the Nasca–Palpa project we can say today that the significance of this transitory phase has clearly been underestimated and that it is a time of change that needs further detailed investigation.

25.8 The Early Nasca Phase (90–325 AD)

The Early Nasca phase can be considered the onset of the cultural florescence in the Nasca region in many respects. During this time the region reached a high settlement density, a discernible political structuring of the settlements evolved, the ceramic and textile production increased in quality and quantity, and the construction of a new type of geoglyph led to the transformation of the whole landscape.

The shape of the settlement pattern for the Early Nasca phase shows the logical continuation of the Initial Nasca developments. The available undeveloped areas in the valleys were systematically turned into arable land. In contrast to the preceding settlement phase, the focus in the Early Nasca phase lies on the large plain formed by the confluence of the Grande, Palpa, and Viscas rivers. There, directly at the valley border the settlements lie strung together one after another. The settlements were unfortified; strategic locations do not seem to have played any role. Apparently the available agricultural land was to be

used most efficiently. This was only possible by means of a well-developed irrigation system. Although we do not have direct proof of irrigation installations, the settlement distribution as well as the obviously high agricultural production and subsequent economical florescence at a time of increasing aridity leave no doubt that a developed irrigation economy, making the still-abundant river water available for agriculture, must have been the basis for this prosperity.

Nonetheless, the inhabitants of the Palpa valleys were well aware of their dependence on the water. It could be proven in the course of the investigations of the Nasca–Palpa project that the geoglyphs of the Nasca period were connected to water and fertility cults (Reindel et al. 2006; Lambers 2006). The construction of geoglyphs increased in the Early Nasca phase and reached a first peak. Geoglyphs should not be understood as mere pictures, however, as has happened thus far, but should be considered action spheres where rituals were held regularly. The best expression for this is small platforms excavated by the project at the terminal points of trapezoids which contained field crops, pottery, textiles, crayfish, shells, and consistently *Spondylus* shells. *Spondylus* have been associated with El Niño events since earliest times and were traded as symbols of water and fertility from the equatorial regions throughout the whole Andean area (Marcos 1986, 2002).

The settlement patterns show a clear hierarchy of settlement types: apart from hamlets and small villages containing stone structures or terraces with wattle and daub (quincha) constructions on them, there are proper settlement centres standing out because of their planned layout, central buildings of special size, and the increased use of adobe bricks. Examples of such regional centres are Llipata at the southern edge of the large plain and Los Molinos in the lower Grande valley. Comparable regional centres are present in the whole Nasca area, for example, Puente Gentil in the Santa Cruz valley, La Ventilla in the Ingenio valley, Cantayoq in the middle Nasca valley, Jumana in the lower Nasca valley, or Tambo Viejo in the Acarí valley. But there is only one large centre which can be considered the overall centre of the whole Nasca region, Cahuachi in the lower Nasca valley. In contrast to other authors (Silverman 1993; Orefici 1993), the results of the Nasca–Palpa project show a pattern of distinct political structuring with definite tendencies towards a beginning regional state (Isla and Reindel 2006b).

Large parts of Los Molinos in the lower Grande valley were excavated as an example of a settlement centre (Fig. 25.7). The motivation for the excavation was Nasca geoglyphs on a slope barely 100 m from the northern part of the settlement (Reindel and Isla 2001). The hope of finding evidence for a relationship between the settlement activity and the geoglyphs, for example, in the form of specialised religious architecture, was not confirmed. Rather, large areas with planned mud brick architecture were uncovered which had terrace walls up to 1.5 m wide and wattle and daub superstructures. The overall design of the complex, the structuring into terraces and long corridors, the form of the bent entries with stairways, as well as many other construction details permit a direct

comparison with the architecture in Cahuachi which reached its bloom at the same time and close ties between the two sites certainly existed. Radiocarbon dating of Los Molinos gives a duration of the Early Nasca phase from 90 to about 325 AD (Unkel 2006; Unkel and Kromer this volume). On the basis of the architectural features a hypothetical reconstruction of one part of the Los Molinos settlement was attempted, which is shown in Fig. 25.7. The size of the habitational units, the scarcity of domestic waste in most rooms, and the existence of apparently central kitchen facilities are an indicator that Los Molinos was the residence of a privileged population.

The plant and animal remains retrieved from the excavation in Los Molinos testify to a broad product range and suggest a diversified subsistence strategy. Maize played a vital role in agriculture, just as did the tuber achira, peanuts, pumpkin, pepper, and miscellaneous fruits. The isotope analysis done within the context of the project showed that meat from llamas kept locally was consumed (Horn et al. this volume). The same analysis also proved there were quite definite differences in the nutrition of the poorer and the richer in Nasca society. Seafood was brought from the 60 km distant coast and numerous obsidian artefacts are evidence of contacts with the highland.

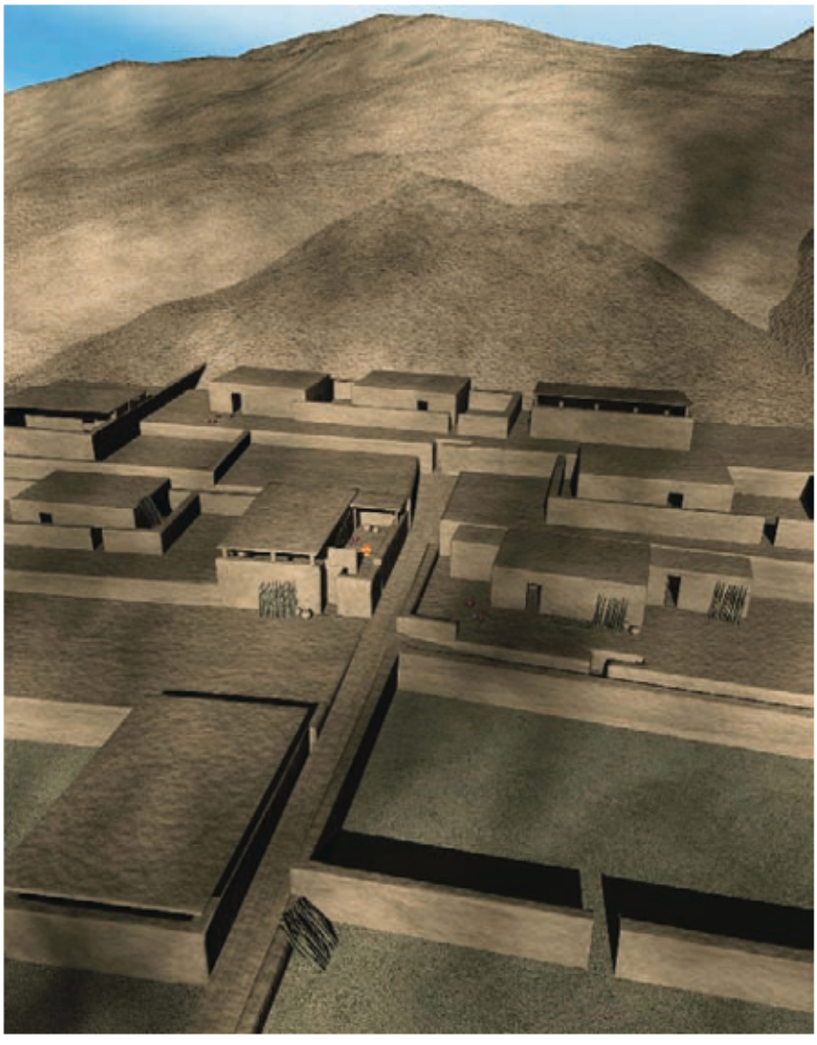

Fig. 25.7 Hypothetical reconstruction of the excavated central area of the Early Nasca settlement Los Molinos (80–325 AD). Wattle and daub constructions were placed on terraces built with adobe retaining walls. (Design: J. Tomkowitz)

25.9 The Middle Nasca Phase (325–440 AD)

During the Middle Nasca phase the settlement centres of the Palpa region shifted to the northern edge of the large plain. On the right bank of the Grande river the La Muña settlement emerged and stretched across the dry slopes of the adjacent hills for several hundred metres from where the plain could easily be controlled. At the same time access to the Grande river as a permanent water source was secured. Apart from the usual settlement terraces numerous adobe buildings can be found in La Muña, some of larger size certainly dedicated to central tasks.

The work of the Nasca–Palpa project concentrated on the southern part of the settlement, where a necropolis with at least twelve monumental graves was located within a walled sector of the site (Reindel and Isla 2001; Isla and Reindel 2006b). The central grave shafts of the burials had already been plundered. But the graves still yielded valuable information concerning the grave architecture and offerings.

A total of six grave structures that were uncovered exhibited a uniform construction model (Isla this volume; Fig. 25.8). Because of their size, their furnishing, their position in a walled sector, and the valuable grave offerings, these graves can be considered elite burials. This adds a vitally important aspect to our concept of the Nasca society: evidently there was a pronounced social hierarchy with an elite. The rich economic resources made possible a society with a division of labour, with specialised craftsmen and people freed from food production for bureaucratic and organisational tasks or the maintenance of religious cults involving the geoglyph construction. This social hierarchy is also reflected in the political hierarchy of the settlement patterns.

Statistical analyses based on the number and duration of use of settlements have shown that the region reached a peak of settlement density in the Middle Nasca phase (Soßna 2007). The Middle Nasca settlements show a similar distribution pattern to the ones from the preceding phase. But a tendency is observable that the settlement foci are shifted to the middle valleys, a trend continued and more accentuated in the Late Nasca phase. This coincides with

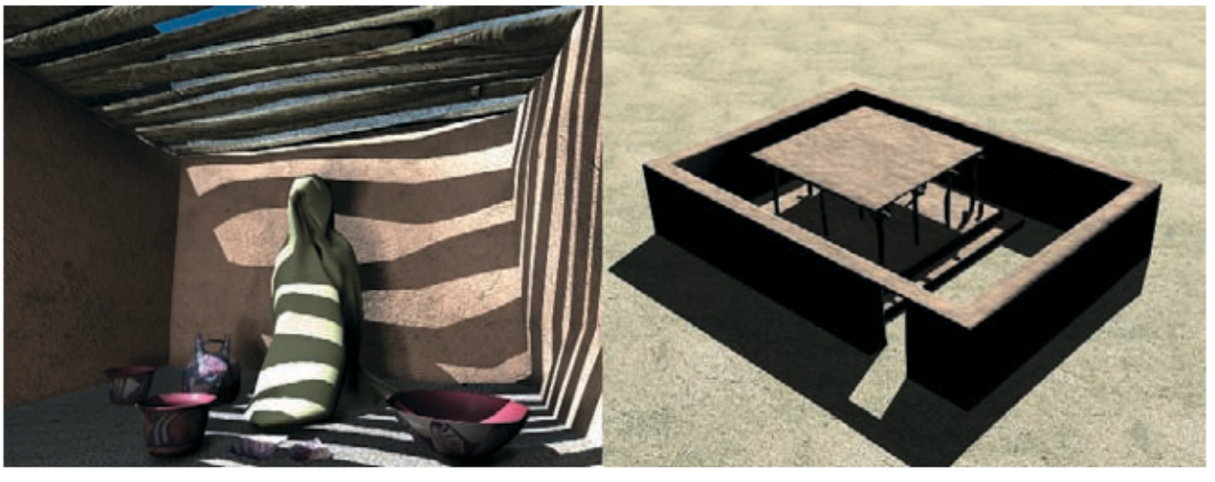

Fig. 25.8 Hypothetical reconstruction of one of the elite tombs of the Middle Nasca necropolis of La Muña (325–440 AD). Left: Grave chamber covered with wooden beams. Right: Funerary architecture with roofed platform and enclosure wall. (Design: J. Tomkowitz)

the increase in aridity which might also explain intensified activities on the geoglyphs probably in connection with difficulties in agriculture.

25.10 The Late Nasca Phase (440–620 AD)

During the Late Nasca phase the settlement shift towards the middle and upper valleys continued. This corresponded to the desert margin shift to the east. Although the middle valleys offered fewer agricultural areas, river water was available more reliably. The large plain at the confluence of the Grande, Viscas, and Palpa rivers was widely abandoned.

According to the palaeoecological reconstruction the region did experience a period of severe aridity at the end of the Late Nasca phase around 600 AD. People tried to counter this process with intensified religious rituals on the geoglyphs. Although not many new geoglyphs were constructed during the Late Nasca phase it seems as though the activities on the geoglyphs increased, especially on the trapezoids with their structures connected to the water and fertility cult (Lambers 2006; Reindel et al. 2006a,b).

A typical site of the Late Nasca phase is Parasmarca (Fig. 25.9). It is located on the right valley margin in the middle Grande valley on a broad alluvial fan

Fig. 25.9 Site map of the Late Nasca settlement of Parasmarca (440–620 AD). The formal layout of the structures on the upper right indicate a planned construction during the establishment of settlement centers in the late phases of Nasca occupation in the upper reaches of the Rio Grande valley

of a dry tributary valley. These locations on the flat alluvial fan surfaces, offering ideal space for planned large-scale building complexes, were preferred spots especially during the Middle and Late Nasca phases, although they were in danger of being destroyed by mudslides caused by occasional heavy rainfalls.

One such complex is situated in the northeasterly part of the alluvial fan of Parasmarca. The regularly spaced terraces, contrasting markedly with the irregular terraces of earlier settlement periods at the site, as well as the extensive walls constructed of local bedrock show that the complex was planned beforehand and constructed in only a short time span. Apparently Parasmarca was built to function as an administrative centre at a time when the main settlement activities shifted to these parts of the valleys.

The pottery encountered in the context of this architecture corresponds to the type termed Nasca 7 and it was the first time this type could be documented in a stratigraphic context (N. Hecht this volume). The ^{14}C dates obtained in Parasmarca plus samples from other contexts with comparable pottery set the duration for the Late Nasca phase from 440 to 620 cal AD (Siegle 2007).

25.11 The Middle Horizon (620–1000 AD)

Although settlements and graves from the Middle Horizon were known from surface surveys and excavations in the more southerly valleys of the Nasca region (Tello 1917; Tello and Mejía 1967; Mejía 2002; Strong 1957; Ubbelohde 1958; Schreiber 1998), in the investigation area of the Nasca–Palpa project only sporadical pottery finds were made from this time during the surface survey (Reindel et al. 1999). The excavation in Los Molinos yielded some simple quincha constructions on the edge of the Nasca settlement (Reindel and Isla 2001). More numerous were Middle Horizon grave finds. First, they were found in Los Molinos (Isla 2001; this volume), then also in Hanaq Pacha (Reindel et al. 2004) and Parasmarca (Reindel 2006). In these graves Nasca traditions were continued but apart from the offerings of a different type of ceramics other innovations, such as multiple burials, were also present (Isla 2001a,b). Through the sampling of finds from settlement and grave contexts the beginning of the Middle Horizon influence in the Palpa valley was ^{14}C-dated to 620 AD. However, the upper limit which should be around 1000 AD could not be determined exactly due to the small number of datable samples of this period (Unkel 2006).

The rectangular complexes thought to be typical for the Middle Horizon have not been found in the Palpa valleys thus far. Only recently, during surface surveys in the upper Viscas valley, was one such settlement encountered. Also, no geoglyphs can be identified with their construction dating clearly to this time. Everything suggests that the region was largely abandoned at the time of the Middle Horizon. Only few people still lived there in simple dwellings and buried their deceased in chosen locations.

This situation can be explained from the palaeoecological findings. Apparently the region was so arid after 600 AD that no agriculture was possible. The desert margin lay high in the Andes and the Palpa valleys turned into a complete desert. This heightened aridity must also have influenced the rivers' water level, so that a situation might have prevailed comparable to the one in the Santa Cruz valley today where river water is available only for a short period of time every few years.

25.12 The Late Intermediate Period (1000–1400 AD)

The climatic situation changed fundamentally during the time of the Late Intermediate period. The humidity increased again and there was another cultural florescence of the region. People returned to the Palpa valleys and built extensive townlike settlements. In contrast to earlier times of intensive settlement of the region, for example, the Early Nasca phase, elevated positions were now preferred, often in combination with settlement parts lying near the mouth of dry valleys although never close to the immediate valley border. The concentration of large settlements and the location some distance from the valley floors indicate that agriculture was no longer the only subsistence source for the inhabitants of the Palpa area but that trading and the interregional exchange became important at a progressive rate.

Pinchango Alto is a typical settlement of this time. It has an extensive settlement part at the base of the Andean foothills on the left side of the Grande river but stretches also to an elevated part far away from any accessible water source (Fig. 25.10; Eisenbeiss this volume). The provisioning with water in this and other Late Intermediate period settlements lying in elevated spots can only have been possible with higher levels of precipitation making water storage possible. The palaeoclimatic investigation showed that indeed the precipitation reached a level between 100 and 150 mm, an amount permitting water storage for drinking water and agricultural use (Mächtle 2007, this volume).

The special location of Pinchango Alto in an area difficult to access as well as numerous large grinding stones and pits within the settlement give way to the speculation that some sort of mining was carried out serving the provision of a supraregional trade network (Stöllner and Reindel 2007; Stöllner this volume). But until now it has not been possible to clarify what was mined although the extraction and working of gold – still practiced in the region today – could be excluded (Schlosser et al. this volume).

Almost all ^{14}C ages from excavations date the Late Intermediate period between 1150 and 1450 AD (Unkel 2006). What happened between 1000 and 1150 AD, that is, between the end of the Middle Horizon and the earliest Late Intermediate period settlement strata observable in Palpa, is unclear. Everything seems to indicate the aridity, and with it the depopulation, lasted well into the twelfth century. Only then, with the increase in humidity and an

Fig. 25.10 Aerial view of the large Late Intermediate period settlement Pinchango Alto (1150–1400 AD). Its location far away from actual water sources indicates that during the Late Intermediate period more water must have been available

improvement of the living conditions, were small agrarian settlements established before the extensive townlike settlements were founded at an explosive rate along the lines of interregional communication.

25.13 The Late Horizon (1400–1532 AD)

The Late Horizon is defined by the expansion of the Inca in the central Andean area. To consolidate and order their power in the empire stretching from northern Chile and Argentina to Colombia, the Inca established administrative centres that normally lay along one of the streets of the widely ramified road system (Hyslop 1984). A pervasion of the local traditions with Incaic traits did not happen normally. Rather, local cultures usually existed parallel to Incaic administrative installations which often are the only places where typical Incaic objects in the so-called imperial Inca style are found.

This situation is reflected in the archaeological settlement distribution of the Palpa valleys. During surface surveys only solitary pottery fragments clearly identifiable as Incaic were found. The only site showing definite architectonic traits of an Inca settlement is Pueblo Nuevo on the left side of the Viscas river between the modern settlements Palpa and Llipata (Fig. 25.11). According to the written sources, dealing with the conquest of the south coast, Pueblo Nuevo

Fig. 25.11 Aerial photo (SAN 524–400) showing the Inka site Pueblo Nuevo (ca. 1470–1532 AD). The site was completely destroyed in the 1950s. In the photo dating to 1944 typical features such as an ample trapezoidal plaza with a possible stone platform (ushnu), a possible long house on the *upper right* (kallanka) and storage units (*lower left*) can be identified

must have been installed around 1440. No settlement centre already in use was chosen but a new administrative site (tambo) was built (Rowe 1945; Menzel 1959). The building complex now is only visible on aerial photographs from 1944. It was levelled completely in the 1950s to make way for agricultural fields. Today, only some stone walls are left to see.

Pueblo Nuevo consisted of a large courtyard surrounded by numerous buildings of varying sizes, among them a storehouse (*qollqa*), a possible 'long-house' (*kallanka*), and a possible ceremonial platform (*ushnu*), all typical construction forms also known from Inca administrative centres in the highlands such as Huanuco Pampa (Morris 1985) or along the coast in Tambo Colorado in the Pisco valley (Uhle 1913; Gasparini and Margolies 1977). Other Inca centres in the Nasca region can be found in Paredones in the Nasca valley (Herrera 1997) and in the Ingenio valley.

Most likely the Late Intermediate period settlements continued into the Inca period. For the Inca it was important to exploit the local resources and social organisation for tribute. No changes had to be made to the local population structure to this end. The agricultural production may have been small again during this time, suffering once more from increasing aridity. The observed settlement spread in the Late Intermediate period, however, indicates an intensive trade based, among others, on regional resources such as, for example,

minerals. The observation of apparently planned structures within settlements with an administrative character, sometimes also storehouses as in the case of Las Colcas, probably built in a later phase of the settlement is striking.

25.14 Conclusion

The synopsis of the results from the different subprojects of the Nasca–Palpa project has yielded a very detailed reconstruction of the settlement history of the Palpa valleys that could be presented here only schematically. The pre-Hispanic settlement history of Palpa can be traced over more than 5000 years, from the earliest forms of sedentary communities followed by the gradual emergence of more complex societies and the height of the Nasca culture, its cultural hiatus, to the reign of the Inca.

A gap we hope to fill in the future still exists between the Middle Archaic and the Initial periods, that is, between 3000 and 1500 BC. All other settlement phases were dated numerically by the Chronometry Project by means of numerous well-contextualised samples. The ideal coordination of natural scientists and archaeologists entering archaeological information from current excavations and long stratigraphies from an area of defined cultures into the calibration and statistical analysis helped immensely in this process. Thus, the Palpa region now possesses certainly one of the best chronologies for prehistoric South America.

The combined research into ecological and cultural changes in one common interdisciplinary project has been able to demonstrate convincingly how important it is to interpret cultural developments against the background of ecological changes. The positioning of the area of investigation on the very sensitive desert margin of the Atacama has proven to be methodologically very advantageous.

The changeable history of the region reflected in the varying settlement patterns over the course of time can also be traced in individual histories. The numerous burials recovered during excavation work offered a good basis for stable isotope research, which showed the long-range exchange relationships of the inhabitants at the base of the Andes with the coast to the west and the mountains to the east. It was also possible to demonstrate that people spent whole phases of their lives in different ecological zones. The palaeogenetic research, still a pioneering discipline in South America, could show the large potential of this relatively new procedure for the investigation of settlement dynamics and migrations of the pre-Hispanic inhabitants. The results indicate that in the course of time considerable movements of populations occurred on the American continent and especially in the Andean area that are reflected in the genetic makeup in the Palpa region.

The geophysical prospection methods, which were newly developed and adapted to the special situation in Peru, have likewise highlighted their large potential for South American archaeology and especially the settlement survey

in Palpa. Particularly the valley floors, where the strong sedimentation of the rivers inhibited a successful surface survey but preserved sites from the destruction of grave robbers, let many finds be expected in the future, especially from earlier phases in the cultural development.

Finally, through the results from all project parts a contribution to the solution of one of the most burning questions in the area of investigation could be made, that is, the history and meaning of the geoglyphs. Against the background of an aridisation process, reaching its climax at around 600 AD and responsible for the very dynamic settlement history, the landscapes covered with geoglyphs amidst the floodplains represent a ritual landscape for water and fertility rituals. With the help from new documentation methods, recording not only the geoglyphs but also their predecessor the petroglyphs, this interpretation was developed from the analysis of an abundance of data. For the dating of the geoglyphs new methods were developed that can likewise be transferred to other stone surfaces. In this way, the history of the development of the geoglyphs can be linked in a meaningful manner to the settlement history and the ecological development of the landscape.

References

AAAI (2008) American Association for Artificial Intelligence. http://www.aaai.org (Accessed 2008-04-16)

Aitken MJ (1974) Physics and Archaeology. Clarendon Press, Oxford

Aitken MJ, Xie J (1992) Optical dating using infrared diodes: young samples. Quatern Sci Rev 11:147–152

Akca D (2007) Least Squares 3D surface matching. PhD thesis. Diss. Nr. 92, Institute of Geodesy and Photogrammetry, ETH Zurich

Akca D, Gruen A (2007) Generalized Least Squares multiple surface matching. ISPRS Workshop on Laser Scanning 2007 and SilviLaser 2007, Espoo Finland, 12–14 September, International Archives of Photogrammetry, Remote Sensing and Spatial Information Sciences, vol 36, Part 3/W52:1–7

Allison MJ (1979) Paleopathology in Peru. Nat Hist 88:74–82

Allison M, Gersten M, Munizaga J, Santoro C, Focacci G (1981) La práctica de la deformación craneana entre los pueblos andinos precolombinos. Chungara Chile 7:238–260

Alva W (1986) Cerámica Temprana en el Valle de Jequetepeque, Norte del Perú. Mat. Allg. Vergl. Arch. 32. München

Alva W (1992) Orfebrería del Formativo. In: Lavalle JA (ed) Oro del Antiguo Perú. Colleción arte y tesoros del Perú, pp 17–116

Alva W (2001) Gold aus dem alten Peru. Die Königsgräber von Sipán. Katalog der Ausstellung Bonn 2000–2001, Kunst- und Ausstellungshalle, Bonn

Alvarez A (1995) La cerámica arqueológica del Ecuador. In: Guinea Bueno M, Bouchard J-F, Marcos J (eds) Cultura y medio ambiente en el área andina septentrional. Quito, pp 434–481

Ambrose SH, Butler BM, Hanson DB, Hunter-Anderson RL, Krueger HW (1997) Stable isotope analysis of human diets in Marianas Archipelago, western Pacific. Am J Phys Anthropol 104:343–361

Anand R, Gilkes R (1987) The association of maghemite and corundum in Darling Range laterites, Western Australia. Austr J Soil Res 25:303–311

Angel L (1984) Health as a crucial factor in the changes from hunting to developed farming in the Eastern Mediterranean. In: Cohen M. and Armelagos G. (eds) Paleopathology at the origins of agriculture. Academic Press, New York, pp 51–73

Angulo P (1995) Ortopedia y traumatología, patología del aparato locomotor. Tomo 2: Afecciones Traumáticas, CONCYTEC, Lima

Anschuetz KF, Wilshusen RH, Scheick CL (2001) An archaeology of landscapes: perspectives and directions. J Archaeol Res 9:157–211

Anthony DW (1990) Migration in Archaeology: The Baby and the Bathwater. Am Anthropol 92:895–914

Araujo AGM, Neves WA, Piló LP, Atui JPV (2005) Holocene dryness and human occupation in Brazil during the "Archaic Gap". Quat Res 64:298–307
Aravena R, Suzuki O, Peña H, Polastri A, Fuenzalida H, Grilli A (1999) Isotope composition and origin of the precipitation in Northern Chile. Appl Geochem 14:411–422
Aravena R, Suzuki O, Pollastri A (1989) Coastal fog and its relation to groundwater in the IV region of northern Chile. Chem Geol (Isot geosci sect) 79:83–91
Argollo J, Mourguiart P (2000) Late Quaternary climate history of the Bolivian Altiplano. Quat Int 72:37–51
Arrowsmith P, Hughes SK (1988) Entrainment and transport of laser ablated plumes for subsequent elemental analysis. Appl Spectrosc 42:1231–1239
Aveni AF (2000a) Between the lines: the mystery of the giant ground drawings of ancient Nasca, Peru. University of Texas Press, Austin
Aveni AF (2000b) Nasca: Eighth wonder of the world? British Museum Press, London
Aveni AF (ed) (1990) The lines of Nazca. American Philosophical Society, Philadelphia
BAE Systems National Security Solutions Inc. (2006) Socet Set User's Manual – Version 5.3
Baker B, Dupras T, Tocheri M (2005) The osteology of infants and children. Texas A&M University Press, Texas
Baker P, Rigsby C, Seltzer G, Fritz S, Lowenstein T, Bacher N, Veliz C (2001) Tropical climate changes and orbital timescales on the Bolivian Altiplano. Nature 409:698–701
Ballesteros R (2002) Traumatología y medicina deportiva. Paraninfo Thompson Learning, Madrid
Baltsavias E (1991) Multi-Photo geometrically constrained matching. PhD Diss. Nr. 49, Institute of Geodesy and Photogrammetry, ETH Zurich
Baltsavias E, Grün A, Van Gool L, Peteraki M (eds) (2006) Recording, Modeling and Visualization of Cultural Heritage. Taylor & Francis Group, London
Bargalló M (1955) La minería y la metalurgia en la América Española durante la época Colonial. Fondo de Cultura Económica, México
Barnes RM (1996) Application of tertiary amines for arsenic and selenium signal enhancement and polyatomic interference reduction in ICP-MS analysis of biological samples. Fresenius J Anal Chem 355:433–441
Barnett T, Chalmers A, Díaz-Andreu M, Ellis G, Longhurst P, Sharpe K, Trinks I (2005) 3D laser scanning for recording and monitoring rock art erosion. International Newsletter on Rock Art (INORA) 41:25–29
Baraybar JP (1987) Cabezas trofeo Nasca: Nuevas evidencias. Gaceta Arqueológica Andina, Perú 15:6–10
Bayes TR (1763) An essay towards solving a problem in the doctrine of chances. Philos Trans R Soc Lond 53:370–418
Becker H (1999) Duo- and quadro-sensor configuration for high-speed/high resolution magnetic prospecting with caesium magnetometer. In: Fassbinder JWE, Irlinger WE (Ed) Archaeological Prospection, Arbeitsh Bayer Landesamt f Denkmalpflege 108, München, pp 100–105
Beja-Pereira A, Caramelli D, Lalueza-Fox C, Vernesi C, Ferrand N, Casoli A, Goyache F, Royo LJ, Conti S, Lari M, Martini A, Ouragh L, Magid A, Atash A, Zsolnai A, Boscato P, Triantaphylidis C, Ploumi K, Sineo L, Mallegni F, Taberlet P, Erhardt G, Sampietro L, Bertranpetit J, Barbujani G, Luikart G, Bertorelle G (2006) The origin of European cattle: evidence from modern and ancient DNA. Proc Natl Acad Sci USA 103(21):8113–8118
Bellot-Gurlet L, Dorighel O, Poupeau G (2008) Obsidian provenance studies in Colombia and Ecuador: obsidian sources revisited. J Archaeol Sci 35:272–289
Bendall C (2003) The application of trace element and isotopic analyses to the study of Celtic gold coins and their metal sources. Diss. Johann Wolfgang Goethe-Universität, Frankfurt
Bendea HF, Chiabrando F, Tonolo FG, Marenchino D (2007) Mapping of archaeological areas using a low-cost UAV the Augusta Bagiennorum Test site. In: CIPA (ed.) XXI International Symposium Proceedings, Athens (on CD-ROM)

Benfer R. (1986) Holocene coast adaptations: Changing demography and health at the fog oasis of paloma, Peru, 5000–7800 B.P. In: Matos R, Turpin S.A. and H.E. Eling (eds) Andean Archaeology. Papers in Memory of Clifford Evans. Monograph XXVII. Institute of Archaeology. University of California, Los Angeles, pp 45–64

Benfer R. (1990) The preceramic period site of paloma, Peru: Bioindications of improving adaptation to sedentism. Latin Am Antiq 1:284–318

Bennett WC (1948) The peruvian co-tradition. In: Bennett WC (ed) A Reappraisal of Peruvian Archaeology. Memoirs of the Society for American Archaeology 4. Menasha, Wisconsin, pp 1–7

Benzoni, Girolamo, Historia del Mondo Nuovo, Venezia 1565 (Reprinted 1572)

Beraldin J-A (2004) Integration of laser scanning and close-range photogrammetry – The last decade and beyond. International Archives of Photogrammetry, Remote Sensing and Spatial Information Sciences & SIS 35(B7):972–983

Berktold A (1997) Geoelektrik – Vierpunkt-Verfahren. In: Beblo M (ed) Umweltgeophysik. Ernst & Sohn, Berlin, pp 97–129

Biermann D (2001) Tejidos de la cultura Nasca - informe intermedio de los objetos textiles de las excavaciones en Palpa. In: Solanilla V (ed) II Jornados internacionales sobre textiles precolombinos. Departamento de Arte de la Universidad Autónoma de Barcelona, Barcelona, pp 347–358

Binford LR (1971) Mortuary Practices: Their study and their potential. In: Brown JA (ed) Approaches to the social dimensions of mortuary practices. Memoirs of the Society for American Archaeology 25. Washington DC, pp 6–29

Binford MW, Kolata AL, Brenner M, Janusek JW, Seddon MT, Abbott MB, Cutis JH (1997) Climate variation and the rise and fall of Andean civilization. Quat Res 47:235–248

Birchall J, O'Connel TC, Heaton THE, Hedges RE (2005) Hydrogen isotopes in animal body protein reflect trophic level. J Animal Ecol 74:877–881

Bird JB (1951) South American radiocarbon dates. Mem Soc Am Archaeol 8:37–49

Bischof H (1998) El Período Inicial, el Horizonte Temprano, el Estilo Chavín y la realidad del proceso formativo en los Andes Centrales. Universidad de Lima (ed) I Encuentro Internacional de Peruanistas. Estado de los estudios histórico-sociales sobre el Perú a fines del siglo XX. Tomo I. Lima, pp 57–70

Bischof H (2000) Cronología y cultura en el formativ centroandino. Estudios Latinoamericanos 20:41–71

Blagg MM (1975) The bizarre innovation in Nasca. Unpublished MA thesis, Department of Art History, University of Texas, Austin

Blais F (2004) Review of 20 years of range sensor development. J Electron Imaging 13:231–240

Blasco Bosqued C, Ramos Gómez J (1980) Cerámica Nazca. Valladolid

Blender (2008) Open source 3D graphics creation website: http://www.blender.org/cms/Home.2.0.html (accessed 29 April 2008)

Blom DE, Janusek JW, Buikstra JE (2003) A reevaluation of human remains from Tiwanaku. In: Kolata A (ed) Tiwanaku and Its Hinterland: Archaeology and Paleoecology Investigations of an Andean Civilization: Volume 2, Urban and Rural Archaeology. Smithsonian Institution Press, Washington, DC, pp 435–446

Bowles J, Gee J, Hildebrand J, Tauxe L (2002) Archaeomagnetic intensity results from California and Ecuador: Evaluation of regional data. Earth Planet Sci Lett 203:967–981

Boyle RW (1979) The geochemistry of gold and its deposits. Geological Survey of Canada Bulletin 280

Brekhus PJ, Armstrong WD (1934) A method for the separation of enamel, dentin, and cementum. J Dent Res 14:23–29

Briones L (2006) The geoglyphs of the north Chilean desert: an archaeological and artistic perspective. Antiquity 80:9–24

Bronk Ramsey C (1995) Radiocarbon and analysis of stratigraphy: The OxCal Program. Radiocarbon 37(2):425–430

Bronk Ramsey C (2001) Development of the radiocarbon calibration program. Radiocarbon 43(2A):355–363
Bronk Ramsey C (2008) Deposition models for chronological records. Quat Sci Rev 27(1–2):42–60
Brown J (1995) Andean mortuary practices in perspective. In: Dillehay TD (ed) Tombs for the living: Andean mortuary practices. Dumbarton Oaks Research Library and Collection, Washington DC, pp 391–405
Browne D (1992) Further archaeological reconnaissance in the Province of Palpa, Department of Ica, Perú. In: Saunders NJ (ed) Ancient America: Contributions to New World archaeology. Oxbow Monograph 24, pp 77–116
Browne D, Silverman H, García R (1993) A cache of 48 Nasca Trophy Heads from Cerro Carapo, Peru. Latin American Antiquity, USA 4:274–294
Buck CE, Millard AR (2004) Tools for constructing chronologies. Springer, London
Buckberry JL, Chamberlain AT (2002) Age estimation from the auricular surface of the ilium: a revised method. Am J Phys Anthropol 119:231–239
Buikstra JE (1991) Out of the appendix and into the dirt: Comments on thirteen years of bioarchaeological research. In: Powell M.L., Bridges P and Wagner A.M. (eds) What mean these bones? Studies in Southeastern Bioarchaeology. The University of Alabama Press, Tuscaloosa and London, pp 172–188
Buikstra JE (2006) Preface. In: Buikstra J and Beck L (eds) Bioarchaeology, the contextual analysis of human remains. Academic Press, San Diego, pp. xvii–xx
Buikstra JE, Tomczak P, Lozada Cerna MC, Rakita GFM (2005) Chiribaya political economy: a bioarchaeological perspective. In: Rakita GFM, Buikstra JE, Beck LA, Willimas S (eds) Interacting with the Dead: Perspectives on mortuary archaeology for the new millennium. University Press Florida, Gainsville, pp 66–80
Buikstra JE, Ubelaker D. (1994) Standards for data collection from human skeletal remains. Arkansas Archaeological Survey Research Series 44, Fayetteville, Arkansas
Burger J, Hummel S, Hermann B, Henke W (1999) DNA preservation: a microsatellite-DNA study on ancient skeletal remains. Electrophoresis 20:1722–1728
Burger RL (1981) The Radiocarbon evidence for the temporal priority of Chavin de Huantar. Am Antiq 46(3):592–602
Burger RL (1985) Prehistoric stylistic change and cultural development at Huaricoto, Peru. National Geographic Research 1(4):505–534
Burger RL, Asaro F, Michel HV, Stross FH, Salazar E (1994) An Initial Consideration of Obsidian Procurement and Exchange in Prehispanic Ecuador. Latin Am Antiq 5,3:228–255
Burger RL, Glascock MD (2000) Locating the quispisisa obsidian source in the department of ayacucho, Peru. Latin Am Antiq 11,3:258–268
Burger RL, Gordon R (1998) Early central andean metalworking from mina perdida, Peru. Science 282/5391:1108–1111
Burger RL, Lau GF, Ponte VM, Glascock MD (2006) The history of prehispanic obsidian procurement in highland Ancash. In: Herrera A, Orsini C, Lane K (eds) La Complejidad Social an la Sierra de Ancash: Trabajos de la primera y segunda Mesa Redonda de Arqueología de la Sierra de Ancash. Milan, pp 103–120
Burger RL, Mendieta Matos R (2002) Atalla: A center on the periphery of the chavin horizon. Latin Am Antiq 13:153–177
Burger RL, Mohr Chávez KL, Chávez SJ (2000) Through the glass darkly: Prehispanic Obsidian Procurement and Exchange in Southern Peru and Northern Bolivia. J World Prehistory 14,3:267–362
Burgess S (1999) Chiribayan skeletal pathology on the South Coast of Peru: Patterns of Production and Comsumption. PhD thesis. Diss. University of Chicago, Illinois
Burmeister S (2000) Archaeology and Migration. Curr Anthropol 41:539–567
Byers S. (2002) Introduction to forensic anthropology. Allyn and Bacon, London
Calaway M (2005) Ice-cores, sediments and civilisation collapse: a cautionary tale from Lake Titicaca. Antiquity 79:778–790

Canfield DE (2001) Biogeochemistry of sulphur isotopes. Rev Min Geochem 2001:607–636
Capasso L, Kennedy K, Wilczak C (1999) Atlas of occupational markers on human remains. Terrano
Carcedo P (1998) Cobre del Antiguo Perú/The copper of Ancient Peru. In: Lavalle JA (ed) Cobre del Antiguo Perú/The copper of ancient Peru. Lima, pp 53–233
Carmichael PH (1988) Nasca mortuary customs: death and ancient society on the south coast of Perú. Ph. D. Diss. Department of Archaeology, University of Calgary, Ann Arbor
Carmichael PH (1995) Nasca burial patterns: social structure and mortuary ideology. In: Dillehay TD (ed) Tombs for the living: Andean mortuary practices. Dumbarton Oaks Research Library and Collection. Washington DC, pp 161–187
Carmichael P, Rowe J (1986) Nasca Pottery Construction in Nawpa Pacha. An International series for Andean Archaeology, Vol. 24, Institute of Andean Studies, Berkeley, 128 pp
Cartajena I, Núnez L, Grosjean M (2007) Camelid domestication on the western slope of the Puna de Atacama, northern Chile. Anthropozoologica 42(2):155–173
Caviedes C (2005) El Niño – Klima macht Geschichte. Wissenschaftliche Buchgesellschaft, Darmstadt
Chandler JH, Bryan P, Fryer JG (2007) The development and application of a simple methodology of recording rock art using consumer-grade digital cameras. Photogramm Rec 22 (117):10–21
Chandler-Ezell K, Pearsall DM, Zeidler JA (2006) Root and tuber phytoliths and starch grains document manioc (Manihot esculenta), arrowroot (Maranta arundinacea), and llerén (Calathea sp.) at the Real Alto site, Ecuador. Econ Bot 60:103–120
Chapdelaine C, Kennedy G, Uceda Castillo S (2001) Neutron activation analysis of metal artefacts from the Moche Site, North Coast of Peru. Archaeometry 43,3:373–391
Chapman R, Klavs R (1981) Approaches to the archaeology of death. In: Chapman R, Kinnes I, Randsborg K (eds) The archaeology of death. Cambridge University Press, New York, pp 1–24
Chauvin A, Garcia Y, Lanos P, Laubenheimer F (2000) Paleointensity of the geomagnetic field recovered on archaeomagnetic sites from France. Phys Earth Planet Inter 120:111–136
Chengyu W, Bush MB, Curtis JH, Kolata AL, Dillehey TD, Binford MW (2006) Deglaciation and Holocene climate change in the western Peruvian Andes. Quatern Res 66:87–96
Chippindale CH, Nash G (2004) The figured landscapes of rock-art: looking at pictures in place. Cambridge University Press, Cambridge
Chwala A, Stolz R, Ijsselsteijn R, Schulze V, Ukhansky N, Meyer HG, Schüler T (2001) SQUID gradiometers for archaeometry. Supercond Sci Technol 14:1111–1114
Cieza de León P de (1553[1880]) Segunda Parte de la crónica del Perú, que trata del señorío de los Incas Yupanquis y de sus grandes hechos y gobernación. Bibliotheca Hispano-Ultramarina 5. Madrid
Clark A (1996) Seeing beneath the soil: Prospecting methods in archaeology. B.T.Batsford Ltd., London
Clarke J, Braginski AI (2004) The SQUID handbook, Vol 1. Wiley-VCH Verlag, Weinheim
Clutton-Brock J (1999) A natural history of domesticated mammals. Cambrige University Press, Cambridge
Conolly J, Lake M (2006) Geographical information systems in archaeology. Cambridge University Press, Cambridge
Cook AG (1987) The middle horizon ceramic offerings from conchopata. Ñawpa Pacha 22–23:49–90
Coplen TB, Hopple JA, Böhlke JK, Peiser HS, Rieder SE, Krouse HR, Rosmann KJR, Ding T, Vocke Jr RD, Revesz KM, Lamberty A, Taylor P, De Bievre P (2003) Compilation of minimum and maximum isotope ratios of selected elements in naturally occurring terrestrial materials and reagents. U.S. Geological Survey Water-Res Investig Rep 01–4222
Cordy-Collins A (1966) An iconographic study of the chavín textiles from the South Coast of Peru: The discovery of a Precolumbian Catechism. Unpublished PhD. Diss. University of California, Los Angeles

Cosmas J, Itagaki T, Green D, Grabczewski E, Gool LV, Zalesny A, Vanrintel D, Leberl F, Grabner M, Schindler K, Karner K, Gervautz M, Hynst S, Waelkens M, Pollefeys M, DeGeest R, Sablatnig R, Kampel M (2001) 3D MURALE: A multimedia system for archaeology. In: Arnold DB, Chalmers A, Fellner DW (eds) Proc. of the international conference on virtual reality, archaeology and cultural heritage. Glyfada, pp. 297–305

Coudrain A, Loubet M, Condom T, Talbi A, Ribstein P, Pouyaud B, Quintanilla J, Dielin C, Dupré B (2002) Données isotopiques (87Sr/86Sr) et changements depuis 15 000 ans sur L'Altiplano andin. Hydrol Sci 47(2):293–306

Craig PP (1992) The chemistry of ancient life – Isotopes as dietary tracers. Perspect Sci 5:21–29

Dansgaard W (1964) Stable isotopes in precipitation. Tellus 16/4:436–468

Date AR, Jarvis KE (1989) Applications of inductively coupled plasma mass spectrometry. In: Date AR, Gray AL, (eds), Blackie, London, pp 43–70

David I, Welch AJE (1956) The oxidation of magnetite and related spinels. Trans Farad Soc. 52:1642–1650

Davidson D (1974; 2001) On the very idea of a conceptual scheme. In: Inquiries into truth and interpretation. 2nd Edition. Oxford University Press, Oxford, New York, pp 183–198

De Jong AFM, Becker B, Mook WH (1986) High-precision calibration of the radiocarbon time scale, 3930–3230 cal BP. Radiocarbon 28:939–942

De Vries H (1958) Variation of the concentration of radiocarbon with time and location on earth. Kon Ned Akad Wetensch Proc Ser 61:267–281

Dell CJ (1972) An occurrence of greigite in Lake Superior sediments. Am Mineral 57:1303–1304

DeNiro MJ, Hastorf CA (1985) Alteration of 15 N/14 N and 13C/12C of plant matter during initial stages of diagenesis: Studies utilizing archaeological specimens from Peru. Geochim Cosmochim Acta 49:97–115

DePiero FW, Trivedi MM (1996) 3-D Computer vision using structured light: design, Calibration, and implementation issues. Adv Comput 43:243–278

Diamond J (2002) Evolution, consequences and future of plant and animal domestication. Nature 418:700–707

Díaz-Andreu M, Brooke C, Rainsbury M, Rosser N (2006) The spiral that vanished: the application of non-contact recording techniques to an elusive rock art motif at Castlerigg stone circle in Cumbria. J Archaeol Sci 33:1580–1587

Dillehay TD (1999) The late pleistocene cultures of South America. Evolution Anthropol 7:206–216

Dillehay TD, Netherly PJ, Rossen J (1989) Middle Preceramic public and residential sites on the forested slope of the western Andes, northern Peru. Am Antiq 54(4):733–759

Dixon EJ (2001) Human colonization of the Americas: timing, technology and process. Quat Sci Rev 20:277–299

Donnan CB (1964) An early house from Chilca, Perú. Am Antiq 30:137–144

Donnan CB (1992) Oro en el arte Moche. In: Lavalle JA (ed) Oro del Antiguo Perú. Colleción arte y tesoros del Perú, pp 119–193

Dornelles CL, Bonatto SL, De Freitas LB, Salzano FM (2005) Is haplogroup X present in extant South American Indians? Am J Phys Anthropol 127:439–448

Drusini A (1987) Análisis de los restos óseos humanos procedentes de Cahuachi y Pueblo Viejo. In Orefici G (ed) Proyecto Nasca 1984–1988. Informe Final de la Campaña 1986. Ms presented to the National Institute of Culture, Lima, pp 513–518

Drusini A (1988) Análisis de los restos óseos humanos procedentes de Cahuachi y Pueblo Viejo. In Orefici G. Proyecto Nasca 1984–1988. Informe Final de la Campaña 1987 pp. 1767–1786. Ms presented to the National Instiurte of Cultura, Lima, pp 1767–1786

Drusini A, M. Rippa Bonati, V. Visconti di Modrone (1988) Studio antropologico dei reperti provenienti dal sito archeologico di Pueblo Viejo, Nasca (Perú). In: Archeologia, Scienza e Società nell'America Precolombiana, Atti del Convegno Internazionale del Centro Italiano Studi e Ricerche Archeologiche Precolombiane, CISRAP, Brescia, pp 53–82

Duller, GAT, Bøtter-Jensen L, Markey BG (1997) A luminescence imaging system based on A CCD Camera. Radiation Measurement 27:91–99

Dunlop DJ, Özdimir O (1997) Rock magnetism: Fundamentals and frontiers. Cambridge

Durrant SF (1999) Laser ablation inductively coupled plasma mass spectrometry: achievements, problems, prospects. J Anal At Spectrom 14:1385–1403

Dussubieux L, Golitko M, Williams PR, Speakman RJ (2007) LA-ICP-MS analysis applied to the characterization of Peruvian Wari ceramics. In: Glascock MD, Speakman RJ, Popelka-Filcoff RS (eds) Archaeological chemistry: Analytical techniques and archaeological interpretation. ACS Symposium Series No. 968. pp 349–363

Ebnöther M (1999) Vom Toten Meer zum Stillen Ozean. Sammlung Ebnöther, Museum zu Allerheiligen Schaffhausen. Hatje, Ostfildern-Ruit

Eerkens JW, Vaughn KJ, Carpenter TR, Conlee CA, Linares Grados M, Schreiber K (2008) Obsidian hydration dating on the South Coast of Peru. J Archaeol Sci 35:2231–2239

Eggert M (2001) Prähistorische Archäologie: Konzepte und Methoden. Francke, Tübingen Basel

Eisenbeiss H (2003) Positions- und Orientierungsbestimmung eines autonomen Helikopters – Vergleich zwischen direkter Georeferenzierung und Aerotriangulation mit Videobilddaten. Diploma Thesis. Universität Dresden

Eisenbeiss H (2004) A mini unmanned aerial vehicle (UAV): System overview and image acquisition. International workshop on processing and visualization using high resolution imagery. International archives of photogrammetry, remote sensing and spatial information sciences, Vol XXXVI-5/W1, 18–20 November, Pitsanulok, Thailand (on CD-ROM)

Eisenbeiss H (2006) Applications of photogrammetric processing using an autonomous helicopter. ISPRS Commission I Symposium, Paris, France, 03–06. July. International Archives of Photogrammetry, Remote Sensing and Spatial Information Sciences, Vol XXXVI-Part1/B, (on CD-ROM)

Eisenbeiss H (2008) The autonomous mini helicopter: A powerful platform for mobile mapping. The International Archives of the Photogrammetry, Remote Sensing and Spatial Information Sciences. Vol. XXXVII. Part B1, Beijing, China, pp 977–983

Eisenbeiss H, Zhang L (2006) Comparison of DSMs generated from mini UAV imagery and terrestrial laser scanner in a cultural heritage applications. ISPRS Commission V Symposium, Image Engineering and Vision Metrology, Dresden, Germany, 25–27. September. International Archives of Photogrammetry, Remote Sensing and Spatial Information Sciences XXXVI(5):90–96

Eisenbeiss H, Baltsavias E, Pateraki M, Zhang L (2004) Potential of IKONOS and QUICKBIRD imagery for accurate 3D point positioning, ortho-image and DSM generation. International Archives of Photogrammetry, Remote Sensing and Spatial Information Sciences, vol 35, Part 3 (and on DVD), XXth ISPRS Congress, 12–23 July, Istanbul Turkey

Eisenbeiss H, Lambers K, Sauerbier M (2007) Photogrammetric recording of the archaeological site of Pinchango Alto (Palpa, Peru) using a mini helicopter (UAV). In: Figueiredo A, Velho GL (eds) The World is in your Eyes. Proceedings of the XXXIII computer applications and quantitative methods in archaeology conference (March 2005 – Tomar, Portugal). Tomar, pp 175–184

Eisenbeiss H, Lambers K, Sauerbier M, Zhang L (2005) Photogrammetric documentation of an archaeological site (Palpa, Peru) using an autonomous model helicopter. Proceedings of the XXth CIPA International symposium, Torino, Italy. International archives of photogrammetry, Remote sensing and spatial information sciences XXXIV(5/C34):238–243

Eisenbeiss H, Sauerbier M, Zhang L, Grün A (2005) Mit dem Modellhelikopter über Pinchango Alto. Geomatik Schweiz 9:510–515

Eitel B (2006) Reaktive Räume. Zeitschrift für Geomorphologie NF Suppl Vol 148:78–80

Eitel B (2007) Kulturentwicklung am Wüstenrand – Aridisierung als Anstoß für frühgeschichtliche Innovation und Migration. In: Wagner GA (2007) Einführung in die Archäometrie. Springer, Berlin Heidelberg New York, pp 301–319

Eitel B, Hecht S, Mächtle B, Schuhkraft G, Kadereit A, Wagner GA, Kromer B, Unkel I, Reindel M (2005a) Geoarchaeological evidence from desert Loess in the Nazca-Palpa Region, Southern Peru: Palaeoenvironmental changes and their impact on pre-Columbian cultures. Archaeometry 47:137–158

Eitel B, Hecht S, Mächtle B, Schukraft G (2004a) Warum verschwand die Nasca-Kultur? Umwelt- und Kulturentwicklung in Süd-Peru. Petermanns Geographische Mitteilungen 148,6:89–92

Eitel B, Kadereit A, Blümel WD, Hüser K, Lomax J, Hilgers A (2006) Fluvial deposits in the Upper Hoanib river catchment, northwestern Namibia: New evidence of environmental changes before and after the Last Glacial Maximum at the eastern Namib desert-margin. Palaeogeograp Palaeoclimat Palaeoecol 234:201–222

Eitel B, Kadereit A, Blümel WD, Hüser K., Kromer B (2005b) The Amspoort Silts, northern Namib Desert (Namibia): Formation, age and palaeoclimatic evidence of river-end deposits. Geomorphology 64:299–314

Eitel B, Mächtle B (2006) Holozäner Umweltwandel in der nördlichen Atacama und sein Einfluss auf die Nasca-Kultur (Südperu). Geographische Rundschau 58:30–36

Eitel B, Mächtle B, Schukraft G (2004b) Geomorphologisch-bodenkundliche Untersuchungen zur Rekonstruktion der Klima- und Landschaftsentwicklung im Umfeld der ehemaligen Siedlungsflächen der Nasca-Kultur/Investigaciones geomorfológicas y edafológicas para la reconstrucción del clima y del paisaje en las antiguas áreas de ocupación de la cultura Nasca. In: Reindel M, Wagner GA (eds) Neue naturwissenschaftliche Methoden und Technologien für die archäologische Forschung in Palpa, Peru/Nuevos métodos y tecnologías para la investigación arqueológica en Palpa, Perú. Publikation zur Feldkonferenz des Projektverbundes Nasca: Entwicklung und Adaption archäometrischer Techniken zur Erforschung der Kulturgeschichte. Lima, pp 15–18

Elias RW, Hirao Y, Patterson CC (1982) The circumvention of the natural biopurification of calcium along nutrient pathways by atmospheric inputs of industrial lead. Geochim Cosmochim Acta 46:2561–2580

Emmerich A (1965) Sweat of the sun and tears of the moon. Seattle

Emmerich A (1992) Sudor del sol y lágrimas de la luna. In: Lavalle JA (ed) Oro del Antiguo Perú. Colleción arte y tesoros del Perú, pp 195–235

Engel FA (1960) Un groupe humain datant de 5000 ans à Paracas, Pérou. Journal de la Société des Americanistes 49:7–35

Engel FA (1963) Notes relatives à des explorations archéologique à Paracas et sur de la côte du Pérou. Travaux de l'Institut Francais des Études Andines 9:1–72

Engel FA (1966) Geografía humana prehistórica y agricultura precolombiana de la Quebrada de Chilca. Lima

Engel FA (1980) Prehistoric Andean Ecology. Man, Settlement and Environment in the Andes. Paloma. New York

Engel FA (1987) De las begonias al maíz. Vida y producción en el Perú antiguo. Lima

Engel FA (1988) Ecología prehistórica andina. El hombre, su establecimiento y el ambiente de los Andes. La vida en tierras áridas y semiáridas. Chilca Pueblo 1. Implementos de hueso. Lima

Engel FA (1991) Un desierto en tiempos prehispánicos. Rio Pisco, Paracas, Río Ica. Lima

Epstein SM, Shimada I (1983) Metalurgia de Sicán: Una Reconstrucción de la Producción de la Aleación de Cobre en El Cerro de los Cementerios, Peru. Beiträge zur Allgemeinen und Vergleichenden Archäologie 5: 379–430

Evans C, Meggers BJ (1960) A New Dating Method Using Obsidian: pt. 2. An Archaeological Evaluation of the Method. Am Antiq 25:253–257

Evans ME, Heller F (2004) Environmental magnetism. Academic Press, Amsterdam

Excoffier L Schneider S (2005) Arlequin ver. 3.0: An integrated software package for population genetics data analysis. Evol Bioinformatics Online 1:47–50

Fassbinder JWE (1994) Die magnetischen Eigenschaften und die Genese ferrimagnetischer Minerale in Böden im Hinblick auf die magnetische Prospektion archäologischer Bodendenkmäler, Leidorf, Buch am Erlbach

Fassbinder JWE (2003) Neuland unterm Magnetometer: Prospektion zur Erforschung vorspanischer Kulturen in Nasca und Palpa, Peru. Denkmalpflege Informationen 125:44–46

Fassbinder JWE (2004) Prospektion in Nasca, Peru. Denkmalpflege Informationen 129:59–60

Fassbinder JWE (2006) Neue Ergebnisse der Magnetometerprospektion auf den Geoglyphen von Nasca und Palpa, Peru. Denkmalpflege Informationen 134:61–62

Fassbinder JWE (2007) Unter Acker und Wadi: Magnetometerprospektion in der Archäologie. In: Wagner GA (ed) Einführung in die Archäometrie. Springer, Berlin Heidelberg New York, pp 53–73

Fassbinder JWE, Ebner D (2007) Schwaches Magnetfeld – starke Befunde: Magnetometerprospektion auf neu entdeckten paracaszeitlichen Siedlungen in Peru. Denkmalpfl Informationen 137:64–67

Fassbinder JWE, Gorka T (2007a) Magnetometry on the geoglyphs of palpa and nasca (Peru). In: Teichert B, Rust C (eds) Nasca-symposium 2006. Zentrum für interdisziplinäre Forschung (ZiF) der Universität Bielefeld. Dresden, pp 71–76

Fassbinder JWE, Gorka T (2007b) Neue Methoden der Magnetometerprospektion für die Archäologie: Das Horizontalgradiometer. Das Arch Jahr Bayern 2006:183–185

Fassbinder JWE, Hecht S (2004) Geophysikalische Untersuchungen zur Erforschung vorspanischer Kulturen in Palpa/Investigaciones geofísicos para el estudio de las culturas prehispánicas en Palpa. In: Reindel M, Wagner GA (eds) Neue naturwissenschaftliche Methoden und Technologien für die archäologische Forschung in Palpa, Peru/Nuevos métodos y tecnologías para la investigación arqueológica en Palpa, Perú. Publikation zur Feldkonferenz des Projektverbundes "Nasca: Entwicklung und Adaption archäometrischer Techniken zur Erforschung der Kulturgeschichte". Lima, pp 19–22

Fassbinder JWE, Reindel M (2004a) Magnetometry on the geoglyphs of Palpa and Nasca (Peru). Geophysical Research Abstracts 6

Fassbinder JWE, Reindel M (2004b) Magnetometry on the geoglyphs of Palpa and Nasca, Peru. 5th EIGG Meeting Recent work in archaeological geophysics, London, pp 22–25

Fassbinder JWE, Reindel M (2005) Magnetometer prospection as research for pre-spanish cultures at Nasca and Palpa, Peru. Proceed 6th International Conference on Archaeological Prospection. Rome, pp 6–10

Fassbinder JWE, Stanjek H (1993) Occurrence of magnetic bacteria in archaeological soil. Archaeologia Polona 31:117–128

Fassbinder JWE, Stanjek H (1994) Magnetic properties of biogenic soil greigite (Fe3S4). Geophys Res Lett 21:2349–2352

Fassbinder JWE, Stanjek H, Vali H (1990) Occurrence of magnetic bacteria in soil, Nature 343:161–163

Fassbinder JWE, Unkel I, Lambers K (2007) A tiny tool for a large line, magnetometry and dating of Nasca Lines in Palpa, southern Peru. Mach M (ed) Proc. of the EU-ARTECH Seminar Munich, pp 27–39

Fehren-Schmitz L (2008) Molekularanthropologische Untersuchungen zur präkolumbischen Besiedlungsgeschichte des südlichen Perus am Beispiel der Palpa-Region. Diss. Universität Göttingen

Fehren-Schmitz L (in prep) Pre-Columbian population dynamics in coastal southern Peru: Diachronic variations of mt-DNA patterns in the Palpa Region revealed by aDNA analysis

Fehren-Schmitz L, Herrmann B, Hölzl S, Horn P, Rossmann A (2004) Molekulare und isotopische Anthropologie zur Rekonstruktion vorspanischer Lebensumstände in Palpa. In: Reindel M, Wagner GA (eds) Neue naturwissenschaftliche Methoden und Technologien für die archäologische Forschung in Palpa, Peru/Nuevos métodos y tecnologías para

la investigación arqueológica en Palpa, Perú. Publikation zur Feldkonferenz des Projektverbundes, Nasca: Entwicklung und Adaption Archäometrischer Techniken zur Erforschung der Kulturgeschichte/Nasca: Desarrollo y Adaptación de Técnicas Arqueométricas ara la Investigación de la Historia Cultural'. Lima, pp 31–34

Fertig J (1997) Seismik – Prinzip der Methode. In: Knödel K, Krummel H, Lange G (eds) Handbuch zur Erkundung des Untergrundes von Deponien und Altlasten. Bd. 3: Geophysik. Berlin Heidelberg, pp 405–445

Fitzpatrick RW, LE Roux J (1976) Pedogenic and solid solution studies on iron-titanium minerals. In: Barler SW (Ed) Proc Int Clay Conf 1975, Mexico City, Wilmette, pp 585–599

Fix AG (2002) Colonization models and initial genetic diversity in the Americas. Hum Biol 74:1–10

Fontugne M, Usselmann P, Lavallée D, Julien M, Hatté C (1999) El Niño Variability in the Coastal Desert of Southern Peru during the Mid-Holocene. Quat Res 52:171–179

Fox JMW, Aitken MJ (1980) Cooling-rate dependency of thermoremanent magnetisation. Nature 283:462–463

Frantz, JH, Schorsch D (1990) Egyptian red gold. Archaeomaterials 4:133–152

Friedel S (1997) Hochauflösende Geoelektrik – Geoelektrische Tomographie. In: Beblo M (ed) Umweltgeophysik. Ernst & Sohn, Berlin, pp 131–151

Frisancho R (1977) Developmental adaptation to high altitude hypoxia. Int J Biometeorol 21, 2:135–146

Frisancho R, Velásquez T, Sánchez J. (1975) Possible adaptive significance of small body size in attainment of aerobic capacity among high altitude Quechua natives. In: Watts E.S, Jonhston F.E, Lasker G.W (eds) Biosocial Interrelations in Population Adaptation, Paris, pp 55–64

Fryer BJ, Jackson SE, Longerich HP (1995) Design, operation and role of the laser-ablation microprobe coupled with and inductively-coupled plasma-mass spectrometer (LAM-ICP-MS) in the earth sciences. Can Mineral 33:303–312

Fuchs PR, Patschke R, Schmitz C, Yenque G (2006): Im Tal der Kultanlagen. Archäologie in Deutschland 3:12–16

Fuselli S, Tarazona-Santos E, Dupanloup I, Soto A, Luiselli D, Pettener D (2003) Mitochondrial DNA diversity in South America and the genetic history of Andean highlanders. Mol Biol Evol 20:1682–1691

Fux P (2007) Das Petroglyphen-Projekt "Chichictara" in Palpa, Peru. Feldarbeiten im Jahr 2006 und Ausblick. Jahresbericht SLSA 2006:189–205

Fux P, Sauerbier M, Peterhans J, Kersten T, Lindstaedt M (2007) Documentation and interpretation of the petroglyphs of Chichictara, Palpa (Peru), using terrestrial laser scanning and image-based 3D modeling. In: Posluschny A, Lambers K, Herzog I (eds) Layers of perception: Proceedings of the 35th Computer Applications and Quantitative Methods in Archaeology Conference, Berlin, Germany, April 2007. Habelt, Bonn, pp 65–71

Gaisecker T (2006) Pinchango Alto: 3D archaeology documentation using the hybrid 3D laser scan system of RIEGL. In: Baltsavias E, Gruen A, Van Gool L, Pateraki M (eds) Recording, Modeling and Visualization of Cultural Heritage. Taylor & Francis, London, pp 459–464

Gaither C (2004). A growth and developmental study of coastal prehistoric Peruvian populations. PhD thesis. Diss. University of Tulane, New Orleans

Galbraith RF, Roberts RG, Laslett GM, Yoshida H, Olley JM (1999) Optical dating of single and multiple grains of quartz from Jinmium rock shelter (northern Australia): Part I, Experimental design and statistical methods. Archaeometry 41:339–395

Gallet Y, Genevey A, Courtillot V (2003) On the possible occurrence of archeo-magnetic jerks in the geomagnetic field over the past three millennia. Earth Planet Sci Lett 214:237–242

Gallet Y, Genevey A, Fluteau F (2005) Does Earth's magnetic field secular variation control centennial climate change? Earth Planet Sci Lett 236:339–347

Galloway A (1999) Broken bones. Anthropological analysis of blunt force trauma. Charles C. Thomas, Springfield
Gander W, Golub G, Strebel R (1994) Least-squares fitting of circles and ellipses. BIT 34:558–578
Garcia F, Moraga M, Vera S, Henriquez H, Llop E, Aspillaga E, Rothhammer F (2006) mtDNA microevolution in Southern Chile's archipelagos. Am J Phys Anthropol 129:473–481
García Soto R, Pinilla J (1995) Aproximacíon a una secuencia de fases con cerámica temprana de Paracas. J Steward Anthropolog Soc 23 (1–2):43–81
Garcilaso de la Vega (1609[1986]) Wahrhaftige Kommentare zum Reich der Inka, nach: Primera parte de los commentarios reales, que tratan del origen de los Yncas, reyes que fueron del Perú. In: Thiemer-Sachse U (ed) Berlin
Garreaud R, Vuille M, Clement AC (2003) The climate of the Altiplano: observed current conditions and mechanisms of past changes. Paleogeogr, Paleoclim, Paleoecol 194:5–22
Gasparini G, Margolies L (1977) Arquitectura Inka. Caracas
Gayton A, Kroeber AL (1927) The Uhle pottery collections from Nazca. University of California Publications in American Archaeology and Ethnology 36:1–46
Geertz C (1973) Thick description: toward an interpretive theory of culture. In: Geertz C (ed) The interpretation of cultures: Selected Essays. Basic Books, New York, pp 3–30
Geertz C (1995) After the fact: two countries, four decades, one anthropologist. Harvard University Press, Cambridge (Massachusetts)
Genevey A, Gallet Y (2002) Intensity of the geomagnetic field in western Europe over the past 2000 years: New data from ancient French pottery. J Geophys Res 107:EPM1.1-EPM1.17
Genovés S (1967) Proportionality of the Long Bones and their relations to Stature among Mesoamericans. Am J Phys Anthropol 26, 1:67–77
Giesso M, Berón MA, Glascock MD (2008) Obsidian in Western Pampas, Argentina: Source Characterization and Provisioning Strategies. International Association for Obsidian Studies Bulletin 38:15–18
Gil A, Tykot R, Neme G, Shelnut N (2006) Maize on the frontier: isotopic and macrobotanical data from central-western Argentina. In: Staller JE, Tykot RH, Benz BF (eds) Histories of Maize: Multidisciplinary Approaches to the Prehistory, Linguistics, Biogeography, Domestication, and Evolution of Maize. Burlington, MA, pp 199–214
Gilbert MT, Binladen J, Miller W, Wiuf C, Willerslev E, Poinar H, Carlson JE, Leebens-Mack JH, Schuster SC (2007) Recharacterization of ancient DNA miscoding lesions: insights in the era of sequencing-by-synthesis. Nucleic Acids Res 35:1–10
Glascock MD (2002) Obsidian provenance research in the Americas. Accounts of Chemical Research 35(8): 611–617
Glascock MD, Speakman RJ, Burger RL (2007) Sources of Archaeological Obsidian in Peru: Descriptions and Geochemistry. In: Glascock MD, Speakman RJ, Popelka-Filcoff RS (eds) Archaeological chemistry: analytical techniques and archaeological interpretation. ACS Symposium Series No. 968. pp 522–552
Goicoechea AS, Carnese FR, Dejean C, Avena SA, Weimer TA, Franco MHLP, Estalote AC, Palatnik M, Salzano FM (2001) Genetic relationships between amerindian populations of argentinia. Am J Phys Anthropol. 115 [2]:133–143
Goldhausen M (2005) Klimaveränderungen im Spiegel regionalen Siedlungsverhaltens? Eine systematische Bevölkerungsverschiebung im 6. Jh. u. Z. an der zentralen Küste von Peru. Ethnograph-archäolog Z 46:59–89
Goldstein L (1981) One-dimensional archaeology and multi-dimensional people: spatial organization and mortuary analysis. In: Chapman R, Kinnes I, Randsborg K (eds) The archaeology of death. Cambridge University Press, New York, pp 53–69
Gondonneau A, Guerra MF, Barrandon JN (1996) Sur Les Traces De L'ór Monnayé: Recherche De Provenances Par LA-ICP-MS. Rev dArchéometrie 20:23–32

Gonfiantini R, Roche M-A, Olivry J-C, Fontes J-C, Zuppi GM (2001) The altitude effect on the isotopic composition of tropical rains. Chem Geol 181:147–167

González, AR (1979) Pre-columbian metallurgy of northwest argentina: Historical development and cultural process. In: Benson EP (ed) Pre-Columbian Metallurgy of South America, Washington, pp 133–202

Goodman N (1976) Languages of art: an approach to a theory of symbols. Hackett Publishing Company, Indianapolis

Gordus AA, Henderson CE, Shimada I (1996) Electron Microprobe and Neutron Activation Analysis of Gold Artifacts from a 1000 A.D. Peruvian Grave Site. In: Orna MV (ed) Archaeological chemistry: Organic, inorganic, and biochemical analysis. American Chemical Society Symposium Series 625. Washington, D.C, pp 83–93

Gorka T, Fassbinder JWE, Lambers K (2007) Magnetometry on the geoglyphs of Palpa and Nasca (Peru). Studijne Zvesti Arch. Ustavu SAV 41:176–179

Görsdorf J, Reindel M (2002) Radiocarbon dating of the Nasca settlements Los Molinos and La Muña in Palpa, Peru. Geochronometria 21:151–156

Goudie AS, Middleton NJ (2006) Desert dust in the global system. Springer, Berlin Heidelberg New York

Gramsch A (2003) Landschaftsarchäologie – ein fachgeschichtlicher Überblick und ein theoretisches Konzept. In: Kunow J, Müller J (eds) Landschaftsarchäologie und geographische Informationssysteme/The archaeology of landscapes and geographic information systems. Brandenburgisches Landesamt für Denkmalpflege und Archäologisches Landesmuseum, Wünsdorf, pp 35–54

Greilich S (2004) Über die Datierung von Gesteinsoberflächen mittels optisch stimulierter Lumineszenz (The dating of stone surfaces using optically stimulated luminescence), PhD thesis. Diss. Universität Heidelberg [download at http://www.ub.uni-heidelberg.de/archiv/4588]

Greilich S, Glasmacher UA, Wagner GA (2002) Spatially resolved detection of luminescence: a unique tool for archaeochronometry. Naturwissenschaften 89:371–375

Greilich S, Glasmacher UA, Wagner GA (2005) Optical dating of granitic stone surfaces. Archaeometry 47:645–665

Greilich S, Harney HL, Woda C, Wagner GA (2006) AgesGalore – a software program for evaluating spatially resolved luminescence data. Radiation Measurement 41:726–735

Greilich S, Kromer B, Unkel I, Wagner GA (2004) Neue Ansätze der Chronometrie in der peruanischen Archäologie: Ortsaufgelöste Luminiszenz- und AMS-Radiokohlenstoff-Datierung/Nuevos conceptos de la cronometría en la arqueología peruana: fechado por luminescencia de alta resolución y fechado de radiocarbono por AMS. In: Reindel M, Wagner GA (eds) Neue naturwissenschaftliche Methoden und Technologien für die archäologische Forschung in Palpa, Peru/Nuevos métodos y tecnologías para la investigación arqueológica en Palpa, Perú. Publikation zur Feldkonferenz des Projektverbundes Nasca: Entwicklung und Adaption archäometrischer Techniken zur Erforschung der Kulturgeschichte. Lima, pp 27–30

Greilich S, Wagner GA (2006) Development of a spatially resolved dating technique using HR-OSL. Radiation Measurement 41:738–743

Greinwald S, Thierbach R (1997) Elektrische Eigenschaften der Gesteine. In: Beblo M (ed) Umweltgeophysik. Ernst & Sohn, Berlin, pp 89–96

Griffin JA (1986) Investigación sobre la unión de los metales. In: Plazas C (ed) Metalurgia de América Precolombina. 45° Congreso Internacional de Americanistas. Bogota, pp 353–366

Grodzicki J (1994) Nasca: Los sintomas geologicos del fenomeno El Niño y sus aspectos arqueologicos. Estudios y Memorias 12. Varsova

Grossman JW (1972) An ancient gold worker's tool kit. The earliest metal technology in Peru. Archaeology 25/4:270–275

Gruen A (1985) Adaptive least squares correlation: a powerful image matching technique. South Afr J of Photogrammetry, Remote Sens Cartograp 14(3):175–187

Gruen A (1999) Photogrammetrische Aufnahmen der Geoglyphen von Nasca, Palpa und San Ignacio. In: Museum Rietberg (Eds) Nasca - Geheimnisvolle Zeichen im Alten Peru. Museum Rietberg, Zurich, pp 5–14

Gruen A (2008) Reality-based generation of virtual environments for Digital Earth. International Digital Earth 1:88–106

Gruen A, Akca D (2005) Least squares 3D surface and curve matching. ISPRS J Photogrammetry and Remote Sensing 59:151–174

Gruen A, Akca D (2007) Calibration and accuracy testing of mobile phone cameras. Proceedings 28th Asian Conference on Remote Sensing (ACRS'07), Kuala Lumpur Malaysia, November 12–16, on CD-ROM

Gruen A, Baltsavias E (1988) Geometrically constrained multiphoto matching. Photogrammetric Engineering and Remote Sensing 54,5:633–641

Gruen A, Brossard J (1997) Photogrammetrische Kampagne Nasca/Palpa 1997. In: Jahresbericht SLSA 1997, pp 163–168

Gruen A, Kocaman S, Wolff K (2007) Geometric validation of ALOS/PRISM images. Proceedings of the First Joint PI Symposium of ALOS Data Nodes for ALOS Science Program in Kyoto Japan, 19–23 November (on CD-ROM)

Gruen A, Murai S (2002) High-resolution 3D modeling and visualization of Mount Everest. ISPRS J Photogrammetry and Remote Sensing 57:102–113

Gruen A, Remondino F, Zhang L (2004a) Photogrammetric reconstruction of the Great Buddha of Bamiyan. Photogrammetric Record 19,107:177–199

Gruen A, Remondino F, Zhang L (2004b) The bamiyan valley: Landscape modeling for Cultural Heritage visualization and documentation. International Archives of Photogrammetry, Remote Sensing and Spatial Information Sciences, vol 34 Part 5/W1, Proc. of the International workshop on processing and visualization using high resolution imagery, Pitsanulok Thailand, November 2004 (on CD-ROM)

Gruen A, Remondino F, Zhang L (2006) The Bamiyan project: multi-resolution image-based modeling. In: Baltsavias E, Gruen A, vanGool L, Pateraki M (eds) Proc of the International Workshop "Recording, Modeling and Visualization of Cultural Heritage", Centro Stefano Franscini, Monte Verita Ascona, Switzerland, 22–27 May 2005, Taylor & Francis, London, pp. 45–54

Gruen A, Roditakis A (2003) Visualization and animation of Mount Everest. International Archives of Photogrammetry, Remote Sensing and Spatial Information Sciences, vol 34, Part 5/W10, International Workshop on Visualization and Animation of Reality-based 3D Models, 24–28 February, Tarasp-Vulpera, Switzerland, on CD-ROM

Gruen A, Sauerbier M, Lambers K (2003) Visualisation and GIS-based analysis of the Nasca geoglyphs. In: Doerr, M., Sarris, A. (eds): The Digital Heritage of Archaeology. Proceedings of the XXX Computer Applications and Quantitative Methods in Archaeology Conference, Hellenic Ministry of Culture. Athens, pp 161–167

Gruen A, Wang X (2002) Integration of landscape and city modeling: The pre-hispanic site Xochicalco. International Archives of Photogrammetry, Remote Sensing and Spatial Information Sciences Int Workshop "Visualization and Animation of Landscape", Kunming China, 26 Feb-1 March, 2002, vol 34, Part 5/W3 (on CD-ROM)

Gruen A, Wolff K (2007) DSM generation with ALOS/PRISM data using SAT-PP. Proc of the IEEE International Geoscience and Remote Sensing Symposium (IGARSS), Barcelona, 23–27 July (on CD-ROM)

Gruen A, Zhang L (2002) Automatic DTM generation from Three-Line-Scanner (TLS) images. Bildteknik/Image Science 2002(1):33–52

Gruen A, Zhang L (2003a) Sensor Modeling for Aerial Triangulation with Three-Line Scanner (TLS) Imagery. Journal of Photogrammtrie, Fernerkundung, Geoinformation 2:85–98

Gruen A, Zhang L (2003b) 3D processing of high-resolution satellite images. Asian Conference on Remote Sensing 2003, Busan Korea, 3–7 November (on CD-ROM)
Gruen A, Zhang L, Eisenbeiss H (2005) 3D processing of high-resolution satellite imagery. Proc ASPRS Annual Conference Baltimore Maryland, 7–11 March (on CD-ROM)
Gruen A, Zhang L, Wang X (2003) Generation of 3D City Models with Linear Array CCD-Sensors). Proc Int Conference on Optical 3D Measurement Techniques, Zurich, September 2003, II:21–31
Grün A, Bär S, Beutner S (2000a) Signale im Sand: 3D-Erfassung und Visualisierung der 'Geoglyphen von Nasca'. In: Schmidt B, Uhlenküken C (eds) Visualisierung raumbezogener Daten: Methoden und Anwendungen. Schriftenreihe des Instituts für Geoinformatik der Westfälischen Wilhelms-Universität vol 8/II. Münster, pp 111–131
Grün A, Bär S, Beutner S (2000b) Signals in the sand: 3-D recording and visualization of the Nasca geoglyphs. International Archives of the Photogrammetry, Remote Sensing and Spatial Information Sciences, 33-B5, pp 53–61
Grün A, Bär S, Beutner S (2000c) Signals in the sand: 3-D recording and visualization of the Nasca geoglyphs. Photogrammetrie-Fernerkundung-Geoinformation 6:385–398
Grün A, Beutner S (2001) The geoglyphs of San Ignacio – new results from the Nasca Project. International Archives of the Photogrammetry, Remote Sen Spatial Inf Sci 34–5/W1, pp 18–24
Grün A, Brossard JC (1998) Photogrammetrische Kampagne Nasca/Palpa 1997. Jahresbericht der Schweizerisch-Liechtensteinischen Stiftung für Archäologische Forschungen im Ausland 1997:163–168
Grün A, Lambers K (2003) The geoglyphs of Nasca: 3-D recording and analysis with modern digital technologies. Acts of the 14th IISPP Congress, University of Liège, Belgium, 2–8.9. 2001, section 1: Theory and methods – general sessions and posters. BAR International Series 1145. Oxford, pp 95–103
Grün A, Sauerbier M, Lambers K (2003) Visualisation and GIS-based analysis of the Nasca geoglyphs. In: Doerr M, Sarris A (eds) The digital heritage of archaeology. Proceedings of the 30th CAA Conference, Heraklion, Crete, April 2002. Hellenic Ministry of Culture, Archive of Monuments and Publications, Athen, pp 161–167
Guillén, S (1995) Las "Cabezas Trofeo": violencia o culto a los muertos en los Andes. Paper presented to the conference "No una sino muchas muertes", held in Mexico, August 1995
Guillén S (2002) Las Momias de la Laguna de los Cóndores. In: González E, León R (eds) Chachapoyas: El Reino Perdido. Lima, pp 345–387
Guillén S, Conlogue G, Bravo A, Seidler H (2004) Las Momias de la Laguna de los Cóndores: Una evaluación radiográfica. Sian 9,15:22–23
Gunn NM, Murray AS (1980) Geomagnetic field magnitude variations in Peru derived from archaeological ceramics dated by thermoluminescence. Geophys J Royal Astron Soc 62:345–366
Günther D, Cousin H, Magyar B, Leopold I (1997) Calibration studies on dried aerosols for laser ablation inductively coupled plasma mass spectrometry. J Anal At Spectrom 12:165–170
Günther D, Hattendorf B (2005) Solid sample analysis using laser ablation inductively coupled plasma mass spectrometry. Trends Anal Chem 24:255–265
Günther D, Jackson SE, Longerich HP (1999) Laser ablation and arc/spark solid sample introduction into inductively coupled Plasma mass spectrometers. Spectrochim Acta Part B 54:381–409
Habermann J, Schilles T, Kalchgruber R, Wagner GA (2000) Steps towards surface dating using luminescence. Radiat Meas 32:847–851
Halgedahl SL, Day R, Fuller M (1980) The effect of cooling rate on the intensity of weak-field TRM in single-domain magnetite. J Geophys Res 85:3690–3698
Halicz L, Günther D (2004) Quantitative analysis of silicates using LA-ICP-MS with liquid calibration. J Anal At Spectrom 19:1539–1545
Hanusch T (2008) A new texture mapping algorithm for photorealistic reconstruction of 3D objects. The International Archives of the Photogrammetry, Remote Sensing and Spatial Information Sciences. Vol XXXVII. Part B5–2, Beijing, China, pp 699–705

Harris EC (1989) Principles of archaeological stratigraphy. 2nd edn, Academic Press, London San Diego
Hartmann, A (1970) Prähistorische Goldfunde aus Europa. Studien zu den Anfängen der Metallurgie, vol 3. Berlin
Hartmann, A (1982) Prähistorische Goldfunde aus Europa II. Studien zu den Anfängen der Metallurgie, vol 5.Berlin
Hauptmann A, Rehren T, Pernicka E (1995) The composition of gold from the Ancient mining district of Verespatak/Rosia Montana, Romania. In: Morteani G, Northover JP (eds) Prehistoric gold in Europe. Cambridge, pp 369–381
Hawkins GS (1974) Prehistoric desert markings in Peru. Natl Geogr Res Rep 1967:117–144
Hecht S (2001) Anwendung refraktionsseismischer Methoden zur Erkundung des oberflächennahen Untergrundes – mit acht Fallbeispielen aus Südwestdeutschland. Stuttgarter Geographische Studien 131. Stuttgart
Hecht S (2003) Differentiation of loose sediments with seismic refraction methods - potentials and limitations derived from case studies. Zeitschr f Geomorph Suppl 132: 89–102
Hecht S (2007) Sedimenttomographie für die Archäologie. In: Wagner GA (ed) Einführung in die Archäometrie. Springer Berlin Heidelberg New York, pp 95–112
Hecht S, Fassbinder JWE (2004) Geophysical and geoarchaeological studies in the northern Atacama desert at Palpa-Nazca, Peru. Geophysical Research Abstracts 6
Hecht S, Fassbinder JWE (2006) Der Blick in den Untergrund: Magnetometrie und Geoelektrische Tomographie in der Geoarchäologie. Geographische Rundschau 58,4 pp 38–45
Heinrich CA, Pettke T, Halter WE, Aigner-Torres M, Audetat A, Günther D, Hattendorf B, Bleiner D, Guillong M, Horn I (2003) Quantitative multi-element analysis of minerals, fluid and melt inclusions by laser-ablation inductively-coupled-plasma mass-spectrometry. Geochimica et Cosmochimica Acta 67:3473–3497
Hernandez M (2006) Space technologies to support the World Heritage Convention. In: Baltsavias E, Grün A, Van Gool L, Peteraki M (eds) Recording, Modeling and Visualization of Cultural Heritage. London, pp 3–9
Herrera F (1997) Trabajos preliminares en Paredones en el valle de Nasca. Tahuantinsuyo 3:119–126
Herrmann B, Hummel S (1995) Ancient DNA: Recovery and Analysis of Genetic Material from Paleontological, Archaeological, Museum, Medical and Forensic Specimens. Springer, Berlin Heidelberg New York
Herwitz SR, Johnson LF, Dunagan SE, Higgins RG, Sullivan DV, Zheng J, Lobitz BM, Leung JG, Gallmeyer B, Aoyagi M, Slye RE, Brass J (2004) Demonstration of UAV-based imaging for agricultural surveillance and decision support. Comput Electron Agr 44:49–61
Hesse B (1982) Archaeological evidence for camelid exploitation in the Chilenean Andes. Säugetierkundliche Mitteilungen 30:201–211
Hillson S (1996) Dental Anthropology. Cambridge University Press, Cambridge
Hillson, S (2000) Dental Pathology. In: A Katzenberg and Sh Saunders (eds) Biological Anthropology of the Human Skeleton Willey-Liss Inc., New York, pp 249–286
Hoffmann-Schimpf B, Tellenbach M (2004) Die Nutzung der Töpferscheibe durch die südamerikanischen Nasca-Indianer. VDR Beiträge zur Erhaltung von Kunst- und Kulturgut 1:99–104
Hohmann C (2006) Informe para el Instituto Nacional de Cultura sobre los trabajos del Proyecto Arqueológico Nasca-Palpa, Temporada de 2006. Unpublished report
Hölzl S, Aberg G, Hedges REM, Horn P, Hull BD, Rummel S, Téreygeol F (2007) Auf Spurensuche in der Vergangenheit – Isotope schreiben Geschichte. In: Wagner GA (2007) Einführung in die Archäometrie. Springer, Berlin Heidelberg New York, pp 263–277
Hölzl S, Horn P, Rossmann A, Rummel S (2004) Isotope-abundance ratios of light (bio) and heavy geo elements in biogenic tissues: methods and applications. In: Heumann KG, Vanhaecke F (eds) Isotope ratio measurements. Anal Bioanal Chem 378:227–228
Hönniger C, Kersten T (2005) Topografische Aufnahme der sächsischen Ringwallanlage Willenscharen mit dem 3D-Laserscanning-System GS100 von Mensi. In: Luhmann T

(ed) Photogrammetrie, Laserscanning, Optische 3D-Messtechnik. Beiträge der Oldenburger 3D-Tage 2005. Wichmann Verlag, Heidelberg, pp 224–231

Horcher A, Visser RJM (2004) "Unmanned Aerial Vehicles: Applications for Natural Resource Management and Monitoring". Council on Forest Engineering Proceedings 2004: Machines and People. The Interface, http://www.cnr.vt.edu/ifo/VT Andy COFE 2004 Drone Paper1.pdf (Accessed 2008-04-16)

Horn P, Hölzl S, Rummel S (2005) Temporal and spatial variations of 87Sr/86Sr in cheeses from Trentino and other regions in Northern Italy. In: Gasperi F, Versini G (eds) Characterisation of typical cheeses from Alpine region: the contribution of research. Quaderni dell Istituto Agrario di San Michele all Adige 1:155–164

Horn P, Hölzl S, Schiegl S, Biermann D, Rummel S (2007) Humans and Llamas from River Oasis around Ica-Palpa-Nasca in prehispanic times: Insights from Isotope values of H, C, N, O, S and Sr. Paper presented to the conference: neue Technologien für die Archäologie, der BMBF-Projektverbund Nasca, Peru, held at Bonn in June 2007

Horn P, Hölzl S, Storzer D (1994) Habitat determination on a fossil stags mandible from the site of Homo erectus heidelbergensis at Mauwer by use of 87Sr/86Sr. Naturwissenschaften 81:360–362

Horn P, Müller-Sohnius D (1999) Comment on "Mobility of Bell Beaker people revealed by strontium isotope ratios of tooth and bone: a study of Southern Bavarian skeletal remains" by Grupe G, Price TD, Schröter P, Söllner F, Johnson CM and Beard BL. Appl Geochem 14:263–269

Hornetz B, Jätzold R (2003) Savannen-, Steppen- und Wüstenzonen. Westermann, Braunschweig

Hostnig R (2003) Arte rupestre del Perú: inventario nacional. CONCYTEC, Lima

Houk RS (1994) Elemental and isotopic analysis by inductively-coupled plasma-mass spectrometry. Acc Chem Res 27:333–339

Hudjashov G, Kivisild T, Underhill PA, Endicott P, Sanchez JJ, Lin AA, Shen P, Oefner P, Renfrew C, Villems R, Forster P (2007) Revealing the prehistoric settlement of Australia by Y chromosome and mtDNA analysis. Proc Nat Acad Sc 104:8726–8730

Hummel S (2003) Ancient DNA Typing: Methods, Strategies and Applications. Springer, Berlin Heidelberg New York

Huntley DJ, Godfrey-Smith DI, Thewalt MLW (1985) Optical dating of sediments. Nature 313:105–107

Huntley DJ, Richards M (1997) The age of the Diring Quriakh archaeological site. Ancient TL 15:48–51

Hyslop J (1984) The Inka Road System. Orlando, FL

Ingold T (1996) Growing plants and raising animals: an anthropological perspective on domestication. In: Harris DR (Ed) The origins and spread of agriculture and pastoralism in Eurasia. London, pp 12–24

Iriarte J (2006) Vegetation and climate change since 14,810 14C yr B.P. in southeastern Uruguay and implications for the rise of early Formative societies. Quat Res 65:20–32

Isbell W (2001) Crecimiento y desarrollo de la capital imperial. In: Cabrera A, Cook J, González-Carré J, Bazán P (eds) Wari – Arte Precolombiano Peruano. Fundaciòn El Monte, Sevilla, pp 99–172

Iscan MY, Loth SR (1986) Determination of age from the sternal rib in white females: a test of the phase method. J Forensic Sci USA 31:990–999

Iscan MY, Loth SR, Wright RK (1984) Age estimation from the rib by phase analysis: white males. J Forensic Sci USA 29:1094–1104

Isla Cuadrado J (1990) La Esmeralda: una ocupación del período arcáico en Cahuachi, Nasca. Gaceta Arqueológica Andina 20:67–80

Isla Cuadrado J (1992) La ocupación Nasca en Usaca. Gaceta Arqueológica Andina 22:119–154

Isla Cuadrado J (2001a) Una tumba Nasca en Puente Gentil, valle de Santa Cruz, Perú. Beiträge zur Allgemeinen und Vergleichenden Archäologie 21:207–239
Isla Cuadrado J (2001b) Huari en Palpa y Nasca: Perspectivas desde el punto de vista funerario. Boletín de Arqueología PUCP 5:555–583
Isla Cuadrado J (2005) Grabsitten an der Südküste Perus: Neue Befunde von der Paracas-, Nasca- und Wari-Kultur. Archäologischer Anzeiger, Jubiläumsband 2004,2:96–98
Isla Cuadrado J, Reindel M (2005) New studies on the settlements and geoglyphs in Palpa, Peru. Andean Past 7:57–92
Isla Cuadrado J, Reindel M (2006a) Una tumba Paracas Temprano en Mollake Chico, valle de Palpa, costa sur del Perú/Ein Grab der frühen Paracas-Zeit in Mollake Chico, Palpa-Tel, Südküste Perus. Zeitschrift für Archäologie Außereuropäischer Kulturen 1:153–181
Isla Cuadrado J, Reindel M (2006b) Burial patterns and sociopolitical organization in Nasca 5 society. In: Isbell W, Silverman H (eds) Andean archaeology III: north and south. Springer, New York, pp 374–400
Isla Cuadrado J, Reindel M, De La Torre JC (2003) Jauranga: un sitio Paracas en el valle de Palpa, costa sur del Perú. Beiträge zur Allgemeinen und Vergleichenden Archäologie 23:227–274
Isla Cuadrado J, Reindel M. (2007) Los Paracas del Sur. Una nueva perspectiva desde los valles de Palpa. In: Instituto Nacional de Cultura (ed) Hilos del Pasado. El aporte francés al legado Paracas. Lima pp 79–91
Issar AS, Zohar M (2004) Climate change – Environment and civilization in the Middle East. Springer, Berlin Heidelberg New York
Jackson A, Jonkers A, Walker M (2000) Four centuries of geomagnetic secular variation from historical records Philos. Trans R Soc 358:957–990
Jacobsen K, Konecny G, Wegmann H (1999) High Resolution Sensor Test Comparison with SPOT, KFA1000, KVR1000, IRS-1C and DPA in Lower Saxony. International Archives of Photogrammetry, Remote Sensing and Spatial Information Sciences, vol 32, Part 4:260–269
Jensen D (2003) Geoglyphs and GIS: modeling transhumance in Northern Chile. In: Doerr M, Sarris A (eds) The digital heritage of archaeology. Proceedings of the 30th Computer Applications and Quantitative Methods in Archaeology Conference, Heraklion, Crete, April 200, pp 179–184
Johnson CM, Beard BL, Albarède F (eds) (2004) Geochemistry of non traditional stable isotopes. Rev Mineral Geochem 55. Min Soc Amer, Wash DC
Johnson GW, Meisner DE, Johnson WL (1990) Aerial Photography of the Nazca Lines. In Aveni, AF, (ed.) The Lines of Nasca, Memoirs of the American Philosophical Society 183, Philadelphia, 273–283
Jones DM (ed) (2007) 3D laser scanning for heritage: advance and guidance to users on laser scanning in archaeology and architecture. English Heritage Publishing, Swindon
Joyce TA (1912) South American Archaeology. G.P. Putnam's Sons, New York
Kadereit A (2002) IR-OSL-datierte Kolluvien als Archive zur Rekonstruktion anthropogen bedingter Landschaftsveränderungen. Das Fallbeispiel Bretten-Bauerbach/Kraichgau. Ibidem-Verlag, Stuttgart
Kadwell M, Fernandez M, Stanley HF, Baldi R, Wheeler JC, Rosadio R, Bruford MW (2001) Genetic analysis reveals the wild ancestors of the llama and the alpaca. Proc. Biol. Sci. 268(1485):2575–2584
Kammerer P, Mara H, Kratzmüller B, Zolda E (2005) Detection and Analysis of Lines on the Surface of Archaeological Pottery. Proc. of EVA'05 – Electronic Imaging & the Visual Arts. Florence, pp. 154–159
Kampel M, Sablatnig R (1999) On 3D Modelling of Archaeological Sherds. In: Sarris N, Strinzis M (eds) Proc. of the International Workshop on Synthetic-Natural Hybrid Coding and Three Dimensional Imaging. Santorini, pp 95–98

Kampel M, Sablatnig R (2004) Automatisierte Dokumentation von Keramikfunden aus Palpa auf der Grundlage eines 3D-Erfassungssystems/La documentación automatizada de cerámica basada en un sistema de registro tridimensional aplicada a hallazgos cerámicos de Palpa. In: Reindel M, Wagner GA (eds) Neue naturwissenschaftliche Methoden und Technologien für die archäologische Forschung in Palpa, Peru/Nuevos métodos y tecnologías para la investigación arqueológica en Palpa, Perú. Publikation zur Feldkonferenz des Projektverbundes Nasca: Entwicklung und Adaption archäometrischer Techniken zur Erforschung der Kulturgeschichte. Lima, pp 39–42

Kaulicke P (1994) Los orígenes de la Civilización Andina. Historia general del Perú, tomo 1. Lima

Keefer DK, de France SD, Moseley ME, Richardson JB, Satterlee DR, Day-Lewis A (1998) Early maritime economy and El Niño events at Quebrada Tacahuay, Peru. Science 281:1833–1835

Keefer DK, Moseley ME, deFrance SD (2003) A 38000-year record of floods and debris flows in the Ilo region of southern Peru and its relation to El Nino events and great earthquakes. Palaeogeography, Palaeoclimatology, Palaeoecology 194:41–77

Keefer DK, Mosley ME (2004) Southern Peru desert shattered by the great 2001 earthquake: Implications for paleoseismic and paleo-El Niño-Sothern Oscillation records. PNAS 101/30:10878–10883

Kellner CM (2002) Coping with Environmental and Social Challenges in Prehistoric Peru: Bioarchaeological Analysis of Nasca Populations. PhD thesis. Diss. University of Santa Barbara, California

Kellner CM, Schoeninger MJ (2008) Waŕis imperial influence on local Nasca diet: The stable isotope evidence. J Anthropol Archaeol 27(2):226–243

Kendall C, McDonnell JJ (eds) (1998) Isotope tracers in catchment hydrology. Elsevier, Amsterdam

Kern H, Reiche M (1974) Peruanische Erdzeichen/Peruvian ground drawings. Kunstraum München e.V., Munich

Kersten T, Przybilla HJ, Lindstaedt M (2006) Integration, Fusion und Kombination von terrestrischen Laserscannerdaten und digitalen Bildern. Workshop "Anforderungen an geometrische Fusionsverfahren", DIN Deutsches Institut für Normung e.V. und Humboldt-Universität zu Berlin, 20. November 2006. Unpublished paper

Keyeux G, Rodas C, Gelvez N, Carter D (2002) Possible migration routes into South America deduced from mitochondrial DNA studies in Colombian Amerindian populations. Hum Biol 74:211–233

Kirsch R, Rabbel W (1997) Seismische Verfahren in der Umweltgeophysik. In: Beblo M (ed) Umweltgeophysik. Ernst & Sohn, Berlin, pp 243–311

Klarich E (2008) Quienes eran los invitados? Cambios temporales y funcionales de los espacios públicos e Pucara como reflejo del cambio de las estratregias de liderazgo durante el Periodo Formativo Tardío. In: Kaulicke P, Dillehay TD (eds) Encuentros: Identidad, Poder y Manejo de Espacios Públicos. Boletín de Arqueología PUCP 9. Lima, pp. 185–204

Klepinger L (1992) Innovative approaches to the study of past human health and subsistence strategies. In: S Saunders and A Katzenberg (eds) Skeletal Biology of Past Peoples: Research Methods. Wiley-Liss Inc, New York, pp 121–130

Kneisel Ch (2003) Electrical resistivity tomography as a tool for geomorphological investigations - some case studies. Zeitschr f Geomorph Suppl 132:37–49

Knudson KJ (2004) Tiwanaku residential mobility in the South Central Andes: identifying archaeological human migration through strontium isotope analysis. Ph. D. Diss. Department of Anthropology, University of Wisconsin, Madison

Knudson KJ, Aufderheide AE, Buikstra JE (2007) Seasonality and paleodiet in the Chiribaya polity of southern Peru. J Archaeol Sci 34:451–462

Knudson KJ, Buikstra JE (2007) Residential mobility and resource use in the Chiribaya polity of southern Peru: strontium isotope analysis of archaeological tooth enamel and bone. Int J Osteoarchaeol 17:563–580

Knudson KJ, Price TD (2007) Utility of multiple chemical techniques in archaeological residential mobility studies: case studies from Tiwanaku- and Chiribay-affiliated sites in the Andes. Am J Phys Anthropol 132:25–39

Knudson KJ, Price TD, Buikstra JE, Blom DE (2004) The use of strontium isotope analysis to investigate Tiwanaku migration and mortuary ritual in Bolivia and Peru. Achaeometry 46:5–18

Kocaman S, Gruen A, Casella V, Franzini M (2007) Accuracy assessment of ADS40 imagery over the Pavia Testsite. Proc of the 28th Asian conference on remote sensing, Kuala Lumpur Malasia, 12–16 November (on CD-ROM)

Kocaman S, Zhang L, Gruen A (2006) Self-calibrating triangulation of airborne Linear Array CCD cameras. Proc EuroCOW 2006 International Calibration and Orientation Workshop, Castelldefels Spain, 25–27 January (on CD-ROM)

Koch PL, Fogel ML, Tuross N (1994) Tracing the diets of fossil animals using stable isotopes. In: Lajtha K and Michener RH (eds) Stable isotopes in ecology and environmental science. Blackwell Sci Pub, Oxford, pp 63–92

Kohn MJ, Cerling TE (2002) Stable isotope compositions of biological apatite. In: Kohn MJ, Rakovan J, Hughes JM (eds) Phosphates: Geochemical, geobiological, and materials importance. Rev Min Geochem 48:455–488

Kolarkar A (1997) Traditional water harvesting systems – Thar desert – Khadins. In: Agarwal A, Narain S (eds) Dying wisdom – Rise, fall and potential of India's traditional water harvesting systems. State of India's Environment 4. Center of Science and Environment, New Delhi, pp 104–143

Kovacheva M, Jordanova N, Karloukovski V (1998) Geomagnetic field variations as determined from Bulgarian archaeomagnetic data. Part II: The last 8000 years. Surv Geophys 19:413–460

Krbetschek MR, Rieser U, Stolz W (1996) Optical dating: some dosimetric properties of natural feldspars, Rad Protect Dosimetry 66:407–412

Kroeber AL (1944) Peruvian Archaeology in 1942. Viking Fund Publication in Anthropology, New York

Kroeber AL (1956) Toward definition of the Nasca style. University of California Publications in American Archaeology and Ethnology 43. Berkeley, pp 327–432

Kroeber AL, Collier D (1998) The archaeology and pottery of Nazca, Peru: Alfred L. Kroeber's 1926 expedition. Carmichael, PH (ed), Altamira Press, Walnut Creek

Kroslakova I, Günther D (2007) Elemental fractionation in laser ablation-inductively coupled plasma-mass spectrometry: evidence for mass load induced matrix effects in the ICP during ablation of a silicate glass. J Anal At Spectrom 22:51–62

Krueger HW and Sullivan (1984) Models for carbon isotope fractionation between diet and bone. In: Turnlund JR, Johnson PE (eds) Stable Isotopes in Nutrition. Am Chem Soc Symp Ser 258. Washington DC

Kruger HC (1990) Hiperostosis porótica en antiguos peruanos del Alto Chillón. Tesis de Bachiller de Medicina, Universidad Peruana Cayetano Heredia. Facultad de Medicina Alberto Hurtado, Lima

Kuper R, Kröpelin S (2006) Climate-controlled Holocene occupation in the Sahara: Motor of Africas evolution. Science 313:803–807

Kupferschmidt D (2008) Viviendo entre dos Horizontes en el Intermedio Tardío. In: Reindel M and Lambers K (Eds) Arqueología de Palpa, Perú: Períodos Nasca, Horizonte Medio e Intermedio Tardío. Forschungen zur Archäologie Außereuropäischer Kulturen. Reichert, Wiesbaden (in press)

Kuramoto J (2001) La Minería Artesanal e Informal en el Perú. Mining, Minerals and Sustainable Development 82:1–47

Kutsch H (1982) Principal features of a form of water-concentrating culture on small-holdings with special reference to the Anti-Atlas. Trierer Geographische Studien 5. Trier

Lake MW, Woodman PE (2003) Visibility studies in archaeology: a review and case study. Environment and Planning B: Planning and Design 30:689–707

Lake MW, Woodman PE, Mithen SJ (1998) Tailoring GIS software for archaeological applications, an example concerning viewshed analysis. J Archaeol Sci 25:27–38

Lalueza C, Perez-Perez A, Prats E, Cornudella L, Turbon D (1997) Lack of founding Amerindian mitochondrial DNA lineages in extinct aborigines from Tierra del Fuego-Patagonia. Hum Mol Genet 6:41–46

Lambers K (2006a) Geoglyphs of the Nasca region: new results from Palpa. In: Shimada I, Baba H, Shinoda K, Ono M (eds) Nasca, wonder of the world. Messages etched on the desert floor. Catalog for an exhibition of the National Science Museum, Tokyo. Tokyo, pp 174–175

Lambers K (2006b) The Geoglyphs of Palpa, Peru: Documentation, Analysis and Interpretation. PhD thesis. Forschungen zur Archäologie Außereuropäischer Kulturen 2. Aichwald

Lambers K, Eisenbeiss H, Sauerbier M, Kupferschmidt D, Gaisecker T, Sotoodeh S, Hanusch T (2007) Combining photogrammetry and laser scanning for the recording and modelling of the late intermediate period site of Pinchango Alto, Palpa, Peru. J Archaeol Sci 34:1702–1710

Lambers K, Sauerbier M (2003) A data model for a GIS-based analysis of the Nasca lines at Palpa (Peru). International Archives of the Photogrammetry, Remote Sensing and Spatial Information Sciences, 34–5/C15 pp 713–718

Lambers K, Sauerbier M (2006) GIS-based visibility studies of the Nasca geoglyphs at Palpa, Peru. In: Baltsavias E, Gruen A, van Gool L, Pateraki M (eds) Recording, modeling and visualization of cultural heritage. Taylor & Francis, London Leiden, pp 249–261

Lambers K, Sauerbier M (2008) A fresh view on the Nasca lines: investigating geoglyph visibility in Palpa (Ica, Peru). In: Clark JT, Hagemeister EM (eds) Digital discovery: exploring new frontiers in cultural heritage. CAA 2006: Computer applications and quantitative methods in archaeology. Proceedings of the 34th conference, Fargo, United States, April 2006. Archaeolingua, Budapest, pp 215–225

Lambers K, Sauerbier M, Grün A (2004) Einsatz von Photogrammetrie und Laserscanning zur Dokumentation von Geoglyphen und Ruinen in Palpa und Nasca/La aplicación de la fotogrametría y el escaneo láser en la documentación de geoglifos y asentamientos arqueológicos en Palpa y Nasca. In: Reindel M, Wagner GA (eds) Neue naturwissenschaftliche Methoden und Technologien für die archäologische Forschung in Palpa, Peru/Nuevos métodos y tecnologías para la investigación arqueológica en Palpa, Perú. Publikation zur Feldkonferenz des Projektverbundes Nasca: Entwicklung und Adaption archäometrischer Techniken zur Erforschung der Kulturgeschichte. Lima, pp 23–26

Lambers K, Sauerbier M, Grün A (in press) Photogrammetric recording, modeling, and visualization of the Nasca lines at Palpa, Peru: an overview. Proceedings of the 32nd CAA Conference, Prato, Italy, 13–17. April 2004. Archaeolingua, Budapest

Landon GV, Brent Seales W (2006) Petroglyph digitization: enabling cultural heritage scholarship. Machine Vision and Applications 17:361–371

Lange G (2005) Gleichstromgeoelektrik. In: Knödel K, Krummel H, Lange G (eds) Handbuch zur Erkundung des Untergrundes von Deponien und Altlasten. Bd. 3: Geophysik. Berlin Heidelberg, pp 128–173

Langer SK (1942) Philosophy in a new key: a study in the symbolism of reason, rite, and art. Harvard University Press, Cambridge, Massachusetts

Lankston RW (1990) High-resolution refraction seismic data acquisition and interpretation. In: Ward SH (ed) Geotechnical and environmental geophysics, Vol 1: Review and tutorial. Society of Exploration Geophysicists, Tulsa, pp 45–73

Lanning EP (1960) Chronological and cultural relationships of early pottery styles in ancient Peru. PhD thesis. Diss. Dept. of Anthropology, University of California, Berkeley

Larsen C.S (1987) Bioarchaeological Interpretations of Subsistence Economy and Behavior from Human Skeletal Remains. In: Schiffer M (ed). Advances in Archaeological Method and Theory. Academic Press, Orlando, pp 339–445

Latorre C, Betancourt JL, Rylander KA, Quade J, Matthei O (2003) A vegetation history from the arid prepuna of northern Chile (22–23°S) over the last 13 500 years. Paleogeography, Paleoclimatology, Paleoecology 194:223–246

Lautaro Nuñez A (1999) Valoración minero-metalúrgica circumpuneña: Minas y mineros para el Inka rey. Estudios Atacameños 18:177–221

Lavallée D, Julien M, Béarez P, Usselmann P, Fontugne M Bolaños A (1999) Pescadores-recolectores arcaicos del extremo sur peruano. Excavaciones en La Quebrada de los burros (Tacna, Perú). Primeros resultados 1995–1997. Bulletin de l'Institut francais d'études Andins 28,1:13–52

Layton R (2001) Ethnographic study and symbolic analysis. In: Whitley DS (ed) Handbook of rock-art research. AltaMira Press, Walnut Creek, California

Le Borgne E (1955) Susceptibilité magnétique anormale du sol superficiel. Ann Geophys 11:399–419

Leach AM, Hieftje GM (2000) Methods for shot-to-shot normalization in laser ablation with an inductively coupled plasma time-of-flight mass spectrometer. J Anal At Spectrom 15:1121–1124

Leach JJ, Allen LA, Aeschliman DB, Houk RS (1999) Calibration of laser ablation inductively coupled plasma mass spectrometry using standard additions with dried solution aerosols. Anal Chem 71:440–445

Lechtman HN (1976) A metallurgical site survey in the peruvian andes. J Field Archaeol 3,1:1–42

Lechtman HN (1979) Issues in Andean Metallurgy. In: Benson EP (ed) Pre-Columbian Metallurgy of South America. Conference at Dumbarton Oaks 1975. Trustees of the Harvard University, Washington, D.C., pp 1–40

Lechtman HN (1988) Traditions and styles in Central Andean metalworking. In: Maddin R (ed) The beginnings of the use of metals and alloys. Cambridge, Mass., pp 344–378

Lechtman HN (1997) El Bronce Arsenical y el Horizonte Medio. In: Varón R, Flores J (eds), Arqueología, Antropología e Historia en los Andes. Homenaje a María Rostworowski. Lima, pp 153–186

Lechtman HN (2003) Middle horizon bronze: Centres and outliers. In: Van Zelst L (ed) Patterns and process. Smithsonian, Maryland, pp 248–268

Lechtman HN (2007) The Inka, and Andean Metallurgical Tradition. In: Burger R, Morris R, Matos Mendieta R (eds): Variations in the expression of inka power. A Symposium at Dumbarton Oaks 1997. Dumbarton Oaks Research Library, Washington DC, pp 313–355

Lechtman HN, Macfarlane AW (2005) La metalurgia del bronce en los Andes Sur Centrales: Tiwanaku y San Pedro de Atacama. Estudios atacameños 30:7–27

Lechtman HN, Macfarlane AW (2006) Bronce y redes de intercambio andino durante el Horizonte Medio: Tiwanaku y San Pedro de Atacama. In: Lechtman H (ed), Esferas de interacción prehistóricas y fronteras nacionales modernas: los Andes sur centrales. Lima, pp 503–539

Lechtman, HN (1978) Issues in Andean Metallurgy. In: Elisabeth Benson (ed) Pre-Columbian Metallurgy of South America. A. Conference at Dumbarton Oaks 1975. Washington D.C., pp 1–40

Legge T (1996) The beginning of caprine domestication in Southwest Asia. In: Harris DR (ed) The origins and spread of agriculture and pastoralism in Eurasia. London, pp 238–262
Lemmens M (2007) Product survey: Terrestrial laser scanner. GIM Int 21:41–45
Leonhardt R, Fabian K (2007) Geomagnetic field variation during the past 5000 years: A global reconstruction. ASI003/IAGA/2007/Perugia, Italy
Leonhardt R, Heunemann C, Krasa D (2004) Analyzing absolute paleointensity determinations: Acceptance criteria and the software ThellierTool4.0. Geochem Geophys Geosystems 5: Q12016
Leonhardt R, Matzka J, Menor EA (2003) Absolute paleointensities and paleodirections from Fernando de Noronha Brazil. Phys Earth Planet Inter 139:285–303
Leonhardt R, Matzka J, Nichols ARL, Dingwell DB (2006) Cooling rate correction of paleointensity determination for volcanic glasses by relaxation geospeedometry. Earth Planet Sci Lett 243:282–292
Lettner M, Mara H, Müller A, Sablatnig R, Singer M, Krenn M (2006) PAT: Profile analysis tool for the Documentation of archaeological finds. Proc. of Electronic Imaging & the Visual Art (EVA'06 Vienna) – Digital Cultural Heritage – Essential for Tourism. Wien, pp 83–90
Leute U (1987) Archaeometry: An introduction to physical methods in archaeology and the history of art. Weinheim, New York
Lewis CM, Buikstra JE, Stone AC (2007a) Ancient DNA and genetic continuity in the south central Andes. Latin Am Antiq 18:145–160
Lewis CM, Lizarraga B, Tito RY, Medina A, Martinez R, Polo S, Caceres AM, Stone AC (2007b) Mitochondrial DNA and the Peopling of South America. Hum Biol 79:159–178
Lewis CM, Tito RY, Lizarraga B, Stone AC (2005a) Land, language, and loci: mtDNA in Native Americans and the genetic history of Peru. Am J Phys Anthropol 127:351–360
Lewis CM, Tito RY., Lizárraga B, Stone AC (2005b) Land, language, and loci: mtDNA in Native Americans and the genetic history of Peru. Am J Phys Anthropol 127:351–360
Lindstaedt M, Kersten T, Sauerbier M, Peterhans J, Fux P (2007) Dokumentation der Petroglyphen von Chichictara durch terrestrisches Laserscanning und digitale Photogrammetrie. Photogrammetrie-Laserscanning, Optische 3D-Messtechnik. In: Luhmann T, Müller C (eds) Beiträge der Oldenburger 3D-Tage 2007 (31.01.-01.02.2007), Oldenburg, Germany. Heidelberg, 328–337
Linford P (2003) Integrated use of Cesium vapour total field and gradiometer magnetometer surveys to maximize data recovery and archaeological interpretation: field experiments from United Kingdom. Archaeol Polonia 41:229–231
Linzen S, Chwala A, Schultze V, Schulz M, Schüler T, Stolz R, Bondarenko N, Meyer H.-G. (2007) A LTS-SQUID System for archaeological prospection and its practical test in Peru. IEEE Trans Appl Superconduct 17:750–755
Liritzis I (1994) A new dating method by thermoluminescence of carved megalithic stone building. Comptes Rendus de l'Académie des Sciences Séries II 319:603–610
Liritzis I, Galloway RB (1999) Dating implications from solar bleaching of ther-moluminescence of ancient marble. J Radioanal Nucl Chem 241:361–368
Liritzis I, Guibert P, Foti F, Schvoerer M (1997) The temple of Apollo (Delphi) strengthens novel thermoluminescence dating method. Geoarchaeology 12:479–496
Liska C (1999) Das Adaptive Lichtschnittverfahren zur Oberflächenkonstruktion mittels Laserlicht. Master Thesis. Vienna University of Technology, Institute of Computer Aided Automation, Pattern Recognition and Image Processing Group, Austria
Llobera M (1996) Exploring the topography of mind: GIS, social space and archaeology. Antiquity 70:612–22
Llobera M (2001) Building past landscape perception with GIS: understanding topographic prominence. J Archaeol Sci 28:1005–1014
Llobera M (2003) Extenting GIS-based visual analysis: the concept of visualscapes. Internat J Geograph Information Sci 17:25–48

Llobera M (2007) Modeling visibility through vegetation. Internat J Geograph Information Sci 21:799–810
Lock G, Harris T (2006) Enhancing predictive archaeological modeling: integrating location, landscape, and culture. In: Mehrer MW, Wescott KL (eds) GIS and archaeological site location modeling. Taylor & Francis Boca Raton, London New York, pp 41–62
Loke MH, Barker RD (1996) Practical techniques for 3D resistivity surveys and data inversion. Geophys Prospecting 44:499–523
Longerich HP, Günther D, Jackson SE (1996a) Elemental fractionation in laser ablation inductively coupled plasma mass spectrometry. Fresenius J Anal Chem 355:538–542
Longerich HP, Jackson SE, Günther D (1996b) Laser ablation inductively coupled plasma mass spectrometric transient signal data acquisition and analyte concentration calculation. J Anal At Spectrom 11:899–904
Longhurst A (1998) Ecological geography of the sea. Academic Press, San Diego (USA)
Lothrop SK (1937) Gold and silver from Southern Peru and Bolivia. J Royal Anthr Inst of Great Britain and Ireland 67:305–325
Lothrop SK (1951) Peruvian metallurgy. In: Sol Tax (ed) Selected Papers of the 29th International Congress of Americanists, vol. 1. Chicago, pp 219–23
Lothrop SK, Mahler J (1957) Late Nazca burials at Chaviña, Perú. Papers of the Peabody Museum of Archaeology and Ethnology 50. Peabody Museum of Archaeology, Cambridge
Lovejeoy O, Meindl R, Pryzbeck R, Mensforth RRYZBECK. (1985) Chronological metamorphosis of the auricular surface of th Ilium: a new method for the determination of adult skeletal age at death. Am J Phys Anthropol 68:15–28
Lovley DR, Stolz JF, North GL, Phillips EJP (1987) Anaerobic production of magnetite by dissimilatory iron-reducing microorganism. Nature 330:252–254
Lumbreras, LG (1981) Arqueología de la América Andina. Lima
Mächtle B (2007) Geomorphologisch-bodenkundliche Untersuchungen zur Rekonstruktion der holozänen Umwelgeschichte in der nördlichen Atacama im Raum Palpa, Südperu. Diss. Heidelberger Geographische Arbeiten 123. Heidelberg
Mächtle B, Eitel B, Kadereit A, Unkel I (2006a) Holocene environmental changes in the norther Atacama desert, southern Peru (14°30'S) and their impact on the rise and fall of pre-Columbian cultures. In: Eitel B (ed) Holocene landscape development and geoarchaeological research. Berlin, Stuttgart, pp 47–62
Mächtle B, Eitel B, Kadereit A, Unkel I (2006b) Holocene environmental changes in the northern Atacama desert, southern Peru (14°30'S) and their impact on the rise and fall of the Pre-Columbian cultures. Zeitschrift für Geomorphologie NF Suppl Vol 142:47–62
Mächtle B, Eitel B, Schukraft G (2008) Cadmium dynamics as a new pedogenic marker for humid phases in desert margin areas? Zeitschrift für Geomorphologie NF (in press)
MacHugh DE, Edwards CJ, Bailey JF, Bancroft DR, Bradley DG (2000) The extraction and analysis of ancient DNA from bone and teeth: a survey of current methodologies. Anc Biomol Vol 3:81–102
Maher BA, Taylor RM (1988) Formation of ultrafine-grained - magnetite in soils. Nature 336:368–370
Maldonado A, Villagran C (2002) Paleoenvironmental Changes in the Semiarid Coast of Chile (32°S) during the last 6200 cal years inferred from a swamp–forest pollen record. Quat Res 58:130–38
Mann S, Sparks NHC, Frankel RB, Bazylinski DA, Jannasch HW (1990) Biomineralization of ferrimagnetic greigite (Fe3S4) and iron pyrite (FeS2) in a magnetotactic bacterium. Nature 343:258–261
Mara H (2003) Automated profile extraction of archaeological fragments. Technical Report PRIP-TR-083. Vienna University of Technology, Institute of Computer Aided Automation, Pattern Recognition and Image Processing Group, Austria. Viena

Mara H (2006) Documentation of rotationally symmetrical archaeological finds by 3D shape estimation. Master Thesis, Technical Report PRIP-TR-103, Vienna University of Technology, Institute of Computer Aided Automation, Pattern Recognition and Image Processing Group, Austria. Viena

Mara H, Hecht N (2005) Analysis of geometry and documentation of NASCA ceramics using 3D-acquisiton. Forum Archaeologiae 37/XII/2005

Mara H, Hecht N (2006) 3D-Acquisition and Analysis of freehand manufactured NASCA Ceramics. Proc. of CAA06: Computer Aplications an Quantitative Methods in Archaeology. Fargo, ND, USA

Mara H, Kampel M (2003) Automated extraction of profiles from 3D Models of archaeological fragments. Proc. of CIPA2003: XIX CIPA Int. Symposium: New Perspectives to Save Cultural Heritage. Antalya, Turkey pp 87–93

Marcos J (2002) Mullo y Pututo para el Gran Caimán: un modelo para el intercambio entre Mesamérica y Andinoamérica. Gaceta Arqueológica Andina 26:13–36

Marcos JG (1986) Intercambio a larga distancia en América: el caso del Spondylus. In: Marcos J (ed) Arqueología de la costa ecuatoriana: nuevos enfoques. Biblioteca Ecuatoriana de Arqueología 1. Quito, pp 197–206

Marcos JG (1988) Real Alto: La historia de un centro ceremonial Valdivia. Biblioteca Ecuatoriana de Arqueología 4,5. Guayaquil

Marota I, Basile C, Ubaldi M, Rollo F (2002) DNA decay rate in papyri and human remains from Egyptian archaeological sites. Am J Phys Anthropol 117:310–318

Marshall G (1964) Examen de algunas muestras Pre-Colombinas de metal/Notes on the examination of some Pre-colombian metal samples. Arqueológicas 7. Lima

Martin DL, DW Frayer (1997) Troubled times. Violence and Warfare in the Past. Gordon and Breach Publishers, Amsterdan

Martino L, Bonomo N, Lascano E, Osella A, Ratto N (2006) Electrical and GPR prospecting at Palo Blanco archaeological site, northwestern Argentina. Geophysics 71:193–199

Mason JA (1926) Dr. Farabee's last journey. Museum J 17(2):128–165

Matos Avalos A (1987) Los petroglifos de Chichictara. Report of the Instituto Nacionál de Cultura. Lima

Mayer EF (1986) Vorspanische Metallwaffen und -werkzeuge in Argentinien und Chile. Armas y herramientas de metal prehispánicas en Argentina y Chile. Materialien zur Allgemeinen und Vergleichenden Archäologie 38. Mainz

Mayer EF (1992) Vorspanische Metallwaffen und -werkzeuge in Ecuador. Armas y herramientas de metal prehispánicas en Ecuador. Materialien zur Allgemeinen und Vergleichenden Archäologie 47. Mainz

Mayer EF (1994) Vorspanische Metallwaffen und -werkzeuge in Bolivien. Armas y herramientas de metal prehispánicas en Bolivia. Materialien zur Allgemeinen und Vergleichenden Archäologie 53. Mainz

Mayer EF (1998) Vorspanische Metallwaffen und -werkzeuge in Peru. Armas y herramientas de metal prehispánicas en Perú. Materialien zur Allgemeinen und Vergleichenden Archäologie 55. Mainz

McClelland-Brown E (1984) Experiments on TRM intensity dependence on cooling rate. Geophys Res Lett 11:205–208

McCormac G, Hogg AG, Blackwell PG, Buck CE, Higham TFG, Reimer PJ (2004) SHCal04 Southern Hemisphere Calibration, 0–11.0 cal kyr BP. Radiocarbon 46(3):1087–1092

McCormac G, Reimer PJ, Hogg AG, Higham TFG, Baillie MGL, Palmer J, Stuiver M (2002) Calibration of the radiocarbon time scale for the southern hemisphere: AD 1850–950. Radiocarbon 44(3):641–651

McElhinny MW, Senayake WE (1982) Variations in the geomagnetic dipole 1: The past 50 000 years. J Geomag Geolelect 34:39–51

Mejia Xesspe T (1942) Actas y trabajos científicos del XXVII Congreso Internacional de Americanistas – Lima 1939, Librería e Imprenta Gil, Lima, 559–569
Mejía Xesspe T (1972) Algunos restos arqueológicos del período Pre-Paracas en el valle de Palpa, Ica. Arqueología y Sociedad 7–8:77–86
Mejía Xesspe T (1976) Sitios Arqueológicos del Valle de Palpa, Perú. San Marcos N.S. 17:23–48
Mejía Xesspe T (2002) Arqueología de la cuenca del Río Grande de Nasca. Cuadernos de Investigación del Archivo Tello 3. Novoa Bellota P (ed). Lima
Melero F, Leon A, Contreras F, Torres J (2003) A new system for interactive Vessel reconstruction and drawing. Proc. of CAA'03: Comput Appl Archaeol, pp 8–12
Mengoni Goñalons GL, Olivera DE, Yacobaccio HD (eds) (2001) Zooarqueología de Camélidos: El Uso de los Camélidos a Través del Tiempo. Buenos Aires
Menzel D (1957) The disjunctive Nasca styles. Unpublished manuscript
Menzel D (1959) The Inca occupation of the south coast of Peru. Southwestern J Anthropol 15:125–142
Menzel D (1964) Style and time in the Middle Horizon. Ñawpa Pacha 2:1–105
Menzel D (1968a) La cultura Huari. Compañía de Seguros Peruano-Suizo, Lima
Menzel D (1968b) New Data on the Huari Empire in the Middle Horizon Epoch 2A. Ñawpa Pacha 6:47–114
Menzel D (1971) Estudios arqueológicos en los valles de Ica, Pisco, Chincha y Cañete. Arqueología y Sociedad 6. Lima
Menzel D, Rowe JH, Dawson L (1964) The Paracas pottery of Ica: a study in style and time. University of California Publications in American Archaeology and Ethnology 50. Berkeley
Merkel J, Shimada I, Swann CP, Doonan R (1994) Pre-hispanic copper alloy production at batán grande, Peru: Interpretation of the analytical data for ore samples. In: Scott DA, Meyers P (eds) Archaeometry of Pre-Columbian Sites and Artifacts. Marina del Rey, CA, pp 199–227
Merriwether DA, Rothhammer F, Ferrell RE (1995) Distribution of the four founding lineage haplotypes in Native Americans suggests a single wave of migration for the New World. Am J Phys Anthropol 98:411–430
Meyer S, Weiss G, von Haeseler A (1999) Pattern of nucleotide substitution and rate heterogeneity in the hypervariable regions I and II of human mtDNA. Genetics 152:1103–1110
Michczynski A, Eeckhout P, Pazdur A (2003) 14C Absolute chronology of pyramid III and the dynastic model at pachacamac, Peru. Radiocarbon 45:59–73
Miller GR, Burger RL (1995) Our father the cayman, our dinner the llama; animal utilization at Chavin de Huantar, Peru. Am Antiq 60(3):421–458
Montelius O (1903) Die älteren Kulturperioden im Orient und in Europa, 1: Die Methode. Stockholm
Montoya M, Garcia W, Caldas J (1994) Geologia de los cuadrangulos de Lomitas, Palpa, Nasca y Puquio. Carta Geológica Nacional 53, Lima
Moorrees C, Faning EA, Hunt E (1963) Age variation of formation stages for ten permanent teeth. J Dental Res 42:1490–1502
Moraga M, Santoro CM, Standen VG, Carvallo P, Rothhammer F (2005) Microevolution in prehistoric Andean populations: chronologic mtDNA variation in the desert valleys of northern Chile. Am J Phys Anthropol 127:170–181
Moraga ML, Rocco P, Miquel JF, Nervi F, Llop E, Chakraborty R, Rothhammer F, Carvallo P (2000) Mitochondrial DNA polymorphisms in Chilean aboriginal populations: implications for the peopling of the southern cone of the continent. Am J Phys Anthropol 113:19–29
Moran EF (2000) Human adaptability: An introduction to ecological anthropology. 2nd Edition. Westview Press, Oxford
Morris C (1985) Huanuco pampa. An Andean City and its Hinterland. London

Moseley ME (1992) The Incas and their ancestors: the archaeology of Peru. Thames and Hudson, London
Mothes P (ed) (1998) Actividad volcánica y pueblos precolombinos en el Ecuador. Quito
Müller-Sohnius D (2007) 87Sr/86Sr for isotope standards of Eimer and Amend (E&A), modern seawater strontium (MSS), and the Standard Reference Material (SRM) 987: development of interlaboratory mean values, procedures of adjusting, and the comparability of results. Geologica Bavarica 110:1–56
Murra, JV (1972) El control "vertical" de un máximo de pisos ecológicos en la economía de las sociedades andinas. In: Iñigo Ortiz de Zuñiga (ed) Visita de la provincia de León de Huánuco en 1562, tomo II: visita de los Yacha y Mitmaqkuna cuzqueños encomendados en Juán Sánchez Falcon. Universidad Nacional Hermilio Valdizán, Facultad de Letras y Educación, Huánuco pp 429–476
Murray AS, Wintle AG (2000) Luminescence dating of quartz using an improved single-aliquot regenerative-dose protocol. Rad Measur 32:57–73
Museo de Arqueologia y Antropologia de la Universidad Nacional Mayor DE SAN Marcas (2002) Arqueología de la cuenca del río Grande. Cuadernos de Investigación del Archivo Tello No 3. Universidad Nacional Mayor de San Marcos, Lima
Nebiker S, Christen M, Eugster H, Flückiger K, Stierli C (2007) Integration von mobilen Geosensoren in kollaborative virtuelle Globen. Dreiländertagung der SGPBF, DGPF und OVG: Von der Medizintechnik bis zur Planetenforschung – Photogrammetrie und Fernerkundung für das 21. Jahrhundert, DGPF Tagungsband Nr. 16. FHNW. Muttenz, 189–198
Nei M (1987) Molecular evolutionary genetics. Columbia University Press, New York
Neubauer W (2001) Images of the invisible – Prospection methods for the documentation of threatened archaeological sites. Naturwissenschaften 88:13–24
Neudecker A (1979) Archäologische Forschungen im Nazca-Gebiet, Peru. Das Tal des Río Santa Cruz in praespanischer Zeit aus der Sicht der Forschungen Professor Dr. Ubbelohde-Doerings im Jahre 1932. Münchner Beiträge zur Amerikanistik 3. Klaus Renner Verlag, Hohenschäftlarn
Nieves AC (2007) Between the river and the pampa: A contextual approach to the rock art of the Nasca valley (Grande River System, Department of Ica, Peru). Diss. (http://catalog.lib.utexas.edu), University of Texas at Austin
Noack K, Thiemer-Sachse U (1991) Altamerikanischer Bergbau. Das Altertum 37/3:166–174
Núñez JA (1986) Petroglifos del Perú: panorama mundial del arte rupestre. 4 vols. Editorial científico-técnica, La Habana
Nuñez L (1992) Cultura y conflicto en los oasis de San Pedro de Atacama. Editorial Universitario, Santiago de Chile
Odah H (1999) Improvement of the secular variation curve of the geomagnetic field in Egypt during the last 6000 years. Earth Planets Space 51:1325–1329
Ogburn DE (2006) Asessing the level of visibility of cultural objects in past landscapes. J Archaeol Sci 33:405–413
Olin JS (ed) (1982) Future direction in archaeometry – a round table. Smithsonian Institution, Washington
Olley J, Caitcheon G, Murray A (1998) The distribution of apparent dose determined by optically stimulated luminescence in small aliquots of fluvial quartz: implications for dating young sediments. Quatern Geochron 17:1033–1040
Orefici G (1983) Los petroglifos de Chichitara. Proyecto S. José. Informe final de la Campaña 1982. Report to the Instituto Nacionál de Cultura. Lima
Orefici G (1992) Nasca: archeologia per una ricostruzione storica. Saggi di archeologia. Editorial Jaca Book, Milan
Orefici G (1993) Nasca: Arte e società del popolo dei geoglifi. Milano
Orefici G, Drusini A (2003) Nasca: hipótesis y evidencias de su desarrollo cultural. Documentos e Investigaciones 2. Brescia, Italia

Orriols X (2004) Generative models for video analysis and 3D range data applications. PhD thesis. Diss. Universidad Autonoma de Barcelona, Spain

Ortlieb L, Vargas G (2003) Debris-flow deposits and El Nino Impacts along the hyperarid southern Peru coast. Fieldiana, Botany, New Series 43:24–51

Ortner D (2003) Identification of pathological conditions in human skeletal remains. 2nd Edition. Smithsonian Institution Press, Washington

Ortner D (2006) Foreword. In: Buikstra J and Beck L (eds.). Bioarchaeology, the contextual analysis of human remains. Academic Press, pp xiii – xv

Osella A, de la Vega M, Lascano E (2005) 3D electrical imaging of an archaeological site using electrical and electromagnetic methods. Geophysics 70

O'Shea J (1981) Social configurations and the archaeological study of mortuary practices: a case study. In: Chapman R, Kinnes I, Randsborg K (eds) The archaeology of death. Cambridge University Press, New York, pp 39–52

Outridge PM, Doherty W, Gregoire DC (1998) Determination of trace elemental signatures in placer gold by laser ablation inductively coupled plasma-mass spectrometry as a potential aid for gold exploration. J Geochem Expl 60:229–240

Paabo S, Poinar H, Serre D, Jaenicke-Despres V, Hebler J, Rohland N, Kuch M, Krause J, Vigilant L, Hofreiter M (2004) Genetic analyses from ancient DNA. Ann Rev Genet 38:645–679

Pakendorf B, Stoneking M (2005) Mitochondrial DNA and human evolution. Ann Rev Genomics Hum Genet 6:165–183

Palang H, Fry G (2003) Landscape interfaces: Introduction. In: Palang H, Fry G (eds) Landscape interfaces: Cultural heritage in changing landscapes. Kluwer, Dordrecht Boston London, pp 1–13

Palmer D (1981) An introduction to the generalized reciprocal method of seismic refraction interpretation. Geophysics 46(11):1508–1518

Pandey D, Gupta A, Anderson D (2003) Rainwater harvesting as an adaption to climate change. Curr Sci 85(1):46–59

Parker Pearson M (2002) The archaeology of death and burial. College Station, Texas

Paul A (1991) Paracas: An ancient cultural tradition on the South coast of Peru. In Paul A (ed), Paracas art and architecture: Object and context in South Coastal Peru. University of Iowa Press, Iowa City, pp 1–31

Pearsall DM (2000) Paleoethnobotany. A handbook of procedures. Second Edition. San Diego

Pearsall DM (2004) Plants and people in ancient ecuador: The ethnobotany of the jama river valley. Wadsworth/Thomson Learning, Case Studies in Archaeology Series. Belmont, CA

Pearson DL, Beletsky L (2002) Brazil: Amazon and Pantanal. The Ecotravellers' Wildlife Guide. Academic Press, London

Pernicka E, Tellenbach M, Schulz GG (2004) Archäologische Goldfunde aus dem Andenraum: Materialuntersuchungen zur Herkunftsbestimmung von Gold mittels LA-ICP-MS/Análisis por medio de LA-ICP-MS para determinar la procedencia de objetos de oro prehispánicos del área andina. In: Reindel M, Wagner GA (eds) Neue naturwissenschaftliche Methoden und Technologien für die archäologische Forschung in Palpa, Peru/Nuevos métodos y tecnologías para la investigación arqueológica en Palpa, Perú. Publikation zur Feldkonferenz des Projektverbundes Nasca: Entwicklung und Adaption archäometrischer Techniken zur Erforschung der Kulturgeschichte. Lima, pp 35–38

Pernicka, E (1999) Trace Element Fingerprinting of Ancient Copper: A Guide to technology or Provenance? In: Young SMM, Pollard AM, Budd P, Ixer RA (eds) Metals in Antiquity. BAR Int Ser 792. Archaeopress, Oxford, pp 163–171

Perry L, Dickau R, Zarrillo S, Holst I, Pearsall DM, Piperno DR, Berman MJ, Cooke RG, Rademaker K, Ranere AJ, Raymond JS, Sandweiss DH, Scaramelli F, Tarble K, Zeidler JA (2007) Starch fossils and the domestication and dispersal of chili peppers (Capsicum spp. L.) in the Americas. Science 315(5814): 986–988

Peters AH (1997) Paracas, topará and early nasca: Ethnicity and society on the South Central Andean Coast. Ph. D. Diss. Dept. of Anthropology, Cornell University Ithaca, Ithaca
Pfeiffer I, Völkel I, Täubert H, Brenig B (2004) Forensic DNA-typing of dog hair: DNA-extraction and PCR amplification. Forensic Sci Int 141(2–3):149–151
Pickhardt C, Becker JS, Dietze HJ (2000) A new strategy of solution calibration in laser ablation inductively coupled plasma mass spectrometry for multielement trace analysis of geological samples. Fresenius J Anal Chem. 368:173–181
Pierce MC, Bertocci GE, Vogeley E, Moreland MS (2004) Evaluating long bone fractures in children: a biomechanical approach with illustrative cases. Child Abuse and Neglect UK 28:505–524
Piperno DR, Pearsall DM (1998) The origins of agriculture in the lowland neotropics. Academic Press, San Diego
Piperno DR (2006) Phytoliths: a comprehensive guide for archaeologists and paleoecologists. AltaMira, Lanham, MD
Piperno DR (2008) Identifying crop plants with phytoliths (and starch grains) in Central and South America; A review and an update of the evidence. Quatern Int, in press
Poli D, Zhang L, Gruen A (2004) Orientation and automated DSM generation from SPOT-5/HRS stereo images. Proc of the 25th ACRS Conference, vol 1. 22–26 November, Chiang Mai Thailand, pp 190–195
Polo de Ondegardo J (1571) Relación de los fundamentos acerca del notable daño que resulta de no guardar a los indios sus fueros, junio 26 de 1571. Colección de libros y documentos referentes a la historia del Perú, notas bibliográficas y concordancias de los textos por Horacio H. Urteaga, tomo III. Lima 1916, pp 45–188
Ponce Sangines C (1970) Las Culturas Wankarani y Chiripa y su relación con Tiwanaku. Academia Nacional de Ciencias de Bolivia, Publicación 25. La Paz
Ponce Sangines C (1980) Panorama de la Arqueología Boliviana. La Paz
Pottmann H, Randrup T (1998) Rotational and helical surface approximation for reverse engineering. Computing 60:307–322
Prescott JR, Hutton JT (1988) Cosmic ray and gamma ray dosimetry for TL and ESR. Nuclear Tracks. Rad Measur 14:223–227
Prescott JR, Hutton JT (1994) Cosmic ray contribution to dose rates for luminescence and ESR dating: Large depths and long-term time variations. Rad Measur 23:497–500
Proulx DA (1968) Local differences and time differences in Nazca pottery. University of California Publications in Anthropology 5. Berkeley
Proulx DA (1970) Nasca gravelots in the Uhle collection from the Ica Valley, Peru. Department of Anthropology, University of Massachusetts, Amherst
Proulx DA (2006) A sourcebook of Nasca ceramic iconography: reading a culture through its art. University of Iowa Press, Iowa City
Pueschel H, Sauerbier M, Eisenbeiss H (2008) A 3D model of Castle Landenberg (CH) from combined photogrammetric processing of terrestrial and UAV-based images. The International Archives of the Photogrammetry, Remote Sensing and Spatial Information Sciences. Vol. XXXVII. Part B6b, Beijing, China, pp 93–98
Pulgar Vidal J (1946) Las Ocho Regiones Naturales del Perú. Lima
Pye K, Sherwin D (1999) Loess. In: Goudie AS, Livingstone I, Stokes S (eds) Aeolian environments, sediments and landforms. Wiley, Chichester, pp 213–238
Quilter J (1989) Life and death at Paloma: Society and mortuary practices in a preceramic peruvian village. Iowa City
Reiche M (1969) Mystery on the Desert. (Eigenverlag) Stuttgart
Reiche M (1993) Contribuciones a la geometría y astronomía en el antiguo Perú. Asociación María Reiche para las líneas de Nasca, Lima
Reidelstuerz P, Link J, Graeff S, Claupein W (2007) UAV (unmanned aerial vehicles) für Präzisionslandwirtschaft. 13. Workshop Computer-Bildanalyse in der Landwirtschaft & 4, Workshop Precision Farming 61:75–84

Reimer PJ, Baillie MGL, Bard E, Bayliss A, Beck JW, Bertrand CJH, Blackwell PG, Buck CE, Burr GS, Cutler KB, Damon PE, Edwards RL, Fairbanks RG, Friedrich M, Guilderson TP, Hogg AG, Hughen KA, Kromer B, McCormac FG, Manning SW, Ramsey CB, Reimer RW, Remmele S, Southon JR, Stuiver M, Talamo S, Taylor FW, van der Plicht J, Weyhenmeyer CE (2004) IntCal04 terrestrial radiocarbon age calibration, 26–0 ka BP. Radiocarbon 46:1029–1058

Rein B, Lückge A, Sirocko F (2004) A major Holocene ENSO anomaly during the Medieval period. Geophys Res Lett 31:L17211

Reindel M (1997) Archäologische Untersuchungen zur Nasca-Kultur und ihren Bodenzeichnungen in Süd-Peru: Bericht über erste Erkundungen im Oktober 1996. Jahresbericht der Schweizerisch-Liechtensteinischen Stiftung für Archäologische Forschungen im Ausland 1996:79–94

Reindel M (2001) Spurensuche im Wüstensand. Archäologie in Deutschland 2001,1:14–19

Reindel M (2004a) 3D-Rekonstruktion der Grabanlagen von La Muña, Peru. In: Baltsavias AE (ed) Commemorative Volume for the 60th Birthday of Prof. Dr. Armin Grün. Zürich, pp 209–212

Reindel M (2004b) Bericht über die Tätigkeit der Kommission für Allgemeine und Vergleichende Archäologie des Deutschen Archäologischen Instituts im Jahr 2003. Ausgrabungen und Forschungen: Peru. Beiträge zur Allgemeinen und Vergleichenden Archäologie 24:245–248

Reindel M (2004c) Landschafts- und Siedlungsgeschichte im Gebiet der Nasca-Kultur/Peru. Geographische Rundschau 56,3:22–29

Reindel M (2004d) Las tumbas de La Muña, Palpa, Perú: una contribución a la discusión acerca de la organización social y política de la cultura Nasca (200 AC – 600 DC). In: Cipolletti MS (ed) Los mundos de abajo y los mundos de arriba: individuo y sociedad en la tierras bajas, en los Andes y más allá. Tomo de homenaje a Gerhard Baer en su 70 cumpleaños. Quito, pp 555–575

Reindel M (2004e) Wüstenzeichungen und Wasserkulte: Geoglyphen und Siedlungsgeschichte in Palpa (Peru). In: Expeditionen in vergessene Welten. 25 Jahre archäologische Forschungen in Amerika, Afrika und Asien. AVA-Forschungen 10, pp 17–47

Reindel M (2005) Pinchango Alto: A Gold Miner's Settlement in Palpa, Southern Peru. In: Eeckhout P, Le Fort G (eds), Wars and Conflicts in Prehispanic Mesoamerica and the Andes. Proceedings of the Conference Brussels 2002. BAR International Series 1385. Oxford, pp 90–98

Reindel M (2006) Ausgrabungen und Forschungen der Kommission für Archäologie Außereuropäischer Kulturen, Bonn: Palpa, Peru. Archäologischer Anzeiger 2006(2):208–211

Reindel M (2007a) Entdeckungen in Amerika: Archäometrische Forschungen in Mexiko, Ekuador und Peru. In: Wagner G (ed) Einführung in die Archäometrie. Springer, Berlin Heidelberg New York, pp 322–338

Reindel M (2007b) The Geoglyphs of Palpa - An Archaeological Approach. In: Teichert B, Rust C (eds) Nasca-Symposium 2006. Zentrum für interdisziplinäre Forschung (ZiF) der Universität Bielefeld. Dresdner Kartographische Schriften 7. Dresden

Reindel M, Eitel B, Wagner GA (2004) Projektverbund Nasca - Entwicklung und Adaption archäometrischer Techniken zur Erforschung der Kulturgeschichte. In: Bundesministerium für Bildung und Forschung (ed) Alte Fragen - neue Antworten. Neue naturwissenschaftliche Methoden und Technologien in den Geisteswissenschaften. Bonn, pp 64–77

Reindel M, Gruen A (2006) The Nasca-Palpa Projekt: a cooperative approach of photogrammetry, archaeometry and archaeology. In: Baltsavias E, Gruen A (eds) Recording, modeling and visualization of cultural heritage. London, pp 21–32

Reindel M, Isla Cuadrado J (1999a) Ausgrabungen in Los Molinos und La Muña: Ergebnisse der Grabungskampagn 1998 des Archäologischen Projektes Nasca-Palpa, Süd-Peru. In: Jahresbericht der Schweizerisch-Liechtensteinischen Stiftung für Archäologische Foschungen im Ausland 1998:123–152

Reindel M, Isla Cuadrado J (1999b) Das Palpa-Tal - Ein Archiv der Vorgeschichte Perus. In: Rickenbach J (ed) Nasca. Geheimnisvolle Zeichen im Alten Peru. Ausstellungskatalog. Zürich, pp 177–198

Reindel M, Isla Cuadrado J (2000) Ausgrabungen in Los Molinos und La Muña. Ergebnisse der Grabungskampagne 1999 des Archäologischen Projektes Nasca-Palpa, Süd-Peru. Jahresbericht der Schweizerisch-Liechtensteinischen Stiftung für Archäologische Forschungen im Ausland 1999:67–95

Reindel M, Isla Cuadrado J (2001) Los Molinos und La Muña. Zwei Siedlungszentren der Nasca-Kultur in Palpa, Südperu. – Los Molinos y La Muña. Dos centros administrativos de la cultura Nasca en Palpa, costa sur del Perú. Beiträge zur Allgemeinen und Vergleichenden Archäologie 21:241–319

Reindel M, Isla Cuadrado J (2003) ¿Globalización en la arqueología? Humboldt 138:18–21

Reindel M, Isla Cuadrado J (2004a) Archäologie und Naturwissenschaften in Palpa/La arqueología y las ciencias naturales en Palpa. In: Reindel M, Wagner GA (eds) Neue naturwissenschaftliche Methoden und Technologien für die archäologische Forschung in Palpa, Peru/Nuevos métodos y tecnologías para la investigación arqueológica en Palpa, Perú. Publikation zur Feldkonferenz des Projektverbundes Nasca: Entwicklung und Adaption archäometrischer Techniken zur Erforschung der Kulturgeschichte. Lima, pp 11–14

Reindel M, Isla Cuadrado J (2004b) Archäologisches Projekt 'Paracas in Palpa', Peru. Bericht über die Grabungskampagne 2003. Jahresbericht der Schweizerisch-Liechtensteinischen Stiftung für Archäologische Forschungen im Ausland 2003:137–156

Reindel M, Isla Cuadrado J (2004c) Bericht über die Grabungskampagne 2003. Jahresbericht der Schweizerisch-Liechtensteinischen Stiftung für Archäologische Forschungen im Ausland (SLSA) 2003:137–156

Reindel M, Isla Cuadrado J (2006a) Archäologisches Projekt 'Paracas in Palpa', Peru – Ausgrabungen und Forschungen im Jahr 2005. Jahresbericht der Schweizerisch-Liechtensteinischen Stiftung für Archäologische Forschungen im Ausland (SLSA) 2005:30–59

Reindel M, Isla Cuadrado J (2006b) Culturas tempranas de la costa sur del Perú: sus evidencias en los valles de Palpa. In: Kaulicke P, Dillehay TD (ed) Procesos y expresiones de poder, identidad y orden tempranos en Sudamérica. Boletín de Arqueología PUCP 10. Lima (in press)

Reindel M, Isla Cuadrado J (2006c) Archäologisches Projekt 'Paracas in Palpa', Peru: Ausgrabungen und Forschungen im Jahr 2005. Jahresbericht der Schweizerisch-Liechtensteinischen Stiftung für Archäologische Forschungen im Ausland 2005:30–59

Reindel M, Isla Cuadrado J (2006d): Reconstructing Nasca social and political structures: a view from Los Molinos and La Muña. In: Shimada I, Baba H, Shinoda K, Ono M (eds) Nasca, wonder of the world. Messages etched on the desert floor. Catalog for an exhibition of the National Science Museum, Tokyo. Tokyo, pp 165–173

Reindel M, Isla Cuadrado J, Lambers K (2006) Altares en el desierto: las estructuras sobre los geoglifos de Palpa. Arqueología y Sociedad 17:179–222

Reindel M, Isla Cuadrado J, Grün A, Lambers K (2001) Neue Erkenntnisse zu Siedlungen, Bodenzeichnungen und Kultplätzen in Palpa, Süd-Peru: Ergebnisse der Feldkampagne 2000 des Archäologischen Projektes Nasca-Palpa. Jahresbericht der Schweizerisch-Liechtensteinischen Stiftung für Archäologische Forschungen im Ausland 2000:81–104

Reindel M, Isla Cuadrado J, Koschmieder K (1999) Vorspanische Siedlungen und Bodenzeichnungen in Palpa, Süd-Peru. Beiträge zur Allgemeinen und Vergleichenden Archäologie 19:313–381

Reindel M, Isla Cuadrado J, Lambers K (2002) Abschließende Untersuchungen zu Geoglyphen und Siedlungen in Palpa, Südperu. Ergebnisse der Feldkampagne 2001 des Archäologischen Projektes Nasca-Palpa. Jahresbericht der Schweizerisch-Liechtensteinischen Stiftung für Archäologische Forschungen im Ausland (SLSA) 2001:37–54

Reindel M, Isla Cuadrado J, Lambers K (2003) Die Arbeiten des Archäologischen Projektes Nasca-Palpa, Peru, im Jahr 2002. Jahresbericht der Schweizerisch-Liechtensteinischen Stiftung für Archäologische Forschungen im Ausland 2002:119–132

Reindel M, Isla Cuadrado J, Lambers K (2004) Archäologisches Projekt "Paracas in Palpa", Peru. Bericht über die Grabungskampagne 2004. Jahresbericht der Schweizerisch-Liechtensteinischen Stiftung für Archäologische Forschungen im Ausland (SLSA) 2004:25–44

Reindel M, Isla Cuadrado J, Lambers K (2006) Los geoglifos de Palpa: documentación, análisis y perspectivas. Boletín de Lima 28,143:73–111

Reindel M, Isla Cuadrado J, Lambers K, Otten H (2007) Los geoglifos de Palpa: documentación y análisis arqueológico. In: Hostnig R, Strecker M, Guffroy J (eds) Actas del Primer Simposio Nacional de Arte Rupestre (Cusco, noviembre 2004). Lima, pp 135–147

Reindel M, Lambers K, Grün A (2003) Photogrammetrische Dokumentation und archäologische Analyse der vorspanischen Bodenzeichnungen von Palpa, Süd-Peru/Documentación fotogramétrica y análisis arqueológico de los geoglifos prehispánicos de Palpa, costa sur del Perú. Beiträge zur Allgemeinen und Vergleichenden Archäologie 23:183–226

Reindel M, Wagner GA (eds) (2004) Neue naturwissenschaftliche Methoden und Technologien für die archäologische Forschung in Palpa, Peru/Nuevos métodos y tecnologías para la investigación arqueológica en Palpa, Perú. Publikation zur Feldkonferenz des Projektverbundes Nasca: Entwicklung und Adaption archäometrischer Techniken zur Erforschung der Kulturgeschichte. Lima

Reinhard J (1996) The Nazca lines: a new perspective on their origin and meaning. 6th ed. Editorial Los Pinos, Lima

Remondino F, El-Hakim S, Gruen A, Zhang L (2008) Developments and performance analysis of image matching for detailed surface reconstruction of heritage objects. IEEE Signal Processing Magazine, Special Issue on Signal Processing in Visual Cultural Heritage, 25(4):55–64

Remondino F, Niederoest J (2004) Generation of high-resolution Mosaic for photo-realistic texture-mapping of cultural heritage 3D models. Proc of the 5th International Symposium on Virtual Reality, Archaeology and Cultural Heritage (VAST), pp 85–92

Remondino F, Zhang L (2006) Surface reconstruction algorithms for detailed close-range object modeling. International Archives of Photogrammetry, Remote Sensing and Spatial Information Sciences, vol 36, part 3, Bonn Germany, 117–123

Renfrew C, Bahn P (1996) Archaeology: theories, methods and practice. 2nd edn. Thames and Hudson, London

Renneberg R (2008) Molekulargenetische Untersuchungen an Überresten präkolumbischer Neuwelt-Camelidae aus dem Palpa-Tal (Peru). Ph. D. Diss. Institute for Historic Anthropology and Human Ecology, University of Göttingen

Rhode M (2006) Habitual Subsistence Practices Among Prehistoric Andean Populations: Fishers And Farmers. PhD thesis. Diss. University of Missouri, Columbia

Rice PM (1987) Pottery analysis: a sourcebook. Chicago, University Press

Richards MB, Macaulay VA, Bandelt HJ, Sykes BC (1998) Phylogeography of mitochondrial DNA in western Europe. Ann Hum Genet 62:241–260

Richards MP, Fuller BT, Sponheimer M, Robinson T, Ayliffe L (2003) Sulphur isotopes in palaeodietary studies: a review and results from a controlled feeding experiment. Int J Osteoarchaeol 13:37–45

Richter C (2007) NascaGIS – An application for cultural heritage conservation. In: Teichert B, Rust C (eds) Nasca Symposium 2006 im Zentrum für interdisziplinäre Forschung der Universität Bieldefeld. Dresdner Kartographische Schriften. Dresden

Rickards O, Martinez-Labarga C, Lum JK, De Stefano GF, Cann RL (1999) mtDNA history of the Cayapa Amerinds of Ecuador: detection of additional founding lineages for the Native American populations. Am J Hum Genet 65:519–530

Riddell, FA, Valdez Cardenas L (1987) Hacha y la ocupación temprana del valle Acarí. Gaceta Arqueológica Andina 16:6–10

Rieser U (1999) Spektrometrie an Feldspäten als Beitrag zur Aufklärung physikalischer Grundlagen der Lumineszenz-Datierungstechnik. Diss. Universität Heidelberg
Rink W, Bartoll J (2005) Dating the geometric Nasca lines in the Peruvian desert. Antiquity 79:390–401
Roark RP (1965) From monumental to proliferous in Nasca Pottery. Ñawpa Pacha 3:1–92
Robinson RW (1994) Recent Excavations at Hacha in the Acarí Valley, Peru. Andean Past 4:9–37
Rogers J, Fox JMW, Aitken MJ (1979) Magnetic anisotropy in ancient pottery. Nature 277:644–646
Roosevelt AC (1991) Moundbuilders of the Amazon. Geophysical Archaeology on Marajo Island, Brazil. Academic Press, San Diego
Roosevelt AC (2007) Geophysical archaeology in the lower Amazon: A Research Strategy. In: Wiseman J, El-Baz F (eds) Remote sensing in archaeology. Interdisciplinary Contributions to Archaeology. New York, pp 443–475
Root W (1949) The metallurgy of the Southern Coast of Peru. Am Antiq 15,1:10–37
Rose J, Burnett B, Blaeuer M, Nassaney M (1984) Paleopathology and the origins of maize agriculture in the lower Mississippi Valley and Caddoan culture areas. In Cohen M and Armelagos G (Eds.) Paleopathology at the Origins of Agriculture. Academic Press, N. York, pp 393–424
Ross K (2007) Geoarchäologisch-bodenkundliche Untersuchungen zu präkolumbischen Bewässerungstechniken im Raum Palpa (nördliche Atacama/Südperu). Unpublished thesis, University of Heidelberg, Geographical Institute
Rostworowski M (1993) Origen religioso de los dibujos y rayas de Nasca. Journal de la Société des Américanistes LXXIX:189–202
Rothhammer F, Llop E, Carvallo P, Moraga M (2001) Origin and evolutionary relationships of native Andean populations. High Alt Med Biol 2:227–233
Rovira Llorens S (1987) Vorkolumbische Metallverarbeitung und Bergbau in den Anden. In: Feest C (Hg.) Gold und Macht. Spanien in der Neuen Welt. Ausstellung anläßlich des 500. Jahrestages der Entdeckung Amerikas. Wien, pp 93–99
Rovira Llorens S (1990) La Metalurgia Americana: Analisis Tecnologico de Materiales Prehispanicos y Coloniales. Madrid
Rovira-Más F, Zhang Q, Reid JF (2005) Creation of three-dimensional crop maps based on aerial stereoimages. Biosystems Eng 90:251–259
Rovira-Más F, Zhang Q, Reid JF (2008) Stereo vision three-dimensional terrain maps for precision agriculture. Comput Electron Agr 60:133–143
Rowe JH (1945) Absolute chronology in the Andean area. Am Antiq 10(3):265–284
Rowe JH (1956) Archaeological explorations in southern Peru, 1954–1955: preliminary report of the fourth University of California Archaeological Expedition to Peru. Am Antiq 22:135–151
Rowe JH (1960a) Cultural Unity and Diversification in Peruvian Archaeology. In: Wallace AFC (ed) Selected Papers of the Fifth International Congress of Anthropological and Ethnological Sciences. Philadelphia. pp 627–631
Rowe JH (1960b) Nuevos datos relativos a la cronología del estilo Nasca. In: Matos Mendieta R (ed) Antiguo Peru, espacio y tiempo. Lima, pp 29–45
Rowe JH (1961) Stratigraphy and seriation. Am Antiq 26:324–330
Rowe JH (1962a) Stages and periods in Archaeological interpretation. Southwestern J Anthropol 18(1):40–54
Rowe JH (1962b) Worsaae's Law and the use of grave lots for archaeological dating. Am Antiq 28:129–137
Rowe JH (1963) Urban Settlements in Ancient Peru. Nawpa Pacha 1:1–28
Rowe JH (1967a) An Interpretation of Radiocarbon Measurements on Archaeological Samples from Peru. In: Rowe JH, Menzel D (eds) Peruvian Archaeology: Selected Readings. Palo Alto, pp 16–30

Rowe JH (1967b) Form and Meaning in Chavín Art. In: Rowe JH and Menzel D (eds) Peruvian Archaeology: Selected Readings. Palo Alto, pp 67–103

Ruppert H (1982) Zur Verbreitung und Herkunft von Türkis und Sodalith in präkolumbischen Kulturen der Kordilleren. Baessler Archiv N. F. 30:69–124

Salazar-Soler C (1991) El Pishtaku entre los campesinos y los mineros en Huancavelica. Bull Institute franc études andines 20(1):7–22

Sandmeier K-J, Liebhardt G (2005) Refraktionsseismik: Iterative Interpretationsmethoden. In: Knödel K, Krummel H, Lange G (eds): Handbuch zur Erkundung des Untergrundes von Deponien und Altlasten. Bd. 3: Geophysik. Berlin Heidelberg, pp 566–572

Sandweiss DH (2003) Terminal Pleistocene through Mid-Holocene Archaeological Sites as Paleoclimatic Archives for the Peruvian coast. Palaeogeography, Palaeoclimatology, Palaeoecology 194:23–40

Sandweiss DH, Maasch KA, Chai F, Andrus CFT, Reitz, EJ (2004) Geoarchaeological evidence for multidecadal natural climatic variability and ancient Peruvian fisheries. Quat Res 61:330–334

Satterlee D, Moseley M, Keefer D, Tapia J (2000) The Miraflores El Niño disaster: convergent catastrophes and prehistoric agrarian change in Southern Peru. Andean Past 6:95–116

Saturno W, Sever TL, Irwin DE, Howell BF, Garrison TG (2007) Putting us on the map: remote sensing investigation of the ancient Maya landscape. In: Wiseman J, El-Baz F (eds) Remote Sensing in Archaeology. Interdisciplinary Contributions to Archaeology. New York, pp 137–160

Sauerbier M (2004) Accuracy of automated aerotriangulation and DTM generation for low textured imagery. International Archives of Photogrammetry, Remote Sensing and Spatial Information Sciences, vol XXXV/B2:521–527

Sauerbier M (2006a) Automated DTM generation for low textured images using multiple primitive multiple-image matching (MPM). In: International Archives of Photogrammetry, Remote Sensing and Spatial Information Sciences, vol XXXVI/B2. on CDROM

Sauerbier M (2006b) GIS-based management and analysis of the geoglyphs in the Nasca region (Peru). International Archives of Photogrammetry, Remote Sensing and Spatial Information Sciences 36–2, pp 73–77

Sauerbier M, Fux P, Lindstaedt M, Kersten T, Peterhans J, Belkaid M (2007) Dokumentation und 3D Modellierung der Petroglyphen von Chichictara (Peru) mittels terrestrischem Laserscanning und Photogrammetrie. In: DGPF Tagungsband 16: 425–433

Sauerbier M, Kunz M, Flühler M, Remondino F (2004) Photogrammetric reconstruction of adobe architecture at Tucume, Peru. Proc of the International Workshop on Processing and Visualization Using High Resolution Imagery, Pitsanoluk Thailand, November, International Archives of Photogrammetry, Remote Sensing and Spatial Information Sciences, vol 36, Part 5/W1 (on CD-ROM)

Sauerbier M, Lambers K (2003) A 3D model of the Nasca lines at Palpa (Peru). International Workshop on Visualization and Animation of Reality-based 3D Models, Tarasp, Switzerland, February 2003. International Archives of the Photogrammetry, Remote Sensing and Spatial Information Sciences, XXXIV-5/W10 (on CD-ROM)

Sauerbier M, Lambers K (2004) From vectors to objects: modeling the Nasca lines at Palpa, Peru. In: Fischer Ausserer K, Börner W, Goriany M, Karlhuber-Vöckl L (eds) Enter the past: the e-way into the four dimensions of cultural heritage. Proceedings of the 31st CAA conference, Vienna, Austria, April 2003. Archaeopress, Oxford, pp 396–399

Sauerbier M, Schrotter G, Eisenbeiss H, Lambers K (2006) Multi-resolution image-based visualization of archaeological landscapes in Palpa (Peru). In: Campana S, Forte M (eds) From space to place: proceedings of the 2nd International Conference on Remote Sensing in Archaeology, CNR, Rome, Italy, December 4–7, 2006. Archaeopress, Oxford, pp 353–359

Scheffer F, Meyer B, Babel,U (1959) Magnetische Messungen als Hilfe zur Bestimmung der Eisenoxide im Boden. Beitr Miner Petrogr 6:371–387
Scheuer L, Black S (2000) Developmental Juvenile Osteology, Academic Press, London
Schilz F (2006) Molekulargenetische Verwandtschaftsanalysen am prähistorischen Skelettkollektiv der Lichtensteinhöhle. Diss. Universität Göttingen
Schlosser S (2004) Archäometrische Untersuchungen zur Herstellungstechnik präkolumbischer Goldobjekte aus Costa Rica. Diploma thesis. Technische Universität Bergakademie Freiberg, Germany
Schmiderer A (2008) Geochemische Charakterisierung von Goldvorkommen in Europa. Diss. Martin Luther Universität Halle Wittenberg, Germany
Schmidt HL (2003) Fundamentals and systematics of the non-statistical distributions of isotopes in natural compounds. Naturwissenschaften 90:537–552
Schreiber KJ (1998) Nasca Research since 1926. In: Carmichael PH (ed) The Archaeology and Pottery of Nazca, Peru. Chicago, pp 261–270
Schultze V, Linzen S, Schüler T, Chwala A, Stolz R, Schulz M, Meyer HG (2008) Rapid and Sensitive Magnetometer Surveys of Large Areas using SQUIDs – the Measurement System and its Application to the Niederzimmen Neolothic Double-ring Ditch Exploration. Archaeological Prospection 15, Issue 2, pp 113–131
Schulz GG (2007) Kleinstbergbau auf Gold im Gebiet von Palpa/Peru. World of Mining 59(1):42–47
Schurr TG (2004) The Peopling of the New World: Perspectives from Molecular Anthropology. Ann Rev Anthropol 33:551–583
Schweigger E (1959) Die Westküste Südamerikas im Bereich des Peru-Stroms. Keysersche Verlagsbuchhandlung, Heidelberg
Schwertmann U, Fechter H (1984) The influence of aluminium on iron oxides. XI. Aluminium-substituted maghemite in soils and its formation. Soil Sci Soc Am J 48:1462–1463
Schwertmann U, Heinemann B (1959) Über das Vorkommen und die Entstehung von Maghemit in nordwestdeutschen Böden. Neues Jahrb Miner Mh 8:174–181
Schwertmann U, Taylor RM (1979) Natural and synthetic poorly crystallized lepidocrocite. Clay Minerals 14:285–293
Scollar I, Tabbagh A, Hesse A, Herzog I (1990) Topics in remote sensing: Archaeological prospecting and remote sensing. Cambridge University Press, Cambridge New York Port Chester Melbourne Sydney
Seler E (1912) Archäologische Reise in Süd- und Mittelamerika 1910/1911. In: Seler E 1915 Gesammelte Abhandlungen zur Amerikanischen Sprach- und Altertumskunde V [reprint of the original article in: Zeitschrift für Ethnologie 44: 201–242], Berlin
Seler E (1923) Die buntbemalten Gefässe von Nazca im südlichen Peru und die Hauptelemente ihrer Verzierung. Gesammelte Abhandlungen zur Amerikanischen Sprach- und Altertumskunde 4:170–338
Service ER (1962) Primitive Social Organization. Random House, New York
Sharp ZD, Atudorei V, Panarella HO, Fernandez J, Douthitt C (2003) Hydrogen isotope systematics of hair: archaeological and forensic applications. J. Arch Sci 30:1709–1716
Shaw J, Yang S, Rolph T, Sun F (1999) A comparison of archaeointensity results from Chinese ceramics using microwave and conventional Thellier's and Shaw's methods. Geoph J Intern 136:714–718
Shepard AO (1956) Ceramics for the archaeologist. Carnegie Institution of Washington Publication, Washington DC
Shimada I, Epstein S, Craig, AK (1982) Batán Grande: a prehistoric metallurgical center in Peru. Science 216:952–959
Shimada I, Merkel JF (1991) Copper-alloy metallurgy in ancient Peru. Scientific Am 265:62–68

Shimada I, Schaaf C B, Thompson L G, Mosley-Thompson E (1991) Cultural Impacts of Severe Droughts in the Prehistoric Andes: Application of a 1,500-Year Ice Core Precipitation Record. World Archaeol 22,3:247–270

Shimada I, Shinoda K, Alva W, Bourget S, Uceda S (2006) Estudios Arqueogenéticos de las Poblaciones Prehispánicas Mochica y Sicán. Arqueología y Sociedad 17:223–254

Shimada I, Shinoda K, Farnum J, Corruccini R, Watanabe H (2004) An integrated analysis of pre-Hispanic mortuary practices. Current Anthropol 45:369–390

Shimada I, Wagner U (2007) Craft Production on the Pre-Hispanic North Coast of Peru: A Holistic Approach and Its Results. In: Skibo J, Grave M Stark M (eds) Archaeology as Anthropology: Theoretical and Methodological Approaches. Tucson, pp 163–197

Shinoda K, Adachi N, Guillen S, Shimada I (2006) Mitochondrial DNA analysis of ancient Peruvian highlanders. Am J Phys Anthropol 131:98–107

Siegle P (2007) Untersuchungen zur absoluten Chronologie der Südküste Perus. Unpublished Masters Thesis. Inst Am Anthropol, University of Bonn

Sieper HP, Kupka HJ, Williams T, Rossmann A, Rummel S, Tanz N, Schmidt HL (2006) A measuring system for the fast simultaneous isotope ratio and elemental analysis of carbon, hydrogen, nitrogen and sulphur in food commodities and other biological material. Rapid Commun Mass Spectrom 20:2521–2527

Silberberg P (2007) www.mypacs.net/cases/RIB-FRACTURES-PROVEN-CHILD-ABUSE-5446625.html

Silva WA Jr, Bonatto SL, Holanda AJ, Ribeiro-dos-Santos AK, Paixao BM, Goldman GH, Abe-Sandes K, Rodriguez-Delfin L, Barbosa M, Paco-Larson ML, Petzl-Erler ML, Valente V, Santos SE, Zago MA (2002) Mitochondrial genome diversity of Native Americans supports a single early entry of founder populations into America. Am J Hum Genet 71:187–192

Silverman H (1977) Estilo y estado: el problema de la cultura Nasca. Informaciones Arqueológicas 1. MNAA, Lima, pp 49–78

Silverman H (1985) Cahuachi: simplemente monumental. Boletín de Lima 7:85–95

Silverman H (1990) Beyond the pampa: the geoglyphs in the valleys of Nazca. Natl Geograph Res 6:435–456

Silverman H (1991) The Paracas Problem: Archaeological Perspectives. In Paul A (ed), Paracas Arts and Architecture. Object and Context in South Coastal Peru. University of Iowa Press, Iowa City, pp 349–414

Silverman H (1993) Cahuachi in the ancient Nasca world. University of Iowa Press, Iowa City

Silverman H (1994) Paracas in Nazca: New Data on the Early Horizon Occupation of the Río Grande de Nazca Drainage, Peru. Latin Am Antiq 5(4):359–382

Silverman H (1996) The Formative Period on the South Coast of Peru: A Critical Review. J World Prehistory 10(2):95–146

Silverman H (2002) Ancient Nasca settlement and society. University of Iowa Press, Iowa City

Silverman H, Proulx D (2002) The Nasca. The peoples of America. Blackwell Publishers, Malden Oxford

Soffel H (1991) Paläomagnetismus und Archäomagnetismus. Springer, Berlin

Soßna V (2007) Siedlungsentwicklung und Siedlungsorganisation der Nasca-Zeit im Raum Palpa, Süd-Peru. Unpublished Masters Thesis. Department of Historical and Cultural Sciences, University of Berlin

Sotoodeh S (2006) Outlier detection in laser scanner points cloud. In: Maas HG, Schneider D (eds.) Proceedings of the ISPRS Commission V Symposium'Image Engineering and Vision Metrology', Dresden, Germany, 25–27 September 2006 XXXVI(5):297–302

Sotoodeh S, Novak D, Sauerbier M, Scaradozzi D, Caiti A, Conte G, Zanoli SM, Drap P, Chapman P, Pascoal AM, Long L, Hanke K (2008) UPGRADE and IMODELASER: Tools and Best Practice for 3D Data Acquisition and Processing for CH in Different

Environments. Paper presented at the Rome Event 2008 of the EPOCH Network of Excellence in Open Cultural Heritage (in press)
Stanish C (2003) Ancient Titicaca : the evolution of complex society in southern Peru and northern Bolivia. Berkeley
Stanjek H (1987) The formation of maghemite and hematite from lepidocrocite and goethite in a cambisol from Corsica, France. Z. Pflanzenernähr Bodenk 150:314–318
Stanjek H, Fassbinder JWE, Vali H, Wägele H, Graf W (1994) Evidence of biogenic greigite (ferrimagnetic Fe3S4) in soil. Europ J Soil Science 45:93–97
Stanley HF, Kadwell M, Wheeler JC (1994) Molecular evolution of the family Camelidae: a mitochondrial DNA study. Proc Biol Sci 256.1345:1–6
Steffen D, Schlunegger F, Preusser F (2007) Correlating sediment aggradation and climate by means of luminescence dating, Valley de Pisco, Peru. Geophys Res Abstracts 9:03347
Stengel HW (1965) Der schwarze Nosob. Wissenschaftliche Forschung in Südwestafrika. 4. Folge. SWA Wiss Ges, Windhoek
Stöllner T, Reindel M (2007) Vorspanische Goldgewinnung im Bereich von Palpa-Nasca? Bericht über eine einwöchige Prospektionskampagne an der Südküste Perus. Der Anschnitt 59,1:2–12
Stolz R, Zakosarenko VM, Fritsch L, Oukhanski N, Meyer HG (2001) Long baseline thin film SQUID gradiometers. IEEE Trans Appl Supercond 11:1257–1260
Stolz R, Zakosarenko VM, Schulz M, Chwala A, Fritsch L, Meyer HG (2004) Magnetic full tensor SQUID gradiometer system for geophysical applications. SEG Expanded Abstracts 23:786–789
Stothert KE (1995) Las albarradas tradicionales y el manejo de aguas en la peninsula de Santa Elena. Miscelánea Antropológica Ecuatoriana 8:131–160
Strong WD (1957) Paracas, Nazca, and Tiahuanacoid Cultural Relationships in South Coastal Peru. Memoirs of the Society for American Archaeology 13. Salt Lake City
Strub PT, Mesias JM, Montecino V, Rutland J (1998) Coastal ocean circulation off western South America. In: Brink K and Robinson A (eds) The sea, vol 11. John Wiley, New York, pp 273–313
Stuiver M, Reimer PJ, Bard E, Burr GS, Hughen KA, Kromer B, McCormac G, Plicht Jvd, Spurk M (1998) INTCAL98 Radiocarbon Age Calibration. Radiocarbon 40,3: 1041–1083
Suchey J (1986) Skeletal Age Standards Derived from an Extensive Multiracial Sample of Modern Americans. Paper presented to the 55° Annual Meeting of the American Association of Physical Anthropologists, Albuquerque
Suess HE (1965) Secular variations in the cosmic-ray produced carbon-14 in the atmosphere and their interpretation. J Geophys Res 70:5937–5952
Supresoft Inc. (2002) Virtuozo User's Manual Version 3.3
Swartz BK, Hurlbutt TS (1994) Space, place and territory in rock art interpretation. Rock Art Research 11,1:13–22
Tainter JA (1978) Mortuary practices and the study of prehistoric social systems. Adv Archaeol Method Theory 1:343–374
Tajima F (1993) Statistical analysis of DNA polymorphism. Jpn J Genet 68:567–595
Tamm E, Kivisild T, Reidla M, Metspalu M, Smith DG, Mulligan CJ, Bravi CM, Rickards O, Martinez-Labarga C, Khusnutdinova EK, Fedorova SA, Golubenko MV, Stepanov VA, Gubina MA, Zhadanov SI, Ossipova LP, Damba L, Voevoda MI, Dipierri JE, Villems R, Malhi RS (2007) Beringian standstill and spread of Native American founders. PloS ONE. 2:e829
Tamura K, Dudley J, Nei M, Kumar S (2007) MEGA4: Molecular Evolutionary Genetics Analysis (MEGA) software version 4.0. MolBiol Evol 24:1596–1599
Taylor JJ, Watling RJ, Shell CA, Ixer RA, Chapman RJ, Warner RB, Cahill M (1995) From gold ores to artifacts in the British Isles: a preliminary study of a new LA-ICP-MS analytical approach. In: Sinclair A, Slater E, Gowlett J (eds) Archaeological Science. Oxbow Monograph Series 64. Oxford, pp 107–111

Teichert B (2007) Astronomical investigations of the Nasca lines. In: Teichert B, Rust C (eds) Nasca Symposium 2006 im Zentrum für interdisziplinäre Forschungen der Universität Bielefeld (ZIF). Bielefeld, pp 87–101

Teichert B and Richter C (2001) The Nasca lines and geoglyphs – on the way to a multimedia GIS. International Archives of Phtotogrammetry, Remote Sensing and Spacial Information Sciences XXXIV-5/W1:24–29

Tello JC (1917) Los Antiguos Cementerios del Valle de Nazca. In: Proceedings of the Second Pan American Scientific Congress, Washington 1915–1916. Vol 1. Washington D. C., pp 283–291

Tello JC (1959) Paracas. Primera Parte. Publicación del Proyecto 8-b del Programa 1941–1942. New York

Tello JC, Mejía Xesspe T (1967) Historia de los Museos Nacionales del Perú 1822–1946. Arqueológicas 10. Museo Nacional de Antropología y Arqueología e Instituto y Museo de Arqueología de la Universidad Nacional Mayor de San Marcos, Lima

Tello JC, Mejía Xesspe T (1979) Paracas. Segunda Parte. Cavernas y Necrópolis. Lima

Theocaris PS, Liritzis I, Galloway RB (1997) Dating of two hellenic pyramids by a novel application of thermoluminescence. J Archaeol Scis 24:399–405

Tite MS (1966) magnetic prospecting near the aequator, Archaeometry 9:24–31

Tobler W (1993) Non-isotropic modeling. Technical Report 93-1, National Center for Geographic Information Analysis. Santa Barbara

Tomasto E (1998) Tratamiento funerario de los niños en el Cementerio Prehispánico de Tablada de Lurín. Tesis para obtener el título de Licenciada en Arqueología. Pontificia Universidad Católica del Perú, Lima

Tomasto E (2005) Tratamiento funerario de los niños en el cementerio prehispánico de Tablada de Lurín (Costa Central del Perú) In: Pontificia Universidad Católica del Perú y Promperú (eds) Arqueología, geografía e historia; Aportes peruanos en el 50 Congreso de Americanistas/Varsovia Polonia 2000, Lima, pp 97–130

Tomczak PD (2003) Prehistoric diet and socioeconomic relationships within the Osmore Valley of southern Peru. J Anthropol Archaeol 22:262–278

Torres MM, Bravi CM, Bortolini MC, Duque C, Callegari-Jacques S, Ortiz D, Bedoya G, Groot DR, Ruiz-Linares A (2006) A revertant of the major founder Native American haplogroup C common in populations from northern South America. Am J Hum Biol 18:59–65

Torroni A, Schurr TG, Cabell MF, Brown MD, Neel JV, Larsen M, Smith DG, Vullo CM, Wallace DC (1993) Asian affinities and continental radiation of the four founding Native American mtDNAs. Am J Hum Genet 53:563–590

Tosi JA (1960) Zonas de Vida Natural en el Perú: Memoria Explicativa Sobre el Mapa Ecológico del Perú Instituto Interamaricano de Ciencias Agrícolas. Boletín Técnico 5 OAS, Zona Andina, Proyecto 39. Lima

Tosovic S (2002) Adaptive 3D Modelling of Objects by combining Shape from Silhouette and Shape from Structured Light. Master Thesis. Vienna University of Technology, Institute of Computer Aided Automation, Pattern Recognition and Image Processing Group, Austria. Vienna

Troll C (1931) Die Geographischen Grundlagen der Andinen Kulturen und des Inkareiches. Iberoamerikanisches Archiv 5. Berlin

Trust BA, Fry B (1992) Stable sulphur isotopes in plants: a review. Plant Cell Environ 15:1105–1110

Trut LN (1999) Early canid domestication: The farm-fox-experiment. Am Scientist 87:160–169

Tung TA (2007) Trauma and violence in the Wari empire of the Peruvian Andes: Warfare, raids, and ritual fights. Am J Phys Anthropol 133:941–956

Tuross N, Warinner C, Kirsanow K, Kester C (2008) Organic oxygen and hydrogen isotopes in a porcine controlled dietary study. Rapid Commun Mass Spectrom 22:1741–1745

Tykot RH (2006) Isotope analyses and the histories of maize. In: Staller JE, Tykot RH, Benz BF (eds) Histories of Maize: Multidisciplinary Approaches to the Prehistory, Linguistics, Biogeography, Domestication, and Evolution of Maize. Burlington, MA, pp 131–142

Ubbelohde-Doering H (1958) Bericht ueber archäologische Feldarbeiten in Peru. Ethnos 23,2–4:67–99

Ubelaker D (1989) Human Skeletal Remains: excavation, analysis, interpretation. Manuals on Archaeology No 2. Smithsonian Institution, Washington

Uda M (1965) On the synthesis of greigite. Am Mineral 50:1487–1489

Uhle M (1913) Zur Chronologie der alten Kulturen von Ica. Journal de la Societe des Americanists de Paris, NS 10:341–367

Uhle M (1914) The Nazca pottery of ancient Peru. Davenport Academy of Sciences vol XIII, Davenport, Iowa, pp 1–16

Underhill PA, Kivisild T (2007) Use of Y Chromosome and Mitochondrial DNA Population Structure in Tracing Human Migrations. Ann Rev Genet 41:539–564

Underhill PA, Passarino G, Lin AA, Shen P, Mirazon LM, Foley RA, Oefner PJ, Cavalli-Sforza LL (2001) The phylogeography of Y chromosome binary haplotypes and the origins of modern human populations. Ann Hum Genet 65:43–62

Unkel I (2006) AMS-14C-Analysen zur Rekonstruktion der Landschafts- und Kulturgeschichte in der Region Palpa (S-Peru)/AMS-14C analyses for the reconstruction of the geomorphological and cultural development of the Palpa region (S-Peru). Heidelberger Geographische Arbeiten 121. Heidelberg

Unkel I, Kadereit A, Mächtle B, Eitel B, Kromer B, Wagner GA, Wacker L (2007) Dating methods and geomorphic evidence of palaeo-environmental changes at the eastern margin of the South Peruvian coastal desert (14°30' S) before and during the Little Ice Age. Quat Int 175:3–28

Unkel I, Kromer B, Reindel M, Wacker L, Wagner GA (2007b) A chronology of the pre-Columbian Paracas- and Nasca-culture in South Peru based on AMS-14C-dating. Radiocarbon 49(2):551–564

Usselmann P, Fontugne M, Lavallée D, Julien M, Hattée C (1999) Estabilidad y rupturas dinámica en el Holoceno de la costa surperuana: el valle de La Quebrada de los burros (departamento de Tacna). Bulletin de l'Institut francais d'études Andins 28,1:1–11

Utecht T (2005) Refraktionstomographie. In: Knödel K, Krummel H, Lange G (eds) Handbuch zur Erkundung des Untergrundes von Deponien und Altlasten. Bd. 3: Geophysik. Berlin Heidelberg: 573–582

UVS International (2008) Unmanned Vehicle Systems International http://www.uvs-international.org (Accessed. 2008-04-16)

Vafiadou A, Murray AS, Liritzis I (2007) Optically stimulated luminescence (OSL) dating investigations of rock and underlying soil from three case studies. J Archaeol Scis 34:1659–1669

Valdez LM (1988) Los camélidos en la subsistencia Nasca: el caso de Kawachi. Boletín de Lima 57:31–35

Valet JP (2003) Time variations in geomagnetic intensity. Rev Geophys 41 doi: 10.1029/2001RG000104:44

Valley JW, Cole DR (eds) (2001). Stable Isotope Geochemistry. Rev Mineral Geochem 43. Min Soc Amer, Washington, DC

van Blyenburg P (1999) UAVs: and Overview. Air Space Eur. I 5/6:43–47

Van der Marel HW (1951) Gamma ferric oxide in sediments. J Sediment Petrol 21:12–21

Vaughn KJ (2000) Archaeological investigations at Marcaya: a village approach to Nasca sociopolitical and economic organization. PhD. Diss. Department of Anthropology, University of California, Santa Barbara

Vaughn KJ, Conlee CA, Neff H, Schreiber KJ (2005) A compositional analysis of Nasca polychrome paints: Implications for craft production on the pre-Hispanic south coast of

Peru. In: Speakman RJ, Neff H (eds) Laser Ablation ICP-MS in Archaeological Research, pp. 138–154. Albuquerque
Vaughn KJ, Conlee CA, Neff H, Schreiber KJ (2006) Ceramic production in ancient Nasca: provenance analysis of pottery from the Early Nasca and Tiza cultures through INAA. J Archaeol Sci 33:681–689
Vaughn KJ, Glascock MD (2005) Exchange of Quispisisa obsidian in Nasca: New evidence from Marcaya. Andean Past 7:93–110
Vaughn KJ, Linares Grados M (2006) 3,000 Years of Occupation in Upper Valley Nasca: Excavations at Upanca. Latin Am Antiq 17(4):595–612
Vaughn KJ, Linares Grados M, Eerkens JW, Edwards MJ (2007) Hematite Mining in the Ancient Americas: Mina Primavera, a 2000 Year Old Peruvian Mine. The Journal of the Minerals, Metals & Materials Society, December 2007:16–20
Vaughn KJ, Neff H (2004) Tracing the clay sources of Nasca polychrome pottery: results from a preliminary raw material survey. J Archaeol Sci 31:1577–1586
Vaughn KJ, Van Gijseghem H (2007) A compositional perspective on the origins of the "Nasca cult" at Cahuachi. J Archaeol Sci 34:814–822
Vavelidis M, Andreou S (2008) Gold and gold working in Late Bronze Age Northern Greece. Nat wiss 95:361–366
Veitch RJ, Hedley IG, Wagner JJ (1984) An investigation of the intensity of the geomagnetic field during Roman times using magnetically anisotropic bricks and tiles. Arch Sci Genéve 37:359–373
Velarde L (1997) La transición Paracas-Nasca en el valle de Chincha. In: Chevalier A, Velarde L and Chenal-Velarde I (eds) L'Amerique du Sud: Des chasseurs-cueilleurs à l'Empire Inca. Actes des journées d'étude d'archéologie précolombienne, Genève, 10–11 october 1997. Archaeopress, Oxford, pp 63–77
Verano JW (1994) Características físicas y biología osteológica de los Moche. In: Uceda S and Mujica E (eds) Moche. Propuestas y Perspectivas. Lima, pp 307–326
Verano JW (1997a) Physical Characteristics and Skeletal Biology of the Moche Population at Pacatnamu. In: Donnan CB, Cock GA (eds) The Pacatnamu Papers, Volume 2: The Moche Occupation. Los Angeles, pp 189–214
Verano JW (1997b) Advances in the Paleopathology of Andean South America. J World Prehistory 11,2:237–268
Verano JW (2003) Human skeletal remains from Machu Picchu: A reexamination of the Yale Peabody Museum's collections. In: Burger RL, Salazar LC (eds), The 1912 Yale Peruvian Scientific Expedition Collections from Machu Picchu: Human and Animal Remains. Publications in Anthropology, Yale University, New Haven, CT, pp 65–118
Verano JW (2003) Trepanation in prehistoric South America: geographical and temporal trends. In: Arnott, Finger and Smith (eds) Trepanation: History, Discovery, Theory. Sweets & Zeitlinger Publishers, Lisse, The Netherlands, pp 223–236
Verano JW (2005) Human skeletal remains from Pikillacta. In: McEwan GF (ed) Pikillacta: The Wari Empire in Cusco. Iowa City, pp 125–130
Verhagen P, Kamermans H, van Leusen M, Deeben J, Hallewas D, Zoetbrood P (2007) First thoughts on the incorporation of cultural variables into predictive modelling. In: Verhagen P (ed) Case studies in archaeological predictive modelling. Leiden University Press, Leiden, pp 203–210
Verwey EJW, Haayman PW (1941) Electronic conductivity and transition point in magnetite. Physics 8:979–982
Visconti di Modrone V (1988) Studio antropologico dei reperti preincaici provenienti dalla zona di Nasca (Perù). Tesis de Doctorado en Sciencias Naturales. Università degli Studi de Milano, Milan
Vogel JS, Southon JR, Nelson DE, Brown TA (1984) Performance of catalytically condensed carbon for use in Accelerator Mass Spectrometry. Nuclear Instrum Methods B5:289–293

Vuille M (1999) Atmospheric circulation over the Bolivian Altiplano during dry and wet periods and extreme phases of the Southern Oscillation. Int J Climatol 19:1579–1600
Wagner GA (ed) (2007) Einführung in die Archäometrie. Springer, Berlin Heidelberg New York
Wagner GA, Glasmacher UA, Greilich S (2005) Spatially resolved dose-rate determination in rocks and ceramics by neutron-induced fission tracks: fundamentals. Radiat Meas 40:26–31
Wagner GA, Greilich S, Kadereit A (2003a) Kaltes Leuchten erhellt die Vergangenheit: Lumineszenzdatierung. Physik in unserer Zeit 34,4:160–166
Wagner U, Häusler W, Shimada I, Wagner FE (2003b) Mössbauer Spectroscopy in South American Archaeology. Hyp Interact 148/149:13–20
Walker P (1994) Is the Battered-Child Syndrome a Modern Phenomenon? Paper presented to the Xth European Meeting of the Paleopathology Association, issued in Göttingen, in September 1994
Walker P, Cook D, Lambert P (1997) Skeletal evidence for child abuse: a physical anthropological perspective. J Forensic Sci 42,2:196–207
Wallace DT (1986a) The Topara tradition: an overview. In: Sandweiss DH Kvietok DP (ed) Perspectives on Andean Prehistory and Protohistory. Papers from the Third Annual Northeast Conference on Andean Archaeology and Ethnohistory. Ithaca, pp 35–47
Wallace J (1986b) Translation theories and the decipherment of Linear B. In: LePore E (ed) Truth and interpretation: perspectives on the philosophy of Donald Davidson. Blackwell, New York
Wang Y, Yang X, Stojic M, Skelton B (2004) Toward higher automation and flexibility in Commercial Digital Photogrammetric System. In: International Archives of Photogrammetry, Remote Sensing and Spatial Information Sciences, vol XXXV/B2, pp 838–840
Ward RH, Salzano FM, Bonatto SL, Hutz MH, Coimbra CEA, Santos R (1996) Mitochondrial DNA Polymorphism in Three Brazilian Indian Tribes. Am J Hum Biol 8:317–323
Wassenaar LI, Hobson KA (2003) Comparative equilibration and online technique for determination of non-exchangeable hydrogen of keratins for use in animal migration studies. Isotopes Environ Health Stud 39:211–217
Watling RJ, Herbert HK, Delev D, Abell ID (1994) Gold fingerprinting by laser-ablation inductively-coupled plasma-mass spectrometry. Spectrochim. Acta Part B 49:205–219
Wegner S (1975) An analysis of vessel shapes and shape changes in phases 6 through 9 of the Nasca sequence. Unpublished manuscript
Wegner S (1976) A Stylistic seriation of Nasca 6 painted pottery designs. Unpublished manuscript
Weisgerber G (2006) Chuquicamata und anderer indianischer Bergbau vor Kolumbus. Der Anschnitt 58,1–2:2–17
Weiss K (1973) Demographic Models for Anthropology. Memoirs of the Society for American Archaeology 27, Issued as Am Antiq 38,2, Part 2
Weiss P (1958) Osteología cultural, primera parte: cabezas trofeos, trepanaciones, cauterizaciones. Universidad Nacional Mayor de San Marcos, Lima
Weiss P (1961) Osteología cultural, segunda parte: Prácticas Cefálicas. Universidad Nacional Mayor de San Marcos, Lima
Wendt A. (2007) Objektraumbasierte simultane multisensorale Orientierung: Dissertation: Deutsche Geodätische Kommission Reihe C, Nr.613
Weng C, Bush MB, Curtis JH, Kolata AL, Dillehay TD, Binford MW (2006) Deglaciation and Holocene climate change in the western Peruvian Andes. Quat Res 66:87–96
Westenthanner M, Adler M, Fehren-Schmitz L, Hummel S (in prep) A New Real Time PCR Strategy to Enable Quantification of Inhibited Low Copy Number DNA Samples
Wester-Ebbinghaus W (1980) Aerial Photography by radio controlled model helicopter. The Photogrammetric Record 55:85–92

Wetter A (2005) Paracas-Keramik aus Jauranga: Grundlagen zur Klassifikation formativzeitlicher Keramik der Südküste Perus. Unpublished Masters Thesis. Institute of American Anthropology, University of Bonn (Ms)

Wheatley D (1995) Cumulative viewshed analysis: a GIS-based method for investigating intervisibility, and its archaeological application. In: Lock G, Stančič Z (eds) Archaeology and Geographical Information Systems: a European perspective. Taylor & Francis, London Bristol, pp 171–185

Wheatley D, Gillings M (2000) Vision, perception and GIS: developing enriched approaches to the study of archaeological visibility. In: Lock G (ed) Beyond the map: archaeology and spatial technology. IOS Press, Amsterdam, pp 1–27

Wheatley D, Gillings M (2002) Spatial technology and archaeology: the archaeological applications of GIS. Taylor & Francis, London New York

Wheeler JC, Russel AJF, Stanley HF (1992) Razas prehispanicas de llamas y alpacas; la medida de lo que se ha perdido. Arch Zootec 41.extra:467–75

Wheeler SM, Williams L, Beauchesne P, Molto JE (2007) Fractured Childhood: A Case of Probable Child Abuse from Ancient Egypt. SAA Bulletin, Newsletter of the Society for Archaeological Sciences 30:6–9

Whitley DS (1998) Cognitive neuroscience, shamanism and the rock art of native California. Anthropology of Consciousness 9,1:22–37

Whitley TG (2004) Spatial variables as proxies for modelling cognition and decision-making in archaeological settings: a theoretical perspective. Internet Archaeology 16. http://intarch.ac.uk/journal/issue16/3/toc.html

Whorf BL (1956) The punctual and segmentative aspects of verbs in Hopi. In: Carroll BJ (ed) Language, Thought and Reality: selected writings of Benjamin Lee Whorf. The Technology Press of Massachusetts Institute of Technology, Cambridge, Massachusetts, 51–56

Wickler W, Seibt U (1998) Kalenderwurm und Perlenpost: Biologen entschlüsseln ungeschriebene Botschaften. Heidelberg

Wieczorek A, Tellenbach M (2002) Exkurs zur Frage der Drehscheibenkeramik. In: Wieczorek A, Tellenbach M (eds) An die Mächte der Natur – Mythen der altperuanischen Nasca-Indianer. Katalog zur Ausstellung im Reiss-Engelhorn-Museum, Mainz, Germany. pp 54– 63

Wilder JA, Kingan SB, Mobasher Z, Pilkington MM, Hammer MF (2004) Global patterns of human mitochondrial DNA and Y-chromosome structure are not influenced by higher migration rates of females versus males. Nat Genet 36:1122–1125

Willerslev E, Cooper A (2005) Ancient DNA. Proc Biol Sci 272:3–16

Williams PR, Couture N, Blom D (2007) Urban Structure at Tiwanaku: Geophysical Investigations in the Andean Altiplano. In: Wiseman J, El-Baz F (eds) Remote Sensing in Archaeology. Interdisciplinary Contributions to Archaeology. New York, pp 423–441

Williams S, Forgey K, Klarich E (2001) An Osteological study of Nasca Trophy Heads collected by A.L. Kroeber during the Marshall Field Expeditions to Peru. Anthropology New Series. USA, 33:1–132

Willis R (2004) Stochastic 3D Geometric Models for Classification, Deformation, and Estimation. PhD thesis. Diss. Brown University, Rhode Island, USA

Wilson L, Pollard AM (2001) The Provenance Hypothesis. In: Brothwell DR, Pollard AM (eds) Handbook of Archaeological Sciences, pp 507–517

Wintle AG (1973) Anomalous fading of thermoluminescence in mineral samples. Nature 245:143–144

Wintle AG, Huntley DJ (1980) Thermoluminescence dating of ocean sediments. Canadian J Earth Sci 17:348–360

Wipf M (2006) Evolution of the Western Cordillera and coastal margin of Peru: evidence from low-temperature thermochronology and geomorphology. Diss. ETH Zürich no. 16383

Witcher RE (1999) GIS and landscapes of perception. In: Gillings M, Mattingly D, van Dalen J (eds) Geographical information systems and landscape archaeology. Oxbow Books, Oxford, pp 13–22

Woda C (2007) Lumineszenz-Datierung an den Externsteinen. In: Jähne R, Linde R, Woda C (eds) Licht in das Dunkel der Vergangenheit. Verlag für Regionalgeschichte, Bielefeld, pp 97–125

Wolfe EF (1981) The Spotted Cat and the Horrible Bird: stylistic change in Nasca 1–5 ceramic decoration. Ñawpa Pacha 19:1–62

Wood JD (1996) The geomorphological characterisation of digital elevation models. PhD thesis. Diss. University of Leicester, http://www.soi.city.ac.uk/~jwo/phd

Yacobaccio HD (2003) Social dimension of camelid domestication in the southern Andes. Anthropozoologica 39,1:237–247

Yang S, Odah H, Shaw J (2000) Variations in the geomagnetic dipole moment over the last 12000 years. Geophys J Int 140:158–162

Yang S, Shaw J, Rolph T (1993) Archeointensity studies of Peruvian Pottery – from 1200 B.C. to 1800 A.D. J Geomag Geoelectr 45:1193–1207

Y-Chromosome Consortium (2002) A nomenclature system for the tree of human Y-chromosomal binary haplogroups. Genome Res 12:339–348

Z/I Imaging Corporation (2002) Image Station Automatic Elevations Help (4.00)

Zaro G, Alvarez AU (2005) Late Chriribaya agriculture and risk management along the Arid Andean Coast of Southern Peru, A.D. 1200–1400. Geoarchaeology 20:717–737

Zeder MA, Hesse B (2000) The initial domestication of goats (Capra hircus) in the Zagros mountains 10,000 years ago. Science 287(5461):2254–2257

Zeil W (1983) Südamerika. Enke, Stuttgart

Zhang L (2005) Automatic digital surface model (DSM) generation from linear array images. Ph. D. Diss., Institute of Geodesy and Photogrammetry, ETH Zurich, Nr. 88

Zhang L, Gruen A (2004) Automatic DSM generation from Linear Array imagery data. XXth ISPRS Congress, 12–23 July Istanbul, Turkey. International Archives of Photogrammetry, Remote Sensing and Spatial Information Sciences, vol 34, Part B3, pp 128–133

Zhou J, Lau KM (1998) Does a monsoon climate exist over South America? J Climate 11:1020–1040

Ziolkowski MS, Pazdur MF, Krzanowski A, Michczynski A (1994) Andes: radiocarbon database for Bolivia, Ecuador and Peru. Warsaw

Zischinsky T, Dorfner L, Rottensteiner F (2000). Application of a new Model Helicopter System in Architectural Photogrammetry. Amsterdam, International Archives of Photogrammetry, Remote Sensing and Spatial Information Sciences XXXIII(B5/2):959–965

Zwicker M (2000) Photogrammetrische auswertung der Siedlung Pinchango im Gebiet Palpa (Peru). Diploma Thesis, ETH Zurich, Switzerland

Index

Absolute chronology, 123, 207–230
Acarí, 8, 137, 142, 419–420, 432, 443, 452
Accelerator mass spectrometer (AMS), 18, 22, 231, 233–235, 244
Active measurement, 347
Administrative centre, 456
Adobe, 27, 32, 80, 83, 87, 100, 125, 129, 130, 132, 135, 220, 233, 297, 299, 443–444, 448, 452, 453, 454
Aerial image, 280, 311, 315
Airborne laser scanner, 347
Albarrada, 41
Alloy, 394–397, 403, 409, 411, 414, 416, 417, 426, 430, 432
Alpaca, 193, 195, 196, 197, 198, 200, 201
Amalgamation, 405
Anaemia, 149, 151, 157
Analytical plotter, 299, 311, 315, 342
Ancient DNA (aDNA), 159–172, 194, 195, 197, 198
Anthropologic*, 5, 11, 141, 192
Anthropology, 2, 5, 142, 143, 159, 160–161, 174
Anticyclone system, 18
Archaeobot*, 6
Archaeoceramology, 13
Archaeochronometry, 205
Archaeointensity, 103, 104, 107, 108–109, 111–113, 115
Archaeological prospection, 6, 49, 87–102
Archaeomagnetic, 103–105, 114–116
Archaeomagnetic jerk (AMJ), 103, 114–116
Archaeometallurgy, 13, 391, 398
Archaeometry, 1, 2–3, 10, 18, 72, 173, 389
Archaic period, 7, 8, 23, 119, 120, 121, 122, 123–124, 136, 143, 145, 149, 163, 167, 439, 440–443
Aridisation, 17, 23, 25, 27, 37, 115, 265, 443, 448, 461
ASTER, 291, 292, 317, 363, 370, 371, 373
Astronomical hypothesis, 329
Atacama, 5, 10, 11, 17–37, 39, 49, 50, 175, 245, 256, 260, 262, 264, 348, 374, 397, 413, 460
Atomic emission spectrometry (AES), 410
Augmented reality, 290
Automation, 234, 290, 294, 309, 345, 379
Axis of rotation, 379, 385, 386, 387

Barbacoa, 125, 129, 130, 132, 134, 138
Batán Grande, 395–397
Bayesian statistic, 235, 242
Bioarchaeolog*, 11, 117, 141–158
Bioarchaeology, 117, 141–143
Biopurification, 189
Bolivia High, 18, 23, 24, 27, 34, 37
Bonding, 416, 433
Burial, 95, 120, 121, 123–131, 134, 136–138, 153–155, 157, 159, 160, 166, 167, 168, 170, 175, 177, 181, 185, 187, 189–191, 196, 202, 273, 280, 384, 393, 398, 400, 413, 442–443, 445, 448–450, 454, 456, 460

14C, 265
Caesium magnetometer, 49, 50, 54, 55, 57, 60, 71, 72, 84, 85
Cahuachi, 8, 26, 133, 196, 451, 452, 453
Calibration, 179, 235, 288, 311, 312, 348, 352, 366, 409, 411, 422–425, 433, 460
Camcorder, 288, 289
Camelid, 6, 45, 173–192, 193–203, 373, 373
Cantayoq, 452
Carapo, 50, 60, 62, 64, 279, 281, 282, 451
Caravansery, 196, 373, 374, 376
Carbonate, 180, 186, 188, 233, 248, 403
CCD, 252, 253, 274, 275, 277, 289, 291, 293, 303

Cerro Blanco, 336, 396
Cerro Carapo, 50, 62, 279, 281, 282
Cerro Colorado, 187
Cerro Llipato, 268
Chakipampa, 134, 241, 242
Char'ki, 195, 201
Chavin, 7, 374
Chilca, 124, 443
Child abuse, 141, 151, 154, 156, 157
Chillo, 106, 199, 200, 202, 265, 403, 419
Chimú, 40, 396, 397
Chincha, 156, 393, 397, 446
Chiribaya, 5, 34, 40, 156
Chromosom*, 160, 162, 164, 166, 168, 193
Chromosomal short tandem repeat, 193
Chromosomal topography, 164
Chromosome, 160, 162, 166
Chronologic*, 2, 3, 7, 12, 13, 18, 20, 21, 69, 122–123, 167, 168, 199, 207–213, 217, 220, 227, 230, 231, 232, 235, 445, 448
Chronology, 2, 11, 13, 21, 106, 123, 207–230, 231–243, 282, 381, 390, 418, 445
Chronometr*, 3, 11, 13, 173, 205, 245, 246, 256–259, 440, 460
Chronometry, 3, 11, 173, 205, 245, 440, 460
Chullpa, 168
Cinnabar, 405
Ciudad Perdida, 9, 32, 33, 40, 41, 42, 43, 44, 45, 46
Climate change, 5, 11, 17–37
Climatic oscillation, 39–46
CMOS, 289
Coca, 178, 183
Cold light, 245–270
Collagen, 177, 178, 187, 190, 191
Complex societies, 6, 7, 8, 17, 460
Computer aided design (CAD), 294, 355
Computer tomography (CT), 380, 381
Cooling rate, 103, 105, 106, 108, 110, 112, 113, 115
Corona, 293
Cost surface, 371, 372, 373
Craft
  production, 4, 444
  specialization, 138
Cranial deformation, 152
Cremation, 153, 445, 449
Cresta de Sacramento, 50, 60, 279, 280, 310, 340
Cryostat, 74, 75
Cultivation terrace, 183
Cultural history, 2, 7, 10, 13, 160, 338, 406, 439–440
Cumulative viewshed calculation, 326, 335
Cupisnique, 417, 418, 427
Cutamalla, 66–68

2D, 87, 90, 92, 94, 95–97, 98, 102, 213, 333, 365
2,5D, 297, 298, 353
2D dipole-dipole survey, 100
3D, 87–102
3D modeling, 287–305, 359–370
4D, 288
4D model, 288
Database, 6, 13, 71, 80, 145, 198, 209, 210, 288, 290, 341, 363, 370, 372, 382
Dawson Seriation, 209, 211, 228
Debris flow, 21, 31, 251, 261, 263, 264, 265, 266
Decapitation, 155, 156
Demography, 141, 142, 143, 145
Dendro*, 234
Desert-margin, 18, 21, 23, 25, 27, 28, 36
Differential GPS, 75, 76, 80, 310, 349, 366
Digital elevation model (DEM), 322, 350
Digital surface model (DSM), 293, 297, 307, 342, 353, 363
Digital terrain model (DTM), 300, 307, 327, 331, 333, 363, 364, 369, 372
Digitization, 287, 296, 303, 365
Disco Verde, 443
DNA
  analysis, 159, 166, 172, 198, 199, 203
  preservation, 164, 168
Domestication, 6–7, 194, 195, 196, 197, 201, 203
Dose-rate determination, 256, 257, 274
Dry valley, 20, 42, 264, 265, 266, 326, 457
Dung effect, 183

Early Horizon, 232, 324, 398, 414
Early Intermediate period, 324, 395, 414
Earth resistivity tomography (ERT), 87, 89–90, 92–95, 102
Electrical resistivity, 89–90, 95
Electromagnetic spectrum, 288
Electron microscopy, 142, 278
El Niño Southern Oscillation (ENSO), 260
Embossing, 398, 413, 415–416
Enamel, 144, 178, 180, 186, 187, 190
Engobe, 213, 214, 215, 216, 220, 228, 450
Erizo, 443

Estaqueria, 66, 77, 81, 82, 83, 84, 85
Evaporation line, 186
Exchange network, 137

Field intensity, 103, 105
Flight planning, 309, 347, 349
Fluvial deposit, 22, 25, 32, 97, 263, 269–270
Fluvial sediment, 23, 87, 92, 93, 94, 96, 263
Fluvial terrace, 92, 93, 94, 95, 96, 263
Fluxgate magnetometer, 73
Formative, 149, 418, 433, 436
Fortification, 401
Four point method, 90
Funerary context, 20, 119–129, 134–138, 141–143, 153, 442, 446
Funerary pattern, 119–120, 139
Funerary practice, 119–139, 148, 157
Funerary ritual, 128

Gender, 122, 123, 141, 157
Generalized reciprocal method (GRM), 90–91
Genetic diversity, 161, 162, 166, 169
Genetic exchange, 170
Genetic marker, 159, 160, 164–166, 172
Genotype, 195, 198
Geoarchaeolog*, 5, 11, 13, 15, 17, 18, 20, 21, 23, 25–27, 32, 33, 37, 87, 88, 89, 245, 327
Geoarchaeology, 15, 18, 88
Geoarchive, 18, 21, 31, 36, 37, 39, 246
Geodesy, 59
Geodet, 36, 342, 357
Geoelectric*, 87, 89, 90, 92, 94–100, 102
Geoglyph, 6, 8, 10, 11, 13, 20, 25, 26, 34, 49–50, 53, 55, 58–65, 68–69, 77, 137, 138, 170, 226, 231, 252, 266, 271, 272, 277, 279–282, 308–310, 317–320, 321–338, 342, 374, 376, 440, 448, 451–452, 454–456, 461
Geographic information system (GIS), 6, 11, 307, 359
Geomagnet*, 11, 69
Geomagnetic field, 11, 49, 56, 103–116
Geomagnetic prospection, 11
Geomatic, 11, 285, 307
Geometrical resolution, 290, 291
Geophysic*, 2, 6, 18, 47, 49–50, 55, 59, 61, 63, 64, 65, 66, 71, 74, 77, 87, 88, 89, 91, 92, 102, 107, 440, 447, 460
Geophysical prospection, 2, 6, 92, 447, 460–461
Georeferenc*, 71, 77, 79, 80, 85, 293, 294, 307, 322, 338, 353
Georeferencing, 293–294
Gilding, 409, 414, 426
Global meteoric water line (GMWL), 185, 186, 187
Global positioning system (GPS), 75, 76, 79, 288, 289, 293, 310, 312, 345, 347, 349, 351, 353, 364, 366, 369
Gold, 393–407, 408–436, 457
Gradiometer, 56–57, 59, 60, 62, 63, 64, 66, 69, 72, 73–75, 78, 79, 81, 84–85
Granitoid stone, 273, 282
Graphitisation, 234
Grave, 97, 121–123, 125, 126, 129, 130, 133, 134, 135, 138, 207, 209–212, 222, 229, 362, 395, 418, 442, 445–446, 448, 454, 456, 461
Guanaco, 193, 195, 198, 200, 201, 202

Hacha, 106, 137, 443
Hanaq Pacha, 9, 121, 128, 130, 132, 134, 138, 167, 168, 176, 199, 229, 240, 456
Haplogroup, 159, 161, 162, 163, 164, 165, 166–168, 169–171
Hd (mitochondrial Haplotype diversity), 23, 45, 169, 442
Helicopter, 339–358
Hiatus, 229, 460
High resolution OSL (HR-OSL), 245, 253, 265–270, 271–272, 275–277, 283
High sensitivity, 27, 72, 265, 410, 411, 420
High spatial resolution sampling, 411
Higuchi viewshed, 326
Histological analysis, 150
Holocene, 7, 17–37, 39, 260, 267
Horizontal gradiometer, 56–57, 60, 62, 63, 64, 66, 69
Huarango, 125, 130, 132, 135, 136
Huari, 27, 40, 176, 412
Huayco, 21, 256, 261–263, 266–267
Husbandry, 194
Hydrological oscillation, 17, 20
Hyperspectral sensor, 288

Ica, 7, 8, 19–22, 106, 119, 128, 175, 191, 192, 208, 210, 228, 232, 272, 370, 393, 395, 397, 398, 406, 409, 412, 416, 419, 420, 443, 445, 446
Ica-Nasca depression, 272
Ica-Nazca region, 17, 23, 27, 36
Iconograph*, 212, 360, 363, 374, 412
Iconography, 196, 212, 217, 230, 232, 359, 372, 376, 377
IKONOS, 292, 300, 301

Image
acquisition, 307, 309, 310, 344, 345, 347, 351, 365–366, 368
-based technique, 287, 290, 297
-matching, 295, 312, 316, 352, 367
Imaging, 274, 275–277, 287, 288, 289, 293, 313
Induced magnetisation, 51, 52–53, 64, 68
Inertial measurement unit (IMU), 288, 293
Inertial navigation system (INS), 289, 345, 347, 351
Infrared-Stimulated Luminescence (IRSL), 248, 251, 253, 256, 260, 262, 265, 266, 268
Initial Nasca, 83, 143, 211, 213–217, 226–230, 232, 236–237, 240, 242–243, 418, 450–451
Initial Period, 8, 20, 23, 28, 105, 106, 111, 113, 115, 119, 121, 123, 125, 137, 143, 167, 181, 191, 231, 233, 236, 237, 241, 395, 439–446
Inka period, 8, 393, 395
Innertropical convergence zone (ITCZ), 235
Intensity curve, 103, 105, 113–115
Intercept-time method, 90–91
Interferometric radar, 288
Irradiation, 247, 249, 251, 253, 268
Irrigation, 32, 40, 65, 267, 269, 270, 325, 336, 341, 448, 452
Isochrone dating, 283
Isotope
abundance ratio, 173
analysis, 142, 151, 410, 453
ratio, 174, 179, 180, 186, 410
signature, 173–192

Jaime, 9, 22, 32, 253, 254, 256, 257, 258, 261, 266, 267–270
Jauranga, 9, 25, 65, 77, 80, 87, 92–95, 106, 121, 125, 126, 128, 137, 167, 168, 169, 175, 199, 200, 202, 229, 231, 233, 236, 238, 239, 240, 261, 263, 269, 373, 446–448, 450, 176, 197
Jumana, 452

Khadin, 33, 41–46

La Esmeralda, 441
La Maquina, 185, 186, 187
La Muña, 167
La Niña, 34, 260, 263
La Paloma, 124
La Ventilla, 106, 452
Lake Titicaca, 27, 115, 395, 414, 415
Landscape
archaeology, 321–323
development, 11, 245–270
Laser, 274, 275, 276, 277, 287–289, 299, 303, 304, 305, 319, 379–390
Laser ablation and inductively coupled plasma-mass spectrometry (LA-ICP-MS), 4, 409–411, 423, 427, 433, 434, 436
Laser ablation (LA), 410–411, 420, 421, 422
Laser scanning, 13, 339–358, 359–377
Las Trancas, 120, 156
Late Horizon, 440, 458–460
Late Intermediate period, 8, 17, 20, 32, 39–40, 42, 45, 63, 103, 105, 106, 114, 121, 181, 196, 199, 202–203, 265, 267, 299, 339, 357, 395, 397–400, 403, 406, 428, 439–440, 457–459
Light detection and ranging (LiDAR), 297
Lightning strike, 49, 53, 56, 60, 62, 68, 69
Linear array sensor, 293
Line of sight (LoS), 333, 334
Little Ice Age, 17, 34, 46, 263–265, 269–270
Llama, 193, 195, 198, 200–202, 449, 453
Llipata, 50, 58, 59, 60, 68, 279, 280, 374, 452, 458
Loess, 17, 21–23, 25, 32, 39, 50, 68, 77, 188, 245, 253, 260–263, 268–270, 374
Loro, 106, 134, 135, 227, 230, 241, 242
Los Batanes, 399, 400, 401
Los Molinos, 9, 77, 81, 106, 121, 128, 130, 131, 134, 138, 166, 167, 168, 175, 182, 185, 187, 192, 199, 200, 202, 211, 214–220, 221, 227–229, 231, 233, 235, 237, 240, 241, 452–453, 456
Low-light luminescence, 274
Lucriche, 9, 121, 134, 135

Magnetic anisotropy, 104, 108, 109–110, 113, 115
Magnetic anomalies, 51, 52, 53, 66, 68, 69, 94, 95–96
Magnetic field, 11, 49, 51, 53–58, 61, 64, 65, 66, 67, 71–75, 84, 98
Magnetic prospecting technique, 55
Magnetic prospection, 11, 71–72, 85, 94
Magnetisation, 51–53, 68, 69, 71, 105, 107, 108–109, 111
Magnetometry, 6, 49, 53–56, 58, 60–62, 65, 69

Magnetomineralogic*, 103, 105, 106, 107, 109
Maize, 5, 131, 150, 174, 182, 183, 187, 189, 191, 192, 453
Marine resource, 185
Mass spectrometry (MS), 4, 410
Mastodonte, 443
Mercury, 405, 432
Metallurg*, 393, 394–398
Metallurgy, 4, 13, 393–395, 397–398, 406, 409, 411, 412–416, 418, 426
Microdrone, 344
Microscopy, 142, 274, 278
Microwave, 289
Middle Horizon, 8, 40, 103, 105, 106, 113, 114, 115, 119, 120, 121, 134–136, 138, 141, 143, 144, 146, 147–152, 156–157, 167–169, 171, 203, 227, 236, 241, 395, 397, 398, 403, 439, 440, 456–457
Migration, 11, 36, 142, 159, 160–163, 170–173, 192, 460
Milling stone, 399
Mina Perdida, 395
Mina Pinchango, 401, 403, 407
Mineralisation, 401, 403, 404
Mineros artesanales, 400, 403, 404
Minimum variance method, 430, 433
Mining, 341, 393, 396, 397, 398, 400, 401–406, 416, 457
Mitochondrial DNA (mtDNA), 160, 164, 165, 193, 197
Mitochondrial genetic marker, 159
Mitochondrial genome, 165
Mitochondrial haplotype diversity (Hd), 169
Moche, 5, 27, 40, 142, 156, 393, 395, 398, 416, 417, 418
Molecular genetic, 160, 161, 164–166, 193–203
Mollake Chico, 9, 125, 137, 153, 167, 236, 238, 373, 398, 436, 445, 446, 450
Monsoon, 17, 27, 34, 36, 260, 264, 267
Monte Grande, 9, 166, 167, 175, 182–192, 370, 373
Mortality, 145–148, 156–157
Mortuary custom, 119, 120, 121, 136, 138
MtDNA haplotype, 161
Mt-haplogroup, 161, 165–168
Mt-haplotype, 161, 162, 168–171
Multielement isotope analysis, 174–176
Multiple areas single section (MASS), 277, 279
Multiple burial, 127, 128, 134, 137, 456
Mummy, 144, 175, 190, 398, 415, 427, 428, 430

Nasca
  chronology, 210, 232, 235–237
  culture, 7–8, 10, 17, 20, 27, 120, 122, 125, 126, 127, 128–129, 134, 136–138, 164, 170, 171, 208, 213, 231, 243, 266, 269, 324, 376, 397, 398, 399, 409, 414, 416, 417, 426, 427, 430, 440, 450, 451, 460
  line, 3, 25, 26, 49, 50, 307–320
  -Palpa project, 3, 8, 9, 10, 12–13, 18, 37, 41, 58, 87, 91, 119–121, 124, 128, 132, 162, 163, 196, 209–210, 212, 271, 282, 307, 343, 364, 400, 406–407, 443, 445–447, 450–452, 454, 456, 460
  period, 11, 13, 25, 26, 83, 98, 105, 109, 130, 138, 143, 164, 168, 170–171, 196, 202, 207–208, 231–243, 376, 388, 397–398, 406, 439, 440, 445, 450–451, 452
  phase, 128, 131, 138, 209, 213–214, 217, 219–226, 228–230, 235–238, 241, 450–457
  style, 7, 207–230, 414, 430, 432
Navigation system, 344–345
Necropolis, 26, 395, 454
Neutron activation analysis (NAA), 4
Nucleotide polymorphism, 164, 193
Numerical chronology, 208, 231–233, 236
Nutrition, 173, 174, 182, 183, 188, 194, 195, 453

Object extraction, 294, 309
Obsidian, 3, 4, 11, 125, 127, 133, 136, 153, 155, 373, 410, 442, 445, 448, 453
Ocucaje, 106, 125, 127, 228, 230, 232, 238, 239, 242, 445, 448, 450
Optically stimulated luminescence (OSL), 3, 245, 246, 271–283
Ore
  deposit, 393, 395, 403, 406, 410
  -formation, 393
Organic fertilisation, 183
Orientation, 83, 123–124, 293, 294, 299, 301, 311–313, 323–326, 331–338, 345, 347, 349, 351, 352, 366, 383–385, 387, 389, 413
Orthoimage, 59, 293–294, 301, 307, 308, 309, 313–319, 339, 340, 347–352, 354, 355, 356, 368
Orthomosaic, 299, 307, 319
Oscillation, 17, 20, 39–46
Osteological analysis, 141–142, 143
Osteology, 142
OxCal, 22, 235–242

Pacapaccari, 167–169, 175, 176, 178, 188–192
Palaeoanthropology, 174
Palaeoclimat*, 17, 23
Palaeoclimatology, 27–30, 34–36, 448, 457
Palaeodose, 253, 254, 268
Palaeogenetic, 18, 161–164, 193, 460
Paleoclimat*, 5, 326, 443
Paleodemography, 142, 143
Paleogen*, 5, 7, 440
Paleogenetic studies, 5, 7
Paleopathology, 142, 143, 145
Paloma, 124, 142, 443
Pampa de Llipata, 50, 279, 280
Pampa de Nasca, 6, 50, 307–320
Pampa de San Ignacio, 50
Paracas
  culture, 7, 8, 17, 25, 26, 124–128, 137, 170, 196, 232, 324, 374, 376, 395, 409, 415, 436, 440, 443, 444–446
  peninsula, 7, 120, 124, 137, 142, 166–169, 182, 183, 185, 188, 190, 191, 192, 232, 397, 419, 428, 430
  period, 77, 80, 105, 111, 113, 125–127, 137, 169, 195, 201, 232, 233, 243, 373, 374, 376, 416, 430, 444–445, 447, 448–449, 450
Parasmarca, 9, 121, 134, 135, 211, 222, 223, 225–229, 241, 455–456
Paredones, 459
Pediment, 19, 20, 21, 25, 31, 50, 272
Periostosis, 144, 150
Pernil Alto, 9, 20, 23, 106, 121, 123–127, 130, 136, 137, 166, 167, 176, 188, 191, 199, 200, 202, 231, 233, 236, 237, 238, 279, 281, 282, 441–445
Petroglyph, 13, 324, 359–377, 448, 461
Phenotype, 195–196
Photogrammetr*, 6, 58, 68, 80, 287–290, 291, 293–295, 299–301, 305, 307, 309, 310, 311, 313, 317, 320, 332, 339, 342–347, 349, 351, 357, 363, 365–367, 370, 377
Photogrammetry, 13, 59, 77, 287–290, 293, 295–299, 304–305, 307–308, 309, 311, 313, 319, 323, 339–358, 359, 365
Physical anthropology, 160
Phytolith, 6, 17, 22, 32, 175, 177, 179, 180, 187–188
Pictometry, 288
Pinchango Alto, 9, 339–358, 399, 400, 401, 457, 458
Pinchango Viejo, 9, 176, 239, 449–450
Pisco, 19, 120, 182, 444, 446, 459
Pit house, 442, 443
Pleistocene, 19, 21, 23, 31, 194, 266, 405
Pluvial phase, 31, 32, 34
Point cloud, 294, 295, 301, 303–304, 305, 347, 348–350, 353, 355, 356, 358, 363, 367, 369
Polymineral fine grain, 248, 249, 251, 260
Polymorphism, 164, 165–166193, 197–198
Pottery
  classification, 211–212
  plate, 383
  style, 105, 106, 111, 208, 209, 221
  wheel, 383, 384
Preablation, 421–422
Precipitation, 19, 21, 27, 31, 33, 39, 45, 50, 89, 185, 186, 422–423, 457
Profile line, 92–93, 379–390
Prospect*, 49–69, 71–85, 87–102, 171, 305, 406, 447, 460
Pueblo Nuevo, 9, 419, 458, 459
Pueblo Viejo, 176, 183, 189, 190, 191, 420
Puente Gentil, 452

Quantitative analysis, 278, 411
Quantum Detection, 72–85
Quebrada, 20, 22, 23, 25, 26, 32, 262, 264–266, 316, 404, 419, 420, 441, 445
Quelccaya, 264
Quimbalete, 405
Quincha (wattle and daub), 451, 452, 456

Radiation, 104, 245–249, 278, 381
Radiocarbon, 3, 11, 18, 31, 32, 105, 111, 122, 123, 231–243, 246, 271, 442, 453
Radiometric, 232, 289, 290, 293, 305
Raster data, 290, 322
Raytracing, 91, 92
Real-time, 76, 164, 290, 298, 317, 318, 320, 345, 350, 354, 370
Relative chronology, 123, 207–230, 281, 390
Reloj Solar, 62, 63
Remanent magnetization, 103
Remote sensing, 2, 6, 49, 288, 290, 291, 304, 305
Resistivity, 6, 53, 65, 87, 89–102
Resolution, 50, 55–56, 71, 72, 74, 75, 85, 88, 90, 91, 96, 98, 102, 104, 115, 116, 172, 194, 252, 253, 265–266, 268, 271, 272, 274, 275, 288, 289, 290, 291, 292, 296, 300, 301, 304, 305, 310, 312, 317–319, 327, 343, 347, 348–350, 352, 353, 355–357, 363, 364, 370, 372, 379, 381, 384, 411, 421
Rock-art, 359–362, 365, 372

San Ignacio, 50, 58, 60, 63–65, 310
San Nicolás, 441
Santa Ana, 175, 441
Saramarca, 403, 404, 405
Satellite, 6, 13, 49, 287, 288, 290, 291–294, 297, 300, 304–305, 310, 317, 319, 327, 352, 363, 367, 370, 373
Satellite image, 13, 49, 288, 290, 291, 294, 300, 304, 305, 310, 317, 327, 352, 363, 373
Sayhua, 176, 188–191
Scanner, 288, 289, 293, 296, 299, 303, 304, 310, 339, 346–351, 353, 356, 358, 363, 364, 365, 379, 381, 382
Scanning, 13, 274, 277, 278, 287, 296, 302, 303, 305, 319, 339–358, 359–377
Schlepp-Effect, 195
Seafood, 174, 182, 184, 185, 187, 191, 192, 453
Secondary burial, 445
Sedentariness, 40, 189
Sedentary, 136, 137, 443, 444, 460
Sediment tomography, 11, 87–89, 91–92, 102
Seismic refraction tomography (SRT), 87, 90–91, 92–95, 102
Sensor technology, 287
Seriation, 207, 209, 211, 228, 448
Settlement
  centre, 452, 454, 459
  history, 11, 230, 398, 401, 439, 440, 460, 461
  pattern, 8, 10, 11, 28, 36, 321, 412, 450, 451, 452, 454, 460
Shell, 22, 122, 124, 127, 133, 373, 442
Shuttle radar topography mission (SRTM), 19, 297
Single-aliquot regenerative (SAR), 251
Sipán, 5, 142, 395, 419
Slag, 56, 283, 397
Social difference, 131, 134, 136, 137
Social differentiation, 131
Socioeconomic complexity, 170–171
Soldering, 398, 413, 416
Solution calibration, 411, 422, 423
South American summer monsoon (SASM), 36, 260
Spacial information system (SIS), 288, 290
Spectral resolution, 291
Spectrometry, 4, 256, 257, 278, 410
Spondylus, 133, 135, 325, 336, 435, 452
Spongiosclerosis, 141, 145, 149–151, 156
SPOT–5, 292, 300
SQUID-Gradiometer, 84
SQUID magnetometer, 58, 66, 108
Stable isotope, 460
Stature, 144, 145, 148–149, 156
Still video, 288–289, 293, 300, 345, 347–349, 351–352, 365
Stratigraph*, 50, 61, 62, 69, 105, 111, 122, 126, 207–213, 219–222, 225, 226, 228, 229, 232, 235, 445, 448, 456
Stratigraphy, 210, 213, 214, 215, 217, 220, 228, 318
Stress indicator, 144–145
Structured light, 287–289, 296, 299, 302–303, 305, 365, 379, 381, 384
Superconducting Quantum Interference Device (SQUID), 71–85, 108

Tachymeter, 342, 369
Tahuantinsuyu, 412
Tambo Viejo, 452
Terrace, 25, 27, 31, 32, 42, 44, 45, 80, 92, 93, 94, 95, 96, 183, 263, 269–270, 405, 444, 445, 449, 451–453, 456
Terrestrial
  laser scanner, 346, 347–348, 358, 363, 365
  measurement, 342
Texture, 289, 294–298, 300–303, 305, 307–320, 347, 348, 350, 354–358, 367, 368–370, 373, 389
Texture mapping, 289, 300, 303, 305, 348, 355, 358
Thellier, 103, 104, 105, 108–110, 112, 505
Thermal experiment, 108
Thermal ionisation mass spectrometer (TIMS), 181
Thermoluminescence (TL), 3, 273
Thermomagnetic, 107, 108, 110
Thermoremanent magnetisation (TRM), 53, 68, 103, 105, 108
Tiahuanaco, 6, 7, 40, 412
Tie point, 304, 309, 311, 312, 313, 351–352, 363, 366
Tissue, 166, 177, 178, 181, 185, 190, 199
Tiwanaku, 5, 397
Tomography, 11, 87–102, 142, 380, 381
Topará, 450
Total field magnetometry, 69
Total field measurement, 54, 57, 58, 60
Trace element, 398, 400, 409–411, 417, 422, 423, 430, 436
Trade, 4, 11, 173, 185, 193, 196, 202, 396, 413, 449, 457, 459–460
Trading, 13, 194, 202, 203, 380, 457

Trapezoid, 49, 50, 53, 57–58, 60–62, 63, 68, 318, 324, 325, 329, 330, 331, 336, 427, 452, 455, 459
Trauma, 141–145, 151–154, 156, 157
Trephination, 141, 151
Triangular irregular network (TIN), 295
Triangulation, 295, 296, 345, 351, 353, 381
Trophy head, 141, 143, 144, 145, 224, 416
Tulin, 405

Ultrasound, 289
Unified modeling language (UML), 370
Universal transverse Mercator (UTM), 79, 80, 288, 310, 311, 330, 331, 333, 334, 364, 366, 369, 370
Unmanned aerial vehicle (UAV), 339, 344
Unwrapped drawing, 381, 388, 389
Urn, 129, 137, 138, 153, 157

Vector, 51, 53, 73, 84, 105, 290, 317, 319, 322, 329, 363, 365, 369, 372
Vesicular layer, 25
Vicuña, 193, 195, 198, 200–202, 398, 416, 418
Viewshed analysis, 323
Virtual axial dipole moments (VADM), 113–115
Virtualization, 287
Virtual reality, 290, 323
Visibility, 56, 321–328, 334–338, 343, 353, 356, 358
Visualization, 288, 290, 294, 298, 303, 305, 356, 367, 370

Wari, 156, 164
Wari culture, 5, 119–121, 134, 138–139, 175, 280
Water harvesting, 32, 33, 39–46
Wattle and daub (quincha), 451–452, 453
Wayurí, 419, 427, 430, 431, 436
Welding, 398, 416, 433

X-ray, 4, 88, 142, 150, 289

Yunama, 60, 61, 68, 77, 81, 87, 92, 95, 96, 97269